UNIVERSIDAD COMPLUTENSE DE MADRID

FACULTAD DE CIENCIAS BIOLÓGICAS

TESIS DOCTORAL

Mecanismos subyacentes a la toxicidad de nanopartículas metálicas: aproximaciones *in vitro e in vivo*

Mechanisms underlying the toxicity of metal nanoparticles : *in vitro* and *in vivo* approaches

MEMORIA PARA OPTAR AL GRADO DE DOCTOR

PRESENTADA POR

Mona Connolly

Directores

José María Navas Antón
María Luisa Fernández Cruz

Madrid, 2017

UNIVERSIDAD COMPLUTENSE DE MADRID

FACULTAD DE CIENCIAS BIOLÓGICAS

Departamento de Bioquímica y Biología Molecular

TESIS DOCTORAL

Mecanismos subyacentes a la toxicidad de nanopartículas metálicas: aproximaciones *in vitro* e *in vivo*

Mechanisms underlying the toxicity of metal nanoparticles: *in vitro* and *in vivo* approaches

MEMORIA PARA OPTAR AL GRADO DE DOCTOR

PRESENTADA POR

Mona Connolly

Directores:

José María Navas Antón

María Luisa Fernández Cruz

Madrid, 2017

Mecanismos subyacentes a la toxicidad de nanopartículas metálicas: aproximaciones *in vitro* e *in vivo*

Mechanisms underlying the toxicity of metal nanoparticles: *in vitro* and *in vivo* approaches.

Tesis Doctoral presentada por Mona Connolly, para optar al grado de Doctor con mención Europea por la Universidad Complutense de Madrid.

El trabajo ha sido realizado en el Instituto Nacional de Investigación y Tecnología Agraria y Alimentaria (INIA) bajo la dirección de los Doctores José María Navas Antón y María Luisa Fernández Cruz y financiado por una acción Marie Curie- "Initial Training Network" (ITN) (FP7-PEOPLE-ITN-2008 Grant Agreement 238701) y el Instituto Nacional de Investigación y Tecnología Agraria y Alimentaria (project AT2011-001).

Madrid, 2017

José María Navas Antón y María Luisa Fernández Cruz, Científicos Titulares de Organismos Públicos de Investigación en el Instituto Nacional de Investigación y Tecnología Agraria y Alimentaria

CERTIFICAN

Que la presente tesis doctoral titulada "Mechanisms underlying the toxicity of metal nanoparticles: *in vitro* and *in vivo* approaches", presentada por Mona Connolly, master en Biotecnología, para optar al grado de Doctor por la Universidad Complutense de Madrid, ha sido realizada bajo su dirección y reúne todos los requisitos necesarios para ser juzgada.

Y para que conste a los efectos oportunos, firman el presente a 30 de enero de 2017

Dr. José María Navas Antón Dra. María Luisa Fernández Cruz

Acknowledgements

My sincerest and most heartfelt thanks goes to my two supervisors Dr José María Navas and Dr Maria Luisa Fernández-Cruz. They have given me guidance and support of such a high standard throughout my studies and their encouragement has ultimately lead to the completion of this thesis.

The experience I have gained from them both and through working within the DETC group at the INIA I will take with me for life and into my future scientific career.

I have been very fortunate to have been part of a Marie Curie training network that has allowed me to meet and share ideas with some of the nicest and dedicated scientists from around the world. Among them, I would like to especially mention Dr Tobias Lammel and Dr Lan Song with whom I have worked closely alongside and have learned a lot from.

On a very personal note to my family for accepting my time spent abroad with the sacrifices that went with it and James for taking the journey with me.

I must also mention the NanoSafety Research group at HWU in Edinburgh who have provided me with a working environment over the past two years that has enabled me to mature and grow in confidence as a scientist.

TABLE OF CONTENTS

Summary

Introduction

Since the turn of the 21st century new materials are emerging through our discovery that well-known materials (e.g. metals) at nanometer scale have extraordinary and surprising properties that could shape our future. Engineered nanomaterials (ENMs) are those man-made materials constituted by particles that have at least one of their dimensions between 1 and 100 nm (EU 2011, ISO 2016). Of course, these limits in size are important for regulatory purposes but when people are working in a laboratory they become wider, and we can talk about NMs of some hundreds of nanometres in size. In any case, before these ENMs full potential can be realised it is our responsibility to ensure that they are engineered as safe materials. This necessity has led to the emergence of nanotoxicology which is by definition the study of the potential toxicological effects of nanomaterials. Presently nanotechnologies are advancing faster than our rate of learning, there are gaps in our knowledge and uncertainties which may lead to as yet unknown risks. Studying the potential toxicological effects (hazards) of nanomaterials as part of a risk assessment is therefore extremely important to deepen our understanding of the potential environmental and health impacts (risks).

Concerns lie in the unpredictable behaviour of materials at nanoscale, their potential widespread distribution in the environment, and translocation within body systems due to their size.

Within this thesis a general introduction (*chapter 1*) gives a detailed background to the area of nanotoxicology and the current regulations we rely on to ensure the sustainable and safe use of ENMs. Specifically it introduces the metal and metal oxide groups of nanoparticles (NPs) used widely both industrially and commercially (namely ZnO, Cu, Ag and Au) and outlines their individual properties, applications and potential risks.

As we embark on a new age, the nano age, the questions which we must strive to answer include: What are the impacts the use of ENMs will have on the environment and are there any concerns to human health from exposure to such materials? The first step in addressing such questions is identifying the potential toxicological effects on organisms (hazard). Studying the potential hazards of these ENMs compared to more traditional chemicals requires a more complex approach and specific methodologies are needed. In liquid media ENMs form suspensions or colloidal systems due to the very nature of particles being present (if ENMs solubilize, then the particulate nature is lost and we would be dealing with the same problems as with conventional chemicals). These systems contain particles dispersed with perhaps some solubilized metal ions. In addition to this general consideration, ENMs present particular physical and chemical properties that make them different from the original bulk material and that influence their behaviour. Of particular importance is their specific surface (surface area) that increases enormously while decreasing the volume (the size) of the NPs. The specific surface area to

volume ratio can increases particles porous nature. This leads to important increments of surface reactivity so that ENMs show a distinct behaviour than the material of origin. Surface chemistry and charge can influence interactions with other particles or with molecules of the medium ENMs are immersed in. Shape and aspect ratio can control persistence.

In the present research we have focused on the possible deleterious effects of nanomaterials by means of the use of *in vitro* approaches based on cultured cells. Since the liver has been identified as an accumulation site for NPs in a number of organisms, liver hepatocytes maintained in primary culture and liver derived cell lines have been employed as *in vitro* test systems in our experiments. *In vitro* test systems may serve as an important component in an integrated testing strategy (ITS) for hazard assessment which focuses heavily on using all appropriate non-animal methods prior to animal testing. Cell lines from various diverse species are available and therefore may provide an important system to test for species susceptibilities and/or species-specific mechanisms of toxicity at the cellular level.

Among the mechanisms underlying the toxicity of ENMs, oxidative stress has emerged as a paradigm that is at the basis of all the observed deleterious effects. Oxidative stress is a cellular state that results from a redox imbalance between the generation of reactive oxygen species (ROS) and the compensatory response from the endogenous antioxidant network. However it is unclear whether oxidative stress associated with nanomaterials is the direct cause of cytotoxicity or a secondary effect of cellular insult. Taking all this into account, in the corresponding sections of this thesis, measurements of oxidative stress related processes and the generation of ROS have been measured and discussed with special care. In particular, in the *research paper 1* an in depth study has been performed to investigate the role of oxidative stress in the toxicity of copper nanoparticles (CuNPs). Also any oxidative disturbances in fish exposed to ZnO NPs have been studied (*research paper 2*).

Specific concerns surrounding metal and metal oxide ENM's is the potential release of high concentrations of metal ions which have already proven to be hazardous. Whether effects are distinct for particle forms or dictated by released ions has yet to be fully elucidated. By comparing NPs dose response curves to those of equivalent concentrations of dissolved metal ions or to those of the fraction of ion released from the ENM under exposure conditions one can begin to determine the role of the dissolved ion in eliciting effects. Considering this, generally, in parallel to the exposure of cells to suspensions of ENM, also exposures to a soluble salt of the metal constituting the ENM have been performed in the present work.

Although the study of the toxicity of individual ENMs is essential to understand their mechanisms of action and assess and manage appropriately their risks, however, in real world situations organisms will be exposed not to a single ENMs but to a mixture of them that interact, influencing mutually their properties and effects. Also as nanotechnologies develop we see the production of materials using a mixture of ENMs, for example in nanocomposites and hybrid materials. It is therefore of high relevance to investigate the potential effects from co-exposures to multiple ENMs or other chemical stressors that coexist in the environment. These aspects have been also tackled in the present thesis by considering the combined toxicity of ENMs based on copper and on zinc. These metals were chosen because they are essential for the organisms and their balance is relied upon for general health. We considered that it was worthwhile to carry out

these experiments due to the complex interdependencies of copper and zinc regulation in the cell.

While *in vitro* tests systems such as cell lines provide a useful tool for such purposes one must question the relevance of such systems to biological outcomes *in vivo*. How do responses seen *in vitro* in cells lines translate to an *in vivo* situation which takes into consideration adaptive responses at the whole organism's levels and toxico-kinetics? *In vivo* studies must be undertaken to answer such questions. Considering these aspects, *in vivo* experiments were carried out using rainbow trout (*research paper 3*). They were exposed to the same ZnO NPs tested for their cytotoxicity and ability to increase ROS levels in fish liver cell lines in *introductory paper 1*. In the *in vivo* study, the distribution of Zn to the liver was analysed and any biochemical disturbances associated with oxidative stress were monitored to determine the *in vitro – in vivo* concordance between these *in vitro* and *in vivo* studies assessing the hazard of ZnO NP exposure.

Taking into account all the aspects previously mentioned, this thesis presents seven published articles, each focusing on testing particular metal or metal oxide ENMs, individually or in mixtures, and using *in vitro* approaches based on a variety of cells and cell lines and *in vivo* approaches based on the use of rainbow trout. The experiments of three of these papers were initially carried out in an attempt to frame and focus adequately our research. So they are grouped as *introductory papers* in chapter 3. Thereafter, each chapter corresponds to a published research paper, tackling one particular aspect of metal ENMs toxicity. These are the articles that constitute the particular and original body of the present thesis.

Objectives

The main aim of this work was to gain information about the mechanisms underlying the toxicity of metal/metal oxide ENM exposure on the liver. We approached this main objective from both human and environmental perspectives. The metal/metal oxide ENMs studied in this research have already been identified as those which should be assessed with high priority due to their widespread use, production volume and commercial importance (OECD, 2010) as well as due to their future emerging applications. They include ZnO, Cu, Ag and Au ENMs.

Another general objective in this work was to address the use and appropriateness of cell lines as alternatives to animal testing and as useful tools for nanoparticle hazard identification both in a screening strategy and to prioritise ENMs for *in vivo* testing.

To achieve these main objectives, first the following preliminary specific objectives (tackled specifically in the preliminary introductory articles) were pursued.

- To investigate the cytotoxic potential of an array of different sized/shaped ENMs (ZnO NPs and CuNPs) and to ascertain if any causal relationships exist between their physico-chemical properties and the toxic responses observed (*introductory papers 1 and 2*).

- To investigate if there are any differences among fish and mammalian cell lines in susceptibility/sensitivity to these ENMs, or if in fact ENMs elicit different mechanism of toxicity (if any) at the cellular level across species (*introductory papers 1 and 2*).

- To determine to what extent the cytotoxicity (if any) is caused by ions formed from NP dissolution or directly by NPs (*research papers 1 and 2*).

- To assess if the combined effect of the ZnO NPs and CuNPs under investigation can differ greatly from that produced by each individual ENM alone (*introductory paper 3*).

These initial objectives allowed us to gain insights into the general mechanisms of toxic action and permitted formulating more specific objectives that were afforded in the research articles that constitute the scaffold of this thesis.

These specific objectives are presented below:

1. To determine the real role of oxidative stress as a causative agent of cytotoxicity of ENMs.

As indicated in the introduction, it has been generally accepted as a paradigm that oxidative stress is the main cause of the toxicity of ENMs. However, oxidative stress could be actually a consequence of the toxicity of ENM instead of its cause. In order to clarify this issue cell lines were exposed to Cu ENMs that induce the production of ROS in cells and its toxicity was assessed under normal conditions and after reducing the level of ROS by activating the anti-oxidative stress defence mechanisms of the cells (*research paper 1*).

2. To compare the sensitivity among different fish cell lines against NP insult and to investigate if cell lines were representative of cells maintained in primary culture.

One of the main problems we have found when initiating the studies investigating the toxicity of ENMs was the selection of the appropriate cell line. We have therefore considered as essential to perform some experiments in order to assess the sensitivity of different cells and cell lines maintained in culture. In *research paper 2*, three rainbow trout cell lines, as well as freshly isolated (primary) liver cells from rainbow trout were used as test systems. AgNPs were chosen in this case as according to predicted environmental concentrations and species sensitivity distributions, AgNPs present one of the highest risks compared to other NPs, particularly in surface waters.

3. To gain information about the relevance of ENM toxicity data obtained *in vitro* with respect to an *in vivo* situation.

Although there is an important amount of data about the toxicity of ENM obtained from *in vitro* approaches, information from *in vivo* studies dealing with ENMs are still scarce. It is therefore essential to carry out some experiments *in vivo* that allows one to generate information about the applicability of *in vitro* data to more realistic *in vivo* situations. Considering this, we performed an *in vivo* study to determine the toxicity and bioaccumulation in rainbow trout of zinc derived from ZnO NPs that were administered to fish through their feed (according to the OECD TG

305)(*research paper 3*). The ZnO NPs used here, were the same as used in previous studies using cell lines, allowing a direct comparison of results obtained using *in vitro* and *in vivo* approaches.

4. To study to what extent modifications in the surface coatings of NPs govern physico-chemical properties and biocompatibility and if the use of different coatings could aid in developing safer ENMs (*research paper 4*).

The surface of NPs can be functionalized in different ways in order to fine tune their physico-chemical or toxicological properties. In this way, we could develop safer ENMs, but also increase the safety of products containing NPs and ensure their low health and environmental impact. Taking this into account, we have monitored *in vitro* differences in the toxicity of Au NPs capped with an array of peptide- biphenyls (*research paper 4*).

Results and Discussion

In chapter 7, a general discussion on the results obtained with metal/metal oxide ENMs (Cu, ZnO, Ag and Au) in the *in vitro* and *in vivo* experiments is presented.

In the introductory articles we observed that ZnO NPs represent an increased hazard compared to CuNPs, when liver cell lines (both mammalian and piscine) are used as test systems. Also we have witnessed a potentiation effect whereby the addition of ZnO NPs leads to an enhanced CuNP cytotoxic effect. The mechanisms underlying the enhancement of toxicity appear to be nanoparticle-specific and associated with the uptake of large concentrations of ZnO NPs within the cell. Interestingly the Zn^{2+} ions released from the nanoparticles did not contribute to the toxic effect. Similarly, in support of particle-specific effects, using a response addition model, we have found that in the case of CuNP suspensions, the nanoparticle fraction highly contributed (together with the ionic fraction) to the cytotoxicity in liver cell lines. To specifically distinguish the contribution of ions and NPs to the toxicity we performed an experiment using different CuNPs with distinct and contrasting dissolution profiles. The high toxicity observed in CuNPs with a low dissolution rate supported the idea that NPs, as such, play a key role in toxicity, independently of (but contributing to) the toxicity caused by ions. NP-specific ROS elicitation from particle suspensions that was not seen following exposures to released ions was also evidenced. In both studies with ZnO and CuNPs there was evidence of uptake of ZnO and CuNPs into cells and their association with intracellular organelles. Therefore in the case of ZnO and CuNPs, the findings presented point to an increased hazard and heightened risk associated with the presence of a nanoparticulate form and to unique biological interactions between cells and these metal NPs.

We have focused heavily on ROS elicitation, and the extent to which oxidative stress plays a role in these metal ENMs pathways of toxicity. The question addressed was if oxidative stress is merely a secondary effect associated with cell death (consequence) or if ROS increase is a key event (or molecular initiating event) in ENMs mechanism of toxicity. In fish cell lines exposed to ZnO NPs, an increase in ROS levels was observed. However, this increase occurred at

concentrations of ZnO NPs higher than those already causing cytotoxicity. In contrast, in cells exposed to CuNPs there was a concentration dependent elevation in the levels of ROS, at concentrations at which cytotoxic effects were observed. Therefore it is likely that ZnO and CuNPs are acting through different mechanisms of cytotoxicity. This suggests that in fact there probably exists a high degree of variability in the mechanisms underlying cytotoxicity among the wide range of ENMs that exist.

In order to find out to what extent oxidative stress dictates toxicity of ENMs we performed some experiments exposing cells to CuNPs, which caused an increase in ROS levels, and simultaneously to an inducer of the aryl hydrocarbon receptor (AhR) which induction pathways are related, among others, with the antioxidant defences of the cells. The induction of AhR led to an increase in glutathione-S-transferase activity and to a decrease in ROS levels in CuNPs exposed cells. When the cells redox status was brought into equilibrium there was evidence of a non-oxidative stress-mediated loss in cell viability. This would suggest that ROS elicitation and oxidative stress, while associated with CuNP exposure, does not appear to be a key event in CuNPs mechanism of cytotoxicity (*research paper 1*). Therefore one must be careful in using oxidative stress as a pathway of toxicity and recognise that other possible modes of action may exist.

Liver cells both mammalian and piscine in origin were incorporated into studies to investigate any species specific differences in responses. Interestingly a clear difference in the sensitivity of cell lines towards CuNPs and ZnO NPs was evidenced (*introductory papers 1 and 2*). Mammalian liver cell lines are more sensitive to toxic effects compared to piscine liver cell lines. We have also observed differences in tolerances to metal ions and therefore the role of metal ions (either released from NPs in the medium environment or intracellularly) may be a key factor in determining differences in sensitivity of cell lines towards ENMs. In particular when comparing responses between mammalian and fish cell lines, mammalian cells are more sensitive to ions whereas fish cells appeared to be more sensitive to the particulate forms.

Following this observation a range of rainbow trout (*Oncorhynchus mykiss*) cell lines were incorporated into a study as sensitive test systems for investigating particle-specific effects of AgNPs (*research paper 2*). Responses were compared to those of primary liver cells isolated from the same species showing good comparability. The robustness of the fish cell lines as *in vitro* cell culture test systems was also increased in this study by incorporating multiple assay systems to the same set of cells. For example, a 3 in 1 cytotoxicity assay (three cytotoxicity assays were performed on the same set of cells) has been incorporated successfully monitoring disturbances in the plasma membrane, on lysosome functioning and on cellular metabolism.

To investigate how results obtained from *in vitro* cell culture tests systems translate on a whole organism level *in vivo* exposures were performed (*research paper 3*). Rainbow trout were fed a diet spiked with ZnO NPs, the levels of Zn in the liver and other organs were measured and the induction of some enzymes of interest measured. Fish exposed to high concentrations of ZnO NPs (1000 mg/kg feed) for 10 days experienced oxidative biochemical disturbances but were also able to maintain redox equilibrium over time during a depuration phase (28 days). Therefore while a link between the ROS elicitation evidenced in fish cell lines and oxidative disturbances

in fish *in vivo* was established, it did not translate to a pathological outcome and oxidative stress levels did not exceed the capability of the fish's endogenous antioxidant/physiological environment to respond. In addition to this, important disturbances to cytochrome P4501A activity were observed, what could point to interferences of metal ENMs with the metabolic capabilities of the organism.

Overall the studies have highlighted that the liver is a major organ of distribution following ENM exposure and that liver cell lines can act as valuable and relevant *in vitro* test systems for NP hazard assessment. Once the toxicity (hazard) of ENM has been identified, these materials can be modified in different ways (e.g. using a variety of coatings) to reduce the hazard and make ENMs more biocompatible. This has been in focus in *research paper 4* presented in this thesis. This study explored the influence of different peptide- biphenyl (PBH) ligands (containing moieties of glycine, cysteine, tyrosine, tryptophan, and methionine) on AuNPs physico-chemical properties and biological responses. Again liver cells provided systems to test differences in toxicity. Depending on the structure of the PBH capping ligand, the behaviour of AuNPs differed both in terms of stability and biocompatibility. PBH-capped AuNP containing trityl-cysteine showed remarkable stability and biocompatibility even in a culture medium environment without serum. Controlling ENMs properties and behaviours through the use of coatings and capping agents in this way could be used as control strategies in order to eliminate or reduce hazard. This level of control, together with an understanding of the ability of ENMs to transverse biological barriers and enter cells, opens up huge opportunities for safely designed ENMs that could be used as carriers of other substances into cells. These delivery systems will have a great impact on modern society with applications that go from biomedicine to agriculture.

Conclusions

The main conclusions obtained from this research are summarized below:

1. Liver cell lines are relevant and valuable test systems that can be used to deepen our understanding of the mechanisms underlying the toxicity of metal ENMs both from an environmental and human health perspective.

2. Important experimental adaptations may need to be taken when testing ENMs using *in vitro* cell culture test systems in order to achieve stable dispersions in the culture media.

3. Technical issues related to the preparation of accurate exposure concentrations outline the necessity of measuring real concentrations instead of using nominal concentrations for estimating cytotoxicity.

4. Interference checks should also be incorporated into the experimental design when testing NPs using *in vitro* cell culture systems to ensure no false positive/negative results due to reactivity or binding of NPs with assay components.

5. The metal ENMs tested can be ranked by their decreasing cytotoxicity to liver cell lines, estimated from the IC_{50} values calculated from responses in liver cells, as Ag>ZnO>Cu>Au.

6. ENMs can enter the cells and appear within membrane enclosed bodies such as lysosomes. In addition, the increased effects with the neutral red assay, which monitors lysosomal functionality, supports that this mechanism can play a key role in the cytotoxicity of NPs.

7. Nanoparticle-specific effects were evidenced highlighting the increased hazard from exposure of liver cells to metal ENMs compared to solely disolved metal ions.

8. Primary particle size does not appear to dictate toxicity as there is no evidence of a size-dependent (nano-specific) cytotoxic relationship.

9. Although it has been claimed that oxidative stress is the most important mechanism of toxicity of ENMs, we have demonstrated that in several cases the toxicity of ENMs is not directly dependent on oxidative stress.

10. Species-specific differences in sensitivity to the cytotoxic effects of ENMs exist that could be related to differences in tolerances of mammalian and piscine cells to metal ions which are released from the ENMs.

11. Fish cell lines do not show necessarily a lower sensitivity than fish liver cells maintained in primary culture so that they appear as a valuable tool for the study of the cytotoxicity of ENMs.

12. ZnO ENMs administered to fish through the diet resulted in the preferential accumulation of Zn in their gills and intestine. Zn distribution to the liver causes oxidative disturbances that are recovered by the organism adaptive responses during depuration.

13. The toxicity of each ENM can be strongly influenced by variations in capping agents which opens the door to safe by design approaches.

Resumen

Introducción

Desde que se descubrió a inicios del siglo XXI que materiales conocidos, tales como los metales, sintetizados en escala nanométrica, presentaban propiedades extraordinarias y sorprendentes, que podrían ser muy beneficiosas y remodelar nuestro futuro, el número de nuevos materiales ha ido aumentando de forma exponencial. Los nanomateriales manufacturados (NMs) son materiales sintetizados por el hombre constituidos por partículas que poseen en al menos una de sus dimensiones un tamaño de entre 1 y 100 nm (ISO, 2016; EU, 2011). Este tamaño es importante desde un punto de vista regulatorio pero, en realidad, cuando se trabaja en el laboratorio estos límites se desdibujan pudiendo hablar de NMs de algunos cientos de nms. En cualquier caso, antes de que el potencial de estos NMs pueda ser conocido por completo, es responsabilidad nuestra asegurar que todo el proceso de desarrollo lleve a la fabricación de materiales seguros. Como consecuencia de esta necesidad ha surgido la nanotoxicología que, por definición, es el estudio de los posibles efectos tóxicos de los NMs. Por el momento, las nanotecnologías están avanzando mucho más deprisa que nuestra capacidad de aprendizaje por lo que existe desconocimiento e incertidumbre sobre los posibles riesgos de estos NMs. Por lo tanto, el estudio de los posibles efectos toxicológicos (peligro) de los NMs, como parte de la evaluación del riesgo, es extremadamente importante para ahondar en nuestro conocimiento de los posibles impactos en la salud medio ambiental y humana (riesgos).

En la actualidad existe una cierta preocupación social por el comportamiento impredecible de los materiales a escala nano, por su distribución generalizada y persistencia en el medio ambiente así como por su capacidad de penetración y de causar efectos adversos en los sistemas vivos.

En la introducción general (capítulo 1) de esta tesis, se presenta el conocimiento actual en el área de la nanotoxicología así como las regulaciones que aseguran el uso sostenible y seguro de los NMS. Esta introducción se centra especialmente en el grupo de nanopartículas (NPs) metálicas y óxido-metálicas de mayor uso industrial y comercial, principalmente las de ZnO, Cu, Ag y Au, describiendo sus propiedades individuales, aplicaciones y posibles riesgos.

Entrando en una nueva era, la nano era, las preguntas que debemos contestar incluyen las siguientes. ¿Cuál será el impacto del uso de los NMs sobre el medio ambiente? ¿Supondrá un problema de salud humana la exposición a los mismos? El primer paso para dar respuesta a estos interrogantes será identificar los posibles efectos adversos en los organismos vivos (peligro). El estudio de los posibles peligros de estos NMs requiere una aproximación más compleja que la que se seguiría con sustancias químicas así como el uso de metodologías específicas. En medios líquidos, los NMs forman suspensiones o coloides (si el NM se solubilizara, la naturaleza particulada de estos materiales se perdería y estaríamos enfrentándonos a los mismos problemas que con las sustancias químicas). Estos sistemas contienen partículas dispersas y quizás algún ion soluble procedente de la mismas. Además, los NMs presentan propiedades físicas y químicas específicas que les hace diferentes del material original de tamaño no nano y que influyen en su comportamiento. Es de especial importancia la superficie específica (área superficial) que aumenta considerablemente al disminuir el volumen (tamaño) de las NPs. La superficie

específica puede también aumentar notablemente en partículas de naturaleza porosa. El aumento de superficie conlleva un incremento significativo de la reactividad superficial de modo que los NMs se comportan de diferente forma que los materiales de origen. De esta forma, no sólo la composición química sino también la carga superficial condicionan las interacciones de las NPs con otras partículas o moléculas presentes en el medio en el que se encuentren. Por otro lado, la forma y el ratio anchura/altura de la NP van a influir profundamente en su persistencia. En la presente investigación nos hemos centrado en los posibles efectos adversos de los NMs por medio del uso de aproximaciones *in vitro* utilizando cultivos celulares. Puesto que el hígado ha sido identificado como un importante órgano diana para las NPs en un buen número de organismos en el presente trabajo se emplearon cultivos primarios de hepatocitos y líneas celulares procedentes de hígado como sistemas de ensayo *in vitro*. Considerando que una estrategia de ensayo integrada (ITS) se basa en el uso de métodos apropiados de ensayo, alternativos al uso experimental de animales, los ensayos *in vitro* son un elemento muy importante para la evaluación del peligro de los NMs. Existen líneas celulares de diversas especies, lo que proporciona un sistema potente para poder ensayar diferencias de susceptibilidad entre especies y/o ensayar los mecanismos de toxicidad propios de cada especie a nivel celular. Entre los mecanismos subyacentes a la toxicidad de NMs, el estrés oxidativo ha emergido como el paradigma responsable de todos los efectos adversos observados. El estrés oxidativo es un estado celular resultante de un desajuste entre la generación de especies de oxígeno reactivas (ROS) y la respuesta adaptativa del sistema endógeno antioxidante. Sin embargo no está claro si el estrés oxidativo asociado con los NMs es la causa directa de citotoxicidad o el efecto secundario al daño celular. Teniendo todo esto en cuenta, en las secciones correspondientes de la tesis, se han estudiado y discutido con especial detalle los procesos relacionados con el estrés oxidativo y la generación de ROS.

En particular, en el *artículo de investigación 1* se realizó un estudio en profundidad para investigar el papel del estrés oxidativo en la toxicidad de las NPs de Cu. Igualmente, se estudiaron las perturbaciones en el metabolismo oxidativo en peces expuestos a NPs de ZnO (*artículo de investigación 3*).

En los NMs metálicos y óxido-metálicos preocupa especialmente la posible liberación de concentraciones elevadas de iones metálicos cuya toxicidad ya es conocida. Queda por elucidar cual es la contribución de la fracción nanoparticulada y de la fracción iónica a la toxicidad global observada. Para determinar el rol de los iones disueltos sobre los efectos observados, se pueden comparar las curvas dosis-respuesta de las NPs frente a las de concentraciones equivalentes de iones metálicos o frente a las de la fracción de ion liberado desde el NM en las condiciones de exposición. Teniendo esto en cuenta, en el presente estudio en la mayoría de los casos las células han sido expuestas a suspensiones de NPs y a una sal soluble del metal correspondiente.

Por otra parte, si bien el estudio de la toxicidad de los NMs individualmente es esencial para entender los mecanismos de acción y evaluar y manejar apropiadamente los riesgos, en las situaciones reales los organismos se verán expuestos a mezclas de NPs que interaccionan entre ellas influyendo mutuamente en sus propiedades y efectos. Además conforme avanzan las nanotecnologías, se están desarrollando materiales con mezclas de NMs, por ejemplo los nanocompuestos y los materiales híbridos. Por lo tanto, es de gran interés investigar los efectos

resultantes de la co-exposición a múltiples NMs o a otros compuestos químicos nocivos que coexisten en el medio ambiente. Estos aspectos también han sido abordados en la presente tesis considerando la toxicidad combinada de NMs compuestos de Cu y de Zn. Estos metales fueron seleccionados pues son esenciales para los organismos y su equilibrio redunda en su salud general. Consideramos que merecía la pena llevar a cabo estos ensayos debido a las complejas interdependencias en la regulación del cobre y zinc en la célula.

Aunque los sistemas de ensayo *in vitro*, tales como las líneas celulares, son una herramienta eficaz para abordar los estudios de toxicidad de NMs, sin embargo es necesario verificar si tales sistemas son representativos de los efectos biológicos originados *in vivo*. ¿Cómo se traducen las respuestas observadas *in vitro* en líneas celulares a situaciones *in vivo* en las que se producen respuestas adaptativas de todo el organismo y toxicocinéticas? Para responder a esta pregunta se deben realizar ensayos *in vivo* y por este motivo, se han realizado ensayos utilizando la trucha arco iris (*artículo de investigación 3*). Se expuso a las truchas a las mismas NPs de ZnO ensayadas en el *artículo introductorio 1* pues se vio que producían citotoxicidad y aumentaban los niveles de ROS en líneas celulares hepáticas de pez. En el estudio *in vivo*, se analizó la distribución de Zn en el organismo así como, a nivel hepático, las alteraciones bioquímicas asociadas a estrés oxidativo para determinar la correspondencia *in vitro – in vivo* de los resultados encontrados en ambos estudios.

Teniendo en cuenta todos los aspectos mencionados anteriormente, esta tesis presenta 7 artículos publicados, cada uno enfocado al ensayo de NMs específicos metálicos u óxido-metálicos, solos o en mezcla, y utilizando aproximaciones *in vitro* mediante una variedad de células (primarias y líneas celulares) e *in vivo* en trucha arco iris. Los experimentos de tres de estos artículos se desarrollaron previamente para contextualizar y dirigir nuestra investigación. Se les ha agrupado como "*artículos introductorios*" en el capítulo 3. Seguidamente, cada capítulo corresponde a un artículo de investigación publicado que aborda un aspecto particular de la toxicidad de NMs. Estos son los artículos que constituyen el trabajo original y específico de la presente tesis.

Objetivos

El principal objetivo de este trabajo fue generar nueva información sobre los mecanismos subyacentes a la toxicidad de nanomateriales metálicos o de óxidos metálicos sobre el hígado. Acometimos este objetivo tanto desde una perspectiva ambiental como de salud humana. Los nanomateriales estudiados fueron aquellos considerados como prioritarios a la hora de ser evaluados debido a su uso generalizado, a su alto volumen de producción, a su importancia comercial (OECD, 2010), o bien a sus posibles aplicaciones futuras. En ellos se incluyen nanomateriales de ZnO, Cu, Ag y Au.

Otro de los objetivos generales de este trabajo consistió en generar información sobre el posible uso de líneas celulares como alternativa a los ensayos animales *in vivo* y como herramientas útiles para la identificación del peligro de los NMs, tanto en el marco de una estrategia global de detección de la toxicidad como a la hora de priorizar los NMs para la realización de ensayos *in vivo* más complejos.

Para alcanzar estos objetivos generales, en primer lugar se persiguieron los siguientes objetivos específicos (abordados en los primeros artículos científicos, que sirven como introductorios):

- Investigar el potencial citotóxico de una serie de nanomateriales de diferentes tamaños y formas (NPs de ZnO y de Cu) y determinar si puede existir algún tipo de relación causal entre sus propiedades físico-químicas y las respuestas tóxicas observadas (*artículos introductorios 1 y 2*).

- Investigar si existen diferencias entre líneas celulares de peces y mamíferos en cuanto a la sensibilidad /susceptibilidad frente a estos NMs, o si, de hecho, los NMs actúan por diferentes mecanismos de toxicidad en células procedentes de diferentes especies (*artículos introductorios 1 y 2*).

- Determinar hasta qué punto la citotoxicidad (si existe) es causada por los iones generados por la disolución de las NPs o directamente por las NPs (*artículos introductorios 1 y 2*).

- Evaluar si los efectos combinados de las NPs de ZnO y Cu investigadas difieren de los causados por cada uno de estos NMs individualmente (*artículo introductorio 3*).

Estos objetivos iniciales nos permitieron generar información sobre los mecanismos subyacentes a los efectos tóxicos observados y nos permitieron formular objetivos específicos que se abordaron en los artículos de investigación que constituyen la estructura fundamental de esta tesis.

Estos objetivos específicos se mencionan a continuación:

1. Determinar el papel real del estrés oxidativo como causa de la citotoxicidad de los NMs.

Como se ha indicado en la introducción, se ha aceptado como una generalidad que el estrés oxidativo es la principal causa de la toxicidad de los NMs. Sin embargo, el estrés oxidativo puede ser, en realidad, consecuencia de la toxicidad. Con el fin de clarificar esta cuestión, se expusieron líneas celulares a NMs de Cu que inducían las producción de ROS en esas células y la toxicidad se evaluó bajo condiciones normales y tras reducir los niveles de ROS mediante la activación de las defensas celulares frente al estrés oxidativo (*artículo de investigación 1*).

2. Comparar la sensibilidad de diferentes líneas celulares de peces frente a la toxicidad de NMs e investigar si esas líneas celulares son representativas de células mantenidas en cultivo primario.

Uno de los mayores problemas que encontramos al iniciar los estudios de toxicidad de NMs fue la selección de una línea celular apropiada. Nos pareció, por lo tanto, imprescindible realizar una serie de experimentos con el fin de evaluar la sensibilidad de distintas líneas celulares y de células mantenidas en cultivo primario. Teniendo esto en cuenta, en el *artículo de investigación 2* se usaron tres líneas celulares de trucha arcoíris y hepatocitos aislados y mantenidos en cultivo primario. En este caso, para los ensayos de citotoxicidad se escogieron NPs de Ag, ya que de acuerdo con estudios recientes, estas NPs presentan uno de los mayores riesgos en comparación con otras NPs, particularmente en aguas superficiales.

3. Obtener información acerca de la relevancia de los datos *in vitro* sobre toxicidad de NMs con respecto a la situación *in vivo*.

Aunque hay una enorme cantidad de datos obtenidos *in vitro* sobre toxicidad de NMs, la información generada en experimentos *in vivo* es todavía muy escasa. Resulta, por lo tanto, imprescindible llevar a cabo experimentos que permitan generar información sobre la aplicabilidad de los datos generados *in vitro* a situaciones más realistas *in vivo*. Siguiendo este razonamiento, llevamos a cabo un experimento para determinar la toxicidad y bioacumulación de NPs de ZnO en trucha tras una exposición *in vivo* (siguiendo la guía técnica 305 de la OCDE) (*artículo de investigación 3*). Las NPs usadas en este caso fueron las mismas que las de los estudios previos con cultivos celulares, lo que permitió una comparación directa de los resultados obtenidos con las aproximaciones *in vitro* e *in vivo*.

4. Estudiar de qué modo las modificaciones en la composición química de la cubierta de los NMs afectan a sus propiedades físico químicas y a su biocompatibilidad y también determinar si el uso de distintas cubiertas puede ayudar al diseño de NMs más seguros.

La superficie de las NPs puede funcionalizarse con distintas sustancias para ajustar las propiedades físico químicas y toxicológicas del NM. De este modo, podríamos desarrollar NMs más seguros, pero también incrementar la seguridad de los productos que contengan esos NMs y asegurar un bajo impacto negativo sobre la salud humana y el medio ambiente. Teniendo esto en cuenta estudiamos, usando cultivos celulares, la toxicidad de NPs de Au cubiertas con una serie de péptidos bifenilos (*artículo de investigación 4*).

Resultados y Discusión

En el capítulo 7 de la tesis se presenta una discusión general sobre los resultados obtenidos en los experimentos *in vitro* e *in vivo* en los que se utilizaron NMs metálicos y óxido-metálicos de Cu, ZnO, Ag y Au.

En los artículos introductorios observamos que las NPs de ZnO presentan un riesgo mayor que las NPs de Cu en líneas celulares de hígado de mamífero y de pez. Además, se produjo un aumento del efecto citotóxico de las NPs de Cu cuando se añadieron NPs de ZnO. Los mecanismos responsables de este incremento de toxicidad parecen ser específicos de la fracción nanoparticulada y estar asociados con una mayor absorción celular de NPs de ZnO. Fue interesante comprobar que los iones Zn^{2+} liberados de las NPs no eran los responsables del efecto tóxico. Igualmente y en apoyo de los efectos específicos de las partículas, mediante el uso de modelos de respuesta aditiva, en el caso de las suspensiones de NPs de Cu, encontramos que la fracción nanoparticulada contribuía de un modo importante, junto con la fracción iónica, al efecto citotóxico observado en las líneas celulares hepáticas. Para poder distinguir de forma específica la contribución de los iones y de las NPs a la toxicidad realizamos un experimento con NPs de Cu de diferentes solubilidades. Se observó una toxicidad elevada en NPs de Cu de baja solubilidad lo que apoyó la hipótesis que las NPs, como tales, juegan un papel importante en la toxicidad, independientemente de, pero contribuyendo a, la toxicidad producida por los

iones. Además se produjo un aumento de ROS tras la exposición a suspensiones de partículas pero no a los iones liberados. En ambos estudios con NPs de ZnO y Cu hubo evidencia de captación celular y unión a orgánulos celulares para ambas NPs. Por lo tanto, en el caso de las NPs de ZnO y Cu, los hallazgos obtenidos apuntan a un incremento del peligro y riesgo por la presencia de formas nanoparticuladas, así como a interacciones biológicas únicas entre las células y estas NPs metálicas.

En la tesis también nos hemos centrado fuertemente en la producción de ROS y en hasta qué punto el estrés oxidativo es responsable de la toxicidad de estos NMs metálicos. La cuestión planteada es si el estrés oxidativo es simplemente un efecto secundario asociado a muerte celular (consecuencia) o si el aumento de ROS es un paso clave (o un evento de iniciación molecular) en los mecanismos de toxicidad de los NMs.

En las líneas celulares de pez, se observó un aumento en los niveles de ROS tras su exposición a NPs de ZnO. Sin embargo este aumento se producía a concentraciones de NPs de ZnO más elevadas que aquellas que ya producían un efecto citotóxico. Por el contrario, en células expuestas a NPs de Cu se produjo, a concentraciones en las que se observaba un efecto citotóxico, un aumento dependiente de la concentración en los niveles de ROS. Aparentemente, las NPs de ZnO y Cu causaban toxicidad por mecanismos diferentes. De hecho, esto sugiere que, entre el amplio abanico de NMs existentes, probablemente exista un elevado grado de variabilidad en los mecanismos responsables de citotoxicidad.

Con el fin de averiguar hasta qué punto el estrés oxidativo dicta la toxicidad de los NMs, realizamos algunos experimentos exponiendo células a NPs de Cu, lo que causó un aumento de los niveles de ROS, y simultáneamente a un inductor del receptor de hidrocarburos aromáticos (AhR) que es responsable, en parte, de la activación de las defensas antioxidantes de las células. La inducción del AhR condujo a un aumento de la actividad del enzima glutatión-*S*-transferasa y a una disminución en los niveles de ROS en las células expuestas a NPs de Cu. Cuando se redujo la concentración de ROS y por lo tanto el estrés oxidativo, continuó apareciendo citotoxicidad, lo que sugiere que, al menos en el caso de las NPs de Cu, esta inducción de ROS no juega un papel fundamental en la citotoxidad (*trabajo de investigación 1*). Por lo tanto, conviene ser cauto al considerar el estrés oxidativo como causa fundamental de la toxicidad de los NMs, teniendo siempre en cuenta que puede haber otros mecanismos inductores de los efectos deletéreos.

Los experimentos se hicieron con líneas celulares de hígado tanto de peces como de mamíferos con el fin de investigar diferencias en las respuestas tóxicas que pudieran estar asociadas a las especies de procedencia. Fue interesante observar que había una clara diferencia de sensibilidad entre líneas celulares frente a las NPs de Cu y de ZnO (*artículos introductorios 1 y 2*), siendo las de mamífero más sensibles que las de peces. También se observaron diferencias en la tolerancia frente a iones metálicos, lo que sugeriría que estos iones (liberados desde las NPs bien al medio de cultivo, bien intracelularmente) pueden ser un factor clave que determine esas diferencias de sensibilidad. Parece ser que las líneas celulares de mamífero son más sensibles a los iones, mientras que las de pez lo serían a la fracción particulada.

Teniendo en cuenta esta observación, en uno de los trabajos se comparó la citotoxicidad de NPs de Ag en varias líneas celulares de trucha arcoíris (*Oncorhynchus mykiss*) y en hepatocitos primarios de la misma especie (*artículo de investigación 2*). Se vio que las líneas celulares daban unas respuestas comparables a las de los hepatocitos primarios. La solidez de los sistemas basados en el uso de líneas celulares además se vio reforzada al incorporar en los ensayos de citotoxicidad hasta tres metodologías diferentes de medida de efectos sobre el mismo conjunto de células. Estos ensayos permitieron detectar alteraciones en la integridad de la membrana plasmática, en la estabilidad de los lisosomas y en la función mitocondrial.

Con el fin de investigar de qué modo los resultados obtenidos *in vitro* pueden aplicarse a un organismo completo, se hicieron experimentos *in vivo* usando trucha arcoíris (*trabajo de investigación 3*). Las truchas se alimentaron con pienso al que se habían añadido NPs de ZnO y se realizaron medidas de los niveles de Zn en hígado y otros órganos, así como de la inducción de algunos enzimas de detoxificación. Los peces expuestos a altas concentraciones de NPs de ZnO (1000 mg/kg pienso) durante 10 días presentaron alteraciones en el metabolismo oxidativo pero fueron capaces de revertirlas durante la fase de depuración (28 días). Por lo tanto, aunque se vio que la inducción de estrés oxidativo detectada *in vitro* también aparecía *in vivo*, no se tradujo en un estado patológico de modo que los niveles de estrés oxidativo no excedieron la capacidad de respuesta antioxidante del pez. Sin embargo, se observaron alteraciones importantes en la actividad del citocromo P4501A, lo que apuntaría a interferencias de los NMs metálicos con la capacidad metabólica del organismo.

En general, todos estos estudios han demostrado que, tras la exposición a los NMs, éstos pueden llegar hasta el hígado y que las líneas celulares procedentes de este órgano constituyen una herramienta muy valiosa para estimar el peligro de estas sustancias. Una vez que ese peligro (la toxicidad) ha sido establecido, se pueden conseguir variaciones en la toxicidad de un determinado NM modificando su superficie mediante la unión a otras moléculas. El *artículo de investigación 4* se centró en este tipo de aproximaciones. Este estudio exploró de qué modo influían en las propiedades físico químicas y en la toxicidad de NPs de Au una serie de ligandos unidos a su superficie. Estos ligandos fueron péptidos bifenilos (PBH) (conteniendo glicina, cisteina, tirosina, triptófano y metionina). Se vio que dependiendo de la estructura del PBH, el comportamiento de las NPs de Au variaba en cuanto a su estabilidad y biocompatibilidad. Las NPs de Au recubiertas con PBHs que contenían tritil-cisteina mostraron una enorme estabilidad y causaron menos toxicidad que las otras NPs. Por lo tanto, el uso de estas cubiertas puede servir para controlar las propiedades y comportamiento de los NMs y para reducir su toxicidad. Este nivel de control, junto con el conocimiento de los mecanismos por los que los NMs atraviesan las membranas biológicas, abre la puerta al diseño de NMs seguros que puedan servir de transportadores de otras sustancias hacia el interior de organismos y células. Este tipo de aplicaciones tendrán un enorme impacto en nuestras sociedades modernas con repercusiones probablemente desde en agricultura hasta en biomedicina.

Conclusiones

Se presentan a continuación las conclusiones más importantes generadas a partir de la investigación realizada:

1. Las líneas celulares obtenidas a partir de hígado constituyen unos sistemas de ensayo de enorme relevancia que pueden usarse para profundizar en nuestro conocimiento sobre los mecanismos subyacentes a la toxicidad de NMs manufacturados, tanto desde una perspectiva ambiental como de salud humana.

2. Al ensayar NMs en cultivos celulares *in vitro* es posible que sea necesario realizar importantes adaptaciones experimentales para conseguir dispersiones estables en el medio de cultivo.

3. El uso de dispersiones de NMs en vez de disoluciones da lugar a problemas técnicos para la consecución de las concentraciones deseadas al realizar diluciones, lo que subraya la necesidad de llevar a cabo medidas de concentraciones reales en vez de utilizar concentraciones nominales.

4. Al estudiar la citotoxicidad de NPs en sistemas celulares *in vitro* es necesario chequear las posibles interferencias de esas NPs con las medidas, interferencias debidas a su reacción o unión con los compuestos usados en el ensayo.

5. Los NMs metálicos utilizados en este estudio pueden ser ordenados siguiendo valores decrecientes de citotoxicidad, estimada a partir de los valores de IC_{50} en líneas celulares de hígado, del siguiente modo: Ag>ZnO>Cu>Au.

6. Los NMs son capaces de entrar en las células apareciendo en el interior de los lisosomas. Además, los importantes efectos observados en las medidas del ensayo de rojo neutro, que refleja alteraciones en el funcionamiento de los lisosomas, sugieren que este mecanismo puede jugar un papel fundamental en la citotoxicidad de las NPs.

7. El tamaño de las partículas no parece ser determinante en la toxicidad puesto que no se ha observado una relación directa entre citotoxicidad y tamaño de las NPs.

8. Se han observado efectos específicos de la fracción nanoparticulada lo que evidencia el mayor peligro de los NMs metálicos para las células de hígado con respecto a los iones metálicos liberados.

9. Aunque se ha propuesto que el estrés oxidativo constituye el mecanismo más importante de citotoxicidad de los NMs, hemos demostrado que en varios casos la citotoxicidad de los NMs no es directamente dependiente del estrés oxidativo.

10. Las diferencias interespecíficas en la sensibilidad a los efectos citotóxicos de los NMs podrían relacionarse con diferencias en la tolerancia de las células de mamíferos y peces a los iones metálicos liberados de los NMs.

11. Las líneas celulares de peces no muestran necesariamente una menor sensibilidad que las células mantenidas en cultivo primario frente a la toxicidad de los NMs, lo que hace de ellas unas valiosas herramientas para el estudio de la citotoxicidad de estas sustancias.

12. La administración de un NM de ZnO a peces a través de la dieta resultó en la acumulación preferencial de Zn en branquias e intestino. Además la llegada de Zn al hígado dio lugar a alteraciones en el equilibrio oxidativo que desaparecieron en la fase de depuración por la respuesta adaptativa del organismo.

13. La toxicidad de cada tipo de NM puede verse fuertemente influenciada por el tipo de agentes de superficie con los que se asocie, lo que abre la puerta a avances en la seguridad de los NMs a través del diseño.

CHAPTER 1:

GENERAL INTRODUCTION

1.1 Nanotoxicology

1.1.1 Its emergence and current state of the field

The engineering and manipulation of materials at a scale a billion times smaller than a metre-at nanometre scale- has led to the emergence of a highly exploitable technology in the last decade known as nanotechnology. This technology exploits the specific properties that materials, commonly referred to as engineered nanomaterials (ENMs), can exhibit at nanometre scale. ENMs are defined as those materials composed of particles having at least one dimension measuring < 100 nm. In this size range materials have a larger specific surface area. In other words the ratio between surface and unit of volume or unit of mass increases enormously compared to the bulk materials. As a consequence they exhibit unique physical properties, chemical reactivity, as well as quantum confinement effects[1] that can give rise to distinct size-dependent properties compared to larger "bulk" materials (Auffan et al. 2009). These distinct, and often new or enhanced, properties have led to their applications in various industries (automobile, construction, electronics, biotechnology and medicine) and incorporation into many (>1,800) consumer products (Project on Emerging Nanotechnologies, 2015[2]).

Nanotoxicology is a very recent discipline that actually emerged at the beginning of the first decade of this century as an important means "to contribute to the development of a sustainable and safe nanotechnology" (Donaldson et al. 2004). By definition, nanotoxicology is the study of the potential toxicological effects of nanomaterials. The disciplines emergence was seen as "timely and necessary" when reports detailing increased toxicity of some ENMs, compared to chemically identical bulk materials, surfaced (Kipen and Laskin 2005, Nel et al. 2006, Oberdörster et al. 2005). This, together with a general lack of information on the potential of ENMs to elicit toxic effects, led to uncertainties and knowledge gaps that needed to be filled. With this realisation, the health, safety, environmental, social and ethical implications of existing and future nanotechnologies became a topic of real concern (Royal Society & Royal Academy of Engineering 2004). Concerns surrounding the potential of materials with altered properties to have adverse effects on both the environment and to human health, associated with increased toxicity, bioavailability or environmental persistence, emerged.

[1] The bulk properties of any material are merely the average of all the quantum forces affecting all the atoms that make up the material. However nanomaterials properties can be controlled by the specific behaviour of individual atoms or molecules.

[2] According to an online global 'Nanotechnology Consumer Products Inventory' maintained by the Project on Emerging Nanotechnologies since 2005 http://www.nanotechproject.org/cpi/products/ accessed July 2015

Today, following intensive research efforts in Europe (under 6th and 7th framework programmes, and currently under Horizon 2020) and internationally, substantial data has emerged to provide evidence that some ENMs have toxicological effects and represent a hazard both to human health and the environment. In the area of human health initial investigations focused on the lung as a possible target organ following reports dating back to 2001 of the pulmonary toxicity of naturally occurring ultrafine particulates[3] (Brown et al. 2001, Donaldson et al. 2001, Donaldson and Tran 2002, Ferin et al. 1990, Oberdörster 2001) and also past concerns surrounding asbestos in the area of fibre toxicology[4]. Reports emerged showing biopersistance and toxicity of engineered fibrous nanotubes of carbon, not unlike asbestos in the lungs of rats and mice (Lam et al. 2004, Muller et al. 2005, Poland et al. 2008, Shvedova et al. 2005). For a range of other types of ENMs, including metal and metal oxides (e.g. copper oxide), toxicity in lung epithelial cells was also evidenced (Eom and Choi 2009, Karlsson et al. 2008, Limbach et al. 2007). However reports also emerged showing cardiovascular effects (systemic effects) following pulmonary exposure (Li et al. 2007) and that other organ systems such as the liver, spleen and even the central nervous system could also be adversely affected following exposure to ENMs through inhalation (Oberdörster et al. 2004, Wang et al. 2008). These observations were among the first to highlight the potential heightened risk of ENMs associated with their ability to translocate to multiple organ systems. Nowadays it is the generally held opinion that ENMs can easily transverse biological barriers and cell membranes into systemic circulation and be redistributed to multiple organs, irrespective of route of exposure[5]. ENMs can be present in sizes small enough to even cross the blood-brain and blood-testis barriers which are designed to be highly selective for protective purposes (Gao et al. 2013, Kim et al. 2008, Kwon et al. 2008, Tang et al. 2008, 2009). Evidence has also emerged to show that ENMs can even cross from mother to baby through the placental membrane, affecting embryonic development and causing pregnancy complications in mice (Pietroiusti et al. 2011, Wick et al. 2010, Yamashita et al. 2011). The precise means by which these particles translocate, distribute and interact with biological systems is an area of intense research, with efforts currently undergoing to assess the potential toxic effects in a wide range of organs and different cell types.

On an environmental level, over the last decade the widespread production, processing, use and disposal of ENMs is leading to their release into the environment. The term "nanowaste" was first coined by Bystrzejewska-Piotrowska and and co-authors in 2009 and according to estimates for 2010 up to 309,000 tonnes of ENMs ended up either in landfill or spread across environmental compartments (soils, 28%; water bodies, 7%; atmosphere, 1.5%) (Keller et al. 2013). The increase in manufacturing or production volumes (some ENMs being produced at >1 million tonnes per annum (Simonet and Valcarel 2009)[6]) will lead to an increase in by-products, emissions and potential contaminants associated with the nanotechnology industry which at present has produced 11.5 million tonnes globally[7]. Many of these ENMs are environmentally

[3] Components of air pollution derived from primary combustion sources that also are in nano-size range.
[4] Asbestos has been proven to cause fibrosis of the lung (asbestosis) and lung cancer (mesothelioma). ENMs such as carbon nanotubes are similar in shape, size, structure and form to asbestos fibres.
[5] Either through inhalation, dermal contact, ingestion or intravenously
[6] Registration of nano Calcium Carbonate (CaC03) under REACH (production between 1-10 tonnes)
[7] According to estimates reported in the European commission staff working paper on Types and uses of nanomaterials, including safety aspects, Brussels, 3.10.2012 SWD(2012) 288 final. Available online: http://ec.europa.eu/health/nanotechnology/docs/swd_2012_288_en.pdf. Last accessed September 2014

bio-persistent and have already been detected in leachates from sea sediment (Hennebert et al. 2011) and at waste sites (wastewater treatment plants, solid waste incineration plants) (Walser et al. 2012, Westerhoff et al. 2011). This, coupled with demonstrations of toxicity of ENMs towards a range of organisms, suggests that at present the uncontrolled environmental release of nanomaterials may pose a risk to all levels of organisation from the soil microbial community (Nogueira et al. 2012) to plants (Lin and Xing 2007, Lee et al. 2010), algae, single-celled organisms to multicellular organisms including aquatic invertebrates and fish (Bondarenko et al. 2013).

1.1.2 Regulatory framework

We rely on regulation to ensure the responsible development of nanotechnology by mitigating the potential risks of nanomaterials. In Europe nanomaterials are included[8], although not mentioned explicitly, under the regulation (EC) No 1097/2006 concerning the Registration, Evaluation, Authorisation and Restriction of Chemicals (REACH) manufactured and imported in the EU. This regulation was established to improve the protection of human health and the environment from the risks that can be posed by chemicals.

Nanomaterials have been entering into the commercial marketplace since the 1990's unlabelled and with a complete lack of consumer awareness. To improve transparency new regulations have been introduced in the cosmetics (EC No. 1223/2009) and food sectors (EC No. 1169/2011). Under these regulations it is obligatory that all ingredients incorporating ENMs be labelled with the word "nano" in brackets. Additionally, under the article 16 of Regulation (EC) No 1223/2009 six months prior to placing a cosmetic product containing nanomaterials on the market, manufacturers, importers, or certain distributors must notify the European Commission and provide chemical safety data (European Commission 2009b).

There are currently 4 registered nanomaterials that are being manufactured or imported at tonnage levels of more than 100 t/year that require registration and chemical safety data (following the latest REACH registration deadline, June 2013). However ENMs are also likely being produced under tonnage threshold levels currently required for registration (<1 t/yr) and chemical safety reporting (<10 t /yr) under REACH. For this reason there is a debate whether nanomaterial regulation under REACH is sufficient or if it needs to be amended to include special provisions for ENMs, because while ENMs may be produced in small quantities they may be widely dispersed across many sectors.

In order to evaluate the risk to human health and the environment from ENMs there is a general consensus that existing test guidelines and risk assessment frameworks can be applied for ENM assessment with some adaptations and refinements (OECD 2014). The European Chemicals Agency (ECHA), which is responsible for implementing REACH regulation, has recognised the regulatory challenges in the risk assessment of nanomaterials. The European Commission's REACH Implementation Projects on Nanomaterials (RIPoNs) have given advice to ECHA on ways to further incorporate nanomaterials into guidance documents. The modification of annexes and technical guidance documents to include specifications for nano is currently under review.

[8] covered by definition of a substance

Nanomaterial regulation is also complicated by the fact that at present there is no harmonised regulatory definition for what a nanomaterial is. Working definitions have been developed by scientific committees of the EU (Scientific Committee on Emerging and Newly Identified Health Risks (SCENIHR)), by the International Organisation for Standardization (ISO) and by EU regulators using different adaptations taking into account aggregation/agglomeration state, and specific properties such as solubility which control biopersistance. A nanomaterial, as defined in Article 2.1(k) of the current legislation on cosmetics products (EC/1223/2009), means "an insoluble or biopersistant and intentionally manufactured material with one or more external dimensions, or an internal structure, on the scale from 1 to 100 nm". While the European commission recommendation proposed the legal definition of a nanomaterial as a "a natural, incidental or manufactured material containing particles, in an unbound state or as an aggregate or as an agglomerate and where, for 50%[9] or more of the particles in the number size distribution, one or more external dimensions is in the size range 1 nm–100 nm (European Commission 2011). Some argue that a size range should not be part of a definition (Schmid et al. 2003) as particles/aggregates >100 nm in size have also shown toxic effects. The appropriateness of such a definition for regulatory purposes is currently being evaluated (Rauscher et al. 2015).

1.2 Metal and metal oxide nanomaterials: Human Health and Environmental risks

In a broad sense ENMs can be grouped into organic (e.g. dendrimers), carbon-based (i.e. allotropic forms of carbon such as fullerenes, carbon nanotubes, or graphene) and metal based (metals/metal oxides) and can be engineered as single particles, fibres, sheets or tube like structures of various sizes and shapes. The metal and metal oxides are an important group as they collectively encompass the vast majority (>75%) of ENMs used both industrially and commercially (Woodrow Wilson database, 2014). Metals are excellent conductors of both heat and electricity. Collectively, their inherent physical and chemical properties have led to metals being used in their bulk form for centuries with a wide variety of applications, from copper wires powering our electrical devices to zinc incorporated into "zinc white" paints. However, the new and enhanced properties conferred upon these materials at nanoscale have led to them becoming highly exploited in modern society. In fact it is estimated that the average person will come into contact (through intentional and/or unintentional exposure) with some form of metal-based ENM in their everyday lives from applying cosmetics or deodorants to ingesting foods containing nanoparticulate additives[10]. Thus, through regular use, disposal and degradation of these consumer products ENMs will be released into the environment.

Ascertaining exposure levels to organisms in the environment and what entity in fact organisms will be exposed to is more challenging. Metal-based ENMs have complex behaviours in natural systems that may present new and as yet understood risks to such environments. Agglomeration state, dissolution, surface modifications and chemical speciation are important processes that control fate, behaviour and transport. While metals are important contaminants of environments worldwide and known to be persistent and non-biodegradable, in some cases metal-based ENMs

[9] it also states that in specific cases and where warranted by concerns for the environment, health, safety or competitiveness the number size distribution threshold of 50% may be replaced by a threshold between 1 and 50%.

[10] Through ingestion alone it has been estimated that daily exposure to nanoparticles could be as high as 40 mg per individual per day (Powell et al. 2010, Lomer et al. 2004). Nanofoods is an area of particular concern with adverse effects evidenced in gastric epithelial cells following exposure to a commonly used food additive TiO_2 NPs (Botelho et al. 2014).

have been shown to have a higher and unique toxic potential compared to metals in their bulk forms. Particularly in the case of metal and metal oxide ENMs, they can be susceptible to dissolution processes and can undergo transformations from nanoparticles to ions. Metal ions such as Ag^{+}, Cu^{2+}, Zn^{2+} released from ENMs will pose toxicity concerns of their own. In fact due to the potential role from both particles and ions, the main risk for the environment is expected from metals and metal oxides (Aschberger et al. 2011). For example metal ions released from ENMs can cause localized toxic effects in the respiratory system of fish through the gills by disturbing ion regulation (Na+ and Cl-) and transport systems (basolateral Na+, K+ATPase, Ca2+ATPase enzyme activity) (Hogstrand and Wood 1996, Lauren and McDonald 1986, Spry and Wood 1989, Verbost et al. 1989, Wood 1992) but also particles can themselves be ingested by aquatic organisms, be transported to the gut epithelium, into the circulatory system and may cause adverse effects. The extent to which metal ions and particles play a role is the subject of an intense scientific debate.

Irrespective of the role of ions or particles, a recent extensive review of toxicological research on nano metals and metal oxides (silver, copper oxide and zinc oxide) report that they are extremely toxic (as defined by Regulation (EC) No 1907/2006) to freshwater aquatic organisms (Bondarenko et al. 2013). Factors such as trophic transfer and biomagnification effects associated with bioaccumulation also come into play when dealing with potentially biopersistant metal-based ENMs. This may lead to not only individual but population and community effects. This has been a major topic in many review papers (Baun et al. 2008, Handy et al. 2008, Klaine et al. 2008, Moore 2006) and research is still very much in its infancy in the area of nanoecotoxicology.

ZnO, Ag and Au ENMs are among representative ENM that have been identified as those which should be assessed with high priority due to their widespread use, production volume and commercial importance (OECD 2010). ENMs of copper (Cu) are attracting attention due to their low cost and ease of availability, that may see their widespread use in the future. Therefore in this thesis the hazard associated with these particular metal-based ENMs was focused on. The properties at nanoscale that have led to their widespread use and the potential human health and environmental risks from exposure, according to toxicity assessments carried out to date, are outlined below.

1.2.1 Zinc oxide (ZnO) ENMs

ZnO has inherent physical and chemical properties that can give rise to a high capacity of light scattering and absorption, high electrical conductivity, excellent optical transmissivity, and often photocatalytic and antibacterial activity. This has led to its use in various and vast applications for centuries. However ZnO ENMs have replaced ZnO in a wide range of both consumer and industrial products due to, in some cases, their enhanced and more desirable properties. For example since the 1990's ZnO ENMs have replaced ZnO in sunscreens as at nanoscale ZnO becomes transparent[11] and thus is more desirable than white opaque ZnO formulations. ZnO exhibits antibacterial properties against an array of pathogens however higher antibacterial activity has been shown at smaller nanoparticle sizes (Jones et al. 2008, Raghupathi et al. 2011).

[11] absorb and scatter light vs reflects and scatters of ZnO

ZnO ENMs highly desirable antibacterial properties are being investigated for their use in the food, textile and medical industry through their incorporation in food packaging, cloths and anti-microbial surface coatings. Global production volumes are between 32,000- 36,000 tonnes per year in 2014[12].

However uncertainties surround ZnO ENMs potential hazards both from a human health and environmental perspective. While it is known that inhalation of ZnO fumes in an occupational setting can cause metal fume fever the potential adverse effects associated with ZnO ENMs are unclear. Sunscreens containing ZnO ENMs have not been approved for use as sprays or in powder form due to concerns over potential toxicity in the lungs. Toxicity in the kidneys and liver following exposure to ZnO ENMs has been shown in inhalation studies with rats (Wang et al. 2010). Therefore important considerations need to be given to hazards particularly in an occupational setting where workers in production facilities may be exposed to high concentrations through inhalation.

Often ZnO ENMs can show heightened photocatalytic activity when they are exposed to UV radiation that can lead to free radicals being formed, which can damage cells. For this reason often they require surface coating[13] in order to prevent any adverse reactions. ZnO ENMs are also present in consumer products that may be ingested (e.g. toothpaste) and thus the gastrointestinal tract may be adversely affected. The hazard associated with exposure can be assessed using various cell types of the tract such as colon cells, with preliminary results suggesting ZnO ENMs are cytotoxic to this cell type (De Berardis et al. 2010) as well as liver cells which are involved in metabolism and excretion (Kermanizadeh et al., 2013, Wang et al. 2011). The mammalian toxicity of ZnO nanoparticles has been reviewed (Vandebriel and De Jong et al. 2012). Cytotoxicity of ZnO ENMs has been demonstrated towards a range of different cell types from different organs; lung epithelial cells (Huang et al. 2010, Hsiao and Huang 2011, Lin et al. 2009, Xia et al. 2008a), kidney cells (Pujalte et al. 2011), colon/intestinal cells (De Berardis et al. 2010, Kang et al. 2013). There are also concerns over possible genotoxic effects with the first reports of DNA damage in a human epidermal cell line being made by Sharma and colleagues in 2009 (Sharma et al. 2009).

The potential heightened risk of ZnO ENMs to the environment lies in the fact that in comparative toxicity studies ZnO ENMs continuously show greater toxicity compared to other metal oxides towards soil and aquatic dwelling organisms (Wu et al. 2013a, Zhu et al. 2008). In fish nanoparticles of ZnO have shown increased bioaccumulation and toxic effects compared to bulk forms (Hao et al. 2013). Evidence of adverse effects suggests that ZnO ENMs may pose a hazard and additional studies to ascertain dose response relationships and to predict possible exposure concentrations will aid in risk assessment.

[12] http://www.futuremarketsinc.com/wp-content/uploads/2015/03/The-Global-Market-for-Copper-Oxide-Nanoparticles-2010-2025.pdf
[13] Coating material includes aluminum hydroxide ($Al[OH]_3$), polymers and inert oxides of silica

1.2.2 Copper (Cu) ENMs

ENMs of copper are of particular high interest due to their low cost, ease of availability and potential for replacing other metal ENMs with similar properties such as silver. Copper is an excellent conductor of heat and electricity[14], it acts as a good catalyst, it has antimicrobial properties, and is produced in large quantities mainly for use in electrical wiring (290-570 tonnes produced globally per year[15]). Cu ENMs have proven to have superior antibacterial properties compared to Ag ENMs (Yoon et al. 2007) and they are being investigated to replace Ag ENMs for use in various industrial applications such as in inks for conductive printing.

While, at present, Cu ENMs are not being produced or applied in such quantities as ZnO or Ag ENMs, their emergence as economically advantageous replacements will inevitably lead to their more widespread use in the future. This will ultimately result in an increase in both human and environmental exposure, making hazard assessments more pertinent. Currently, hazard assessments for Cu ENMs are scarcer than for other metal and metal oxide ENMs. However, most strikingly the visual observations of grave toxicological effects of Cu ENMs on the kidney, liver and spleen in mouse models *in vivo* have been highlighted by Meng et al. (2007) and Chen et al. (2006) with heightened toxic efficacy at nanoscale compared to bulk counterparts. From an environmental perspective, Cu ENM waterborne exposures performed in rainbow trout have caused pathologies in many organs including the brain (Al-Bairuty et al. 2013, Shaw et al. 2012).

Copper ENMs can be oxidised and thus can exist as cupric oxide (CuO) nanoparticles. In fact most studies have focused on the hazards associated with CuO ENM despite Cu ENMs being more favourable due to the loss of conductivity as oxide forms. These studies have shown that CuO ENMs are also more toxic than bulk counterparts (Semisch et al. 2014, Wang et al. 2012) and can be more toxic than other metal oxides (Karlsson et al. 2008).

Toxic effects have been linked to the release of high concentrations of cupric ions either at the cell surface (Karlsson et al. 2013) or intracellularly (Studer et al. 2010). However lower acute toxicity has been observed following Cu ENM exposure compared to soluble forms of copper ($CuCl_2$,$CuNO_3$,$CuSO_4$) in fish (Grosell et al. 2007) suggesting unique heightened hazard from particle exposure.

Copper is also a redox active metal capable of producing hydroxyl radical by Haber-Weiss[16] and Fenton-like reactions[17]. Redox cycling between different valence states on the surface of Cu ENMs can also lead to the generation of reactive oxygen species producing pro-oxidant effects. The induction of both inflammatory responses and of oxidative DNA damage have been described as cellular effects mediated by CuO ENMs (Ahamed et al. 2010, Cho et al. 2010, Fahmy and Cormier 2009, Studer et al. 2010). Thus, oxidative stress has been proposed as the major mechanism of toxicity associated with Cu based ENM exposure.

[14] second only to silver in the table of elements for the best electrical conductivity properties, with over half of all globally produced (20 million tonnes per year) copper going into electrical wiring.
[15] http://www.futuremarketsinc.com/wp-content/uploads/2015/03/The-Global-Market-for-Copper-Oxide-Nanoparticles-2010-2025.pdf
[16] a reaction between oxidized metal ion and H_2O_2 to induce OH•
[17] In this reaction a transition metal ion reacts with H_2O_2 to yield OH• and an oxidized metal ion

Collectively Cu ENMs potential widespread use, their high redox activity and toxicity reported from studies to date warrant further investigations.

1.2.3 Silver (Ag) ENMs

Silver has been known for centuries for its germicidal properties and it is Ag ENMs distinct high and broad spectrum antimicrobial activity[18] that has led to their incorporation into a growing list of consumer products (> 400 nano silver incorporated products). They are currently the most commercialized ENM, used for antimicrobial and disinfection purposes in wide sectors including health, food storage and the textile industry. In contrast to elements such as copper, zinc, and iron which are essential in trace amounts for organisms, silver has no biological function. In fact in its ionic form (and bioavailable) silver is one of the most toxic metals. Micro-organisms and aquatic life are particularly susceptible to silver nanoparticle toxicity (Rai et al. 2012, Sohn et al. 2015). This represents a potential hazard, as through consumer use some products containing Ag ENMs have the potential to directly release Ag ENMs and silver ions into the environment and water systems. In fact the release of Ag ENMs from socks and textiles already has been documented (Benn and Westerhoff 2008, Geranio et al. 2009) and they have been reported in sewage sludge in the form of silver sulfide (Potera 2010). Therefore Ag ENMs released into aquatic environments may adversely affect a range of aquatic organisms by acting as a source of toxic ions or eliciting distinct toxic effects themselves. According to current environmental risk assessments, based on modelling predicted environmental concentrations (PEC) and taking into account species sensitivity distributions, Ag ENMs show one of the highest risks compared to other ENMs, particularly in surface waters (Gottschalk et al. 2013). They also have been shown as acutely toxic to a range of freshwater organisms according to the Globally Harmonized System of Classification and Labelling of Chemicals (Sohn et al. 2015).

Silver ENM toxicity assessments performed to date show toxic effects in aquatic invertebrates, algae and fish (Fabrega et al. 2011). For example Ag ENMs have been shown to affect early life stage development in fish with hatching delays, decreased survival rates, physical deformities and cardiovascular defects reported (Asharani et al. 2011, Bar-llan et al. 2009, Kashiwada et al. 2012). They have also been shown to accumulate in plants and animals (Park 2013, Scown et al. 2010). For example in rainbow trout exposures Ag ENMs were highly concentrated in the liver (Scown et al. 2010). This would suggest whole ecosystem-level (plants, micro-organisms) impacts following the intentional[19]/unintentional release of Ag ENMs into the environment.

[18] antimicrobial efficacy against even multidrug-resistant and highly pathogenic bacteria (Rai et al. 2012) and even have been studied for their application in combating the HIV virus (Elehiguerra et al. 2005, Lara et al. 2005).

[19] Adverse effects have already been seen following application of wastewater treatment biosolids containing Ag ENMs to the land as fertilizer (Colman et al. 2013).

1.2.4 Gold (Au) ENMs

The focus of Au ENMs application has mainly been in the area of biomedicine. Gold in its bulk form has been used in biomedicine since the 1950s and is well recognised as being safe for use. Au ENMs are now being investigated heavily for their use in an extensive range of potential biomedical applications such as drug delivery systems. However, unlike the bright lustrous colour of gold in its bulk form, suspensions of gold nanoparticles appear as different shades of red or blue at 10-200 nm scale. This is due to the collective oscillation of surface electrons upon irradiation with light known as surface plasmon resonance. This surface plasmon resonance means that Au ENMs can absorb and scatter light with a high extinction coefficient (very intensely) and this has led to applications in sensing, bio-imaging and colorimetric assays for diagnostics.

Au ENMs also can be easily functionalised through surface modifications and thus this widens the application window of Au ENMs. Au ENMs can also be functionalised with organic molecules such as peptides and even DNA and in fact such an approach is seen as promising for drug delivery and gene therapy. Research today is focused on developing such functionalisation's to target certain cell type's (e.g. tumour cells in cancer therapy). By using different surface coatings, for example bovine serum albumin (BSA) or glutathione (GSH), different biodistribution patterns have been evidenced (Zhang et al. 2012). The biocompatibility of such approaches must be addressed however, as even for such a seemingly inert material as gold, particle size can influence biological effects (Brown et al. 2008). There are some conflicting results with regard to the biocompatibility of Au ENMs with evidence of both toxicity (Connor et al. 2005) and biocompatibility (Shukla et al. 2005) and even some studies showing that different surface groups/chemistries can dictate responses (Goodmann et al. 2004). Also distinct size dependent toxicities have been reported for Au ENMs of smaller sizes (1-2 nm) (Pan et al. 2007, Tsoli et al. 2005). Acute inflammation and apoptosis in the liver of rats following intravenous administration has also been reported (Cho et al. 2009).

1.2.5 Risks from co-exposures to metals

Metals such as copper and zinc play very important roles in the body and they are found distributed among thousands of proteins where they act as co-factors. They also have a close interrelationship (Osredkar J and Sustar N 2011). Zinc can compete with copper for absorption and binding sites on albumin (Bal et al. 1998). A high intake of zinc may result in decreased assimilation of copper as zinc stimulates synthesis of metallothionein which preferentially binds copper in the cytosol and reduces Cu absorption in the intestine and prevents hepatic accumulation (Fischer et al. 1981, 1983, Fosmire 1990, Hall et al. 1979, L'Abbe & Fischer 1984, Nielson and Winge 1984). Therefore very high doses of zinc can lead to serious and potentially fatal copper deficiency. For example when animals are fed high doses of zinc, their systems became incapable of absorbing enough copper to maintain health. In one study pregnant sheep's reproductive performance was severely impaired and an increase in the incidence of nonviable lambs was witnessed following being fed diets high in zinc (750 mg/kg) (Campbell & Mills 1979). For this reason uptake of both metals must be very tightly regulated and a balanced

copper/zinc ratio[20] maintained. Silver has also been observed to alter copper metabolism (Hirasawa et al. 1994). In particular there is evidence to suggest silver salts cause embryotoxicity through altering the copper-transporting function of ceruloplasmin (Shavlovski et al. 1995). There are also instances of synergistic interrelationships in the environment between metals where one may increase or decrease the bioavailability of another. For instance, there is evidence that the presence of nano titanium dioxide may increase the accumulation of cadmium in carp (*Cyprinius carpio*) (Zhang et al. 2007).

Taken together, along with the fact that already the simultaneous presence of different metal and metal oxide nanomaterials in the environment has been reported (Bolyard et al. 2013, Bystrzejewska-Piotrowaka et al. 2009), this raises considerable concerns about the potential adverse effects of co-exposure. At present this is an area of research in which there is a lack of data both on the co-occurrence of ENMs in the environment and associated hazards.

1.3 Nanomaterial hazard assessment

A hazard is defined as an inherent property of an agent or situation having the potential to cause adverse effects when an organism, system or (sub) population is exposed to that agent (OECD 2004). Hazard identification is the first step in the process of risk assessment and it involves investigating a dose-response relationship and establishing half maximal lethal/effect/inhibitory concentration ($LC_{50}/EC_{50}/IC_{50}$ respectively) values from these relationships. Other concentrations values, as those provoking a lethality effect or inhibition of the effect ($LC_X/EC_X/IC_X$ respectively) can also be calculated. No-observed effect concentrations (NOEC) and the lowest observed effect concentrations (LOEC) can also be estimated from these dose-responses. From these hazard values and, by applying a safety factor to protect all the organisms of a certain environmental compartment from a short and a long-term exposure, a predicted no effect concentration (PNEC) is established.

1.3.1 Approaches & methodology

Nanomaterial toxicity assessment requires a more complex approach compared to traditional chemicals due to the vast amount of parameters that can control potential toxic effects. If one looks at the actual physical and chemical properties of these materials, there really are many factors, not just size, but their shape, agglomeration/aggregation state and chemical reactivity that will dictate how the material interacts with its environment and ultimately the biological response (toxic efficacy). A multidisciplinary approach is needed and a strong focus in ENM hazard assessment is placed on establishing so called property-effect relationships in order to ascertain what is driving toxicity. ENM hazard assessment is complicated further by the broad range of extremely heterogenous ENMs, even among the metal-based group, which necessitates testing on a case by case basis. Experimental considerations need to be specifically made due to technical issues posed by particulate forms or interaction of particles with assay reagents and readout interferences. Particle dispersion methods may potentially alter ENMs characteristics and thus, mechanism of action and behaviour in biological systems. It is of upmost importance

[20] the optimal copper/zinc ratio in serum or plasma is 0.70 - 1.00.

to standardize particle dispersion methods and investigate the impact of different dispersion preparation methods on the cytotoxicity, genotoxicity and ecotoxicity of selected ENMs.

1.3.2 Physico-chemical characterisation

"How meaningful are the results of nanotoxicity studies in the absence of adequate material characterisation?" (Warehit et al. 2008).

The importance of particle characterisation was first realised by researchers in an era when large quantities of toxicological data was emerging, often unreproducible and with conflicting results and erroneous conclusions (Murdock et al. 2008, Montes-Burgos et al. 2010, Oberdörster et al. 2005, Powers et al. 2006). Nowadays physico-chemical characterisation is recognised as an essential prerequisite to nanotoxicity studies for two reasons. Firstly, because defining ENM properties is fundamental to the interpretation of a toxicological effect. Secondly, to facilitate comparative studies with particles that have the same properties and behaviour and thus ensure that results obtained are reproducible and meaningful.

ENMs can be synthesised with an array of different sizes, shapes and functionalities that have been shown to affect biological activity. Particle size will have an effect on the translocation of particles from exposure sites to the rest of the body, cellular uptake and particle processing once inside the cell and their subsequent elimination. The surface area-to-volume ratio is also a function of particle size, with smaller particles having a larger surface area per volume than larger particles which may result in increased reactivity (in fact this is the fundamental assumption of the laws that govern nanomaterials). Shape will also dictate how and if particles are taken up by cells, with particles with different aspect ratios (diameter x length), showing different uptake rates and toxicities (Huang et al. 2010, Hsiao and Huang 2011). For example if ENMs with high aspect ratios and with long fibre-like morphologies (such as carbon nanotubes) are attempted[21] to be taken up by phagocytic cells they can protrude from compartments leading to unclosed phagosomes and leakage of cell contents, ultimately resulting in inflammatory responses (Brown et al. 2007). Such a process has been identified for asbestos like fibres and called frustrated phagocytosis (Davis et al. 1986).

Surface charge can influence the interaction of particles with biomolecules (protein corona formation), as well as their uptake into cells, with greater permeabilization for cationic positively charged particles across negatively charged cell membranes. The particles polarity and hydrophobic/hydrophilic nature will also influence clearance with hydrophobic particles being recognised as foreign and their quick clearance by the mononuclear phagocyte system (MPS), while hydrophobic particles generally have a much longer circulation time. Particles can be susceptible to dissolution, particularly metal and metal oxide ENMs, releasing ions into suspensions or intracellularly that can also contribute to toxicity. Therefore monitoring ion release becomes increasingly important. ENMs can also have different tendencies to aggregate/agglomerate in suspension. Single particles have a tendency to associate with each other either physically (through van der Waals or electrostatic forces) or through chemical bonds, forming aggregates or agglomerates respectively. The state of agglomeration or aggregation will

[21] Fibers greater than 10–20 μm in length are longer than a macrophage can engulf.

influence how the nanomaterials are "seen" by and interact with cells (cellular uptake and processing). In contrast to dose -dependent toxicity seen for conventional chemicals, at higher concentrations ENMs may form bigger or more agglomerates/aggregates reducing their bioavailability and their toxicity. Distinct biological effects can exist for aggregates/agglomerates and primary particles. Large aggregates/agglomerates may produce more local effects while primary particles may distribute to produce systemic effects to multiple systems. Often ENMs suspensions are composed of a heterogeneous population with broad size distributions of aggregates/agglomerates (different sizes) as well as single particles with each of these subpopulations producing distinct effects (Gatoo et al. 2014).

All of the above mentioned properties influence biological action and these properties themselves can be influenced by the composition of biological matrices (pH, ionic strength, osmolarity, protein content), by storage conditions and mechanical treatment prior to testing. It is now common practice to use ultrasonic treatment for optimal dispersion of hard to disperse ENMs such as TiO2 and ZnO. Also often stabilisers such as albumin or serum are added that are shown to improve the dispersion by producing small agglomerates of primary particles with narrow size variations (Vippola et al. 2009) and stable suspensions (Tantra et al. 2010). While there is no standardised protocol some research suggests that particle size reduction depends on the applied energy per volume of the dispersion (specific energy), also that the sequence of sonication and stabiliser addition is important in order to prevent reagglomeration, and that the required amount of stabilizer depends on the total surface area of the particles in the dispersion (Bihari et al. 2011).

Also these abiotic factors/experimental conditions such as pH, salt content, amino acids and proteins will have a direct effect on ENM behaviour in terms of dispersion stability and dissolution as well as aggregation/agglomeration state. Under physiological conditions (and in artificial medium environments that mimic such conditions) ENMs will come in contact with proteins and other macromolecules that have been shown to coat them forming a protein corona (Cedervall et al. 2007). Such a corona is dictated by the different proteins present and can influence cellular uptake and trafficking (Walczyk et al. 2010). As well as this the presence of organic compounds such as sulfate, nitrate, ammonia or chloride and their interaction with metal ions can lead to chemical transformations. For example both copper and zinc ions can combine with sulfate and nitrate molecules to form salts and thus be present as metalorganic complexes (Massey et al. 1975). AgNPs, due to the high chemical reactivity of Ag0 with dissolved O_2, and Ag^+ with anions like Cl^- often transform into silver chloride (Levard et al. 2012).

All of these factors can influence toxicity in terms of bioavailability, cellular uptake (Kettler et al. 2014) and metal ion insult. Therefore it is imperative to characterise ENM physico- chemical properties and behaviour in suspensions/exposure environments.

Optical methods such as dynamic light scattering (DLS) is an important technique in this sense as they can measure particles or particle population's hydrodynamic size in suspension. DLS gives measured hydrodynamic size distributions of particles/ aggregates/agglomerates in suspension according to time dependent fluctuations in scattered light intensity caused by particles random motion (Brownian motion) in suspension. The Stokes–Einstein equation then relates the timescale of fluctuations to the equivalent-sphere hydrodynamic diameter of the

particle. Its ease of use allows one to monitor particle suspension stability over an exposure period. The particles/aggregates/agglomerates physical form and morphology can be directly visualised by high powered microscopes (for instance transmission electron microscopes, TEMs) that utilise electron beams instead of light and use electron diffraction to produce high resolution images down to the 1 nanometer scale.

While many studies have sought to correlate certain properties with biological effects there is no defined set of key determinants emerging as more strongly related to toxicity than others.

Nanoparticles can be functionalised through coating or capping with surfactants or biomolecules such as peptides which can control ENM behaviour and improve biocompatibility. For example Fe doping of ZnO NPs is seen as a possible safe design strategy for preventing ZnO toxicity (George et al. 2010). Also using a manganese coating to reduce the unwanted photo-activity of TiO_2 in sunscreens is being applied. Peptides in particular can be used in a programmable fashion with different sequences of amino acids providing the building blocks for ligand molecules that can be optimized to stabilize nanoparticles. One can also make use of the biological functionality of certain peptides, by controlling specific cellular uptake routes, as reported for Au nanoparticles (de la Fuente & Berry 2005, Nativo et al. 2008) , as well as modulating the reaction of the immune system towards nanoparticles by different peptide coatings (Bastus et al. 2009). Particularly in the area of biomedicine there is enormous potential in designing particles which are stable, biocompatible and easily functionalised for targeting cells or interacting with other biomolecules.

1.3.3 Test systems

Toxicity of chemicals and/or nanomaterials should be assessed through established assay protocols that must be set up and accepted by a number of laboratories (at the national or international level) guaranteeing the robustness, accuracy and replicability of the obtained results. This data would then be applied for the risk assessment of chemicals or nanomaterials. A number of regulatory agencies play an essential role in the development of these tests. From the Environmental Protection Agency (EPA) of the US to the International Standardization Organization (ISO), probably the Organization for Economic Cooperation and Development (OECD) is the agency taking a leading role at this level due to its size and international influence (34 countries grouping the biggest economies and most developed regions of the world). Although this agency is internationally known and recognized, mostly due to its economical surveys and predictions, it has an essential function in the development of internationally agreed instruments in a variety of areas including chemical regulation. At this level, the OECD has developed an entire program devoted to chemical safety. In this framework the OECD has set up test guidelines (TG) for the testing of chemicals. They are internationally accepted as standard methods to assess potential harmful effects of chemicals on humans and environment. “Test Guidelines are covered by the Mutual Acceptance of Data, implying that data generated in the testing of chemicals in an OECD member country, or a partner country having adhered to the Decision, in accordance with OECD Test Guidelines and Principles of Good Laboratory Practice (GLP), be accepted in other OECD countries and partner countries having adhered to the

Decision"[22]. These guidelines have been deemed generally applicable when testing ENMs, with in some cases the need for ENM specific amendment or guidance (OECD 2014).

The majority of these test guidelines for human health involve *in vivo* testing using animals, usually rodents (mice or rats). Test guidelines pertaining to ecotoxicity and environmental fate of substances involve different organisms at various levels of biological and environmental organization (earthworms and soil micro-organisms, algae and cyanobacteria, midges, springtail, aquatic and terrestrial plants, daphnia species, frogs, bees, birds and fish). Fish represent higher trophic level organisms in aquatic ecosystems and for this reason they are routinely used in toxicity assessment. Guidelines for fish toxicity testing include a 96 h acute lethality test (OECD TG 203, OECD 1992), effects on specific developmental and life stages (TG 212, TG 210, TG 215)(OECD 1998, 2000) and bioaccumulation studies/bio-concentration studies (TG 305)(OECD 2012c). However standard *in vivo* test methods that rely heavily on the use of animals, such as those mentioned, are not seen as feasible options to meet the testing required to fill information gaps under REACH legislation for all existing and new chemicals including ENMs. The 3Rs principle to replace, reduce, and refine animal testing (Russell and Burch 1959) has been implemented in the EU Directive 2010/63/EU on the protection of animals used for scientific purposes[23]. Also according to the European REACH legislation 'testing on vertebrate animals shall only be undertaken as a last resort' (Article 25, REACH). Furthermore, on a regulatory level, as of March 11th 2009 an amendment to the EU cosmetics directive came into force which bans animal testing of cosmetics or their raw ingredients. Therefore investigating the potential value of alternative non-animal testing systems becomes extremely relevant and of high interest. Alternative methods to animal testing including *in vitro* test systems are currently being validated and introduced. Analysts forecast the global *in vitro* toxicity testing market in Europe will grow at a compound annual growth rate of 15.84 percent over the period 2013-2018 (Research and Markets 2014).

1.3.3.1 Animal models (*in vivo* testing)

In vivo testing provides a means to assess toxicity on a whole organism level with the interplay of a full repertoire of body systems and functions. Presently it is the only means by which to obtain toxicokinetic/pharmacokinetic information concerning the processes of absorption, bio-distribution, metabolism and excretion of ENMs; areas in which currently very little is known. Since the pioneering studies with fish, showing that nanoparticles (fullerenes) in aquatic environments can be toxic (Oberdörster et al. 2004), these studies have been followed by a number of research groups (for instance, Smith et al. 2007, Federichi et al. 2007, Griffitt et al. 2007, and Scown et al. 2010 using SWCNT, TiO_2, Cu ENMs and Ag ENMs, respectively), with evidence of pathologies and toxic effects. However studies are in their infancy and up until now most of them have been performed using waterborne exposures despite the high relevance of dietary exposure for ENM testing and the OECD test guideline No. 305 adaptation to reflect this.

There is also a lack of studies investigating the bioaccumulation of ENMs in fish, their tissue distribution and retention times. Metals are non-biodegradable and therefore it is important to

[22] http://www.oecd-ilibrary.org/environment/oecd-guidelines-for-the-testing-of-chemicals_chem_guide_pkg-en

[23] almost 150 million € in funding has been provided under the EU's 6th and 7th Research Framework Programmes to advance the development and validation of 3Rs methods and testing strategies for regulatory purposes (Alternative testing strategies Progress Report 2010).

investigate bioaccumulation. Behavioural and physiological indicators of sublethal toxicity have been associated with bioaccumulation of metals in fish (Boyle et al. 2013, Handy et al 1999). Investigations into whether such affects present themselves with metal ENMs are in their infancy. However reports have shown that nanoparticles of ZnO hyperaccumulated compare to ZnO in its bulk form in juvenile carp (Hao et al. 2013). The risk from nanoparticles bioaccumulating, as opposed to bulk forms, is that dissolution properties, along with their small size at nanoscale, may facilitate their entry into systemic circulation resulting in potential effects on multiple organs.

1.3.3.2 Alternative cell culture based models (*in vitro* testing)

In vitro test systems using cell cultures are being investigated as alternatives to animal testing. Cell culture refers to the growing of cells derived from tissues in a favourable artificial environment outside of the body "*in vitro*". Freshly isolated cells are referred to as primary cultures. These cultures proliferate until confluency and generally do not possess the ability to be subcultured. However they provide a more superior model of the *in vivo* situation. Cell lines on the other hand are cells which have acquired, either spontaneously or through experimental manipulation, the ability to proliferate either for a finite time or indefinitely in continuous culture. A large number of cell lines exist (>4,000) from different species, tissues and cell types, available at the depository of the American type culture collection (ATCC) or at the European collection of authenticated cell cultures (ECACC) and they represent a valuable resource.

In particular fish cell culture has developed rapidly since Wolf and Quimby established the first fish cell line, RTG-2, in the 1960s (Wolf and Quimby 1962). Since then a repertoire of cell lines from different organ systems of the rainbow trout have been established representing a very valuable resource: rainbow trout gill cell line, RTgill-W1; rainbow trout liver, RTL-W1; a rainbow trout spleen cell line, RTS34; Rainbow trout gut cell line, RTgut-GC1; a rainbow trout macrophage cell line (RTS11); and the rainbow trout hepatoma cell line RTH-149. Also other cell lines from other fish species have been developed.

In vitro cell cultures are also seen as fundamental tools for mechanistic studies at the cellular level, providing a means to investigate the mode of toxic action (MOA) of substances. Particularly in the case of ENMs, given the wide diversity of materials and the fact that different forms of the same nanomaterial can have different toxicological properties, there is a need to assess them on a case by case basis. Such assessments require a robust approach.

Cell lines as test systems are both time and cost effective and they provide a platform for high throughput testing. Cell lines also provide a controlled testing environment for mechanistic investigations at the cellular level. Recent evaluations of safety assessment of ENMs indicated that *in vitro* assays may be useful, but mainly for screening and the evaluation of specific mechanistic pathways (ECETOC 2006, Oberdörster et al. 2005). However, to be applicable in risk assessment, these assays need to be validated and their relevance for *in vivo* hazard identification needs to be demonstrated. Currently the proposed use of cell lines are yet under validation for nanomaterial toxicity assessment[24] however they can be used as a non-standard

[24] RTLW1 gill cell line is currently being validated.

methods to provide toxicological data that can be used in a weight of evidence approach of an integrated testing strategy according to the Commission Regulation (EC) No 134/2009 concerning the Registration, Evaluation, Authorisation and Restriction of Chemicals (REACH) (European Commission 2009a).

The appropriateness of *in vitro* test systems using cell cultures has been questioned for ENM toxicity assessment. These questions concern their compatibility when using ENMs and their value in predicting an *in vivo* response. Cell lines can express phenotypes that are very distinct from the cells from which they were originated. Therefore studies comparing responses between cell lines and cells freshly isolated will aid in establishing the value of particular cell lines and if they are representative models.

1.4 Nanomaterials as potential hepatotoxicants

1.4.1 The liver as a relevant target organ for metal nanomaterials

In order to produce meaningful and relevant data *in vitro* it is important to carefully consider exposure routes and possible target sites. According to possible direct ENM exposure routes (inhalation, dermal contact and ingestion) the lungs, skin and gastrointestinal tract are target organs. However ENMs have been evidenced to cross biological barriers moving from these sites of exposure into systemic circulation and reaching other organs (secondary exposure sites). Among these organs the liver, kidneys and spleen show the highest retention of ENMs that pass into systemic circulation. This may be related to their predominant role in the reticuloendothelial system and clearance of foreign objects from the blood.

The liver plays a major role in the uptake, storage, metabolism, redistribution and excretion of many substances and this may include ENMs. In particular, in the case of metals such as copper, the liver is central to maintaining a balance by incorporating copper into newly synthesised caeruloplasmin, metallothionein or cuproproteins for transport and storage and ensuring excess is excreted using the biliary excretion pathway[25] (Wijmenga and Klomp 2004). The fact that the liver has been identified as one of the major secondary organs of distribution following exposure to a range of metal ENMs (Au ENMs) (De Jong et al. 2008, AgNPs; Sung et al. 2009) both in mice (Wang et al. 2007, Xie et al. 2010) and in fish (Choi et al. 2010, Handy et al. 2008a, 2008b, Kashiwada 2006, Ramsden et al. 2009, Scown et al. 2009) points to its central role in handling ENMs and as a potential site for toxicity.

The liver is a central organ in the circulatory system receiving blood from the gastrointestinal tract and spleen (portal vein) as well as arterial blood from the hepatic artery. Therefore once in circulation, ENM will be carried with the blood through the liver. In the liver of mammals blood circulates through a capillary network of blood vessels known as sinusoids. These sinusoids are lined with endothelial cells (liver sinusoidal endothelial cells (LSECs)) and have fenestrations or "pores" that filter the nutrient rich blood coming from the heart through the portal vein. The LSEC's are responsible for filtering macromolecules from the blood and therefore represent an important line of defence. Lipoproteins and smaller molecules pass through these pores to the

[25] Under normal physiological conditions about 98% of copper excretion is via the bile and the remaining 2% is via the urine (Linder and HazeghAzam 1996).

perisinusoidal space or space of Disse and subsequently to the hepatocytes, which are the main cells responsible for the livers metabolic functions. Fenestrations are usually between 100-150 nm depending on the animal species and therefore ENMs in this size range and below may easily access hepatocytes. Uptake of polystyrene nanoparticles (20 nm) by hepatocytes and there localisation in cytosolic compartments has been demonstrated (Johnston et al. 2010). How hepatocytes and other liver cells may process ENMs has yet to be fully elucidated. Biliary excretion by hepatocytes is an important detoxifying mechanism of many heavy metals by the liver and therefore metal ENM processed by these cells may potentially be excreted into the bile. ENM association with bile canaliculi of hepatocytes has been documented and the biliary excretion of quantum dots has been shown to be an extremely slow and inefficient process (Choi et al. 2007), thus, the organ may be exposed for a prolonged time. If nanoparticles are present in large aggregates, >150 nm in size, they also may be taken up by liver macrophages, also known as Kupffer cells, which are located on top of and between endothelial cells and are in direct contact with the blood. Kupffer cells are part of the RES, they take up particles by phagocytosis and rely exclusively on intracellular degradation for particle removal. Particles that are not broken down by intracellular processes and taken up by Kupffer cells will remain within the cell and will therefore be retained by the body. Results from *in vivo* studies would suggest that the liver may be exposed to ENM for a prolonged time (Tseng et al. 2012) with associated hepatic pathologies[26].

The liver in fish also has very important functions in the elimination of metals however one important consideration is that the gills also play a role. Despite this discrepancy exposures performed in fish show the liver as a major organ of accumulation (Salari-Joo et al. 2013, Wu et al. 2013b) and that the liver burden following waterborne exposure to nanomaterials is twice that of the gills (Scown et al. 2010). In fish the liver has the same general circulatory component and physiological role as in mammals with analogous metabolic function and detoxification systems (small differences that may affect the rate, pattern and or extent of toxicity that occur in a fish compared to mammal is discussed more in detail in the discussion section and also some architectural differences exist[27] (Di Giulio and Linton 2008)).

Within the liver parenchyma hepatocytes are sites of major metabolic transformations and for this reason may be particularly vulnerable to ENM insult. Reports have emerged that ENMs have the potential to interfere with the normal functioning of cytochrome P450 (CYP) enzyme activities that are related with the metabolism of endogenous and exogenous substances (Balasubramanian et al. 2010, Kulthong et al. 2012, Lamb et al. 2010, Sereemaspun et al. 2008). Few studies have demonstrated or monitored this effect *in vivo.* For instance, one report showed changes in rats following 2 months of Au ENM intravenous administration (Balasubramanian et al. 2010). The mechanism underlying this phenomenon has not been fully elucidated but may have major consequences for the organism and xenobiotic metabolism.

[26] In juvenile carps severe hepatic pathologies were reported by Hao et al. 2009 after 21 days of exposure to TiO2 ENMs with evidence of necrotic and apoptotic hepatocytes. Similarily Federici et al. (2007) reported some hepatocytes with apoptotic bodies in *O. mykiss* following exposure to TiO_2 ENMs.

[27] There is a lack of lobular pattern and an absence of functional metabolic zonation in the liver paranchyma of fish and only the basal side of hepatocytes face sinusoids. Fish may also have lower capacity to metabolise xenobiotic substances, as they have a lower liver perfusion rate and produce bile at much slower rate. (Di Giulio and Linton 2008).

1.4.2 Liver cell culture models (liver cell lines and primary culture)

Liver cell lines composed of cells derived from neoplastic tissues taken from explants or that have de-differentiated in some way from the original cell types are available and represent valuable resources as *in vitro* test systems. Both liver cell lines mammalian (for instance, Huh-7, Huh 6, Huh 4 and HepG2) and piscine (for instance, ZFL, from zebra fish, *Danio rerio*, or RTH-149, from rainbow trout, cell lines) in origin are available and therefore can be used to evaluate the cytotoxicity of ENMs. They could also constitute an important tool to evaluate interspecies differences in sensitivities.

Methods for isolating specific cell types from the liver have also been well established and usually involve a two-step collagenase perfusion technique (Berry and Friend 1969, Seglen 1976). However their use as test systems is limited due to a number of factors, including the heterogeneity of cells from one isolation to another and quality of cells isolated. Unlike cell lines, they have a very finite lifespan grown under culture conditions *in vitro* and even have a tendency to dedifferentiate into different cell types during *in vitro* culture. However, they have the great advantage of showing unaltered cellular functioning and metabolism that reflect the real situation of the cell in the organism *in vivo*.

1.5 Mechanistic insights into the toxicity of nanomaterials at the cellular level

ENMs can be in the order of ten thousand times smaller than a human cell with their specific physico-chemical properties controlling unique nanoparticle-cellular interactions (Verma and Stellacci 2009). They can be taken up by multiple endocytotic pathways (clathrin- and caveolae-receptor mediated, phagocytosis, micropinocytosis, pinocytosis) and in some cases non-endocytotic “passive” routes such as diffusion or through ion channels or pores. The precise pathways by which these ENMs are taken up by cells, how they are processed (intracellular trafficking) and their potential mechanisms of toxicity have not been fully elucidated. Uptake and processing mechanisms have been shown to be cell type specific (dos Santos et al. 2011, Xia et al. 2008b) and can even depend on the specific cell cycle phase (Kim et al. 2012). Depending on their uptake route, ENMs can be found free in the cytosol or undergoing various cascades of intracellular trafficking steps (being taken up/released from endosomes /lysosomes or within such membrane bound vesicles). ENM have been frequently reported to be held in membrane bound vesicles. Conditions in these compartments can lead to unpredictable behaviour of some ENMs, such as their dissolution and increased redox activity, causing disruption to cellular ion and redox homeostasis.

It must also be noted that ENMs do not necessarily need to be taken up to cause cytotoxic effects associated with cell surface interaction and mechanical damage (Karlsson et al. 2013). However once uptaken ENMs have been shown to interact with multiple cellular organelles (mitochondria, lysosomes) including the nucleus which can result in cellular dysfunction and DNA damage. ENMs which enter the nucleus may directly interact with nuclear DNA, as ENMs at the lowest nm range (1-2 nm) are the same size as the width of base pairs that make up our DNA. Au ENMs specifically in this size range have been shown to cause increased cytotoxicity to various cell

types, possibly due to interaction with DNA grooves (Pan et al. 2007, Schmid 2008). Genotoxicity has been reported for a wide range of metal and metal oxide ENMs (Ahamed et al. 2010, CuO; Akhtar et al. 2016, CuO ENMs).

Biochemical assays can be applied to cell cultures to investigate cytotoxicity at the cell membrane or specific organelle sites as well as according to a general loss in metabolic activity. Imaging techniques such as TEM can be used to investigate nanoparticle- cell interaction, cellular uptake and intracellular distribution/fate and in this way complement biochemical based assay systems. Induced coupled plasma mass spectroscopy (ICP-MS) can be used as a quantitative approach to measure ENM cellular uptake. Using such an approach one can gain an understanding of possible mechanisms underlying a cytotoxic response.

1.5.1 Cytotoxicity assessment using multiple endpoints

Using *in vitro* cell culture, assays can be applied in a high throughput and robust fashion to assess toxicity according to multiple endpoints. As a physical barrier and critical portal of entry for ENMs the cells membrane integrity is one of the most frequently assessed endpoints of toxicity. Traditional cytotoxicity assays, which have been used in this research to monitor such an endpoint, include the LDH assay as an indicator of membrane integrity according to the release of lactate dehydrogenase (LDH) and the use of carboxyfluorescein diacetate, acetoxymethyl ester (CFDA-AM) dye allowing its hydrolysis by intracellular esterases and measuring its conversion product (carboxyfluorescein).

At a specific organelle level, the functioning of mitochondria, taking into account its primary role in energy production and regulation of cell death, are key to monitor. Mitochondrial dysfunction associated with reduced cellular ATP delivery, increased reactive oxygen species production, loss of mitochondrial membrane potential, and triggering of apoptosis pathways in a mitochondria mediated pathway of toxicity has been reported following metal and metal oxide ENM exposure (Hsin et al. 2008, Piao et al. 2011, Siddiqui et al. 2013). One of the most commonly used tetrazolium salt based assay systems[28], the 3-(4,5-dimethylthiazol-2-yl)-2,5-diphenyltetrazolium bromide (MTT) assay, was employed in this work to assess reduction in specific mitochondrial function as an endpoint of toxicity (Mosmann 1983). As a measure of general metabolic activity alamar blue and resazurin reduction assays (RRU), which both quantify cellular viability based on the reduction of the reporter dye resazurin to resorufin by cellular metabolic processes, can be used (O'Brien et al. 2000).

Once taken up, ENMs have been evidenced in some instances to be directed to the endosomal/lysosomal processing pathway where they can either escape from endosomes (proton sponge effect) or are degraded by lysosomal enzymes. Through this process ENM have been reported to cause destabilization of lysosomes and permeabilization of lysosomal membranes. Researchers have highlighted lysosomal dysfunction as an emerging mechanism of toxicity for ENMs (Stern et al. 2012). Thus the neutral red uptake assay which serves to assess lysosomal

[28] Other tetrazolium salt based assay systems include (MTS, XTT, WST-8, WST-1),

functionality by cells ability to retain a neutral red dye (Borenfreund and Puerner 1985) may be very relevant for ENM cytotoxicity assessment.

Some of these assays can also be applied in combination affording the characterisation of different endpoints on the same set of cells. However applying these assay systems for the cytotoxicity assessment of ENMs, as opposed to conventional chemicals and drugs, requires a more particular approach. Interaction of ENMs with assay components and interference with readouts of assay systems such as those listed above has been well documented (Worle-Knirsch et al. 2006). Specific examples include inactivation of the LDH enzyme by copper and silver ENMs (and potentially their ions) (Han et al. 2011), the extracellular reduction of the MTT tetrazolium salt to formazan by TiO_2 (Holder et al. 2012) and the adsorption of highly cationic dyes such as neutral red (NR) to nanoclays (Felbeck et al. 2013). Some ENMs also show intrinsic light absorbing (Au ENMs absorb light in the visible region, ~520 nm), and scattering properties that can lead to optical interferences with absorbance, or fluorescence readouts. As one is often dealing with insoluble particulate materials, this can also lead to physical interferences. Such interferences can lead to either false positives or false negatives and a perceived increase or decrease in toxicity, respectively.

Despite a number of authors outlining their concerns (Kong et al. 2011, Stone et al. 2009) the majority of studies do not account for potential interference of ENMs (Ong et al. 2014). This has serious implications for confidence in the generated data. Checking for such interferences associated with adsorption capacity, reactivity, and agglomeration state and including appropriate controls is critical in order to obtain reliable data and ensure assay compatibility. Interferences are often assay and ENM-specific and therefore interference needs to be assessed on a case by case basis. Adaptation of assay protocols to include additional washing steps may also be adequate to overcome potential interferences.

Dosimetry may also be affected by NP agglomeration/aggregation and settling once ENM suspensions are prepared in exposure medium (e.g. biological culture medium) (Teeguarden et al. 2007). In the case of metal ENMs they tend to have a “sticky” nature which can result in their strong adherence to experimental equipment when handling. Taking both these issues into consideration it is imperative to measure real exposure concentrations to get a more accurate dose metric.

1.5.2 Reactive oxygen species generation and oxidative stress -The oxidative stress paradigm

ENM-induced reactive oxygen species (ROS) generation and oxidative stress-mediated cytotoxicity is the most widely proposed mechanism of toxicity, especially in the case of metal and metal oxide nanoparticles.

ROS are chemical species derived from molecular oxygen that contain one or more unpaired electrons making them highly reactive. The superoxide anion radical ($O_2^{\bullet-}$), peroxide (O_2^{-2}) hydrogen peroxide (H_2O_2) and hydroxyl radical ($^{\bullet}OH$) are all examples of ROS. They are constantly being produced endogenously as intermediates or by products of cellular oxidative metabolism and other biochemical processes, but they can also be generated by ENMs. In this last case, ROS generation can occur directly on the particles surface through redox chemistry, if

there are active electron donor or acceptor groups or if surfaces become photo-activated by UV light as seen for ZnO (Ma et al. 2011) and TiO_2 NPs (Marcone et al. 2012). Particularly in the case of metal NPs that are susceptible to dissolution, ions of redox-active metals, such as copper, can catalyse the oxidation of H_2O_2 to the highly reactive hydroxyl radical (•OH) through Fenton and Harber-Weiss type chemical reactions (Cu^+ and H_2O_2 generate $Cu_2^+ + OH^- + OH$) (Valko et al. 2005). Such ions can interact with NADPH (nicotinamide adenine dinucleotide phosphate reduced) oxidases from the plasma membrane or mitochondria, disturbing the electron transport chain and generating highly reactive superoxide anions (Klotz & Sies 2009). If particles themselves reach the mitochondria, high levels of ROS also can result from nano-particulate disruption at this site, which houses the cells major stores of endogenous ROS (Turrens 2003).

Cells respond to such ROS insults with compensatory responses involving anti-oxidant networks. However, if the cell endogenous antioxidant network becomes overwhelmed or depleted by high concentrations of ROS, oxidative damage to biomolecules such as lipids, proteins and DNA will result and cells will experience oxidative stress. Oxidative stress was first proposed by Sies in 1991 and was defined as "a disturbance in the pro-oxidant –anti-oxidant balance in favour of the former, leading to potential damage" (Sies 1991). Oxidative stress is involved in the pathogenesis of many diseases, in the brain causing dementia and Alzheimer's, in the joints causing arthritis, in the blood vessels causing heart disease, in the nerves causing multiple sclerosis (MS), myasthenia gravis and amyotrophic lateral sclerosis (ALS), and in the gut causing colitis, irritable bowel syndrome (IBS) and Krohn's disease. It is thought to precede an inflammatory response that ultimately leads to cell death either by apoptosis or necrosis.

Indeed a hierarchical oxidative stress model has been proposed to explain ENM toxicity and oxidative stress has become an established paradigm for NP toxicity (Li et al. 2003, Xia et al. 2006). According to this model, following ROS insult, cells activate signalling pathways that lead to the expression of genes coding for antioxidants involved in mounting an anti-oxidative response. The nuclear erythroid-2-related factor (Nrf2) signalling pathway is one of these pathways and is responsible for the transcription of various antioxidant genes encoding for a range of cytoprotective enzymes and proteins, including phase II detoxifying enzymes such as glutathione-S-transferase (GST), the stress-protein heme oxygenase 1 (HO-1) and also key constituents involved in the synthesis of glutathione (GSH) (Alam et al. 1999, Itoh et al. 1999, Lu 2013). GSTs are an important group of enzymes that catalyse the nucleophilic addition of GSH to electrophiles and products of oxidative stress, making them less reactive and more soluble. HO-1 catalyzes the breakdown of heme into iron, carbon monoxide, and biliverdin. Biliverdin is then reduced to bilirubin, an antioxidant, via biliverdin reductase. Glutathione is the most abundant cellular antioxidant, involved in the conjugation of ROS and maintaining redox status through the glutathione redox system. In this system, under basal conditions, cells ratio of reduced to oxidised glutathione (GSH/GSSG) is 100:1 (Zitka et al. 2012). Any change in this ratio can be used as an indicator of imbalanced cellular redox status and oxidative insult. Similarly, measurements of the mentioned GST or HO-1 activities or of the corresponding gene expression can be a very valuable tool to assess if the cells are mounting an antioxidant response against an oxidative insult. Also through an understanding of such pathways responses can be manipulated (e.g. upregulated) in order to determine the role oxidative processes play in ENMs mechanism of toxicity. For example the transcription of GST is also triggered when the aryl

hydrocarbon receptor (AhR) is activated. The AhR is an important transcription factor involved principally in xenobiotic metabolism through the transcription of cytochrome P450 monooxygenases (CYP1A1) but its activation also plays a role in anti-oxidant defence. In fact recent evidence suggest that there is an overlap between target genes that encode for GST (GSTA2) that requires activation of both AhR and Nrf2 pathways (Ma et al. 2004) and that there is an interplay between these two pathways in which there is an AhR-dependent activation of Nrf2 (Dietrich 2016). Using this understanding there is a potential for studies to be performed to test if oxidative stress is a specific mechanism of toxicity for specific ENMs by increasing the cells antioxidant capacity though AhR-mediated activation and checking for a protective effect. In fact such an approach was taken in the research paper 3 presented within this thesis to test the role of oxidative stress in CuNPs mechanism of cytotoxicity.

According to the proposed oxidative stress model, if the cells antioxidant network is overwhelmed or antioxidants become depleted a tier 2 inflammatory and subsequently a tier 3 apoptotic response will ensue, ultimately leading to cytotoxicity. Therefore according to this pathway the levels of ROS following nanoparticle insult are critical in dictating the cellular response. Therefore, the measurement of intracellular levels of ROS can be essential in determining the role of oxidative stress in cytotoxicity. For that, a variety of probes have been developed. For instance, 2', 7' dichlorofluorescin diacetate (DCFH-DA) has been widely used as a marker for oxidative stress (Wang and Joseph 1999). This compound diffuses through the cell membrane where it is enzymatically de-acetylated by intracellular esterases to the non-fluorescent DCF-H. DCF-H in the presence of ROS is converted to the highly fluorescent DCF.

Studies point to oxidative stress as being mechanistically important particularly for the metal and metal oxide group of ENMs. For ZnO NPs there have been reports of oxidative DNA damage (Lin et al. 2009, Sharma et al. 2012). Similarly oxidative damage has been evidenced for CuO ENMs (Karlsson et al. 2008) and for TiO_2 (Reeves et al. 2008). For Ag ENMs both ROS-dependent and independent pathways of toxicity have been proposed (Chairuangkitti et al. 2012, Kim et al. 2011). In many studies there have been no reports of oxidative stress or ROS generation and in fact anti-oxidative effects have been seen. Therefore a more detailed assessment is needed. The key question that needs to be addressed is to what degree oxidative stress dictates toxicity and by which mechanisms do ENMs cause oxidative stress. The other essential question that we must also pose is if oxidative stress constitutes merely a secondary effect associated with cell death or if it is a key player in NPs toxicity. In many studies evidence of elevated levels of ROS is suggested to be a sign that cytotoxicity is likely to be mediated through oxidative stress. While this can be an important indicator of cellular stress it may be associated with cell death and not constitute a causative factor.

CHAPTER 2

OBJECTIVES

The main aim of this work is to gain information about the mechanisms underlying the toxicity of metal/metal oxide ENM exposure on the liver. We have approached this main objective from both human and environmental perspectives. The metal/metal oxide ENMs studied in this research have already been identified as those which should be assessed with high priority due to their widespread use, production volume and commercial importance (OECD 2010) as well as due to their future emerging applications. They include ZnO, Cu, Ag and Au ENMs.

A range of liver cell lines were employed as *in vitro* test systems and afforded the application of multiple biochemical based assays to gain mechanistic insights into any observed cytotoxicity.

An underlying objective in this work was to address the use and appropriateness of *in vitro* cell lines as alternatives to animal testing and as useful tools for nanoparticle hazard identification both in a screening strategy and to prioritise ENMs for *in vivo* testing.

Preliminary studies presented in introductory papers 1, 2 amd 3 were performed first as a foundation upon which to build on achieveing the main objective of gaining some insight into the mechanisms underlying the toxicity of a ENMs. Studies were devised

- To investigate the cytotoxic potential of an array of different sized/shaped ENMs (ZnONPs and CuNPs) and to ascertain if any causal relationships exist between their physico-chemical properties and the biological responses observed (*introductory papers 1 and 2*).

- To investigate if there are any differences among fish and mammalian cell lines in susceptibility/sensitivity to these ENMs according to the species in which the cell line was isolated, or if in fact ENMs elicit different mechanism of toxicity (if any) at the cellular level across species (*introductory papers 1 and 2*).

- To determine to what extent the cytotoxicity (if any) is caused by ions formed from NP dissolution or directly by NPs (*introductory papers 1 and 2*).

- To assess if the combined effect of the ZnONPs and CuNPs under investigation can differ greatly from that produced by each individual ENM alone (*introductory paper 3*).

The results from these initial studies allowed us to characterise the cytotoxic potential of the ENMs and provided information needed to design studies to gain insights into the general mechanisms of toxic action of ZnO NPs and CuNPs. These further studies constitute the main backbone of this thesis and they were performed to meet the specific objectives presented below.

1. To determine the real role of oxidative stress as a causative agent of cytotoxicity of ENMs.

   As indicated in the introduction, it has been generally accepted as a paradigm that oxidative stress is the main cause of the toxicity of ENMs. However, oxidative stress could be actually a consequence of the toxicity of ENM instead of its cause. In order to clarify this issue cell lines were exposed to CuNPs that induce the production of ROS in cells and toxicity was assessed under normal conditions and after reducing the level of ROS by activating the anti-oxidative stress defense mechanisms of the cells (*research paper 1*).

2. To compare the sensitivity among different fish cell lines against NP insult and to investigate if cell lines were representative of cells maintained in primary culture.

   One of the main challenges we have found when designing studies to investigate the cytotoxic potential of ENMs was in selecting the most appropriate cell line as a test system. To address this issue we have performed a study to assess the sensitivity of different cells and cell lines maintainted in culture. In *research paper 2* all available cell lines, as well as freshly isolated (primary) liver cells from rainbow trout were used as test systems. AgNPs were chosen in this case, as according to current environmental risk assessments based on modelling predicted environmental concentrations and taking into account species sensitivity distributions AgNPs present one of the highest risks compared to other NPs, particularly in surface waters.

3. To gain information about the relevance of ENM toxicity data obtained *in vitro* with respect to an *in vivo* situation.

   Although there is an important amount of data concenring the toxicity of ENMs obtained from *in vitro* approaches, information from *in vivo* studies dealing with ENMs is still scarce. It is therefore essential to carry out some experiments *in vivo* to evaluate the applicability of *in vitro* data to more realistic *in vivo* situations. Taking this into consideration, we performed an *in vivo* study to determine the toxicity and bioaccumulation of zinc derived from ZnONPs to rainbow trout fed ZnO NPs (according to the OECD TG 305) (*research paper 3*). The ZnO NPs used here were the same as those used in previous studies when testing cytotoxicty towards cell lines, and therefore allowed a direct comparison of results obtained using *in vitro* and *in vivo* approaches.

4. To study to what extent modifications in the surface coatings of NPs govern physico-chemical properties and biocompatibility and if the use of different coatings could aid in developing safer ENMs.

   The surface of NPs can be functionalized in different ways in order to fine tune their physico-chemical or toxicological properties. In this way, we could develop safer ENMs, but also increase the safety of products containing NPs and ensure their low health and environmental impact (by increasing safety in the manufacturing processes, the use of

the products, and their recycling or spillage). Taking this into account, we have monitored *in vitro* differences in the toxicity of AuNPs capped with an array of peptide- biphenyls (*research paper 4*).

CHAPTER 3

An introductory investigation into the cytotoxicity of ZnO NPs and CuNPs in both mammalian and piscine liver cell lines and their potential potentiating effect when co-exposed.

Chapter 3 is an introductory chapter constituted by three articles that served to generate initial results and to propose a general objective for the thesis. This chapter presents an investigation into the cytotoxicity of ZnO NPs (*introductory paper 1*) and CuNPs (*introductory paper 2*) towards both mammalian and piscine liver cell lines and their potential potentiating effect when co-exposed (*introductory paper 3*). Copper and zinc are two essential trace metals required by all living organisms in ionic form and in low concentrations to carry out important biological processes necessary for survival. Cellular zinc and copper homeostasis is achieved through tight regulation. The biological activity of ZnO NPs and CuNPs and whether nanoparticles of zinc and copper are regulated with such efficiency has yet to be determined. Liver cell lines were chosen as experimental models/test systems for ZnO NP and CuNP hazard assessment as the liver is an important detoxification site and site for NP distribution once in systemic circulation. A range of NPs with different primary particle sizes and shapes were used, in order to ascertain if any causal relationship exists between such physico-chemical properties and biological responses. Exposures using reference ions, in the form of copper metal salts or released zinc ion fractions, were performed, in parallel, to investigate the contribution of metal ions released form NPs to effects. Often in toxicology investigating hazard to the environment and human health form separate and distinct lines of investigation however within this thesis the use of both mammalian and piscine liver cell lines provided an opportunity to investigate potential differences in susceptibility across species. Important species-specific differences in susceptibility exist, that appear to be dictated by the role of dissolved ion in NP cytotoxicity and the distinct differences in sensitivity for the different mammalian and piscine cells. Also the potential hazard associated with the co-occurrence of both ZnO NPs and CuNPs in the environment and the potentiation effects associated with co-exposure was highlighted (*introductory paper 3*).

Introductory paper 1: Comparative cytotoxicity induced by bulk and nanoparticulated ZnO in the fish and human hepatoma cell lines PLHC-1 and Hep G2.

Introductoy paper 2: Species-specific toxicity of copper nanoparticles among mammalian and piscine cell line.

Introductory paper 3: The potentiation effect makes the difference: Non-toxic concentrations of ZnO nanoparticles enhance Cu nanoparticle toxicity *in vitro.*

Nanotoxicology, August 2013; 7(5):935–952
© 2013 Informa UK, Ltd.
ISSN: 1743-5390 print / 1743-5404 online
DOI: 10.3109/17435390.2012.676098

informa
healthcare

Comparative cytotoxicity induced by bulk and nanoparticulated ZnO in the fish and human hepatoma cell lines PLHC-1 and Hep G2

Maria Luisa Fernández-Cruz[1], Tobias Lammel[1], Mona Connolly[1], Estefania Conde[2], Ana Isabel Barrado[2], Sylvain Derick[3], Yolanda Perez[4], Marta Fernandez[2], Christophe Furger[3] & Jose Maria Navas[1]

[1]*Instituto Nacional de Investigación y Tecnología Agraria y Alimentaria (INIA), Departamento de Medio Ambiente, Carretera de la Coruña Km 7 Madrid, Spain,* [2]*CIEMAT Avda. Complutense 40, Madrid, Spain,* [3]*NOVALEADS, 10 avenue de l'Europe, Ramonville, France and* [4]*Departamento de Química Inorgánica y Analítica (E.S.C.E.T.), Universidad Rey Juan Carlos, Móstoles, Madrid, Spain*

Abstract

The increasing presence of ZnO nanoparticles (NPs) in consumer products may be having a dramatic impact in aquatic environments. The evaluation of ZnO NP toxicity represents a great challenge. This study aimed at evaluating the cytotoxic effect of micro- and nanosized ZnO in a fish and a mammalian hepatoma cell line. A detailed characterisation of the particles in exposure media showed that ZnO NPs formed large aggregates. ZnO cytotoxicity was evaluated with a battery of *in vitro* assays including LUCS, a new approach based on DNA alteration measurements. In fish cells, ZnO NP aggregates contributed substantially to the cytotoxic effects whereas toxicity in the human cells appeared to be mainly produced by the dissolved fraction. ROS production did not contribute to the observed cytotoxicity. This work also showed that measuring concentrations of NPs is essential to understand the mechanisms underlying their toxicity.

Keywords: *In vitro*, nanoparticles, oxidative stress, ICP-MS, LUCS

Introduction

Metal oxide nanoparticles (NPs) are receiving increasing attention in material sciences and nanotechnology-based industries for a large variety of applications leading to the increasing presence of NPs in commercial products. Among NPs, ZnO is frequently used in personal care products such as sunscreens, ceramics, rubber processing, waste water treatment and even as a fungicide (Wong et al. 2010). Due to the increasing volumes of consumer products containing ZnO NPs, the probability that they will enter the environment and particularly the aquatic ecosystems is heightened. It has been suggested that the use of TiO_2, ZnO and Fe_2O_3 in sunscreens represents, by itself, a potential discharge of 250 tonnes/year into the marine environment (Wong et al. 2010). Moreover, the potential risks towards occupational workers and consumers are not clearly established. Thus, it is urgent to assess NPs real ecotoxicological impacts. While there has been an increasing number of research articles focused on the impact of these NPs on human health, there is less knowledge on their potential toxicity to wildlife and aquatic biota.

The biological activity of NPs is dependent on many factors, some of which include size, shape and surface properties that are different from their larger sized counterparts. These physico-chemical properties will influence the NPs tendency to agglomerate or aggregate, as well as their ability to adsorb onto surfaces. NPs behaviour will not only be a function of the surface chemistry of the NPs, but will also be affected by the composition of NPs, the presence of any coatings, the dissolution of material from the particle surface into solution and the presence of any soluble substances in the preparation. A particular concern for metal-based NPs, regarding their small size and large surface area, is the dissolution of metal ions from the surface of the particle. This process may eventually lead to the complete dissolution of the particle leaving only metal ions remaining in solution (Handy et al. 2008a; Dhawan & Sharma 2010). For all these reasons, NPs require much more extensive particle characterisation than other chemical compounds. Incomplete characterisation will hinder attempts to find a correlation between various biological effects and particle properties, leading to the misinterpretation of results (Handy et al. 2008a). These properties have to be considered carefully, thus appropriate analytical techniques must be applied to measure size, shape and state of aggregation or agglomeration and to quantify the real NP concentration.

In vitro assays based on cell lines are employed as one of the first steps for understanding the toxicity and mechanism of action of a compound. ZnO NPs have been shown to produce *in vitro* cytotoxic, genotoxic, inflammatory and oxidative stress

Correspondence: María Luisa Fernández Cruz, Instituto Nacional de Investigación y Tecnología Agraria y Alimentaria (INIA), Departamento de Medio Ambiente, Carretera de la Coruña Km 7.5, E-28040 Madrid, Spain. Tel: +34 91 3478788. Fax: +34 91 3474008. E-mail: fcruz@inia.es

(Received 13 December 2011; accepted 10 March 2012)

responses in different mammalian cells (Xia et al. 2008; Yang et al. 2009; Huang et al. 2010; Song et al. 2010; De Berardis et al. 2010; Yuan et al. 2010; Hsiao & Huang 2011; Pujalté et al. 2011). Studies in mammalian cell lines also attributed the toxicity of ZnO NPs, at least in part, to their solubility, the latter leading to Zn ion formations (Xia et al. 2008; De Berardis et al. 2010; Song et al. 2010). It was also proposed that the production of reactive oxygen species (ROS) is the main factor responsible for the observed cytotoxicity (Xia et al. 2008; Sharma et al. 2009; De Berardis et al. 2010; Huang et al. 2010; Song et al. 2010). The contribution of the size and shape to the mammalian cytotoxicity of different ZnO NPs has also been reported, but different conclusions have been reached (Lin et al. 2009; Deng et al. 2009; Hsiao & Huang 2011).

A limited amount of studies have been carried out in aquatic organisms and fish cell lines. It has been reported that ZnO NPs are toxic to isolated trout hepatocytes (Scown et al. 2010), *Daphnia magna* (Adams et al. 2006, Heinlaan et al. 2008) as well as zebrafish embryos and larvae (Zhu et al. 2008, 2009). Acute toxicity studies of ZnO NPs and bulk ZnO in different marine organisms such as algae, crustaceans and medaka fish, concluded that the toxicity of ZnO NPs could be mainly attributed to dissolved Zn ions (Franklin et al. 2007; Wong et al. 2010). However, other authors ascribed the toxicity also to ZnO NPs and the bulk ZnO themselves. This was the case in adult zebrafish (Xiong et al. 2011), *Daphnia magna* (Wiench et al. 2009), the bacterium *Vibrio fischeri*, the branchipod *Thamnocephalus platyurus* (Heinlaan et al. 2008) and the microalga *Pseudokirchneriella subcapitata* (Aruoja et al. 2009).

The main objective of this work was to determine if ZnO NPs exhibit differences in their mechanisms of toxic action in a fish and in a mammalian hepatoma cell line. These cell lines have been selected because the liver plays an essential role in detoxification processes and because this organ has been identified as one of the major target organs of NPs, particularly in fish (Handy et al. 2008a, b; Kashiwada 2006). For fish, the PLHC-1 cell line has been chosen because culture conditions (30°C, 5% CO_2 atmosphere) are closer to those of most of the mammalian hepatoma cell lines used up until now in cytotoxicity studies. A battery of cytotoxicity assays covering different mechanisms of toxicity has been employed. In order to better characterise these mechanisms, the observed toxicity was related to the size and the shape of the NPs and with the possible effect of the fraction corresponding to the dissolved NPs. In addition to the usual cytotoxicity assays, LUCS (light-up cell signal), a new fluorescent method addressing DNA alteration status has been used. This method relies on the light-induced fluorescence intensity enhancement of a DNA binding dye. It has been recently applied with success in cytotoxicity studies using Hep G2 cells (Derick et al. 2009). This assay was utilised in this work in order to acquire new cytotoxicity information at the DNA level, as well as to evaluate its sensitivity and possible application in fish cells.

Methods

Particles

Three commercial ZnO NPs differing in size were tested and compared with the bulk material. The ZnO fine powder <5 μm (99.9% purity), ZnO nanopowder <100 nm and ZnO nanopowder 6% aluminium-doped <50 nm (BET) (97% purity) (referred to in this work as ZnO, nZnO-1 and nZnO-2, respectively) were purchased from Sigma-Aldrich (Madrid, Spain). The ZnO nanopowder 20–30 nm (BET) (referred to as nZnO-3) was from Tecnan (Madrid, Spain).

Chemicals

Ultraglutamine 1 (200 mM), L-glutamine (200 mM), fetal bovine serum (FBS), penicillin and streptomycin (P/S) (10 000 U/ml/10 mg/ml), non-essential amino acids 100X (NEAA), cell culture EMEM (Eagle's Minimum Essential Medium) and α-MEM (Alpha-Minimum Essential Medium) media were purchased from Lonza (Barcelona, Spain). 4,5-Dimethylthiazoyl-(2-yl)-2,5-diphenyltetrazolium bromide (MTT), neutral red (NR) solution (0.33%), 6-carboxy-2′7′-dichlorofluorescein diacetate (DCFH-DA), chloramine-T trihydrate, 2-propanol and glacial acetic acid were from Sigma-Aldrich (Madrid, Spain). Ethanol was from Panreac (Barcelona, Spain). EvaTOX kit (Evakit; 5 mM solution in DMSO) for LUCS assay was from Novaleads (Ramonville, France). Trace analysis grade nitric acid 65% (Scharlau, Madrid, Spain) was purified by sub-boiling distillation in a Milestone Duopur (Milestone Srl., Italy).

Cell culture

The fish and the human hepatocellular carcinoma cell lines, PLHC-1 (derived from topminnow fish (*Poeciliopsis lucida*) and Hep G2 were obtained from the American Type Culture Collection (ATTC) (Manassas, VA, USA). The PLHC-1 cell line was cultured in α-MEM supplemented with 5% FBS, 1% P/S and 1% L-glutamine. Hep G2 cells were cultured in EMEM supplemented with 10% FBS, 1% P/S, 1% ultraglutamine and 1% NEAA. PLHC-1 and Hep G2 cells were grown in a 5% CO_2 atmosphere at 30 and 37°C, respectively.

Exposure to NPs

PLHC-1 and Hep G2 cells were seeded in 96-well plates (Costar, VWR, Spain) at an initial cell number of 5×10^4 and 7.5×10^4 cells/well, respectively. After 24 h, the cells were exposed to serial dilutions (0.78–100 μg/ml) of the four different ZnO particles. Particle suspensions of 100 μg/ml were prepared in serum-free medium and vortexed for 1 min just before applying them to the cells. In order to investigate to which extent the dissolved ZnO fraction, in which Zn ions released from the particle surface may be present, contributes to the cytotoxicity, both cell lines were exposed to the supernatants of centrifuged ZnO particle suspensions. These supernatants were prepared with a 100 μg/ml particle suspension in serum-free medium and incubated for 24 h at 30 or 37°C to reproduce the time of exposure to the NPs. Subsequently, these suspensions were centrifuged for 10 min at 1000 *g* (Orto Alresa, Lince R). After the 24-h exposure period, the treated cells were analysed for cytotoxic effects by means of different assays.

Particle characterisation

Particle characterisation was performed on all the particle suspensions obtained after serial half dilutions of the initial

one (100 μg/ml) in serum-free culture medium. This particle characterisation was also performed in the supernatants obtained after centrifugation of the 100 μg/ml particle suspensions. To select the speed of centrifugation, initially 100 μg/ml particle suspensions were centrifuged at 1000 *g* for 10 min or at 180 000 *g* for 1 h, after a 24-h incubation period at 30 or 37°C (to imitate exposure conditions). After centrifugation Zn concentration was measured in supernatants by means of inductively coupled plasma mass spectrometry (ICP-MS). Since differences in the Zn concentration between both supernatants were negligible, in order to facilitate the experimental work, cell exposure and further detailed characterisation were performed only in the supernatant obtained after centrifugation at 1000 *g*.

Transmission electron microscopy

Transmission electron microscopy (TEM) was performed to morphologically characterise the particle suspensions. Both pristine particles as well as particles incubated in serum-free culture media for 24 h at 30 or 37°C were analysed. The samples were prepared by dropping aliquots of the particle suspensions onto carbon-coated copper grids and leaving the solvent to evaporate. Subsequently, the samples were analysed using a JEOL 2100 HT (JEOL Ltd., Japan) operated at an accelerating voltage of 200 kV with integrated energy dispersive X-ray (EDX) spectroscopy (Oxford Inca). The size of the particles (ferret diameter) in the TEM micrographs was measured using the image processing and analysis software ImageJ (National Institutes of Health, USA).

Dynamic light scattering

Dynamic light scattering (DLS) was used as a method to determine the hydrodynamic size of the particles in solution, using a Zetasizer Nano-ZS (Malvern Instruments Ltd., UK). Measurements were performed in the suspensions and in the supernatants at different concentrations directly after preparation and after 24 h incubation at 30 or 37°C. Medium without particles was used as a control and to record any background signals that may arise from medium components. Before preparing the samples the instrument temperature was set to 37°C for EMEM preparations and to 30°C for α-MEM preparations. Four independent measurements were taken with each measurement consisting of six runs, each of 20 s duration.

Inductively coupled plasma mass spectrometry

The Zn concentration in each well of the treated plates, the original particle suspension (100 μg/ml) and the supernatants obtained after centrifugation of the original particle suspension at 1000 *g* for 10 min or after ultracentrifugation at 180 000 *g* for 2 h was determined by means of an ICP-MS Thermo X-Series II (Thermo Scientific, Bremen, Germany) equipped with a quadrupole mass analyser and an electron multiplier detector. A Meinhard nebuliser with Scott (Ryton) spray chamber (Elemental Scientific Inc., Omaha, NE, USA) and a peristaltic pump were used for sample introduction. The optimisation of plasma-operating parameters and mass calibration were performed with a certified multi-element solution Tune A (As, Ba, Be, Bi, Ce, Co, In, Li, Ni, Pb and U) supplied by Analytika Ltd. (Czech Republic). The sample solutions were quantified by external calibration; three isotopes of Zn (^{64}Zn, ^{66}Zn and ^{68}Zn) were used for measurements to discard the presence of isobaric interferences. An internal standard (Ga) was used in order to check instrumental stability and to correct potential effects of the matrix on the signal. Calibration standard solutions of Zn and internal standard solution of Ga were prepared daily with the appropriate dilution of 1000 mg/l Zn in 2% (v/v) and 1000 mg/l Ga in 2% (v/v) stock standard solutions (Alfa Aesar, Ward Hill, MA, USA), respectively. High purity water (>18 MΩ cm^{-1}) obtained from a Milli-Q Element A10 Century (Millipore Ibérica, Spain) was used. For the analysis of Zn concentrations in the exposed cells, the medium from each well was transferred into polypropylene flasks. The wells were washed twice with nitric acid 2% (v/v) for the digestion of the cells and for collecting the remaining ZnO NPs present in the wells. The rinses were added to the respective sample media, and the latter filled up with nitric acid 2% (v/v) to a final volume of 10 ml. Just before ICP-MS analysis, samples were ultrasonicated for 5 min. Limits of detection (LOD) and limits of quantification (LOQ) were calculated as being 3 and 10 times the standard deviation of the blank, respectively, considering as such the Hep G2 and PLHC-1 media, prepared as the samples. The LOD for the three isotopes ranged from 0.21 to 0.32 μg/l and the LOQ from 0.71 to 1.1 μg/l. The instrumental response was linear over the calibration range used for the measurements from 0.1 to 100 μg/l, with a relative standard deviation (RSD) <2%.

Cytotoxicity assays

MTT and NRU assay

The MTT assay evaluates the mitochondrial activity and was performed according to the method of Mosmann (1983) based on the enzymatic conversion of the MTT tetrazolium salts to formazan crystals. The neutral red uptake (NRU) assay was used to determine the lysosomal membrane integrity following Borenfreund and Puerner (1985). After exposure, the medium was replaced with 100 μl of phenol red-free MEM containing MTT (0.5 mg/ml) or NR (0.1 mg/ml). The plates were incubated for 2 or 4 h, respectively. The formazan crystals were dissolved by adding isopropanol whereas the retained NR dye was extracted with 1% glacial acetic acid in 50% ethanol. The absorbance was measured at 570 or 550 nm (MTT or NRU, respectively) using a microplate reader (Genios, TECAN, Männedorf, CH). Results were expressed as percentage of the control.

Lactate dehydrogenase leakage

The leakage of the cytoplasm enzyme lactate dehydrogenase (LDH) is commonly used as an indicator of xenobiotic-related damage of the cellular membrane. After the 24-h exposure period, the LDH activity in the medium and the cells was measured following the method of Liu et al. (2010). Culture medium was removed and stored at 4°C for immediate analysis. Cells were washed with phosphate buffered saline (PBS) and the plates frozen by immersion in liquid nitrogen and stored at -20°C for 1 h to obtain a cell lysate. LDH enzymatic activity was measured in both the culture

medium and the cell lysate. In this method, LDH catalyses the reduction of pyruvate to lactate with simultaneous oxidation of NADH to NAD^+. The rate of NADH decrease, which is directly proportional to LDH activity, was measured at 340 nm in a temperature-controlled microplate reader set to 30 or 37°C for PLHC-1 or Hep G2, respectively. The quantity of LDH leaked from the cells into the culture medium was expressed as percentage of the total amount of LDH determined in the medium and cell samples.

LUCS assay

Nucleic acid alterations were measured by means of the Novaleads LUCS assay, according to Derick et al. (2009). EvaTOX quantifies alterations in DNA organisation. This assay is based on the LUCS process patented method (PCT/EP2009/050235). Briefly, cells are exposed to a proprietary fluorescent DNA dye solution (EvaKit). Under normal (untreated) conditions, the combined effect of LED-based light (10 s) on a DNA-bound fluorescent dye leads to a fluorescent intensity enhancement, an effect that is lost after DNA damage response. For this assay, the cells were seeded into black 96-well plates (Greiner, Dismalab, Madrid, Spain). After 24 h of exposure, the medium was removed and replaced by 100 µl of a 4 µM EvaKit stain solution (prepared in serum-free culture medium). Subsequently, the PLHC-1 and Hep G2 cells were incubated at the corresponding temperature for 20 or 30 min, respectively. A first reading of the fluorescence (R1) was done at 485 nm excitation and 535 nm emissions in a microplate reader. The cells were illuminated for 10 s at 470 nm with a LED-based device (LED-based aDAPter, Novaleads, Ramonville, Fr). The fluorescence was then read over 20 min at 1 min intervals. For data analysis, the values obtained at the time at which no further increase in fluorescence occurred (usually after 10–15 min; R2) were divided by the respective values obtained in R1. In order to compare data, R2/R1 ratios were normalised between 0 and 100% considering the control R2/R1 value as 100% and R2/R1 = 1 as 0%.

ROS assay

Intracellular ROS production was determined by using the dichlorofluorescein (DCF) assay (Wang & Joseph 1999). DCFH-DA (100 µM) in phenol red and serum-free EMEM medium was added after the incubation period and maintained during 30 min at 37°C in the dark. Chloramine-T, an effective inducer of oxidative stress, was used as a positive control, with cells being exposed to concentrations in the range of 0.3–10 mM for 24 h. Fluorescence was measured at 485 nm excitation and 535 nm emission at 37°C using a microplate reader. Fluorescence readings were taken every 15 min for 60 min with the plates being incubated at 37°C with 5% CO_2 between measurements. Oxidative stress was expressed as the percentage increase in fluorescence over a 60-min period.

Statistical analyses

Data are represented as mean ± standard error of the mean (SEM) of three to five independent experiments (in each experiment, each concentration was applied by triplicate in the culture plates). Significant differences among treatments were determined by one-way repeated measures analysis of variance (RMANOVA, $p < 0.05$). Previously, normality of the distribution was checked by means of the Shapiro-Wilk test and homoscedasticity by means of Bartlett's test. Means of treatments were contrasted with respect to the control group using Dunnett's test. For pairwise comparisons, a Student's t-test was used. The statistics were performed with the GraphPad Prism version 4.00 program for Windows (GraphPad Software, San Diego, CA, USA). The effective concentration for 50% maximal response (EC_{50}) was calculated using Sigma Plot version 8.0 (Jandel Scientific, San Rafael, CA, USA). The estimation of the concentration–response function and the calculation of the IC_{50} (concentration causing a 50% of inhibition with respect to the controls) were done by fitting the assay results to a regression model equation for a sigmoid curve:

$$y = \max / (1 + e^{-[(x - IC_{50})/b]}) + \min$$

where max is the maximal response observed, b is the slope of the curve and min the minimal response.

Results

Characterisation of ZnO particles

TEM analysis

TEM analysis was performed to determine the morphology and the size distribution of ZnO particles. TEM micrographs of pristine ZnO particles are shown in Figure 1. Different morphologies were observed in the four different ZnO particle powders used. Three types: polyhedral, rod-like and near-spherical-shaped particles, all showing clear edges and corners coexisted in each sample. Figure 2 shows the size distribution calculated from TEM images. The average length of the ZnO particles was 165, 51, 35 and 33 nm, for ZnO, nZnO-1, nZnO-2 and nZnO-3, respectively, with a median of 120, 40, 27 and 29 nm and a 75% percentile of 181, 66, 44 and 41 nm. ZnO particles incubated in EMEM and α-MEM media were also analysed by TEM (Figure 3). The TEM images were acquired after 24 h of incubation of the 100 µg/ml suspensions in media at 37 or 30°C (Figure 3). Some differences with respect to the pristine particles (Figure 1) were observed. In general, the particles in the culture media presented considerably more aggregation and were more irregular in shape with corners less defined than the primary powder. The EDX spectrum of the ZnO particle suspended in the EMEM medium clearly indicated the presence of calcium together with zinc (Figure 4).

Dynamic light scattering

DLS was used to measure the hydrodynamic sizes of the particles in the culture media used for exposures. Measurements could only be obtained for concentrations ≥25 µg/ml. In addition, size distribution profiles were similar at each concentration. Therefore, only the hydrodynamic sizes and size distribution widths of the highest concentration (100 µg/ml) are presented in Table I. According to the instrument

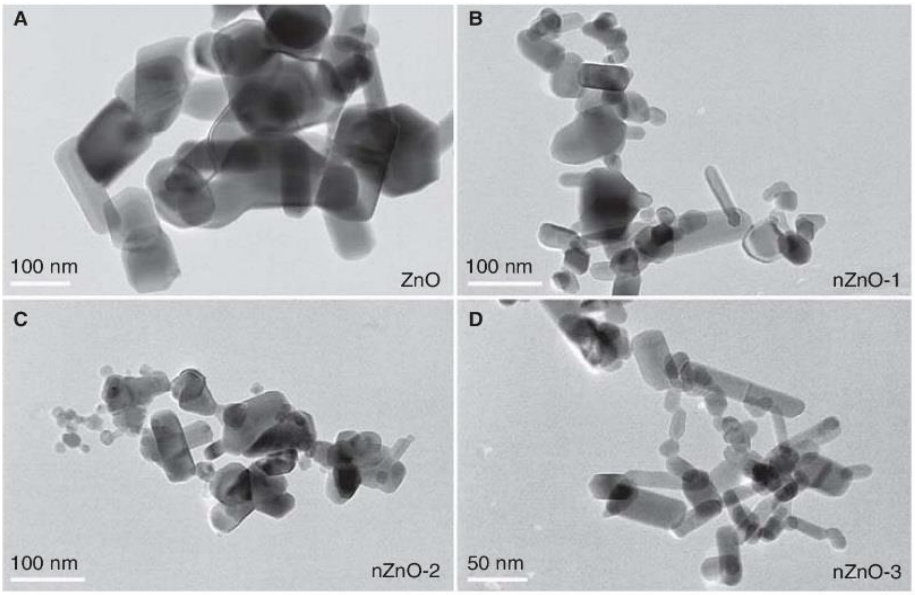

Figure 1. TEM micrographs of the pristine forms of the four different ZnO particles: A) ZnO, B) nZnO-1, C) nZnO-2 and D) nZnO-3. Scale bars are 100 nm for A, B and C, and 50 nm for D.

specifications, not all particles present in the suspensions were in the detectable size range. The instrument reported samples of very high polydispersity and aggregates with diameters >6000 nm present. At the position selected, the maximum signal within the instrument range of detection was 80%. In general, the hydrodynamic size of each ZnO suspension was similar in both media at time zero but differed after 24 h incubation (Table I). At time zero, ZnO, nZnO-1 and nZnO-2 formed aggregates of similar sizes ranging from 1134 to 1421 nm and from 957 to 1978 nm in EMEM and α-MEM medium, respectively. However, nZnO-3 formed larger size aggregates (2978 and 2504 nm in both media, respectively) in spite of the very similar size of the nZnO-2 and nZnO-3 pristine forms. After 24 h, similar

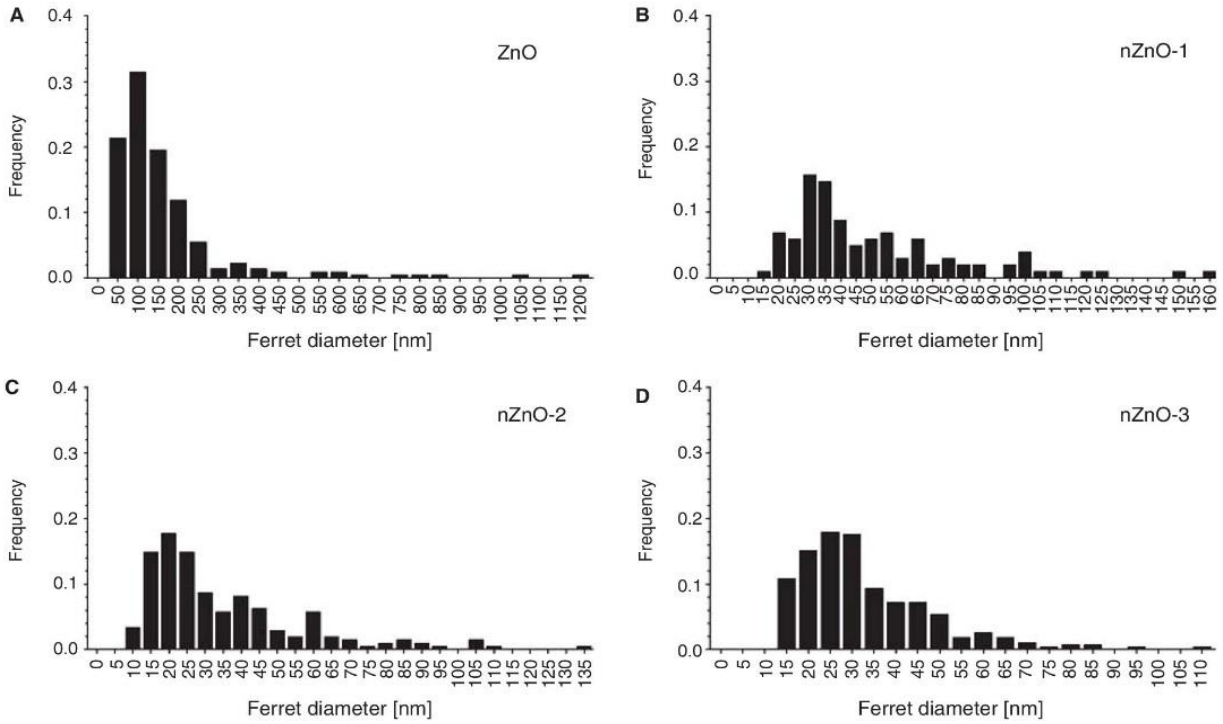

Figure 2. Frequency distribution of particle sizes (ferret diameter) derived from TEM micrographs of the pristine ZnO particles.

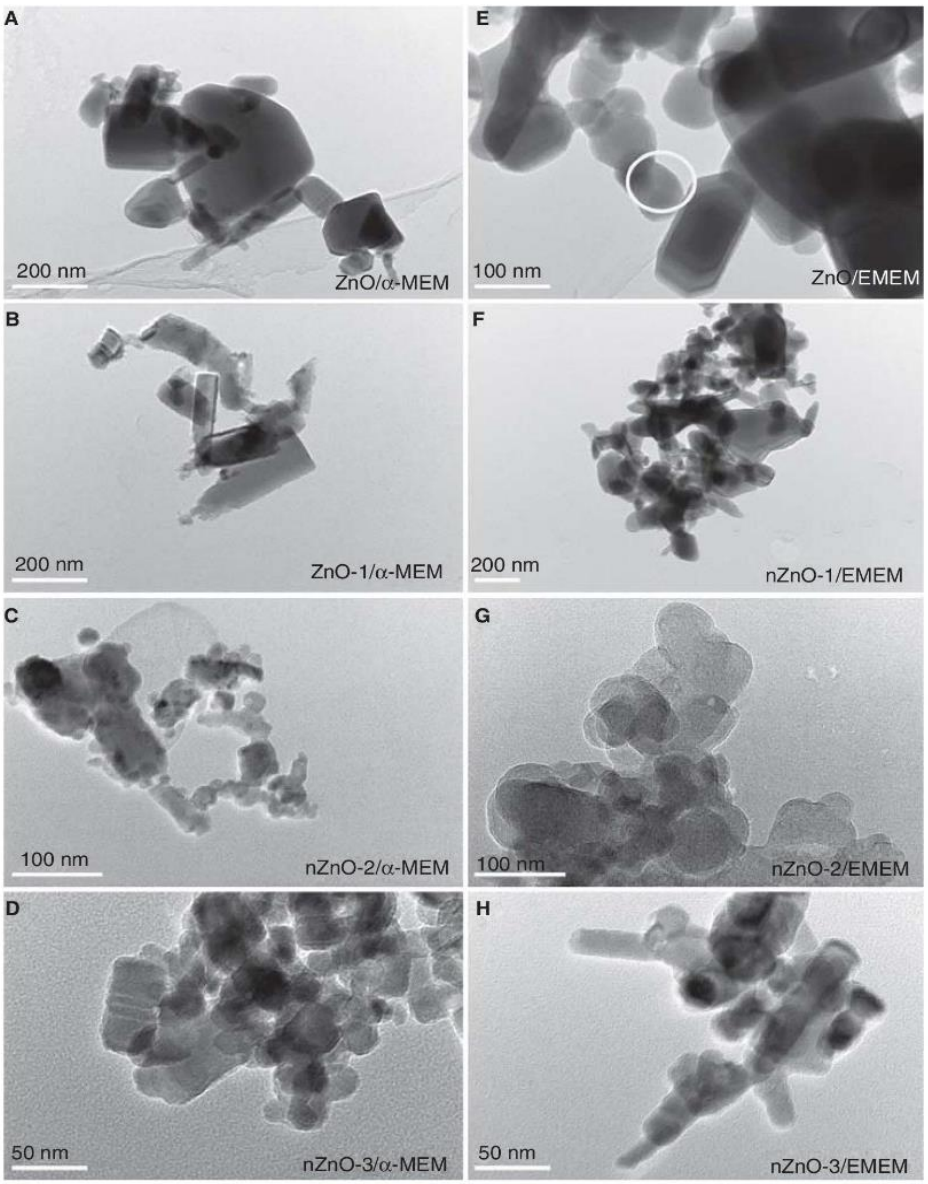

Figure 3. TEM images of ZnO particles after incubation in different cell culture media: A, B, C and D) ZnO, nZnO-1, nZnO-2 and nZnO-3 incubated for 24 h in α-MEM, respectively; E, F, G and H) ZnO, nZnO-1, nZnO-2 and nZnO-3 incubated for 24 h in EMEM, respectively. The white circle in E) marks the particle, which was exemplarily analysed by EDX spectroscopy (cf. Figure 4). The scale bars are 200 nm for A, B and F, 100 nm for C, E and G and 50 nm for D and H.

sizes as in time zero could be observed for ZnO and nZnO-1 particles in both media. The nZnO-2 NPs were found to form aggregates of similar size than nZnO-3 NPs in the EMEM medium (2166 and 2481 nm, respectively). However, these later NPs behaved very differently in the α-MEM after 24 h. The nZnO-2 NPs seemed to de-agglomerate (from 1978 to 1091 nm), whereas the nZnO-3 increased considerably its size (from 2504 to 3753 nm). Since the apparatus indicated a very high degree of polydispersity, smaller particles could be present but their signal may be overshadowed by these bigger ones.

DLS measurements were also taken from the supernatants of the particle suspensions following centrifugation at 1000 *g* for 10 min. After centrifugation, a pellet of particles was evident on visual inspection. Control media were also incubated for 24 h and centrifuged as described. According to the DLS profiles of the control media (Figure 5), some medium components could be detected at very low intensity. These profiles could be used as background controls to distinguish medium components from possible ZnO particles remaining in solution after centrifugation. Both medium controls presented different distribution profiles that differed from the particle profiles in the supernatants indicating the presence of NPs. In α-MEM medium, a particle population from approximately 30–100 nm could be measured for the four NPs that didn't appear in the medium control. In the EMEM, this clear difference could not be observed, except for the nZnO-3 NPs that exhibited a population between

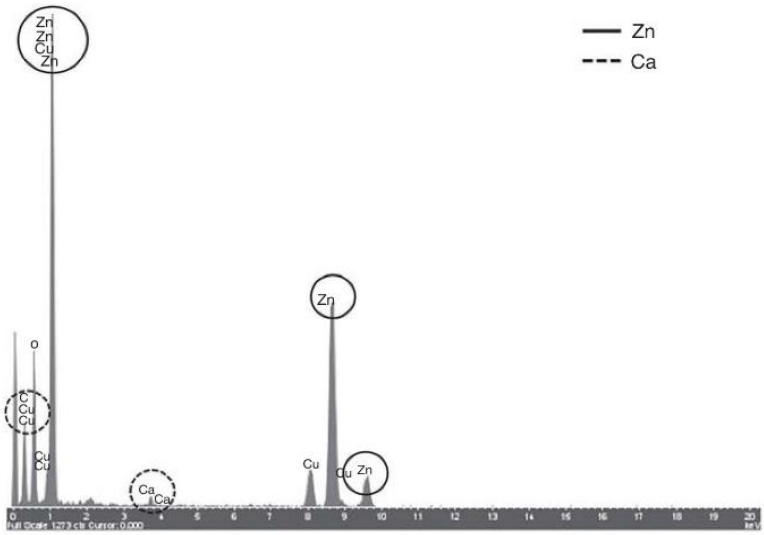

Figure 4. EDX spectrum of the surface of a ZnO particle incubated for 24 h in cell culture medium (cf. Figure 3E, white circle).

50 and 200 nm and for the bulk ZnO with a population down around 20–50 nm, albeit, at relatively low intensity (Figure 5).

ICP-MS analysis

Total concentration of ZnO in the 100 μg/ml particle stock suspensions ranged between 108 and 128 μg/ml (Table II). The different 100 μg/ml suspensions were maintained for 24 h at 30 or 37°C to reproduce the conditions of exposure and then centrifuged at 1000 *g* or ultracentrifuged at 180 000 *g*. Total ZnO concentrations were measured in both supernatants and were found to be similar, indicating that even ultracentrifugation is not able to remove the dissolved fraction further. The concentration of Zn measured by ICP-MS in the supernatants and expressed as ZnO ranged from 3.8 to 7.7 μg/ml in the Hep G2 medium (EMEM) and from 28.3 to 43.3 μg/ml in the PLHC-1 medium (α-MEM) (Table II). To compare the toxic effects produced by the dissolved NPs and/or Zn ions, cells were exposed to serial half dilutions of only the centrifuged (1000 *g*) stock solutions. The concentrations of ZnO, as prepared by serial dilutions of the stock suspensions and subsequently used to treat the cells, are presented in Table II. These concentrations were obtained by measuring the level of Zn present in each well after the assay was performed in both cell lines (Hep G2 (two repetitions) and in PLHC-1). The concentrations in both assays were similar and reproducible data were obtained between replicates. The mean and standard deviation of these measurements are presented in Table II. The most limiting step is achieving a concentration of 100 μg/ml in the highest exposure concentration well. We measured a loss of 50–60% of the concentration probably due to the rapid sedimentation of the non-dissolved NPs and aggregates during the 100 μl aliquot collection from the stock suspension for cell exposure. Just after shaking the stock suspensions, we could observe a deposition of non-dissolved NPs beginning after 20 s and a clear precipitate in less than 60 s. Despite a twofold serial dilution, the real concentrations were 1.7–3.7 times lower than expected. The lower nominal doses (0.39, 0.78 and 1.56 μg/ml) exhibited a similar measured concentration as those from the controls. Zn is an important element required by many cellular enzymes and it is present in relatively high background levels in cells and tissues. Since ICP-MS cannot distinguish between ZnO and any other form of Zn present in the cells, therefore, lower ZnO particle doses may be hidden by background levels of Zn in cells. The concentrations indicated in Table II for the cell lines exposed to half dilutions of the centrifuged stock solutions are estimates from those measured in the supernatants of the stock solution. The results indicate that PLHC-1 cells have been exposed to very similar concentrations before and after centrifugation, contrary to Hep G2 cell line, which have been exposed to lower concentrations after centrifugation.

Cytotoxicity of ZnO particles to PLHC-1 and Hep G2 cell lines

MTT reduction

The cytotoxicity of the suspensions of the four ZnO particles as well as of the supernatants obtained after centrifugation is shown in Figure 6. Real concentrations are indicated in brackets together with nominal concentrations in the text and in the figures. In the PLHC-1 cell line, the bulk materials and the three NP suspensions provoked a significant reduction of cell viability (Figure 6A) with non-observed effect concentrations (NOECs) values of 25 (7), 12.5 (5), 6.25 (2) and 12.5 (6) μg/ml for ZnO, nZnO-1, nZnO-2 and nZnO-3, respectively. In the case of the Hep G2 cells (Figure 6B), NOEC values of 25 (7), 25 (9), 25 (7) and 12.5 (6) μg/ml were obtained after exposure to the suspensions for ZnO, nZnO-1, nZnO-2 and nZnO-3, respectively. Thus, differences between PLHC-1 and Hep G2 cells in NOEC values appeared only for nZnO-1 and nZnO-2. In addition, no significant differences in cytotoxicity between both cells lines were observed except at the highest concentration (Figure 6A and 6B). At this concentration, loss in cell viability detected in Hep G2 was

Table I. Particle sizes (nm) measured by DLS in EMEM and α-MEM media immediately after preparation and 24 h after incubation under the respective culture conditions.

	EMEM medium (Hep G2 cells)				α-MEM medium (PLHC-1 cells)			
	0 h		24 h		0 h		24 h	
Sample	Size	Width	Size	Width	Size	Width	Size	Width
ZnO	1421	263	1564	216	957	179	859	93
nZnO-1	1134	183	1060	141	1123	141	1280	123
nZnO-2	1260	204	2166	317	1978	420	1091	139
nZnO-3	2978	746	2481	527	2504	920	3753	877

α-MEM, alpha-Minimum Essential Medium; DLS, dynamic light scattering; EMEM, Eagle's Minimum Essential Medium.

much stronger than in PLHC-1 cells, with significantly lower values in the bulk material, nZnO-1 and nZnO-3. PLHC-1 cells exposed to the supernatants also exhibited significant decreases in cell viability resulting in NOEC values of 25 (10), 12.5 (5), 25 (10), and 25 (10) μg/ml for ZnO, nZnO-1, nZnO-2 and nZnO-3, respectively (Figure 6C). In the case of Hep G2 cells treated with the supernatants, the NOEC values detected were 50 (3), 50(3), 100 (6) and 100 (6) μg/ml for ZnO, nZnO-1, nZnO-2 and nZnO-3, respectively (Figure 6D). Taking into account the NOEC values obtained for measured concentrations (Table III), PLHC-1 cells were similarly sensitive to the suspensions and the dissolved fraction, except for nZnO-2 where the non-dissolved fraction (aggregates and suspended NPs)

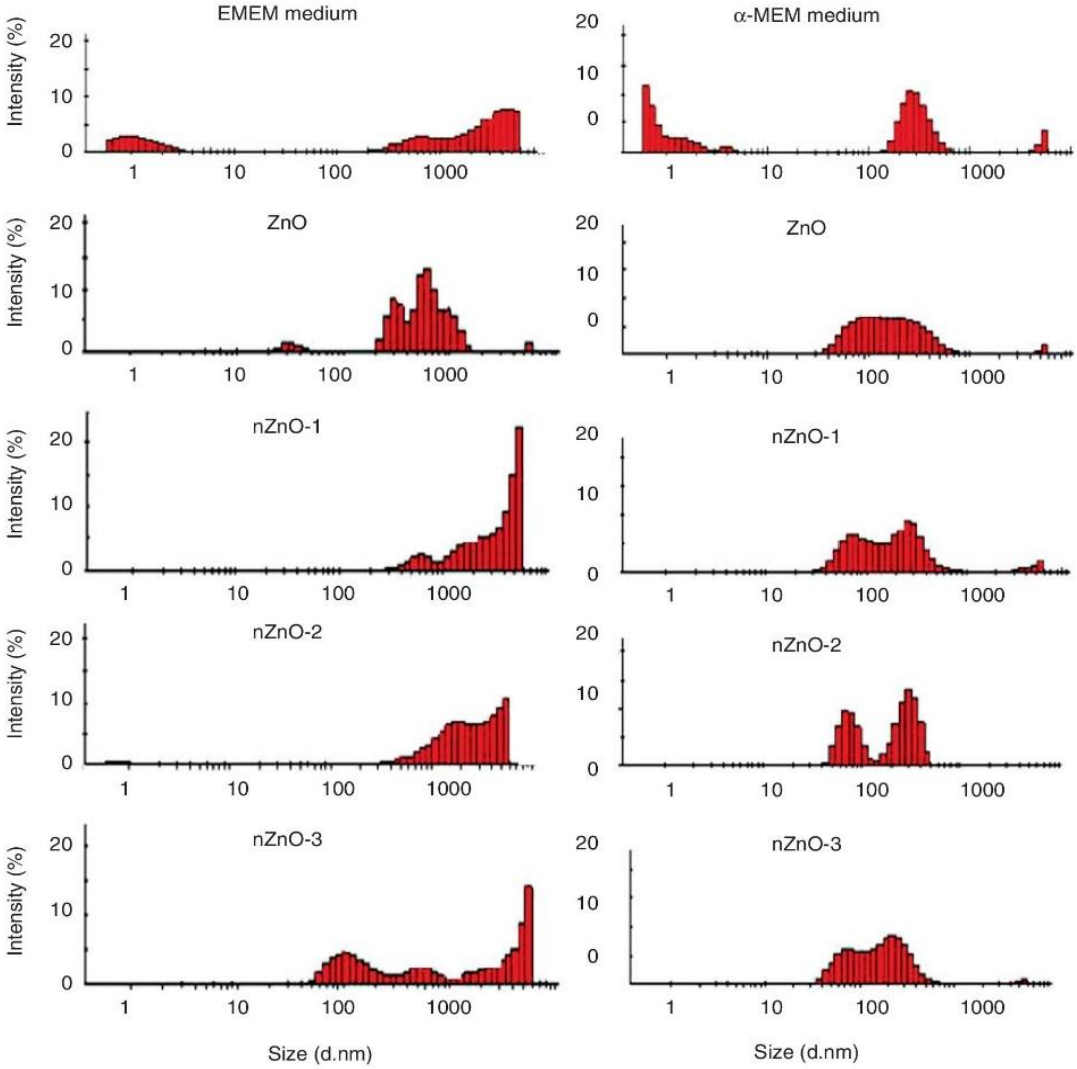

Figure 5. DLS size distribution profile of the supernatants obtained by centrifugation (1000 rpm for 10 min) of the ZnO particle suspensions prepared in EMEM and α-MEM medium (100 μg/ml) incubated for 24 h at 37 and 30°C, respectively.

Table II. Measured concentrations of total Zn by ICP-MS expressed as μg ZnO per ml.

		ZnO concentration in freshly prepared medium PS (100 μg/ml) and in the Sup after centrifugation at 1000 or 180 000 *g*									
		PS	1000 *g* Sup	180 000 *g* Sup				PS	1000 *g* Sup	180 000 *g* Sup	
ZnO	EMEM	113	4.5	4.1	ZnO	α-MEM		128	30.1	28.3	
nZnO-1	EMEM	108	4.3	3.8	nZnO-1	α-MEM		124	40.7	35.6	
nZnO-2	EMEM	109	7.2	7.1	nZnO-2	α-MEM		125	40.8	35.7	
nZnO-3	EMEM	110	7.7	7.3	nZnO-3	α-MEM		123	43.3	41.7	
Mean ± SD		110 ± 2.2	5.9 ± 1.8*	5.6 ± 1.9	Mean ± SD			125 ± 2.2	38.7 ± 5.9*	35.3 ± 5.5	
		ZnO concentration in Hep G2 and PLHC-1 cells treated with PS									
Nominal concentrations[1]		Control	0.39	0.78	1.56	3.12	6.25	12.5	25	50	100
		Measured concentrations[2]									
ZnO	Mean ± SD	0.87 ± 0.46	1.4 ± 0.16	0.67 ± 0.17	1.1 ± 0.06	1.4 ± 0.13	1.8 ± 0.54	3.3 ± 0.74	6.8 ± 0.52	13.7 ± 0.87	40.5 ± 0.66
	Dil. factor[4]		0.48	1.6	1.2	1.3	1.8	2.0	2.0	2.9	
nZnO-1	Mean ± SD	0.94 ± 0.43	1.3 ± 1.2	0.77 ± 0.12	1.4 ± 0.07	1.7 ± 0.26	2.6 ± 0.81	4.7 ± 0.91	9.4 ± 0.55	18.5 ± 0.76	50.9 ± 5.5
	Dil. factor[4]		0.59	1.9	1.2	1.5	1.8	2.0	1.9	2.7	
nZnO-2	Mean ± SD	0.62 ± 0.26	0.53 ± 0.42	0.64 ± 0.42	0.63 ± 0.37	1.3 ± 0.51	2.2 ± 0.50	3.5 ± 0.90	7.6 ± 3.07	15.6 ± 7.1	58.4 ± 18.7
	Dil. factor[4]		1.2	0.98	2.1	1.7	1.6	2.1	2.1	3.7	
nZnO-3	Mean ± SD	0.78 ± 0.23	0.63 ± 0.51	0.84 ± 0.63	0.95 ± 0.55	1.8 ± 0.91	3.7 ± 0.71	6.3 ± 2.1	12.2 ± 4.9	24.9 ± 10.5	51.7 ± 16.1
	Dil. factor[4]		1.3	1.1	1.9	2.0	1.7	1.9	2.0	2.1	
		Estimated ZnO concentration in the Sup obtained alter 1000 *g* centrifugation and used for the exposure in Hep G2 and PLHC-1 cells[3]									
α-MEM					0.60	1.2	2.4	4.8	9.7	19.4	38.7 ± 5.9*
EMEM								0.74	1.5	3.0	5.9 ± 1.8*

[1]Nominal concentrations are the expected one for treatments; [2]The mean of the measured concentrations are an average of two replicates in Hep G2 cell lines and one measurement in PLHC-1 cell lines; [3]The concentrations indicated for the cell lines exposed to half dilutions of the centrifuged stock solution are estimates from the mean* of the four measured concentrations corresponding to each particle after 1000 *g* centrifugation; [4]Dilution factor.
α-MEM, alpha-Minimum Essential Medium; EMEM, Eagle's Minimum Essential Medium; PS, particle suspensions; Sup, supernatants.

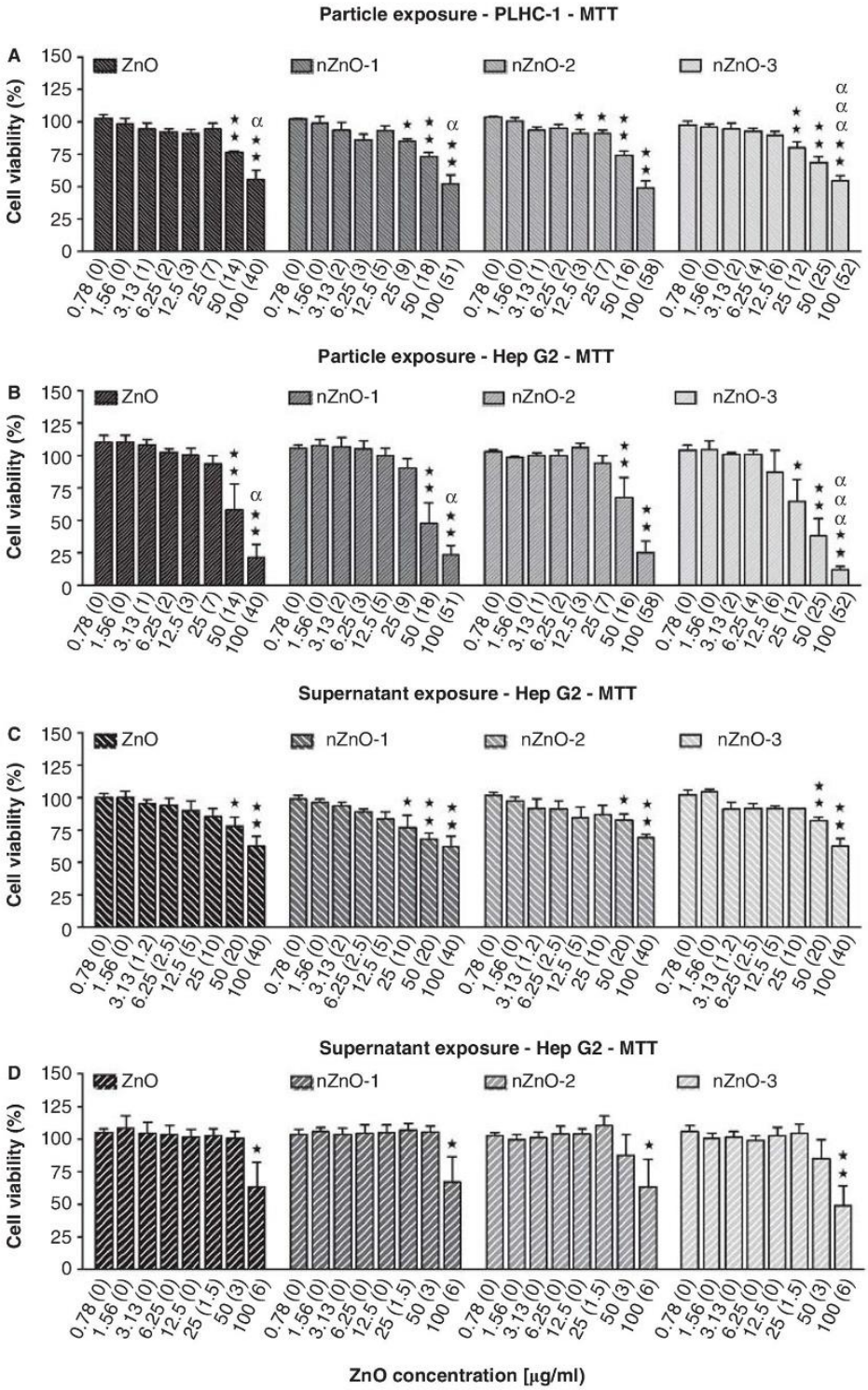

Figure 6. Cytotoxicity of ZnO particles suspensions and supernatants in PLHC-1 and Hep G2 cells after 24 h exposure as determined with the MTT assay. Results are expressed as percentage of viability compared with the control. The measured concentration that corresponds to each nominal concentration is shown in brackets. A value of zero indicates that the measured concentrations were similar to those measured in control media without ZnO. Data are represented as the mean ± SEM of at least three independent experiments. Different symbols are used to indicate statistical significant differences (simple, double and triple superscripts correspond to $p < 0.05$, $p < 0.01$ and $p < 0.001$, respectively), asterisks (*) are used to indicate differences with respect to the controls, α is used to indicate differences between both cell lines.

Table III. NOECs obtained for PS and Sup exposures of fish and mammalian cell lines by means of the different cytotoxicity assays taking into account measured concentrations.

	MTT				NR				LDH				LUCS	
	PLHC-1		Hep G2		PLHC-1		Hep G2		PLHC-1		Hep G2		PLHC-1	HEP G2
NOEC (μg/ml)	PS	Sup	PS	Sup	PS	Sup	PS	Sup	PS	Sup	PS	Sup	PS	PS
ZnO	7	10	7	3	7	>40	14	3	7	20	3	3	14	7
nZnO-1	5	5	9	3	18	>40	18	3	9	20	9	3	18	9
nZnO-2	2	10	7	3	7	>40	7	3	7	10	16	3	16	7
nZnO-3	6	10	6	3	12	>40	12	3	12	10	12	3	25	6

LDH, lactate dehydrogenase leakage assay; LUCS, light-up cell signal assay; MTT, 4,5-dimethylthiazoyl-(2-yl)-2,5-diphenyltetrazolium bromide reduction assay; NOEC, non-observed effect concentration; NR, neutral red uptake assay; PS, particle suspension; Sup, supernatant.

produced a higher toxicity. By contrast, Hep G2 cells were more responsive to the dissolved ions and NPs (Table III). The relatively weak toxic effect that the studied ZnO particles provoked in the PLHC-1 cells did not allow a full dose–response curve to be established and the calculation of respective IC_{50} values (Table IV). Thus, the different-sized ZnO particles could not be ranked in terms of their absolute toxicity towards PLHC-1. This analysis could be performed with the results following exposures in the Hep G2 cell line. The IC_{50} calculated with the nominal concentrations for ZnO, nZnO-1, nZnO-2 and nZnO-3 were 53.6, 48.9, 65.2 and 34.0 μg/ml, respectively, showing the nZnO-3 as the most toxic (Table IV). However, the IC_{50} for real concentrations were 16.3, 18.6, 26.6 and 16.7 μg/ml, showing a similar toxicity for the NPs and the bulk material (Table IV).

NR uptake

The cytotoxicity after exposure of the fish and the human hepatoma cell lines to the suspended and centrifuged ZnO suspensions measured by the NR assay is shown in Figure 7. The NOECs for the PLHC-1 cells exposed to the particle suspensions were 25 (7), 50 (18), 25(7) and 25(12) μg/ml for ZnO, nZnO-1, nZnO-2 and nZnO-3, respectively (Figure 7A). For Hep G2, the NOECs were 50 (14), 50 (18), 25 (7) and 25 (12) μg/ml for ZnO, nZnO-1, nZnO-2 and nZnO-3, respectively (Figure 7B). When the NOECs obtained with the real concentrations were compared (Table III), the PLHC-1 cells appeared to be more sensitive to the bulk material (7 μg/ml) than the Hep G2 cell line (14 μg/ml) but the NOECs in both cell lines were identical for the three NPs (18, 7 and 12 μg/ml for nZnO-1, nZnO-2 and nZnO-3, respectively). However, the toxic responses caused by nZnO-2 and nZnO-3 were significantly stronger in Hep G2 than in PLHC-1 cells at the highest doses (Figure 7A, 7B). The exposure to the supernatants didn't produce any cytotoxicity in the PLHC-1 cell line (Figure 7C). The NOECs after exposure of Hep G2 cells to the supernatants were 50 (3) μg/ml for the four particles (Figure 7D). Taking into account the NOEC values obtained for measured concentrations (Table III), PLHC-1 cells were more sensitive to the suspensions than to the dissolved fraction whereas the Hep G2 cells were more sensitive to the dissolved fraction. No IC_{50} values could be calculated (Table IV).

LDH leakage

The membrane cytotoxic effects of the particle suspensions and supernatants are shown in Figure 8. The NOECs of PLHC-1 cells after NP suspension exposure were 25 (7), 25 (9), 25 (7) and 25 (12) μg/ml and with the supernatants exposure, 50 (20), 50 (20), 25 (10) and 25 (10) μg/ml for ZnO, nZnO-1, nZnO-2 and nZnO-3, respectively (Figure 8A, 8C). For the Hep G2 cell line, the NOECs after NP suspension exposure were 12.5 (3), 25 (9), 50 (16) and 25 (12) μg/ml for ZnO, nZnO-1, nZnO-2 and nZnO-3, respectively and with the supernatants 50 (3) μg/ml for the four particles (Figure 8B, 8D). Taking into account the NOECs from real concentrations, the fish cell line was more sensitive to the ZnO and nZnO-1 suspensions than to the corresponding supernatants. However, these cells responded similarly to the suspensions and supernatants of the nZnO-2 and nZnO-3 NPs (Table III). By contrast, the human cell line was more sensitive to the supernatants of the NPs, but showed similar sensitivity to the bulk material suspension and to the corresponding supernatant (Table III). As shown in Figure 8, treatment of PLHC-1 and Hep G2 cells with the different ZnO particles resulted in a dose-dependent LDH leakage. Table IV summarises the respective IC_{50} calculated from the full dose–response curve obtained. Using nominal concentrations, the values for PLHC-1 were 43.3, 39.5, 50.5 and

Table IV. IC_{50} calculated from the cytotoxicity assay results after PS exposure of fish and mammalian cell lines.

	MTT				NR				LDH				LUCS			
	PLHC-1		Hep G2		PLHC-1		Hep G2		PLHC-1		Hep G2		PLHC-1		Hep G2	
IC_{50} (μg/ml)	Nominal	Real	Nominal	Real	Nominal	Real	Nominal	Real	Nominal	Real	Nominal	Real	Nominal	Real	Nominal	Real
ZnO	nd	nd	53.6	16.3	nd	nd	nd	nd	43.3	12.2	26.4	7.6	93.0	36.3	44.1	12.1
nZnO-1	nd	nd	48.9	18.6	nd	nd	nd	nd	39.5	14.1	42.0	15.2	52.9	18.9	27.7	9.8
nZnO-2	nd	nd	65.2	26.6	nd	nd	nd	nd	50.5	16.2	60.1	18.4	94.9	55.8	33.7	9.7
nZnO-3	nd	nd	34.0	16.7	nd	nd	nd	nd	43.7	21.7	48.8	24.3	93.7	48.5	17.4	8.3

LDH, lactate dehydrogenase leakage assay; LUCS, light-up cell signal assay; MTT, 4,5-dimethylthiazoyl-(2-yl)-2,5-diphenyltetrazolium bromide reduction assay; nd, IC_{50} could not be calculated; NR, neutral red uptake assay; PS, particle suspension.

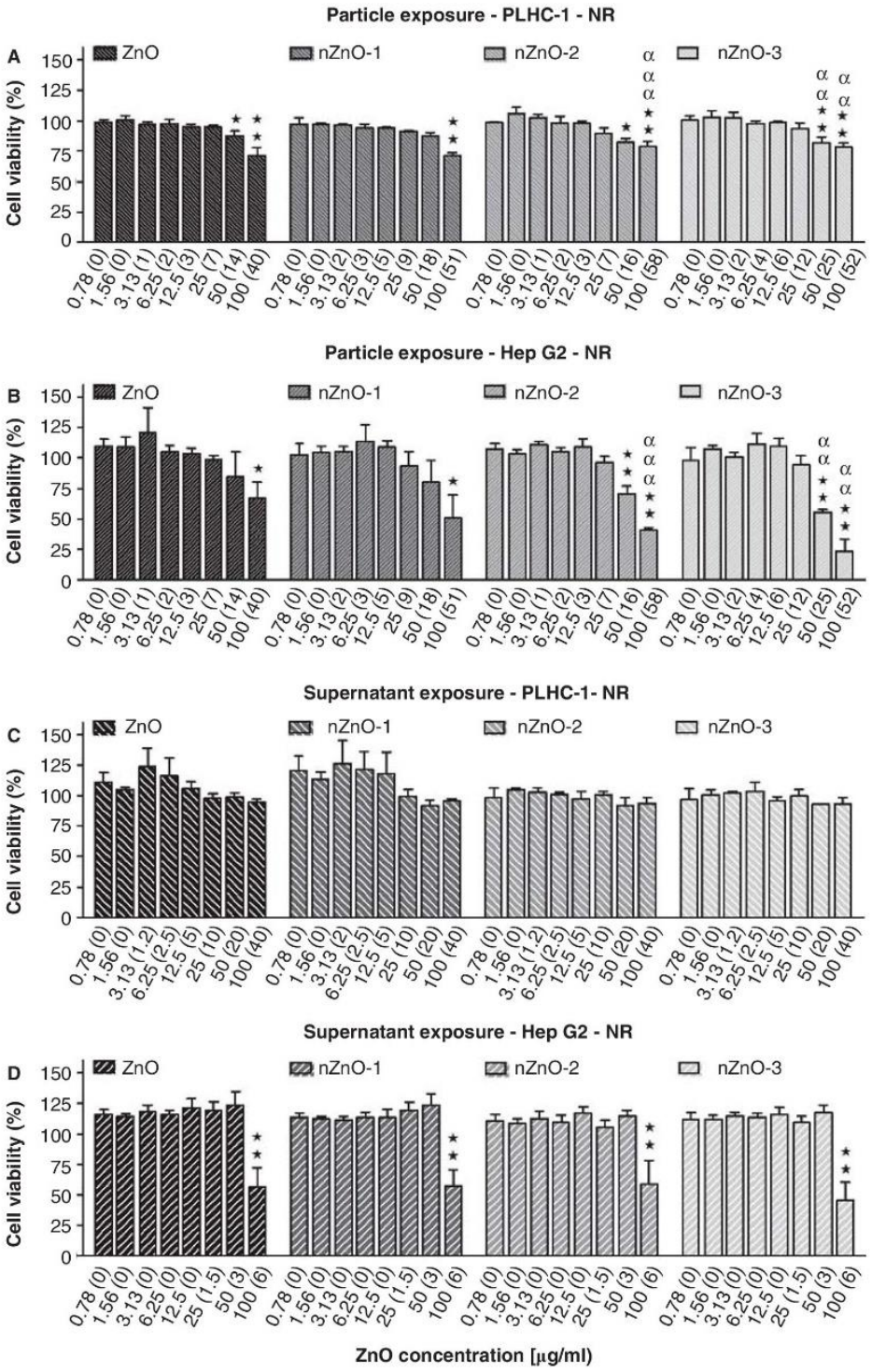

Figure 7. Effects of ZnO particles suspensions and supernatants on PLHC-1 and Hep G2 cell viability after 24 h exposure as determined with the NR assay. Results are expressed as the percentage of viability compared with the control. The measured concentrations corresponding to the nominal concentrations are shown in brackets. A value of zero indicates that the measured concentration was similar to the one measured in control media without ZnO. Data are represented as mean ± SEM of at least three independent experiments. Different symbols are used to indicate statistical significant differences (simple, double and triple superscripts correspond to $p < 0.05$, $p < 0.01$ and $p < 0.001$, respectively), asterisks (*) are used to indicate differences with respect to the controls, α for differences between particle suspension exposures for each concentration in both cell lines.

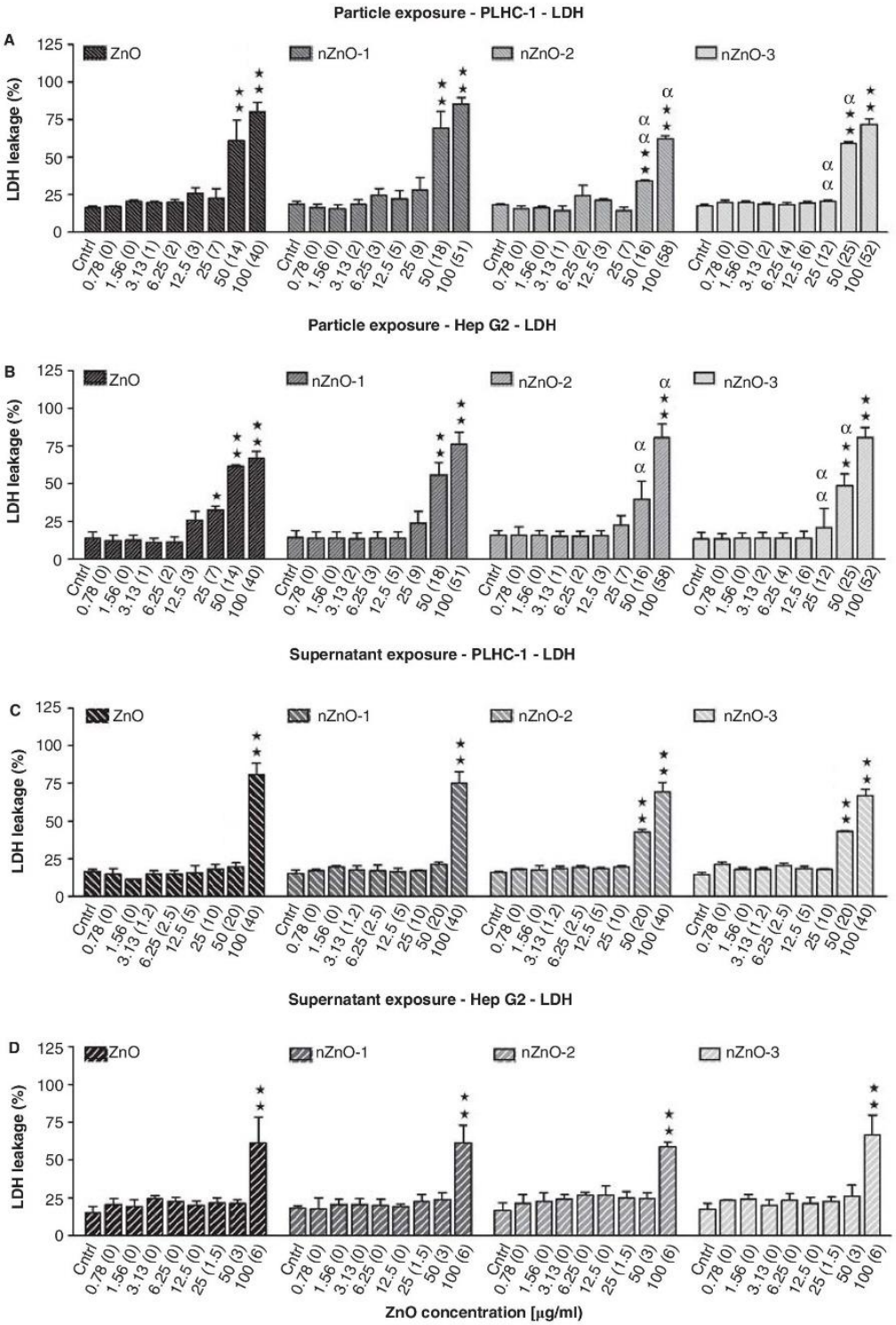

[leakage expressed as percent of control after exposure to serial dilutions of ZnO particle suspensions or supernatants in Hep G2 cells. The measured concentration that corresponds to each nominal concentration is represented in brackets. ro indicates that the measured concentration was similar to the one measured in control media without ZnO. Columns mean ± SEM of at least three independent experiments. Different symbols are used to indicate statistical significant imple and double superscripts correspond to $p < 0.05$ and $p < 0.01$, respectively). Asterisks (*) were used to indicate ith respect to the controls, α for differences between particle suspension exposures for each concentration in both cell lines.

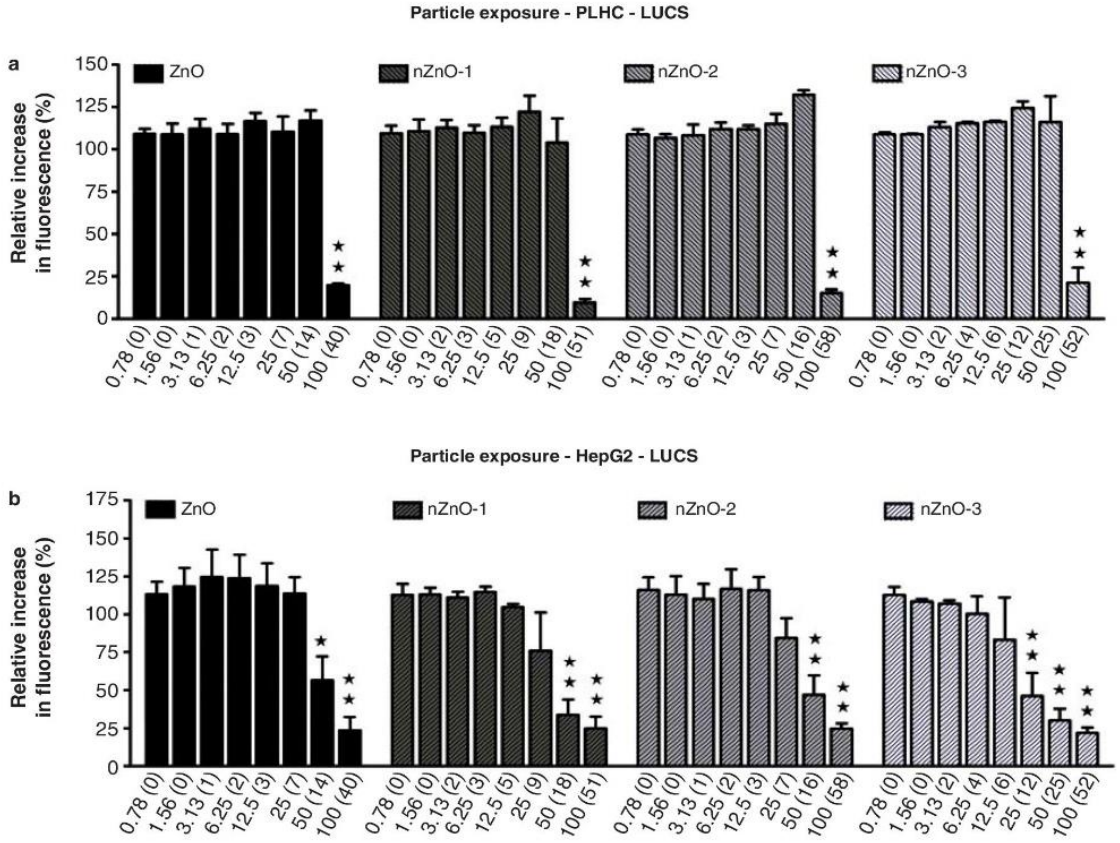

Figure 9. Effects of ZnO particles suspensions on PLHC-1 and Hep G2 cells after a 24 h exposure as determined with the new LUCS assay, measuring DNA alteration level. The data are presented as the mean ± SEM of at least three independent experiments. Significant differences with respect to the controls are indicated with asterisks ($^{*}p < 0.05$ or $^{**}p < 0.01$).

43.7 μg/ml for ZnO, nZnO-1, nZnO-2 and nZnO-3, respectively, whereas the values were 12.2, 14.1, 16.2 and 21.7 μg/ml when calculated using real concentrations. The IC_{50} values corresponding to the Hep G2 cell line were 26.4, 42.0, 60.1 and 48.8 μg/ml with nominal concentrations and 7.6, 15.2, 18.4 and 24.3 μg/ml with real concentrations. When considering the measured concentrations to which cells have been exposed, both cell lines showed similar sensitivity to the four NPs.

LUCS assay

ZnO, nZnO-1, nZnO-2 and nZnO-3 showed no cytotoxicity over a wide range of nominal concentrations (0.78–50 μg/ml) in PLHC-1 cells (Figure 9A). However, at the highest nominal concentration (100 μg/ml) a sharp drop, to values lower than 20%, could be observed for all particles. The ZnO particles were more toxic to the Hep G2 cell line (Figure 9B) with NOEC nominal values of 25 μg/ml for ZnO, nZnO-1 and nZnO-2 and lower for nZnO-3, and NOEC real values of 7, 9, 7 and 6 μg/ml, respectively. The IC_{50} values of the particles in these cell lines are shown in Table IV. For the fish cells, IC_{50} values were of 93.0 (36.3), 52.9 (18.9), 94.9 (55.8) and 93.7 (48.5) μg/ml for ZnO, nZnO-1, nZnO-2 and nZnO-3, respectively. The IC_{50} for the mammalian cells were 44.1 (12.1), 27.7 (9.8), 33.7 (9.7) and 17.4 (8.3) μg/ml for ZnO, nZnO-1, nZnO-2 and nZnO-3, respectively (Table IV). With respect to the signal dynamics of the LUCS assay, the increase in fluorescence induced by photo-bleaching of the sample was found to be lower in the PLHC-1 cells than in the Hep G2 cells. While in Hep G2 cells R2/R1 ratios of

Table V. Sensitivity of the LUCS assay with respect to other cytotoxicity assays as calculated from the IC_{50} ratios.

	PLHC-1		Hep G2		Hep G2	
	LDH/LUCS		MTT/LUCS		LDH/LUCS	
IC_{50} ratios (μg/ml)	Nominal	Real	Nominal	Real	Nominal	Real
ZnO	0.5	0.3	1.2	1.3	0.6	0.6
nZnO-1	0.7	0.5	1.8	1.9	1.5	1.6
nZnO-2	0.5	0.3	1.9	2.7	1.8	1.9
nZnO-3	0.5	0.4	1.9	2.0	2.8	2.9

LDH, lactate dehydrogenase leakage assay; LUCS, light-up cell signal assay; MTT, 4,5-dimethylthiazoyl-(2-yl)-2,5-diphenyltetrazolium bromide reduction assay.

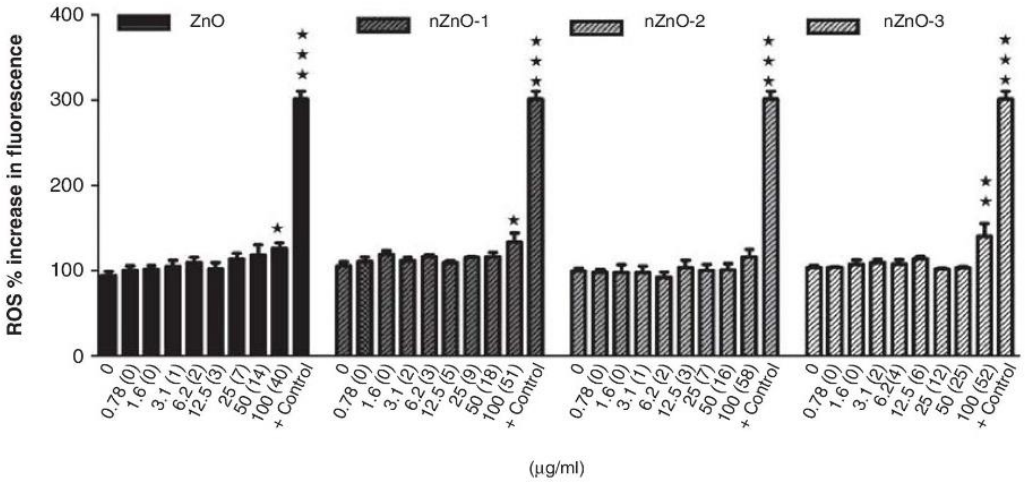

Figure 10. Effects of ZnO particles suspensions on ROS generation by PLHC-1 after a 24 h exposure period. The data are represented as the mean ± SEM of at least three independent experiments. Asterisks (*) represent significant differences ($*p < 0.05$;$**p < 0.01$) with respect to the controls. Chloramine-T (567.5 µg/ml) was used as positive control (+ control).

1.7–2.0 were reached, ratios in the assays carried out with PLHC-1 cells were usually between 1.4 and 1.7. Taking into account that if the R2/R1 ratios range from 1.0 (maximal intoxication) to 2.0 (control), a deviation of 0.1 in the R2/R1 ratio corresponds to a change of 10% in the resulting cytotoxicity values, whereas in the R2/R1 ratios only range from 1.0 to 1.7, this deviation corresponds to a change of 14% in the resulting cytotoxicity values. The sensitivity of the different assays with respect to the LUCS was evaluated by calculating the IC_{50} ratios (Table V). In the Hep G2 cell line, the LUCS assay was found to be more sensitive than the MTT and LDH assays to the effects of the three NPs. However, in the fish cell line it was less sensitive than the LDH assay. If considering the concentrations not producing any effect in the fish cell lines, NOECs were higher with the LUCS assay than with the MTT, NR and LDH assays (Table III). However, the LUCS assay was found to be as sensitive as the MTT assay and together more sensitive than NR and LDH assays in the human cell line.

ROS production

The NPs nZnO-1 and nZnO-3 and the bulk material increased the production of ROS at the highest concentration used, 100 µg/ml, in the PLHC-1 cell line (Figure 10). However, these particles were not able to induce ROS production in the Hep G2 cell line (data not shown).

Discussion

One of the most critical steps in *in vitro* as well as in *in vivo* toxicity studies is the preparation of the NPs suspensions in the media or vehicles used. Previous studies described different methods to prepare NP suspension, either directly in the medium by simple agitation (Yang et al. 2009; Yuan et al. 2010), by using bath sonication (Huang et al. 2010; Pujalté et al. 2011; Song et al. 2010; Xiong et al. 2011) or by probe sonication (De Berardis et al. 2010; Hsiao & Huang 2011). Other authors used filtration (De Berardis et al. 2010) or stabilisers such as bovine serum albumin (Tantra et al. 2010; Yang et al. 2009) to eliminate possible aggregates. However, it was recently recommended to not discard these aggregates since their implication in the toxicity of ZnO NPs in embryo and adult zebrafish (Bai et al. 2010; Xiong et al. 2011) and human cells (Yuan et al. 2010) was demonstrated. Moreover, it has been described that ZnO NPs rapidly form very large aggregates in deionised water (2990, 6820 and 11,400 nm for concentrations of 1, 10 and 100 µg/ml) that are not easy to disperse after stirring, sonication, using pH variations or even following ultrasonic disruption (Tso et al. 2010). Degen and Kosec (2000) found that ZnO suspensions could not be electrostatically stabilised because the colloidal ZnO particles were transformed into Zn ions. Because of these previously reported results, and to have a more realistic scenario of exposure conditions in an aquatic environment, in this work the cells were exposed to freshly prepared NPs suspensions dispersed by vortex for 1 min in culture medium without FBS.

To understand the mechanisms underlying the toxicity of NPs, it is essential to perform a thorough characterisation of their physico-chemical properties (Handy et al. 2008a). In this study, the size and shape of the pristine forms were observed by means of TEM. Since polyhedral, rod-like and near-spherical shapes were found to coexist in all tested particle forms, no definite conclusion could be made concerning the implication of the shape on toxicity. The average dimensions in length of the pristine NPs measured by TEM were 165, 51, 35 and 33 nm, for ZnO, nZnO-1, nZnO-2 and nZnO-3, respectively. Thus, the expected microsized particle was very close to the nanometre range and the NPs nZnO-2 and nZnO-3 presented similar average diameters. TEM images of ZnO particles suspended in medium showed aggregated particles with irregular shapes and corners less defined. Such changes in morphology have been explained by other authors as being attributed to the adsorbance of the ions present in the medium on the surface of ZnO particles (Fang et al. 2010; Yin 2010). Particle size was also studied by

DLS in the medium suspensions freshly prepared and after 24 h incubation. Large sizes (>1 μm) could be measured by DLS at time 0 and 24 h. It was observed that the two smallest particles nZnO-2 and nZnO-3 tend to form the largest aggregates in suspension and have a wider size distribution profile (>2000 nm). The size of the aggregates of the bulk material was lower (859–1564 nm). Our results are in close agreement with those of Wong et al. (2010) who found that ZnO NPs tended to form aggregates in the micrometre range (2.3 ± 1.6 μm) in seawater, and these aggregates were bigger than those formed by its bulk counterpart (1.7 ± 1.2 μm). By contrast, in the study of Hsiao and Huang (2011) using ZnO NPs prepared by a precipitation or a solvothermal method, the smaller-sized ZnO particles aggregated to smaller secondary sizes than the larger NPs. These differences may be attributed to the regular shapes of the NPs used in this last study. Others authors also found that ZnO NPs formed large aggregates in algal media (Franklin et al. 2007) or in serum-free RPMI 1640 culture medium (Pujalté et al. 2011).

As ZnO particles are not soluble in aqueous solutions and form large aggregates on preparation, homogenous dispersions with reproducible concentrations are probably difficult to obtain. It is, therefore, essential to have an accurate estimation of the real concentrations used in the experiments. This has been achieved successfully in this work by means of ICP-MS. To our knowledge, this is the first time that this measurement has been carried out in cytotoxicity studies. From our findings the real concentrations for ZnO NPs were between 1.7 and 3.8 times lower than the nominal ones. Such findings must be kept in mind when interpreting toxicity results.

It has also been described that ZnO NPs can dissolve into Zn ions. The solubility of ZnO in aqueous media can show important variations ranging from 3.7 μg/ml in seawater (Wong et al. 2010) to 5.8–7.2 μg/ml in serum-free DMEM medium (Hsiao et al. 2011) and up to 15 μg/ml in complete DMEM medium (Xia et al. 2008). Since some Zn ions can be released into solution from the particles, a controversy surrounding the role played by these ions on toxicity remains. In the present study this was investigated. ZnO suspensions with the highest concentration used in the exposure experiments (100 μg/ml) were incubated for 24 h at the corresponding temperatures allowing the dissolution of Zn in media. Thereafter, suspensions were centrifuged at two different speeds and the concentration of Zn in the supernatants was measured by ICP-MS. Concentrations obtained in both supernatants were similar, indicating that the lowest speed was enough to remove any particle in suspension, and therefore this speed was selected for further experiments. After centrifugation, ZnO concentrations exhibited important differences depending on the medium used. Values measured were ~6 μg/ml in EMEM and reached 40 μg/ml in α-MEM. This could be explained by a greater aggregation of the NPs at a higher temperature in the EMEM or by the presence of other medium substances that can stabilise the suspension in the α-MEM. In addition, the DLS measurements of the supernatants showed the presence of a NP population in the α-MEM medium (20–100 nm) that couldn't be clearly observed in the EMEM medium except for the ZnO-3 NP (50–200 nm). These NPs, together with the ions, could also be responsible for the toxicity caused by the supernatants. Other authors have also suggested that the toxicity observed in zebrafish (Bai et al. 2010; Xiong et al. 2011), *Daphnia magna* (Wiench et al. 2009), bacteria and branchipods (Heinlaan et al. 2008), microalgae (Aruoja et al. 2009) and in a human cell line (Yuan et al. 2010) could not only be attributed to the Zn ions but also to the presence of NPs in the exposure media.

In this work, different cytotoxicity assays have been performed to look into different end points. Results obtained with the MTT assay have shown that the PLHC-1 cell line was more sensitive than the Hep G2 cell line, but only with nZnO-1 and nZnO-2 freshly prepared suspensions. Nevertheless, for the highest concentrations used in the bulk material and in the NPs the effect observed in Hep G2 was significantly stronger than in PLHC-1. No differences in sensitivity between both cell lines could be observed with the NR or LDH assays. However, the LUCS assay indicated a higher sensitivity of the human cell line to ZnO particles than that of the fish one. Results also gave indications concerning the contribution of suspended and dissolved NPs and ions to the toxicity. Treatment of PLHC-1 with ZnO suspensions before and after centrifugation have shown, in the MTT, NR and LDH assays, that these cells were generally more sensitive to the particle suspensions than to the dissolved NPs and ions present in the supernatants. This result points to the involvement of aggregates in the toxicity of ZnO NPs to PLHC-1 cells. Bai et al. (2010) attributed the toxicity in zebrafish embryos in part to the large nZnO aggregates that might block the pore canals of the chorion, resulting in hypoxia to the developing embryos. By contrast, the measured concentrations indicated that Hep G2 cells are more responsive to supernatants than suspended NPs. It could be easier for dissolved NPs or ions to enter the Hep G2 cells when aggregates are not present. In addition, cells treated with supernatants are exposed to the dissolved ions and colloidal NPs longer, than those treated with the suspensions. Song et al. (2010), after exposing mouse macrophage cell lines to ZnO particle suspensions and to supernatants, concluded that the toxic effect at dosages under 10 μg/ml was mainly due to dissolved zinc ions whereas when the concentration of ZnO particles exceeded 40 μg/ml, the enhancement of cytotoxicity was mainly caused by ZnO particles. Similarly, De Berardis et al. (2010) also found in human colon carcinoma cells that cytotoxicity induced by Zn ions was only slightly lower than that induced by ZnO NPs.

Differences in cytotoxicity between nominal and measured concentrations clearly indicate that the estimation of real concentrations is essential to avoid misinterpretations and erroneous conclusions.

One of the aims of this study was to test the applicability of the LUCS test in a fish cell line. Positive results were obtained in PLHC-1 cells, showing that ZnO particles are able to trigger DNA alteration in fish cells. Results obtained with LUCS in the Hep G2 cell line suggested that the three NPs are able to disrupt the DNA helicoidal conformation with a higher intensity than the bulk material. In the case of PLHC-1 cells, when all assays were compared, only LDH and LUCS allowed for IC_{50} evaluation with a better sensitivity

seen using the LDH assay. However, in the case of Hep G2, IC_{50} were evaluated with MTT, LDH and LUCS assays with a better sensitivity of the latter assay as shown by ratio calculations. If we consider NOEC values, the MTT assay was the most sensitive for the fish cell line whereas the LUCS and MTT assays were most sensitive in the human cell line.

The NPs nZnO-1, nZnO-3 and the bulk material provoked a significant increase in ROS production in the PLHC-1 cell line. However, none of the particles were able to induce ROS production in the Hep G2 cell line in contrast with other studies in mouse or human cell lines where ZnO NPs were able to generate ROS at concentrations ranging from 5 to 100 μg/ml (Yang et al. 2009; Huang et al. 2010; Song et al. 2010). This difference could be explained by the low concentration of ZnO (6 μg/ml) detected in the EMEM supernatants that probably correspond to Zn ions that need to be present and the need of NPs and Zn ions to enter into the cell to generate ROS as previously suggested (Song et al. 2010; Yuan et al. 2010; Yang et al. 2009). Nevertheless, a main implication of zinc ions in the oxidative stress response has been discarded by these authors as well as by Gojova et al. (2007) and Pujalté et al. (2011). It has been reported that although ROS plays an important role in the toxicity of NPs, it is not necessarily the main factor of cytotoxicity of ZnO particles, but the cytotoxic response (Xia et al. 2008; Song et al. 2010; Wong et al. 2010). This might also be the case in this work. The observed cytotoxicity appeared not to be dependent on the induction of oxidative stress.

The relevance of these experimental data to ZnO NPs exposures *in vivo* remains to be elucidated. The acute toxicity of metal NPs is not always explained, or only partly explained, by the presence of free metal ions. The results of the present work indicate a different sensitivity of both cell lines to the aggregates versus the dissolved fraction. In fish, the dissolution of metal ions from the surface of the particle as well as the presence of dissolved ZnO NPs and large aggregates will determine and influence absorption (dietary versus respiratory or dermal exposure) as well as their presence in different organs. Some studies indicate that the most probable uptake mechanism of NPs is by endocytosis (Handy et al. 2008c; Shaw & Handy 2011). In this regard, fish may be more vulnerable than mammals, since fish guts are able to take up much larger materials by endocytosis across the gut (Handy et al. 2008c). Additionally, their presence in the surface of gills can produce pathologies and toxicity in the internal organs without their direct presence in those tissues (Shaw & Handy 2011). The body distribution, metabolism and excretion of metal NPs is poorly documented in fish, but hepatic excretion into the bile seems a more likely mechanism, rather than mainly by renal or branchial excretion (Handy et al. 2008c). Evidence suggests that metal NPs can be found in a range of organs including the gill, liver, intestine and brain (Handy et al. 2008a, b) and all of them could be targets for NPs and explain or help to explain NP toxicity *in vivo*. Further studies on the possible absorption of the aggregates and the dissolved fraction in fish will allow a better understanding of the risk of these ZnO NPs to the aquatic environment.

Conclusions

In the present study, the toxic effects of ZnO NPs were not clearly related either with the size or the shape of the used NPs, this latter due to the heterogeneity of the commercial ZnO particles used. However, it is important to take into account that different sizes and shapes of ZnO NPs can coexist in the aquatic environment and contribute collectively to specific toxic effects. ZnO NPs formed large aggregates in culture medium that highly contribute to the toxicity observed in the fish cell line. The effects observed in the human cell line seem to be mainly due to the dissolved ZnO fraction. These results support the idea that, in order to have realistic conditions which consider all possible mechanisms of action, experiments involving exposure to ZnO NPs in aqueous suspensions should be performed without homogeneous dispersion of the NPs. It has been also shown that it is essential to measure real concentrations to avoid making erroneous conclusions when only nominal concentrations are considered.

A battery of end points should be measured to study the cytotoxicity of NPs. In this work, we have introduced the LUCS test, a test to measure toxicity based on DNA alteration. It provides us with extra information regarding cellular events. From the classical cytotoxicity assays used, the MTT gave the highest sensitivity in both cell lines. However, the newly developed LUCS assay appeared to be even more sensitive in the Hep G2 cell line. From both cell lines, the human one appeared to be more sensitive than the piscine one. Of particular interest is the fact that the LUCS has been shown to be applicable to other cell lines than the mammalian ones in which it was originally established. The results from this study also indicated that ROS production is not the main factor causing cytotoxicity of ZnO particles, but cellular damage at the mitochondrial and DNA levels.

Further studies in fish *in vivo* to address the consequences of environmental exposures to these NPs are needed.

Acknowledgements

This work was supported by the Spanish Ministerio de Medio Ambiente y Medio Rural y Marino (grant number AEG07-060). T Lammel was funded by FP7-PEOPLE-ITN 2008 ECO (Environmental ChemOinformatics) (Project ref. 238701).

Declaration of interest

The authors report no conflicts of interest. The authors alone are responsible for the content and writing of the paper.

References

Adams LK, Lyon DY, Alvarez PJJ. 2006. Comparative eco-toxicity of nanoscale TiO_2, SiO_2, and ZnO water suspensions. Water Res 40:3527–3532.

Aruoja V, Dubourguier H, Kasemets K, Kahru A. 2009. Toxicity of nanoparticles of CuO, ZnO and TiO2 to microalgae Pseudokirchneriella subcapitata. Sci Total Environ 407:1461–1468.

Bai W, Zhang ZY, Tian WJ, He X, Ma YH, Zhao YL, et al. 2010. Toxicity of zinc oxide nanoparticles to zebrafish embryo: a physicochemical study of toxicity mechanism. J Nanopart Res 12:1645–1654.

Borenfreund E, Puerner JA. 1985. Toxicity determined in vitro by morphological alterations and neutral red absorption. Toxicol Lett 24:119–124.

De Berardis B, Civitelli G, Condello M, Lista P, Pozzi R, Arancia G, et al. 2010. Exposure to ZnO nanoparticles induces oxidative stress and cytotoxicity in human colon carcinoma cells. Toxicol Appl Pharmacol 246:116–127.

Degen A, Kosec M. 2000. Effect of pH and impurities on the surface charge of zinc oxide in aqueous solution. J Eur Ceram Soc 20: 667–673.

Deng XY, Luan QX, Chen WT, Wang YL, Jiao Z. 2009. Nanosized zinc oxide particles induce neural stem cell apoptosis. Nanotechnology 20:115101.

Derick S, Tocanne JF, Morin B, Narbonne JF, Furger C. 2009. DAP, a new fluorescent cell-based assay which predicts human acute toxicity to 82% [Abstract 501]. In 7th World Congress on Alternatives to Animal Experimentation, vol. 26, 130 Rome (Italy); 30 August-3 September, 2009.

Dhawan A, Sharma V. 2010. Toxicity assessment of nanomaterials: methods and challenges. Anal Bioanal Chem 398:589–605.

Fang X, Yu R, Li B, Somasundaran P, Chandran K. 2010. Stresses exerted by ZnO, Ce O(2) and anatase TiO(2) nanoparticles on the Nitrosomas europaea. J Colloid Interface Sci 348:329–334.

Franklin NM, Rogers NJ, Apte SC, Batley GE, Gadd GE, Casey PS. 2007. Comparative toxicity of nanoparticulate ZnO, bulk ZnO, and ZnCl2 to a freshwater microalga (Pseudokirchneriella subcapitata): the importance of particle solubility. Environ Sci Technol 41:8484–8490.

Gojova A, Guo B, Kota RS, Rutledge JC, Kennedy IM, Barakat AL. 2007. Induction of inflammation in vascular endothelial cells by metal oxide nanoparticles: effect of particle composition. Environ Health Perspect 115:403–409.

Handy RD, Owen R, Valsami-Jones E. 2008a. The ecotoxicology of nanoparticles and nanomaterials: current status, knowledge gaps, challenges, and future needs. Ecotoxicology 17:315–325.

Handy RD, Kammer FVD, Lead JR, Hassellöv M, Owen R, Crane M. 2008b. The ecotoxicology and chemistry of manufactured nanoparticles. Ecotoxicology 17:287–314.

Handy RD, Henry TB, Scown TM, Johnston BD, Tyler CR. 2008c. Manufactured nanoparticles: their uptake and effects on fish-a mechanistic analysis. Ecotoxicology 17:396–409.

Heinlaan M, Ivask A, Blinova I, Dubourguier HC, Kahru A. 2008. Toxicity of nanosized and bulk ZnO, CuO and TiO2 to bacteria Vibrio fischeri and crustaceans Daphnia magna and Thammnocephalus platyurus. Chemosphere 71:1308–1316.

Hsiao IL, Huang YJ. 2011. Effects of various physicochemical characteristics on the toxicities of ZnO and TiO2 nanoparticles toward human lung epithelial cells. Sci Total Environ 409:1219–1228.

Huang CC, Aronstam RS, Chen D, Huang Y. 2010. Oxidative stress, calcium homeostasis, and altered gene expression in human lung epithelial cells exposed to ZnO nanoparticles. Toxicol In Vitro 24: 45–55.

Kashiwada S. 2006. Distribution of nanoparticles in the see-through Medaka (Oryzias latipes). Environ Health Perspect 114:1697–1702.

Lin WS, Xu Y, Huang CC, Ma YF, Shannon KB, Chen DR, et al. 2009. Toxicity of nano- and micro-sized ZnO particles in human lung epithelial cells. J Nanopart Res 11:25–39.

Liu J, Zhang W, Jing H, Popovich DG. 2010. Bog Bilberry (Vaccinium uliginosum L.) extract reduces cultured Hep-G2, Caco-2, and 3T3-L1 cell viability, affects cell cycle progression, and has variable effects on membrane permeability. J Food Sci 75:103–107.

Mosmann T. 1983. Rapid colorimetric assay for cellular growth and survival: application to proliferation and cytotoxicity assays. J Immunol Methods 65:55–63.

Pujalté I, Passagne I, Brouillaud B, Tréguer M, Durand E, Ohayon-Courtès C. 2011. Cytotoxicity and oxidative stress induced by different metallic nanoparticles on human kidney cells. Part Fibre Toxicol 8:1–16.

Scown TM, Goodhead RM, Johnston BD, Moger J, Baalousha M, Lead JR, et al. 2010. Assessment of cultured fish hepatocytes for studying cellular uptake and (eco)toxicity of nanoparticles. Environ Chem 7:36–49.

Sharma V, Shukla RK, Saxena N, Paramar D, Das M, Dhawan A. 2009. DNA damaging potential of zinc oxide nanoparticles in human epidermal cells. Toxicol Lett 185:211–218.

Shaw BJ, Handy RD. 2011. Physiological effects of nanoparticles on fish: a comparison of nanometals versus metal ions. Environ Int 37:1083–1097.

Song W, Zhang J, Guo J, Zhang J, Ding F, Li L, et al. 2010. Role of the dissolved zinc ion and reactive oxygen species in cytotoxicity of ZnO nanoparticles. Toxicol Lett 199:389–397.

Tantra R, Tompkins J, Quincey P. 2010. Characterisation of the de-agglomeration effects of bovine serum albumin on nanoparticles in aqueous suspension. Colloids Surf B 75:275–281.

Tso CP, Zhung CM, Shih YH, Tseng YM, Wu SC, Doong RA. 2010. Stability of metal oxide nanoparticles in aqueous solutions. Water Sci Technol 61:127–133.

Wang H, Joseph JA. 1999. Quantifying cellular oxidative stress by dichlorofluorescein assay using microplate reader. Free Radic Biol Med 27:612–616.

Wiench K, Wohlleben W, Hisgen V, Radke K, Salinas E, Zok S, et al. 2009. Acute and chronic effects of nano- and non-nano-scale TiO2 and ZnO particles on mobility and reproduction of the freshwater invertebrate Daphnia magna. Chemosphere 76:1356–1365.

Wong SWY, Leung PTY, Djurisic AB, Leung KMY. 2010. Toxicities of nano zinc oxide to five marine organisms: influences of aggregate size and ion solubility. Anal Bioanal Chem 396:609–618.

Xia T, Kovochich M, Liong M, Madler L, Gilbert B, Shi H, et al. 2008. Comparison of the mechanism of toxicity of zinc oxide and cerium oxide nanoparticles based on dissolution and oxidative stress properties. ACS NANO 2:2121–2134.

Xiong D, Fang T, Yu L, Sima X, Zhu W. 2011. Effects of nano-scale TiO2, ZnO and their bulk counterparts on zebrafish: Acute toxicity, oxidative stress and oxidative damage. Sci Total Environ 409:1444–1452.

Yang H, Liu C, Yang D, Zhang H, Xi Z. 2009. Comparative study of cytotoxicity, oxidative stress and genotoxicity induced by four typical nanomaterials: the role of particle size, shape and composition. J Appl Toxicol 29:69–78.

Yin H, Casey PS, McCall MJ, Fenech M. 2010. Effects of surface chemistry on cytotoxicity, genotoxicity, and the generation of reactive oxygen species induced by ZnO nanoparticles. Langmuir 26:15399–15408.

Yuan JH, Chen Y, Zha HX, Song LJ, Li CY, Li JQ, et al. 2010. Determination, characterization and cytotoxicity on HELF cells of ZnO nanoparticles. Colloids Surf B 76:145–150.

Zhu XS, Zhu L, Duan ZH, Qi RQ, Li Y, Lang YP. 2008. Comparative toxicity of several metal oxide nanoparticle aqueous suspensions to Zebrafish (Danio rerio) early developmental stage. J Environ Sci Health A 43:278–284.

Zhu X, Wang J, Zhang X, Chang Y, Chen Y. 2009. The impact of ZnO nanoparticle aggregates on the embryonic development of zebrafish (Danio rerio). Nanotechnology 20:195103.

Nanotoxicology, June 2014; 8(4):383–393
© 2014 Informa UK, Ltd.
ISSN: 1743-5390 print / 1743-5404 online
DOI: 10.3109/17435390.2013.790997

informa
healthcare

Species-specific toxicity of copper nanoparticles among mammalian and piscine cell lines

Lan Song[1], Mona Connolly[2], Maria L. Fernández-Cruz[2], Martina G. Vijver[1], Marta Fernández[3], Estefanía Conde[3], Geert R. de Snoo[1], Willie J.G.M. Peijnenburg[1,4], & Jose M. Navas[2]

[1]Institute of Environmental Sciences (CML), University Leiden, Leiden, The Netherlands, [2]Departamento de Medio Ambiente, Instituto Nacional de Investigación y Tecnología Agraria y Alimentaria (INIA), Carretera de la Coruña Km 7.5, E-28040 Madrid, Spain, [3]CIEMAT. Avda. Complutense 40, 28040 Madrid, Spain and [4]National Institute for Public Health and the Environment, Bilthoven, The Netherlands

Abstract

The four copper nanoparticles (CuNPs) with the size of 25, 50, 78 and 100 nm and one type of micron-sized particles (MPs) (~500 nm) were exposed to two mammalian (H4IIE and HepG2) and two piscine (PLHC-1 and RTH-149) cell lines to test the species-specific toxicities of CuNPs. The results showed that the morphologies, ion release and size of the particles all played an important role when investigating the toxicity. Furthermore, the authors found that the particle forms of CuNPs in suspensions highly contribute to the toxicity in all exposed cell lines whereas copper ions (Cu^{2+}) only caused significant responses in mammalian cell lines, indicating the species-specific toxicity of CuNPs. This study revealed that the morphologies, ion release rate of NPs as well as the species-specific vulnerabilities of cells should all be considered when explaining and extrapolating toxicity test results among particles and among species.

Keywords: copper nanoparticles, mammalian and fish cell lines, size and morphology of NPs, species-specific cytotoxicity, reactive oxygen species

Introduction

Considering the wide application of copper nanoparticles (CuNPs) in a variety of fields, such as in facial spray, as additives in lubricants, in metallic coating and inks, anode materials for lithium ion batteries (Cioffi et al. 2005; Guo et al. 2002; Lei et al. 2008; Liu et al. 2004), CuNPs can enter into diverse environmental compartments and be taken up by organisms through intake of water, food and even from soil by plant species resulting in reduced seedling growth (Lee et al. 2008). Therefore, the potential risks from exposure to CuNPs must be further investigated.

Various studies showed that CuNPs can cause a diversity of toxic effects to biological systems. CuNPs showed a size- and concentration-dependent toxicity to dorsal root ganglion neurons of rat (Prabhu et al. 2010). Lei et al. (2008) claimed that CuNPs could cause scattered dot hepatocytic necrosis and widespread renal proximal tubule necrosis in the rat. Chen et al. (2006) showed that only CuNPs can induce toxicological effects and severe pathological injuries to the kidney, liver and spleen of mice when compared with copper at micrometer size. It is already known that the toxicity caused by micro copper is lower than the toxicity of CuNPs and the toxicity caused by copper ions in CuNPs media and the toxicity of copper oxide NPs cannot be simply explained by Cu ions released into the cell medium (Chen et al. 2006; Karlsson et al. 2008). However, little attention has been paid to species-specific NP toxicity and only a limited number of studies have quantified the toxicity contribution of the particle form of NPs and released ions to the total toxicity of particle suspensions (Patra et al. 2007). Therefore, the sensitivity of four different hepatoma cell lines, two mammalian and two piscine in origin, exposed to four sizes of CuNPs and one type of micron-sized copper particles (MPs), was investigated in this study. The aim is to evaluate the species-specific acute toxicity of CuNPs at the cellular level and to evaluate the toxicity contribution of the particle form of CuNPs and ions to the total toxicity of particle suspensions, respectively. Uptake of NPs is not investigated in this study since uptake of NPs cannot always and also is not the only pathway to cause acute toxicity to cells (George et al 2009). For instance, a large amount of uptake may not cause any toxic effect due to the inert characterisation of NPs or the high tolerability of cells (Connor et al. 2005). Cytotoxic effects and reactive oxygen species (ROS) levels were correlated with the physico-chemical properties of the CuNPs and the cell types. Liver being the critical organ for copper storage, homeostasis and excretion of several species and an inherited disorder of copper metabolism can cause Wilson's

Correspondences: Lan Song, Institute of Environmental Sciences (CML), University Leiden, Leiden, The Netherlands. E-mail: song@cml.leidenuniv.nl and Jose M. Navas, Departamento de Medio Ambiente, Instituto Nacional de Investigación y Tecnología Agraria y Alimentaria (INIA), Carretera de la Coruña Km 7.5, E-28040 Madrid, Spain. E-mail: jmnavas@inia.es

(Received 26 July 2012; accepted 25 March 2013)

disease in humans (Tao & Gitlin, 2003). Therefore, hepatocytes were chosen as the cell lines for this research. The preliminary hypotheses of this study are: 1) size or shape of CuNPs can influence their toxicity; 2) the toxicity of CuNPs can be related to the type of the cells that they are exposed to; 3) ion release is not the dominant factor inducing toxicity of CuNPs.

Materials and methods

Chemicals and reagents

CuNPs of 25, 50 and 100 nm sizes were purchased from IoLiTec, Inc., Germany. CuNPs of 78 nm as well as the MPs (nominal size of MPs is 500 nm) were purchased from NanoAmor®, USA (Houston, TX , USA). All particles are uncoated. The resazurin *in vitro* toxicology assay kit, 6-carboxy-2′7′-dichlorofluorescein diacetate (DCFH-DA) probe and copper (II) nitrate hydrate ($Cu(NO_3)_2$) were purchased from Sigma Aldrich, Madrid, Spain. Ethanol was from Panreac (Barcelona, Spain). Ultraglutamine 1 (200 mM), L-glutamine (200 mM), foetal bovine serum (FBS), penicillin and streptomycin (P/S) (10,000 U/ml/ 10 mg/ml), non-essential amino acids 100X (NEAA), sodium pyruvate (100 mM), Eagle's Minimum Essential Media (EMEM) for cell culture and Alpha Minimum Essential Media (α-MEM) were purchased from Lonza (Barcelona, Spain). Phenol-red free, serum free Minimum Essential Media (MEM) was sourced from PAN Biotech GmbH, Germany. Analysis grade nitric acid 65% from Scharlau (Barcelona, Spain) purified by sub-boiling distillation in a Milestone Duopur (Milestone srl., Italy) and high purity water (>18 MΩ/cm) obtained from a Milli-Q Element A10 Century (Millipore Ibérica, Spain) were used for inductively coupled plasma mass spectrometry (ICP-MS) analysis.

Preparations of CuNPs

Stock copper suspensions (200 μg/ml) of the four types of CuNPs (25, 50, 78 and 100 nm), of the MPs and of $Cu(NO_3)_2$ were freshly prepared and dispersed in culture media used for culturing each cell line (Supplementary 1) using sonication for 10 min in an S 40 H Elmasonic water bath sonicator (Elma, Germany). The MPs were included to compare the toxicity of nano/microparticles. $Cu(NO_3)_2$ was used as a positive control and the response curves of $Cu(NO_3)_2$ were used to calculate the effects of copper ions (Cu^{2+}) present in copper suspensions.

Physico-chemical characterisation

Dynamic light scattering

The size distributions of all particles at 200 μg/ml were measured directly after preparation (0 h) in four types of culture media and after 24 h incubation under relevant culture conditions (see cell cultures section) by dynamic light scattering (DLS) on a Zetasizer Nano-ZS instrument (Malvern, Instruments Ltd., UK). Three independent measurements were taken with each measurement consisting of four measurements. The different types of culture media were also included in measurements to act as background controls as the presence of large proteins and other media components may affect the DLS measurements. Any peaks detected in the same size range as those found in the media were attributed to media components (Supplementary 2). This instrument was also used to ensure that there were no CuNPs but only copper ions in the supernatants of centrifuged media suspensions in the copper ion release experimental setup (see Actual exposure concentrations and copper ion release section). A Zetasizer Nano-ZS instrument was also used to try to measure the zeta potential of nanoparticles in culture medium (200 μg/ml). However due to the high (>9 mS/cm) conductivity of EMEM, medium quality criteria could not be met and measurements were aborted.

Transmission electron microscopy

Transmission electron microscopy (TEM) analysis was used to characterise the morphology and size distribution of copper suspensions after 24 h incubation. Analysis was only performed in one type of culture medium, EMEM culture medium, because the DLS measurements showed that the different media compositions and temperatures did not influence the hydrodynamic size profiles of the CuNPs. TEM was also used to characterise the primary particle size of the copper suspensions using ethanol as a dispersant. This allowed us to compare profiles and analyse the impact of the media. A JEOL 2100 HT (JEOL Ltd., Japan) TEM was used, operating at an accelerating voltage of 200 kV with integrated energy dispersive X-ray (EDX) spectroscopy (EDX) (Oxford Inca, UK). Stock copper suspensions (200 μg/ml) were deposited onto copper grids and images of CuNPs in ethanol and following 24 h of incubation in EMEM culture medium were collected. Morphology and size distribution of CuNPs were analysed by ImageJ (National Institutes of Health, Bethesda, MD, USA). Size distribution analysis was only performed when individual well-defined NPs could be determined.

Actual exposure concentrations and copper ion release

The actual exposure concentrations of copper suspensions (including both CuNPs, MPs suspensions and $Cu(NO_3)_2$ solution, five concentrations) were prepared freshly and measured using ICP-MS with a quadrupole-based instrument (Thermo X-Series II – Thermo Scientific, Bremen, Germany). Many studies report the release of metal ions as a contributing factor to the toxicity of NPs (Jiang et al. 2009, Wang et al. 2009), therefore the ion release from all copper suspensions (200 μg/ml) in the four different culture media under four culture conditions were quantified using ICP-MS (Supplementary 3). One ml CuNPs suspensions were sampled at time 0, 24 and 48 h after incubation and centrifuged at 13,362 *g* for 20 min, at 4°C (5415 R series centrifuge, Eppendorf, Germany) to remove CuNPs from suspensions (Fernández-Cruz et al. 2012). The supernatants were analysed using DLS to confirm that all CuNPs were removed. The supernatants were then analysed using ICP-MS. Copper ion release (%) was calculated as percentage of the total copper concentration.

Cell cultures

Four liver cell lines were used in this study, two mammalian in origin; a rat hepatoma (H4IIE) and a human hepatocellular carcinoma (HepG2) and two from fish; the topminnow fish (*Poeciliopsis lucida*) hepatocellular carcinoma (PLHC-1) and rainbow trout (*Oncorhynchus mykiss*) hepatoma (RTH-149). All cell lines were obtained from the American Type Culture Collection (ATTC) (Manassas, VA, USA). According to the cell type, the EMEM culture media was supplemented with necessary components for optimum cell growth (Supplementary 1). H4IIE and HepG2 were cultured at 37°C, PLHC-1 and RTH-149 were cultured at 30 and 20°C, respectively. A 5% CO_2 atmosphere was applied to all culture conditions. The media was changed every 48 h and cells were split one to two times per week using 0.5% trypsin/0.02% EDTA.

Cell exposure

Due to different growth rates and morphologies, cells were seeded in 96-well plates (Greiner-Bio one, CellStar, Spain) with different densities (2.5×10^4 cells/well for H4IIE, 7.5×10^4 for HepG2 and 5×10^4 for RTH-149 and PLHC-1) in 100 µl culture media per well under each culture condition, respectively. After 24 h, the culture media was removed and the cells were washed with phosphate buffer saline (PBS). Cells were exposed to all copper suspensions and the $Cu(NO_3)_2$ using the nominal concentration range of 12.5–200 µg/ml immediately following 10 min water bath sonication. A cell free 96-well plate with the same generated nominal concentration range was also prepared for each culture media and used to measure copper concentration by ICP-MS to determine the actual exposure concentrations.

Toxicity evaluation

Cytotoxicity

The assay based on the ability of mitochondrial oxidoreductases to reduce the indicator dye resazurin (7-hydroxy-3H-phenoxazin-3-one-10 oxide) to resorufin has been used (O'Brien et al. 2000). After 24 h exposure under relevant incubation conditions, the medium was removed and the cells were washed once with PBS; 100 µl culture media together with 5 µl of resazurin dye was added to the wells. Fluorescence intensity (532 nm excitation and 595 nm emission) was quantified on a GENios microplate reader (Tecan, Männendorf, Switzerland) after 2 h incubation. Potential interference of all copper suspensions with the fluorescence of the indicator dyes was checked by preparing a plate with corresponding concentration ranges as exposures (12.5–200 µg/ml) but without cells and quantifying the fluorescence intensity of wells after 2 h. Cellular toxicity (%) was calculated as the decrease in fluorescence intensity and expressed as a percentage of control.

Oxidative stress

Intracellular ROS production was determined using the fluorescent probe DCFH-DA. The probe was prepared in phenol-red free, serum free MEM media (100 µM) under dark conditions just prior to carrying out the assay. Culture media was removed from the exposed cells following the exposure timeframe (24 h) and cells were washed with PBS. The DCFH-DA probe was loaded to the wells, dark conditions were maintained and the plates were incubated under culture conditions for 30 min. Following the 30 min period cells were washed twice with PBS to remove any extracellular probe. Cells were then reconstituted with phenol-red free, serum free MEM media. Fluorescence (485 nm excitation and 530 nm emission) was measured on a GENios microplate reader immediately upon reconstitution and then 60 min after incubation under respective culture conditions. Potential interferences of copper suspensions with the fluorescence of the probe were checked by preparing a sample plate of copper suspensions without cells and quantifying the fluorescence intensity of wells after 60 min. Oxidative stress (%) was calculated as the percentage of fluorescence increase over 60 min.

Data analysis and statistics

Statistics

All exposures were performed in triplicate, with the mean ± standard deviation of three independent tests being represented in the final results. The data were analysed by one-way ANOVA followed by Dunnett's *post hoc*-test (treatment vs. control) in SigmaPlot® 12.0 (Systat Software Inc., Chicago, IL, USA). The normality and homoscedasticity of all data was checked prior to carrying out statistical analysis.

The calculation of the IC_{50} (concentration causing a 50% of inhibition with respect to the controls) caused by copper suspensions and by $Cu(NO_3)_2$ (resazurin assay) was performed by SPSS 16.0 using the function of the Probit regression (IBM SPSS, Armonk, NY, USA). The statistical significances ($p < 0.05$) were compared among different particles and among different cell lines using TTest2 (Matlab, MathWorks, Natick, MA, USA), respectively. The results are listed in Supplementary 6. The dose–response curves of oxidative stress production (exposure concentration range: 12.5–200 µg/ml) were plotted in Figure 1. The increase of ROS production (%) caused by 50 and 80 µg/ml (measured exposure concentration) of each copper suspension was calculated from the fitted curve in order to further compare the different responses among cell lines. These values were then used for pairwise comparisons to detect significant differences in the abilities of the different sized NPs to increase ROS production. Multiple comparisons among groups were carried out using a one-way ANOVA followed by a Holm-Sidak method ($p < 0.05$). This allowed determining any size-dependent differences in toxicity as well as providing a statistical way for species-dependent sensitivity analysis.

Toxic contribution of the particle form of CuNPs and Cu^{2+}

Both the Cu^{2+} and the particle form of CuNPs contribute to the toxicity of copper suspensions in living cell lines. The toxicity of Cu^{2+} in copper suspensions can be determined by the concentration–response curve of $Cu(NO_3)_2$. The actual concentrations of Cu^{2+} released by CuNPs (200 µg/ml) have been measured by ICP-MS (see Actual exposure concentrations and copper ion release section). When calculating the contribution of Cu^{2+} and CuNPs to the overall toxicity

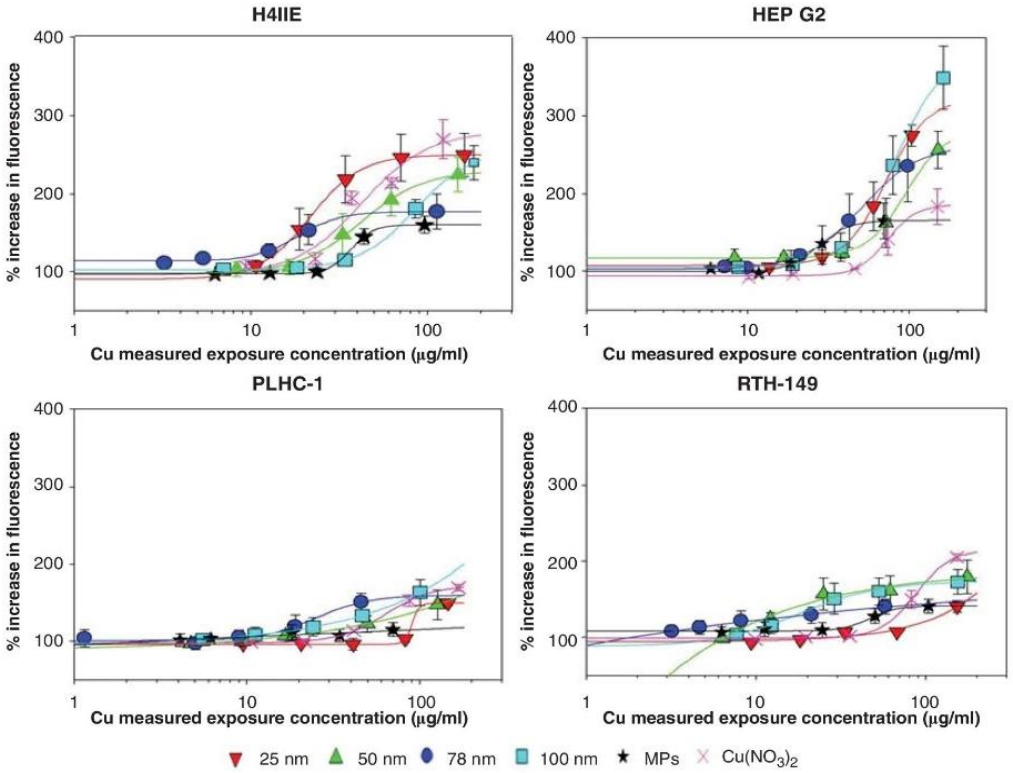

Figure 1. Intracellular ROS levels in the four cell lines following 24 h exposure to the different copper suspensions and $Cu(NO_3)_2$. ROS levels are quantified by measuring the % of increase in fluorescence with respect to the control (100%). Results are expressed as means ± standard error of the mean. Standard curves are presented using a four parameter logistic function to fit the data to a sigmoidal curve.

of the suspensions, it was assumed that the release of copper ions is independent of the concentration of CuNPs. Subsequently, the toxicity of Cu^{2+} (E_{Cu}^{2+}) in the copper suspensions could be determined according to the concentration–response curve of $Cu(NO_3)_2$. Furthermore, it is assumed that there are no interactions between Cu^{2+} and CuNPs.

The total toxicity of copper suspensions was assessed experimentally. Therefore, the toxic effect of the particle form of the CuNPs (E_{CuNPs}) can be estimated using the response addition model (Backhaus et al. 2000):

$$E_{CuNPs} = 1 - [(1 - E_{total}) / (1 - E_{Cu}^{2+})] \qquad (1)$$

Where E_{total} represents the total cell toxicity caused by the copper suspensions. E_{CuNPs} and E_{Cu}^{2+} represent the cell toxicity caused by the particle form of CuNPs and Cu^{2+}, respectively.

The cellular toxicity (%) caused by copper suspensions was plotted as a function of the total copper concentration, together with the corresponding toxic contribution of the particle form of CuNPs and Cu^{2+}. The IC_{50} caused by copper suspensions and the IC_{50} caused by the particle form in each copper suspension were plotted together with the IC_{50} values caused by $Cu(NO_3)_2$. The IC_{20}, IC_{50} and IC_{80} caused by the particle form of each suspension were calculated and listed together with the IC_{20}, IC_{50} and IC_{80} of copper suspensions for comparison in the Supplementary 5.

Results

Physico-chemical characterisation of CuNPs

Transmission electron microscopy

Figure 2 shows the TEM micrographs of the copper particles indicating the size, shape and distribution status in ethanol and after 24 h incubation in culture media. The results revealed that none of the CuNPs appear in the specified size according to the suppliers. The pristine CuNPs are present as aggregates and therefore it is very difficult to differentiate individual NPs to determine their size from TEM images except for the MPs. CuNPs of 25, 50 and 100 nm are spherical particles but are present in aggregates of irregular shape that appear conjoined. The 78 nm CuNPs interestingly appear to have rod-shaped nanostructures visible within aggregates. The MPs aggregates have a defined shape, distinctly spherical with a rough surface in nature. After 24 h incubation under culture conditions, 25, 50 and 100 nm CuNPs retain the aggregate status with a lighter appearance. The form of the 78 nm CuNPs after 24 h incubations was similar as the initial forms. The MPs retain their rough edged appearance with lighter appearances as well but the size decreased by a factor of 10 according to size distribution analysis from TEM images. The mean size at 0 h was 360.2 nm with more than 85% of the particles between 200 and 600 nm. However, after 24 h incubation in culture media, 90% of the MPs were smaller than 60 nm and the mean size decreased to 35 nm (Supplementary 4).

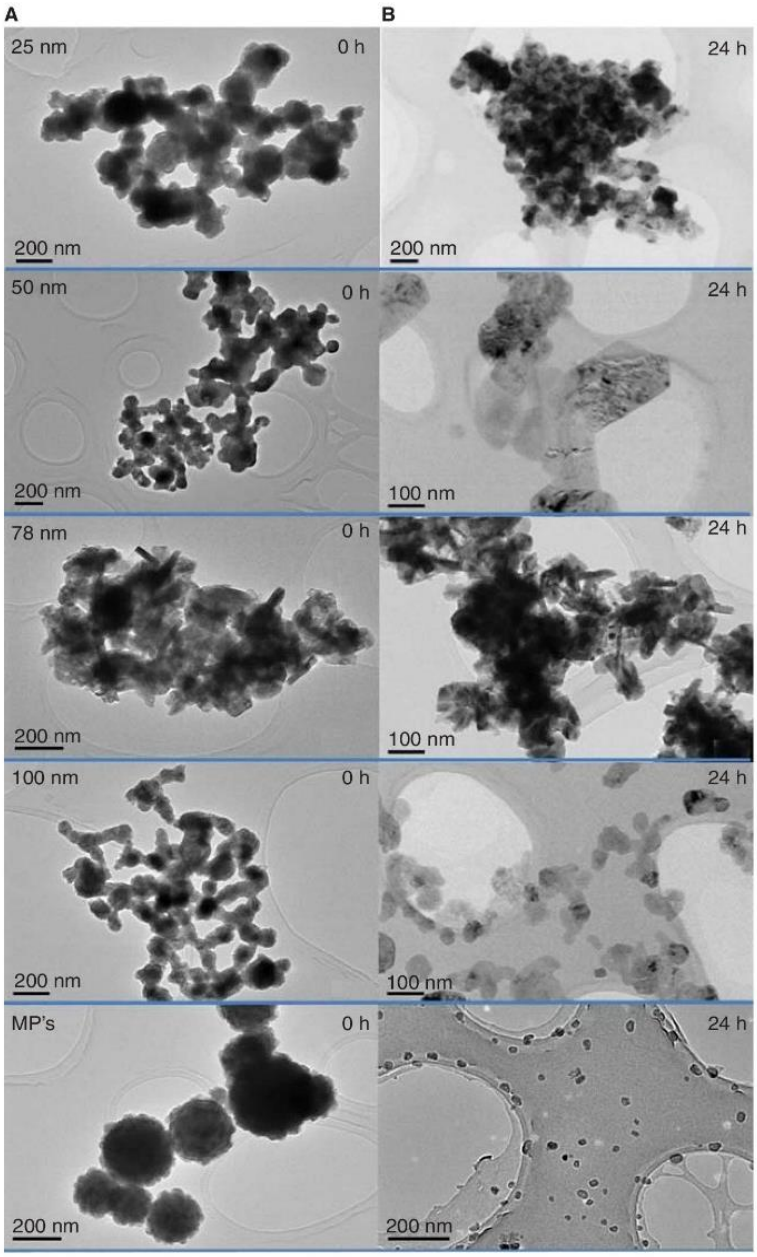

Figure 2. TEM images of copper particles (A) in their pristine form (prepared in ethanol) and (B) following 24 h incubation in EMEM culture medium under culture conditions (37°C/5% CO_2). Scale bars indicate size (nm).

Dynamic light scattering

The hydrodynamic sizes of suspensions before and after 24 h incubation in the four culture media are presented in Figure 3. The results illustrate that all the copper particles are present largely in aggregates with sizes 200–700 nm in diameter depending on the type of particles. Slight differences in sizes were measured in the different culture media, with no apparent trend or temperature/media compositions influencing factor seen. Following 24 h of incubation, the general trend was a decrease in the hydrodynamic diameters of the particles under each culture condition. The 78 nm CuNPs showed higher stability than all other particles under culture conditions, with similar sizes at 0 and 24 h after incubation, which is consistent with the TEM results. The DLS profiles of all the supernatants showed that there are no peaks except the media profiles, indicating no particles present in the supernatants after centrifugation and the measured copper concentration using ICP-MS in the supernatants were solely copper ions.

Actual exposure concentration and ion release

Measured concentrations of copper suspension versus nominal exposure concentrations are presented in Table I. Measured concentrations are the mean of four measurements in

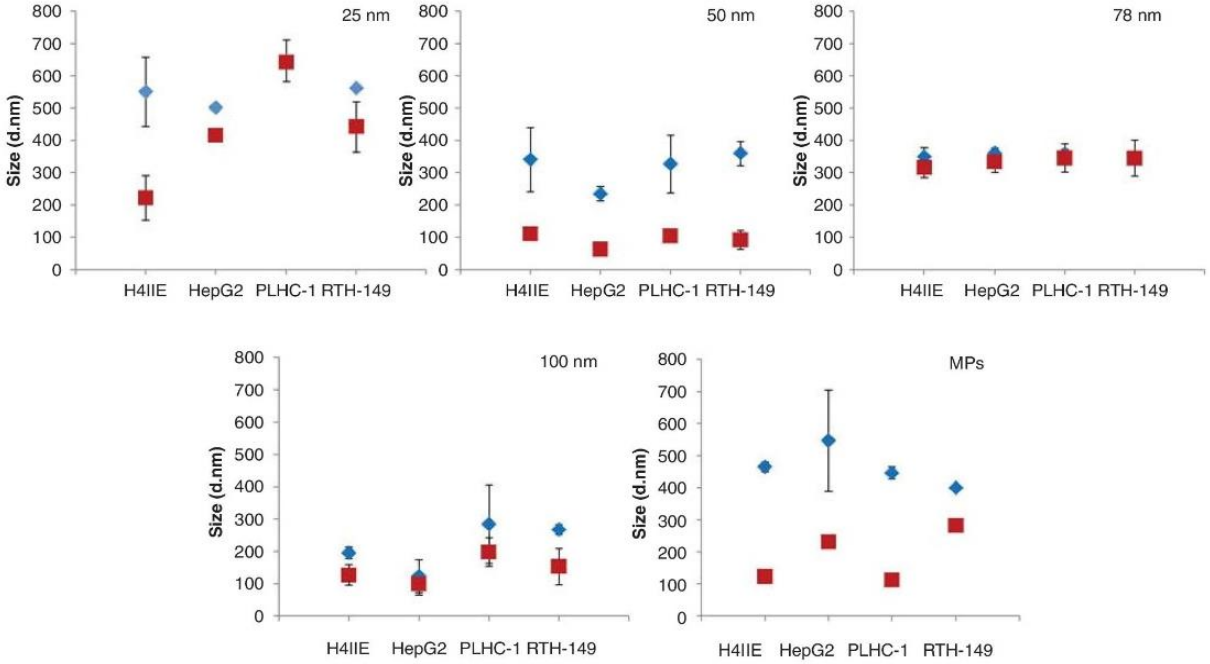

Figure 3. Size distributions of the copper particles measured by DLS directly after preparation (0 h) and after incubation (24 h) in four different culture media, designated H4IIE (37°C), HepG2 (37°C), PLHC-1 (30°C) and RTH-149 (20°C) according to the which cell line it is used for. Results are expressed as means ± standard deviation.

different culture media. The measured copper concentrations in experimental media deviated from 23% to 55% from the desired nominal concentrations depending on the CuNPs. The 78 nm CuNPs and the MPs showed the largest deviations, possibly due to the difficulties encountered in their manipulation (partly due to visible adherence of the particles to the plastic). Therefore, all responses in toxicity assays are correlated with the measured concentrations in this study.

The ICP-MS results showed that there were no significant differences in measured ion release rates between the different media. Therefore, the mean of four measurements in different media and standard deviation (SD) are shown in Figure 4A. Ion release profiles were distinct for all CuNPs. The release of copper ions was time-dependent. At 0 h copper ions were present at low levels in particle suspensions of 200 μg/ml, with Cu^{2+} concentrations ranging from 2 ± 1 to 45 ± 3 μg/ml depending on the types of copper particles. The dissolution rate was very fast in the first 24 h, with the majority of ions being released in the culture media during this time period. The 78 nm CuNPs showed the lowest rate of dissolution among all suspensions. Figure 4B illustrates the percentage of ion release from CuNPs and the MPs calculated as a percentage of the measured total copper concentration. Only 23 ±15% of 78 nm CuNPs was present as dissolved Cu^{2+} after 24 h. The 50 and 100 nm CuNPs showed similar percentages of dissolution, approximately 41%. Approximately 70–80% of 25 nm CuNPs and the MPs were dissolved after 24 h. The ion release of all CuNPs slows down after 24 h. Only 3% and 11% of 25 and 78 nm suspensions, respectively, were released as ions during the later 24 h. The percentage of Cu^{2+} released by 50 and 100 nm CuNPs was very similar after 48 h (approximately 50%). However, about 98% of the MPs were dissolved after 48 h.

Toxicity evaluation

Cellular toxicity

There was a clear dose–effect relationship after exposure of the different cell lines with the different copper suspensions. Values of the IC_{50} for each copper suspension and of the IC_{50} for each particle form in each suspension in different cell

Table I. Nominal exposure concentration ranges vs. the measured concentration (ICP-MS) ranges expressed as mean ± standard deviation (μg Cu/ml of medium suspension).

	Nominal exposure concentration (μg/ml)				
Measured concentration (μg/ml)	12.5	25	50	100	200
25 nm CuNPs	9.8 ± 1.0	17.8 ± 3.0	34.4 ± 5.2	70.2 ± 9.4	153.1 ± 6.1
50 nm CuNPs	7.0 ± 1.8	13.6 ± 3.5	28.2 ± 9.4	61.2 ± 8.9	150.4 ± 20.0
78 nm CuNPs	3.6 ± 2.5	6.8± 2.3	13.7 ± 5.2	28.7 ± 10.7	89.2 ± 29.5
100 nm CuNPs	7.2 ± 1.3	15.1 ± 4.0	31.2 ± 5.9	66 ± 19.2	150.2 ± 34.9
MPs	5.6 ± 1.0	10.4 ± 2.9	21.2± 3.4	39.2 ± 9.5	100.0 ± 16.9

Measured concentrations are a mean of four measurements from four different culture media.
CuNPs: copper nanoparticles; ICP-MS: inductively coupled plasma mass spectrometry; MPs: micron-sized particles.

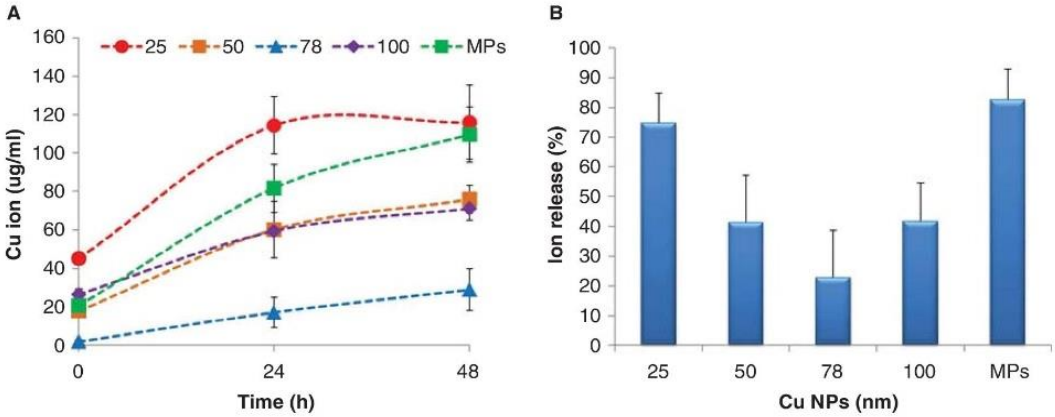

Figure 4. Copper ion release profiles for the copper suspension (a) over time and (b) the ion release after 24 h incubation, expressed as percentage of the total copper suspension concentration. Results are expressed as means ± standard deviation.

lines are plotted in Figure 5. The IC_{50} of $Cu(NO_3)_2$ to each cell line was plotted as a reference in this figure. The corresponding significant statistical analyses between different particles and between different cell lines are shown in Supplementary 6. There is a strong contrast between the sensitivities of cell lines to copper suspensions. In general, the mammalian cell lines are more sensitive than the piscine cell lines, most strikingly in the case of exposure to $Cu(NO_3)_2$ and 25 nm CuNPs. The lowest IC_{50} was seen following exposure to 25 nm in the H4IIE cell line. Exposure to the MPs induced a lower IC_{50} value in both the mammalian cell lines and the piscine cell lines as compared with the CuNPs. The piscine cell line RTH-149 shows the highest resistance to all copper suspensions and $Cu(NO_3)_2$. The lowest IC_{50} was 74 ± 14 µg/ml when RTH-149 was exposed to the MPs.

Toxic contribution of the particle form of CuNPs and Cu^{2+}

The IC_{50} of the particle form in each suspension in different cell lines was much lower than the IC_{50} of the Cu^{2+} ions, except when H4IIE was exposed to the 78 nm CuNP (Figure 5). The IC_{50} of the particle form of 78 nm CuNPs is 77 ± 17 µg/ml for the H4IIE cell line, whereas the IC_{50} of the Cu^{2+} is 54 ± 9 µg/ml for H4IIE cells; 25 nm CuNPs and the MPs were the most toxic particles to all cell lines. The lowest value of the IC_{50} 4 ± 3 µg/ml was found when H4IIE was exposed to MPs, and the second lowest value of IC_{50} was 7 ± 1 µg/ml when HepG2 cells were exposed to 25 nm CuNPs. RTH-149 shows the highest resistance to all copper particles.

The cellular toxicity(%) caused by copper suspensions is plotted against the total copper concentration (measured values) in Figure 6, together with the corresponding toxic

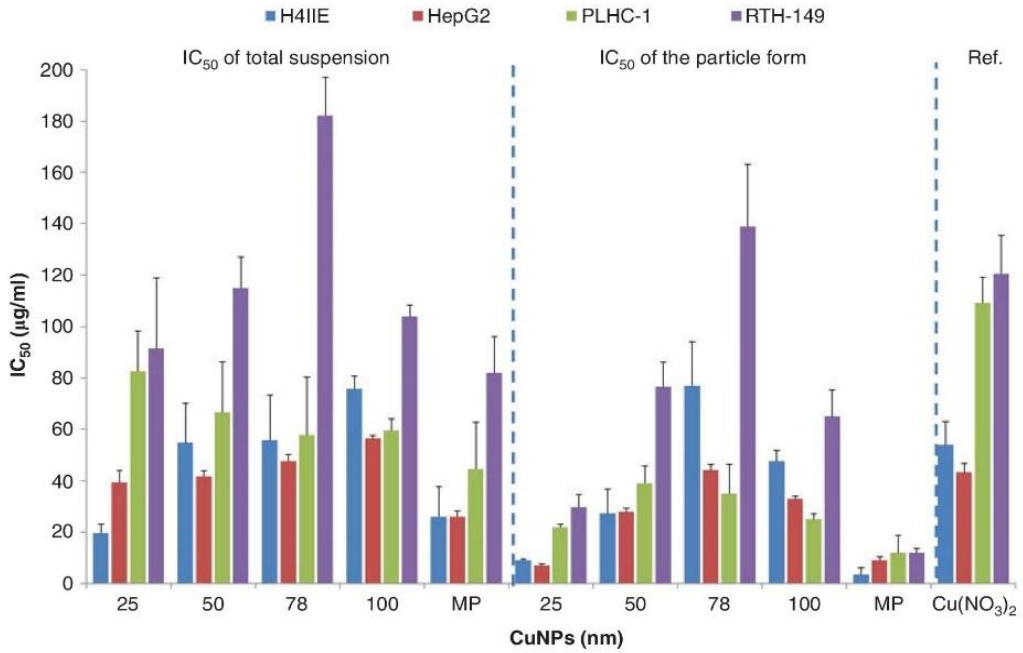

Figure 5. The IC_{50} caused by each copper suspension and the IC_{50} caused by the particle form in each copper suspensions to mammalian (H4IIE, HepG2) and piscine cell lines (PLHC-1 and RTH-149). The IC_{50} of $Cu(NO_3)_2$ for four types of cell lines is shown separately. Results are expressed as means ± standard deviation.

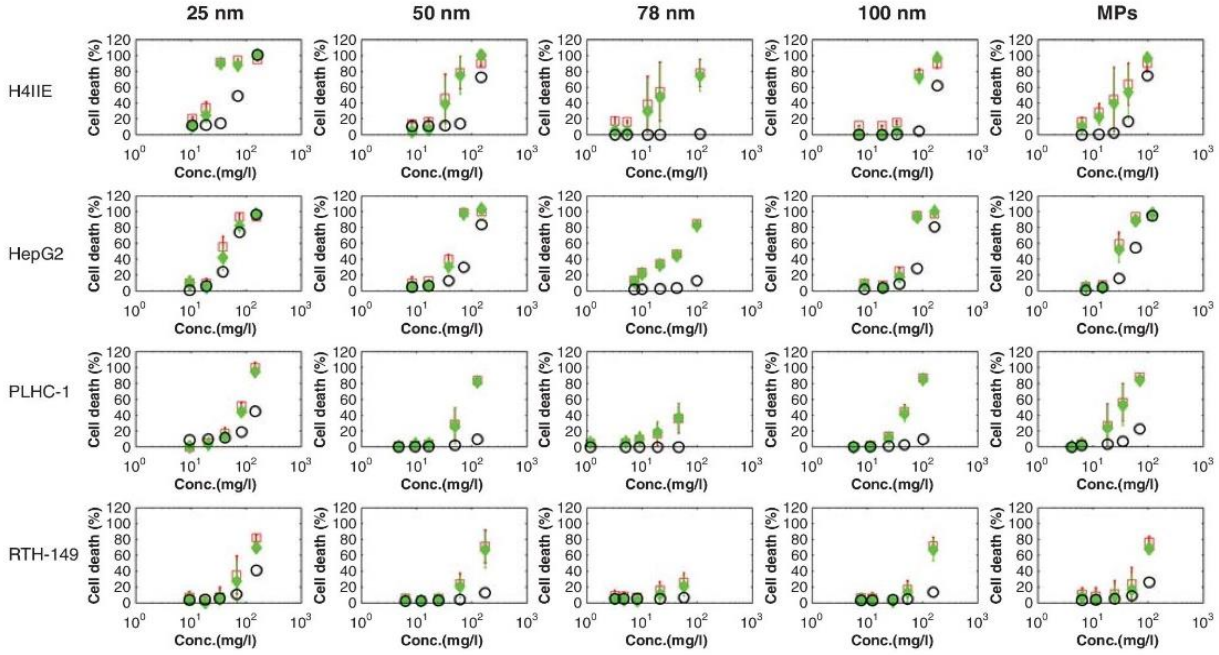

Figure 6. The total cellular toxicity (%) caused by copper suspensions (red, square), and the cellular toxicity (%) caused by particle forms of each copper suspension (CuNPs) (green, solid diamond) and Cu^{2+} (blue, circle) plotted against the total copper concentrations, respectively. Results are expressed as means ± standard deviation.

contribution of the particle form of CuNPs and Cu^{2+}, respectively. The particle form of CuNPs significantly contributed to the toxicity of the copper suspensions in all four cell lines. However, the toxic contribution of Cu^{2+} and of the particle form of CuNPs is dependent on the type of CuNPs and cell lines. The IC_{50} of Cu^{2+} in $Cu(NO_3)_2$ in mammalian cell lines (54 ± 9 μg/ml for H4IIE and 43 ± 4 μg/ml for HepG2) was about half of the value found for piscine cell lines (109 ± 10 μg/ml for PLHC-1 and 120 ± 15 μg/ml for RTH-149). Cu^{2+} only significantly contributed to the total toxicity in the H4IIE and HepG2 cell lines exposed to 25, 50, 100 nm CuNPs and the MPs as shown in Figure 6. Cu^{2+} exhibited little toxicity to the total toxicity when H4IIE and HepG2 exposed to 78 nm CuNPs, because of the low levels of Cu^{2+} in the 78 nm suspensions. The piscine cell lines showed a high resistance to Cu^{2+} in all cases.

The IC_{20}, IC_{50} and IC_{80} of $Cu(NO_3)_2$, of the copper suspensions and of the particle form in each copper suspension when exposed to each cell line are given in Supplementary 5. The particle form of CuNPs can cause 20% of cellular toxicity at much lower concentration compared with $Cu(NO_3)_2$ in most of cases (Supplementary 5). For instance, the particle form of the 25 nm CuNPs and of the MPs can cause 20% cellular toxicity at 6 ± 2 and 4 ± 0 μg/ml to HepG2 cell lines, respectively. But the IC_{20} of $Cu(NO_3)$ is 18 ± 2 μg/ml to HepG2 cell lines, which is three times higher (less toxic) than the IC_{20} of the particle form of the 25 nm CuNPs and the MPs.

ROS levels

The ability of copper suspensions and $Cu(NO_3)_2$ to elicit the generation of intracellular ROS was also investigated. Curves representing the response of each cell line to all copper particles and $Cu(NO_3)_2$ are compared in Figure 1. The ability of CuNPs to increase intracellular ROS levels is concentration and cell type dependent. The corresponding responses to two different concentrations (50 and 80 μg/ml) are extrapolated from the fitted curves to compare the different responses of different cell lines (Supplementary 7). Although no differences in ROS generation were detected among cell lines after exposure to low concentrations, at the highest concentrations the mammalian cell lines (H4IIE and HepG2) exhibited a higher sensitivity to CuNPs than the piscine cell lines used in this study. Mammalian cell line H4IIE responses are significantly different ($p < 0.01$) from both piscine responses upon exposure to the 25 nm CuNPs and $Cu(NO_3)_2$. The 25 nm CuNPs elicit the highest increase in ROS levels in H4IIE compared with all other suspensions, even above those elicited by $Cu(NO_3)_2$. However, there is no significant difference of ROS response among cell line when exposed to other CuNPs. Furthermore, the difference of ROS generation among CuNPs in same cell lines is not apparent. The results showed that only the ROS response of 25 nm in H4IIE is significantly different ($p < 0.05$) from the response to the 100 nm CuNPs for the 50 μg/ml dose. And only the 78 nm CuNPs elicits an increased response significantly different ($p < 0.05$) from the 25 nm NP and the MPs in the PLHC-1 cell line for the 80 μg/ml.

Discussion

Behaviour of NPs in culture media

It was found that all tested CuNPs aggregated immediately in the culture media. All CuNPs and the MPs underwent

dissolution releasing copper ions under exposure conditions, however to different extents depending on the type of CuNPs. The increase in dissolution rates over time is consistent with the fact that the hydrodynamic sizes of CuNPs in culture media decreased after 24 h, as shown by the DLS and TEM measurements. This suggests that the decrease in size of the CuNPs is due to dissolution. The net surface area may be a dominating factor affecting ion release of CuNPs. The smaller the NPs, the larger the net surface area. The large dissolution rate of 25 nm CuNPs could be explained by the largest net surface area. The rough surface of MPs causes fast decomposition of MPs. Therefore, the size of MPs decreases sharply as the net surface area and ion release rate of MPs increases dramatically. Much lower Cu^{2+} ion levels and constant morphologies were detected before and after 24 h incubations of 78 nm CuNPs which may be due to the 78 nm CuNPs being rod-shaped according to the TEM observation. The net surface area of rod-shaped particles is much smaller compared with the same amount of spherical CuNPs according to mathematic calculation. Therefore, the rod shape of 78 nm CuNPs has much lower dissolution compared with other CuNPs.

Although (Liu and Hurt 2010) reported that the ion release rates of silver NPs can increase with temperature in the range 0–37°C, no clear relationship was found between the rate of ion release, temperature (20, 30 and 37°C) and the original size of the CuNPs in this study (Figure 3). The ionic strengths of the culture media for all cell lines are expected to be quite similar (Supplementary 1). It is also difficult to conclude if the ion strength of the culture media has clear impact on Cu^{2+} ion release from Figure 3. Further studies are needed to investigate the effect of temperature and different compositions of culture mediums on aggregation size and the rate of ion release of CuNPs.

Physical properties and toxicities of CuNPs suspensions

The toxicity of CuNPs suspensions (except MPs) in mammalian cell lines increased with a decrease of the nominal size of the particles (Figure 5, left part). The toxicity of CuNPs showed the same trend in RTH-149 when the nominal particle size of the particle is less than 100 nm. If we only consider the IC_{50} caused by the particle form of 25, 50, 78 nm CuNPs suspensions, then the toxicity of CuNPs increased with the decrease of nominal particle size in H4IIE, HepG2 and RTH-149 cell lines (Figure 5, middle part). Therefore, the original size could be one of parameters which affect the toxicity of CuNPs suspensions. However, the particles were present as big aggregates in the culture media and all particles went through dissolution processes. Whereas also the shape of the particles was different (78 nm CuNPs is rod, the rest of CuNPs is spherical). Furthermore, there is no significant difference of toxicities between different copper suspensions in PLHC-1 cell lines (Supplementary 6). No correlation could be established between the initial size of aggregates or the aggregates after dissolution and the toxicity of CuNPs suspensions. Therefore, the size of particle matters, but size is not the only dominant factor regarding the toxicity of CuNPs.

Both the particle form of CuNPs and Cu^{2+} are responsible for the adverse effects observed for the copper suspensions (Figure 6). However, the particle form of CuNPs was the dominant source of toxicity of copper suspensions in all cases. Cu^{2+} only contributed significantly when mammalian cell lines exposed to 25, 50, 100 nm CuNPs and the MPs. The $IC_{50(particle)}$ found for the particle form of 25 nm CuNPs and the MPs was extremely low due to the large surface area of the particles before (25 nm) and especially after dissolution. The high surface reactivity of CuNPs can cause oxidative stress via the Fenton reaction or induce mitochondrial depolarisation of cells (Karlsson et al. 2009). The high ion concentrations also caused severe damage to all cells. Therefore, the total toxicities were quite high in both cases. All copper suspensions and $Cu(NO_3)_2$ can generate a high level of ROS following 24 h exposure, indicating that ROS may be the potential mechanism causing cell toxicity in both cases. In addition, all copper suspensions generated higher ROS levels than $Cu(NO_3)_2$ in HepG2 and some CuNPs also produced higher ROS levels than $Cu(NO_3)_2$ in the other cell lines. These results indicate that the particle form of CuNPs also plays an important role in ROS production to cells in all suspensions.

Morphology of CuNPs is one of the important properties affecting their toxicity. Compared with spherical CuNPs, the rod particle form of CuNPs (78 nm) expressed quite low toxicity to H4IIE and HepG2 cell lines. Rod-shaped particles have a smaller surface area as compared with the same quantity of spherical-shaped particles according to the mathematic calculation. Therefore, the lower toxicity of the rod particle form of 78 nm CuNPs can be explained by the low reactivity of the surface area of the rod-shaped particles. In addition, there is evidence that spherical NPs are easier to be taken up by H4IIE cells than rod-shaped NPs (Arnida et al. 2010). Singh et al. (2007) reported that the spherical shape of CuNPs facilitates physical interaction with cells, allowing them to be more efficiently attached to the surface of cells and be taken up more efficiently through endocytosis, specifically pinocytosis processes.

Species-specific toxicity of CuNPs suspensions

The uptake and toxicities of CuNPs were associated with the properties of the cells. The RTH-149 cell lines have higher resistance to toxicity of copper suspensions compared with mammalian cell lines and PLHC cell lines in general. The ROS generation in piscine cell lines was lower than the ROS generation in mammalian cell lines. Particularly, the IC_{50} of 25 nm CuNPs suspensions and of $Cu(NO_3)_2$ in mammalian cell lines was two times lower than the IC_{50} of piscine cell lines, indicating the higher vulnerability of mammalian cell lines. The mammalian cells were susceptible to both the particle form of CuNPs and Cu^{2+} in the suspensions, but piscine cells seem to be only vulnerable to the particle form of CuNPs (Figure 6). The particle form of CuNPs can induce severe damage to all cell lines, revealing the low resistance of all cell lines to CuNPs in particle forms. The different toxicities of copper ions to all tested cell lines were due to variations in biological properties and the responses of the four cell lines. Copper ions can be metabolised in hepatoma

cells and be transferred in metallothionein by reduced glutathione (Chen et al. 2006). The overloading of copper ions leads to cellular toxicity. Cu^{2+} contributes significantly when exposed to mammalian cells but little effect was found on piscine cells indicating that piscine cells have greater abilities to metabolise and transport copper ions than mammalian cells. Therefore, species-specific cell features significantly affect the toxicity profile of copper suspensions.

The sizes and the shapes of different cells are different. The average diameter of HepG2 ranges from 1.5 to 3.5 μm and they normally grow in clusters because of the irregular cytoplasmic expansions and microvilli on the plasma membranes connecting them (Bouma et al. 1989). PLHC-1 cell lines have round shapes and these cells appear loosely organised and form monolayers of 4–8 μm thick in culture (Hightower & Renfro, 1988). H4IIE cells have the fastest growth rate compared with the rest of the cell lines and RTH-149 is the only one with fabric shapes, multiple nuclei and connecting filaments. All these factors can also affect the exposure, uptake and toxicity of CuNPs and Cu^{2+}. Also the culture conditions of the cell lines are different, and the metabolism inside the cells may proceed slower at lower temperatures, all of which may affect the uptake of CuNPs and their level of toxicity. For instance, the higher resistance of the piscine cell lines and in particular of the RTH-149 cell line to the toxicity of copper suspensions compared with the other cell lines used could be related with the lower temperature of culture of the piscine cell lines, and in particular of RTH-149 cells. The properties of cells and the exposure conditions should therefore also be taken into account when discussing the toxicity of the CuNPs.

Conclusions

By investigating the behaviour and toxicity of CuNPs using four different cell lines, this study revealed that the toxicity of CuNPs cannot be simply linked with a single physicochemical property of CuNPs. The decrease in particle size can be linked to the toxicity of CuNPs, but the morphologies of CuNPs and the species-specific vulnerabilities of cells also play important roles in evaluating the toxicity profile of CuNPs. The particle form of CuNPs highly contributes to the toxicity in all copper suspensions whereas copper ions only caused significant impacts on mammalian cell lines. More research should be carried out to investigate the mechanisms of uptake and toxicity of NPs in different species regarding the specific properties of cell lines, the contribution of particle and ion form of NPs as well as the exposure conditions. It is clear that the extrapolation of toxicities among species and different test concentrations needs to be handled carefully.

Acknowledgements

L Song and M Connolly have contributed equally to this work. Both of them are sponsored by the Environmental ChemOinformatics Marie Curie Initial Training Network (ECO-ITN) within the seventh research framework programme of the European Union (238701). MG Vijver is supported via VENI grant (863.08.023) awarded by The Netherlands Organization for Scientific Research (NWO). Part of the work was performed within the framework of the RIVM sponsored project "IRAN" and the INIA project AT2011-0001.

Declaration of interest

The authors declare that they have no conflict of interest.

References

Arnida Malugin A, Ghandehari H. 2010. Cellular uptake and toxicity of gold nanoparticles in prostate cancer cells: a comparative study of rods and spheres. J Appl Toxicol 30:212–217.

Backhaus T, Scholze M, Grimme LH. 2000. The single substance and mixture toxicity of quinolones to the bioluminescent bacterium Vibrio fischeri. Aquat Toxicol 49:49–61.

Bouma ME, Rogier E, Verthier N, Labarre C, Feldmann G. 1989. Further cellular investigation of the human hepatoblastoma-derived cell line HepG2: morphology and immunocytochemical studies of hepatic-secreted proteins. In Vitro Cell Dev Biol 25:267–275.

Chen Z, Meng H, Xing G, Chen C, Zhao Y, Jia G, et al. 2006. Acute toxicological effects of copper nanoparticles in vivo. Toxicol Lett 163:109–120.

Cioffi N, Ditaranto N, Torsi L, Picca RA, Sabbatini L, Valentini A, et al. 2005. Analytical characterization of bioactive fluoropolymer ultra--thin coatings modified by copper nanoparticles. Anal Bioanal Chem 381:607–616.

Connor EE, Mwamuka J, Gole A, Murphy CJ, Wyatt MD. 2005. Gold nanoparticles are taken up by human cells but do not cause acute cytotoxicity. Small 1:325–327.

Fernández-Cruz ML, Lammel T, Connolly M, Conde E, Barrado AI, Derick S, et al. 2012. Comparative cytotoxicity induced by bulk and nanoparticulated ZnO in the fish and human hepatoma cell lines PLHC-1 and Hep G2. Nanotoxicology 0:1–18.

George S, Pokhrel S, Xia T, Gilbert B, Ji Z, Schowalter M, et al. 2009. Use of a rapid cytotoxicity screening approach to engineer a safer zinc oxide nanoparticle through iron doping. ACS Nano 4:15–29.

Guo K, Pan Q, Wang L, Fang S. 2002. Nano-scale copper-coated graphite as anode material for lithium-ion batteries. J Appl Electrochem 32:679–685.

Hightower LE, Renfro JL. 1988. Recent applications of fish cell culture to biomedical research. J Exp Zool 248:290–302.

Jiang W, Mashayekhi H, Xing B. 2009. Bacterial toxicity comparison between nano- and micro-scaled oxide particles. Environ Pollut 157:1619–1625.

Karlsson HL, Cronholm P, Gustafsson J, Moller L. 2008. Copper oxide nanoparticles are highly toxic: a comparison between metal oxide nanoparticles and carbon nanotubes. Chem Res Toxicol 21:1726–1732.

Karlsson HL, Gustafsson J, Cronholm P, Möller L. 2009. Size-dependent toxicity of metal oxide particles—A comparison between nano- and micrometer size. Toxicol Lett 188:112–118.

Lee WM, An YJ, Yoon H, Kweon HS. 2008. Toxicity and bioavailability of copper nanoparticles to the terrestrial plants mung bean (Phaseolus radiatus) and wheat (Triticum aestivum): Plant agar test for water -insoluble nanoparticles. Environ Toxicol Chem 27:1915–1921.

Lei R, Wu C, Yang B, Ma H, Shi C, Wang Q, et al. 2008. Integrated metabolomic analysis of the nano-sized copper particle-induced hepatotoxicity and nephrotoxicity in rats: a rapid in vivo screening method for nanotoxicity. Toxicol Appl Pharmacol 232:292–301.

Liu G, Li X, Qin B, Xing D, Guo Y, Fan R. 2004. Investigation of the mending effect and mechanism of copper nano-particles on a tribologically stressed surface. Tribol Lett 17:961–966.

Liu J, Hurt RH. 2010. Ion release kinetics and particle persistence in aqueous nano-silver colloids. Environ Sci Technol 44:2169–2175.

O'Brien J, Wilson I, Orton T, Pognan F. 2000. Investigation of the Alamar Blue (resazurin) fluorescent dye for the assessment of mammalian cell cytotoxicity. Eur J Biochem 267:5421–5426.

Patra HK, Banerjee S, Chaudhuri U, Lahiri P, Dasgupta AK. 2007. Cell selective response to gold nanoparticles. Nanomedicine 3:111–119.

Prabhu BM, Ali SF, Murdock RC, Hussain SM, Srivatsan M. 2010. Copper nanoparticles exert size and concentration dependent toxicity on somatosensory neurons of rat. Nanotoxicology 4:150–160.

Singh S, Shi T, Duffin R, Albrecht C, Van Berlo D, Höhr D, et al. 2007. Endocytosis, oxidative stress and IL-8 expression in human lung epithelial cells upon treatment with fine and ultrafine TiO_2: Role of the specific surface area and of surface methylation of the particles. Toxicol Appl Pharmacol 222:141–151.

Tao TY, Gitlin JD. 2003. Hepatic copper metabolism: insights from genetic disease. Hepatology 37:1241–1247.

Wang H, Wick RL, Xing B. 2009. Toxicity of nanoparticulate and bulk ZnO, Al2O3 and TiO_2 to the nematode Caenorhabditis elegans. Environ Pollut 157:1171–1177.

Supplementary materials available online

Supplementary 1
Supplementary 2
Supplementary 3
Supplementary 4
Supplementary 5
Supplementary 6
Supplementary 7

Science of the Total Environment 505 (2015) 253–260

Contents lists available at ScienceDirect

Science of the Total Environment

journal homepage: www.elsevier.com/locate/scitotenv

The potentiation effect makes the difference: Non-toxic concentrations of ZnO nanoparticles enhance Cu nanoparticle toxicity *in vitro*

Lingxiangyu Li [a], María Luisa Fernández-Cruz [b], Mona Connolly [b], Estefanía Conde [c], Marta Fernández [c], Michael Schuster [d], José María Navas [b,*]

[a] State Key Laboratory of Environmental Chemistry and Ecotoxicology, Research Center for Eco-Environmental Sciences, Chinese Academy of Sciences, Beijing 100085, China
[b] Departamento de Medio Ambiente, Instituto Nacional de Investigación y Tecnología Agraria y Alimentaria (INIA), Madrid 28040, Spain
[c] Centro de Investigaciones Energéticas, Medioambientales y Tecnológicas (CIEMAT), Madrid 28040, Spain
[d] Department of Chemistry, Technische Universität München, Garching 85747, Germany

HIGHLIGHTS

- ZnONPs at non-toxic concentrations increased the toxicity of CuNPs *in vitro*.
- ZnONPs of larger size provoked a stronger synergistic effect with CuNPs.
- The synergistic effect was attributed to the particle fraction of ZnONPs.

ARTICLE INFO

Article history:
Received 5 August 2014
Received in revised form 17 September 2014
Accepted 6 October 2014
Available online 15 October 2014

Editor: Kevin V. Thomas

Keywords:
ZnONPs
CuNPs
HepG2
Potentiation effect
Cytotoxicity assays

ABSTRACT

Here we examined whether the addition of a non-toxic concentration (6.25 μg/mL) of zinc oxide nanoparticles (ZnONPs: 19, 35 and 57 nm, respectively) modulates the cytotoxicity of copper nanoparticles (CuNPs, 63 nm in size) in the human hepatoma cell line HepG2. The cytotoxic effect of CuNPs on HepG2 cells was markedly enhanced by the ZnONPs, the largest ZnONPs causing the highest increase in toxicity. However, CuNPs cytotoxicity was not affected by co-incubation with medium containing only zinc ions, indicating the increase in toxicity might be attributed to the particle form of ZnONPs. Transmission electron microscopy (TEM) revealed the presence of CuNPs and ZnONPs inside the cells co-exposed to both types of NP and outflow of cytoplasm through the damaged cell membrane. Inductively coupled plasma mass spectrometry (ICP-MS) determined an increase in the concentration of zinc and a decrease in that of copper in co-exposed cells. On the basis of these results, we propose that accumulation of large numbers of ZnONPs in the cells alters cellular membranes and the cytotoxicity of CuNPs is increased.

1. Introduction

Over the last two decades, a large number of engineered metal-containing nanomaterials with varying particle sizes have covertly entered our daily lives. According to the Nanotechnology White Paper published by the US-EPA, metal oxides are the most widely used engineered nanomaterials (U.S. EPA, 2007). Among the various engineered nanomaterials, zinc oxide nanoparticles (ZnONPs) are widely used all over the world (Gottschalk et al., 2009). Consequently, ZnONPs have inevitably entered the milieu, thus raising concerns about the potential threats they pose to the environment and public health. Copper nanoparticles (CuNPs) are commonly used as superconductors and catalysts. They are applied to lithium ion electrode materials, bioactive coatings, and liquid films. Given such wide use of these NPs, there is a high risk of their release into the environment and of exposure to humans and wildlife.

The divalent ion forms of Zn and Cu are nutritionally essential for all living organisms as they are cofactors for a number of enzymes. However, when present in excess, these metals can cause adverse effects (Regoli and Principato, 1995; Wilson et al., 2012). The toxicity of zinc and copper has long been recognized, and a number of studies have already addressed issues related to the bioavailability, bioaccumulation, and deleterious activities of soluble forms of these two metals (Babich and Stotzky, 1978; Jonas, 1989). The mutual interactions of zinc and copper at the nutritional level are also well known. These metals mutually inhibit absorption in the intestine (Hall et al., 1979; Hogstrand, 2011). This effect is caused by feed-back mechanisms affecting metal regulatory proteins. For instance, an increase in cellular copper can lead to the down-regulation of zinc importer proteins and channels

* Corresponding author. Tel.: +34 91 3474155; fax: +34 91 3474008.
E-mail address: jmnavas@inia.es (J.M. Navas).

http://dx.doi.org/10.1016/j.scitotenv.2014.10.020
0048-9697/

(Qiu and Hogstrand, 2005) and the up-regulation of metallothionein as a zinc buffering protein (Westin and Schaffner, 1988). Interestingly, inhibitory effects of zinc on copper uptake in the intestine have also been observed (Wapnir and Balkman, 1991).

Although the possible deleterious effects of high or low concentrations of these metals are recognized, there is a considerable knowledge gap about the toxic effects of nanoparticles (NPs) whose structure is based on zinc or copper (Li et al., 2014; Ma et al., 2014). In order to shed light on this field, we recently performed in-depth studies in a variety of hepatic cell lines of mammalian and piscine origin in an attempt to determine the contribution of ionic and NP fractions to the cytotoxicity of ZnONPs and CuNPs (Fernandez-Cruz et al., 2013; Song et al., 2014). We revealed the complexity of the toxic effects of these nanomaterials and showed that although the toxicity is influenced by the metal (Zn or Cu) ions released during the dissolution of NPs in the culture medium, the NP itself greatly contributes to the toxicity observed.

Organisms are exposed to soluble zinc and copper ions in the natural environment. In this regard, these previous studies raised the question about the possible interaction between ZnONPs and CuNPs in the environment and about the mutual influence of these materials on their toxicity. Indeed, the simultaneous presence of both kinds of nanomaterials in the environment has already been reported, for instance in wastewater effluents (Bolyard et al., 2013; Gystrzejewska-Piotrowaka et al., 2009), thus raising considerable concerns about the potential adverse effects of co-exposure. Interactions between these materials may occur at the NP level, but NPs of each material may also influence the processes or toxicity caused by the ions released by the other. A number of studies have addressed the possible modulation of the activity of ions or chemicals by NPs. For instance, Tan et al. (2012) showed that TiO_2NPs enhance the uptake and retention of zinc and cadmium in *Daphnia magna*, and Torre-Roche et al. (2013) demonstrated that exposure of *Cucurbita pepo* (zucchini) and *Glycine max* (soybean) to silver nanoparticles (AgNPs) leads to a significant reduction in the uptake of *p,p′*-DDE. However, with some exceptions (Guo et al., 2009; Tang et al., 2013), little attention has been given to the effects of co-exposure to ZnONPs and CuNPs.

Here we sought to study the mutual influence of ZnONPs and CuNPs on the toxicity of these particles *in vitro* using a human hepatoma cell line, HepG2. The data obtained here will serve to set the basis for more realistic and complex experiments *in vivo*.

2. Materials and methods

2.1. Chemicals

We used one type of CuNPs (50 nm according to the manufacturer, IoLiTec, Inc., Germany) and three types of ZnONPs (with sizes of 25, 50 and 100 nm according to the manufacturer, Sigma-Aldrich, Madrid, Spain). All particles were uncoated. With the exceptions indicated below, all chemicals were supplied by Sigma-Aldrich and all the products for cell culture by Lonza (Barcelona, Spain). A detailed description of the materials and chemicals is included in the Supplementary Material.

2.2. Cell culture and exposure

The HepG2 cell line was obtained from the American Type Culture Collection (ATCC, Manassas, VA, USA). Cells (5×10^5 cells/mL) were cultured in Eagle's minimum essential medium (EMEM) supplemented with 10% fetal bovine serum (FBS), 1% penicillin/streptomycin (P/S), 1% ultraglutamine and 1% non-essential amino acids 100× (NEAA) and exposed to NPs in 96-well plates (Greiner Bio-one GmbH) following the method previously described (Fernandez-Cruz et al., 2013).

Stock CuNPs and ZnONPs suspensions of 200 μg/mL were freshly prepared and dispersed in serum-free medium using sonication for 10 min in an S 40H Elmasonic water bath sonicator (Elma, Germany). Afterwards, vortexing for 1 min was used before applying suspensions to the cells, as described in Song et al. (2014) and Fernandez-Cruz et al. (2013) respectively. A volume of 100 μL of NP suspension in serum-free medium was added to each well. Final concentrations of CuNPs ranging from 0.39 to 25.0 μg/mL were applied alone or together with 6.25 μg/mL ZnONPs (a non-toxic concentration for HepG2 cells, as determined by Fernandez-Cruz et al., 2013). For NP co-exposure, CuNPs and ZnONPs suspensions were first mixed (v/v = 1:1) and then added to the culture wells. As a control, cells exposed to serum-free medium were used. Exposure lasted for 48 h, after which the medium was removed, and three cytotoxicity assays were performed.

To establish the contribution of Zn ions to the toxicity caused by ZnONPs, cells were also co-exposed to CuNPs and to supernatants obtained after centrifugation (5500 rpm for 2 h at 4 °C) of ZnONPs suspensions. A Lince R centrifuge (Orto Alresa, Spain) was used for this purpose.

2.3. Cytotoxicity assays and protein measurements

We checked for possible interference of NPs with the wavelengths used to perform the measurements in the assays. No interaction at any of the concentrations used was detected.

The 4,5-dimethylthiazoyl-(2-yl)-2,5-diphenyltetrazolium bromide (MTT) assay, which evaluates effects on mitochondrial activity, was done following the method described by Mosmann (1983), which is based on the enzymatic conversion of MTT salts to formazan crystals. After removal of the medium, the cells were washed twice with PBS, and 100 μL of phenol red-free MEM containing MTT (0.5 mg/mL) was added to each well. The plates were incubated for 2 h at 37 °C. The formazan crystals were then dissolved by adding 100 μL of isopropanol. Absorbance was measured at 570 nm using a Genios microplate reader (TECAN, Männedorf, CH).

The 6-carboxy-2′7′-dichlorofluorescein diacetate (CFDA) assay was performed following Schirmer et al. (1997). CFDA is an esterase substrate that living cells can convert into a polar fluorescent dye. Its release outside of the cell and consequent reduction of concentration inside the cell is indicative of damage to the plasma membrane. After washing the exposed cells twice with PBS, we added 100 μL of phenol red-free MEM containing CFDA reagent to each well. After a 30-min incubation at 37 °C, fluorescence was measured at an excitation wavelength of 485 nm and an emission wavelength of 530 nm using a TECAN microplate reader.

The neutral red uptake (NRU) assay was done following Borenfreund and Puerner (1985). Since NR is accumulated in functional lysosomes in living cells, this test allows the assessment of lysosomal membrane integrity. After 48 h of exposure, the cell medium was removed, and the cells were washed twice with PBS. Next, 100 μL of phenol red-free MEM containing NR dye (0.1 mg/mL) was added to each well. The plates were incubated for 2 h at 37 °C, and the medium containing the NR dye was removed. The retained NR dye was extracted with 100 μL of 1% glacial acetic acid in 50% ethanol. Absorbance was measured at 550 nm using a TECAN microplate reader.

Total protein content was measured using the fluorescamine method (Udenfriend et al., 1972). Fluorescence was measured using a TECAN microplate reader at excitation/emission wavelengths of 360 and 450 nm.

2.4. Microscopy analyses

Transmission electron microscopy (TEM) was used to determine the size of pristine CuNPs and ZnONPs and of these NPs in suspensions (100 μg/mL) obtained in serum-free EMEM. For TEM analysis of pristine NPs, ethanol was used as a dispersant. A JEOL 2100 HT (JEOL Ltd., Japan) model operating at an accelerating voltage of 200 kV was used. Ultrathin sections of cells were analyzed by TEM to reveal the intracellular

accumulation/distribution of NPs and possible ultrastructural modifications. The method used has been described in Lammel et al. (2013), which is briefly shown in the Supplementary Materials. A JEOL 1010 JEM (JEOL) microscope operating at an acceleration voltage of 100 kV with integrated energy dispersive X-ray (EDX) spectroscopy (Oxford INCA) was used.

2.5. Inductively coupled plasma mass spectrometry

The cellular concentration (we were unable to distinguish between the inside and the surface of the cell) of zinc and copper was determined by inductively coupled plasma mass spectrometry (ICP-MS), as described in Fernandez-Cruz et al. (2013) and in Song et al. (2014). Details of the method have been included in the Supplementary Material. For this analysis, cells were exposed to CuNPs and ZnONPs in 6-well plates (Greiner Bio-one GmbH) and were cultured at an initial density of 1.25×10^6 cells/well in a total volume of 2.5 mL of medium per well. Exposure experiments were done as previously described. After exposure, the culture medium was removed, and cells were rinsed twice with PBS (2.5 mL/well) to remove the NPs remaining in the wells before cell collection for metal analyses.

2.6. Statistical analysis

Results obtained in the co-exposure experiments with each CuNPs concentration and a fixed ZnONPs concentration (6.25 μg/mL) were compared with the toxicity results corresponding to cells exposed to the CuNPs alone at the corresponding concentration. The normality and homoscedasticity of all data were checked by the Shapiro–Wilk test and Bartlett's test, respectively. For comparisons, a parametric repeated measurements-analysis of variance (RM-ANOVA) followed by a Dunnett's post hoc test was applied. The concentration–response function and IC_{50} (Inhibition Concentration 50, defined for the cytotoxicity assays as the concentration causing a 50% inhibition with respect to the maximal response observed in the controls) were estimated by fitting the cytotoxicity results to a regression equation for a sigmoidal curve: $y = \max/[1 + (x / IC_{50})\ b] + \min$, (where max is the maximal response observed, b is the slope of the curve, and min is the minimal response). SigmaPlot 12.0 (Systat Software Inc., Chicago, IL, USA) was used for all the statistical analysis and to calculate the IC_{50} values.

3. Results

3.1. Nanoparticle shape and size

TEM images revealed that the pristine CuNPs were spheroidal (Fig. S1A in the Supplementary Material), with a mean diameter of 63 ± 16 nm. Fig. 1A shows the size distribution histogram obtained from 145 measurements. ZnONPs were trapezoidal with round borders, and the mean sizes of three ZnONPs were 19 ± 4, 35 ± 11 and 57 ± 16 nm, respectively (Fig. S1B, C and D). The size frequency distribution histograms of pristine ZnONPs (n = 145) are shown in Fig. 1B, C and D.

In addition, we further characterized the size of NPs in the serum-free culture medium used for the cytotoxicity test. TEM micrographs revealed that the NPs in the medium showed a higher degree of aggregation than pristine particles (Fig. S2). The frequency size distribution of each NP in culture medium was determined by dynamic light scattering (DLS). Particle sizes of CuNPs and ZnONPs measured by DLS were 265,

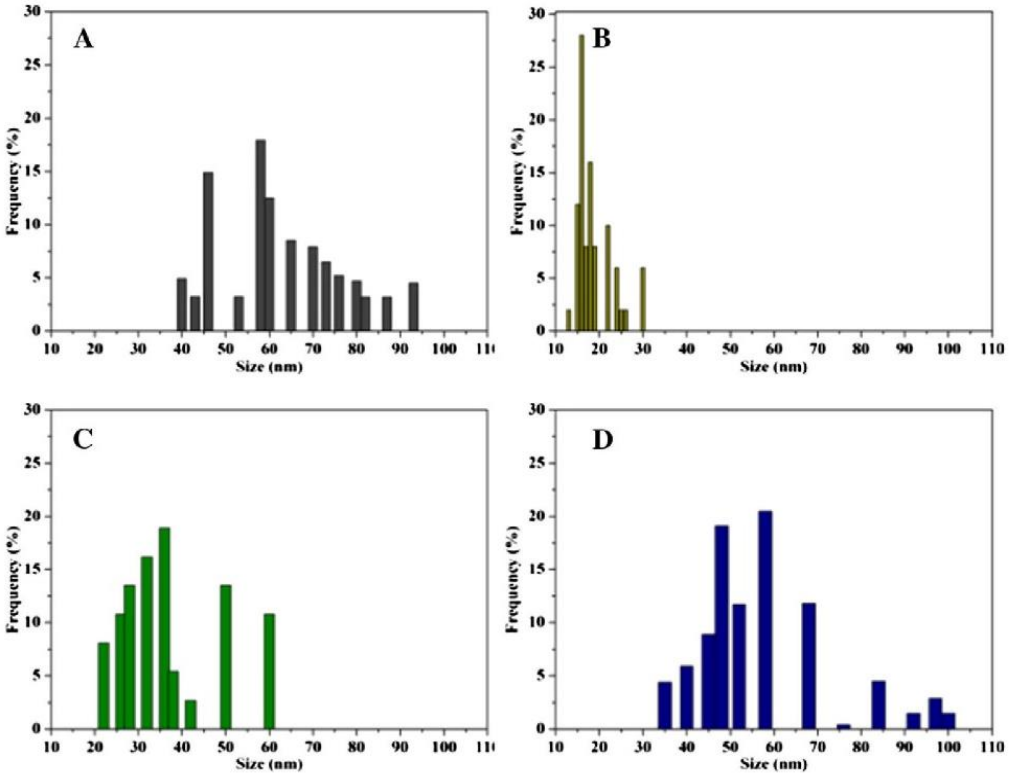

Fig. 1. Primary particle size distribution histograms of NPs used in this study. (A) CuNPs (40–93 nm), (B) ZnONPs (13–30 nm), (C) ZnONPs (22–60 nm), and (D) ZnONPs (35–100 nm).

1134, 1260 and 2978 nm respectively, which has been reported in our previous studies (Fernandez-Cruz et al., 2013; Song et al., 2014).

3.2. Effects of a non-toxic concentration of ZnONPs on the cytotoxicity of CuNPs

HepG2 cells exposed to CuNPs alone showed a concentration-dependent drop in viability when measured by the MTT assay, with a marked decrease at concentrations of 12.5 μg/mL or higher (Fig. 2A). None of the ZnONPs caused cytotoxicity in HepG2 cells, thereby indicating that the cells showed a normal mitochondrial function.

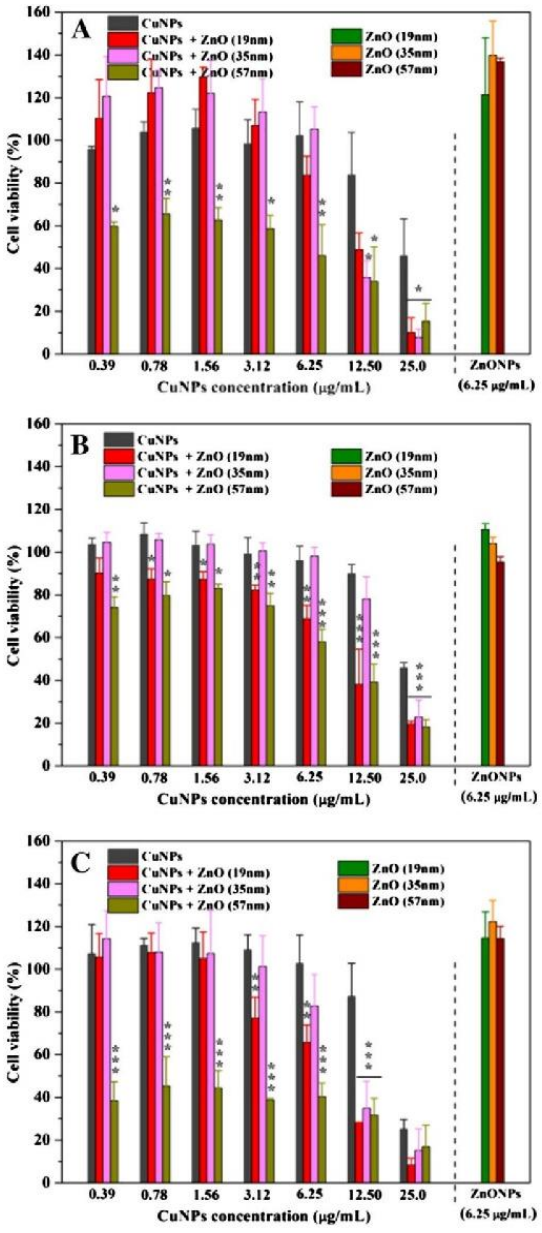

Fig. 2. Data obtained from cytotoxicity assays for CuNPs and ZnONPs. The concentrations of CuNPs ranged from 0.39 to 25.0 μg/mL, and those of ZnONPs were fixed at 6.25 μg/mL. (A) MTT assay, (B) CFDA assay, and (C) NRU assay. Results are expressed as percentage of viability compared with the control cells (*i.e.* cells without toxicant). Values represent the mean ± standard deviation of at least three independent experiments. Asterisks denote differences with respect to the effect produced by the CuNPs alone at each concentration tested (one-way RM-ANOVA followed by Dunnett's test): * $p < 0.05$, ** $p < 0.01$ and *** $p \leq 0.001$.

Surprisingly, the addition of ZnONPs to the CuNPs caused a clear increase in toxicity. Moreover, we found that the reduction in cell viability was related to the size of the ZnONPs. For the smallest ones (19 nm), significant differences in cell viability ($p < 0.05$) with respect to the cells exposed to CuNPs alone were observed only at the highest CuNPs concentration (25.0 μg/mL), while ZnONPs with a diameter of 35 nm led to a significant ($p < 0.05$) decrease in viability with respect to cells treated with CuNPs alone at a concentration of 12.5 μg/mL. The largest ZnONPs (57 nm, 6.25 μg/mL) caused a significant ($p < 0.05$) increase in toxicity with respect to cells exposed only to CuNPs at a concentration of 0.39 μg/mL (Fig. 2A).

In the CFDA and NRU assays, exposure to CuNPs alone caused a decrease in cell viability only at the highest CuNPs concentration (25.0 μg/mL). The results of these assays also showed enhanced cytotoxicity of CuNPs in HepG2 cells after addition of ZnONPs (Fig. 2B and C). In the CFDA assay, addition of ZnONPs with a diameter of 19 nm led to a significant ($p < 0.05$) decrease in cell viability with respect to cells exposed to CuNPs concentrations of 0.78 μg/mL or higher. ZnONPs with a size of 35 nm caused an increase ($p < 0.001$) in the cytotoxicity produced by a CuNPs concentration of 25.0 μg/mL. Finally, the largest ZnONPs (57 nm) led to a decrease ($p < 0.01$) in cell viability compared to that of the lowest CuNPs concentration tested (0.39 μg/mL).

In the case of the NRU assay, ZnONPs (19 nm) led to an increase ($p < 0.01$) in the cytotoxicity produced by the CuNPs when present at a concentration of 3.12 μg/mL; the ZnONPs (35 nm) caused this effect ($p < 0.001$) at a CuNPs concentration of 12.5 μg/mL; and the largest ZnONPs (57 nm) led to a reduction ($p < 0.001$) in cell viability at a CuNPs concentration of 0.39 μg/mL.

The IC_{50} values corresponding to CuNPs alone and also to co-exposure to CuNPs and ZnONPs of different sizes were calculated for the MTT assay (Fig. 3). The IC_{50} corresponding to the co-exposure to CuNPs and the largest ZnONPs (57 nm) was lower than that calculated after exposure to CuNPs alone or after co-exposure to CuNPs and the smallest ZnONPs (19 or 35 nm).

3.3. Species-specific contribution of ZnONPs to the enhanced cytotoxicity of CuNPs

We used the MTT assay to evaluate and compare the cytotoxicity of CuNPs alone with that of the supernatants obtained after centrifugation of ZnONPs and also with that of the mixtures of ZnONPs supernatants

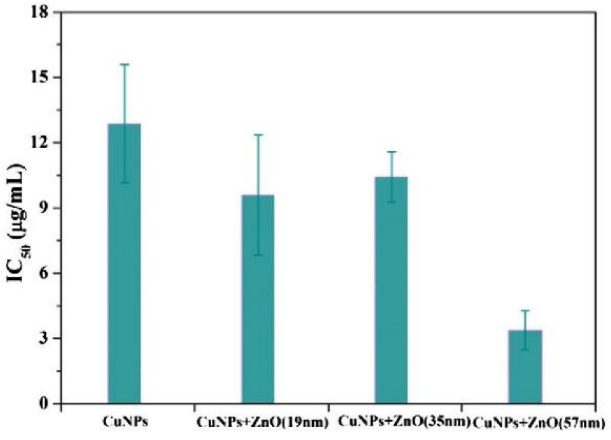

Fig. 3. IC_{50} calculated after exposure of HepG2 cells to CuNPs alone or to CuNPs (0.39–25.0 μg/mL) plus ZnONPs at a concentration of 6.25 μg/mL, according to the results from the MTT assay.

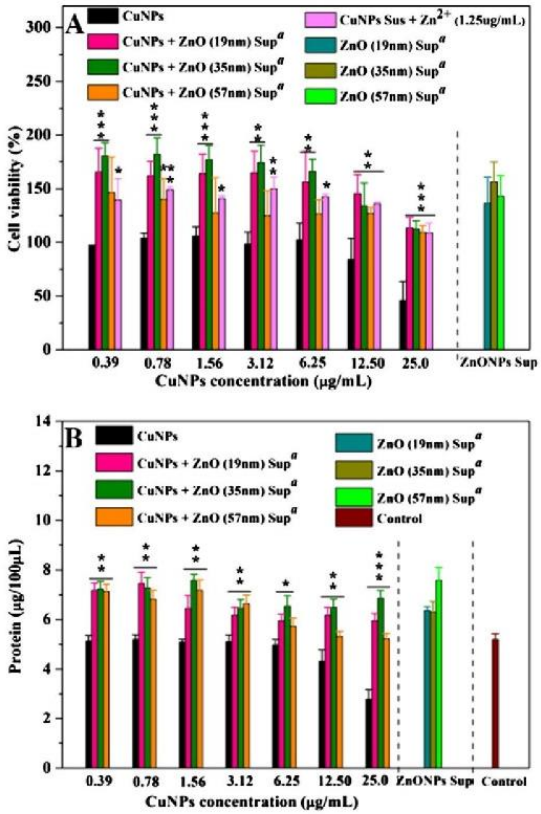

Fig. 4. (A) Viability of HepG2 cells exposed to ZnONPs supernatants (Sup) and CuNPs, as shown by the MTT assay. Results are expressed as percentage of viability compared to the control (*i.e.*, cells without toxicant). (B) Protein content of HepG2 cells co-exposed to ZnONPs supernatants and CuNPs. Values represent the mean ± standard deviation of at least three independent experiments. Asterisks denote statistically significant differences with respect to the effect produced by the CuNPs alone at each concentration tested (one-way RM-ANOVA followed by Dunnett's test); * $p < 0.05$, ** $p < 0.01$ and *** $p \leq 0.001$. [a]: The ZnONPs supernatants were obtained by centrifugation of ZnONPs suspensions.

and CuNPs (Fig. 4). DLS did not reveal the presence of any particle in these supernatants (Fig. S3), therefore zinc detected was present only in its ionic form (Table S1). The viability of HepG2 cells co-exposed to a mixture of ZnONPs supernatants and CuNPs was not reduced compared to that of cells exposed to CuNPs alone (Fig. 4A). On the contrary, an increase in cellular viability was observed, which led to significant ($p < 0.001$ to $p < 0.05$) differences for most of the supernatant co-exposure experiments. We also found that this effect was caused by addition of zinc sulfate as a source of zinc ion (Fig. 4A).

To determine whether the increase in viability observed in the MTT assay was related to an increase in the number of cells, optical microscopy observations were made and the protein content of the wells was measured. Exposure to ZnONPs supernatants (alone or together with CuNPs) caused a massive layer of hyper-confluent cells covering the bottom of the wells. At the same time, a substantial increase in the protein content of the wells was observed in cells treated with ZnONPs supernatants alone or when co-exposed to CuNPs (Fig. 4B).

3.4. Effects on HepG2 cell morphology and membrane

TEM was used to observe NP uptake and alterations of cell morphology or membrane integrity caused by individual NPs and mixtures. In the case of cells exposed to CuNPs alone at a concentration of 6.25 μg/mL, small particle clusters were observed dispersed in the cytosol (Fig. 5A). Once the NPs had entered the cell, the presence of vesicles surrounding some of these clusters suggested that intracellular processing mechanisms were operating (Fig. 5B). The cells treated with ZnONPs alone also showed particle uptake, with NPs present in the cytoplasm and without evidence of membrane disruption (Fig. 5C). TEM micrographs of HepG2 cells co-exposed to CuNPs and ZnONPs with a diameter of 19 nm showed the cytoplasm full of membrane-bound vesicular processing bodies with a large number of particles inside (Fig. 5D). Regarding co-exposure to CuNPs and larger ZnONPs (57 nm), we detected vesicles containing small particles (Fig. 5E). These particles exhibited a morphology similar to that of the particles observed when cells were exposed to these CuNPs alone. This finding is shown in the inset at the bottom of image 5E. Also, large amounts of bigger particles resembling ZnONPs in their pristine form (top inset Fig. 5E) were present but not surrounded by any membrane (therefore we assume that they were not undergoing processing, Fig. 5E and F). EDX analysis allowed the positive identification of only copper (Fig. 5E). The detection of zinc was not possible, possibly due to the high background readings for osmium used during cell fixation. However, the morphology and size of some of the particles strongly suggest the presence of ZnONPs.

3.5. ICP-MS measurement

In order to obtain additional data to clarify the mechanisms behind the enhancement of toxicity observed in the co-exposure experiments, the total copper and zinc content of HepG2 cells after 48 h of exposure was determined by means of ICP-MS after the acid digestion.

The copper content of cells exposed to CuNPs alone increased from 1.4 to 1.6 μg copper/mg cellular protein when the nominal concentration of CuNPs in the exposure medium increased from 6.25 to 25.0 μg/mL (Fig. 6). When cells were co-exposed to 6.25 μg/mL CuNPs and to ZnONPs of different sizes, the cellular copper content ranged from 0.28 to 0.43 μg copper/mg cellular protein. The zinc content in the co-exposed cells increased with the increasing CuNPs concentration in the cell medium.

The zinc concentrations in the supernatants obtained after centrifugation of ZnONPs (6.25 μg/mL) in medium (Table S1) ranged from 0.18 to 0.25 μg/mL, which implies that the dissolution of ZnONPs in serum-free EMEM was less than 4% in this study.

4. Discussion

Previous studies have reported that the size, shape, and surface coatings of NPs are major factors affecting their bioavailability and toxicity. However, these NP features, in turn, are influenced by the composition of the media used in toxicity assays (George et al., 2012; Song et al., 2014). In this study, NPs showed a higher degree of aggregation than originally observed in the pristine preparations. This finding can be attributed to the culture media, EMEM, which contains high amounts of a variety of ions (1.8 mM of Ca^{2+}, 0.8 mM of Mg^{2+}, 5.4 mM of K^+, and 135 mM of Na^+) (Table S2) that favors such aggregation.

Here we found that the combination of two distinct NPs at concentrations causing no or very limited cytotoxic effects when present alone led to a strong enhancement of toxicity. Potentiation phenomena have been described for a variety of chemicals in a number of systems (for instance studies of Smith et al. (2013) in *D. magna* and Torre-Roche et al. (2013) in *C. pepo* and *G. max*). However, few data are available on such effects after exposure to a mixture of NPs (Chen et al., 2008; Tang et al., 2013).

In cells co-exposed to CuNPs and ZnONPs, the content of copper decreased with respect to that present after exposure to CuNPs alone, as determined by ICP-MS measurements. This finding suggests that copper is not responsible for the observed toxicity. At the same time, a considerable rise in the cell content of zinc was observed, accompanied by an increase in toxicity. Variations in copper and zinc cellular content could

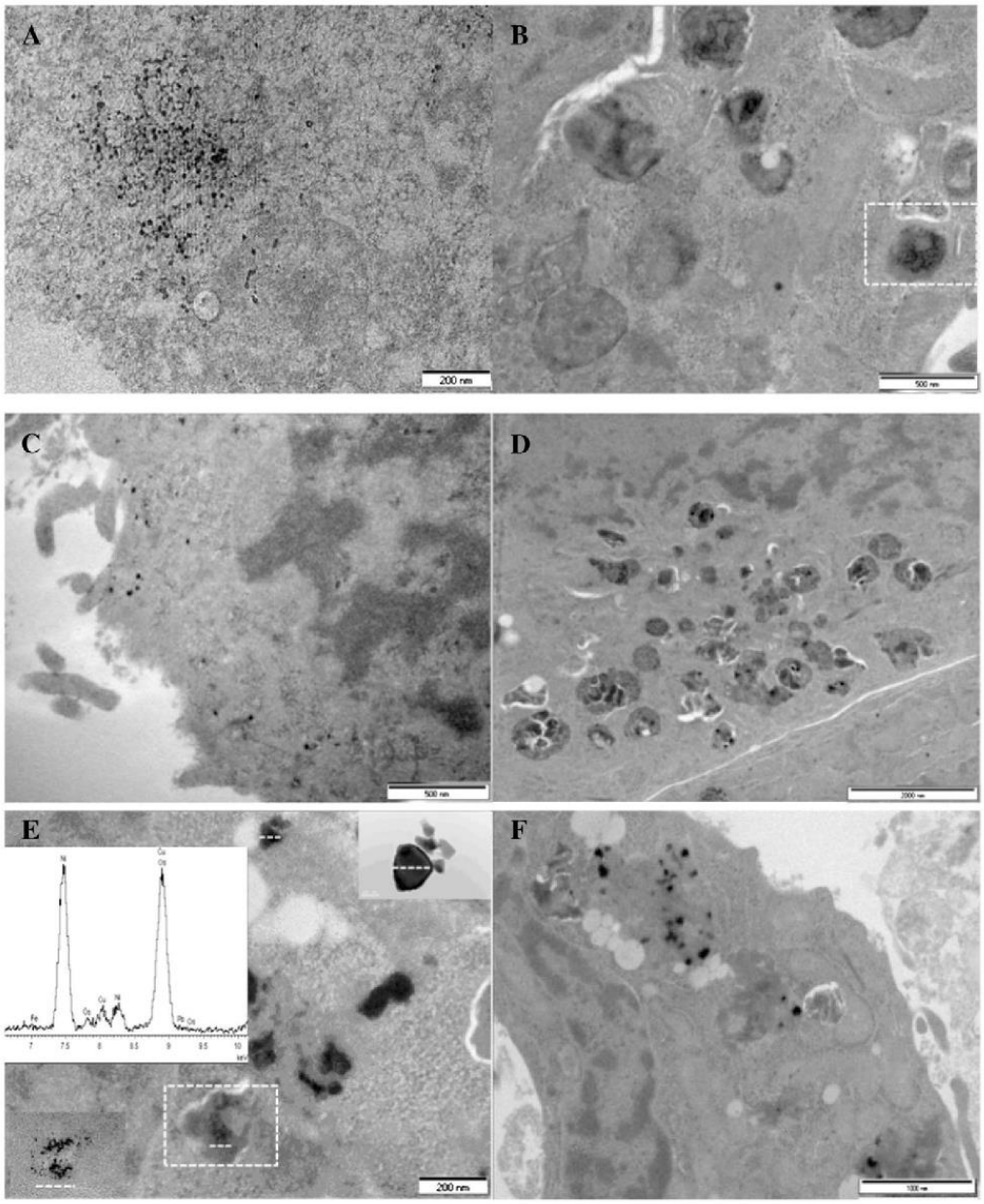

Fig. 5. TEM images of HepG2 cells after 48-h exposure experiments. (A–B) HepG2 cells exposed to CuNPs alone (6.25 μg/mL). CuNPs were observed in the cytoplasm (A) and being processed by autophago/lysosomal machinery (white box) (B). (C) HepG2 cells exposed to ZnONPs (19 nm, 6.25 μg/mL) alone. The ZnONPs accumulated in the cytoplasm and appeared to be processed by endo/lysosomal machinery. (D–F) HepG2 cells co-exposed to CuNPs (6.25 μg/mL) and ZnONPs (19 nm, 6.25 μg/mL) (D) or (57 nm, 6.25 μg/mL) (E and F). Insets in (E) present EDX analysis and CuNPs (bottom) and ZnONPs (top) images extracted from micrographs of cells exposed only to CuNPs or to ZnONPs, respectively, and indicate that these NPs show a similar size and shape as those observed in the co-exposure experiments.

be attributable to NPs or to soluble ions. TEM analysis indicated the presence of NPs that were similar in shape to the pristine CuNPs or ZnONPs. In addition, EDX analysis corroborated the presence of CuNPs inside the cells. These approaches thus confirmed the internalization of both kinds of NP into the cell. Although we cannot draw a conclusion about the mechanism by which ZnONPs or CuNPs are taken into the cell on the basis of the TEM images obtained, we found no evidence supporting endocytosis. We recently reported that graphene nanoplatelets penetrate HepG2 and PLHC cells without any apparent endocytosis (Lammel et al., 2013). Since the mechanism of cellular internalization of CuNPs and ZnONPs was not in the scope of this study, we performed no further studies in this direction; however, our results open up new avenues of research to elucidate this phenomenon.

To shed light on the mechanisms underlying the enhancement of toxicity observed after addition of ZnONPs and the increase in cellular zinc content, we attempted to differentiate the contribution of ZnONPs and of zinc ions to the elevated cytotoxicity. For this purpose, we

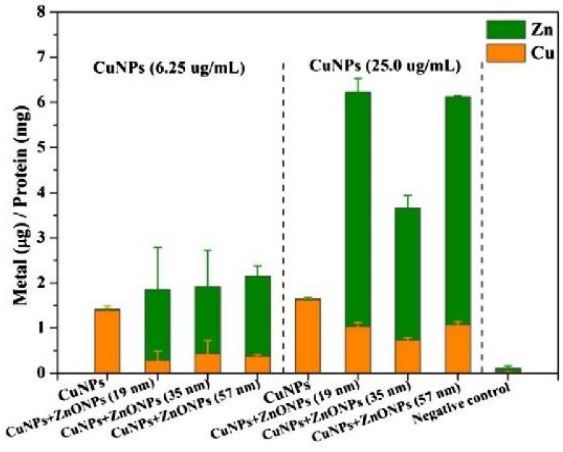

Fig. 6. Total zinc and copper content in HepG2 cells exposed to CuNPs alone or co-exposed to CuNPs and ZnONPs, as determined by ICP-MS.

performed co-exposure experiments using supernatants free of ZnONPs, as shown by DLS measurements, but containing zinc ions, as determined by ICP-MS analysis. Although the release of zinc ions has been proposed as the primary mechanism of ZnONPs toxicity in aquatic organisms (Franklin et al., 2007; Yoon et al., 2007), not only did co-exposure of HepG2 cells to ZnONPs supernatants and CuNPs not cause an increase in cytotoxicity, it led to greater cell viability. In previous studies using ZnONPs or CuNPs individually, we reported that cytotoxicity cannot be explained only by the ions released and that the direct interaction of NPs with cells is essential to induce the cytotoxicity of nanomaterials (Fernandez-Cruz et al., 2013; Song et al., 2014). The increase in cell viability after exposure to ZnONPs supernatants might be related to the nature of zinc as an essential element which, at the low concentrations (0.18–0.25 μg/mL) detected in the supernatants, exerts a positive effect on cell homeostasis and on the tolerance of HepG2 cells to CuNPs. A hormetic effect of zinc ions on the toxic impact of AgNPs on HepG2 cells and *Escherichia coli* has been reported (Kawata et al., 2009; Xiu et al., 2012). The presence of low amounts of zinc ions may activate cell repair mechanisms against these noxious substances, thus compensating the deleterious effects of the exposure.

It must be noted here that we were unable to establish a relationship between the zinc concentration of the supernatants and ZnONPs size. In a previous study, we found that the amount of copper ions released from CuNPs was not determined by NPs size (Song et al., 2014). This finding implies that, in addition to NP size, other factors contribute to the dissolution of these particles. Therefore, the toxicity caused by any nanomaterial is either directly or indirectly dependent on size.

The decrease in cellular content of copper after co-exposure to CuNPs and ZnONPs suggests that zinc competes with copper for cell uptake. It appears that this competition can lead to a preferential internalization of ZnONPs, leading to a decrease in the total content of copper inside the cell, which may also contribute to the detrimental effects observed. The mutual inhibition of the intestinal absorption by these two elements has already been reported (Hall et al., 1979; Hogstrand, 2011). Similarly, the inhibition of copper uptake has been reported in Caco-2 cells (Arredondo et al., 2006). In this cell line, an excessive intake of zinc results in overt copper deficiency, which has been exploited beneficially for the treatment of Wilson's disease to prevent copper accumulation (Barone et al., 1998).

In cells exposed to CuNPs alone, TEM analysis allowed observation of the presence of NPs surrounded by cellular membranes with a structure that could be assimilated to autophagosomes. In the co-exposure experiments, these kinds of membrane structures were seen only around NPs similar in shape and size to those inside the cells exposed solely to CuNPs. However, these membrane structures were not found in cells exposed to ZnONPs alone, neither were they detected around NPs similar to ZnONPs in the micrographs of cells in the co-exposure experiments. These observations suggest that the CuNPs processing route is not affected by the presence of ZnONPs but rather that the opposite is occurring. Therefore, it is possible that zinc levels increase to reach a critical concentration that affects cell homeostasis, leading to cell death. As stated earlier, since supernatants containing only zinc ions did not cause toxicity when co-incubated with CuNPs, we deduce that the contribution of zinc to the toxicity was produced only by the nano-particulate fraction. TEM micrographs showed a number of relatively large ZnONPs aggregates or agglomerates inside the cells and close to the plasma membranes. These aggregates were not surrounded by membranes and therefore were not being processed by the cellular machinery. It is therefore plausible that these unprocessed ZnONPs damaged the cell membranes, thus causing cell death.

It has been widely considered that the toxicity of NPs is highly dependent on their size, with smaller NPs being more cytotoxic, which is generally attributed to an increase in their specific surface (Kim et al., 2012; Maurer-Jones et al., 2013; Unrine et al., 2010). However, the results of the co-exposure experiments performed in the present work differ from those obtained in studies using individual NPs. Here, addition of ZnONPs with the largest size (57 nm) to CuNPs caused the highest cytotoxicity in HepG2 cells. These findings are in agreement with the idea that the interaction of large ZnONPs aggregates with the membrane is one of the factors driving toxicity (Vakurov et al., 2013; Vandebriel and De Jong, 2012). Moreover, they indicate that the exposure of cells to combinations of NPs introduces new factors that greatly contribute to determining the global toxicity of the mixture.

5. Conclusion

Here we addressed the potentiation effect of ZnONPs at the non-toxic concentration and CuNPs on the cytotoxicity of HepG2 cells. We observed an enhancement of toxicity, thus pointing to a potentiation effect. We found that the enhancement of CuNPs toxicity produced by the addition of ZnONPs is attributable to the nano-particulate fraction (and not to zinc ions) and is influenced by the size of the ZnONPs. In addition, microscopy studies and the measurement of cellular concentrations of zinc and copper indicated that the build-up of large unprocessed ZnONPs aggregates or agglomerates might explain the increase in toxicity observed.

Although potentiation effects are considered when evaluating risk in specific cases, such as in workplace exposure or for pesticide residues in food and feed (Smith et al., 2013), most regulatory frameworks for chemicals continue to focus on the testing of single substances. However, here we demonstrate that the combined toxicity of several substances—a realistic scenario—can differ greatly from that produced by each individual substance alone.

Conflict of interest

No conflict of interest exists in the submission of this manuscript 'The potentiation effect makes the difference: Non-toxic concentrations of ZnO nanoparticles enhance Cu nanoparticle toxicity in vitro'.

Acknowledgments

The authors thank Luis Alte Garcia-Olias (INIA, Spain) for assistance with cell cultures. This work was funded through INIA project AT2011-001.

Appendix A. Supplementary data

Supplementary data to this article can be found online at http://dx.doi.org/10.1016/j.scitotenv.2014.10.020.

References

Arredondo M, Martinez R, Nunez MT, Ruz M, Olivares M. Inhibition of iron and copper uptake by iron, copper and zinc. Biol Res 2006;39:95–102.

Babich H, Stotzky G. Toxicity of zinc to fungi, bacteria, and coliphages: influence of chloride ions. Appl Environ Microbiol 1978;36:906–14.

Barone A, Ebesh O, Harper R, Wapnir R. Placental copper transport in rats: effects of elevated dietary zinc on fetal copper, iron and metallothionein. J Nutr 1998;128:1037–41.

Bolyard SC, Reinhart DR, Santra S. Behavior of engineered nanoparticles in landfill leachate. Environ Sci Technol 2013;47:8114–22.

Borenfreund E, Puerner JA. Toxicity determined in vitro by morphological alterations and neutral red absorption. Toxicol Lett 1985;24:119–24.

Chen B, Dai Y, Wang X, Zhang R, Xu W, Shen H, et al. Synergistic effect of the combination of nanoparticulate Fe_3O_4 and Au with daunomycin on K562/A02 cells. Int J Nanomedicine 2008;3:343–50.

Fernandez-Cruz ML, Lammel T, Connolly M, Conde E, Barrado AI, Derick S, et al. Comparative cytotoxicity induced by bulk and nanoparticulated ZnO in the fish and human hepatoma cell lines PLHC-1 and Hep G2. Nanotoxicology 2013;7:935–52.

Franklin NM, Rogers NJ, Apte SC, Batley GE, Gadd GE, Casey PS. Comparative toxicity of nanoparticulate ZnO, bulk ZnO, and ZnCl2 to freshwater microalgae (*Pseudokirchneriella subcapitata*): the importance of particle solubility. Environ Sci Technol 2007;41:8484–90.

George S, Lin S, Ji Z, Thomas CR, Li L, Mecklenburg M, et al. Surface defects on plate-shaped silver nanoparticles contribute to its hazard potential in a fish gill cell line and zebrafish embryos. ACS Nano 2012;6:3745–59.

Gottschalk F, Sonderer T, Scholz RW, Nowack B. Modeled environmental concentrations of engineered nanomaterials (TiO_2, ZnO, Ag, CNT, Fullerenes) for different regions. Environ Sci Technol 2009;43:9216–22.

Guo B, Zebda R, Drake SJ, Sayes CM. Synergistic effect of co-exposure to carbon black and Fe_2O_3 nanoparticles on oxidative stress in cultured lung epithelial cells. Part Fibre Toxicol 2009;6. http://dx.doi.org/10.1186/1743-8977-6-4.

Gystrzejewska-Piotrowaka G, Golimowaki J, Urban PL. Nanoparticles: their potential toxicity, waste and environmental management. Waste Manag 2009;29:2587–95.

Hall AC, Young BW, Bremner I. Intestinal metallothionein and the mutual antagonism between copper and zinc in the rat. J Inorg Biochem 1979;11:57–66.

Hogstrand C. Zinc. In: Wood CM, Farrell AP, Brauner CJ, editors. Homeostasis and toxicology of essential metals. Book Series: Fish PhysiologyNew York, USA: Academic Press; 2011. p. 135–200.

Jonas RB. Acute copper and cupric ion toxicity in an estuarine microbial community. Appl Environ Microbiol 1989;55:43–9.

Kawata K, Osawa M, Okabe S. *In vitro* toxicity of silver nanoparticles at noncytotoxic doses to HepG2 human hepatoma cells. Environ Sci Technol 2009;43:6046–51.

Kim T, Kim M, Park H, Shin US, Gong M, Kim H. Size-dependent cellular toxicity of silver nanoparticles. J Biomed Mater Res A 2012;100A:1033–43.

Lammel T, Boisseaux P, Fernández-Cruz ML, Navas JM. Internalization and cytotoxicity of graphene oxide and carboxyl graphene nanoplatelets in the human hepatocellular carcinoma cell line HepG2. Part Fibre Toxicol 2013;10:1–21.

Li S, Pan X, Fan ZY, Wallis LK, Chen ZL, Diamond SA. Comparison of the phototoxicity of TiO_2 nanoparticle and graphene–TiO_2 nanoparticle composite in *Daphnia magna* and *Oryzias latipes*. Chemosphere 2014;112:62–9.

Ma H, Wallis LK, Li S, Cañas-Carrell JE, Parra AM, Diamond SA. Toxicity of zinc oxide nanoparticles: role of particle dissolution and photocatalytic reactive oxygen species (ROS) production. Environ Pollut 2014;193:165–72.

Maurer-Jones MA, Gunsolus IL, Murphy CJ, Haynes CL. Toxicity of engineered nanoparticles in the environment. Anal Chem 2013;85:3036–49.

Mosmann T. Rapid colorimetric assay for cellular growth and survival: application to proliferation and cytotoxicity assays. J Immunol Methods 1983;65:55–63.

Qiu A, Hogstrand C. Functional expression of a low-affinity zinc uptake transporter (FrZIP2) from pufferfish (*Takifugu rubripes*) in MDCK cells. Biochem J 2005;390:777–86.

Regoli F, Principato G. Glutathione, glutathione-dependent and antioxidant enzymes in mussel, *Mytilus galloprovincialis*, exposed to metals under field and laboratory conditions: implications for the use of biochemical biomarkers. Aquat Toxicol 1995;31:143–64.

Schirmer K, Chan AGJ, Greenberg BM, Dixon DG, Bols NC. Methodology for demonstrating and measuring the photocytotoxicity of fluoranthene to fish cells in culture. Toxicology In vitro 1997;11:107–19.

Smith KEC, Schmidt SN, Dom N, Blust R, Holmstrup M, Mayer P. Baseline toxic mixtures of non-toxic chemicals: "solubility addition" increases exposure for solid hydrophobic chemicals. Environ Sci Technol 2013;47:2026–33.

Song L, Connolly M, Fernandez-Cruz ML, Vijver MG, Fernandez M, Conde E, et al. Species-specific toxicity of copper nanoparticles among mammalian and piscine cell lines. Nanotoxicology 2014;8:383–93.

Tan C, Fan W, Wang W. Role of titanium dioxide nanoparticles in the elevated uptake and retention of cadmium and zinc in *Daphnia magna*. Environ Sci Technol 2012;46:469–76.

Tang Y, Li S, Qiao J, Wang H, Li L. Synergistic effects of nano-sized titanium dioxide and zinc on the photosynthetic capacity and survival of *Anabaena* sp. Int J Mol Sci 2013;14:14395–407.

Torre-Roche RDL, Hawthorne J, Musante C, Xing B, Newman LA, Ma X, et al. Impact of Ag nanoparticle exposure on p,p′-DDE bioaccumulation by *Cucurbita pepo* (zucchini) and *Glycine max* (soybean). Environ Sci Technol 2013;47:718–25.

U.S. EPA. Nanotechnology White Paper. EPA 100/B-07/001. Washington, DC: U.S. Environmental Protection Agency, Science Policy Council; 2007.

Udenfriend S, Stein S, Böhlen P, Dairman W, Leimgruber W, Weigele M. Fluorescamine: a reagent for assay of amino acids, peptides, proteins, and primary amines in the picomole range. Science 1972;178:871–2.

Unrine JM, Tsyusko OV, Hunyadi SE, Judy JD, Bertsch PM. Effects of particle size on chemical speciation and bioavailability of copper to earthworms (*Eisenia fetida*) exposed to copper nanoparticles. J Environ Qual 2010;39:1942–53.

Vakurov A, Mokry G, Drummond-Brydson R, Wallace R, Svendsen C, Nelson A. ZnO nanoparticle interactions with phospholipid monolayers. J Colloid Interface Sci 2013;404:161–8.

Vandebriel RJ, De Jong WH. A review of mammalian toxicity of ZnO nanoparticles. Nanotechnol Sci Appl 2012;5:61–71.

Wapnir RA, Balkman C. Inhibition of copper absorption by zinc. Effect of histidine. Biol Trace Elem Res 1991;29:193–202.

Westin G, Schaffner W. A zinc-responsive factor interacts with a metal-regulated enhancer element (MRE) of the mouse metallothionein-I gene. EMBO J 1988;12:3763–70.

Wilson M, Hogstrand C, Maret W. Picomolar concentrations of free zinc(II) ions regulate receptor protein-tyrosine phosphatase β activity. J Biol Chem 2012;287:9322–6.

Xiu Z, Zhang Q, Puppala HL, Colvin VL, Alvarez PJJ. Negligible particle-specific antibacterial activity of silver nanoparticles. Nano Lett 2012;12:4271–5.

Yoon KY, Byeon JH, Park JH, Hwang J. Susceptibility constants of *Escherichia coli* and *Bacillus subtilis* to silver and copper nanoparticles. Sci Total Environ 2007;373:572–5.

CHAPTER 4

Testing the oxidative stress pathway of toxicity for CuNPs in a liver cell line.

Chapter 4 is entitled: Testing the oxidative stress pathway of toxicity for CuNPs in a liver cell line. In this chapter, through *research article 1*, the extent to which the cytotoxic effect of CuNPs is governed by oxidative stress was investigated. Liver cells exposed to CuNPs produce high levels of reactive oxygen species (ROS) (*introductory paper 2*). The generation of ROS and consequent oxidative stress is regarded as a relevant mechanism for nanoparticle toxicity. This is plausible for CuNPs as the copper ion is a redox-active metal and also if taken up by the cell NPs disruption of the mitochondria may lead to the release of endogenous ROS stores. To investigate the extent to which the ion or NP contributes to ROS generation two CuNPs with high and low dissolution profiles were included in the study. Results revealed ROS elicitation was CuNP-specific. Also it was important to question if an increase in intracellular ROS was the cause or consequence of cellular damage that leads to cytotoxicity. To answer this question liver cells were challenged with high reactive oxygen species (ROS) levels following CuNP exposure, while at the same time the aryl hydrocarbon receptor (AhR) gene battery of cellular antioxidant defence was activated by the ligand ß-Naphthoflavone (BNF). We hypothesised that through simultaneous activation of the AhR signalling pathway, and its gene battery, by BNF the anti-oxidative response would be upregulated and the cells redox status brought back into equilibrium following CuNP insult. Interestingly despite ROS abrogation and redox balance the levels of cell viability did not increase. This result supports the hypothesis that the reduced viability of H4IIE liver cells following exposure to CuNPs occurs independently of intracellular ROS and redox status and other pathways of NP cytotoxicity must be explored.

Research paper 1: Recovery of redox homeostasis altered by CuNPs in H4IIE liver cells does not reduce the cytotoxic effects of these NPs: an investigation using aryl hydrocarbon receptor (AhR) dependent antioxidant activity.

Chemico-Biological Interactions 228 (2015) 57–68

Contents lists available at ScienceDirect

Chemico-Biological Interactions

journal homepage: www.elsevier.com/locate/chembioint

Recovery of redox homeostasis altered by CuNPs in H4IIE liver cells does not reduce the cytotoxic effects of these NPs: An investigation using aryl hydrocarbon receptor (AhR) dependent antioxidant activity

Mona Connolly, María Luisa Fernández-Cruz, José María Navas *

Instituto Nacional de Investigación y Tecnología Agraria y Alimentaria (INIA), Carretera de la Coruña Km 7.5, Madrid, Spain

ARTICLE INFO

Article history:
Received 5 September 2014
Received in revised form 26 November 2014
Accepted 7 January 2015
Available online 21 January 2015

Keywords:
Copper nanoparticles (CuNPs)
Oxidative stress
H4IIE
Aryl hydrocarbon receptor (AhR)
ß-Naphthoflavone (ßNF)
Co-incubation

ABSTRACT

The generation of reactive oxygen species (ROS) and consequent oxidative stress is regarded as a relevant mechanism for nanoparticle toxicity. In cells, the activation of the aryl hydrocarbon receptor (AhR) triggers a cascade of defence responses against oxidative stress. By increasing AhR dependent cellular anti-oxidant activity, we tested the extent to which the cytotoxic effect of copper nanoparticles (CuNPs) is governed by oxidative stress. H4IIE rat hepatoma cells were challenged with high ROS levels after exposure to CuNPs, while the AhR-induced cellular anti-oxidant defence was simultaneously activated by the AhR ligand beta-Naphthoflavone (ßNF). Activation of phase II detoxification enzymes (as glutathione-S-transferases, GSTs) and anti-oxidants (glutathione, GSH) led to a complete abrogation of CuNP-induced ROS production. However, a concurrent reduction in cytotoxicity was not detected, thereby indicating that CuNPs exert non-oxidative stress mediated cytotoxic effects. Transmission electron microscopy analysis pointed to a direct physical perturbation of cellular structures by CuNPs, thus contributing to their cytotoxicity. Our observations highlight that distinct mechanisms underlie the toxicity of ions and NPs and indicate that while ROS elicitation is CuNP-specific, the cytotoxic action of these particles may not be directly related to their pro-oxidative activity. These findings have important implications with respect to the oxidative stress paradigm used to explain NP toxicity.

1. Introduction

The increasing use of nano-sized materials in a variety of products has raised serious concerns about the possible release of this new class of anthropogenic contaminants into the environment [1]. Consequently, the assessment of the risks associated with these substances has become of great importance. Toxicity assessments using CuNPs currently lags behind research efforts made for other nanomaterials. However research that has been performed shows striking evidence of grave toxicological effects of CuNPs on the kidney, liver and spleen in mouse models [2]. This, along with the fact that heightened toxic efficacy of Cu at nanoscale compared to bulk counterpart has been highlighted, points to possible increased hazards associated with nanoforms [3].

The mechanisms underlying CuNPs toxic insults (and many other nanomaterials) are currently under debate. Together with the physical damage of cell membranes caused by direct contact with NPs [4,5], one of the most accepted theories to explain the toxicity of these particles is the oxidative stress paradigm [6]. Countless studies point to and highlight the association between increased reactive oxygen species (ROS) levels and cytotoxicity after exposure to NPs [7–9].

Oxidative stress is the result of a redox imbalance between the generation of ROS and the compensatory metabolic response of the endogenous anti-oxidant networks of the cell. Cells respond to ROS

Abbreviations: CuNP, copper nanoparticle; ROS, reactive oxygen species; AhR, aryl hydrocarbon receptor; ßNF, ß-Naphthoflavone; αNF, α-Naphthoflavone; GST, glutathione-S-transferase; GSH, glutathione; GSSG, oxidised glutathione; Nrf2, nuclear factor erythroid-2-related factor; HO-1, heme oxygenase-1; SnPP, tin protoporphyrin IX; TEM, transmission electron microscopy; AREs, anti-oxidant response elements; XREs, xenobiotic response elements; LOEC, lowest observed effect concentration; CYP1A1, cytochrome P450, family 1, subfamily A, polypeptide 1; RR, resazurin reduction; EROD, 7-ethoxyresorufin-*O*-deethylase; MTT, 3-[4,5-dimethylthiazol-2-yl]-2,5 diphenyl tetrazolium bromide; P/S, penicillin and streptomycin; EMEM, Eagle Minimum Essential Medium; NEAA, non-essential amino acids; BSA, bovine serum albumin; DLS, dynamic light scattering; PBS, phosphate-buffered saline; FBS, foetal bovine serum; NADPH, β-nicotinamide adenine dinucleotide 2′-phosphate reduced tetrasodium salt hydrate.

* Corresponding author at: Departamento de Medio Ambiente, Instituto Nacional de Investigación y Tecnología Agraria y Alimentaria (INIA), Carretera de la Coruña Km 7.5, E-28040 Madrid, Spain. Tel.: +34 91 347 41 55/87 75; fax: + 34 91 347 40 08.

E-mail addresses: connolly.mona@inia.es (M. Connolly), fcruz@inia.es (M.L. Fernández-Cruz), jmnavas@inia.es (J.M. Navas).

http://dx.doi.org/10.1016/j.cbi.2015.01.012
0009-2797/

insult by activating signalling pathways that trigger the expression of genes that participate in the anti-oxidative response. One such pathway involves the activation of the nuclear factor erythroid-2-related factor (Nrf2), which is responsible for the induction of genes that hold anti-oxidant response elements (AREs) in their promoters. These genes encode for a range of cytoprotective enzymes, including phase II detoxifying enzymes such as glutathione-S-transferase (GST), the stress-protein heme oxygenase 1 (HO-1), and also key players in the synthesis of glutathione (GSH) [10–12]. GSTs catalyse the nucleophilic addition of GSH to electrophiles, making them less reactive and more soluble.

The induction of phase II GST and other detoxification activities directed at reducing oxidative stress is also triggered by other transcription factors, as for instance the aryl hydrocarbon receptor (AhR) [13]. This receptor can be activated by a variety of xenobiotics sharing some structural features (polycyclic aromatic compounds that can easily take a planar conformation) [14,15]. This receptor induces genes that hold xenobiotic response elements (XREs) in their promoter regions. A prototypical AhR activator used in a variety of studies is ß-Naphthoflavone (ßNF). Activation of AhR results in an increase in phase I cytochrome P4501A (CYP1A) mono-oxygenase enzyme induction involved in oxidation reactions but also of phase II GST detoxification activity [13]. CYP1A can be evidenced at the enzymatic level by measuring the associated ethoxyresorufin-*O*-deethylase (EROD) activity. Recent data provide evidence for a cross-talk between the Nrf2 pathway and the pathway leading to the induction of XRE-driven genes by the AhR [14,16–18]. Unlike the AhR, the Nrf2 transcription factor is not ligand activated, rather it responds to xenobiotics and endogenous compounds that are thiol reactive, such as reactive oxygen species or electrophilic insults.

A variety of modes of toxicity have been suggested for metal ions and NP fractions [19,20]. The relative contribution of free ions to NP toxicity and ROS generation is debatable and the role of dissolution in nanoparticle toxicity further increases the complexity of this process. Kim and colleagues [21] provide evidence that NP cytotoxicity is caused by NP-specific oxidative stress responses, independently of the toxicity of ions. Other studies support the hypothesis that the toxic effects of these particles are simply due to the release of ions into the surrounding environment, with a limited material effect [22], while others argue joint action [23,24]. Recent papers also suggest that ROS-independent mechanisms involving cell cycle arrest are associated with NP toxicity [25] and that oxidative stress is merely a secondary effect of direct physical damage by NPs [26,27]. Also, metal NPs show anti-oxidative properties that promote cell survival under conditions of oxidative stress. For example, cerium oxide (CeO_2) and yttrium oxide (Y_2O_3) have been reported to exhibit ROS scavenging capacity and neuroprotective activity in rodent nervous system HT22 cells [28,29].

Copper is a redox active metal. It directly catalyses the formation of ROS through redox cycling between different valence states either through Haber-Weiss reactions or Fenton chemistry [30]. Copper capacity to stimulate Nrf2-dependent transcriptional activity and induce HO-1 activity has been reported [30,31]. In a previous study, we showed that copper nanoparticles (CuNPs) induce high levels of ROS in a variety of mammalian and piscine cell lines [32]. Following this line of work, the main objective of the present work was to determine if CuNP cytotoxicity is associated with the observed increase in ROS levels. We have exposed H4IIE cells (a rat hepatoma cell line) to two of the previously used CuNPs (CuNP 25 and CuNP 78, with 25 and 78 nm in size, respectively), or to $Cu(NO_3)_2$, used as a source of ions that served as a control, and characterised the induction of ROS. Then to test to what extent the cytotoxic effect of CuNPs is governed by ROS generation and oxidative stress we increased endogenous cellular antioxidant activity through activation of the AhR signalling pathway. We have chosen ß-Naphthoflavone (ßNF), as a prototypical AhR inducer for the co-incubation experiments. Co-incubations allowed us to simultaneously study the responses of H4IIE cells to activation of the ßNF detoxification pathway and CuNP-induced ROS generation. We characterised the redox status in cells exposed to CuNPs and to $Cu(NO_3)_2$ alone and compared the responses with those obtained after simultaneous co-incubation with the AhR ligand ßNF.

2. Materials and methods

2.1. Chemicals and reagents

Uncoated CuNPs of 25 and 78 nm (CuNP 25 and CuNP 78), in size according to the manufacturer's information, were purchased from IoLiTec, Inc. (Heilbronn, Germany) and NanoAmor® USA (Houston, TX, USA), respectively. L-Glutamine (200 mM), foetal bovine serum (FBS), penicillin, and streptomycin (10,000 U/mL, 10 mg/mL, respectively) (P/S), 100X non-essential amino acids (NEAA), and Eagle's Minimum Essential Medium (EMEM) were purchased from Lonza (Barcelona, Spain). Phenol-red free, serum-free Minimum Essential Medium (MEM) was supplied by PAN Biotech GmbH, (Aidenbach, Germany). Acetonitrile (HPLC grade) was provided by Panreac (Barcelona, Spain). Bovine serum albumin (BSA) was purchased from Merck group KGaA (Darmstadt, Germany). Glutaraldehyde (Electron Microscopy grade, 25%), osmium tetroxide, and Spurr's resin were from TAAB Laboratories Equipment Ltd. (Aldermaston, UK). Paraformaldehyde (16%) was sourced from Electron Microscopy Sciences (Hatfield, UK). All other chemicals and reagents used, including ßNF and α-Naphthoflavone (αNF), were supplied by Sigma Aldrich (Madrid, Spain).

2.2. Cell culture conditions

The rat hepatoma cell line H4IIE was cultured in EMEM supplemented with 10% FBS, 1% P/S, 1% L-glutamine, and 1% NEAA at 37 °C in a humidified atmosphere of 5% CO_2. Cells were seeded at a density of 2.5×10^4 cells/well in 96-well plates (Greiner Bio-One GmbH, Germany). For TEM analysis, they were seeded on poly-L-lysine-coated glass coverslips (BD Biosciences, Erembodegem, Belgium) in 24-well plates (Greiner Bio-One GmbH, Germany).

2.3. Nanoparticle preparation and physico-chemical characterisation

We prepared 200 μg/mL suspensions of CuNP 25 and CuNP 78 in EMEM (10% FBS) directly prior to exposure experiments. In order to improve dispersion, the suspensions were sonicated for 10 min in a water bath sonicator (S 40 H Elmasonic, Elma, Germany). Dynamic light scattering (DLS) using a Zetasizer Nano-ZS apparatus (Malvern Instruments Ltd., Malvern, UK) was then used to measure the hydrodynamic size of the particles upon dispersion (time 0) and after 24 h of incubation under culture conditions (37 °C/5% CO_2). Supernatants were prepared from these NP suspensions after a 24 h incubation under cell-free culture conditions and 20 min centrifugation at 13,362×*g* (5415 R series centrifuge, Eppendorf, Hamburg, Germany), as described by Song and colleagues [32]. These supernatants contained only copper ion fractions, as shown by DLS analysis. The ion concentration in each CuNP suspension was determined in a previously published study [32], which established the dissolution rate of a 200 μg/mL suspension of CuNPs. In the present study, DLS was also performed with suspensions of CuNPs co-incubated with ßNF (2.5 μM) for 24 h in order to characterise the size distribution of NPs in co-incubation experiments. Size distributions are reported on the basis of the mean of four

measurements per sample and three independent measurements and were calculated using Zetasizer Software version 6.34 (Malvern Instruments Ltd).

2.4. Exposures

Cells were exposed for 24 h to a range of CuNP suspensions, their supernatants, the Cu salt $Cu(NO_3)_2$, and ßNF and αNF solutions, alone or in co-incubation experiments. For comparative purposes, results corresponding to $Cu(NO_3)_2$ are presented in relation to the concentration (μg/mL) of copper content (and not of the salt). Serial half dilutions (1:2) of the working CuNPs and $Cu(NO_3)_2$ suspensions were performed directly in the 96-well culture plate, giving a nominal concentration range of between 0.78 and 200 μg/mL. However, instead of nominal concentrations, we used true exposure concentrations when presenting our results. These concentrations were determined by inductively coupled plasma mass spectrometry (ICP-MS), and were published elsewhere [32]. These concentrations ranged between 0.5 and 153 μg/mL for CuNP 25, between 0.1 and 89 μg/mL for CuNP 78, and between 0.5 and 159 μg/mL of Cu content for $Cu(NO_3)_2$. Cu ion fractions were prepared from the supernatants of serial half dilutions of CuNP suspensions prepared in microfuge tubes. The concentration of Cu ion in the supernatants of the 200 μg/mL CuNP 25 and CuNP 78 suspensions was 112 and 20 μg/mL, respectively. Thus the concentration ranges of Cu ion tested in the supernatants prepared for each concentration of CuNP ranged from 0.37 to 112 μg/mL for CuNP 25 and 0.02 to 20 μg/mL for CuNP 78.

Cells were also exposed to serial dilutions of ßNF (concentration range of 0.078 to 20 μM with a dilution factor of 2) originally prepared in dimethyl sulfoxide (DMSO). The maximal DMSO concentration of 0.1% (v/v) in medium was added to the control cells and did not impair cell viability. Simultaneous 24 h co-exposures to CuNPs plus ßNF or the Cu salt plus ßNF were also performed. Cells were exposed simultaneously to 2.5 μM ßNF plus a sublethal concentration of CuNP 25 (0.5–17.8 μg/mL), CuNP 78 (0.25–13.7 μg/mL) or $Cu(NO_3)_2$ (0.5–42 μg/mL). In cell viability and ROS production assays, the effects on cells pre-incubated for 1 h with the AhR antagonist αNF (25 μM), prior to co-incubation for a further 24 h with CuNPs plus ßNF or with $Cu(NO_3)_2$ plus ßNF, were also assessed. A HO-1 inhibitor, tin protoporphyrin IX (SnPP) (5 μM), was also used to study the contribution of this enzyme to ROS elicitation and anti-oxidant activity. Cells were pre-incubated for 1 h with this compound prior to co-incubation for a further 24 h with CuNPs plus ßNF or with $Cu(NO_3)_2$ plus ßNF. The working concentrations of αNF and SnPP were prepared from stock solutions (10 mM in DMSO). The copper ion fractions of supernatants were not used in co-incubation experiments, instead a copper salt $Cu(NO_3)_2$ was included in all assays to differentiate between the effects of the NPs and ions in the co-incubation experiments.

2.5. Cell viability

Viability was quantified after exposure to individual chemicals, nanoparticles or supernatants, or after co-exposure experiments, using the resazurin assay described by O'Brien and colleagues [33]. The principle of this assay is based on the reduction of resazurin to resorufin by cellular mitochondrial oxidoreductases, and it was performed as described in [32]. Fluorescence was measured at 532 nm excitation and 595 nm emission wavelengths in a TECAN Genios microplate reader (Tecan Group Ltd., Männedorf, Switzerland). Interference of all copper suspensions with the fluorescence of the indicator dye was checked without observing any kind of alterations in the readouts (the same as in [32]). A decrease in the intensity of resorufin fluorescence was taken as an indicator of reduced cellular metabolic activity, and results are expressed as a percentage of the fluorescence of control cells.

2.6. ROS levels

Intracellular ROS levels in cells exposed to CuNPs, their supernatants, $Cu(NO_3)_2$, ßNF, αNF, or SnPP and cells in co-incubation experiments with ßNF, αNF, or SnPP were measured using the 6-carboxy-2′7′ dichlorofluorescein diacetate (DCFH-DA) probe reported by Wang and Joseph [34] and following [32]. Fluorescence at 485 nm excitation and 530 nm emission wavelengths was measured in a TECAN Genios microplate reader every 15 min up to a 75 min endpoint. Potential interferences of copper suspensions with the fluorescence of the probe were previously checked by preparing a sample plate of copper suspensions without cells and quantifying the fluorescence intensity of wells after 75 min [32]. No interference was observed. ROS levels were quantified on the basis of the percentage increase in fluorescence over time and are presented as percentages of the fluorescence of untreated control cells.

2.7. Protein content

Protein content was measured in cells after exposure to ßNF, CuNP 25, CuNP 78, or $Cu(NO_3)_2$ alone and in co-incubation with ßNF (2.5 μM). Protein content was determined following Udenfriend [35] using the fluorescamine method and measuring fluorescence at 360 nm excitation and 450 nm emission wavelengths in a TECAN Genios microplate reader. BSA was used as a standard. Interference of copper suspensions with fluorescamine was checked after an incubation experiment exactly under the same conditions but without cells. NPs did not influence the readouts. This assay was used as an indicator of toxicity and served for comparative purposes, particularly in incubations involving ßNF, in which reductions of cellular metabolic activity were observed. It also served to normalise GST and EROD activities and also to quantify GSH and HO-1 levels to express values per mg of protein.

2.8. EROD activity

The catalytic activity of CYP1A was measured by means of EROD activity following the method of Burke and Mayer [36]. In addition, following Lubet and colleagues [37], dicumarol was included to maintain the stability of the resorufin produced, ensuring that reduction by cytoplasmic β-nicotinamide adenine dinucleotide 2′-phosphate reduced (NAD(P)H) quinone acceptor oxidoreductase (NQO1) did not occur. EROD levels were measured in cells exposed to ßNF, or to CuNP 25, CuNP 78 or $Cu(NO_3)_2$ alone and in co-incubation with ßNF (2.5 μM). Inhibition of EROD activity by αNF using a concentration range of 0.2–25 μM was also analysed. After removal of exposure medium, washing with PBS, and cell lysis by liquid nitrogen, we added a reaction mixture comprising 100 μL/well of PBS (pH 7.5) containing 7-ethoxyresorufin (1.25 μM), dicumarol (20 μM) and NADPH (1.4 μM) to each well. Resorufin fluorescence was measured at 532 nm excitation and 590 nm emission wavelengths in the TECAN Genios microplate reader. Subsequently, fluorescamine was added to each well to measure the protein content, as described in the previous section. Possible interference of nanoparticles with fluorescence readouts was discarded considering the lack of interference with the fluorescent product resorufin observed in the resazurin cytotoxicity assay.

2.9. GSH/GSSG ratio

GSH and GSSG (oxidised glutathione) were measured using a modified method of Allen and colleagues [38]. Following 24 h of

exposure to ßNF, sublethal concentrations of CuNP 25, CuNP 78 or $Cu(NO_3)_2$ alone and in co-incubations with ßNF (2.5 μM), cells were washed twice with PBS, freeze-thaw lysed for 1 h and sonicated for 15 s in a S 40 H Elmasonic water bath sonicator (Elma, Germany). Lysed cells were re-suspended in 100 μL of sodium phosphate reaction buffer (143 mM, pH 7.5 supplemented with 6.3 mM ethylenediaminetetraacetic acid, EDTA). Next, 25 μL aliquots of the lysed cell suspensions were used to determine protein content while another 25 μL was transferred to a new plate, and 50 μl of ice-cold sulfosalicylic acid (SSA) solution (5% w/v) was added to each well in order to remove any interfering proteins. Samples were collected in microfuge tubes and centrifuged (13,362×g) for 30 min. Supernatants were then used to determine total GSH content. To assay only GSSG content, lysed samples were suspended in reaction buffer containing 4-vinylpyridine (0.5 μmol/L) to scavenge GSH. For the determination of GSH and GSSG, the total reaction volume per well of a 96-well plate was 150 μL, consisting of 25 μL of sample/standard and 125 μL of a reaction mixture of glutathione reductase (229 U/mL), NADPH (2.39 mM) and 5′5 dithiobis [2-nitrobenzoic acid] (DTNB) (0.01 M) prepared in sodium phosphate buffer. The conversion of DTNB to 5′-thiol-2-nitrobenzoic acid (TNB) by the oxidation of GSH to GSSG was monitored by measuring absorbance at 405 nm every min over a 10-min time frame in a TECAN microplate reader. Concentrations of total GSH and GSSG were then determined using GSSG standard curves, and values were normalised to protein content. The concentration of GSH was then calculated from subtracting GSSG from total GSH-GSSG concentrations. The results are presented as the GSH/GSSG ratio. No interference of NPs with fluorescence readouts was observed. This is normal taking into account that possible proteins and CuNPs were removed in the centrifugation step.

2.10. Glutathione-S-transferase activity (GST) assay

First, we measured GST activity in cells after exposure to ßNF. Next, activity was determined in cells exposed to CuNP 25, CuNP 78 or $Cu(NO_3)_2$ alone and in co-incubation with ßNF (2.5 μM). The assay was performed using a method previously described by Habig and colleagues in 1974 [39] with slight modifications for a 96-well plate format [40]. The product of conjugation of GSH to 1-chloro-2,4-dinitrobenzene (CDNB), namely glutathione dinitrobenzene (GS-DNB), was measured at 340 nm absorbance in a TECAN microplate reader. Stock concentrations of CDNB (100 mM) were prepared in ethanol (0.1% v/v ethanol) and stored at −20 °C. Cell lysates were prepared as outlined above. The total reaction volume per well of a 96-well plate was 200 μL, consisting of 10 μL of sample and 190 μL of a reaction mixture of CDNB (1 mM) and GSH (10 mM) prepared in potassium phosphate assay buffer (pH 6.5). Changes in absorbance per min were converted into nanomoles of CDNB conjugated per min per mg of protein. Possible interferences of the CuNPs with the fluorescence readouts were discarded taking into account the consistency of the results and the very low quantities of NPs that could be remaining in the 10 μL samples used.

2.11. Heme-oxygenase (HO-1) levels

HO-1 protein levels were measured using a commercial ELISA kit (#ADI-EKS-810A) specific for rat HO-1 purchased from Enzo Life Sciences (Madrid, Spain). HO-1 levels were measured after exposure to CuNPs or $Cu(NO_3)_2$ alone or in co-incubation with 2.5 μM of ßNF. The medium was aspirated, and cells were washed twice with PBS, freeze-thaw lysed, and sonicated for 15 s in an S 40 H Elmasonic water bath sonicator to further lyse and detach them from the culture plate. The cell lysate was then suspended in 1 mL of kit extraction reagent supplemented with 0.1 mM of the protease inhibitor phenylmethylsulfonyl fluoride (PMSF) and kept on ice for 30 min to allow extraction. The suspension was then centrifuged at 13,362×g for 10 min, and the supernatant was diluted 1:10 using the kit sample diluent. The assay was performed following the manufacturer's instructions. HO-1 protein levels were quantified by measuring absorbance at 450 nm in a TECAN microplate reader. The concentration of HO-1 in the samples was then calculated against a HO-1 standard curve and expressed as ng/mL/mg protein.

2.12. Cellular uptake and intracellular distribution

The uptake and intracellular distribution of the CuNPs was visualised by means of transmission electron microscopy (TEM). This technique also served to compare signs of toxicity in cells after exposure to CuNPs alone and in co-incubation with ßNF. After a 24-h exposure to CuNP 25 (9.8 μg/mL) and CuNP 78 (6.8 μg/mL) alone and in co-incubation with ßNF (2.5 μM), cells were fixed in 3.7% paraformaldehyde/2.5% glutaraldehyde, post-fixed using 1% osmium tetraoxide, and embedded in Spurr's resin. Millonig buffer (phosphate buffer 0.1 M, pH 7.3) was used for the washing steps between fixations. After fixation, samples were dehydrated with gradual increases in concentrations of acetone (30–100%). Samples were then embedded by means of a gradual infiltration of Spurr's epoxy resin/acetone at ratios of 1:3, 1:1 and 3:1 (v/v), each for 1 h, and subsequently of pure resin (100%) overnight. The resin was then replaced with fresh resin and incubated at 60 °C for a further 48 h for the final polymerisation step. Ultrathin (60 nm) sections were cut using an ultramicrotome (Ultracut E Leica, Leica Microsystems, Wetzlar, Germany) equipped with a diamante knife. In order to prepare the sections for viewing, they were stained with 1% uranyl acetate in bi-distilled water, followed by Reynolds' lead citrate. Images were acquired with a transmission electron microscope (JEOL 1010 JEM, JEOL Ltd, Tokyo, Japan) operating at an acceleration voltage of 100 kV. Untreated cells and cells exposed to 2.5 μM ßNF served as negative and positive controls, respectively. Micrographs were analysed using Olympus Soft Imaging, Si Viewer version 5.1 (Olympus soft imaging solutions GmbH, Münster, Germany).

2.13. Statistical analysis

All exposures were performed in triplicate, and data are represented by the mean ± standard error of the mean (SEM) of at least three independent experiments. SigmaPlot®12.0 software (Systat Software Inc, San Jose, CA, United States) was used for all statistical analysis. To calculate the IC_{50} (concentration causing 50% inhibition with respect to the controls) values, we fitted the results to a regression model equation for a sigmoid curve: $y = \max/[1 + e - (x - IC_{50})/b)] + \min$, where max is the maximal response observed, b is the slope of the curve, and min is the minimal response. Normality of the data distributions was checked by means of the Shapiro-Wilk test. The homogeneity of variances was checked automatically by the programme. Since the data were normal and homoscedastic, we performed a one-way repeated measures analysis of variance (RM-ANOVA) followed by a Dunnett's post hoc-test, thus allowing the detection of significant difference from control values and the establishment of the lowest observed effect concentration (LOEC). Cell responses to co-incubation experiments involving ßNF and αNF were compared with the respective activity of those exposed solely to CuNPs and $Cu(NO_3)_2$ using a one-way analysis of variance (ANOVA), followed by a Holm-Sidak post hoc test, or using a t-test when only two groups were compared. In all cases, statistically significant differences were considered when p was <0.05.

3. Results

3.1. Physico-chemical characterisation

The hydrodynamic diameters of CuNP 25 and CuNP 78 were 565 ± 30 and 289 ± 7, respectively directly after dispersion. After 24 h of incubation, the hydrodynamic diameters were 177 ± 20 nm and 282 ± 4 nm, respectively. These results are consistent with those reported in [32] that used the same CuNP preparations. According to these authors, CuNP 25 has a high dissolution rate over 24 h under our experimental conditions: 73% of total Cu concentration is present as dissolved ion, while CuNP 78 shows a slow dissolution rate with only 23% of total concentration as dissolved ion. Our DLS measurements, comparing size distributions at time 0 and after 24 h of incubation, corroborate the contrasting dissolution profiles of CuNP 25 and CuNP 78. Size distributions in co-incubations with ßNF did not differ from those of suspensions of CuNPs alone. Supernatants collected after centrifugation of CuNP suspensions contained only the dissolved ion fractions, as DLS did not show the presence of NPs in suspension.

3.2. Contribution of ion and nanoparticulate fraction to CuNP toxicity and ROS elicitation

3.2.1. Viability

Fig. 1A shows the cell viability after a 24 h exposure to NP suspensions and supernatant ion fractions. Exposure to CuNP 25 suspensions or to its ion fractions caused a similar reduction in viability, with IC_{50} values of 29 ± 1 μg/mL and 26 ± 4 μg/mL, respectively. Viability was lost when cells were exposed to 70.2 μg/mL of CuNP 25. At this concentration, the corresponding concentration of released ion (51.2 μg/ml) also abrogated cell viability. For CuNP 78, the IC_{50} was 22 ± 4 μg/mL. In contrast to CuNP 25, the Cu ion concentration in fractions from high concentrations of CuNP 78 suspensions (89.2 μg/mL) was only 6.6 μg/mL. Exposure to this concentration of ions had no effect on cell viability. The reference salt, $Cu(NO_3)_2$, whose toxicity was caused only by released ions, led to similar profiles of reduced cell viability to those observed for the CuNPs and ion fractions of CuNP 25. However, the IC_{50} for the salt was higher (59 ± 6 μg/mL).

3.2.2. ROS levels

CuNP 25 and 78 suspensions at concentrations of 9.8 μg/mL and 6.8 μg/mL or higher, respectively, produced a significant ($p < 0.05$) increase in ROS levels with respect to controls (Fig. 1B). ROS levels were only significantly ($p < 0.05$) increased at high concentrations of ions (51.2 μg/mL) in fractions from CuNP 25 suspensions (70.2 μg/mL). Copper ions (6.6 μg/ml) released from the highest CuNP 78 concentrations did not cause an increase in ROS. $Cu(NO_3)_2$ at concentrations $\geqslant$21 μg/mL caused a significant ($p < 0.05$) increase in ROS levels.

3.3. Effects of ßNF

Preliminary studies were conducted with a full concentration range of ßNF (0.078–20 μM) to investigate the cytotoxicity of this compound. For all concentrations tested, protein levels and levels of viability did not drop below 80% of those detected in controls (data not shown). A dose-dependent increase in EROD activity was observed. Higher EROD activity ($p < 0.05$) compared to the controls was detected at ßNF concentrations $\geqslant$1.25 μM, reaching maximum activity at 5 μM (Fig. 2A). Therefore 2.5 μM ßNF was chosen for co-incubation experiments as this concentration produced a similar degree of EROD activity to the maximum observed levels without any cytotoxic effect.

Cells exposed to concentrations of ßNF ranging from 0.15 to 20 μM exhibited a significant ($p < 0.05$) and concentration-dependent increase in GST activity (Fig. 2B). There was no evidence of any effect on the GSH/GSSG ratio or ROS levels in cells exposed to increasing concentrations of ßNF (0.078–20 μM) (data not shown).

3.4. Co-incubation effects of CuNPs or $Cu(NO_3)_2$ plus ßNF

Having established the cellular responses to ßNF exposure, we examined the effects of simultaneous co-incubation of ßNF with sublethal concentrations of CuNPs and with the $Cu(NO_3)_2$ salt. In

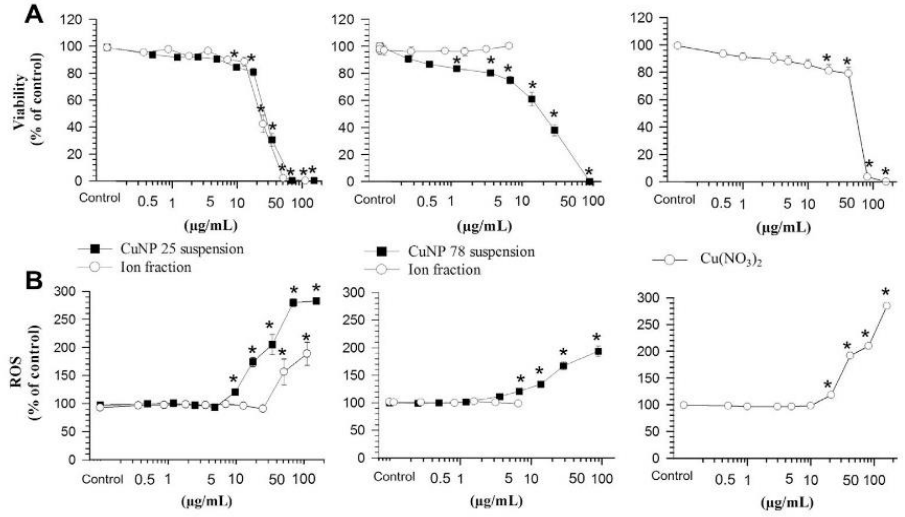

Fig. 1. Viability and ROS levels after exposure to CuNPs and released ion fractions. Viability (A) and ROS levels (B) in the H4IIE cell line following 24 h of exposure to CuNP 25 and CuNP 78 suspensions and the ion fractions released from both CuNP suspensions. These responses are compared to those achieved in response to a copper salt, $Cu(NO_3)_2$ (far right), which serves as a reference for cellular responses to copper ions. Asterisks indicate significant differences from untreated control $p < 0.05$. The concentrations presented are not nominal but measured concentrations for the two CuNP suspensions, their ion fractions, and the $Cu(NO_3)_2$ salt (corresponding to copper concentration).

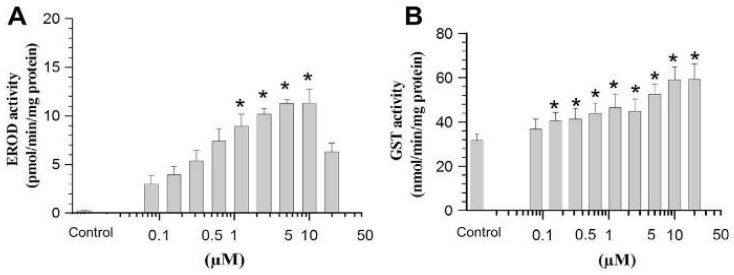

Fig. 2. Cellular response to ßNF exposure. The induction of EROD (A) and GST (B) activities in H4IIE cells following 24 h of exposure to a full concentration range of ßNF (0.08–20 μM). Asterisks denote significant differences from control untreated basal levels for $p < 0.05$.

addition, in some cases αNF was also used in the co-incubation experiments. This chemical is an AhR antagonist [41,42] and its application served to discriminate the effects mediated by this receptor.

3.4.1. Cell viability

Fig. 3A presents cell viability after co-incubation with CuNPs plus ßNF or with $Cu(NO_3)_2$ plus ßNF and also following pre-treatment with αNF, as shown by the resazurin assay. The LOEC after a 24 h exposure to CuNP 25 was 9.8 μg/mL. Following co-incubation with 2.5 μM ßNF, the LOEC decreased to 4.9 μg/mL. Cells exposed to CuNP 78 exhibited a dose-dependent reduction in viability, with a LOEC of 1.2 μg/mL. This value remained the same when the cells were co-incubated with ßNF, with no significant difference between the two exposures. The LOEC after exposure to $Cu(NO_3)_2$ was 21 μg/mL. Interestingly, we did not detect a reduction in viability at this concentration or even at higher concentrations (42 μg/mL) when cells were co-incubated with ßNF. Protein content analysis corroborated these results (Fig. 3B). Pre-exposure to αNF resulted in decreased cell viability (Fig. 3A), which was lower ($p < 0.05$) than that detected for cells treated with the highest concentrations of CuNP 25, CuNP 78 and $Cu(NO_3)_2$ alone and in co-incubation with 2.5 μM ßNF. For the CuNP 78, pre-exposure of cells to αNF led to reduced cell viability ($p < 0.05$) with respect to cells exposed only to this NP also at lower concentrations (1.2 μg/mL or higher concentrations of CuNP 78).

3.4.2. ROS levels

Fig. 3C compares the levels of intracellular ROS after a 24 h exposure to CuNPs or $Cu(NO_3)_2$ alone, in the presence of the AhR

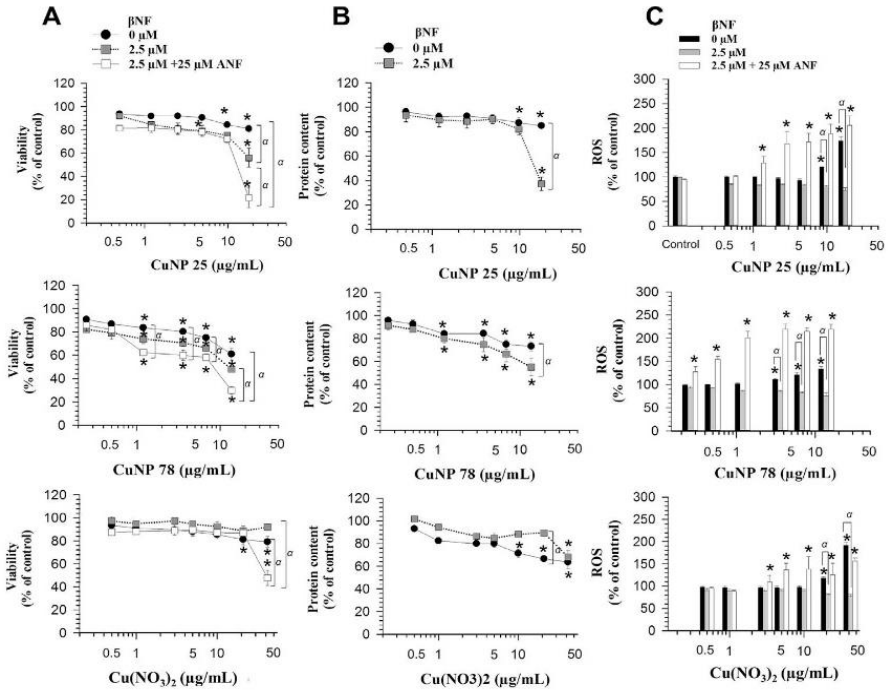

Fig. 3. Viability, protein content, and ROS levels in co-incubations of CuNPs or $Cu(NO_3)_2$ plus ßNF. Viability (A), protein content (B) and ROS levels (C) in H4IIE cell line following 24 h of exposure to CuNP 25, CuNP 78, and $Cu(NO_3)_2$ alone or in co-incubation with 2.5 μM of ßNF. Also presented are responses following 1 h pre-exposure to the AhR antagonist αNF (25 μM) prior to co-incubation with ßNF (A and C). Results of $Cu(NO_3)_2$ are presented in relation to the copper concentration. Asterisks denote significant differences with respect to the controls for $p < 0.05$, whereas α indicates significant differences ($p < 0.05$) in responses between exposure to NPs alone and in co-incubation with ßNF alone or together with αNF.

agonist ßNF, and following pre-treatment with the AhR antagonist αNF. αNF alone did not cause any increase in ROS levels in a complete range of concentrations up to 25 μM (data not shown). Neither ßNF alone nor in co-incubation with αNF increased intracellular ROS levels at the concentrations used, 2.5 μM and 25 μM, respectively (see control in CuNP 25 graph of Fig. 3C). The LOEC for CuNP 25, CuNP 78 and $Cu(NO_3)_2$ exposures were 9.8, 3.4, and 21 μg/mL, respectively. Co-incubation with ßNF abrogated the CuNP-induced intracellular levels of ROS and also the ROS elicited by $Cu(NO_3)_2$. Subsequently, in order to confirm that this effect was AhR activation-dependent, we pre-treated cells with αNF (25 μM) for 1 h prior to co-incubation with CuNPs plus ßNF or $Cu(NO_3)_2$ plus ßNF. Pre-treatment with αNF caused an increase in ROS levels, which were even greater than those measured after exposure to CuNPs alone, with LOEC values reduced to 1.2 μg/mL, 0.1 μg/mL, and 3 μg/mL for CuNP 25, CuNP 78 and $Cu(NO_3)_2$, respectively.

3.5. GSH/GSSG ratio

To determine the mechanisms underlying the decrease in ROS levels observed in the co-incubations with ßNF, we monitored the changes induced by the CuNPs and $Cu(NO_3)_2$ on GSH status and the effects of ßNF co-exposure on these levels. Results are presented as GSH/GSSG ratios, with a reduction in ratio indicating high levels of GSSG, a redox imbalance, and cells under oxidative stress. Exposure to CuNPs 25 and 78 alone resulted in a concentration-dependent decrease in the GSH/GSSG ratio in H4IIE cells (Fig. 4) that was statistically significant ($p < 0.05$) at exposure concentrations of 1.2 μg/mL and 0.25 μg/mL, respectively. Cells exposed to $Cu(NO_3)_2$ exhibited a decrease ($p < 0.05$) in the GSH/GSSG ratio only at concentrations ⩾42 μg/mL. However, cells exposed to CuNPs or $Cu(NO_3)_2$ plus ßNF exhibited increases in GSH levels, as reflected by the increase in the GSH/GSSG ratios to basal redox homeostatic control ratios. In some cases, ratios higher ($p < 0.05$) than ßNF 2.5 μM control ratios were observed.

3.6. EROD activity

Co-incubation of cells with a constant concentration of ßNF (2.5 μM) and increasing concentrations of αNF (0.2–25 μM) caused complete inhibition of EROD activity by αNF at 25 μM (data not shown), thus confirming an antagonistic effect. Exposures to the CuNPs and $Cu(NO_3)_2$ alone did not result in cellular EROD activity (data not presented). Co-incubations were also performed to study the potential modulatory effect of the CuNPs and the Cu salt on the induction of EROD activity by ßNF. No effects were observed (data not shown).

3.7. GST activity

Exposure to CuNP 25 and $Cu(NO_3)_2$ alone caused an increase ($p < 0.05$) in GST activity only at 10 μg/mL CuNP 25 (20% increase over control) and 21 μg/mL $Cu(NO_3)_2$ (19% increase over control) (Fig. 5). In contrast, at the lowest concentration tested (0.25 μg/mL), CuNP 78 significantly ($p < 0.05$) increased GST activity levels from control levels. These levels remained elevated (by an average 27 ± 3%) up to concentrations ⩾6.8 μg/mL. At higher CuNP 78 concentrations, GST activity returned to basal control levels. Exposure to 2.5 μM of ßNF increased GST enzymatic activity significantly ($p < 0.05$) by 35 ± 8% from constitutive control levels (Fig. 2B). In almost all cases, GST levels were higher ($p < 0.05$) in cells co-exposed to ßNF and CuNP 78 or $Cu(NO_3)_2$ than those observed in cells exposed to CuNP 78 or to $Cu(NO_3)_2$ alone. In contrast, no significant differences were found in GST activity between cells exposed to CuNP 25 and those co-incubated with 2.5 μM of ßNF.

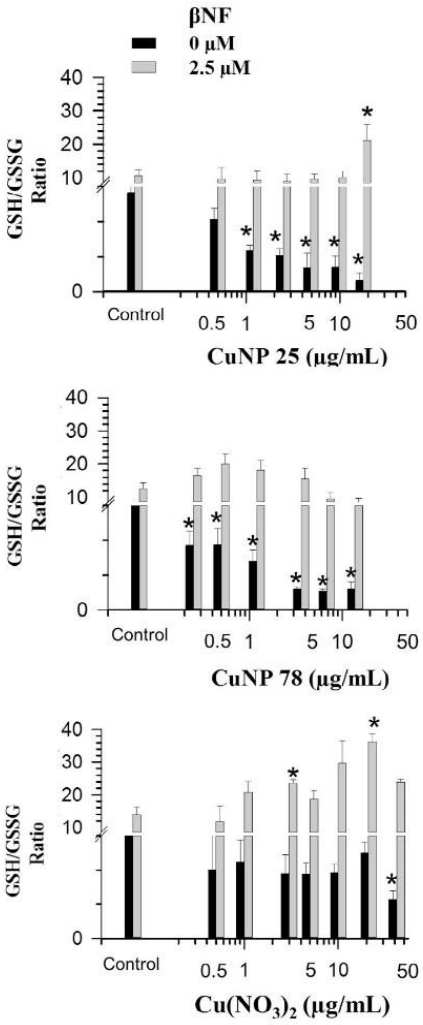

Fig. 4. GSH/GSSG ratio in co-incubations of CuNPs or $Cu(NO_3)_2$ plus ßNF. Ratios of reduced to oxidised glutathione (GSH/GSSG) following exposure to a sublethal concentration range of CuNP 25, CuNP 78, and the copper salt $Cu(NO_3)_2$ alone and in co-incubation with 2.5 μM of ßNF. Results of $Cu(NO_3)_2$ are presented in relation to the copper concentration. Asterisks denote significant differences with respect to the control ($p < 0.05$).

3.8. Heme oxygenase-1 (HO-1) levels

The incubation of cells with ßNF alone did not lead to an increase in HO-1 from basal control levels (11.25 ± 0.5 and 11.95 ± 0.1 ng/ml/mg protein, respectively) (Fig. 6). A concentration-dependent increase in HO-1 was observed in cells exposed to CuNPs or $Cu(NO_3)_2$. Exposure to the highest CuNP 25 and CuNP 78 concentrations (17.8 and 13.7 μg/mL, respectively) caused 46- and 35-fold increases in HO-1 levels with respect to controls. In contrast, only at $Cu(NO_3)_2$ concentrations ⩾42 μg/mL was there an increase ($p < 0.05$) in this variable. Co-incubations with ßNF had no effect on HO-1 levels induced by CuNPs or $Cu(NO_3)_2$.

Using SnPP, we also examined the effect of inhibiting HO-1 on cell viability and ROS levels. Pre-treatment with SnPP (5 μM) had no effect on viability or ROS levels in co-incubation experiments (data not shown).

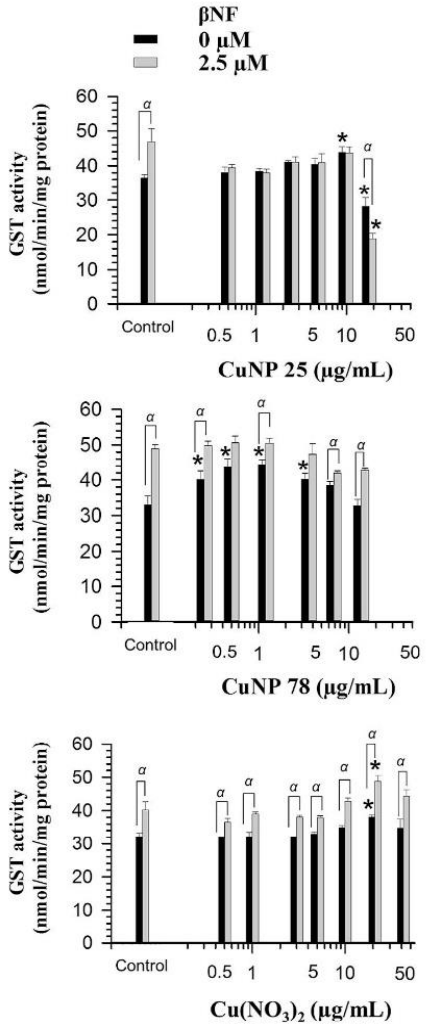

Fig. 5. Glutathione-S-transferase (GST) activity in co-incubations of CuNPs or $Cu(NO_3)_2$ plus ßNF. GST activity following exposure to sublethal concentration ranges of CuNP 25, CuNP 78, and the copper salt $Cu(NO_3)_2$ alone and in co-incubation with 2.5 μM of ßNF. Control untreated levels as well as levels after exposure to ßNF alone are also presented. Results of $Cu(NO_3)_2$ are presented in relation to the copper concentration. Asterisks denote significant differences with respect to controls ($p < 0.05$), while α indicates significant difference in responses between exposures to NPs alone and in co-incubation with ßNF ($p < 0.05$).

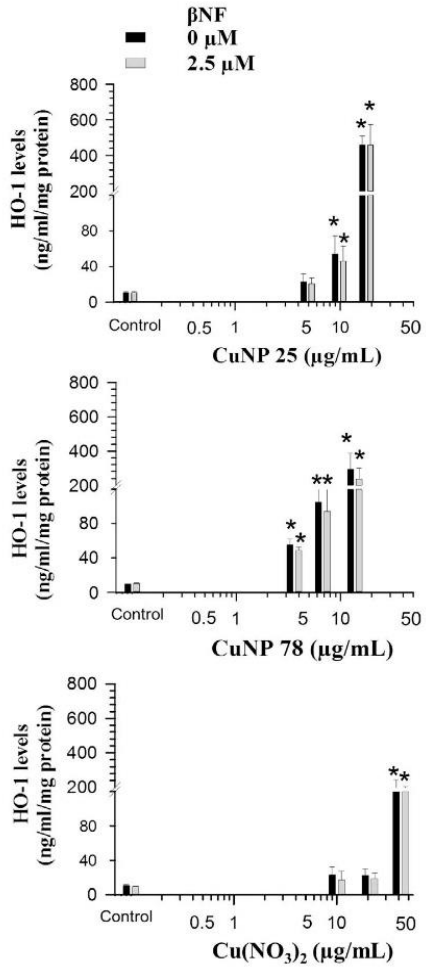

Fig. 6. Heme-oxygenase-1 (HO-1) protein levels in co-incubations of CuNPs or $Cu(NO_3)_2$ plus ßNF. The levels of inducible HO-1 protein following exposure to 4.9, 9.8 and 17. 8 μg/mL of CuNP 25, 3.6, 6.8 and 13.7 μg/mL of CuNP 78, and 10, 21 and 42 μg/mL of the copper salt $Cu(NO_3)_2$ alone and in co-incubation with 2.5 μM of ßNF are shown. Control untreated levels, as well as levels after exposure to ßNF alone, are also indicated. Results of $Cu(NO_3)_2$ are presented in relation to the copper concentration. Asterisks denote statistically significant differences with respect to the controls for $p < 0.05$.

3.9. Cellular uptake and intracellular distribution

To study the uptake and internalisation of the CuNPs when cells were exposed to CuNP 25 and CuNP 78 alone and when in co-incubation with ßNF, we used TEM. Fig. 7 shows TEM micrographs corresponding to H4IIE cells exposed to CuNP 25 (9.8 μg/mL) and CuNP 78 (6.8 μg/mL) for 24 h. In Fig. 7A and B, CuNP 25 and CuNP 78 have been taken up into the cells but remain in large aggregates sequestered within vacuoles of the peripheral cytoplasm. TEM micrographs of cells co-incubated with CuNPs plus ßNF (2.5 μM) showed similar CuNP distribution in membrane vesicles. CuNP aggregates were also found scattered in the cytoplasm, translocating across into the perinuclear region and in close proximity to the endoplasmic reticulum in both CuNP exposures alone and in co-exposures with ßNF.

4. Discussion

In this study we used two CuNPs with distinct ion dissolution profiles [32] but both able to generate high intracellular ROS levels associated with a redox imbalance in H4IIE cells. First, we compared the contribution of ions released from the CuNPs to the cytotoxicity of these particles and to ROS elicitation. Interestingly, comparison of the CuNP 25 and CuNP 78 exposures revealed that the profiles of the NP suspensions and Cu ion fractions differed. While there was evidence of ion-based toxicity for CuNP 25 (high dissolution rate), ROS elevation was associated mainly with the NP fraction. For the CuNP 78 (low dissolution rate), the decrease in cell viability and ROS production was caused exclusively by the NPs, without any apparent contribution of the ions. The low concentrations of copper ions (⩽6.6 μg/mL) present in the CuNP 78 ion fractions did not elicit any toxic effects or increase in ROS. Also, both types of CuNP presented higher toxicity and elicited

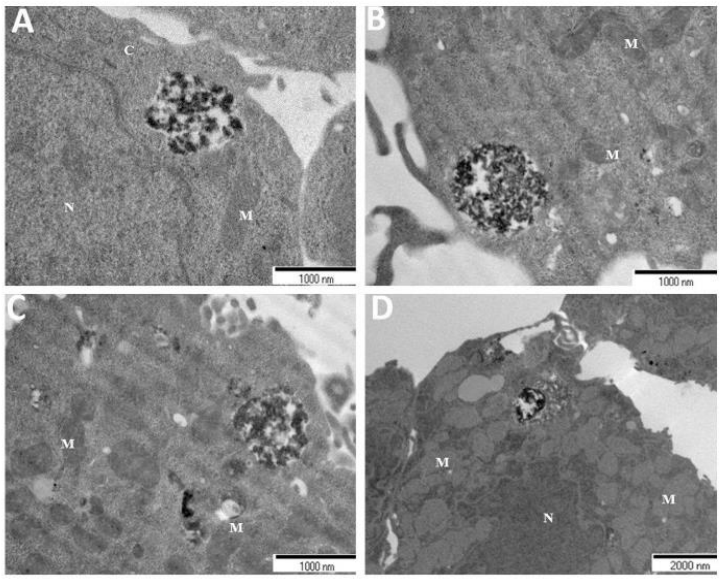

Fig. 7. TEM micrographs of H4IIE cells after exposure to CuNPs and co-incubations with ßNF. Transmission electron microscopy (TEM) micrographs showing uptake and compartmentalisation in vacuoles in the cytoplasm of H4IIE cells following 24 h exposure to CuNP 78 (6.8 μg/mL) (A) and CuNP 25 (9.8 μg/mL) (B). The intracellular distribution of CuNP 78 and CuNP 25 in co-incubation with ßNF (2.5 μM) can be seen in micrographs C and D, respectively. C, M, and N stand for cytoplasm, mitochondria, and nucleus, respectively (A–D).

ROS at lower concentrations than the $Cu(NO_3)_2$ salt. Taken together, these results suggest that CuNPs play a key role, independent of the ions released, in increasing ROS and decreasing cell viability. These results corroborate findings from studies investigating the contribution of CuO NPs and released ions to cytotoxicity that have highlighted a significant role for particle forms [43–45]. Minocha and Mumper have also proposed a unique particle effect for CuNPs targeting the cell membrane which was not evident following exposure to a copper salt [46]. Using gene expression profiles, Poynton and colleagues [19] proposed unique mechanisms of action in the case of ZnO NPs and zinc ions from $Zn(SO)_4$. However, in the present study, it must be taken into account that, if NPs are taken up, the intracellular environment (specifically pH) will affect their dissolution rate. Consequently, extracellular dissolution does not reflect what may be occurring intracellularly. Ion release studies have only been performed extracellularly in culture medium at pH 7 due to limitations in analytical techniques. Therefore, NP uptake and subsequent internal ion release cannot be excluded, in what is known as a Trojan horse-type mechanism where NPs may act as carriers for ions [47]. Researchers have used cell permeable Cu-chelators (desferoxamine and D-penicillamine) to investigate if intracellular Cu^{2+} was involved in toxic mechanism. Failure of chelation to mitigate cytotoxicity led them to conclude that the biological effect of CuO is not mediated by Cu^{2+} release either extracellularly or intracellularly [48]. Regardless of the specific contribution of NPs and ions intracellularly, our findings reveal that NP exposure is required for ROS elicitation.

We also observed that exposure to CuNP 25 and CuNP 78 at concentrations as low as 1.2 μg/mL led to a decrease in the GSH/GSSG ratio, indicative of cells under oxidative stress. At the same time, a clear dose-dependent induction of the anti-oxidant HO-1 protein was observed, indicating that the cellular Nrf2 anti-oxidant signalling pathway was activated in response to this oxidative insult. GST activity was also significantly induced in cells exposed to the CuNPs. The induction of GST activity and increased HO-1 protein levels were attained at much lower concentrations of CuNP 78 than CuNP 25 (0.25 and 9.8 μg/mL for GST and 3.6 and 9.8 μg/ml for HO-1, respectively). CuNP 78 suspension is presenting a greater challenge to the H4IIE cells, and this could explain the higher anti-oxidant response generated. Nevertheless, the increases detected in such anti-oxidants do not protect cells from the cytotoxicity caused by CuNP 78 and CuNP 25 at concentrations of 1.2 and 9.8 μg/mL, respectively.

In an attempt to increase the anti-oxidative capacity of cells and thus prevent a cytotoxic effect derived from oxidative stress, we used ßNF to activate the AhR signalling pathway and its detoxification enzymes. The concentration selected (2.5 μM) significantly induced AhR-related EROD activity, with an associated increase in GST activity without substantial toxic effects. In co-incubations with ßNF CuNP-associated ROS production was abrogated and accompanied by an increase in GSH/GSSG ratios to basal levels, indicative of a recovery of cellular redox homeostasis. However, these phenomena did not confer protection against the cytotoxic effects of CuNPs, but rather slightly increased cytotoxicity levels, possibly through an additive effect in toxicity. In contrast, we observed protection from the toxic effects of $Cu(NO_3)_2$ when cells were co-incubated with ßNF. The redox balance was also maintained, and the cytotoxic effects were abrogated at all the dose levels tested. This observation further highlights the distinct mechanisms of toxicity of ions and NPs and implies that the cytotoxic action of CuNPs is not directly related to their pro-oxidative action. Similarly, in another study, microsomal GST overexpression abrogated ROS levels and reversed the cytotoxicity of SiO_2 NPs in MCF-7 cells but showed no anti-oxidant effects or protection from ZnO nanoparticle insult [49]. The authors hypothesise that differences in dissolution properties influence mechanisms of toxicity and that GST upregulation protects cells only against NP-induced lipid peroxidation.

To unveil the true role of AhR activation in determining this anti-oxidative response, we examined the effect of pre-exposure with the AhR receptor antagonist (αNF). After pre-treatment with αNF ROS production increased significantly and cell viability decreased significantly, compared with responses to CuNPs alone or in co-incubation with ßNF. These results support the role of AhR activation in the anti-oxidative effect.

Together with the AhR, the Nrf2/ARE pathway is responsible for inducing detoxification enzymes, such as GSTs, and a vast number of cytoprotective gene products such as y-glutamyl-cysteine ligase, glutathione reductase and the cysteine transporter, all involved in GSH biosynthesis [50–52]. Joint activation of AhR- and Nrf2-regulated phase II GST and GSH synthesis would explain the high GSH/GSSG ratios in co-incubation, which were even higher than the levels induced by ßNF alone. However, according to HO-1 analysis as a marker of Nrf2 activity, ßNF did not activate Nrf2 directly. In contrast, HO-1 levels were elevated in CuNP-exposed cells. Literature reports a direct relationship between cellular oxidative stress and inducible HO-1 [53]. HO-1 levels were elevated in cells exposed to much lower concentrations of CuNPs than when exposed to the Cu salt (9.8, 3.6 and 42 μg/mL for CuNP 25, Cu NP 78 and Cu salt, respectively). Co-incubation with ßNF did not affect the HO-1 induction observed after exposure to CuNPs or $Cu(NO_3)_2$. This observation would imply that a HO-1 induction was initiated as a direct response to CuNP or $Cu(NO_3)_2$ exposure and not by the associated ROS insult. Similarly, Sikorski and colleagues [54] suggested that the observed increase in HO-1 protein and mRNA levels in human renal proximal tubular epithelial cells after exposure to Cd was associated with a direct activation of Cd responsive elements (CdREs) in the promoter region of the HO-1 gene and not with the activation of stress-related responsive elements. We further studied the relationship between HO-1, ROS levels, and cell viability using the HO-1 inhibitor SnPP [41]. HO-1 inhibition with 5 μM of SnPP had no effect on ROS levels or viability in cells exposed to CuNPs or in co-incubation with ßNF.

Taken together, these results support the hypothesis that the reduction in viability of H4IIE cells after exposure to CuNPs is only partly dependent on levels of intracellular ROS. TEM micrographs showing internalised CuNP aggregates suggest a direct physical perturbation of cellular organelles in dictating NP toxicity. ßNF does not inhibit NP uptake with particles visible in membrane bound vesicles.

Our results also allow us to gain insight into the possible interference caused by CuNPs and associated ROS on CYP1A activity, although this question was not in the scope of this study. Given that CYP1A activity is involved in metabolising ßNF and other potentially harmful chemicals, such as polycyclic aromatic hydrocarbons (PAHs), any alteration in biotransformation capacity could potentially alter the mutagenicity and carcinogenicity of these compounds. Sereemaspun and colleagues [42] first reported the inhibition of CYP enzymes by metallic NPs (AuNPs and AgNPs) in 2008. Since then, other studies have corroborated these findings [55] and suggest that even polystyrene NPs, due to their small size, uptake, and access to the endoplasmic reticulum, can inhibit CYP activity [56]. Cu-specific suppression of CYP1A activity induced by the persistent environmental contaminant 2,3,7,8-Tetrachlorodibenzo-*p*-dioxin (TCDD) has been reported [57]. Also in a study carried out using primary hepatocytes from catfish (*Heteropneustes fossili*), exposure to $CuSO_4$ inhibited EROD activity induced by ßNF [58]. The authors claimed that this effect was related to a reduction in GSH levels induced by ßNF.

It has been observed that some CYP1A substrates uncouple the catalytic cycle of CYP1A, leading to the formation of ROS within the active site and inactivation of the enzyme [59]. Consequently, increased GSH concentrations could reduce ROS levels, thus allowing the normal functioning of CYP1A. In fact, Oliveira and colleagues [60] reported that GSH protects against heavy metal inhibition of CYP1A activity in sea bass. Their results showed that by introducing GSH (0.5 μM), EROD inhibition by Cu^{2+}, Hg^{2+} as well as Zn^{2+}, was significantly reduced. In the present study we did not detect any modulation of ßNF-induced CYP1A activity by CuNPs or Cu ions. Interspecies differences and the high levels of GSH detected in the co-incubations with ßNF may prevent the inhibition of CYP1A, as observed by other authors. We are also aware that there are distinct outcomes according to the exposure strategy used [61] and the type of metal and specific organic compounds being applied [62–64].

5. Conclusions

Using two CuNPs with high and low dissolution profiles, here we have shown that NP and ion forms have distinct modes of action. We have shown that ROS elicitation is NP-specific. Co-incubation with ßNF brings H4IIE cells into redox homeostasis. This effect is achieved through the activation of the AhR pathway, GST enzymatic up-regulation, and GSH increase. The abrogation of the anti-oxidative effect of ßNF in the presence of the AhR antagonist αNF strongly suggests that the this receptor contributes to the observed reduction of ROS to basal levels in response to CuNP insult. Despite ROS abrogation and redox balance, levels of cell viability did not increase. Taken together, these results support the hypothesis that the reduced viability of H4IIE cells following exposure to CuNPs occurs independently of intracellular ROS and redox status. TEM images evidenced CuNP uptake into the cell, resulting in the disruption of normal cellular function. Further studies are required to elucidate if ßNF co-exposure influences the way in which cells process NPs. Our results question the use of ROS elicitation and the oxidative stress paradigm as indicators of NP toxicity. While the induction of ROS and oxidative injury have been widely accepted as a vital mechanistic paradigm to explain NP toxicity, other patterns of injury should also be considered.

Conflict of Interest

The authors declare that there are no conflicts of interest.

Transparency Document

The Transparency document associated with this article can be found in the online version.

Acknowledgements

This research was made possible through the support provided by the European Commission under the FP7 framework programme Marie Curie Initial Training Network FP7-PEOPLE-ITN-2008 238701 Environmental ChemOinformatics (ITN-ECO) and the INIA project AT2011-001. The authors thank the staff of the *Centro Nacional de Microscopía Electrónica* (Madrid, ES) for technical assistance with the preparation and analysis of TEM samples (Fernández Larios A and García Gil ML).

References

[1] F. Gottschalk, B. Nowack, The release of engineered nanomaterials to the environment, J. Environ. Monit. 13 (2011) 1145–1155.
[2] Z. Chen, H. Meng, G. Xing, C. Chen, Y. Zhao, G. Jia, T. Wang, H. Yuan, C. Ye, F. Zhao, Z. Chai, C. Zhu, X. Fang, B. Ma, L. Wan, Acute toxicological effects of copper nanoparticles in vivo, Toxicol. Lett. 163 (2006) 109–120.
[3] H. Meng, Z. Chen, G. Xing, H. Yuan, C. Chen, F. Zhao, C. Zhang, Y. Wang, Y. Zhao, Ultra-high reactivity and grave nanotoxicity of copper nanoparticles, J. Radioanalyt. Nucl. Chem. 271 (2007) 595–598.
[4] C.A. Poland, R. Duffin, I. Kinloch, A. Maynard, W.A.H. Wallace, A. Seaton, V. Stone, S. Brown, W. Macnee, K. Donaldson, Carbon nanotubes introduced into the abdominal cavity of mice show asbestos-like pathogenicity in a pilot study, Nat. Nanotechnol. 3 (2008) 423–428.
[5] T. Lammel, P. Boisseaux, M.L. Fernández-Cruz, J.M. Navas, Internalization and cytotoxicity of graphene oxide and carboxyl graphene nanoplatelets in the human hepatocellular carcinoma cell line Hep G2, Part. Fibre Toxicol. 12 (2013) 10–27.

[6] T. Xia, M. Kovochich, J. Brant, M. Hotze, J. Sempf, T. Oberley, C. Sioutas, J.I. Yeh, M.R. Wiesner, A.E. Nel, Comparison of the abilities of ambient and manufactured nanoparticles to induce cellular toxicity according to an oxidative stress paradigm, Nano Lett. 6 (2006) 1794–1807.
[7] A. Nel, T. Xia, L. Mädler, N. Li, Toxic potential of materials at the nanolevel, Science 311 (2006) 622–627.
[8] N. Li, T. Xia, A.E. Nel, The role of oxidative stress in ambient particulate matter-induced lung diseases and its implications in the toxicity of engineered nanoparticles, Free Radic. Biol. Med. 44 (2008) 1689–1699.
[9] H.J. Eom, J. Choi, Oxidative stress of silica nanoparticles in human bronchial epithelial cell, Beas-2B, Toxicol. In Vitro 23 (2009) 1326–1332.
[10] J. Alam, D. Stewart, C. Touchard, S. Boinapally, A.M. Choi, J.L. Cook, Nrf2, a Cap'n'Collar transcription factor, regulates induction of the heme oxygenase-1 gene, J. Biol. Chem. 274 (1999) 26071–26078.
[11] K. Itoh, T. Ishii, N. Wakabayashi, M. Yamamoto, Regulatory mechanisms of cellular response to oxidative stress, Free Radic. Res. 31 (1999) 319–324.
[12] S.C. Lu, Glutathione synthesis, Biochim. Biophys. Acta 1830 (2013) 3143–3153.
[13] J.D. Hayes, D. Pulford, The glutathione S-transferase supergene family: regulation of GST and the contribution of the isoenzymes to cancer chemoprotection and drug resistance, Crit. Rev. Biochem. Mol. Biol. 30 (1995) 445–600.
[14] J.D. Hayes, A.T. Dinkova-Kostova, M. McMahon, Cross-talk between transcription factors AhR and Nrf2: lessons for cancer chemoprevention from dioxin, Toxicol. Sci. 111 (2009) 199–201.
[15] C.L. Waller, J.D. McKinney, Three dimensional quantitative structure–activity relationships of dioxins and dioxin-like compounds: model validation and Ah receptor characterization, Chem. Res. Toxicol. 8 (1995) 847–858.
[16] P.A. Münzel, S. Schmohl, F. Buckler, J. Jaehrling, F.T. Raschko, C. Köhle, K.W. Bock, Contribution of the Ah receptor to the phenolic antioxidant-mediated expression of human and rat UDP-glucuronosyltransferase UGT1A6 in Caco-2 and rat hepatoma 5L cells, Biochem. Pharmacol. 66 (2003) 841–847.
[17] R.L. Yeager, S.A. Reisman, L.M. Aleksunes, C.D. Klaassen, Introducing the "TCDD inducible AhR-Nrf2 gene battery", Toxicol. Sci. 111 (2009) 238–246.
[18] S. Kalthoff, U. Ehmer, N. Freiberg, M.P. Manns, C.P. Strassburg, Interaction between oxidative stress sensor Nrf2 and xenobiotic-activated aryl receptor in the regulation of the human phase II detoxifying UDP-glucuronosyltransferase 1A10, J. Biol. Chem. 285 (2010) 5993–6002.
[19] C.H. Poynton, M.J. Lazorchak, A.C. Impellitteri, E.M. Smith, K. Rogers, M. Patra, A.K. Hammer, J.H. Allen, D.C. Vulpe, Differential gene expression in *Daphnia magna* suggests distinct modes of action and bioavailability for ZnO nanoparticles and Zn ions, Environ. Sci. Technol. 45 (2011) 762–768.
[20] S.I.L. Gomes, S.C. Novais, J.J. Scott-Fordsmand, W. de Coen, A.M. Soares, M.J. Amorim, Effect of Cu-Nanoparticles versus Cu-salt in *Enchytraeus albidus* (Oligochaeta): differential gene expression through microarray analysis, Comp. Biochem. Physiol. C: Toxicol. Pharmacol. 155 (2012) 219–227.
[21] S. Kim, E.J. Choi, J. Choi, Oxidative stress-dependent toxicity of silver nanoparticles in human hepatoma cells, Toxicol. In Vitro 23 (2009) 1076–1084.
[22] B.J. Shaw, G. Al-Bairuty, R.D. Handy, Effects of waterborne copper nanoparticles and copper sulphate on rainbow trout, (*Oncorhynchus mykiss*): physiology and accumulation, Aquat. Toxicol. 116–117 (2012) 90–101.
[23] K. Kawata, M. Osawa, S. Okabe, In vitro toxicity of silver nanoparticles at noncytotoxic doses to HepG2 human hepatoma cells, Environ. Sci. Technol. 43 (2009) 6046–6051.
[24] M.L. Fernández-Cruz, T. Lammel, M. Connolly, E. Conde, A. Barrado, S. Derick, Y. Perez, M. Fernandez, C. Furger, J.M. Navas, Comparative cytotoxicity induced by bulk and nanoparticulated ZnO in the fish and human hepatoma cell lines PLHC-1 and Hep G2, Nanotoxicology 7 (2013) 935–952.
[25] P. Chairuangkitti, S. Lawanprasert, S. Roytrakul, S. Aueviriyavit, D. Phummiratch, K. Kulthong, P. Chanvorachote, R. Maniratanachote, Silver nanoparticles induce toxicity in A549 cells via ROS-dependent and ROS-independent pathways, Toxicol. In Vitro 27 (2013) 330–338.
[26] A.A. Shvedova, A. Pietroiusti, B. Fadeel, V.E. Kagan, Mechanisms of carbon nanotube-induced toxicity: focus on oxidative stress, Toxicol. Appl. Pharmacol. 261 (2012) 121–133.
[27] T. Lammel, J.M. Navas, Graphene nanoplatelets spontaneously translocate into the cytosol and physically interact with cellular organelles in the fish cell line PLHC-1, Aquatic Toxicol. 150 (2014) 55–65.
[28] D. Chung, Nanoparticles have health benefits too, New Sci. 179 (2003) 2410–2416.
[29] D. Schubert, R. Dargusch, J. Raitano, S.W. Chan, Cerium and yttrium oxide nanoparticles are neuroprotective, Biochem. Biophys. Res. Commun. 342 (2006) 86–91.
[30] N. Ercal, H. Gurer-Orhan, N. Aykin-Burns, Toxic metals and oxidative stress. Part I. Mechanisms involved in metal-induced oxidative damage, Curr. Top. Med. Chem. 1 (2001) 529–539.
[31] S.O. Simmons, C.Y. Fan, K. Yeoman, J. Wakefield, R. Ramabhadran, NRF2 oxidative stress induced by heavy metals is cell type dependent, Curr. Chem. Genomics. 5 (2011) 1–12.
[32] Y. Dewa, J. Nishimura, M. Muguruma, M. Jin, Y. Saegusa, T. Okamura, M. Tasaki, T. Umemura, K. Mitsumori, Molecular expression analysis of β-Naphthoflavone-induced hepatocellular tumors in rats, Toxicol. Pathol. 37 (2009) 446–455.
[33] L. Song, M. Connolly, M.L. Fernández-Cruz, M.G. Vijver, M. Fernández, E. Conde, G.R. de Snoo, W.J. Peijnenburg, J.M. Navas, Species specific toxicity of copper nanoparticles among mammalian and piscine cell lines, Nanotoxicology 8 (2014) 383–393.
[34] J. O'Brien, I. Wilson, T. Orton, F. Pognan, Investigation of the Alamar Blue (resazurin) fluorescent dye for the assessment of mammalian cell cytotoxicity, Eur. J. Biochem. 267 (2000) 5421–5426.
[35] H. Wang, J.A. Joseph, Quantifying cellular oxidative stress by dichlorofluorescein assay using microplate reader, Free Radic. Biol. Med. 27 (1999) 612–616.
[36] S. Udenfriend, S. Stein, P. Böhlen, W. Dairman, W. Leimgruber, M. Weigele, Fluorescamine A: reagent for assay of amino acids, peptides, proteins, and primary amines in the picomole range, Sci. New Ser. 178 (1972) 871–872.
[37] M.D. Burke, R.T. Mayer, Ethoxyresorufin: direct fluorimetric assay of a microsomal O-dealkylation which is preferentially inducible by 3-methylcholanthrene, Drug Metab. Dispos. 2 (1974) 583–588.
[38] R.A. Lubet, R.W. Nims, R.T. Mayer, J.W. Cameron, L.M. Schechtman, Measurement of cytochrome P-450 dependent dealkylation of alkoxy-phenoxazones in hepatic S9s and hepatocyte homogenates: effects of dicumarol, Mutat. Res. Lett. 142 (1985) 127–131.
[39] S. Allen, J.M. Shea, T. Felmet, J. Gadra, P.F. Dehn, A kinetic microassay for glutathione in cells plated on 96-well microtiter plates, Methods Cell Sci. 22 (2001) 305–312.
[40] W.H. Habig, M.J. Pabst, W.B. Jakoby, Glutathione S-transferases: the first enzymatic step in mercapturic acid formation, J. Biol. Chem. 249 (1974) 7130–7139.
[41] S. Tiwari, K. Pelz-Stelinskik, S.R. Mann, L.L. Stelinski, Glutathione transferase and cytochrome P450 (general oxidase) activity levels in candidatus liberibacter asiaticus-infected and uninfected Asian citrus psyllid (Hemiptera: Psyllidae), Ann. Entomol. Soc. Am. 104 (2011) 297–305.
[42] R.J. Wong, H.J. Vreman, S. Schulz, F.S. Kalish, N.W. Pierce, D.K. Stevenson, In vitro inhibition of heme oxygenase isoenzymes by metalloporphyrins, J. Perinatol. 31 (Suppl. 1) (2011) S35–S41.
[43] A. Sereemaspun, P. Hongpiticharoen, R. Rojanathanes, P. Maneewattanapinyo, S. Ekgasit, W. Warisnoicharoen, Inhibition of human cytochrome P450 enzymes by metallic nanoparticles: a preliminary to nanogenomics, Int. J. Pharmacol. 4 (2008) 492–495.
[44] K. Midlander, P. Cronholm, H.L. Karlsson, K. Elihn, L. Moller, C. Leygraf, I.O. Wallinder, Surface characteristics, copper release, and toxicity of nano and micrometer-sized copper and copper(II) oxide particles: a cross-disciplinary study, Small 5 (2009) 389–399.
[45] H.L. Karlsson, P. Cronholm, J. Gustafsson, L. Moller, Copper oxide nanoparticles are highly toxic: a comparison between metal oxide nanoparticles and carbon nanotubes, Chem. Res. Toxicol. 21 (2008) 1726–1732.
[46] S.K. Misra, S. Nuseibeh, A. Dybowska, D. Berhanu, T.D. Tetley, E. Valsami-Jones, Comparative study using spheres, rods and spindle-shaped nanoplatelets on dispersion stability, dissolution and toxicity of CuO nanomaterials, Nanotoxicology 8 (2014) 422–432.
[47] S. Minocha, R.J. Mumper, Effect of carbon coating on the physico-chemical properties and toxicity of copper and nickel nanoparticles, Small 8 (2012) 3289–3299.
[48] L.K. Limbach, P. Wich, P. Manser, R.N. Grass, A. Bruinink, W.J. Stark, Exposure of engineered nanoparticles to human lung epithelial cells: influence of chemical composition and catalytic activity on oxidative stress, Environ. Sci. Technol. 41 (2007) 4158–4163.
[49] B. Fahmy, S.A. Cormier, Copper oxide nanoparticles induce oxidative stress and cytotoxicity in airway epithelial cells, Toxicol. In Vitro 23 (2009) 1365–1371.
[50] J. Shi, H.L. Karlsson, K. Johansson, V. Gogvadze, L. Xiao, J. Li, T. Burks, A. Uheida, A. Garcia-Bennett, M. Muhammed, S. Mathur, R. Morgenstern, V. Kagan, B. Fadeel, Microsomal glutathione transferase 1 protects against toxicity induced by silica nanoparticles but not by zinc oxide nanoparticles, ACS Nano 6 (2012) 1925–1938.
[51] A.C. Wild, H.R. Moinova, R.T. Mulcahy, Regulation of gamma-glutamylcysteine synthetase subunit gene expression by the transcription factor Nrf2, J. Biol. Chem. 274 (1999) 33627–33636.
[52] M.K. Kwak, N. Wakabayashi, K. Itoh, H. Motohashi, M. Yamamoto, T.W. Kensler, Modulation of gene expression by cancer chemopreventive dithiolethiones through the Keap1-Nrf2 pathway. Identification of novel gene clusters for cell survival, J. Biol. Chem. 278 (2003) 8135–8145.
[53] T. Ishii, K. Itoh, S. Takahashi, H. Sato, T. Yanagawa, Y. Katoh, S. Bannai, M. Yamamoto, Transcription factor Nrf2 coordinately regulates a group of oxidative stress-inducible genes in macro-phages, J. Biol. Chem. 275 (2000) 16023–16029.
[54] L.A. Applegate, P. Luscher, M.R. Tyrrell, Induction of heme oxygenase: a general response to oxidant stress in cultured mammalian cells, Cancer Res. 51 (1991) 974–978.
[55] E.M. Sikorski, T. Uo, R.S. Morrison, A. Agarwal, Pescadillo interacts with the cadmium response element of the human heme oxygenase-1 promoter in renal epithelial cells, J. Biol. Chem. 281 (2006) 24423–24430.
[56] W. Warisnoicharoen, P. Hongpiticharoen, S. Lawanprasert, Alteration in enzymatic function of human cytochrome P450 by silver nanoparticles, Res. J. Environ. Toxicol. 5 (2011) 58–64.
[57] E. Fröhlich, T. Kueznik, C. Samberger, E. Roblegg, C. Wrighton, T.R. Pieber, Size-dependent effects of nanoparticles on the activity of cytochrome P450 isoenzymes, Toxicol. Appl. Pharmacol. 242 (2010) 326–332.
[58] M. Benedetti, D. Fattorini, G. Martuccio, M. Nigro, G. Regoli, Interactions between trace metals (Cu, Hg, Ni, Pb) and 2,3,7,8-tetrachlorodibe nzo-p-dioxin

in the Antarctic fish Trematomus bernacchii: oxidative effects on biotransformation pathway, Environ. Toxicol. Chem. 28 (2009) 818–825.
[59] C.M. Ghosh, R. Ghosh, K.A. Ray, Impact of copper on biomonitoring enzyme ethoxyresorufin-o-deethylase in cultured catfish hepatocytes, Environ. Res. 86 (2001) 167–173.
[60] J.J. Schlezinger, R.D. White, J.J. Stegeman, Oxidative inactivation of cytochrome P450 1A (CYP1A) stimulated by 3,3′,4,4′-tetrachlorobiphenyl: production of reactive oxygen by vertebrate CYP1As, Mol. Pharmacol. 56 (1999) 588–597.
[61] M. Oliveira, M.A. Santos, M. Pacheco, Glutathione protects heavy metal-induced inhibition of hepatic microsomal ethoxyresorufin O-deethylase activity in *Dicentrarchus labrax* L, Ecotoxicol. Environ. Saf. 58 (2004) 379–385.
[62] W. Wei, X.F. Li, X.N. Li, X.M. Chen, A.L. Liu, W.Q. Lu, Oxidative stress and cell cycle change induced by coexposed PCB126 and benzo[a]pyrene to human hepatoma (HepG2) cells, Environ. Toxicol. 27 (2012) 316–320.
[63] H.M. Korashy, A.O. El-Kadi, Modulation of TCDD-mediated induction of cytochrome P450 1A1 by mercury, lead, and copper in human HepG2 cell line, Toxicol. In Vitro 22 (2008) 154–158.
[64] D.D. Vakharia, N. Liu, R. Pause, M. Fasco, E. Fessette, Q. Zhang, L.S. Kaminsky, Polycyclic aromatic hydrocarbon/metal mixtures: effect on PAH induction of CYP1A1 in human HepG2 cells, Drug Metab. Dispos. 29 (2001) 999–1006.

CHAPTER 5

Investigating the hazard associated with Ag ENMs in aquatic environments using available liver cell lines and primary hepatocytes from rainbow trout.

The research article presented in chapter 5 focuses on the hazard associated with AgNPs reaching freshwater environments. According to current environmental risk assessments based on modelling predicted environmental concentrations (PEC) and taking into account species sensitivity distributions, AgNPs present one of the highest risks compared to other NPs, particularly in surface waters. Fish are particularly susceptible to the toxic effects of silver ions and, with knowledge gaps regarding the contribution of dissolution and unique particle effects to AgNP toxicity, they represent a group of vulnerable organisms. Using primary liver cells and available cell lines from rainbow trout the cytotoxicity of AgNPs and the silver salt $Ag(NO_3)_2$ was tested. Results were used to compare the sensitivities between cell lines, to investigate if responses in liver cell lines were representative of primary liver cells behaviour and to shed light on the mechanisms underlying observed toxic responses (if any). Multiple assay systems were applied to the same set of cells to monitor plasma membrane damage, lysosome functioning and cellular metabolic activity increasing the robustness of the *in vitro* cell culture test system and providing valuable information on potential mechanisms of cytotoxicity of AgNPs. In particular the role of the lysosome in AgNPs mechanism of cytotoxicity was highlighted and lysosomal damage pinpointed as an important indicator for detecting NP-specific effects.

Research paper 2: Comparative Cytotoxicity Study of Silver Nanoparticles (AgNPs) in a Variety of Rainbow Trout Cell Lines (RTL-W1, RTH-149, RTG-2) and Primary Hepatocytes.

Int. J. Environ. Res. Public Health **2015**, *12*, 5386-5405; doi:10.3390/ijerph120505386

OPEN ACCESS

International Journal of
Environmental Research and Public Health
ISSN 1660-4601
www.mdpi.com/journal/ijerph

Article

Comparative Cytotoxicity Study of Silver Nanoparticles (AgNPs) in a Variety of Rainbow Trout Cell Lines (RTL-W1, RTH-149, RTG-2) and Primary Hepatocytes

Mona Connolly [1], Maria-Luisa Fernandez-Cruz [1], Alba Quesada-Garcia [1], Luis Alte [1], Helmut Segner [2] and Jose M. Navas [1,*]

[1] Instituto Nacional de Investigación y Tecnología Agraria y Alimentaria (INIA), Carretera de la Coruña Km 7.5, E-38040 Madrid, Spain; E-Mails: connolly.mona@inia.es (M.C.); fcruz@inia.es (M.-L.F.-C.); quesada.alba@inia.es (A.Q.-G.); luis.alte@inia.es (L.A.)

[2] Faculty of Vetsuisse, Centre for Fish and Wildlife Health, University of Berne, Länggassstr. 122, Postfach 8466, CH-3001 Bern, Switzerland, E-Mail: helmut.segner@vetsuisse.unibe.ch

* Author to whom correspondence should be addressed; E-Mail: jmnavas@inia.es; Tel.: +34-913-474-155; Fax: +34-913-474-008.

Academic Editor: Mónica Amorim

Received: 26 March 2015 / Accepted: 12 May 2015 / Published: 20 May 2015

Abstract: Among all classes of nanomaterials, silver nanoparticles (AgNPs) have potentially an important ecotoxicological impact, especially in freshwater environments. Fish are particularly susceptible to the toxic effects of silver ions and, with knowledge gaps regarding the contribution of dissolution and unique particle effects to AgNP toxicity, they represent a group of vulnerable organisms. Using cell lines (RTL-W1, RTH-149, RTG-2) and primary hepatocytes of rainbow trout (Oncorhynchus mykiss) as *in vitro* test systems, we assessed the cytotoxicity of the representative AgNP, NM-300K, and AgNO3 as an Ag+ ion source. Lack of AgNP interference with the cytotoxicity assays (AlamarBlue, CFDA-AM, NRU assay) and their simultaneous application point to the compatibility and usefulness of such a battery of assays. The RTH-149 and RTL-W1 liver cell lines exhibited similar sensitivity as primary hepatocytes towards AgNP toxicity. Leibovitz's L-15 culture medium composition (high amino acid content) had an important influence on the behaviour and toxicity of AgNPs towards the RTL-W1 cell line. The obtained results demonstrate that, with careful consideration, such an *in vitro* approach

can provide valuable toxicological data to be used in an integrated testing strategy for NM-300K risk assessment.

Keywords: AgNPs; cytotoxicity; rainbow trout (Oncorhynchus mykiss); *in vitro* cell lines; primary hepatocyte

1. Introduction

Among the plethora of nanoparticles (NPs) already on the market, silver nanoparticles (AgNPs) are being used in more products (>400) than any other manufactured nanomaterial (MN) [1]. AgNPs' antimicrobial properties, catalytic activity and conductivity have led to their wide application in biomedicine, electronics, the food sector (in packaging materials), and even the textile industry. Mueller and Nowack provided an estimate of a worldwide production of 500 tonnes per annum in 2008, however with continued growth in the industry, this would be significantly higher today [2]. There is evidence to suggest that AgNPs are currently being released into the aquatic environment simply through the use of consumer products containing them [3–5]. This, along with the fact that the toxicity of AgNPs has been demonstrated in a range of aquatic organisms [6], with reported LC50s <0.1 mg/L, highlights an environmental risk that warrants careful assessment. According to current environmental risk assessments based on modelling predicted environmental concentrations (PEC) and taking into account species sensitivity distributions, AgNPs present one of the highest risks compared to other NPs, particularly in surface waters [7].

Fish are particularly susceptible to the toxic effects of metal ions such as silver [8,9] that could be released from NPs. There have been significant advancements in the amount of AgNP toxicity studies performed in fish, using for instance zebrafish (Danio rerio) [10–12], Japanese medaka (Oryzias latipes) [13,14], sheephead minnow (Cyprinodan variegatus) [15] or rainbow trout (Oncorhynchus mykiss) [16]. The reported LC50 values from these studies were very different ranging from 0.089 µg/mL to 250 µg/mL. This leads to discrepancies in their classification as being toxic or very toxic to the environment according to the European Council directives 67/548/EEC [17] and its further amendment by the Regulation (EC) No 1272/2008 on the classification, labelling and packaging (CLP) of substances and mixtures (directive 2008/112/EC) [18].

Fish cells maintained in primary culture or as immortalized cell lines can represent an economically feasible robust *in vitro* testing system to meet the high number of substances to be tested, including MNs. A large number of fish cell lines exist from different species, tissues and cell types, however they have only been used in a limited number of studies for nanoparticle toxicity assessment [19–22]. Although such *in vitro* models are yet under validation, information gathered from non-validated *in vitro* systems can still be used in a weight of evidence approach of an integrated testing strategy according to the Commission Regulation (EC) No 134/2009 concerning the Registration, Evaluation, Authorisation and Restriction of Chemicals (REACH) [23]. Ethical reasons and the fulfilment of the 3Rs' principles (replacement, reduction and refinement) also favour the application of cells in culture. Finally, the ease of maintenance and reproducibility of results makes these systems the ideal tool for studies devoted to determining possible mechanisms underlying the toxicity of chemicals and MNs.

However, when using an *in vitro* approach, it is important to carefully consider exposure routes and possible target sites to produce relevant data.

In vivo exposures in fish have shown that AgNPs can accumulate in the liver [24,25]. Furthermore, after waterborne exposure to AgNPs, it has been shown that the liver burden of silver was approximately twice that of the gills [26], demonstrating that if the NPs are taken up by fish, they will translocate to the liver as a major site of clearance regardless of the route of exposure. Thus, in the present study, we have employed liver cell lines from rainbow trout, RTH-149 and RTL-W1 as relevant test systems to determine the toxicity of AgNPs *in vitro*. In addition, and for comparative purposes, a rainbow trout gonadal cell line (RTG-2) was also used. Since one of the main limitations of cell lines is the lack of functional receptors or enzymes leading to the disappearance of essential metabolic routes, in this work primary hepatocytes were included to assess differences in sensitivity among continuous cell lines and primary cells whose liver-specific metabolic functions are conserved. Previous studies comparing responses to AgNP exposure in a human hepatocellular cell line and primary hepatocytes showed very good correlation [27].

The main objective of this work was therefore to determine the toxicity of AgNPs in liver cells of rainbow trout as a model system and to shed light on the mechanisms underlying the observed toxic response (if any). This information ultimately would be useful and pertinent in an integrated intelligent testing strategy for AgNP risk assessment. The lack of standardisation for MN testing, confounded by the fact that different MNs have been used with different cappings and coatings, may explain why up until now there have been huge variations in reported toxicities of NPs. To facilitate future comparisons with this study, we have used a representative manufactured silver nanomaterial (NM-300K) which was tested in the testing programme overseen by the OECD Working Party on Manufactured Nanomaterials [28]. As it is still not clear whether the effects of AgNPs are dominated by released silver ions or are caused by the unique properties of the particles themselves, we have assessed in parallel the toxicity of $AgNO_3$ which acts as a source of Ag+. In this study, liver cell lines appeared to be a sensitive test system when compared to primary hepatocytes, what has important practical implications taking into account the ease of maintenance and culture of cell lines. The simultaneous use in the same plate of three assay systems evidencing three different mechanisms of toxic action appeared as very appropriate to determine the cytotoxic activity of AgNPs.

2. Experimental Section

2.1. Chemicals and Reagents

Fetal bovine serum (FBS), ultraglutamine 1 (200 mM), L-glutamine (200 mM), penicillin and streptomycin (P/S) (10,000 U/mL/10 mg/mL), phosphate-buffered saline (PBS), Trypsin/Ethylene diaminetetraacetic acid (EDTA) (17,000 U trypsin/L, 200 mg/l EDTA), non-essential amino acids (NEAA)100X, Eagle's minimal essential medium (EMEM), Minimum Essential Medium (MEM) Alpha (α-MEM) and Leibovitz's L-15 medium were purchased from Lonza (Barcelona, Spain). Serum-free/phenol red-free MEM (MEM(-)) used was from PAN Biotech, Aidenbach, Germany. Ethanol was from Panreac (Barcelona, Spain). Neutral red (NR, 3-amino-7-dimethylamino-2-methylphenanzine hydrochloride) solution (3.3 g/L), silver nitrate ($AgNO_3$), EDTA, sodium pyruvate and bovine serum

albumin (BSA) were supplied by Sigma-Aldrich (Madrid, Spain). AlamarBlue® dye and the 5-Carboxyfluorescein diacetate-acetoxymethyl ester (CFDA-AM) probe were from Life Technologies (Madrid, Spain).

For primary hepatocyte isolation Venofix® A perfusion cannulae (15 × 0.5 mm length) (B. Braun Melsungen AG, Melsungen, Germany) were used. Liquid heparin (5000 U.I heparin / 1 mL) was sourced from Drossapharm AG/SA Basel, Switzerland. Ethyl 3-aminobenzoate methanesulfonate anaesthetic (MS-222), collagenase (collagenase IV from Clostridium histolyticum), calcium- and magnesium-free GIBCO® Dulbeccos Phosphate Buffered Saline (DPBS), calcium chloride (CaCl2), and trypan blue (0.4%) solution were supplied by Sigma-Aldrich (Buchs, Switzerland). Sefar PETEX Nylon screens (mesh size 50 µm, 105 µm, 250 µm) were purchased from Sefar AG (Heiden, Switzerland). The peristaltic pump used for perfusion was an ISMATEC® IPC High Precision Multichannel Dispenser and was supplied by IDEX Health & Science (Wertheim, Germany). Medium 199 (M199) (with Earle's salts, L-glutamine and sodium bicarbonate), used for culturing the primary hepatocytes, was purchased from Sigma Aldrich (Madrid, Spain).

2.2. Nanoparticles

The representative silver nanomaterial NM-300K was provided by the European Commission Joint Research Centre (JRC) (Ispra, Italy) in the framework of the FP7 Project MARINA (Managing Risks of Nanomaterials) project. Vials contained 2 mL of an already dispersed AgNP suspension with 10.16% Ag content. Samples were stored at room temperature (~20 °C) under dark conditions. Prior to use, vials were shaken vigorously to ensure homogeneity. The exact concentration of nano-silver was measured (mg per mL) according to the handling procedure for weighing and sample introduction outlined in the JRC scientific and technical report on the characterisation, stability and homogeneity of this nanomaterial [29]. Exposure concentrations of the NM-300K dispersion were prepared directly in culture medium with no intermediate dilution in ultrapure water. We were also provided with the NM-300K sample dispersant (NM-300KDIS); an aqueous dispersant with stabilizing agents, consisting of 4% w/w each of polyoxyethylene glycerol trioleate and polyoxyethylene and sorbitan mono-Laurat (Tween 20). This dispersant acted as a vehicle control in all assays to test for any effects from the dispersant only.

2.3. Physico-Chemical Characterization of Nanoparticles

Dynamic light scattering (DLS) was applied to characterise the size distribution of AgNPs following suspension (time 0) and, after 24 h incubation in the corresponding cell culture, medium was put under appropriate culture conditions (according to cell line or primary hepatocytes being exposed). A Zetasizer Nano-ZS (Malvern Instruments Ltd., Malvern, UK) was used. Measurements were performed with the highest NM-300K exposure suspension concentrations (93.5 µg/mL). Size distributions are reported according to the mean of three independent measurements per sample, with each measurement consisting of four individual readings, and calculated using Zetasizer Software version 6.34 (Malvern Instruments Ltd). Due to the potential masking of smaller particles by using only intensity measurements, hydrodynamic sizes were also presented according to volume and number weighted distributions taking into account the AgNPs refractive index. The width and average

size of NM-300K size distributions were also taken into account according to the polydispersity index (PdI) and Z-average values, respectively. Measurements with only culture media were used as background controls as the presence of large proteins, and other media components will give size distribution readings. The NM-300K dispersion was also diluted in ultrapure Milli-Q water (93.5 μg/mL) to determine the size distribution prior to suspension in culture medium. MEM(-) was also employed in a preliminary study to investigate the stability of NM-300K in medium without serum.

2.4. Cell Line Culture

An array of cell lines derived from the rainbow trout were used in this study. RTL-W1, a rainbow trout liver cell line that appears to be derived from biliary preductural epithelial cells [30] was a generous gift from Dr. Bols and Dr. Lee [31]. The RTH-149 rainbow trout hepatoma cell line [32] and RTG-2, a fibroblast-like gonadal cell line [33] were obtained from the American Type Culture Collection (ATTC) (Manassas, VA, USA). The RTL-W1 cell line was cultured in L-15 medium supplemented with 1% L-glutamine and 1% penicillin/streptomycin. Both RTH-149 and RTG-2 cell lines were cultured in EMEM with Earle's balanced salts and with 1% L-glutamine, 1% penicillin/streptomycin and additionally either 1% sodium pyruvate in the case of RTH-149 or 1% NEAA for the RTG-2 cell line. The former and latter were termed EMEM(Pyr) and EMEM(NEAA), respectively. All media were supplemented with 10% FBS. Complete media formulations can be found in Supplementary Information Table 1.

All cell lines were cultured at 20 °C and, in the case of RTH-149 and RTG-2 cell lines, under 5% CO_2 atmosphere. Cell cultures were maintained in 75 cm^2 culture flasks (Greiner Bio-one, CellStar, Frichenhausen, Germany) and routinely split one to two times per week using 0.5% trypsin/0.02% EDTA. Experiments were carried out on confluent cell monolayers obtained with a seeding density of 2.5 × 104 cells in 100 μL of culture media after 24 h of culture in 96-well plates (Greiner-Bio one, CellStar, Spain).

2.5. Primary Hepatocyte Isolation and Culture

For hepatocyte isolation, juvenile rainbow trout weighing on average 210 ± 5 g and measuring 22 ± 4 cm in length were used. Trout were sacrificed using MS-222 (150 mg/L). A two-step perfusion method and collagenase digestion was used followed by mechanical dissociation of the liver tissue [34–36]. Following isolation, hepatocytes were seeded in 24 well culture plates (TPP, Trasadingen, Switzerland) at an optimum seeding density of 50×10^4 cells/ well (400 μL). The primary trout hepatocytes were cultured at 16 °C for 24 h in M199 medium supplemented with 10% FBS prior to exposures.

2.6. Exposures

Values of LD50 and IC50 reported in the literature after exposure of rainbow trout and rainbow trout cell lines to AgNPs range between 2.5 and 31 μg/mL [16,37]. To cover this reported range of concentrations, the highest and lowest concentrations chosen in the present study were 93.5 μg/mL and 0.73 μg/mL. Taking into account the possibility that cells could show a different sensitivity to the Ag ion than to AgNPs, a wider concentration range was chosen for the Ag ion going from 0.0345 μg/mL

Ag to 345 µg/mL Ag. The NM-300K original dispersion was diluted 1/1000 in the corresponding culture medium (depending on cell line/primary hepatocytes) to create the highest exposure concentration (93.5 µg/mL). From this, a 1/2 serial dilution produced the exposure concentration range used: 0.73 to 93.5 µg/mL. In these experiments, exposures were also performed with $AgNO_3$ which acted as a reference Ag+ ion source to compare with nanoparticle effects. For $AgNO_3$, exposures were performed using a 1/10 serial dilution of the highest exposure concentration, 345 µg/mL of Ag, until reaching the lowest exposure concentration of 0.0345 µg/mL of Ag. For ease of interpretation and comparative purposes, $AgNO_3$ exposure concentrations are presented with their respective µg/mL of silver content. Suspensions were also prepared of the dispersant (NM-300KDIS) in culture medium using initially a 1/1000 dilution to mimic the method used to create the highest NM-300K exposure concentration, and then diluted using a factor of 2. Cells exposed to dispersant only acted as a vehicle control in all assays. Cell lines and primary hepatocytes were exposed for 24 h before cytotoxicity assays were performed. This time frame was considered as appropriate to determine cytotoxicity allowing comparisons among cell lines and assay systems.

2.7. Cytotoxicity Assessment Using AlamarBlue, CFDA-AM and Neutral Red Uptake (NRU) Assay

We have employed a 3 in 1 fluorometric-based assay system that incorporates a 96-well plate layout and facilitates the simultaneous use of three assays to monitor different endpoints of cytotoxicity following 24 h exposure to $AgNO_3$ and NM-300K [38]. AlamarBlue, a CFDA-AM probe and neutral red dye were applied to the same set of cells to monitor metabolic activity, plasma membrane integrity and lysosome functionality, respectively. Cells were first treated with 100 µL of an alamarBlue/CFDA-AM working solution (1.25% v/v AlamarBlue and 4 µM CFDA-AM) prepared in MEM(-) for 30 min under dark conditions. Fluorescence intensity of the AlamarBlue and CFDA-AM conversion products, resorufin and carboxyfluorescin, respectively, were measured at 532 and 590 nm or 485 and 535 nm excitation (exc.) and emission (em.) wavelengths, respectively, using a microplate reader (Tecan Genios, Tecan Group Ltd., Männedorf, CH). Subsequently, the reagents were removed and cells were washed once with PBS before being treated for 1 h with 100 µL of a NR working solution (0.03 µg/mL) prepared in MEM(-) again under dark conditions. After this incubation period, the NR solution was removed and cells washed with PBS. Any retained NR was extracted using 150 µL of an acidified (1% glacial acetic acid) 50% ethanol/49% Milli-Q water solution and fluorescence was measured at 532 nm exc. and 680 nm em. (Tecan Genios microplate reader).

2.8. Interference

In order to assess any potential particle auto-fluorescence or quenching at the fluorescence wavelengths used in the cytotoxicity assays readouts, fluorescence readings of nanoparticle suspensions without cells were taken at 532 nm exc./590 nm em. for the AlamarBlue assay, 485nm exc./535 nm em. for the CFDA-AM assay and 532 nm exc./680 nm em. for the NRU assay. Readings were also taken with exposed cells after two washing steps with PBS to assess if the amount of nanoparticles present after washing (either adhered to the cell surface or taken up) is great enough to cause any potential interference. Furthermore, readings were taken of washed cells suspended in maximum concentrations of assay conversion products (resorufin (1 µM), 5-CF (4µM) and NR

(0.03 mg/mL)) prepared in MEM(-) to assess if the concentration of nanomaterial (NM) that remains in/on cells after washing could interfere with assay conversion products fluorescence.

2.9. Statistics

Data are represented as the mean ± standard error of the mean (SEM) of at least three independent experiments. In each of these experiments, exposure of cells to each of the concentrations of nanoparticle, the salt or the control medium was performed in triplicate. For all statistical analyses, the SigmaPlot® 12.0 software (Systat Software Inc, San Jose, CA, United States) was used. To calculate IC50 (concentration causing a 50% inhibition with respect to the controls) values, results were fitted to a regression model equation for a sigmoid curve: y = max/[1+e-(x-IC50)/b)] + min, where max is the maximal response observed, b is the slope of the curve and min the minimal response. Normality of the data distributions was checked by means of a Shapiro-Wilk test. The homogeneity of variances was checked automatically by the program. Since the data were normal and homoscedastic, a one-way repeated measures analysis of variance (RM-ANOVA) followed by a Dunnett's post hoc test was performed, allowing the detection of significant difference from control values and the establishment of the lowest observed effect concentration (LOEC) ($p < 0.05$).

3. Results

3.1. Physico-Chemical Characterisation

The size distribution of silver nanoparticles in the aqueous dispersion and culture media (MEM(-), L-15, EMEM(pyr), EMEM(NEAA) and M199) was characterised using DLS directly after preparation and after 24 h to check stability (Table 1). Hydrodynamic sizes are presented according to intensity, volume and number weighted distributions taking into account the AgNPs refractive index.

DLS analysis shows that aqueous dispersions of NM-300K (93.45 µg/mL) have a stable but polydisperse size distribution (PdI 0.473) with two distinct populations according to intensity distributions with average hydrodynamic diameters of 6 ± 1 nm and 54 ± 6 nm. However, when volume and number distributions are taken into consideration, NM-300K aqueous dispersions show a population averaging 25 ± 3 nm and 4 ± 1 nm, respectively, with a maximum hydrodynamic diameter. These distributions appear as stable after 24 h. In contrast, in serum free MEM(-), the silver nanoparticles aggregate and sediment out of solution over time. DLS analysis of particles that remain in suspension after 24 h reveal that bigger populations, 467 ± 56 nm in diameter, are present. Volume and number measurements show that, together with these particles (570 ± 30 nm), there are also particles present with maximum hydrodynamic diameters of 29 ± 3 and 24 ± 3 nm, respectively.

Table 1. Size distribution of the NM-300K dispersion in the various culture medium suspensions used in exposure studies characterised by dynamic light scattering (size distribution by intensity, volume and number).

NM-300K Suspension (93.5 µg/mL)				Hydrodynamic Size by Intensity					Hydrodynamic Size by Volume		Hydrodynamic Size by Number
Medium Type (Cells)	**Temp (°C)**	**Cl Ion (mM)**	**Cysteine */ Cystine Content (µM)**	**Time (h)**	**PdI**	**Z-Av (d.nm ± sd)**	**Peak 1 (d.nm ± sd) (%)**	**Peak 2 (d.nm ± sd) (%)**	**Peak 1 (d.nm± sd) (%)**	**Peak 2 (d.nm± sd) (%)**	**Peak 1 (d.nm ± sd) (%)**
MilliQ Water	20	–	–	T0	0.473	36 ± 7	6 ± 1 (14)	54 ± 6 (86)	4 ± 1 (98)	25 ± 3 (2)	4± 1 (100)
				T24	0.484	36 ± 10	6 ± 1 (9)	56 ± 3 (91)	4 ± 2 (97)	30 ± 4 (3)	3 ±1 (100)
MEM(-)	20	75.7	99	T0	0.453	44 ± 12	6 ± 1 (10)	62 ± 8 (90)	5 ± 1 (95)	30 ±6 (5)	4 ± 1(100)
				T24	0.569	188 ± 72	467± 56 (54)	42 ± 3 (46)	29 ± 3 (90)	570 ±30(10)	24 ±3 (100)
L-15 (RTL-W1 *)	20	88.0	990 *	T0	0.418	34 ± 1	7 ± 1 (8)	53 ± 3 (92)	5.8 ± 1 (93)	28 ± 3 (7)	5 ± 1 (100)
				T24	0.234	209 ±4	254 ± 27 (100)		294 ± 36 (100)		136 ± 13(100)
EMEM (pyr) (RTH-149)	20	75.7	99	T0	0.529	58 ± 2	9 ± 2 (9)	70 ± 9 (91)	7 ± 1 (95)	24 ± 7 (5)	5 ± 2(100)
				T24	0.441	53 ± 1	9 ± 1 (11)	83 ± 2 (89)	8 ± 1 (96)	23 ± 3 (4)	6 ± 1(100)
EMEM (NEAA) (RTG-2)	20	75.7	99	T0	0.455	53 ± 3	8 ± 1 (7)	79 ± 7 (93)	5 ± 1 (97)	21 ± 7 (3)	4 ± 1 (100)
				T24	0.297	43 ± 1	7 ± 2 (5)	64 ± 7 (95)	6 ± 2 (92)	26 ± 8 (8)	5 ± 2 (100)
M199 (primary hepatocytes)	16	75.3	5 * /83	T0	0.430	35 ± 1	6 ± 2 (6)	58 ± 3 (94)	5 ± 1 (92)	26 ± 6 (8)	4 ± 1 (100)
				T24	0.428	35 ± 1	6 ± 1 (8)	58 ± 4 (92)	5 ±1 (96)	26 ± 2 (4)	4 ± 1 (100)
Mean size distribution				T0	0.458	45 ± 12	7.5 ± 1 (7)	65 ± 12 (93)	6 ± 1 (94)	24 ± 3 (6)	5 ± 1 (100)
* excluding RTL-W1 culture medium L-15				T24 *	0.389	44 ± 9	7.3 ± 2 (8)	68 ± 13 (92)	6 ± 2 (95)	25 ± 2 (5)	5 ± 1 (100)

In L-15 medium, visual observation confirmed evidence of sedimentation and darkening of the NM-300K suspension (Supplementary Materials Figure S1). DLS measurements considering intensity readouts in this medium showed particles in suspension 254 ± 27 nm with average diameter. There was no evidence of smaller populations even when representing distributions in terms of volume or number. A PdI value of 0.234 confirmed that the silver nanoparticles are present in single populations of bigger sizes in this medium. With the exception of L-15, in all complex culture media (*i.e.*, EMEM (pyr), EMEM(NEAA) and M199) used for the cell lines and primary hepatocytes exposures the NM-300K dispersion is stable over 24 h and the frequency size distribution showed no important differences among media (see Table 1 for all details). Taking the mean size distribution for all medium suspensions, hydrodynamic diameters and respective intensity percentages for the populations are 7.5 ± 1 nm (7%) and 65 ± 12 nm (93%) in intensity distribution, 6 ± 1 nm (94%) and 24 ± 3 nm (6%) for volume distribution and 5 ± 1 nm (100 %) in number distribution. Very similar values are obtained after 24 h of incubation (Table 1). Size distribution frequency curves of the NM-300K dispersion in the different complex culture medium suspensions after 24 h incubation can be found in Supplementary Materials Figure S2.

3.2. Interference

The NM-300K dispersion in cell free suspensions had no fluorescence emission on their own. However, concentration dependent reductions in fluorescence units were seen due to both solution turbidity and possible physical interference from particles sedimented out of solution in the case of L-15 culture medium (see Supplementary Materials Figure S3). When NM-300K suspensions were incubated with cells under exposure assay conditions, and the washing steps were applied as in the cytotoxicity assays, the quantity of NM that remained in both stable (EMEM (pyr), EMEM (NEAA), M199) and sedimented (L-15) suspensions was not great enough to interfere with the fluorescent signal or mask the fluorescent product (resorufin, 5-CF or NR dye) signal.

3.3. Cytotoxicity of $AgNO_3$ and NM-300K

Dispersant alone (NM-300KDIS) at the concentrations corresponding to the exposure assays did not provoke any cytotoxic effect in any of the assay systems used.

3.3.1. AlamarBlue Assay

The cytotoxicity results obtained with this assay for all cell lines and primary hepatocytes following exposure to $AgNO_3$ and NM-300K are presented in Figure 1 and Table 2. The IC50 values following 24 h exposure to $AgNO_3$ and NM-300K are presented in (Table 2). For $AgNO_3$, the RTL-W1 cell line exhibited the highest IC50 value (10.9 µg/mL) while the other cells used in these experiments exhibited much lower IC50 values (1.1–2 µg/mL). Taking LOEC values into account, the primary hepatocytes showed increased sensitivity (LOEC = 0.34 µg/mL) with respect to the other cell lines (Figure 1 (a)).

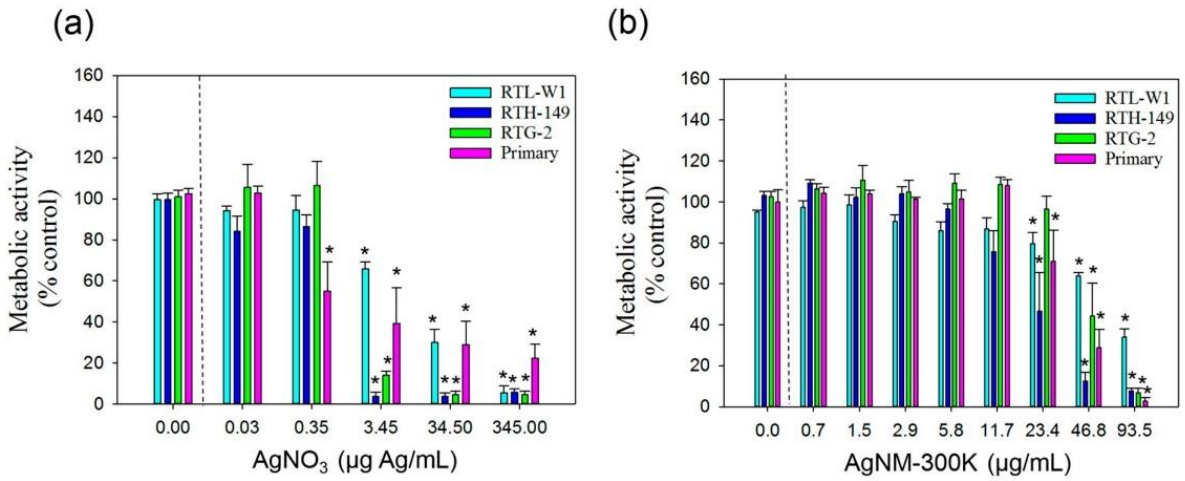

Figure 1. Cytotoxicity of $AgNO_3$ and AgNPs NM-300K according to AlamarBlue assay. (**a**) Cytotoxicity measured using the AlamarBlue assay and metabolic activity as endpoint of toxicity in liver cell lines (RTL-W1 and RTH-149), a gonadal cell line (RTG-2) and primary hepatocytes from rainbow trout following 24 h exposure to $AgNO_3$; (**b**) silver nanomaterial NM-300K. Cells exposed to concentration 0 received the maximal concentration of the dispersant and served as control. Values represent the mean ± standard error of the mean (SEM) (n = 3); * denotes statistically significant differences from control ($p < 0.05$).

Table 2. IC50 (µg /mL) values calculated from the different cytotoxicity assay systems in the rainbow trout cell lines and primary hepatocytes after exposure to $AgNO_3$ and NM-300K.

Assay system	**AlamarBlue**		**CFDA-AM**		**NRU**	
	$AgNO_3$	NM-300K	$AgNO_3$	NM-300K	$AgNO_3$	NM-300K
Cell line	IC_{50} (µg/mL)					
RTL-W1	11	75.9	32.2	15.9	10.9	10.7
RTH-149	1.1	19.8	1.4	21.8	0.4	24.9
RTG-2	2.8	41.7	1.3	43.1	1.0	37.2
Primary hepatocytes	2.0	30.6	2.7	37.7	3.8	45.2

After exposure to NM-300K, the RTL-W1 cell line showed higher IC50 values (75.9 µg/mL) than the other cells (19.8 µg/mL to 41.7 µg/mL). Primary hepatocytes, RTH-149 and RTL-W1 exhibited similar LOEC values (23.4 µg/mL). The LOEC value recorded for the RTG-2 gonadal cell lines was 46.8 µg/mL (Figure 1 (b)).

3.3.2. CFDA-AM Assay

Curves showing concentration dependent effects obtained with this assay are presented in Figure 2, whereas IC50 values of these curves are shown in Table 2. Again, the RTL-W1 cell line had the highest IC50 and the LOEC value for the RTL-W1 cell line following AgNO3 exposure was 10-fold higher (34.52 µg/mL) than for primary hepatocytes, RTH-149 and RTG-2 cell lines (3.45 µg/mL) (Figure 2 (a)).

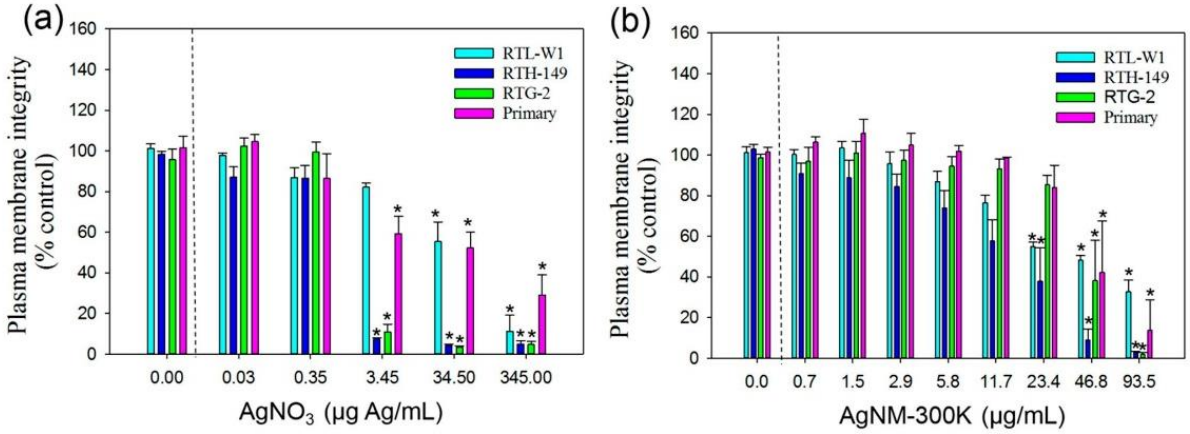

Figure 2. Cytotoxicity of $AgNO_3$ and AgNPs NM-300K according to CFDA-AM assay; (**a**) Cytotoxicity measured using the CFDA-AM assay and plasma membrane integrity as endpoint of toxicity in liver cell lines (RTL-W1 and RTH-149), a gonadal cell line (RTG-2) and primary hepatocytes from rainbow trout following 24 h exposure to $AgNO_3$; (**b**) silver nanomaterial NM-300K. Cells exposed to concentration 0 received the maximal concentration of the dispersant and served as control. Values represent the mean ± standard error of the mean (SEM) (n = 3); * denotes statistically significant differences from control ($p < 0.05$).

In contrast to responses to $AgNO_3$, the RTL-W1 cell line showed the lowest IC50 value following NM-300K exposure (Table 2). Thus, according to IC50 values in this assay, the cell sensitivity for NM-300K toxicity follows the order: RTL-W1 > RTH-149 > Primary hepatocytes > RTG-2. Both liver cell lines (RTH-149 and RTL-W1) showed lower LOEC values (23.4 µg/mL) than primary hepatocytes and RTG-2 cells (46.8 µg/mL) (Figure 2(b)).

3.3.3. Neutral Red Uptake Assay

Concentration response curves according to this assay system for the cell lines and hepatocytes following exposure to $AgNO_3$ and NM-300K are presented in Figure 3. Similarly to the previous assays, the highest IC50 value for $AgNO_3$ was recorded for the RTL-W1 cell line but all the fish cells showed a NOEC of 3.45 µg/mL (Figure 3(a)).

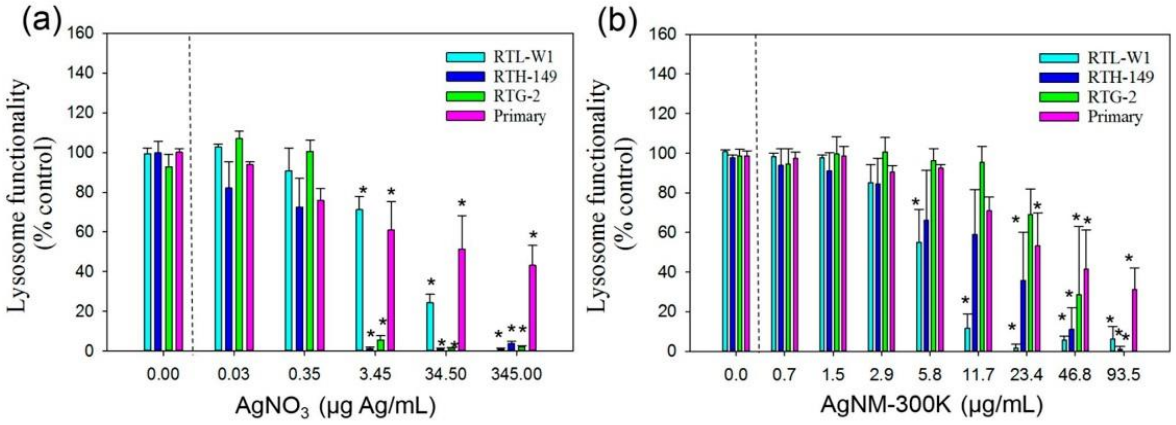

Figure 3. Cytotoxicity of $AgNO_3$ and AgNPs NM-300K according to NRU assay; (**a**) Cytotoxicity measured using the NRU assay and lysosome functionality as toxicity endpoint in liver cell lines (RTL-W1 and RTH-149), a gonadal cell line (RTG-2) and primary hepatocytes from rainbow trout following 24 h exposure to AgNO3; (**b**) silver nanomaterial NM-300K. Cells exposed to concentration 0 received the maximal concentration of the dispersant and served as control. Values represent the mean ± standard error of the mean (SEM) (n = 3); * denotes statistically significant differences from control ($p < 0.05$).

For the AgNP, the RTL-W1 was the most sensitive showing lower IC50 and LOEC values than the other cells (Table 2 and Figure 3(b)). The LOEC value for the RTL-W1 cell line was 5.8 µg/mL according to the NRU assay (Figure 3(b)). In contrast, the RTG-2 cell line showed the lowest sensitivity towards NM-300K exposure according to a recorded LOEC value of 46.8 µg/mL.

4. Discussion

In this study, we have tested the toxicity of $AgNO_3$ and AgNPs (using the representative silver nanomaterial NM-300K from the JRC Nanomaterials Repository) towards rainbow trout liver cell lines (RTL-W1, RTH-149), a gonadal cell line (RTG-2) and primary hepatocytes. For chemicals in general, *in vitro* systems are still being validated and their regulatory applicability is still being explored, taking into account, in particular, their value in predicting *in vivo* responses. In the case of NMs, that possibly present additional confounding factors, the use of *in vitro* systems raises new concerns. We sought to address these issues.

Prior to nanoparticle cytotoxicity assessment, it is essential to take into consideration the possible interference between *in vitro* assay systems and nanomaterials [39–42]. In this work, this issue was carefully assessed and it was shown that the amount of NM-300K that remained inside or adhered to the cells was not great enough to cause interference with the used cytotoxicity assays.

According to DLS analysis, NM-300K suspensions prepared in EMEM (RTH-149, RTG-2 cells) and M199 (primary hepatocytes) were stable over the 24 h exposure period. Taking volume distributions as the most accurate representation, due to intensity masking of smaller particles and number distributions favouring smaller particles, the NM-300K size distribution in culture medium is

composed of 95% of particles with an average diameter of 7 ± 1 nm and 5% 25 ± 2 nm in diameter. This guarantees a real exposure to nanoparticulate material. All media were supplemented with FBS which appeared to ensure stability. In contrast to other media suspensions, particles prepared in L-15 medium (RTL-W1 cells) experienced aggregation formation and precipitated out of solution over the 24 h exposure timeframe. L-15 has high levels of thiol containing amino acids including cysteine and methionine which are strong Ag+ complexing ligands known to form Ag–S covalent bonds with AgNPs. It also has a higher chloride content that could favour the formation of silver chloride compounds that could precipitate out of solution [43]. Therefore, although L-15 is widely used as a cell culture medium and has been used previously in nanoparticle toxicity studies with fish cells [19,44] results of this study would suggest that it should be applied with maximal caution in these kinds of approaches. As seen in this study and also highlighted by Yue and colleagues [45], the choice of cell culture medium can affect AgNP physico-chemical behaviour and thus is likely to also have a direct effect on toxicity.

In this study, $AgNO_3$ was included as a Ag+ ion source to investigate differences in the toxicity of Ag+ ions and AgNPs and also if differences in sensitivities to Ag+ exist between different cell lines and hepatocytes. Previous studies with CuNPs and ZnO NPs demonstrated an increased sensitivity of mammalian cell lines with respect to fish cell lines to nanoparticle toxicity, possibly due to differences in their sensitivity to ions released from the nanoparticles rather than to nanoparticle effects [46,20]. There is also debate surrounding the influence of Ag+ ion on nanoparticle toxicity and conflicting results showing either that nanoparticles are more or less toxic than equivalent concentrations of Ag+ [47,48]. In this study, in general, cytotoxic effects were observed at lower concentrations of $AgNO_3$ than NM-300K, which suggests a higher toxicity of ions.

IC50 values corresponding to $AgNO_3$ for RTH-149, RTG-2 and primary hepatocytes ranged from 0.4 to 3.8 μg/mL across all toxicity endpoints. This is in agreement with Farkas and colleagues [49] who showed an IC50 of 1.1 μg/mL following $AgNO_3$ exposures using rainbow trout primary hepatocytes and the AlamarBlue assay system. In contrast, the RTL-W1 liver cell line was distinctly the least sensitive, and the toxic potency of $AgNO_3$ was around 10-fold lower (IC50 ranging from 10.9 to 32.2 μg/mL) than in the rest of the cells used in this study. As previously discussed, the difference in sensitivity and susceptibility in this cell line is most likely related with decreased bioavailability and complexing of the Ag+ ions in L-15 medium. This important observation has also been made by Dayeh and colleagues [50] when using L-15 medium and testing the toxicity of copper sulphate ($CuSO_4$) and copper chloride ($CuCl_2$) in fish cells, where toxicity was absent but appeared when using amino acid free minimal medium (L15/ex). This draws attention to the important influence of medium composition on metal ion toxicity in cell lines *in vitro*. Kermanizadeh and co-authors reported IC50 values of 14.06 and 31.25 μg/mL for NM-300K toxicity in human renal proximal tubule epithelial cells (HK-2) following exposure in different mediums [51]. A similar phenomenon has been reported for AgNP toxicity studies *in vivo* towards rainbow trout fry with LOEC values ranging from 0.7 to 25 μg/mL, increasing with increasing water salinity [52]. Therefore, medium composition/exposure environment can be a key factor not only in influencing particle behaviour but in dictating toxicity.

A concentration dependent reduction in viability following exposure to NM-300K (0.73 to 93.5 μg/mL) in all cell lines and primary hepatocytes was observed. IC50 values ranged from 10.7 to 75.9 μg/mL according to the specific cell line and toxicity assay endpoint used. Despite its apparent

increased resistance to $AgNO_3$, the RTL-W1 cell line proved particularly susceptible to toxic effects of NM-300K when measured as lysosomal damage (NRU assay, with the lowest IC50 value recorded: 10.7 µg/mL) or membrane disruption (CFDA-AM assay, with an IC50 of 15.9 µg/mL). However, the IC50 values according to the AlamarBlue assay were the highest recorded (IC50 75.9 µg/mL). Similarly Gaiser and co-authors [53] showed lower IC50 values using the lactate dehydrogenase (LDH) leakage assay which measures loss of membrane integrity compared to the AlamarBlue assay (8 µg/mL *vs.* 64 µg/mL respectively) using the same NM-300K particles in the human hepatic cell line C3A. This may point to a specific mechanism of toxicity for the NM-300K suspensions targeting membranes, particularly those of lysosomes. It is possible that the bigger aggregates present in RTL-W1 culture medium (L-15) can cause lysosomal damage at lower exposure concentrations. In fact, lysosomal perturbation has been reported for a variety of NMs (reviewed in [54]) and is seen as an emerging mechanism of NM toxicity. According to a study by Yue and colleagues [45], using the RTgill-W1 rainbow trout gill cell line, lysosomal membrane integrity was also a significantly more sensitive toxicity endpoint for citrate capped AgNPs. Furthermore, they have also shown that cysteine can protect against metabolic activity and membrane damage but not lysosomal damage in the case of AgNPs, thus corroborating our findings in this study. This could be due to different uptake mechanisms of these aggregated AgNPs and, while outside of the scope of this study, this warrants further investigation.

When comparing the responses of the continuous cell lines to the primary hepatocytes in general primary cells showed comparable sensitivity both to Ag+ and AgNPs. However, when LOEC values were taken into account, primary cells showed increased sensitivity to Ag+ according to the AlamarBlue assay system which measures metabolic activity. The lack of any noticeable difference in the physico-chemical properties of AgNPs in media used for primary hepatocyte exposures suggests that the exposure environment did not contribute to this increased sensitivity. Primary cells exhibit metabolic pathways and capacities quite similar to the cells in original tissues, while continuous cell lines have lost some of them. This can be associated with higher detoxification capabilities (and therefore lower sensitivity to toxic action of substances) but also with higher sensitivities (to the toxic action of substances) due to alterations of any of the very closely related metabolic pathways or due to a favored uptake rate of Ag+. Any or a combination of these factors could explain the differences in sensitivity that would need to be addressed in future studies. Interestingly, the increased sensitivity is only seen following exposure to $AgNO_3$ and not when exposed to AgNPs suggesting that possessing full metabolic processes (e.g. cytochrome P450–mediated oxidation) may not be particularly significant for the toxicology of NPs. This point has also been made by other authors [53] when comparing responses to AgNPs in rat liver models *in vitro* and *in vivo*.

In vitro studies are always limited with respect to *in vivo* approaches by not being able to represent different tissue specific toxic insults, adaptive responses at whole organism levels and toxicokinetics [55]. As a consequence, they show in general lower sensitivity than *in vivo* systems [56,57]. The recently reported LC50 value in juvenile rainbow trout following 48 h AgNP exposure was 3.13 µg/mL [16]. In our study, IC50 values ranged from 10.7 to 75.9 µg/mL, representing three to 24-fold higher values than that reported in *in vivo* LC50. Apart from the obvious metabolic and complexity differences between *in vitro* and *in vivo* systems, one factor that helps to explain the higher IC50 values is that the actual concentrations of bioavailable AgNPs in this study are most likely much lower due to the presence of

serum proteins in the culture media. Massarsky and co-authors, also using rainbow trout primary hepatocytes, only report subtle responses to 31 µg/mL of AgNPs when bovine serum albumin was present in the exposure medium [37]. In contrast, studies using serum free medium recorded IC50 values between 2.5 and 4.9 µg/mL in rainbow trout primary hepatocytes [49]. In our study, we have used serum due to its physiological relevance and to reflect conditions in the circulatory environment which the nanoparticles would be exposed to prior to distribution in the liver. Incorporation of FBS also ensured the exposure of cells to stable AgNP preparations. All this must be taken into account in the future development of standard guidelines for *in vitro* tests in order to increase the predictive value of *in vitro* studies for *in vivo* responses. For now, working with well-defined representative NMs, choosing cell lines from relevant target tissues and using a battery of cytotoxicity assays, as in the present study, can be very useful in toxicity ranking and as pre-screening to help regulators in making the decision to avoid particular *in vivo* assays. It is also evident that the applied approach represents an invaluable tool for mechanistic studies.

5. Conclusions

Up until now, the cytotoxicity of the NM-300K silver representative nanomaterial has not been tested in liver cells of fish. In this comparative study, liver cell lines (RTH-149, RTL-W1) proved as sensitive test systems when compared to primary hepatocytes following exposure to NM-300K. Considering the ease of maintenance and culture of cell lines compared with primary hepatocytes, this has important practical implications for the integration of such a tool into intelligent testing strategies for the hazard assessment of nanoparticles. However, further work is necessary to determine the applicability of this tool to other NPs using other cellular systems that could be more representative of particular conditions or environments.

Using the simultaneous application of three different assay systems (AlamarBlue, CFDA-AM and NRU) proved a valuable means to assess cytotoxicity according to different targets of toxic action. The lowest IC50 was recorded using the NRU assay and the RTL-W1 cell line (10.7 µg/mL) and, thus, points to lysosomal damage as an important indicator for detecting nanoparticle specific effects. It must be noted, however, that cell culture medium composition had a strong influence on the behaviour and toxicity of Ag+ and AgNPs, causing precipitation or limiting their bioavailability and leading to a reduction of or increase in toxicity according to particular tests applied. Therefore, while such an *in vitro* testing approach was easily applicable careful consideration must be made regarding the influence of cell culture medium composition when using cellular *in vitro* systems for observing toxicity of NPs. Choosing culture media with similar compositions for exposures will ensure the same NM presentation to respective cell lines being tested and facilitate an accurate comparative toxicity assessment.

Acknowledgments

This research was performed under the European Commission 7th framework project MARINA (Grant Agreement No. 263215) with financial support also from the Instituto Nacional de Investigación y Tecnología Agraria y Alimentaria (INIA) project AT2011-001. All authors wish to acknowledge Anja Möller and all the staff in the centre for Fish and Wildlife Health (FIWI) at the

Vetsuisse Faculty of the University of Bern for their assistance when working with rainbow trout and isolating primary hepatocytes.

Author Contributions

Mona Connolly, Jose M. Navas and Maria-Luisa Fernandez-Cruz conceived and designed the experiments; Mona Connolly, Luis Alte and Alba Quesada-Garcia performed the experiments; Mona Connolly analyzed the data; Helmut Segner provided the training in primary hepatocyte cell culture and facilities in which exposures to primary hepatocytes were performed and also was involved in the design of these experiments. Mona Connolly wrote the paper. Maria-Luisa Fernandez-Cruz, Helmut Segner, and Jose M. Navas were involved in critical revision and editing of the manuscript.

Conflicts of Interest

The authors declare no conflict of interest.

References

1. Woodrow Wilson Database, 2014. Nanotechnology consumer product inventory. Woodrow Wilson International Centre for Scholars. Available online: http://www.nanotechproject.org/cpi/ website (accessed on 10 October 2014).
2. Mueller, N.C.; Nowack, B. Exposure modeling of engineered nanoparticles in the environment. *Environ. Sci. Technol.* **2008**, *42*, 4447–4453.
3. Benn, T.M.; Westerhoff, P. Nanoparticle silver released into water from commercially available sock fabrics. *Environ. Sci. Technol.* **2008**, *42*, 4133–4139.
4. Geranio, L.; Heuberger, M.; Nowack, B. The behavior of silver nanotextiles during washing. *Environ. Sci. Technol.* **2009**, *43*, 8113–8118.
5. Kaegi, R.; Sinnet, B.; Zuleeg, S.; Hagendorfer, H.; Mueller, E.; Vonbank, R.; Boller, M.; Burkhardt, M. Release of silver nanoparticles from outdoor facades. *Environ. Pollut.* **2010**, *158*, 2900–2905.
6. Fabrega, J.; Luoma, S.N.; Tyler, C.R.; Galloway, T.S.; Lead, J.R. Silver nanoparticles: Behaviour and effects in the aquatic environment. *Environ. Int.* **2011**, *37*, 517–531.
7. Gottschalk, F.; Kost, E.; Nowack, B. Engineered nanomaterials in water and soils: A risk quantification based on probabilistic exposure and effect modeling. *Environ. Toxicol. Chem.* **2013**, *32*, 1278–1287.
8. Wood, C.M.; Hogstrand, C.; Galvez, F.; Munger, R.S. The physiology of waterborne silver toxicity in freshwater rainbow trout (Oncorhynchus mykiss): 1. The effects of ionic Ag+. *Aquat. Toxicol.* **1996**, *35*, 93–109.
9. Hogstrand, C.; Galvez, F.; Wood C.M. Toxicity, silver accumulation and metallothionein induction in freshwater rainbow trout during exposure to different silver salts. *Environ. Toxicol. Chem.* **1996**, *15*, 1102–1108.
10. Bilberg, K.; Hovgaard, M.B.; Besenbacher, F.; Baatrup, E. In vivo toxicity of silver nanoparticles and silver ions in zebra fish (Danio rerio). *J. Toxicol.* **2012**, doi:10.5620/eht.e2014021.

11. Choi, J.E.; Kim, S.; Ahn, J.H.; Youn, P.; Kang, J.S.; Park, K.; Yi, J.; Ryu, D.Y. Induction of oxidative stress and apoptosis by silver nanoparticles in the liver of adult zebra fish. *Aquat. Toxicol.* **2010**, *100*, 151–159.
12. Griffitt, R.J.; Luo, J.; Gao, J.; Bonzongo, J.-C.; Barber, D.S. Effects of particle composition and species on toxicity of metallic nanomaterials in aquatic organisms. *Environ. Toxicol. Chem.* **2008**, *27*, 1972–1978.
13. Chae, Y.J.; Pham, C.H.; Lee, J.; Bae, E.; Yi, J.; Gu, M.B. Evaluation of the toxic impact of silver nanoparticles on Japanese medaka (Oryzias latipes). *Aquat. Toxicol.* **2009**, *94*, 320–327.
14. Wu, Y.; Zhou, Q.; Li, H.; Liu, W.; Wang, T.; Jiang, G. Effects of silver nanoparticles on the development and histopathology biomarkers of Japanese medaka (Oryzias latipes) using the partial-life test. *Aquat. Toxicol.* **2010**, *100*, 160–167.
15. Griffitt, R.J.; Brown-Peterson, N.J.; Savin, D.A.; Manning, C.S.; Boube, I.; Ryan, R.A.; Brouwer, M. Effects of chronic nanoparticulate silver exposure to adult and juvenile sheepshead minnows (Cyprinodon variegatus). *Environ. Toxicol. Chem.* **2012**, *31*, 160–167.
16. Johari, S.A.; Kalbassi, M.R.; Soltani, M.; Yu, I.J. Toxicity comparison of colloidal silver nanoparticles in various life stages of rainbow trout (Oncorhynchus mykiss). *Iran. J. Fish. Sci.* **2013**, *12*, 76–95.
17. EU Directive 67/548/EEC on the classification, packaging and labelling of dangerous substances of 27 June 1967 on the approximation of laws, regulations and administrative provisions relating to the classification, packaging and labelling of dangerous substances. Available online: http://eur-lex.europa.eu/homepage.html (accessed on 15 November 2014).
18. Regulation (EC) No 1272/2008 on the classification, labelling and packaging of substances and mixtures; amending and repealing Directives 67/548/EEC and 1999/45/EC, and amending Regulation (EC) No 1907/2006. EU directive 2008/112/EC amending Council Directives 76/768/EEC, 88/378/EEC, 1999/13/EC and Directives 2000/53/EC, 2002/96/EC and 2004/42/EC in order to adapt them to Regulation (EC) No 1272/2008 on classification, labelling and packaging of substances and mixtures. Available online: http://eurlex.europa.eu/legalcontent/EN/TXT/?qid=1401782728680&uri=CELEX:32008R1272 (accessed on 15 November 2014).
19. Fernández, D.; García-Gómez, C.; Babín, M. In vitro evaluation of cellular responses induced by ZnO nanoparticles, zinc ions and bulk ZnO in fish cells. *Sci. Total Environ.* 2013, *452–453*, 262–274.
20. Song, L.; Connolly, M.; Fernández-Cruz, M.L.; Vijver, M.G.; Fernández, M.; Conde, E.; de Snoo, G.R.; Peijnenburg, W.J.; Navas, J.M. Species-specific toxicity of copper nanoparticles among mammalian and piscine cell lines. *Nanotoxicology* **2014**, *8*, 383–393.
21. Vo, N.T.; Bufalino, M.R.; Hartlen, K.D.; Kitaev, V.; Lee, L.E. Cytotoxicity evaluation of silica nanoparticles using fish cell lines. *In Vitro Cell Dev. Biol. Anim.* **2014**, *50*, 427–38.
22. Taju, G.; Abdul-Majeed, S.; Nambi, K.S.; Sahul-Hameed, A.S. In vitro assay for the toxicity of silver nanoparticles using heart and gill cell lines of Catla catla and gill cell line of Labeo rohita. *Comp. Biochem. Physiol. Pt. C* **2014**, *161*, 41–52.

23. Commission Regulation (EC) No 134/2009 amending Regulation (EC) No. 1907/2006 of the European Parliament and of the Council on the Registration, Evaluation, Authorisation and Restriction of Chemicals (REACH) as regards Annex XI. Available online: http://eur-lex.europa.eu/legalcontent/EN/TXT/?qid=1401782624095&uri=CELEX:32009R0134 (accessed on 15 November 2014)
24. Salari-Joo, H.; Kalbassi, M.R.; Yu, I.J.; Lee, J.H.; Johari, S.A. Bioaccumulation of silver nanoparticles in rainbow trout (Oncorhynchus mykiss): Influence of concentration and salinity. *Aquat. Toxicol.* **2013**, *140–141*, 398–406.
25. Wu, Y.; Zhou, Q. Silver nanoparticles cause oxidative damage and histological changes in medaka (Oryzias latipes) after 14 days of exposure. *Environ. Toxicol. Chem.* **2013**, *32*, 165–173.
26. Scown, T.M.; Santos, E.M.; Johnston, B.D.; Gaiser, B.; Baalousha, M.; Mitov, S.; Lead, J.R.; Stone, V.; Fernandes, T.F.; Jepson M.; *et al.* Effects of aqueous exposure to silver nanoparticles of different sizes in rainbow trout. *Toxicol. Sci.* **2010**, *115*, 521–534.
27. Kermanizadeh, A.; Gaiser, B.K.; Ward, M.B.; Stone, V. Primary human hepatocytes *versus* hepatic cell line: assessing their suitability for *in vitro* nanotoxicology. *Nanotoxicology* **2013**, *7*, 1255–1271.
28. OECD-WPMN, Series on the Safety of Manufactured Nanomaterials, List of manufactured nanomaterials and list of endpoints for phase one of the OECD testing programme, No. 6-ENV/JM/MONO (2008)13/REV, Organisation for Economic Co-operation and Development, Paris, France. Available online: http://search.oecd.org/officialdocuments/publicdisplaydocumentpdf/?cote=ENV/JM/MONO(2008)13/REV&docLanguage=En (accessed on 20 November 2014).
29. Klein, C.; Comero, S.; Stahlmecke, B.; Romazanov, J.; Kuhlbusch, T.; van Doren, E.; de Temmerman, P.-J.; Mast, J.; Wick, P.; Krug, H.; *et al. NM-Series of Representative Manufactured Nanomaterials: NM-300 Silver Characterisation, Stability, Homogeneity*; Publications Office of the European Union: City of Luxembourg, Luxembourg, 2011.
30. Malhão, F.; Urbatzka, R.; Navas, J.M.; Cruzeiro, C.; Monteiro, R.A.; Rocha, E. Cytological, immunocytochemical, ultrastructural and growth characterization of the rainbow trout liver cell line RTL-W1. *Tissue Cell.* **2013**, *45*, 159–174.
31. Lee, L.E.; Clemons, J.H.; Bechtel, D.G.; Caldwell, S.J.; Han, K.B.; Pasitschniak-Arts, M.; Mosser, D.D.; Bols, N.C. Development and characterization of a rainbow trout liver cell line expressing cytochrome P450-dependent monooxygenase activity. *Cell. Biol. Toxicol.* **1993**, *9*, 279–294.
32. Fryer, L.; McCain, B.; Leong, J. A cell line derived from Rainbow Trout (Salmo gairdneri) *Hepatoma. Fish Pathol.* **1981**, *15*, 193–200.
33. Wolf, K.; Quimby, M.C. Established eurythermic line of fish cells *in vitro*. *Science* **1962**, *135*, 1065–1066.
34. Mommsen, T.P.; Moon, T.W.; Walsh, P.J. Hepatocytes: Isolation, maintenance and utilization. In *Biochemistry and Molecular Biology of Fishes*: *Analytical techniques*; Hochachka, P.W., Mommsen, T.P, Eds.; Elsevier: Amsterdam, Netherlands, 1994; Volume 3, pp. 355–373.
35. Segner, H. Isolation and primary culture of teleost hepatocytes. *Comp. Biochem. Physiol. Pt. A* **1998**, *120*, 71–81.

36. Navas, J.M.; Segner, H. Vitellogenin synthesis in primary cultures of fish liver cells as endpoint for *in vitro* screening of the (anti)estrogenic activity of chemical substances. *Aquatic Toxicol.* **2006**, *80*, 1–22.
37. Massarsky, A.; Abraham, R.; Nguyen, K.C.; Rippstein, P.; Tayabali, A.F.; Trudeau, V.L.; Moon, T.W. Nanosilver cytotoxicity in rainbow trout (Oncorhynchus mykiss) erythrocytes and hepatocytes. *Comp. Biochem. Physiol. Pt. C* **2014**, *159*, 10–21.
38. Dayeh, V.R.; Schirmer, K.; Lee, L.E.J.; Bols, N.C. Rainbow trout gill cell line microplate cytotoxicity test. In *Small-Scale Freshwater Toxicity Investigations*; Blaise, C., Férard, J.F., Eds.; Springer Netherlands: Berlin, Germany, 2005; Volume 1, pp. 473–503.
39. Han, X.; Gelein, R.; Corson, N.; Wade-Mercer, P.; Jiang, J.; Biswas, P.; Finkelstein, J.N.; Elder, A.; Oberdörster, G. Validation of an LDH assay for assessing nanoparticle toxicity. *Toxicology* **2011**, *287*, 99–104.
40. Kroll, A.; Pillukat, M.H.; Hahn, D.; Schnekenburger, J. Interference of engineered nanoparticles with *in vitro* toxicity assays. *Arch. Toxicol.* **2012**, *86*, 1123–1136.
41. Samberg, M.E.; Oldenburg, S.J.; Monteiro-Riviere, N.A. Evaluation of silver nanoparticle toxicity in skin *in vivo* and keratinocytes *in vitro*. *Environ. Health Perspect.* **2010**, *118*, 407–413.
42. Wörle-Knirsch, J.M.; Pulskamp, K.; Krug, H.F. Oops they did it again! Carbon nanotubes hoax scientists in viability assays. *Nano Lett.* **2006**, *6*, 1261–1268.
43. Grosell, M.; Hogstrand, C.; Wood, C.M.; Hansen, H.J. A nose-to-nose comparison of the physiological effects of exposure to ionic silver *versus* silver chloride in the European eel (Anguilla anguilla) and the rainbow trout (Oncorhynchus mykiss). *Aquat. Toxicol.* **2000**, *48*, 327–342.
44. George, S.; Lin; S.; Ji, Z.; Thomas, C.R.; Li, L.; Mecklenburg, M.; Meng, H.; Wang, X.; Zhang, H.; Xia, T.; Hohman, J.N.; Lin, S.; Zink, J.I.; Weiss, P.S.; Nel, A.E. Surface defects on plate-shaped silver nanoparticles contribute to its hazard potential in a fish gill cell line and zebra fish embryos. *ACS Nano* **2012**, *6*, 3745–3759.
45. Yue, Y.; Behra, R.; Sigg, L.; Fernández-Freire, P.; Pillai, S.; Schirmer, K. Toxicity of silver nanoparticles to a fish gill cell line: Role of medium composition. *Nanotoxicology* **2015**, *9*, 54–63.
46. Fernández-Cruz, M.L.; Lammel, T.; Connolly, M.; Conde, E.; Barrado, A.I.; Derick, S.; Perez, Y.; Fernandez, M.; Furger, C.; Navas, J.M. Comparative cytotoxicity induced by bulk and nanoparticulated ZnO in the fish and human hepatoma cell lines PLHC-1 and Hep G2. *Nanotoxicology* **2013**, *7*, 935–952.
47. Asghari, S.; Johari, S.A.; Lee, J.H.; Kim, Y.S.; Jeon, Y.B.; Choi, H.J.; Moon, M.C.; Yu, I.J. Toxicity of various silver nanoparticles compared to silver ions in Daphnia magna. *J. Nanobiotechnol.* **2012**, *10*, 14.
48. Lubick, N. Nanosilver toxicity: Ions, nanoparticles—Or both? *Environ. Sci. Technol.* **2008**, doi:10.1021/es8026314.
49. Farkas, J.; Christian, P.; Urrea, J.A.; Roos, N.; Hassellöv, M.; Tollefsen, K.E.; Thomas, K.V. Effects of silver and gold nanoparticles on rainbow trout (Oncorhynchus mykiss) hepatocytes. *Aquat. Toxicol.* **2010**, *96*, 44–52.
50. Dayeh, V.R.; Lynn, D.H.; Bols, N.C. Cytotoxicity of metals common in mining effluent to rainbow trout cell lines and to the ciliated protozoan, Tetrahymena thermophila. *Toxicol. Vitro* **2005**, *19*, 399–410.

51. Kermanizadeh, A.; Vranic. S.; Boland, S.; Moreau, K.; Baeza-Squiban, A.; Gaiser, B.K.; Andrzejczuk, L.A.; Stone, V. An *in vitro* assessment of panel of engineered nanomaterials using a human renal cell line: Cytotoxicity, pro-inflammatory response, oxidative stress and genotoxicity. *BMC Nephrol.* **2013**, doi:10.1186/1471-2369-14-96.
52. Kalbassi, M.R.; Salari-joo, H.; Johari, A. Toxicity of silver nanoparticles in aquatic ecosystems: Salinity as the main cause in reducing toxicity. *Iran. J. Toxicol.* **2011**, *5*, 436–443.
53. Gaiser, B.K.; Hirn, S.; Kermanizadeh, A.; Kanase, N.; Fytianos, K.; Wenk, A.; Haberl, N.; Brunelli, A.; Kreyling, W.G.; Stone, V. Effects of silver nanoparticles on the liver and hepatocytes *in vitro*. *Toxicol. Sci.* **2013**, *131*, 537–547.
54. Stern, S.T.; Adiseshaiah, P.P.; Crist, R.M. Autophagy and lysosomal dysfunction as emerging mechanisms of nanomaterial toxicity. *Part. Fibre. Toxicol.* **2012**, doi:10.1186/1743-8977-9-20.
55. Mothersill, C.; Austin, B. *In Vitro Methods in Aquatic Ecotoxicology*; Springer and Praxis Publishing: Chichester, UK, 2003; pp. 381–384.
56. Castano, A.; Bols, N.; Braunbeck, T.; Dierickx, P.; Halder, M.; Isomaa, B.; Kawahara, K.; Lee, L.E.J.; Mothersill, C.; Pärt, P.; *et al.* The use of fish cells in ecotoxicology. Report and recommendations of the ECVAM workshop 47. *Atla-Altern. Lab Anim.* **2003**, *31*, 317–351.
57. Segner, H.; Lenz, D. Cytotoxicity assays with the rainbow trout R1 cell line. *Toxicol. Vitro* **1993**, *7*, 537–540.

CHAPTER 6

Investigating the hazard associated with ZnO NPs in aquatic environments using rainbow trout and a dietary exposure according to the OECD Test No. 305.

In chapter 6 the hazard associated with ZnO NPs reaching aquatic environments and being taken up by fish is investigated. According to *in vitro* studies performed assessing the cytotoxicity of a range of ENMs using a range of liver cell lines, ZnO NPs are the most hazardous (lowest IC_{50}). While NP dissolution and the release of ions can contribute to cytotoxicity, the presence of large ZnO NP aggregates highly contributed to the toxicity observed in the fish cell line. An increase in ROS levels was also measured in fish liver cells exposed to ZnO NPs. This increase in ROS was also specific for fish cells. Therefore in order to test how this response translates to what may occur on a whole organism level an *in vivo* exposure study (OECD TG 305) was performed using the same ZnO NPs. Rainbow trout (*Oncorhynchus mykiss*) were fed feed spiked with ZnO NPs over a 2 week period. Such an exposure route was chosen, as according to the recommendation for application of TG 305 to ENM testing, dietary spiking should be favoured. The tissue distribution and depuration pattern of Zn as well as any associated redox balance disturbances in fish following exposure to ZnO NPs was measured. High Zn levels in plasma and the livers of groups exposed to the higher dose ZnO NPs (1000 mg/kg) were measured. While levels were quickly eliminated during depuration, we observed biochemical disturbances associated with oxidative stress in the liver (decreased GSH/GSSG ratios) and interactions with the cytochrome P450 (CYP) enzyme activities (increased EROD activity). No lethality was observed and no differences among groups were observed in fish growth (weight and length) or in the hepatosomatic index. Therefore it appears the level of biochemical disturbance (decrease in GSH/GSSG ratios) which may have been associated with oxidative stress did not exceed the capability of the fish's endogenous antioxidant/physiological environment to respond. A positive concordance was evidenced between ROS increase in liver cells and oxidative disturbances seen in the liver of fish however ultimately an organism's adaptive capability must be considered in predicting an adverse outcome.

Research paper 3: Tissue distribution of zinc and subtle oxidative stress effects after dietary administration of ZnO nanoparticles to rainbow trout.

Science of the Total Environment 551–552 (2016) 334–343

Contents lists available at ScienceDirect

Science of the Total Environment

journal homepage: www.elsevier.com/locate/scitotenv

Tissue distribution of zinc and subtle oxidative stress effects after dietary administration of ZnO nanoparticles to rainbow trout

Mona Connolly [a], Marta Fernández [b], Estefanía Conde [b], Fernando Torrent [c], José M. Navas [a], María L. Fernández-Cruz [a,*]

[a] Instituto Nacional de Investigación y Tecnología Agraria y Alimentaria (INIA), Crta. de la Coruña, km. 7,5, 28040 Madrid, Spain
[b] Centro de Investigaciones Energéticas, Medioambientales y Tecnológicas (CIEMAT), Av. Complutense, 40, 28040 Madrid, Spain
[c] E.T.S. Ingenieros de Montes, Universidad Politécnica de Madrid, Campus Montegancedo, Calle ciruelos, s/n, 28660 Boadilla del Monte, Madrid, Spain

HIGHLIGHTS

- Dietary exposure to ZnO NPs; no effect on growth or in the hepatosomatic index
- Zn translocation into systemic circulation and distribution to liver and gills
- Bioaccumulation of high levels of Zn in the intestine and gills
- Redox imbalances associated with distribution to liver and gills

GRAPHICAL ABSTRACT

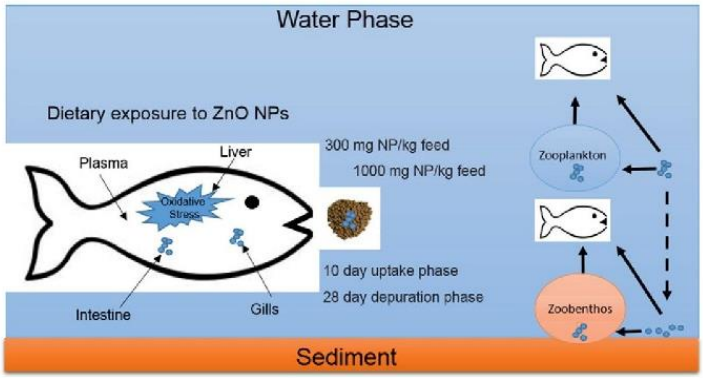

ARTICLE INFO

Article history:
Received 4 December 2015
Received in revised form 25 January 2016
Accepted 27 January 2016
Available online 13 February 2016

Editor: D. Barcelo

Keywords:
Rainbow trout (*Oncorhynchus mykiss*)
Zinc oxide nanoparticles (ZnO NPs)
Dietary exposure
Bioaccumulation
Tissue distribution
Oxidative stress

ABSTRACT

The increasing use of ZnO nanoparticles (ZnO NPs) in different fields has raised concerns about the possible environmental risks associated with these NPs entering aquatic systems. In this study, using a dietary exposure route, we have analysed the tissue distribution and depuration pattern of Zn as well as any associated redox balance disturbances in rainbow trout (*Oncorhynchus mykiss*) following exposure to ZnO NPs (20–30 nm). Fish were fed a diet spiked with ZnO NPs prepared from a dispersion in sunflower oil at doses of 300 or 1000 mg ZnO NPs/kg feed for 10 days. This uptake phase was followed by a 28 days depuration phase in which fish from all groups received untreated feed. While no overt signs of toxicity were observed and no important effects in fish growth (weight and length) or in the hepatosomatic index among groups were recorded, we observed high levels of Zn bioaccumulation in the gills and intestine of exposed fish following exposure to both dose levels. Zn levels were not eliminated during the depuration phase and we have evidenced oxidative stress responses in gills associated with such long term ZnO NPs bioaccumulation and lack of elimination. Furthermore, exposures to higher doses of ZnO NPs (1000 mg/kg feed) resulted in Zn distribution to the liver of fish following 10 days of exposure. Fish from this exposure group experienced biochemical disturbances associated with oxidative stress in the liver and ethoxy-resorufin-*O*-deethylase (EROD) activity which may point to the ability of ZnO NPs or its ions to interfere with cytochrome P450 metabolic processes.

* Corresponding author at: Departamento de Medio Ambiente, Instituto Nacional de Investigación y Tecnología Agraria y Alimentaria (INIA), Ctra. de la Coruña km 7.5, 28040 Madrid, Spain.
E-mail address: fcruz@inia.es (M.L. Fernández-Cruz).

http://dx.doi.org/10.1016/j.scitotenv.2016.01.186
0048-9697/

1. Introduction

ZnO together with TiO_2 and SiO_2 nanoparticles (NPs) are among the most industrially and commercially utilised groups of engineered nanomaterials (NMs). At one point worldwide production for ZnO NPs was estimated to be 10–100 folds higher than that for any other NM with outputs of between 550 and 5550 tonnes/year (Piccinno et al., 2012). They have essentially replaced their bulk counterparts in a range of personal care products, sunscreens and cosmetics in favour of "enhanced" properties at nanoscale. Their unique bacteriostatic and fungicidal properties have favoured their introduction into paints and even food packaging (Espitia et al., 2012). Similarly for their more preferable dissolution kinetics the use of nanoformulations of ZnO in fertilisers is being tested (DeRosa et al., 2010; Milani et al., 2012). ZnO in its bulk form is also used as a feed supplement of zinc for different farmed species including fish. The contents of Zn required for fish feed range between 15 and 150 mg Zn/kg feed (19–187 mg ZnO/kg feed) (EFSA FEEDAP Panel, 2014). Recently the use of the nanoform of ZnO as a source of dietary Zn has been investigated in carp with good results (Faiz et al., 2015). However it is still unclear if and to what extent the replacement of such "bulk" metal oxides with nanoforms may represent a hazard to such organisms and to the wider environment. Aquatic environments are particularly susceptible as they act as sinks for most environmental contaminants.

NM's behaviour in such environments will be governed by their inherent physico-chemical properties as well as by environmental conditions (such as water temperature, hardness, and pH) that will influence aggregation state, dissolution properties and ultimately the toxic potential to organisms (Keller et al., 2010; Reed et al., 2012).

ZnO NPs acute toxicity has been demonstrated in studies across a wide range of taxonomic groups from different trophic levels in aquatic ecosystems including bacteria, algae, invertebrates and fish (Bondarenko et al., 2013; Ma et al., 2013). 96 h lethal concentrations (LC50) reported for *Danio rerio* (zebrafish) are 1.79 and 3.97 μg/mL (Yu et al., 2011; Zhu et al., 2008). Lower trophic level organisms (crustaceans and algae) in general show increased sensitivity and lower LC50 values. Heinlaan and colleagues reported a 96 h LC50 of 0.18 μg/mL for *Thamnocephalus platyurus* (Heinlaan et al., 2008) while 72 h EC50s of 0.042 μg/mL have been shown for microalgae *Pseudokirchneriella subcapitata* (Aruoja et al., 2009). However reliable ecological risk assessments require information not only on the threshold concentration for toxicity but also on the risk of bioaccumulation and any latent physiological effects or biochemical disturbances.

Being at the top of the aquatic food chain, fish are particularly susceptible to the exposure to NMs. Mesocosm studies (Bradford et al., 2009; Ferry et al., 2009) have demonstrated the transfer of NMs from the water column to sediments and subsequently into food webs. There are already reports of high levels of accumulation in *Daphnia magna*, a common food source for fish, following NM exposure (TiO_2 and ZnO) (Adam et al., 2014; Zhu et al., 2010). Ingestion of these species by organisms at higher trophic levels (fish) in aquatic ecosystems will lead to a direct dietary exposure route and possible biomagnification effects. However, at present reports on bioaccumulation of NMs in fish, their tissue distribution and retention times are scarce. It has been observed, for instance, that rainbow trout (*Oncorhynchus mykiss*) exposed using a dietary route to TiO_2 NMs for either 21 (Johnston et al., 2010) or 56 days (Ramsden et al., 2009), showed no effects on growth or food intake but some subtle physiological and biochemical disturbances including the depletion in levels of Cu in the brain and spleen tissues and decreases in Na^+–K^+–ATPase activity. In the case of ZnO NPs, bioaccumulation has been observed in the gill, liver, intestine, and brain of juvenile carp (*Cyprinus carpio*) following waterborne exposure (Hao et al., 2013). In goldfish (*Carassius auratus*) exposed to 2 mg/L of ZnO NPs for 30 days, NPs appeared to accumulate preferentially in the gills, but also in the liver (Fan et al., 2013). In the case of ZnO NPs, the fact that they are poorly soluble in water and tend to aggregate rapidly in aqueous suspension (Degen and Kosec, 2000; Tso et al., 2010) would imply that they settle in sediments. In fact according to modelled predicted environmental concentrations freshwater sediments represent major sinks for ZnO NPs compared to other NMs with accumulation concentration ranges between 30 and 4800 μg/kg predicted following a 14 year timeframe (2000–2014) (Gottschalk et al., 2015). As a consequence ZnO NPs would either be taken up by fish as particles associated with sediments/organic material or by feeding on exposed lower trophic level organisms. Therefore in this study we decided to use rainbow trout as a model fish species, being on the top of the food chain in fresh water ecosystems, to study the bioaccumulation of ZnO NPs after dietary exposure to reflect a more environmentally realistic situation.

To date biochemical disturbances associated with ZnO NPs bioaccumulation in fish show signs of oxidative stress involvement (Hao and Chen, 2012; Xiong et al., 2011; Zhao et al., 2013). *In vitro* studies in fish cell lines also point to oxidative stress as a mechanism of toxicity associated with ZnO NPs exposure (Fernández et al., 2013; Fernández-Cruz et al., 2013). While the underlying mechanism remains to be elucidated, many studies point to the role of ion release in mediating toxicity apart from that of the NP. Indeed heavy metal ion toxicity and oxidative stress in fish has been extensively documented and if released from ZnO NPs may lead to high local concentrations of toxic ions in tissues at sites of NM bioaccumulation. Furthermore, metal ions including Zn^{2+} have also been found to modulate several enzyme activities including cytochrome P450 (CYP) enzyme catalysed activities such as ethoxyresorufin-*O*-deethylase (EROD), associated with CYP1A (Bozcaarmutlu and Arinç, 2004; Oliveira et al., 2004). CYP1A enzymes play a major role in the metabolism of potentially toxic chemicals and environmental contaminants and any alteration in the CYP system could have important consequences. Oxidative stress is also seen to be responsible for this modulation (Elbekai and El-Kadi, 2005). Therefore in order to explorethe presence of these possible biochemical disturbances related to oxidative stress following ZnO NPs uptake glutathione balance (reduced to oxidised glutathione, GSH/GSSG), glutathione-*S*-transferase (GST) activity and EROD activity were analysed. To our knowledge this study is the first to address the dietary exposure hazard from ZnO NPs in the rainbow trout. Experiments were performed according to OECD test guideline for assessing bioaccumulation in fish using dietary exposure (OECD, 2012).

2. Materials and methods

2.1. Materials and chemicals

ZnO nanopowder 20–30 nm without coating (Brunauer–Emmett–Teller (BET)) was used for exposures and sourced from Tecnan (Madrid, Spain). These NPs have been previously characterised (Fernández-Cruz et al., 2013) and in their pristine form consist of polyhedral, rod-like and near-spherical-shaped particles. Particles had an average length of 33 nm according to transmission electron microscopy (TEM) analysis. All chemicals and reagents used were purchased from Sigma Aldrich (Madrid, Spain) unless otherwise stated.

2.2. Fish and ZnO NPs dietary exposure

Rainbow trout (*O. mykiss*) juveniles (mean initial weight and length of 20 ± 3 g and 13 ± 1 cm) were kept in 1 × 0.25 × 0.4 m^3 rectangular 80 L tanks supplied with flow-through water taken from an artesian well and maintained under natural conditions of photoperiod and temperature (water hardness was 140 mg/L and pH 8.0). The temperature oscillated during the whole experiment between 17.6 °C and 19.3 °C whereas the oxygen content between 7.5 and 8.6 mg/L. The faeces were cleaned 1 h after the treatments. The mortality at the end of the experiment was lower than 10%.

Fish were fed daily at a rate of 2% of their body weight during the 38 days that the experiment lasted. A commercial diet for trout, Inicio

Plus 887 (BIOMAR Iberia, S.A., Dueñas, Spain), with pellets of 1.9 mm in diameter and a lipid content of 18% was used. Two different exposure concentrations of the ZnO NPs, 300 or 1000 mg ZnO NPs/kg feed (6 or 20 mg ZnO NPs/kg body weight) were used. These doses were chosen taking into account the normal Zn contents in feed and the toxic levels of Zn for fish that should not be achieved. In parallel a control group received fish feed spiked with sunflower oil only (carrier blank). Thirty fish per group were fed once a day. The exposure period lasted for ten consecutive days and was followed by a 28 days depuration phase in which fish from all groups received untreated feed. Following OECD TG305 (OECD, 2012) the start of the test is defined as the time of first feeding with spiked food (day 1) and the first experimental day of uptake runs from the time of first feeding with spiked food to shortly before (e.g. one hour) the second feeding with spiked food. In practise the uptake phase ends shortly before (e.g. one hour) the first feeding with unspiked test substance (day 11 of the experimental period) as the fish will continue to digest spiked food and absorb the test substance in the intervening 24 h.

All the experiments were performed according to the EU and national legislation for the use of laboratory animals after receiving a favourable report of the INIA ethical committee for animal experimentation.

2.3. Preparation of pellets spiked with ZnO NPs

The ZnO nanopowder was dispersed in sunflower oil at a concentration of 6 mg/ml to prepare 300 mg ZnO NPs/kg feed or of 20 mg/mL for the 1000 mg ZnO NPs/kg feed. Pellets were thereafter soaked in these spiked oils using 250 μl of oil per 5 g of feed. Sunflower oil was selected as ZnO NPs dispersed better than in olive oil. In order to have an idea of the size and aggregation of the NPs in these suspensions, measurements by dynamic light scattering (DLS) using a Zetasizer Nano-ZS (Malvern Instruments Ltd., UK) were performed. However no data could be obtained because of highly unstable heterogeneous suspensions with polydispersity indexes equal to 1, which did not meet quality criteria for a correct measurement. Zn concentration was measured in the soaked pellets (1000 mg/kg) and in the pellets submerged in water after 0, 2, 5, 10 and 30 min and 1 and 5 h.

2.4. Sampling

Five fish from each experimental or control group were randomly sampled at days 1 and 11 (just before the beginning and at the end of the uptake phase, as explained above), as well as at days 12, 19, 27, and 39 (depuration phase). They were anaesthetized using tricaine methanesulfonate (MS-222) at a concentration of 100 mg/L of water. Fish weights and lengths were recorded. Blood samples (between 0.5 and 1 mL) were collected from the caudal vein plexus and centrifuged immediately (4 °C, 20 min at 800 ×*g*) using a 5415 R series centrifuge (Eppendorf, Germany). Tissue samples (liver, gills, muscle, stomach and intestine) were taken, weighed, and stored at −20 °C together with plasma samples until analysis of Zn contents by ICP-MS. Stomach and intestine samples were washed prior to weighing and storage in order to remove any remnants of ZnO NPs spiked feed. Other samples of liver and gill were weighed and immediately frozen in liquid nitrogen and stored at −80 °C until analysis of enzymatic activities.

2.5. Zn levels analysis in feed and tissues

Levels of Zn in feed, tissues and plasma were measured by an inductively coupled plasma mass spectrometer (ICP-MS) Thermo iCap Q (Thermo Scientific, Bremen, Germany) equipped with a quadrupole mass analyser and an electron multiplier detector. A Meinhard nebulizer with Scott (Ryton) spray chamber (Elemental Scientific Inc., USA) and a peristaltic pump was used for sample introduction. The dissolution of the samples was accomplished by acid digestion with a mixture of HNO_3 and H_2O_2 (105 °C, overnight) in Parr reactors. The sample solutions were quantified by external calibration; three isotopes of Zn (66Zn, 67Zn and 68Zn) were used for measurements to discard the presence of isobaric interferences. Internal standard (Gallium) was used in order to check instrumental stability and to correct potential effects of matrix in the signal. The measured data were expressed as μg Zn/g tissue or feed (fresh weight).

2.6. Accumulation analysis

The chemical assimilation efficiency (α, absorption of test substance across the gut) was calculated with the formula:

$$\alpha = \left[\left(C_{0,m} * k_2\right)/\left(I * C_{food}\right)\right] * \left[1/\left(1-e^{-k2t}\right)\right]$$

where: $C_{0,m}$ is the measured concentration in fish at time zero of the depuration phase (mg/kg).

k_2 is the overall (not growth-corrected) depuration rate constant (1/day).

I is the food ingestion rate constant (g food/g fish/day). I was not adjusted for fish growth as fish didn't grow significantly ($P < 0.05$) during the uptake and depuration phases.

C_{food} is the concentration in food (mg/kg food).

t is the duration of the feeding period (day).

α is unitless but it is normally expressed as a percentage rather than a fraction.

The overall depuration rate constant k_2 was estimated using mean sample concentrations from the depuration phase subtracting the basal Zn levels measured in the control group at the corresponding time of sampling. These values were adjusted to a linear regression of ln(concentration) versus time. The slope of the regression line is an estimate of the depuration rate constant k_2.

A dietary biomagnification factor (BMF_d) representing only the dietary exposure but not a dietary and water combined exposure could be calculated by the formula,

$$BMF_d = (I * \alpha)/k_2.$$

The estimation of the time (days) to reach the 50% depuration ($t_{½}$) of Zn was estimated with the formula $t_{½} = 0.693/k_2$.

2.7. Preparation of tissue samples and biochemical analysis

EROD and GST activities and the ratio of GSH/GSSG were monitored as biomarkers of toxicity and oxidative stress in both liver and gill tissues. Liver and gill samples were weighed and cut into two fragments. One fragment was used for EROD and GST analysis while the other was prepared for total glutathione (tGST) and GSSG analysis. Tissue fragments used for EROD and GST analysis were homogenised in 1 mL of ice cold homogenisation buffer (0.1 M Tris HCL pH 7.5, 1 mM ethylenediaminetetraacetic acid (EDTA), 0.25 M sucrose, 150 mM KCL, 20% *v*/v glycerol solution). A protease inhibitor cocktail (phenylmethylsulfonyl fluoride, PMSF, 0.125 mM, dithiothreitol, DTT, 1 mM and 5 μg/mL of pepstatin A, aprotinin and leupeptin) was added to the homogenisation buffer directly prior to sample addition. Tissues were manually cut and sonicated using water bath sonication (S 40 H Elmasonic, Elma, Germany) for 15 s to create a tissue homogenate. Homogenates were then centrifuged at 6704 ×*g* in a 5415 R series Eppendorf centrifuge for 10 min at 4 °C. The resulting supernatant was then centrifuged at 15,682 ×*g* for 60 min also at 4 °C using the same centrifuge. The supernatant was used for GST analysis and the resulting pellet for EROD analysis (Valdehita et al., 2012).

For tGSH and GSSG analysis tissue samples were homogenised in the same homogenisation buffer and protease cocktail but with the addition of 1:2 *v*/v 5% 5-sulfosalicyclic acid to remove interfering proteins. Tissues were also cut and sonicated (15 s) before undergoing one

centrifugation step (15,682 ×g for 30 min) at 4 °C to obtain the supernatant used for analysis.

Biochemical analyses were performed for each of the five fish sacrificed at each sampling point. All samples prepared from the fish of each exposure group of the same sampling day were assayed together using different wells of a 96-well plate (Greiner Bio-One GmbH, Germany). EROD activity was measured following the method of Burke and Mayer (1974). Fluorescence of the product formed, resorufin, was measured at 530 nm excitation and 590 nm emission in a Tecan-Genios microplate reader (Tecan Group Ltd., Männedorf, Switzerland). Microsomal protein concentrations were quantified using a fluorescamine-based assay (Udenfriend et al., 1972) and bovine serum albumin as a standard. EROD activities are expressed as pmol resorufin/min/mg protein.

GST activity was measured according to the general method described by Habig et al. (1974) with slight modifications for a 96-well plate format (Tiwari et al., 2011). The total reaction volume per well was 200 μL consisting of 20 μL sample and 180 μL of a reaction mixture of 1-chloro-2,4-dinitrobenzene (CDNB) (1 mM) and reduced glutathione (GSH) (10 mM) prepared in potassium phosphate assay buffer (pH 6.5). The product of conjugation of GSH with CDNB was measured at 340 nm absorbance in a Tecan-Genios microplate reader. Changes in absorbance per minute were converted into nanomoles of CDNB conjugated per min and presented as nmoles/min/mg tissue.

Both total glutathione (tGSH) and oxidised glutathione (GSSG) were measured according to the modified method of Allen et al. (2001). The assay is based on the sequential oxidation of GSH by 5, 5`-dithiobis 2-nitrobenzoic acid (DTNB) and reduction by reduced nicotinamide adenine dinucleotide phosphate (NADPH) in the presence of glutathione reductase (GR) (Griffith, 1980). Samples were diluted in assay buffer (sodium phosphate buffer/EDTA (143 mM/6.3 mM)) using a 1:20 and 1:10 dilution factor for tGSH and GSSG analysis, respectively. The total reaction volume per well was 150 μL consisting of 25 μL sample/standard and 125 μL of a reaction mixture of GR (229 U/mL), NADPH (2.39 mM) and DTNB (0.01 M) prepared in assay buffer. The reaction was monitored by measuring the 5`-thiol-2-nitrobenzoic acid (TNB) product formation at 405 nm absorbance every min over a 10 min time frame in a Tecan-Genios microplate reader. The concentration of tGSH was calculated from a GSH standard curve and represented as μM GSH/mg tissue. Levels of GSSG were measured in the same way with 1 h pre-incubation of samples and standards with 2 μL of 4-vinyl pyridine solution per 100 μL of sample prior to analysis. Levels of reduced glutathione (GSH) were calculated by subtracting the amount of GSSG from tGSH content and the ratio of GSH/GSSG was calculated.

2.8. Statistical analysis

The hepatosomatic index (HSI) was calculated according to the formula:

$$HSI = [\text{liver weight (g)}/\text{body weight (g)}] \times 100.$$

All the data are presented as means ± standard error of the mean (SEM) of measurements taken from five fish from control or experimental groups in each sampling point. Significant differences ($P < 0.05$) among control and exposure groups from each sampling day were determined by using one-way ANOVA followed by a Dunnett's Post hoc test. In the case of Zn levels measured in exposure groups at day 12 statistical analysis was performed between control Zn levels measured at day 11 and these exposure groups.

Statistical analysis was performed using SigmaPlot 12.0 (Systat Software Inc., Chicago, IL, USA). Normality of the data distributions were checked by means of a Shapiro–Wilk test and data were checked automatically by the programme for equal variance ($P < 0.05$).

3. Results

3.1. Zn levels analysis in feed

Content of Zn in control feed as measured by inductively coupled-mass spectrometry (ICP-MS) was 84 ± 3 mg Zn/kg feed (105 mg ZnO/kg feed) ($n = 6$). Measured concentrations of Zn in the 300 and 1000 mg ZnO NPs/kg treated pellets were 274 ± 21 mg Zn/kg feed (341 ± 26 mg ZnO/kg feed) and 720 ± 40 mg Zn/kg feed (896 ± 50 mg ZnO/kg feed), respectively ($n = 6$), indicating no important differences with respect to nominal concentrations. Pellets in contact with water during a 5 h period didn't release ZnO NPs to the water. Also, it was observed that trout ingested the pellets in less than 2 min after feeding.

3.2. Fish growth and condition

No overt signs of toxicity in fish were observed throughout the experiment. Similar hepatosomatic indices were calculated for the control and treatment groups at the end of the uptake phase and during depuration (Table 1). All fish increased in weight (Fig. 1a) and length (Fig. 1b) from an initial mean weight and length of 26 ± 3 g, 13 ± 1 cm at day 1 to the ranges 41–50 g in weight and 14.7–15.5 cm in length at the end of the experiment (day 39) in the three groups. Significant differences ($P = 0.047$) between control and treatment groups were only seen in the case of the 300 mg ZnO NPs/kg treatment group with lower body weights compared to the control group at day 11 (the end of the uptake phase) (Fig. 1a). Throughout the depuration phase fish showed similar increases in body weight as the control group. Exposure to the higher dose (1000 mg ZnO NPs/kg feed) did not cause any significant reductions in body weight directly following exposure or throughout the depuration phase.

3.3. Zn tissue accumulation/depuration

Fig. 2 shows the levels of Zn in plasma, liver, gill and intestine of control and treatment groups following a 10 day exposure period (day 11) and during a 28 day depuration phase (day 12 to day 39). Following dietary exposure elevated Zn levels were found in plasma and in the intestine, liver and gills. Animals exposed to 1000 mg ZnO NPs/kg feed exhibited significantly higher Zn levels in plasma ($P = 0.0014$) and liver ($P = 0.003$) than controls, but these differences disappeared during the depuration phase (Fig. 2a, b). In the gills and intestine there was evidence of significant bioaccumulation for both treatment groups following exposure and throughout the depuration phase (Fig. 2c, d). However, no increase in residue levels of Zn in muscle and stomach could be observed (data not shown).

The α, $t_{½}$ and BMF could only be measured in the liver and plasma of fish treated with the highest dose as no depuration was obtained in the gut and gills tissues. Results indicated an assimilation of the substance of 30% and no biomagnification in plasma and liver (BMF of 0.01 and 0.04, respectively). The 50% depuration was faster in plasma than in liver (1.5 and 4 days, respectively).

Table 1
Hepatosomatic indices calculated for fish from control and treatment groups.

Hepatosomatic index				
	Day	Control	300 mg/kg	1000 mg/kg
Uptake phase	1		2.14 ± 0.20[a]	
	11	1.50 ± 0.13	1.83 ± 0.11	1.54 ± 0.08
Depuration phase	12		1.53 ± 0.14	1.74 ± 0.18
	19	1.90 ± 0.19	1.79 ± 0.11	1.91 ± 0.24
	27	2.38 ± 0.52	2.38 ± 0.15	2.03 ± 0.06
	39	2.84 ± 0.17	2.56 ± 0.22	3.21 ± 0.33

Values are presented as mean ± SEM ($n = 5$).
[a] Mean of all fish from all groups.

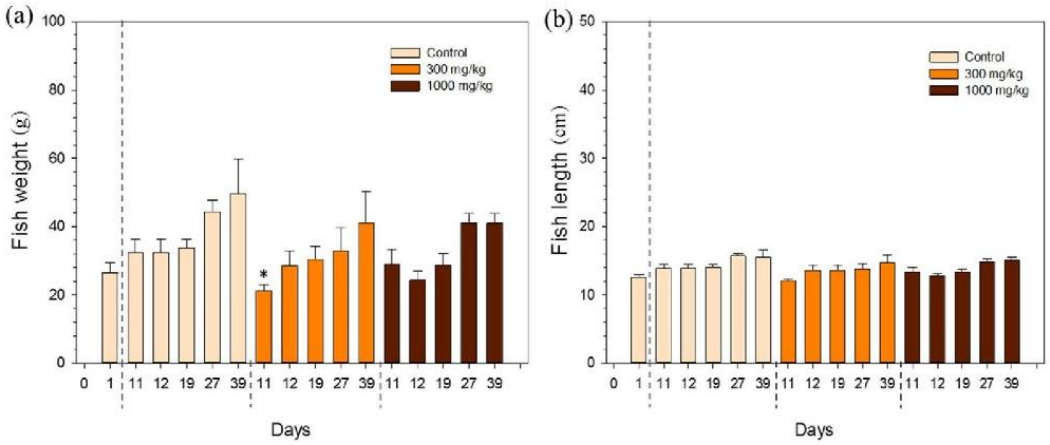

Fig. 1. Fish weight (a) and length (b) in control and ZnO NPs treatment groups (300 and 1000 mg ZnO NPs/kg feed) following uptake (day 1–11) and during the depuration phase. Bars represent the mean ± SEM (n = 5). Significant differences between control and treatment groups on the same respective sampling day are represented as *P(<0.05) according to a one-way ANOVA, Dunnetts post hoc test.

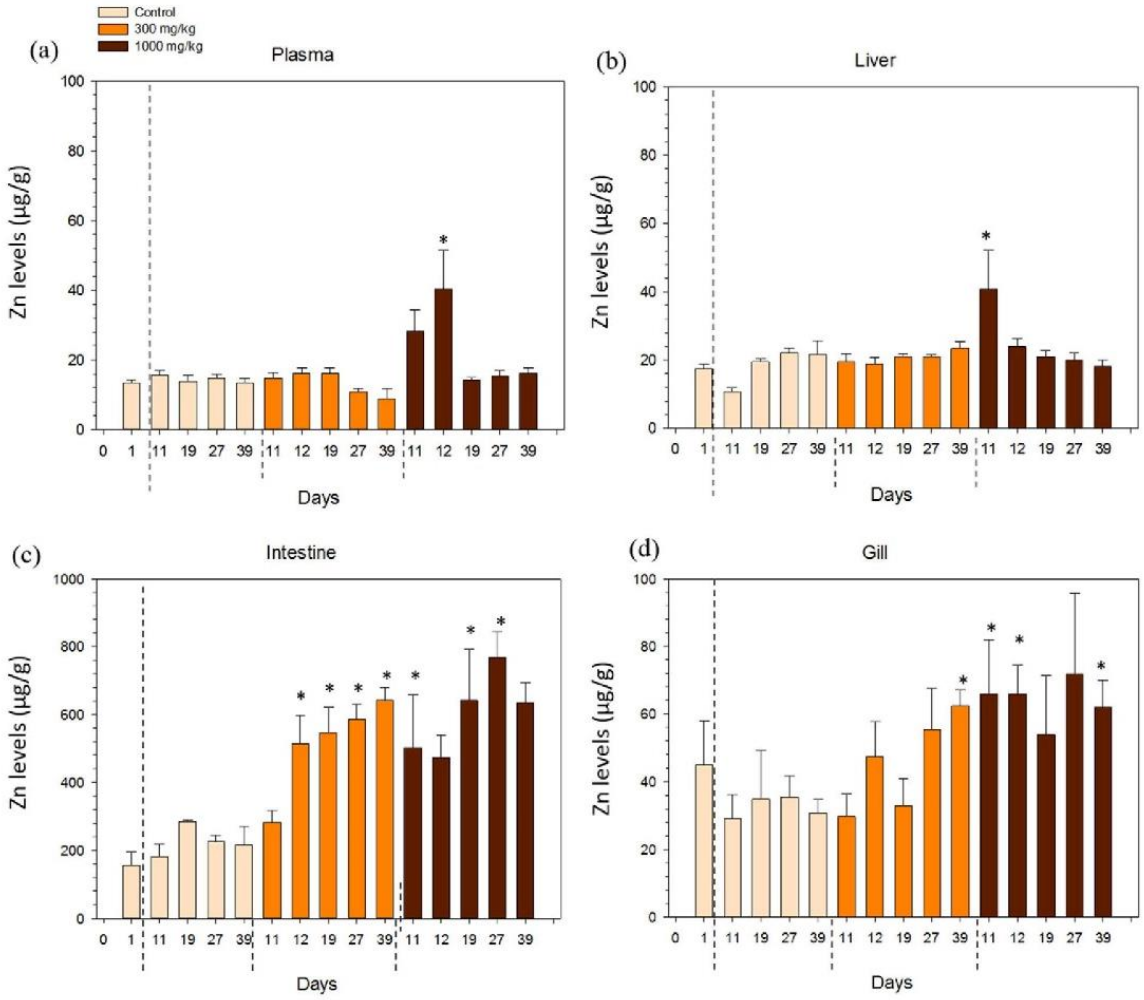

Fig. 2. Levels of Zn measured in tissues samples of (a) plasma, (b) liver, (c) intestine and (d) gill of control and treatment groups following uptake (day 1–11) and during the depuration phase. Bars represent the mean ± SEM (n = 5). Significant differences between the control and treatment groups at the same respective sampling day are represented as *P(<0.05) according to a one-way ANOVA, Dunnetts post hoc test. The control group at day 11 was used to compare treatment groups at days 11 and 12 as no significant deviations in Zn levels are expected within 24 h.

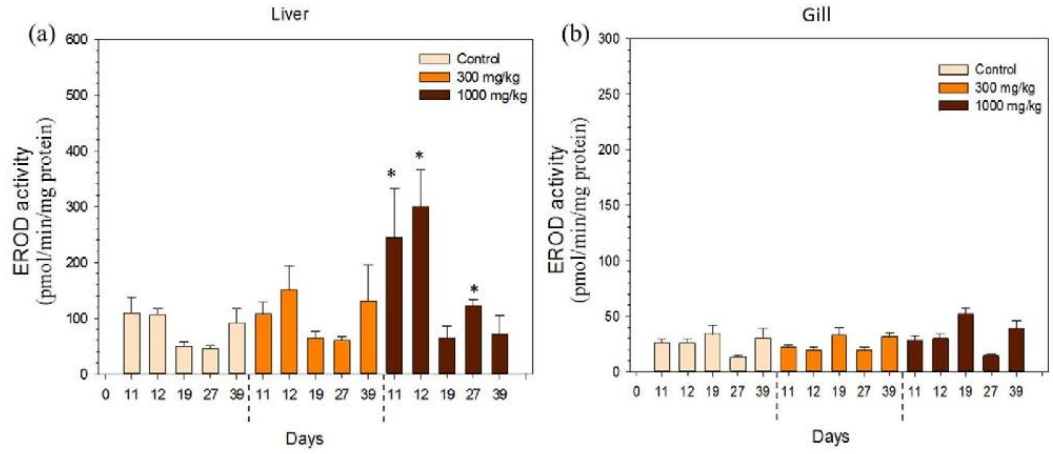

Fig. 3. EROD activity in samples of microsomal fractions prepared from homogenised tissues of the livers (**a**) and gills (**b**) of control and treatment groups (300 and 1000 mg ZnO NPs/kg feed) sampled at the last day of the uptake phase (day 11) and at days 12, 19, 27 and 39 during depuration. Bars represent the mean ± SEM (n = 5). Significant differences between the control and treatment groups on the same respective sampling day are represented as * P(<0.05) according to a one-way ANOVA, Dunnetts post hoc test.

3.4. Biochemical analysis

3.4.1. EROD activity

3.4.1.1. Liver. Basal levels of EROD activity in the liver tissues of the control group ranged from 40 to 140 pmol/min/mg protein (Fig. 3a). Exposure to 300 mg ZnONPs/kg feed did not affect liver EROD activity. Contrastingly at day 11 and 12, the last day of exposure period and one day into the depuration phase, fish exposed to the higher dose of 1000 mg ZnO NPs/kg feed showed significantly (P = 0.016 and P = 0.013, respectively) higher levels of EROD activity (245 ± 88 pmol/min/mg protein and 300 ± 65 pmol/min/mg protein, respectively) than controls. However by day 19 (8 days into the depuration period) EROD activity levels dropped back down to basal control levels. Some significant (P = 0.013) increase (122 ± 10 pmol/min/mg protein) was seen at day 27. At day 39 (28 days into the depuration phase) EROD activities in the control group and exposure group were similar.

3.4.1.2. Gill. Basal levels of EROD activity in the gill tissues of the control group ranged from 20 to 40 pmol/min/mg protein (Fig. 3b). There was no evidence of an increase or decrease in EROD activity in the ZnO NPs exposed groups in gill tissues of rainbow trout.

3.4.2. Glutathione S transferase (GST) activity

3.4.2.1. Liver. Basal levels of GST activity in the liver tissues of the control group ranged from 700 to 1100 nmol/min/mg tissue (Fig. 4a). Following exposure to 300 mg ZnO NPs/kg feed GST activity was significantly increased compared to control levels at day 11 (1233 ± 82 nmol/min/mg tissue, 35% increase, P = 0.009). At day 12, already in the depuration phase, an important increase in GST activity was observed (1340 ± 122 nmol/min/mg tissue, 23% increase) with respect to control levels, although no statistical significance (P = 0.149) was detected. At day 19 and 27 GST activity levels had decreased to control basal levels but at day 39 GST activity levels increased again significantly (P = 0.001) to 1138 ± 54 nmol/min/mg tissue.

Following exposure to 1000 mg ZnO NPs/kg feed GST activity was significantly increased following 24 h of depuration and at the end of the depuration phase (days 12 and 39). At day 12 GST activity levels were 1472 ± 181 nmol/min/mg tissue compared to control levels of 1090 ± 52 nmol/min/mg tissue, representing a 35% increase (P =

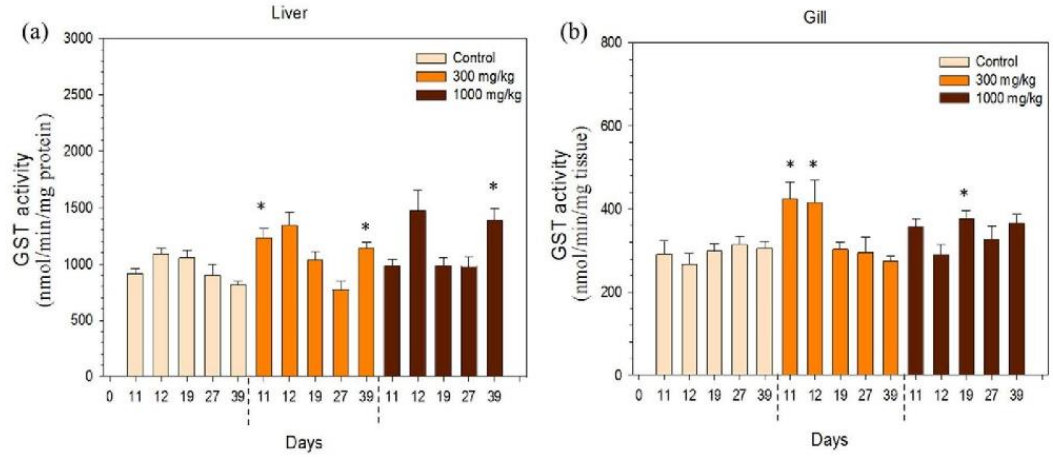

Fig. 4. GST activity in samples of cytosolic fractions prepared from homogenised tissues of the livers (**a**) and gills (**b**) of control and treatment groups (300 and 1000 mg ZnO NPs/kg feed) sampled at the last day of the uptake phase (day 11) and at days 12, 19, 27 and 39 during depuration. Bars represent the mean ± SEM (n = 5). Significant differences between the control and treatment groups on the same respective sampling day are represented as * P(<0.05) according to a one-way ANOVA, Dunnetts post hoc test.

0.006). At day 19 and 27 during depuration GST activity levels did not differ from control levels. At the end of depuration phase (day 39), GST activity was at 1390 ± 104 nmol/min/mg tissue, representing a 71% significant (P = 0.009) increase from respective control levels sampled on the same day.

3.4.2.2. Gill. Levels of GST activity in the gill tissues of the control group ranged from 220 to 340 nmol/min/mg tissue (Fig. 4b). Following exposure to 300 mg ZnO NPs/kg feed GST activity was significantly increased compared to control levels at day 11 (424 ± 41 nmol/min/mg tissue, 46% increase (P = 0.024)) and 12 (416 ± 55 nmol/min/mg tissue, 56% increase (P = 0.035)) during the depuration phase. At day 19, 27 and 39 GST activity levels had decreased to control levels with no significant differences between exposure and control groups being detected. In the 1000 mg ZnO NPs/kg feed group no significant differences from respective control levels were seen in any sampling day (11, 12, 19, 27 and 39) following exposure or during the depuration phase exposure groups. GST activity ranged from 290 ± 25 nmol/min/mg tissue (day 12) to 377 ± 19 nmol/min/mg tissue (day 19).

3.4.3. GSH/GSSG ratio

3.4.3.1. Liver. The GSH/GSSG ratio in the liver tissues of the control group ranged from values of 50 to 60 (Fig. 5a). For the animals receiving 300 mg ZnO NPs/kg feed sampled at days 11, 12 and 19 there was no significant difference in GSH/GSSG ratios with respect to controls. At day 27 the ratio begins to decrease (34 ± 11) and significantly (P = 0.037) lower ratios compared to control levels appeared at day 39 (25 ± 5).

Following exposure to the higher dose of 1000 mg ZnO NPs/kg feed GSH/GSSG ratios were significantly (P = 0.037) lower compared to control levels at day 11 of sampling with values of 46 ± 6 and 24 ± 2 recorded for the treated and control group respectively. At day 12 the ratios for exposure and control groups were 46 ± 6 (P = 0.049) and 33 ± 9 respectively. Ratios of GSH/GSSG remained significantly reduced from control levels at day 19 (P = 0.047) and day 27 (P = 0.034) during the depuration phase. At day 39 there is evidence of a slight increase in the ratio (39 ± 7) approaching control levels.

3.4.3.2. Gill. The GSH/GSSG ratio in the gill tissues of the control group ranged from values of 25 to 35 (Fig. 5b). For the 300 mg ZnO NPs/kg feed group there is evidence of a subtle transient increase in ratios over the first 8 days of the depuration period (day 11: 16 ± 6, day 12: 25 ± 5, day 19: 34 ± 6) after which the ratio decreased (day 27: 18 ± 3) reaching significantly (P = 0.007) lower ratios than controls at day 39 (8 ± 2).

The same phenomenon was seen in fish exposed to 1000 mg ZnO NPs/kg feed. During the first 8 days of the depuration period (days 12 and 19) a subtle increase, while non-significant, is observed (day 11, 25 ± 11; day 12, 33 ± 7; and day 19, 41 ± 10). At days 27 and 39 ratios (16 ± 2 and 14 ± 2 respectively) have decreased to levels significantly lower than those of control fish (P = 0.003 and P = 0.025, respectively).

4. Discussion

This study represents the first investigation into bioaccumulation and oxidative stress effects following dietary exposure to ZnO NPs in rainbow trout. In general investigations using the dietary exposure route to NM in vertebrate fish are scarce (Fraser et al., 2011; Johnston et al., 2010; Ramsden et al., 2009) despite evidence to suggest that dietary intake is a likely uptake route for higher trophic level aquatic organisms such as fish. Therefore in this study we considered the dietborne exposure route as being more environmentally relevant as well as acting as a controlled means of exposure.

Fish received pellets spiked with ZnO NPs. The exposure route was considered strictly dietborne as all feed was directly ingested by fish within seconds of administration. No signs of toxicity were observed during the dietary exposure period with fish growth (weight and length) in general not deviating from control groups and no differences in the hepatosomatic index being recorded among experimental groups. Zn is an essential micronutrient for fish required at certain concentrations for maximal growth (Ogino and Yang, 1978) and its assimilation is highly regulated (Bury et al., 2003). The current evaluated maximum tolerable dose of Zn for fish is 250 mg Zn/kg feed (312.5 mg ZnO/kg feed) with ZnO regarded as a safe source of Zn in feed (EFSA, 2012). However it appears that rainbow trout can tolerate very high levels of dietary ZnO without any apparent effects on growth or overt toxicity. Using whole-body responses such as growth depression as a parameter of impaired performance, dietary zinc concentrations up to 1700 mg/kg were tolerated by rainbow trout (Wekell et al., 1983). However, physiological parameters such as blood hematocrit and haemoglobin indicated that dietary zinc concentrations of 1000 mg/kg compromised the health of rainbow trout (Knox et al., 1984).

The presence of NMs accumulated in rainbow trout tissue following both dietary and waterborne NM exposure (TiO2, SWCNT, Cu NP) has

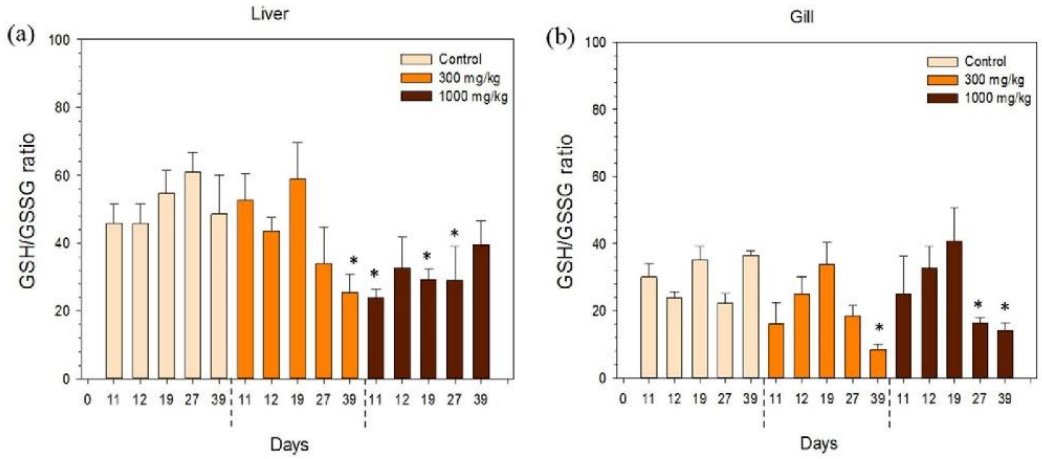

Fig. 5. GSH/GSSG ratios in liver (**a**) and gill (**b**) tissue samples of control and treatment groups (300 and 1000 mg ZnO NPs/kg feed) sampled at day 11 of the uptake phase and at days 12, 19, 27 and 39 during depuration. Bars represent the mean ± SEM (n = 5). Significant differences between the control and treatment groups on the same respective sampling day are represented as * P(<0.05) according to a one-way ANOVA, Dunnetts post hoc test.

been reported mainly in the gill, liver and gut but also in the brain (Fraser et al., 2011; Johnston et al., 2010; Ramsden et al., 2009; Shaw et al., 2012; Smith et al., 2007). In the case of ZnO NPs, higher accumulation in juvenile carp than in the case of the bulk material has been observed (Hao et al., 2013). In the present study we have analysed levels of Zn in plasma and tissue samples of the liver, gills, muscle, stomach and intestine of rainbow trout juveniles. Due to technical constraints (ICP-MS only measures the metal content) we cannot differentiate the form of the accumulated Zn (NPs and/or dissolved Zn). Zn levels higher than in the control group could be observed for both dose treatments in gut and gills and at the highest dose in plasma and liver but no differences could be observed in stomach and muscle. Zn was depurated within 1.5 and 4 days from the plasma and liver of the fish group treated with the highest dose, and no biomagnifications occurred in these tissues. However, the ingestion of ZnO NPs at both doses results in the presence and accumulation of Zn levels in the gut and gills during the whole depuration phase. In the case of the intestine, this finding points to a lack of complete assimilation and elimination from the intestine. The absorption across the gut was only 30%. This finding either indicates ZnO NPs transport from the intestine into circulation, or dissolution of Zn^{2+} ion from the ZnO NPs leading to absorption of Zn^{2+} to the plasma, and subsequent distribution to liver and gills. In rats, it has been suggested that the absorption of ZnO NPs could be facilitated by their dissolution in the acidic gastric fluid, so that released Zn^{2+} can easily diffuse into the blood stream and subsequently be translocated to the liver (Cho et al., 2013). Alternatively if uptaken by endocytosis NPs may be enclosed in cellular vesicles, which show acid conditions that are known to facilitate the dissolution of ZnO NPs (Cho et al., 2011; Kao et al., 2012). In fact the dissolution of vesicular ZnO NPs and subsequent Zn^{2+} leakage into the cytosol followed by the collapse in mitochondrial membrane potential has been detailed in a mechanical toxicological pathway of ZnO NPs proposed in rats by Kao et al. (2012). The dissolution of ZnO NPs was also used to explain their depuration from the body of *D. magna* (Li and Wang, 2013). However, Bacchetta and colleagues reported ZnO NPs disruption of the intestinal barrier facilitating the translocation of NPs to other tissues using the amphibian *Xenopus laevis* as a test species (Bacchetta et al., 2014).

Studies using waterborne exposure have also reported some uptake into the intestine from fish ingesting NPs. Federici et al. (2007) and Smith et al. (2007) using histological observations evidenced, in the case of TiO_2, milky suspensions while for SWCNT visible aggregates were present in the gut lumen of rainbow trout. Both reported associated intestinal pathologies; erosion of villi and inflammation, fusion and vacuolation of mucosa, stressing the need for environmental risk assessments using dietary exposures of NMs. While the pathway of intestinal Zn^{2+} uptake has not been fully characterised in rainbow trout, there is evidence that it is a high-capacity low-affinity transport pathway highly regulated to ensure Zn^{2+} homeostasis (Glover and Hogstrand, 2002). Increased mucus secretion from the intestinal wall is seen as a regulatory mechanism to control uptake. There have been reports of Zn^{2+} accumulation in the intestine and different processing mechanisms dictated by exposure route in rainbow trout (Sappal and Kamunde, 2009). Distinct from waterborne uptake there is a tendency for dietborne Zn^{2+} to be sequestered in metabolically detoxified pools rendering the metal less biologically available and preventing translocation. Such a phenomenon could explain the high levels of Zn bioaccumulation in the intestine witnessed throughout the depuration period following ZnO NPs exposure in this study.

Our results also indicate that gill Zn levels are significantly higher than control levels, most prominently in the high exposures groups, following exposure. Zn levels remain elevated in these groups even after 28 days of depuration. However the levels of Zn are 100 fold lower than levels measured in the intestine which may suggest that the gill is only a secondary organ of bioaccumulation. Studies have also shown high levels of Zn^{2+} in the gill following dietary exposure of Zn^{2+} to rainbow trout (Sappal et al., 2009).

Biochemical disturbances related with oxidative stress have been associated with NP accumulation in rainbow trout tissues (Federici et al., 2007 (TiO_2); Shaw et al., 2012 (CuNPs)). Also when comparing ZnO NPs and bulk ZnO effects in fish distinct and more potent effects of NPs on antioxidant defence have been reported (Hao et al., 2013; Xiong et al., 2011). The gill and liver are reported to be the most sensitive organs to ZnO NPs (Hao and Chen, 2012) therefore in this study we have monitored biochemical activities in these tissues, despite high levels of accumulation in the intestine. Exposure to lower concentrations (300 mg/kg) of ZnO NPs were well tolerated and regulated by the fish with evidence of GST detoxification enzyme activity and the maintenance of redox status both in the gill and liver. However following 10 days of depuration sustained high levels of bioaccumulation and lack of elimination from tissues led to a change in Zn tolerance. There was no longer evidence of heightened GST activity above control levels. Instead cells GSH/GSSG ratios decreased, what could be indicative that antioxidant defences were becoming overwhelmed, although measurements of oxidative damage would have been necessary to confirm this.

The administration of the highest ZnO NPs concentration (1000 mg/kg feed) led to a loss in redox balance with decreased GSH/GSSG ratios at different days of the recovery period in the liver, and at days 27 and 39 of the experiment in the gills. At the same time, a lack of GST activity above control levels was observed in general, with a significant increase in this activity only at day 39 in the liver and 19 in the gill. This effect coincides with the presence of high levels of Zn in gills along the depuration period and at day 11 in liver tissues. High levels of Zn could lead to the depletion of GSH through conjugation which could in turn suppress GST synthesis inhibiting the antioxidant defence system and thus leading to oxidative stress. This concentration dependent inhibition in antioxidant defence has been reported in tissues of carp exposed to TiO2 and ZnO NPs (Hao and Chen, 2012; Hao et al., 2013). In the present study Zn was quickly eliminated from the liver following 24 h of depuration. Simultaneously we observed subtle increase in the GSH/GSSG ratio in the liver and GST upregulation suggesting the recovery of the cellular antioxidant defence system.

In the group exposed to 1000 mg ZnO NPs/kg feed we also observed an induction of EROD activity in the liver but not in gills, corroborating the essential role of the liver in detoxification processes. EROD activity is dependent on CYP1A, whose expression is regulated by the aryl hydrocarbon receptor (AhR). At the same time, induction of oxidative stress causes the activation of AhR that regulates the expression of genes directly related with the cellular antioxidant defences, as these of GSTs. There is strong evidence that in the case of metal ions, including Zn^{2+}, EROD induction is oxidative stress mediated and regulated through the AhR (Bozcaarmutlu and Arinç, 2004; Elbekai and El-Kadi, 2005). We hypothesise that ZnO NPs provide high concentrations of available Zn^{2+} to the liver causing an increase in EROD activity. There have been very few studies looking at the effects of metal NPs on EROD activity. One such study has shown increased *cyp1a2* gene expression in the gills of rainbow trout exposed to silver NPs (Scown et al., 2010). This may have important consequences, especially in the case of co-exposures of fish to ZnO NPs and chemicals that activate the AhR or that are bioactivated by the AhR pathway.

5. Conclusion

In this study using a dietborne exposure route, to mimic a more realistic chronic exposure scenario, we have analysed the tissue distribution and depuration pattern of Zn as well as any associated redox balance disturbances in rainbow trout following dietary exposure to ZnO NPs. We observed high levels of bioaccumulation in the gills and intestine of exposed fish following exposure and throughout the depuration phase. No overt signs of toxicity were evidenced. Whether or not zinc accumulation and reallocation in particular tissues could be part of the allostatic organismal response to cope with toxicity or is

just a reflection of such toxicity has to be addressed. Measurements of GSH/GSSG ratio and GST detoxification activity showed that at lower concentrations the upregulation of GST detoxification enzymes ensure redox equilibrium. However we begin to see oxidative stress responses associated with long term ZnO NPs bioaccumulation and lack of elimination during depuration.

Most noteworthy, exposure to higher concentrations of ZnO NPs resulted in Zn translocation into systemic circulation and distribution to the liver following 10 days of exposure. While levels were quickly eliminated during depuration we observed disturbances in the antioxidant defence system resulting in cellular oxidative stress. These high concentrations were also capable of inducing EROD activity in the liver. If we take this as a specific biomarker for CYP1A activity this may have important consequences, especially in the case of chemicals which are bioactivated by the AhR pathway.

Acknowledgements

The authors thank Luis Alte Garcia-Olias (INIA, Spain) for his assistance with fish tissue sampling. This work was funded through INIA project AT2011-001.

References

Adam, N., Schmitt, C., Galceran, J., Companys, E., Vakurov, A., Wallace, R., Knapen, D., Blust, R., 2014. The chronic toxicity of ZnO nanoparticles and $ZnCl_2$ to *Daphnia magna* and the use of different methods to assess nanoparticle aggregation and dissolution. Nanotoxicology 8 (7), 709–717.

Allen, S., Shea, J.M., Felmet, T., Gadra, J., Dehn, P.F., 2001. A kinetic microassay for glutathione in cells plated on 96-well microtiter plates. Methods Cell Sci. 22 (4), 305–312.

Aruoja, V., Dubourguier, H.C., Kasemets, K., Kahru, A., 2009. Toxicity of nanoparticles of CuO, ZnO and TiO_2 to microalgae *Pseudokirchneriella subcapitata*. Sci. Total Environ. 407 (4), 1461–1468.

Bacchetta, R., Moschini, E., Santo, N., Fascio, U., Del Giacco, L., Freddi, S., Camatini, M., Mantecca, P., 2014. Evidence and uptake routes for zinc oxide nanoparticles through the gastrointestinal barrier in *Xenopus laevis*. Nanotoxicology 8 (7), 728–744.

Bondarenko, O., Juganson, K., Ivask, A., Kasemets, K., Mortimer, M., Kahru, A., 2013. Toxicity of Ag, CuO and ZnO nanoparticles to selected environmentally relevant test organisms and mammalian cells in vitro: a critical review. Arch. Toxicol. 87 (7), 1181–1200.

Bozcaarmutlu, A., Arinç, E., 2004. Inhibitory effects of divalent metal ions on liver microsomal 7-ethoxyresorufin O-deethylase (EROD) activity of leaping mullet. Mar. Environ. Res. 58 (2–5), 521–524.

Bradford, A., Handy, R.D., Readman, J.W., Atfield, A., M¨uhling, M., 2009. Impact of silver nanoparticle contamination on the genetic diversity of natural bacterial assemblages in estuarine sediments. Environ. Sci. Technol. 43 (12), 4530–4536.

Burke, M.D., Mayer, R.T., 1974. Ethoxyresorufin in direct fluorometric assay of a microsomal O-de-ethylation which is preferentially inducible by 3-methylcholanthrene. Drug Metab. Dispos. 2 (6), 583–588.

Bury, R.N., Walker, A.P., Glover, N.C., 2003. Nutritive metal uptake in teleost fish. J. Exp. Biol. 206, 11–23.

Cho, W.S., Duffin, R., Howie, S.E., Scotton, C.J., Wallace, W.A., Macnee, W., Bradley, M., Megson, I.L., Donaldson, K., 2011. Progressive severe lung injury by zinc oxide nanoparticles; the role of Zn^{2+} dissolution inside lysosomes. Part. Fibre Toxicol. 8, 27.

Cho, W.S., Kang, B.C., Lee, J.K., Jeong, J., Che, J.H., Seok, S.H., 2013. Comparative absorption, distribution, and excretion of titanium dioxide and zinc oxide nanoparticles after repeated oral administration. Part. Fibre Toxicol. 10, 9.

Degen, A., Kosec, M., 2000. Effect of pH and impurities on the surface charge of zinc oxide in aqueous solution. J. Eur. Ceram. Soc. 20, 667–673.

DeRosa, M.C., Monreal, C., Schnitzer, M., Walsh, R., Sultan, Y., 2010. Nanotechnology in fertilizers. Nat. Nanotechnol. 5 (2), 91.

EFSA, 2012. Scientific Opinion on safety and efficacy of zinc compounds (E6) as feed additive for all animal species: Zinc oxide, based on a dossier submitted by Grillo Zinkoxid GmbH/EMFEMA. EFSA J. 10 (11), 2970 (www.efsa.europa.eu/en/efsajournal/doc/2970.pdf).

EFSA FEEDAP Panel (EFSA Panel on Additives and Products or Substances used in Animal Feed), 2014r. Scientific opinion on the potential reduction of the currently authorised maximum zinc content in complete feed. EFSA J. 12 (5), 3668.

Elbekai, R.H., El-Kadi, A.O., 2005. The role of oxidative stress in the modulation of aryl hydrocarbon receptor-regulated genes by As^{3+}, Cd^{2+}, and Cr^{6+}. Free Radic. Biol. Med. 39, 1355–1367.

Espitia, P.J.P., Soares, N.F.F., Coimbra, J.S.R., Andrade, N.J., Cruz, R.S., Medeiros, A.A.E., 2012. Zinc oxide nanoparticles: synthesis, antimicrobial activity and food packaging applications. Food Bioprocess Technol. 5 (5), 1447–1464.

Faiz, H., Zuberi, A., Nazir, S., Rauf, M., Younus, N., 2015. Zinc oxide, zinc sulfate and zinc oxide nanoparticles as source of dietary zinc: comparative effects on growth and hematological indices of juvenile grass carp (*Ctenopharyngodon idella*). Int. J. Agric. Biol. 17 (3), 568–574.

Fan, W., Li, Q., Yang, X., Zhang, L., 2013. Zn subcellular distribution in liver of goldfish (carassius auratus) with exposure to zinc oxide nanoparticles and mechanism of hepatic detoxification. PLoS One. 8 (11), e78123.

Federici, G., Shaw, B.J., Handy, R.D., 2007. Toxicity of titanium dioxide nanoparticles to rainbow trout (*Oncorhynchus mykiss*): gill injury, oxidative stress, and other physiological effects. Aquat. Toxicol. 84 (4), 415–430.

Fernández, D., García-Gómez, C., Babín, M., 2013. In vitro evaluation of cellular responses induced by ZnO nanoparticles, zinc ions and bulk ZnO in fish cells. Sci. Total Environ. 1 (452–453), 262–274.

Fernández-Cruz, M.L., Lammel, T., Connolly, M., Conde, E., Barrado, A.I., Derick, S., Perez, Y., Fernandez, M., Furger, C., Navas, J.M., 2013. Comparative cytotoxicity induced by bulk and nanoparticulated ZnO in the fish and human hepatoma cell lines PLHC-1 and Hep G2. Nanotoxicology 7 (5), 935–952.

Ferry, J.L., Craig, P., Hexel, C., Sisco, P., Frey, R., Pennington, P.L., Fulton, M.H., Scott, I.G., Decho, A.W., Kashiwada, S., Murphy, C.J., Shaw, T.J., 2009. Transfer of gold nanoparticles from the water column to the estuarine food web. Nat. Nanotechnol. 4, 441–444.

Fraser, T.W., Reinardy, H.C., Shaw, B.J., Henry, T.B., Handy, R.D., 2011. Dietary toxicity of single-walled carbon nanotubes and fullerenes (C60) in rainbow trout (*Oncorhynchus mykiss*). Nanotoxicology 5 (1), 98–108.

Glover, C.N., Hogstrand, C., 2002. In vivo characterization of intestinal zinc uptake in freshwater rainbow trout. J. Exp. Biol. 205 (1), 141–150.

Gottschalk, F., Lassen, K., Kjoelholt, J., Christensen, F., Nowack, B., 2015. Modeling flows and concentrations of nine engineered nanomaterials in the Danish environment. Int. J. Environ. Res. Public Health 12 (5), 5581–5602.

Griffith, O.W., 1980. Determination of glutathione and glutathione disulfide using glutathione reductase and 2-vinylpyridine. Anal. Biochem. 106 (1), 207–212.

Habig, W.H., Pabst, M.J., Jakoby, W.B., 1974. Glutathione S-transferases: the first enzymatic step in mercapturic acid formation. J. Biol. Chem. 249 (22), 7130–7139.

Hao, L., Chen, L., 2012. Oxidative stress responses in different organs of carp (*Cyprinus carpio*) with exposure to ZnO nanoparticles. Ecotoxicol. Environ. Saf. 80, 103–110.

Hao, L., Chen, L., Hao, J., Zhong, N., 2013. Bioaccumulation and sub-acute toxicity of zinc oxide nanoparticles in juvenile carp (*Cyprinus carpio*): a comparative study with its bulk counterparts. Ecotoxicol. Environ. Saf. 91, 52–60.

Heinlaan, M., Ivask, A., Blinova, I., Dubourguier, H.C., Kahru, A., 2008. Toxicity of nanosized and bulk ZnO, CuO and TiO_2 to bacteria *Vibrio fischeri* and crustaceans *Daphnia magna* and *Thamnocephalus platyurus*. Chemosphere 71 (7), 1308–1316.

Johnston, B.D., Scown, T.M., Moger, J., Cumberland, S.A., Baalousha, M., Linge, K., van Aerle, R., Jarvis, K., Lead, J.R., Tyler, C.R., 2010. Bioavailability of nanoscale metal oxides TiO_2, CeO_2, and ZnO to fish. Environ. Sci. Technol. 44 (3), 1144–1151.

Kao, Y.Y., Chen, Y.C., Cheng, T.J., Chiung, Y.M., Liu, P.S., 2012. Zinc oxide nanoparticles interfere with zinc ion homeostasis to cause cytotoxicity. Toxicol. Sci. 125 (2), 462–472.

Keller, A.A., Wang, H., Zhou, D., Lenihan, H.S., Cherr, G., Cardinale, B.J., Miller, R., Ji, Z., 2010. Stability and aggregation of metal oxide nanoparticles in natural aqueous matrices. Environ. Sci. Technol. 44 (6), 962–1967.

Knox, D., Cowey, C.B., Adron, J.W., 1984. Effects of dietary zinc intake upon copper metabolism in rainbow trout (*Salmo gairdneri*). Aquaculture 40 (3), 199–207.

Li, W.M., Wang, W.X., 2013. Distinct biokinetic behavior of ZnO nanoparticles in *Daphnia magna* quantified by synthesizing ^{68}Zn tracer. Water Res. 47 (2), 895–902.

Ma, H., Williams, P.L., Diamond, S.A., 2013. Ecotoxicity of manufactured ZnO nanoparticles—a review. Environ. Pollut. 172, 76–85.

Milani, N., McLaughlin, M.J., Stacey, S.P., Kirby, J.K., Hettiarachchi, G.M., Beak, D.G., Cornelis, G., 2012. Dissolution kinetics of macronutrient fertilizers coated with manufactured zinc oxide nanoparticles. J. Agric. Food Chem. 60 (16), 3991–3998.

OECD, 2012. OECD Guideline for Testing of Chemicals 305: Bioaccumulation in Fish: Aqueous and Dietary Exposure. Organisation for Economic Co-operation and Development (OECD), Paris, France (http://www.oecd-ilibrary.org/content/book/9789264185296-en).

Ogino, C., Yang, Y.G., 1978. Requirement of rainbow trout for dietary zinc. Bull. Jpn. Soc. Sci. Fish. 44, 1015–1018.

Oliveira, M., Santos, M.A., Pacheco, M., 2004. Glutathione protects heavy metal-induced inhibition of hepatic microsomal ethoxyresorufin O-deethylase activity in *Dicentrarchus labrax* L. Ecotoxicol. Environ. Saf. 58 (3), 379–385.

Piccinno, F., Gottschalk, F., Seeger, S., Nowack, B., 2012. Industrial production quantities and uses of ten engineered nanomaterials in Europe and the world. J. Nanoparticle Res. 14, 1109.

Ramsden, S.C., Smith, J.T., Shaw, J.B., Handy, D.R., 2009. Dietary exposure to titanium dioxide nanoparticles in rainbow trout, (*Oncorhynchus mykiss*): no effect on growth, but subtle biochemical disturbances in the brain. Ecotoxicology 18, 939–951.

Reed, R.B., Ladner, D.A., Higgins, C.P., Westerhoff, P., Ranville, J.F., 2012. Solubility of nano-zinc oxide in environmentally and biologically important matrices. Environ. Toxicol. Chem. 31 (1), 93–99.

Sappal, R., Kamunde, C., 2009. Internal bioavailability of waterborne and dietary zinc in rainbow trout, *Oncorhynchus mykiss*: preferential detoxification of dietary zinc. Aquat. Toxicol. 93 (2–3), 166–176.

Sappal, R., Burka, J., Dawson, S., Kamunde, C., 2009. Bioaccumulation and subcellular partitioning of zinc in rainbow trout (*Oncorhynchus mykiss*): cross-talk between waterborne and dietary uptake. Aquat. Toxicol. 91 (4), 281–290.

Scown, T.M., Santos, E.M., Johnston, B.D., Gaiser, B., Baalousha, M., Mitov, S., Lead, J.R., Stone, V., Fernandes, T.F., Jepson, M., van Aerle, R., Tyler, C.R., 2010. Effects of aqueous exposure to silver nanoparticles of different sizes in rainbow trout. Toxicol. Sci. 115 (2), 521–534.

Shaw, B.J., Al-Bairuty, G., Handy, R.D., 2012. Effects of waterborne copper nanoparticles and copper sulphate on rainbow trout, (*Oncorhynchus mykiss*): physiology and accumulation. Aquat. Toxicol. 116–117, 90–101.

Smith, C.J., Shaw, B.J., Handy, R.D., 2007. Toxicity of single walled carbon nanotubes to rainbow trout, (*Oncorhynchus mykiss*): respiratory toxicity, organ pathologies, and other physiological effects. Aquat. Toxicol. 82, 94–109.

Tiwari, S., Pelz-Stelinskik, K., Mann, S.R., Stelinski, L.L., 2011. Glutathione transferase and cytochrome P450 (general oxidase) activity levels in *Candidatus Liberibacter asiaticus*-infected and uninfected Asian citrus psyllid (Hemiptera: Psyllidae). Ann. Entomol. Soc. Am. 104, 297–305.

Tso, C.P., Zhung, C.M., Shih, Y.H., Tseng, Y.M., Wu, S.C., Doong, R.A., 2010. Stability of metal oxide nanoparticles in aqueous solutions. Water Sci. Technol. 61 (1), 127–133.

Udenfriend, S., Stein, S., Böhlen, P., Dairman, W., Leimgruber, W., Weigele, M., 1972. Fluorescamine: a reagent for assay of amino acids, peptides, proteins, and primary amines in the picomole range. Science 178, 871–872.

Valdehita, A., Fernández-Cruz, M.L., Torrent, F., Navas, J.M., 2012. Differences in the induction of CYP1A and related genes in cultured rainbow trout *Oncorhynchus mykiss*. Additional considerations for the use of EROD activity as biomarker. J. Fish Biol. 81 (1), 270–287.

Wekell, J.C., Shearer, K.D., Houle, C.R., 1983. High zinc supplementation of rainbow trout diets. Prog. Fish Cult. 45 (3), 144–147.

Xiong, D., Fang, T., Yu, L., Sima, X., Zhu, W., 2011. Effects of nano-scale TiO_2, ZnO and their bulk counterparts on zebrafish: acute toxicity, oxidative stress and oxidative damage. Sci. Total Environ. 409 (8), 1444–1452.

Yu, L.P., Fang, T., Xiong, D.W., Zhu, W.T., Sima, X.F., 2011. Comparative toxicity of nano-ZnO and bulk ZnO suspensions to zebrafish and the effects of sedimentation, •OH production and particle dissolution in distilled water. J. Environ. Monit. 3 (7), 1975–1982.

Zhao, X., Wang, S., Wu, Y., You, H., Lv, L., 2013. Acute ZnO nanoparticles exposure induces developmental toxicity, oxidative stress and DNA damage in embryo–larval zebrafish. Aquat. Toxicol. 136–13, 49–59.

Zhu, X.S., Zhu, L., Duan, Z.H., Qi, R.Q., Li, Y., Lang, Y.P., 2008. Comparative toxicity of several metal oxide nanoparticle aqueous suspensions to zebrafish (*Danio rerio*) early developmental stage. J. Environ. Sci. Health, Part A: Tox. Hazard. Subst. Environ. Eng. 43 (3), 278–284.

Zhu, X., Chang, Y., Chen, Y., 2010. Toxicity and bioaccumulation of TiO_2 nanoparticle aggregates in *Daphnia magna*. Chemosphere 78 (3), 209–215.

CHAPTER 7

An investigation into the hazard associated with AuNPs and the influence of different peptide capping's on stability and biological activity in a liver cell line.

In chapter 7, we focus on AuNPs, ENMs which are being intensely investigated for their potential use in biomedicine due to their light absorbing and scattering properties at nanoscale. Obviously prior to their application any potential hazards associated with their use must be investigated and their biocompatibility must be assured. The use of coatings and capping agents in the rational design of ENMs is seen as an approach both to functionalise and to achieve safer NPs by design. In research paper 4, using AuNPs as an example, we investigate how ENMs properties and behaviour can be manipulated as desired. A detailed physico-chemical characterisation of an array of AuNPs capped with different peptide- biphenyl moieties containing (glycine (Gly), cysteine (Cys), tyrosine (Tyr), tryptophan (Trp) and methionine (Met)) under cell culture conditions was performed. How the cappings influence stability in such an environment and dictate activity towards liver cells was assessed. One PBH-capped AuNP preparation, namely (Au[(Gly-Tyr-TrCys)2B]), showed unique stability under biological conditions and distinct biological activity. The remarkable stability provided by such a capping agent may prove useful in the future design of AuNPs for drug delivery systems or simply to control ENM behaviour in biological matrices.

Research paper 4: Peptide-biphenyl hybrid-capped AuNPs: stability and biocompatibility under cell culture conditions.

Connolly et al. Nanoscale Research Letters 2013, 8:315
http://www.nanoscalereslett.com/content/8/1/315

Nanoscale Research Letters
a SpringerOpen Journal

NANO EXPRESS Open Access

Peptide-biphenyl hybrid-capped AuNPs: stability and biocompatibility under cell culture conditions

Mona Connolly[1], Yolanda Pérez[2*], Enrique Mann[3], Bernardo Herradón[3], María L Fernández-Cruz[1*] and José M Navas[1]

Abstract

In this study, we explored the biocompatibility of Au nanoparticles (NPs) capped with peptide-biphenyl hybrid (PBH) ligands containing glycine (Gly), cysteine (Cys), tyrosine (Tyr), tryptophan (Trp) and methionine (Met) amino acids in the human hepatocellular carcinoma cell line Hep G2. Five AuNPs, Au[(Gly-Tyr-Met)$_2$B], Au[(Gly-Trp-Met)$_2$B], Au[(Met)$_2$B], Au[(Gly-Tyr-TrCys)$_2$B] and Au[(TrCys)$_2$B], were synthesised. Physico-chemical and cytotoxic properties were thoroughly studied. Transmission electron micrographs showed isolated near-spherical nanoparticles with diameters of 1.5, 1.6, 2.3, 1.8 and 2.3 nm, respectively. Dynamic light scattering evidenced the high stability of suspensions in Milli-Q water and culture medium, particularly when supplemented with serum, showing in all cases a tendency to form agglomerates with diameters approximately 200 nm. In the cytotoxicity studies, interference caused by AuNPs with some typical cytotoxicity assays was demonstrated; thus, only data obtained from the resazurin based assay were used. After 48-h incubation, only concentrations ≥50 μg/ml exhibited cytotoxicity. Such doses were also responsible for an increase in reactive oxygen species (ROS). Some differences were observed among the studied NPs. Of particular importance is the AuNPs capped with the PBH ligand (Gly-Tyr-TrCys)$_2$B showing remarkable stability in culture medium, even in the absence of serum. Moreover, these AuNPs have unique biological effects on Hep G2 cells while showing low toxicity. The production of ROS along with supporting optical microscopy images suggests cellular interaction/uptake of these particular AuNPs. Future research efforts should further test this hypothesis, as such interaction/uptake is highly relevant in drug delivery systems.

Keywords: Gold nanoparticles; Hep G2; ROS; Autophagy; Cytotoxicity

Background

At the forefront of many lines of research in drug delivery are the endless possibilities of gold nanoparticles (AuNPs) [1-4]. These molecules are readily taken up by cells, and they therefore provide a valuable means for drug delivery, with reports of efficient transport across the blood–brain barrier in mice [5] and nuclear penetration in the human HeLa cell line [6]. At nanoscale, the properties conferred upon such an otherwise inert metal in its bulk form are surprising. It is precisely these unique properties that offer potential in fields as diverse as diagnostics, anti-cancer therapies, catalysts and fuel cells. One avenue that has been studied exhaustively in recent years is the use of coatings and capping agents in the rational design of NPs, both to stabilise and functionalise these nanoparticles. Specific capping agents can lead to the self-assembly of NPs into ordered 'superstructures' creating different shapes [7], and by altering the capping structure, different arrangements can be achieved. In terms of biocompatibility, when using a polyvinyl alcohol capping agent, AuNPs do not show toxicity in zebrafish, despite being taken up into embryos and evidence of bioaccumulation [8]. These observations highlight the use of capping agents as an approach to achieve safer NPs. We recently proposed the use of peptide-biphenyl hybrid (PBH) ligands as capping agents [9]. PBHs have a biphenyl system and two amino acid/peptide fragments, and they present key characteristics, such as dynamic properties in solution [10], ordered structures in the solid phase [11] and biological activity as calpain inhibitors [12]. Some of these properties arise from the presence of

* Correspondence: yolanda.cortes@urjc.es; fcruz@inia.es
[2]Universidad Rey Juan Carlos, Tulipán s/n, Móstoles, Madrid 28933, Spain
[1]Departamento de Medio Ambiente, Instituto Nacional de Investigación y Tecnología Agraria y Alimentaria (INIA), Carretera de la Coruña Km 7.5, Madrid 28040, Spain
Full list of author information is available at the end of the article

amino acid residues, as well as aromatic rings, that are able to participate in a variety of non-covalent bonds, including hydrogen bonds [13,14] and arene interactions [15,16]. In addition, the conformational flexibility around the aryl-aryl single bond allows the PBH to adopt its structure in order to obtain the most favourable interactions with other chemical species, thus achieving high biological activity [17]. In peptidomimetics, this approach is considered a novel way to tailor NPs to have desired physico-chemical properties, which could contribute, for example, to advances in biomedical applications for AuNPs as drug delivery systems. A molecule can be designed in such a way as to benefit from structure-activity relationships and to attain higher levels of stability and/or biocompatibility. In a study on the design of peptide capping ligands for AuNPs, Lévy et al. [18] reported that peptide chain length, hydrophobicity and charge strongly influence NP stability. Here, we capped AuNPs with various PBH ligands and studied how the ligand structures influence the stability and the physico-chemical properties of the AuNPs under cell culture conditions and how they affect the biological response.

The huge discrepancies in reports on NP toxicity may be related to their different stabilities under various experimental conditions, leading to distinct physico-chemical properties that directly influence the effect of these particles. Given the unique and unpredictable behaviour of NPs in different environments [19,20], we performed a detailed physico-chemical analysis, a prerequisite for any NP toxicity study. Distinct NP properties, such as size, shape, aggregation state, zeta potential and dispersibility, along with the inherent composition of the NPs themselves, all influence the degree of toxicity [21-23]. To study the interaction between these PBH-capped AuNPs and biological systems, we undertook cytotoxicity studies. Many articles have demonstrated a close relationship between size and toxicity for AuNPs [24,25]. Findings suggest that size not only can influence uptake but may also dictate the possible interaction with DNA grooves [26,27], thus leading to AuNPs of different sizes showing distinct mechanisms of toxicity. For instance, AuNPs of 1.4 and 1.2 nm in diameter, thus differing by only 0.2 nm, show different pathways of toxicity in HeLa human cervix carcinoma cell lines, causing cell death by necrosis and apoptosis, respectively [28]. AuNPs have reported LC_{50} values of 65 to 75 μg/ml in *Daphnia magna* [29]. According to Farkas et al. [30], these particles are potent inducers of reactive oxygen species (ROS) in rainbow trout hepatocytes, with concentrations of 17.4 μg/ml increasing ROS production threefold as early as 2 h post-exposure. However, there have also been reports of AuNP biocompatibility, suggesting cell-selective responses following AuNP exposure that may be related to specific mechanisms of toxicity. Cell death through apoptosis has been reported in the human lung carcinoma cell line A549 after exposure to AuNPs, with no evidence of cytotoxicity in BHK21 (baby hamster kidney), Hep G2 (human hepatocellular liver carcinoma) or MDCK (canine epithelial kidney) cell lines [31,32]. These observations may be explained by AuNP interaction with cellular stress response mechanisms on a genetic level [33], which may dictate the cells capacity to prevent cytotoxic effects.

To further our understanding of AuNP interaction with biological systems and the properties that may govern biocompatibility, after performing a detailed physico-chemical characterisation of all the PBH-capped AuNPs, we used an *in vitro* approach to assess the possible toxic effects and the oxidative stress potential of these particles. We focused on how the structure of the capping PBH used affects NP size and stability over time under a range of conditions *in vitro*. Differences in NP behaviour when suspended in cell culture medium with serum and without serum were examined. This approach allowed us to compare any changes in the physico-chemical properties of the NPs that may be associated with the interaction of the agent with fetal bovine serum and protein coating. Given that the liver is one of the main sites of AuNP bioaccumulation following intravenous injection [34,35]; we chose a human hepatocellular carcinoma cell line (Hep G2) as the most appropriate and relevant test system. NPs have been described to interfere with assays, and some reviews report the limitations of certain assay systems [36] and that AuNPs even have the capacity to quench or enhance fluorescence depending on the plasmon field and dipole energy [37]. Also, gold can bind biological thiols such as glutathione [38,39]. Therefore, in this study, close attention was paid to any potential interference of AuNPs with the assay systems.

Methods

Chemicals and reagents

The synthesis and characterisation of PBHs are described in detail in Additional file 1. The chemicals used for AuNP synthesis, such as hydrogen tetrachloroaurate (III) trihydrate ($HAuCl_4{\cdot}3H_2O$), sodium borohydride ($NaBH_4$), ethanol, 2-propanol and dimethyl sulfoxide-d_6 were purchased from Sigma-Aldrich (Madrid, Spain).

For biocompatibility studies, Eagle's minimum essential medium (EMEM), ultra glutamine 1 (200 mM in 0.85% NaCl solution), non-essential amino acids 100 X (NEAA), fetal bovine serum (FBS), penicillin/streptomycin (10,000 U/ml/10 mg/ml) and trypsin EDTA (200 mg/l EDTA, 17,000 U trypsin/l) were all sourced from LONZA (Barcelona, Spain). MEM and EMEM without phenol red were purchased from PAN Biotech GmbH (Aidenbach, Germany). High-grade purity water (>18 MΩ cm) obtained from a Milli-Q Element A10 Century (Millipore Iberia, Madrid, Spain) was used in all the

experiments. All other chemicals were purchased from Sigma-Aldrich.

Synthesis of AuNPs

Five AuNPs, (Au[(Gly-Trp-Met)$_2$B], Au[(Gly-Tyr-TrCys)$_2$B], Au[(Gly-Tyr-Met)$_2$B], Au[(Met)$_2$B] and Au[(TrCys)$_2$B]) (Figure 1), were synthesised following the methodology described by Pérez et al. [9] (see Additional file 1). Thus, each PBH (50 μmol) was dissolved in ethanol (20 ml, 2.5 mmol/l) and was added to a solution of $HAuCl_4$ (50 ml, 0.5 mmol/l) in 2-propanol under stirring. After 30 min, a freshly prepared aqueous solution of $NaBH_4$ (4 ml, 50 mmol/l) was added slowly. The mixture was stirred for 2 h at room temperature to afford a red-brown colloidal gold solution. The AuNPs were precipitated by centrifugation for 15 min at 6,000 rpm. The black-brown precipitate was washed with 2-propanol to remove the free ligand and then dried under vacuum. The PBH-capped AuNPs obtained were stable to some cycles of precipitation and re-dispersion and could be easily dispersed in water.

Physico-chemical characterisation of AuNPs

Transmission electron microscopy

Transmission electron microscopy (TEM) images of the synthesised AuNPs were obtained using a Philips Tecnai 20 operating at 200 kV (FEI, Eindhoven, The Netherlands). AuNPs were also examined after their suspension in culture medium without serum (EMEM/S-) at time 0 and 24 h using a LEO-910 microscope (Carl Zeiss, Oberkochen, Germany) operating at an accelerating voltage of 80 kV and equipped with a digital camera Gatan Bioscan 792 (Gatan Inc., Pleasanton, CA, USA). The samples for TEM characterisation were prepared by placing and evaporating a drop of the AuNPs in 2-propanol, or in medium, on carbon-coated copper grids (200 mesh). Average particle sizes were obtained by measuring the diameters of 150 particles.

Nuclear magnetic resonance

^{1}H nuclear magnetic resonance (NMR) and ^{13}C NMR spectra were recorded on Varian Mercury-400 and Varian Inova-300 instruments (Agilent Tecnologies, Santa Clara, CA, USA). Chemical shift (δ) constants are indicated in hertz. ^{1}H NMR spectra were referenced to the chemical shift of TMS (δ = 0.00 ppm). ^{13}C NMR spectra were referenced to the chemical shift of the deuterated solvent. The following abbreviations are used to explain multiplicities: s = singlet, d = doublet, t = triplet, q = quartet, m = multiplet, br = broad. The spectra of the ligands and the AuNPs were collected in dimethyl sulfoxide-d_6 (DMSO-d_6).

Elemental analysis

The amount of PBH capped on the AuNPs was estimated by elemental analysis of C, H, N and S. Combustion analyses were performed on an EA 1180-Elemental Analyzer (Carlo Erba, Milan, Italy).

Fourier transform infrared spectroscopy

Fourier transform infrared (FT-IR) spectra in the range of 600 to 4,000 cm^{-1} were recorded using a Nicolet-550 FT-IR spectrophotometer (Thermo Fisher, Hudson, NH, USA). The analysis was done in the solid state. Thirty-two scans were used to record the IR spectra.

UV–vis spectroscopy

Ultraviolet–visible (UV–vis) spectroscopy measurements of the AuNP samples were recorded on a Cary-500 spectrophotometer (Agilent Tecnologies, Santa Clara CA, USA) within the range 300 to 900 nm. The samples were prepared, using water as solvent, at 100 μg/ml. UV–vis

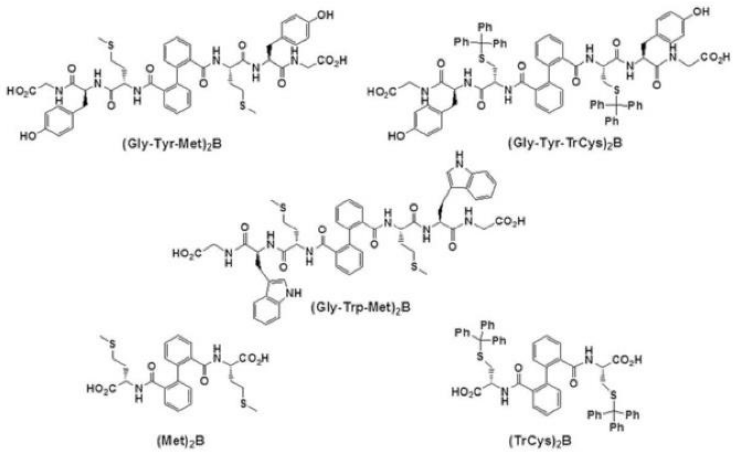

Figure 1 Peptide-biphenyl hybrid (PBH) ligands used in this study, Tr = Trityl, B = 2, 2′-(bis)carbonylbiphenyl.

measurements were also taken after suspension of the AuNPs in EMEM/S+ and EMEM/S- at a concentration of 100 μg/ml and at time-point 0 and 2, 4 and 24 h after incubation at 37°C.

Dynamic light scattering

Dynamic light scattering (DLS) was used to determine the hydrodynamic size of NPs in solution, using a Zetasizer Nano-ZS (Malvern Instruments Ltd., Worcestershire, UK). Measurements of the hydrodynamic size of the NP suspensions (100 μg/ml) in Milli-Q water and in EMEM biological medium with serum (EMEM/S+) and without serum (EMEM/S-) were taken at time 0 and at 24 h under exposure conditions (37°C and 5% CO_2). Careful attention was paid to distinguish measurements of background serum proteins from NP agglomerates in suspensions prepared in EMEM/S+. In addition, to study stability over time and the state of particles during the cell exposure timeframe in EMEM/S-, we conducted a kinetic study. DLS measurements were taken directly after the AuNPs were suspended (time 0) and at 2, 4, 24 and 48 h of incubation in exposure conditions. Three independent analyses were performed, and the mean ± standard deviation (SD) was used to represent results. Four measurements were taken in each independent analysis, with each measurement consisting of six runs, each lasting 10 s. The average from each of these measurements was calculated using Zetasizer series software 6.20 (Malvern Instrument). The instrument was set to automatically select the best conditions for measurements. A kinetic study was not performed in EMEM/S+ because of evidence of a stable suspension from time 0 to 24 h under exposure conditions when serum was present.

Zeta potential

Zeta potential measurements were performed to determine the stability of the PBH-capped AuNPs in Milli-Q water and in the different medium suspensions (EMEM/S+ and EMEM/S-). A Malvern Zetasizer Nano-ZS and folded capillary cells (Malvern Instruments Ltd., Worcestershire, UK) were used. One-millilitre aliquots of AuNP suspensions (100 μg/ml) were taken directly after preparation and 24 h after incubation in the different media. Due to the limitations of high salt content in both medium suspensions, zeta potential measurements were performed only in Milli-Q water. Three independent measurements were taken, and the mean ± SD is presented.

Optical microscopy and visual sedimentation of AuNP suspensions

An inverted light microscope Axiovert 25 (Carl Zeiss, Madrid, Spain) equipped with a Canon EOS 1000D (Canon, Madrid, Spain) camera was used to take images. NP suspensions (0.781 to 100 μg/ml) were prepared in EMEM/S+ and EMEM/S- medium, and 100-μl aliquots of each concentration were suspended in 96-well plates. Suspensions were viewed 24 h after incubation in exposure conditions (37°C/5% CO_2). A recent study carried out by Cho et al. [40] highlights the importance of considering sedimentation when carrying out NP toxicity studies *in vitro*. Those authors reported that different concentrations of NPs in the bottom of culture plates or 'interaction zones' caused by distinct ratios of sedimentation to diffusion velocities can result in variations in uptake. To detect differences in dispersion and sedimentation between the PBH-capped AuNPs in EMEM/S+ and EMEMS/S- medium, photographs were taken of the AuNP suspensions (100 μg/ml) in 1.5-ml tubes after 24-h incubation under exposure conditions.

Cell culture and AuNP exposure

Human liver hepatocellular carcinoma cells (Hep G2) were from the American Type Culture Collection (Manassas, VA, USA). These cells were cultured in EMEM medium supplemented with 10% FBS, 1% penicillin/streptomycin, 1% ultraglutamine and 1% NEAA. They were incubated at 37°C with 5% CO_2 in a humidified incubator. For AuNP exposure, cells were plated at densities of 7.5×10^4 cells per millilitre in 96-well tissue culture microtiter plates (Greiner-Bio one, CellStar, Madrid, Spain) and subsequently incubated for 24 h. After this period, cells were exposed to a series of concentrations of the five AuNP preparations for either 2 or 24 h for ROS production studies or for 24 or 48 h for the cytotoxicity studies. AuNP suspensions were prepared in high-grade Milli-Q water to achieve a stock concentration of 1,000 μg/ml. All stock preparations were stored at 4°C. AuNP working concentrations were prepared from the 1,000 μg/ml stock preparations in EMEM/S + or EMEM/S-. Given the different size and stability profiles found for the AuNPs when suspended in these two types of medium, as shown by UV–vis, DLS and TEM analysis, we performed exposures in medium with and without serum. Working concentrations ranged from 0.781 to 100 μg/ml and were prepared using serial half dilutions. The final concentration of water in EMEM medium did not cause any osmotic imbalance. For each assay, three independent experiments were performed, with exposures carried out in triplicate for each concentration. Untreated cells in culture medium were used as negative controls in all experiments, while a serial half dilution of chloramine-T was used to produce a concentration range between 0.325 and 10 mmol/l, which was used as a positive control.

Toxicity studies

Interference of AuNPs in toxicity assays

NP suspensions of each concentration tested were prepared in EMEM medium, phosphate-buffered saline

(PBS) and sulfosalicyclic acid dihydrate (SSA) 5% (*w*/*v*) or MEM phenol red-free medium, depending on the assay system being used, and included in the assay as another control to check possible AuNP absorbance at the corresponding wavelengths. Very high dose-dependent interferences were observed at the wavelengths used for the methyl thiazol tetrazolium (MTT) and neutral red uptake assay (NRU) assays. Some measurements were carried out after washing the cells to determine if this washing could lead to a reduction in the number of remaining AuNPs and consequently in the interference. We also examined whether the AuNPs used in this study interacted with glutathione. For that, a cell-free experiment was set up in which a constant concentration (8 μmol/l) of glutathione was incubated with a range of AuNP concentrations for 2 h. The glutathione content was then measured as described below.

Cytotoxicity

Methyl thiazol tetrazolium and neutral red uptake assays The MTT [(4,5-dimethylthiazoyl-2-yl)-2,5-diphenyltetrazolium bromide)] reduction assay, based on the conversion of tetrazolium salts to formazan crystals, was used to evaluate cell viability on the basis of mitochondrial activity, following the method described by Mosmann [41]. The NRU assay was used to determine the accumulation of neutral red dye in the lysosomes of viable, uninjured cells [42]. After the 24-h exposure, cells were incubated for 3 h with 500 μg/ml MTT reagent or for 2 h with 100 μg/ml neutral red dye, depending on the assay being performed. The resulting formazan crystals and remaining neutral red dye were dissolved with isopropanol or 1% glacial acetic acid in 50% ethanol, respectively. The absorbance of each well was read at 550 and 570 nm for the NRU and MTT assays, respectively, using a Tecan GENios plate reader (Tecan Group Ltd., Männedorf, Switzerland).

Resazurin assay The method described by O' Brien et al. [43], based on the reduction of resazurin to resorufin by mitochondrial oxidoreductases, was used. Cells were exposed to the AuNPs for 24 h, suspensions were removed, and cells washed with PBS and then treated with 20% (*v*/*v*) of resazurin dye reagent prepared in EMEM medium. The plate was then placed in a 37°C/5% CO_2 incubator for 2 h, after which the fluorescence intensity was read at 532-nm excitation and 595-nm emission wavelengths using a Tecan GENios plate reader. Results are represented as a percentage of the control. To study whether there was any further reduction in viability, cytotoxicity was also analysed after 48 h of exposure.

Images of cell condition At 2 and 24 h of exposure, images of the cells treated with NPs were taken and analysed for signs of cytotoxicity. An inverted light microscope (Axiovert 25, Carl Zeiss) equipped with a camera was used to take images. Evidence of cytoskeleton rounding or a change in normal shape compared to untreated controls was regarded as a sign of cytotoxicity. Also, to determine the degree of cytotoxicity, we compared the morphology of cultured cells with that of cells exposed to the positive control chloramine-T.

Oxidative stress

Quantification of reactive oxygen species Intracellular ROS production was determined using the dichlorofluorescein (DCF) assay [44]. Stock aliquots of 2', 7'-dichlorofluorescein diacetate (DCFH-DA) were prepared in dimethyl sulfoxide (DMSO) (100 mM) and diluted 1:1,000 in MEM phenol red-free medium to a final concentration of 100 μM, 0.1% (*v*/*v*) DMSO. After the exposure period (2 or 24 h), the medium and exposure compounds were removed, and cells were washed with PBS. Next, 100 μM of DCFH-DA probe was added to each well. The plate was incubated at 37°C/5% CO_2 in the dark for 30 min. After the incubation period, the DCFH-DA probe was removed, and the cells were washed twice with PBS. MEM phenol red-free medium was then added to the cells, and the fluorescence was measured at 485-nm excitation and 535-nm emissions (Tecan GENios plate reader). Fluorescent readings were taken immediately (time 0) and every 15 min over 60 min, with the plates maintained under dark conditions and incubated under exposure conditions (37°C/5% CO_2) between measurements. ROS production was calculated as the percentage increase in fluorescence per well over a 60-min period using the formula [(Ft60 − Ft0)/Ft0 × 100], where Ft60 and Ft0 are the fluorescence measured at time 60 and 0 min, respectively. This result was finally expressed as percentage of the control.

Reduced glutathione/oxidised glutathione ratio The assay protocol was set up based on the optimised microtiter plate method used by Allen et al. [45]. Following the 24-h exposure, cells were lysed, and 50 μl of PBS was then added to each well. Twenty-five microlitres of cell suspension was transferred to a new 96-well plate and used to assay for protein content. To the other 25 μl of lysed cells, we added 50 μl of ice-cold 5% (*w*/*v*) SSA diluted in Milli-Q water in order to remove any interfering proteins from the sample. Of this suspension, 25 μl was used to assay for total glutathione (reduced glutathione + oxidised glutathione ratio - GSH + GSSG) content, while the other 25 μl was treated with 4-vinylpyridine 0.5 μmol/l, a scavenger of GSH, to assay the GSSG content. One hundred twenty-five microlitres of reaction buffer (PBS 143 mmol/l containing 6.3 mmol/l EDTA at pH 7.4, 229 U/ml GSH reductase, 2.39 mmol/l β-nicotinamide adenine dinucleotide phosphate (NADPH) and 0.01 mol/l 5, 5'-dithiobis (2-

nitrobenzoic acid) (DTNB)) was added to each 25-μl suspension. The conversion of DTNB to 5'-thiol-2-nitrobenzoic acid (TNB) by the oxidation of GSH to GSSG was monitored by measuring absorbance at 405 nm every min over 10 min using a Tecan GENios plate reader. The rate of conversion, measured by the slope of the curve, was proportional to the concentration of glutathione in the sample. A standard curve with different concentrations of GSSG was used to calculate the glutathione contents in the samples.

Statistical analysis

For all the assays used, we performed three independent experiments with exposures carried out in triplicate for each concentration. The values shown are expressed as mean ± standard error of the mean (SEM). Sigma Plot 12 software (Systat Software Inc, CA, USA) was used for statistical analysis. The normality of the distribution was checked by means of the Shapiro-Wilk test. Equal variance was not assumed by the software and was tested (F test). A one-way repeated measures analysis of variance (RM-ANOVA) was carried out, followed by a *post hoc* Dunnett's test with $P < 0.05$ or $P < 0.01$.

Results

Physico-chemical characterisation of PBH-capped AuNPs

The AuNPs were synthesised using PBHs as capping ligands (Figure 1). In a previous study [9], we used PBHs containing cysteine (Cys), tyrosine (Tyr) and glycine (Gly) amino acids to form stable AuNPs: Au[$(TrCys)_2B$] and [$(Gly\text{-}Tyr\text{-}TrCys)_2B$]. In the present study, we demonstrate that the amino acids methionine (Met) and tryptophan (Trp) are also useful to prepare stable functionalised AuNPs such as Au[$(Met)_2B$], Au[$(Gly\text{-}Tyr\text{-}Met)_2B$] and Au[$(Gly\text{-}Trp\text{-}Met)_2B$]. TEM images of the PBH-capped AuNPs and the corresponding size distribution histograms are shown in Figure 2. The micrographs show isolated near-spherical NPs with diameters of 1.5, 1.6, 2.3, 1.8 and 2.3 nm for Au[$(Gly\text{-}Tyr\text{-}Met)_2B$], Au[$(Gly\text{-}Trp\text{-}Met)_2B$], Au[$(Met)_2B$], Au[$(Gly\text{-}Tyr\text{-}TrCys)_2B$] and Au[$(TrCys)_2B$], respectively. The NPs stabilised with the bulkiest PBHs were smaller. This observation may be attributable to the steric bulk of the ligand controlling NP growth.

TEM images combined with elemental analysis were used to estimate the molecular formula of the PBH-capped AuNPs (Table 1). The AuNPs prepared with PBHs containing Met residue were stabilised with a lower number of ligands on each AuNP surface compared to the AuNPs capped with other PBH ligands. A direct comparison of Au[$(Met)_2B$] and Au[$(TrCys)_2B$] revealed fewer ligands for the Met-containing PBH-AuNP, despite both having the same diameter. ^{1}H NMR spectra and FT-IR absorption spectra of free PBHs and of the PBH-capped AuNPs were measured to identify the interactions between the gold surface and the capping ligand. The NMR spectra of the AuNPs showed broad signals compared to the free PBHs. Figure 3 shows ^{1}H NMR spectra of Au[$(Gly\text{-}Tyr\text{-}Met)_2B$] and its free PBH $(Gly\text{-}Tyr\text{-}Met)_2B$ in DMSO-d_6. The signal of the H-α of the Met residue appeared at approximately 1.5 ppm in the PBH $(Gly\text{-}Tyr\text{-}Met)_2B$ NMR spectrum and was significantly broadened in that of Au[$(Gly\text{-}Tyr\text{-}Met)_2B$]. A similar line broadening was also observed in the NMR spectrum of Au[$(Gly\text{-}Trp\text{-}Met)_2B$] (Figure 3) and of Au[$(Met)_2B$] (see Additional file 2: Figure S1). These observations indicate that the PBH was attached to the gold surface through the Met residue [46]. Analogous results were observed for the NMR spectra of Au[$(Gly\text{-}Tyr\text{-}TrCys)_2B$] and Au[$(TrCys)_2B$] [9], where the sulphur atom of the TrCys residue is involved in the surface binding.

The FT-IR spectra are shown in Figure 4. For Au[$(Gly\text{-}Tyr\text{-}Met)_2B$], Au[$(Gly\text{-}Trp\text{-}Met)_2B$] and Au[$(Met)_2B$], the band caused by the C = O stretching mode of the carboxylic group was absent. However, two bands were observed around 1,600 and 1,398 cm^{-1}, assigned to the asymmetric and symmetric stretching vibrations of carboxylate anions [48]. These results suggest that the carboxylic groups are also involved in PBH interactions with the gold surface. Significant changes were observed in the amide I band in the spectra of capped NPs compared with those of the free PBHs. For Au[$(Gly\text{-}Tyr\text{-}Met)_2B$] and Au[$(Gly\text{-}Trp\text{-}Met)_2B$], the amide I band red shifted to 1,639 and 1,649 cm^{-1}, respectively, however, the amide band II appeared in the same position at 1,515 and 1,523 cm^{-1}, respectively. For Au[$(Met)_2B$], the band assigned to amide I blue shifted to about 1,600 cm^{-1} and the amide II band red shifted to 1,543 cm^{-1}. These findings indicate that conformational changes occur in the structure of the capping ligands attached to the NPs. Similar conclusions were drawn from the IR spectra of Au[$(Gly\text{-}Tyr\text{-}TrCys)_2B$] and Au[$(TrCys)_2B$] [9].

Physico-chemical characterisation of PBH-capped AuNPs under culture conditions

UV–vis absorption spectroscopy

Figure 5 shows the UV–vis absorption spectra of AuNPs in Milli-Q water at time 0 and in EMEM/S- taken at different time points under assay conditions (37°C and 5% CO_2). The spectrum in water, at a concentration of 100 μg/ml, shows the surface plasmon resonance (SPR) band in the range of 505 to 519 nm, characteristic of colloidal gold. The position of the SPR band was established as a function of particle size, stabilising ligand and solvent dielectric [49]. The SPR band of the UV–vis spectra of AuNPs (100 μg/ml) in EMEM/S- changed over time. The UV–vis spectra of the AuNPs after 24-h incubation

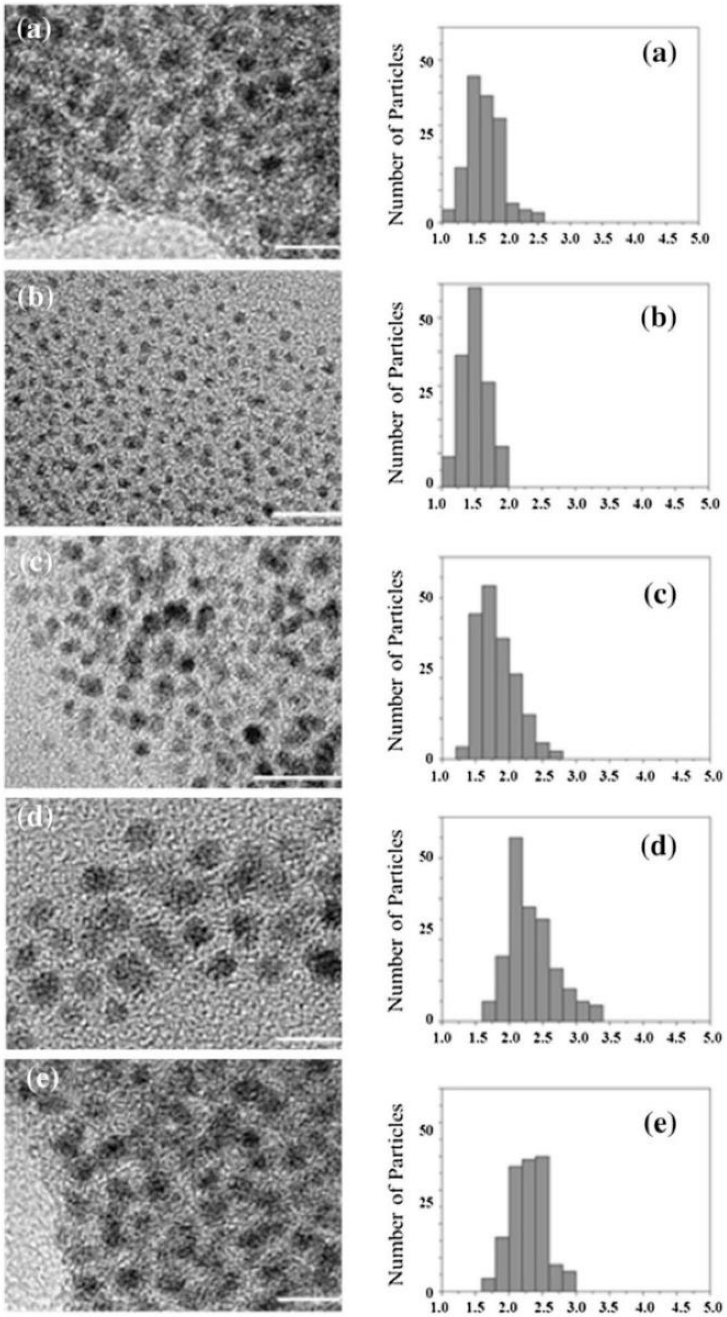

Figure 2 TEM images and size histograms of PBH-capped AuNPs. (a) Au[(Gly-Trp-Met)$_2$B], **(b)** Au[(Gly-Tyr-TrCys)$_2$B], **(c)** Au[(Gly-Tyr-Met)$_2$B], **(d)** Au[(Met)$_2$B] and **(e)** Au[(TrCys)$_2$B] [Scale bars: 10 nm for **(a)** and **(b)**; and 5 nm for **(c)**, **(d)** and **(e)**].

showed a slight broadening of the SPR band, in the range of 550 to 800 nm, indicating the aggregation of NPs in EMEM/S- medium as a result of the presence of salts in the medium. The band was also red shifted to 525 nm, in the case of Au[(Gly-Trp-Met)$_2$B] and Au [(Gly-Tyr-Met)$_2$B], and close to 560 nm for Au[(Gly-Tyr-TrCys)$_2$B], Au[(Met)$_2$B] and Au[(TrCys)$_2$B]. The red shift of the SPR band can be induced by a change in the refractive index that surrounds the AuNPs or by aggregation of NPs [50] caused by the presence of chemical or biological analytes in the culture medium. In addition, in the case of Au[(Gly-Trp-Met)$_2$B], Au [(Gly-Tyr-Met)$_2$B] and Au[(Met)$_2$B], which contain methionine, a minimal decrease in the intensity band was

Table 1 Structural characteristics of the AuNPs from elemental analysis and TEM data

AuNP	Size (nm)	Calculated m/n[a] from %N[b]	Number of Au atoms[c]	PBH units per Au nanoparticle	Mw
Au[(Gly-Trp-Met)$_2$B]	1.6	0.062	126	8	32,106
Au[(Gly-Tyr-TrCys)$_2$B]	1.8	0.22	180	40	90,397
Au[(Gly-Tyr-Met)2B]	1.5	0.064	104	7	27,100
Au[(Met)$_2$B]	2.3	0.154	375	57	102,625
Au[(TrCys)$_2$B]	2.3	0.26	375	97	164,377

Bold emphasis is used to signal the most stable AuNP; [a]*m*, Number of PBH units; *n*, Number of Au atoms; [b]%N from elemental analysis; [c]estimated supposing spherical particles and applying $N = 30.89602$ D3 [47].

observed over time. This decrease was associated with the structure and optical properties of gold. The amino acids of the culture medium were adsorbed on the surface of Au[(Gly-Trp-Met)$_2$B], Au[(Gly-Tyr-Met)$_2$B] and Au[(Met)$_2$B], and this effect might mask the optical absorption of these NPs [51]. AuNPs containing methionine were stabilised with a lower number of ligands and may have the capacity to link more molecules of amino acid on their surfaces. In comparison, the UV–vis spectra of AuNPs in EMEM/S+ (100 μg/ml) (see Additional file 3: Figure S2) did not show any change in the range of 550 to 800 nm. These spectra revealed no noticeable aggregation in preparations of AuNPs in EMEM/S+. Nevertheless, some decreases in the band intensities occurred over time in all cases, thereby indicating the adsorption of serum proteins from the medium [52].

Zeta potential

To study changes in AuNP stability, on the basis of electrostatic interaction, zeta potential measurements were performed. Due to the high salt content of EMEM/S+ and EMEM/S- media, measurements were performed only in Milli-Q water. Measurements were taken just after preparation of AuNP suspensions (100 μg/ml), at initial time (T0) and 24 h after incubation under assay conditions. The five AuNP preparations used in this study, namely Au[(Gly-Trp-Met)$_2$B], Au[(Gly-Tyr-TrCys)$_2$B], Au[(Gly-Tyr-Met)$_2$B], Au[(Met)$_2$B] and Au[(TrCys)$_2$B], showed zeta potentials of −31.6 ± 2.02, −37 ± 1.04, −36 ± 1.12, −39 ± 1.07 and −43.3 ± 1.13 mV, respectively (Table 2). All zeta potentials were negative and remained negative over time.

DLS was used to measure the hydrodynamic diameters of NPs in Milli-Q water and in medium suspension (100 μg/ml). DLS measurements were taken just after suspension (T0) and after 24 h incubations (T24) under assay conditions. In water, all AuNP preparations formed agglomerates, showing characteristic maximum intensity hydrodynamic diameters of ≤200 nm (Table 2). The Au[(Gly-Tyr-Met)$_2$B] also appeared as larger agglomerates, with a maximum intensity diameter of 591 nm at time 0, while Au[(Met)$_2$B] presented an additional NP population of only 38 nm in diameter. Using the size distribution of the AuNPs in water as a reference, we observed an increase in hydrodynamic size for all the AuNP preparations when incubated in EMEM/S+ and EMEM/S-, but to different extents. The average increase in hydrodynamic size for all the NP preparations in EMEM/S+ was 85 ± 26 nm at time 0 (Table 2). An exception was AuNPs Au[(Met)$_2$B], which did not increase in size in this medium. Also, with respect to the other three NPs, the larger agglomerates of Au[(Gly-Tyr-Met)$_2$B] underwent a much larger increase in size from 591 to 987 nm. The hydrodynamic sizes of Au[(Gly-Trp-Met)$_2$B] in water and EMEM/S+ are noticeably smaller than found for Au[(Gly-Tyr-Met)$_2$B]. These differences could be attributed to the presence, in the PBH ligand (Gly-Trp-Met)$_2$B, of the additional anchoring site, indole NH group of the Trp reside, which may be contributing to the stabilisation of this nanoparticle. All AuNP preparations remained in the same state in water and EMEM/S+ over 24 h, with no change in their size distribution profiles from those measured directly after preparation (Table 2). In contrast, for AuNPs incubated in EMEM/S-, a time-dependent increase in size was detected (Table 2). At time 0 (T0), the average increase in size in EMEM/S- was 86 ± 21 nm, similar to the distribution of most PBH-capped NPs in EMEM/S+, except Au[(Met)$_2$B], which experienced extensive agglomeration at time 0 (1,568 nm) with smaller fluctuations in its maximum hydrodynamic diameter over 24 h in EMEM/S- (1,368 nm). The Au[(Gly-Trp-Met)$_2$B], Au[(Gly-Tyr-Met)$_2$B] and Au[(TrCys)$_2$B] showed a time-dependent increase in size distribution, represented by agglomerates of 1,239, 1,230 and 908 nm after 24 h of incubation, respectively (Table 2). Au[(Gly-Tyr-TrCys)$_2$B] was the only preparation of AuNP that remained in the same relative size distribution profile over time and with the same maximum intensity hydrodynamic diameter (±54 nm) after a 24-h incubation in EMEM/S-. A kinetic study was performed to monitor changes in the AuNP suspensions (100 μg/ml) over time (Figure 6). DLS measurements were taken just after NP suspension in EMEM/S- and after 2-, 4-, 24- and 48-h incubations under assay conditions. The size distribution profiles for each preparation in EMEM/S- at each time point are represented in Figure 6, which shows an increasing tendency of agglomeration for all the AuNPs, except Au[(Gly-Tyr-TrCys)$_2$B], which remained stable over time.

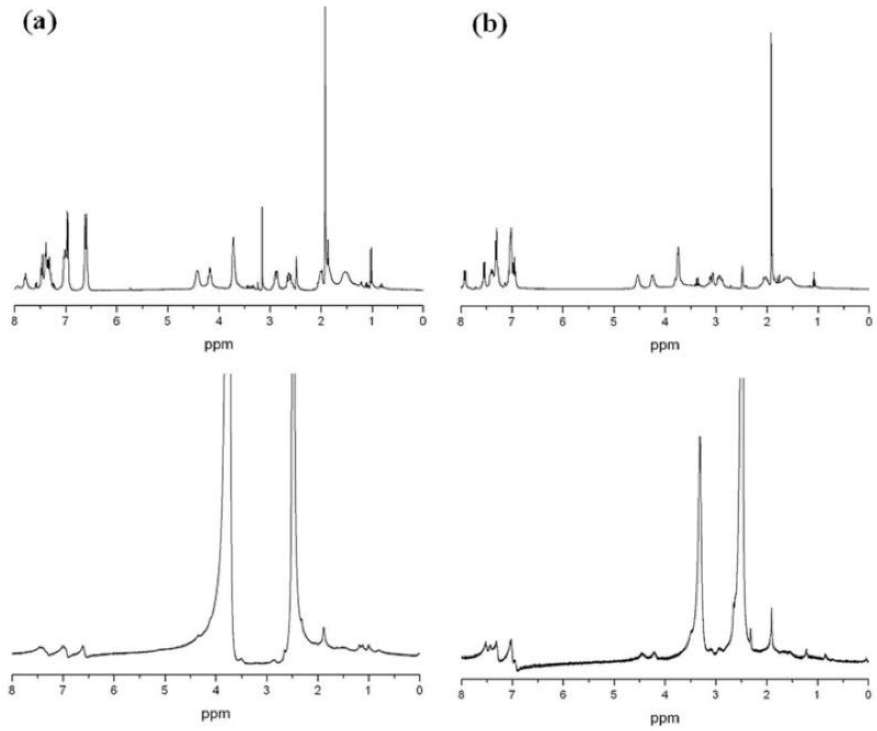

Figure 3 ^{1}H NMR spectra of free PBHs and PBH-capped AuNPs. (a) Free PBH (Gly-Tyr-Met)$_2$B (top) and ^{1}H NMR spectrum of AuNP Au[(Gly-Tyr-Met)$_2$B] (bottom) in DMSO-*d6*, and **(b)** ^{1}H NMR spectrum of free PBH (Gly-Trp-Met)$_2$B (top) and ^{1}H NMR spectrum of AuNP Au[(Gly-Trp-Met)$_2$B] (bottom) in DMSO-*d6*.

Transmission electron microscopy

Transmission electron micrographs were taken of the PBH-capped AuNPs after suspension in EMEM/S- medium (T0) and after 24 h of incubation (T24) under assay conditions (37°C/5% CO_2). Representative TEM images of Au[(Gly-Tyr-TrCys)$_2$B], Au[(TrCys)$_2$B] and Au [(Gly-Tyr-Met)$_2$B] are shown in Figure 7. Figure 7a,c shows TEM micrographs of Au[(TrCys)$_2$B] and Au[(Gly-Tyr-TrCys)$_2$B] directly after suspension, respectively. Both images reveal isolated NPs with the same size (1 to 3 nm) in the absence of medium. After 24 h of incubation, Au[(Gly-Tyr-TrCys)$_2$B] and Au[(TrCys)$_2$B] (Figure 7b,d) showed agglomeration and a clear interaction of individual NPs with medium components, as determined from TEM images. By comparing the micrographs, the highest degree of agglomeration in the case of Au[(Gly-Tyr-Met)$_2$B] (Figure 7e,f) after suspension in medium can be appreciated. Therefore, one would expect the surface chemistry of these NPs upon interaction with media not to be the same as for the NPs initially prepared [53].

Optical microscopy and visual sedimentation of AuNP suspensions

Large distinctive agglomerates of micrometre scale were observed for all AuNP preparations when viewed under an optical microscope (Figure 8), with the exception of Au[(Gly-Tyr-TrCys)$_2$B] (Figure 8b). Also upon visual observation of the AuNP suspensions in the different medium suspensions after 24 h of incubation, we made some key observations regarding sedimentation over time. After 24 h of incubation in EMEM/S-, Au[(Gly-Trp-Met)$_2$B], Au[(Gly-Tyr-Met)$_2$B], Au[(Met)$_2$B] and Au [(TrCys)$_2$B] sedimented out of solution, as determined by the presence of a pellet at the bottom of the tubes. Au [(Gly-Tyr-TrCys)$_2$B] remained dispersed in solution, having a visibly darker appearance in suspension. In the case of the serum-containing medium, EMEM/S+, sedimentation was less apparent. AuNP Au[(Gly-Tyr-TrCys)$_2$B], along with Au[(Met)$_2$B] and Au[(TrCys)$_2$B], had a visibly darker appearance, thereby suggesting different dispersion rates for these particles when serum was present.

Toxicity studies

Interference of AuNPs with toxicity assays

AuNP concentration-dependent interference was detected with the toxicity assays used in this study (Figure 9). In the case of the commonly used MTT and NRU assays, absorbance is used as the assay readout. Concentration-dependent interference by control samples containing AuNPs without cells was observed at both of the wavelengths used, 570 and

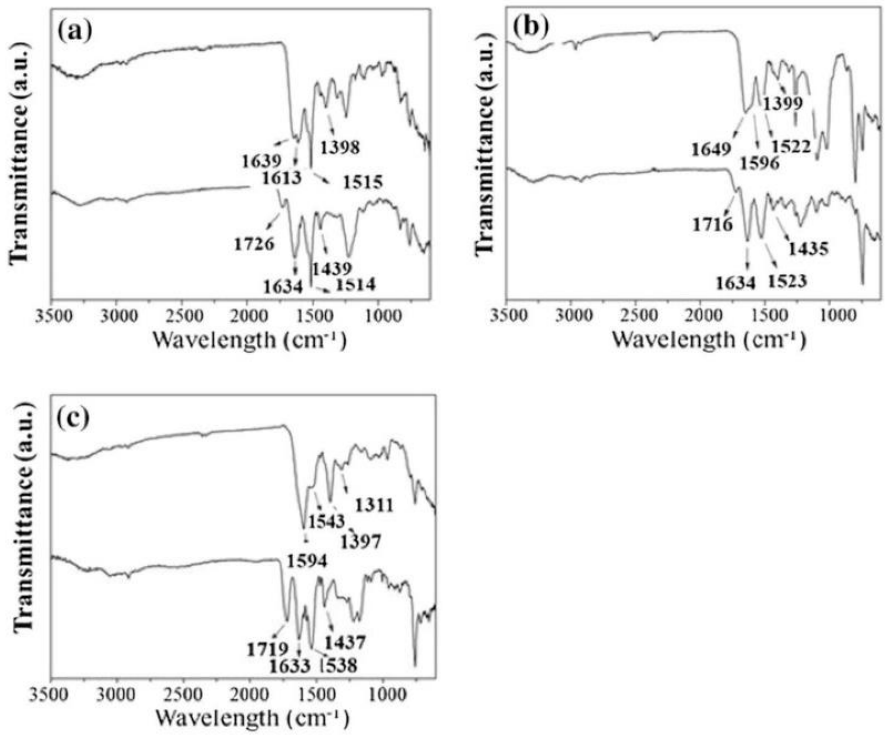

Figure 4 FT-IR spectra for free PBHs and PBH-capped AuNPs. (a) Free PBH (Gly-Tyr-Met)$_2$B (bottom) and AuNP Au[(Gly-Tyr-Met)$_2$B] (top), **(b)** free PBH (Gly-Trp-Met)$_2$B (bottom) and AuNP Au[(Gly-Trp-Met)$_2$B] (top) and **(c)** free PBH (Met)$_2$B (bottom) and AuNP Au[(Met)$_2$B] (top).

550 nm, as a result of the absorbance of AuNPs at the same wavelengths (Figure 9a,b). A concentration-dependent increase in absorbance levels was evident from a 6.25 μg/ml exposure concentration, which reached a 500% increase at the highest concentration used in this study (100 μg/ml) for both wavelengths. The removal of the media and washing with PBS did not lead to a significant reduction in interferences to levels that permitted the assays to be used appropriately. To combat interferences seen using absorbance as endpoint readout, a cytotoxicity assay using resazurin and its fluorescent product was applied. AuNP-only controls suspended in EMEM medium were included and interference was detected. We observed a concentration-dependent decrease in the levels of fluorescence as a result of AuNP interference (Figure 9c). At the highest concentration of AuNP, levels decreased by 11% to 24% depending on the AuNP in question. Au[(Gly-Tyr-TrCys)$_2$B] exhibited the highest level of interference. The results were interpreted with care in order to avoid drawing erroneous conclusions. Cytotoxicity was assumed only when the decrease in fluorescence was lower than possible interference levels. We also examined whether the AuNPs used in this study interacted with the glutathione assay. AuNPs absorbed at the wavelength used in this assay (405 nm). A dose-dependent increase appeared for some of them at concentrations of 1.56 μg/ml (data not shown) or higher. Additionally, when glutathione was incubated with a range of AuNP concentrations for 2 h the level of free glutathione decreased as the concentration of AuNPs increased (Figure 9d). Therefore, this assay was not considered suitable for studying the oxidative stress potential of the AuNPs. However, no interference was observed with the ROS production assay (data not shown).

Cytotoxicity

Methyl thiazol tetrazolium and neutral red uptake assays The MTT and NRU assays could not be performed as there was AuNP interference at the wavelengths used in these tests (570 and 550 nm, respectively) (Figure 9a,b).

Resazurin assay Cytotoxicity assays were performed with cells incubated in EMEM/S+ and EMEM/S- after 24- and 48-h exposure periods. Only results with cells incubated in EMEM/S- are shown in Table 3, as clear evidence of cytotoxicity in cells exposed to AuNPs in EMEM/S+ could not be determined because of high interference levels in this assay under these conditions (Figure 9c). Cytotoxicity is expressed as percentage of live cells (viability) compared to the untreated control (100%). At the highest concentration (100 μg/ml), all AuNP preparations caused approximately 10% decrease in viability. This was the highest decrease in viability recorded after 24 h of incubation for

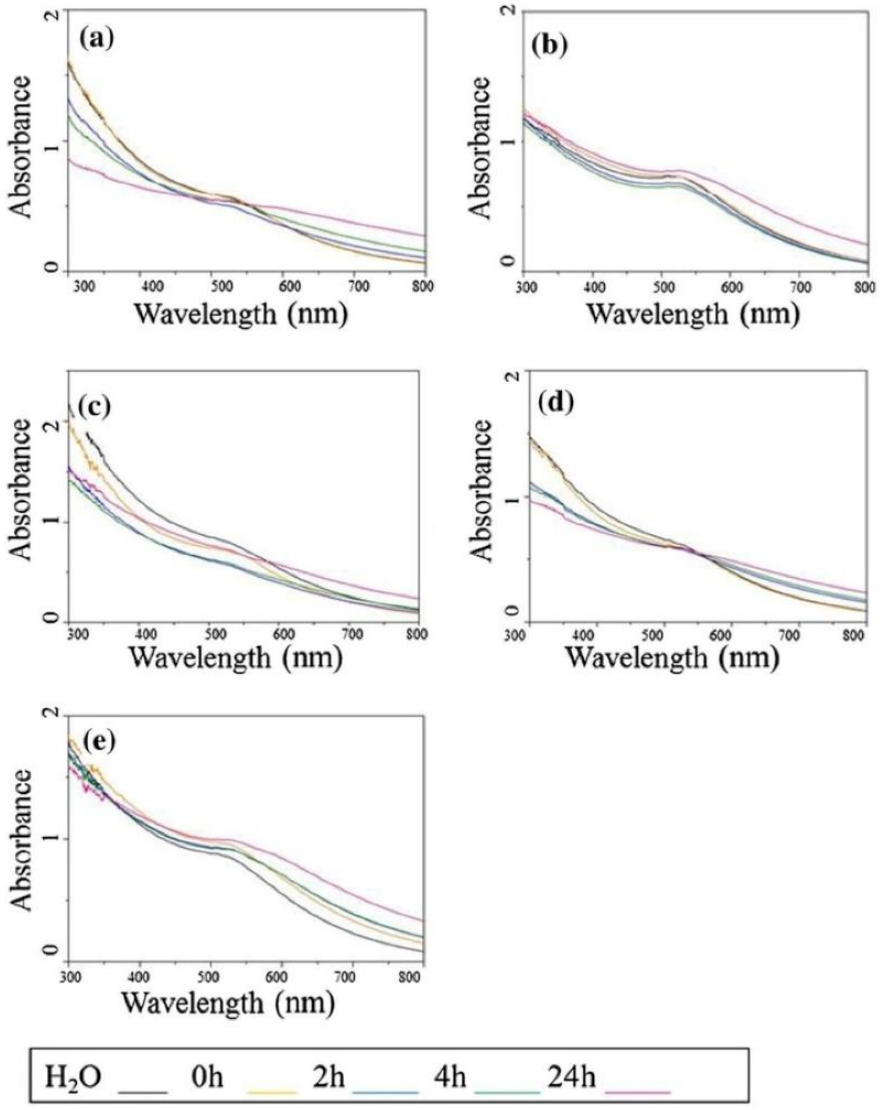

Figure 5 UV–vis absorption spectra of AuNPs. (a) Au[(Gly-Tyr-Met)$_2$B], **(b)** Au[(Gly-Tyr-TrCys)$_2$B], **(c)** Au[(Gly-Trp-Met)$_2$B], **(d)** Au[(Met)$_2$B] and **(e)** Au[(TrCys)$_2$B], in water and EMEM/-, each at a concentration of 100 μg/ml and at time point 0 and 2, 4 and 24 h of incubation at 37°C.

the AuNP preparations tested. This decrease in viability was not higher than that recorded for the cell-free AuNP-only controls in the interference studies (11% to 24% decrease). Therefore, the reduction in viability is perceived to be a result of NP interference and cannot be reported as cytotoxicity. After 48 h of incubation, the level of cytotoxicity for Au[(Gly-Tyr-Met)$_2$B], Au[(Met)$_2$B] and Au [(TrCys)$_2$B] increased significantly for the two highest doses of 50 and 100 μg/ml ($p < 0.01$). Viability was reduced to levels beyond which AuNP interference may be responsible. A significant decrease ($p < 0.01$) in cell viability was observed for the AuNP Au[(Gly-Trp-Met)$_2$B] only at the highest dose (100 μg/ml). Exposure to AuNP Au [(Gly-Tyr-TrCys)$_2$B] also resulted in a reduction in viability over time but not below interference levels. This observation thus suggests that this AuNP presents increased biocompatibility.

Images of cell condition An optical microscope was used to view the cells and NPs in EMEM/S- at various time points throughout the exposure. The study was performed only for exposures using EMEM/S- because of evidence of higher instability and toxicity of AuNPs under these conditions. Figure 10 shows Hep G2 cells after 24 h of incubation with NP concentrations of 100 μg/ml. The AuNPs Au[(Met)$_2$B] formed large agglomerates that covered almost the entire well (Figure 10f). While this phenomenon made it difficult to view the cells, evidence

Table 2 Physico-chemical properties of PBH-capped AuNPs (100 μg/ml) under different conditions over time

	Milli-Q water			EMEM/S+		EMEM/S-	
	T0	T24	T0	T0	T24	T0	T24
AuNP	**Size**[a]	**Size**	**Zeta**[b]	**Size**	**Size**	**Size**	**Size**
	nm	nm	mV	nm	nm	nm	nm
Au[(Gly-Trp-Met)$_2$B]	148 ± 2	148 ± 1	−31.6 ± 2.0	242 ± 4	243 ± 6	233 ± 15	1,239 ± 26
Au[(Gly-Tyr-TrCys)$_2$B]	143 ± 1	143 ± 1	−37 ± 1.4	261 ± 1	261 ± 2	251 ± 15	195 ± 2
Au[(Gly-Tyr-Met)$_2$B]	591 ± 73	507 ± 65	−36 ± 1.1	987 ± 205	987 ± 207	407 ± 21	1,230 ± 8
	161 ± 5	150 ± 12		203 ± 13	201 ± 9		
Au[(Met)$_2$B]	229 ± 23	228 ± 10	−39 ± 1.1	190 ± 13	190 ± 4	1568 ± 28	1,368 ± 25
	38 ± 6	40 ± 3		27 ± 9	28 ± 3		
Au[(TrCys)$_2$B]	205 ± 1	205 ± 1	−43.2 ± 1.1	261 ± 3	260 ± 4	271 ± 23	908 ± 23
							97 ± 3

T0 represents measurements directly after preparation and T24 measurements 24 h after incubation under cell exposure conditions (37°C, 5% CO_2). Average values of three independent measurements are presented (mean ± SD). Bold emphasis is used to signal the most stable AuNP; DLS, dynamic light scattering.
[a]Hydrodynamic size (Size); [b]zeta potential (Zeta) of AuNPs in Milli-Q water.

of cell rounding was observed when compared to the untreated cells (Figure 10a). However, the cells most dramatically affected were those exposed to Au[(Gly-Tyr-TrCys)$_2$B] and Au[(TrCys)$_2$B] (Figure 10d,g, respectively). Unique and distinct dark assemblages in the cells exposed to Au[(Gly-Tyr-TrCys)$_2$B] (Figure 10d) were evident. The size of Au[(Gly-Tyr-TrCys)$_2$B] agglomerates did not permit NP visualisation in a cell-free Au[(Gly-Tyr-TrCys)$_2$B] suspension (Figure 8). This observation led us to believe that the assemblies, visible when Au[(Gly-Tyr-TrCys)$_2$B] was in contact with cells (Figure 10d), are a result of cell damage or are formed from cellular interaction with these AuNPs. The cells exposed to Au[(TrCys)$_2$B] (Figure 10g) showed the characteristic appearance of cells treated with chloramine-T (Figure 10b), the chemical used in this study as a positive control. The cells rounded completely into a blister-like structure. However, the AuNPs did not appear to interact with the cells and instead were suspended in the medium. The morphology of Hep G2 cells incubated with Au[(Gly-Trp-Met)$_2$B] was comparable with that of untreated cells, despite the presence of some dark assemblages (Figure 10c). Cells exposed to Au[(Gly-Tyr-Met)$_2$B] (Figure 10e) also seemed to retain healthy cellular features, with NPs settled on clear areas of the 96-well plate, thereby suggesting limited NP-cellular interaction.

Oxidative stress

Quantification of reactive oxygen species A concentration-dependent increase in ROS in Hep G2 cells exposed to the two highest doses (50 and 100 μg/ml) of AuNPs in EMEM/S- was evident and significant as early as 2 h and increased after 24 h of exposure (Figure 11a,b). Exposure to Au[(Gly-Tyr-TrCys)$_2$B] for 24 h produced the highest increase in ROS levels, showing a 150% increase after exposure to the highest concentration tested (100 μg/ml) (Figure 11b). Au[(Gly-Tyr-Met)$_2$B] showed the lowest oxidative potential, with only a 40% increase in ROS level after 24 h of exposure. Exposure assays after 24 h using EMEM/S+ (Figure 11c) led to a reduction in ROS production in Hep G2 cells in comparison with EMEM/S- for all AuNP preparations after the same period. Most dramatically, the capacity of Au[(Gly-Trp-Met)$_2$B] and Au[(Met)$_2$B] to elicit ROS generation disappeared while the ability of Au[(Gly-Tyr-TrCys)$_2$B], Au[(Gly-Tyr-Met)$_2$B] and Au[(TrCys)$_2$B] to elicit an oxidative stress response was attenuated, with a significant difference in responses, as measured statistically.

Reduced glutathione/oxidised glutathione ratio This assay could not be performed due to AuNP interference with the system (Figure 9d). There is a concentration-

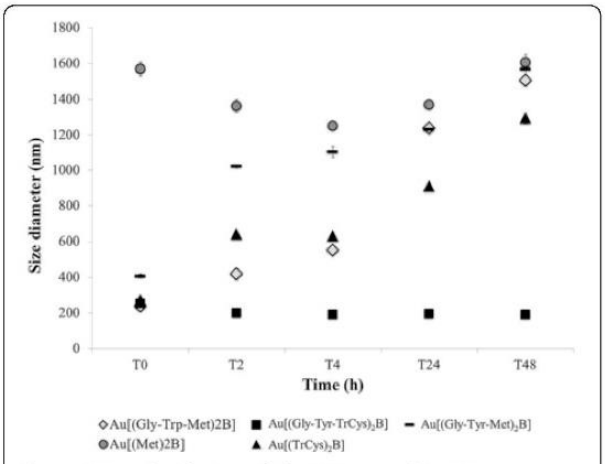

Figure 6 Size distribution of the PBH-capped AuNP preparations (100 μg/ml) in EMEM/S- over time using DLS. Maximum intensity hydrodynamic diameter (nm) measured directly after preparation (T0) and at 2 h (T2), 4 h (T4), 24 h (T24) and 48 h (T48) of incubation are shown.

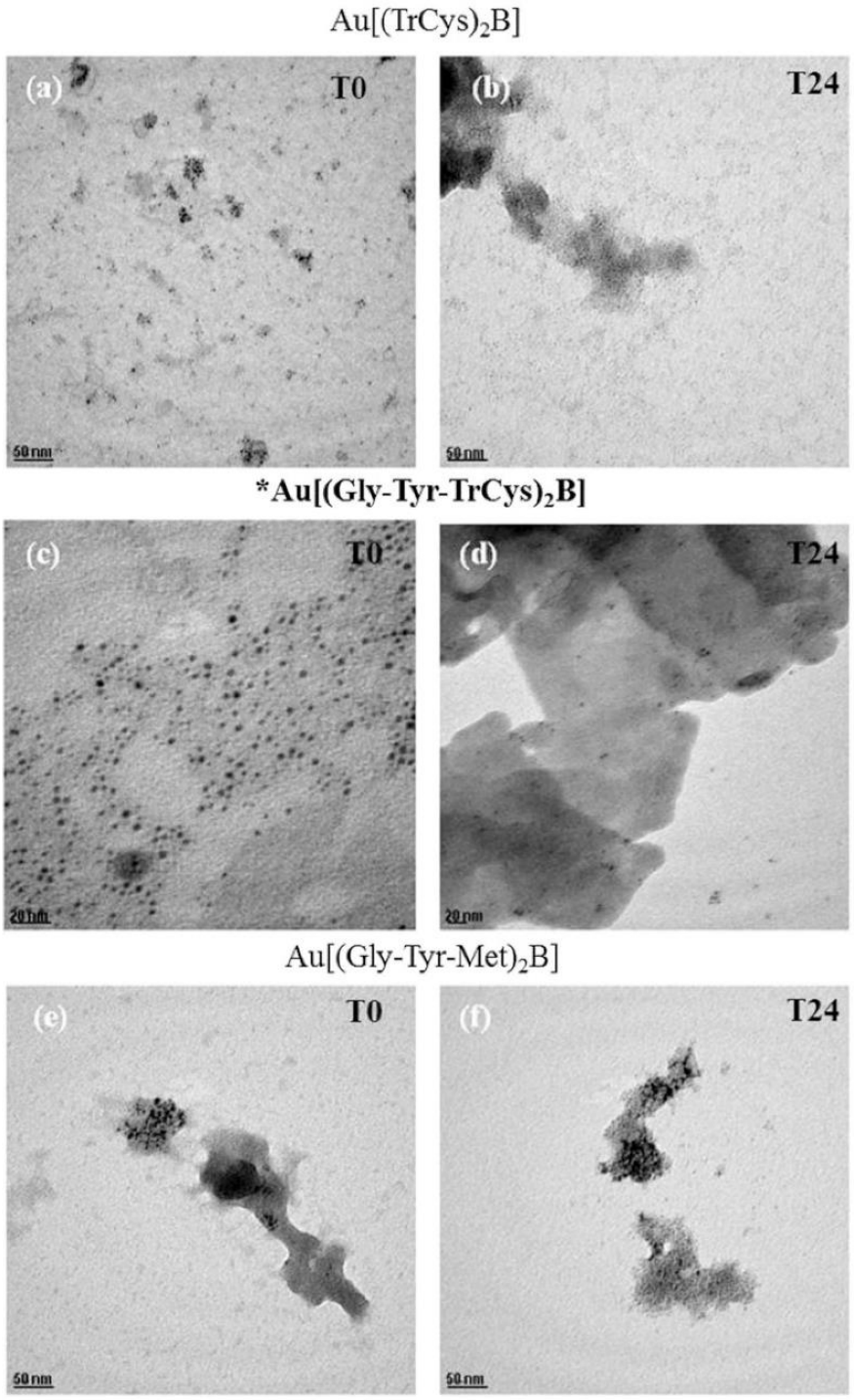

Figure 7 TEM images of AuNPs in EMEM/S- after preparation. (a) Au[$(TrCys)_2B$], **(c)** Au[$(Gly\text{-}Tyr\text{-}TrCys)_2B$] and **(e)** Au[$(Gly\text{-}Tyr\text{-}Met)_2B$], and at 24 h of incubation; **(b)** Au[$(TrCys)_2B$], **(d)** Au[$(Gly\text{-}Tyr\text{-}TrCys)_2B$] and **(f)** Au[$(Gly\text{-}Tyr\text{-}Met)_2B$] [Scale bar **(c)** and **(d)** is 20 nm, and for all other images, scale bar is 50 nm]; asterisk and bold letters are used to signal the most stable AuNP.

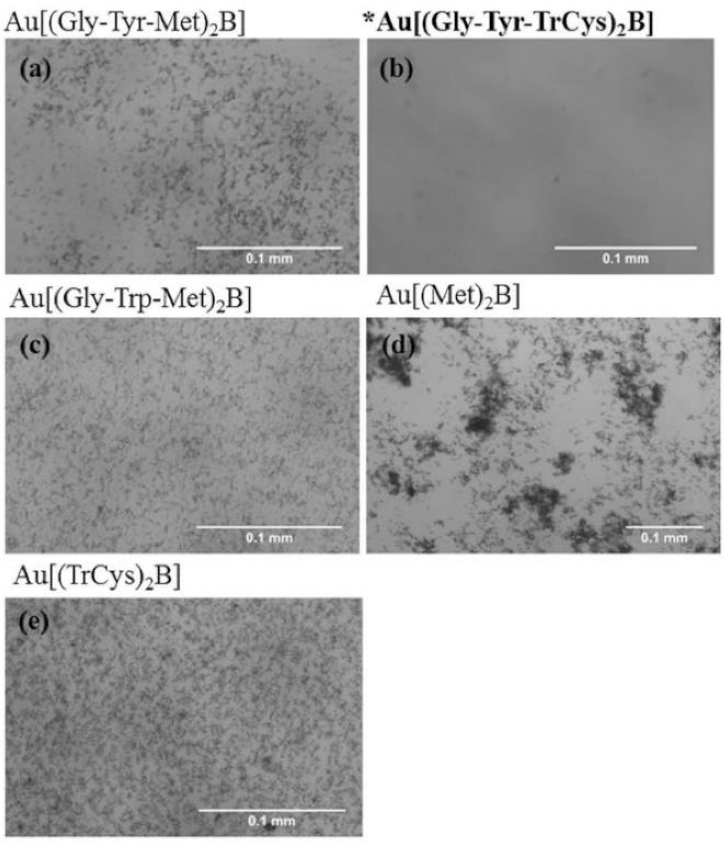

Figure 8 PBH-capped AuNPs (100 μg/ml) after 24-h incubation in EMEM/S- as viewed using optical microscope. (a) $Au[(Gly\text{-}Trp\text{-}Met)_2B]$, **(b)** $Au[(Gly\text{-}Tyr\text{-}TrCys)_2B]$, **(c)** $Au[(Gly\text{-}Tyr\text{-}Met)_2B$, **(d)** $Au[(Met)_2B$ and **(e)** $Au[(TrCys)_2B]$; asterisk and bold letters are used to signal the most stable AuNP.

dependent decrease in the rate of conversion (slope) of DTNB to TNB caused by the interaction of the AuNPs with glutathione.

Discussion

In this study, we have made some important observations concerning the biological behaviour of PBH-capped AuNPs. Depending on the structure of the PBH capping ligand, the behaviour of AuNPs differed both in terms of stability and biocompatibility. The PBH-capped AuNPs used in this study associated in different ways, forming agglomerates of different sizes under culture conditions, as demonstrated through DLS measurements, UV–vis analysis and optical imaging. The stability of these particles over time is dictated by both the structure of the PBH ligand and the surrounding medium. Even the smallest of changes in ligand structure can lead to great differences in AuNP behaviour. We detected clear differences in the hydrodynamic size of AuNPs in EMEM/S+ and EMEM/S-. In the former, all the AuNP preparations experienced a uniform increase in hydrodynamic size, possibly because of serum coating forming a corona, as proposed for other NPs [54,55], but these preparations remained in a stable size distribution over 24 h. It would appear that the serum coating prevented further interaction between the individual AuNPs over time. In agreement with this finding, Ehrenberg et al. [56] demonstrated protein binding to polystyrene particles (100 nm) with COOH functional groups within seconds with stable protein-coated NPs after as little as 30 min and these NPs remained stable for the entire test period (4 h). According to our UV–vis and DLS analyses, all PBH-capped AuNPs form stable agglomerates under culture conditions when serum was present. However, considerations are needed when serum is not present. In this case, the structure of the PBH greatly influences the stability and biocompatibility of the AuNP. In EMEM/S-, the characteristic hydrodynamic size distribution profiles of all the NP preparations increased considerably in a time-dependent manner, with the exception of $Au[(Gly\text{-}Tyr\text{-}TrCys)_2B]$. This PBH-capped AuNP had the same hydrodynamic size distribution profile range (150 to 260 nm) in EMEM/S- as in a water suspension and in medium containing serum. Thus, the hydrodynamic size decreased approximately 40 nm upon incubation. This reveals that

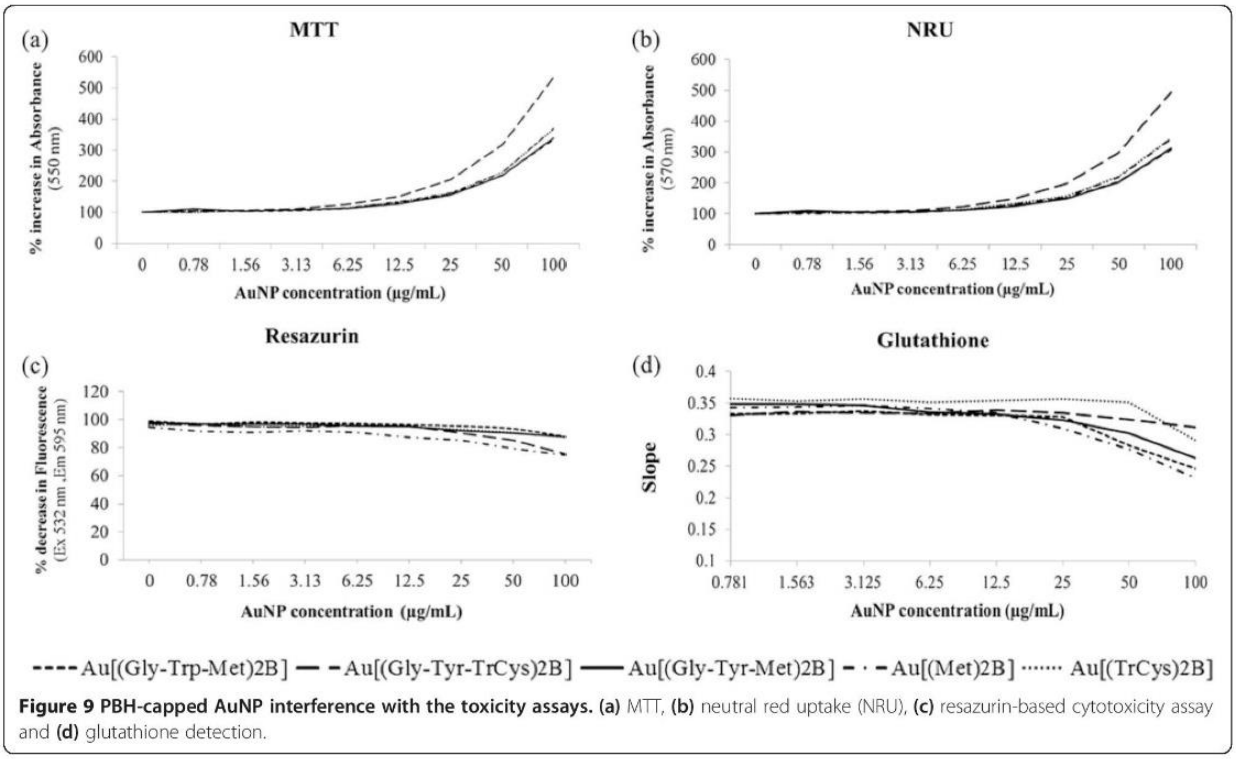

Figure 9 PBH-capped AuNP interference with the toxicity assays. (a) MTT, **(b)** neutral red uptake (NRU), **(c)** resazurin-based cytotoxicity assay and **(d)** glutathione detection.

Table 3 Cytotoxicity of PBH-capped AuNPs following 24- and 48-h exposure (EMEM/S-), using resazurin assay

		Exposure concentration (µg/ml)			
Exposure duration	**AuNP**	**12.5**	**25**	**50**	**100**
Au[(Gly-Trp-Met)$_2$B]	24 h	97 ± 1	97 ± 1*	96 ± 1*	94 ± 0.3**[a]
Viability (%)	48 h	98 ± 1	98 ± 2	91 ± 1	69 ± 4**[a]
Measured interference (%)		96 ± 2	95 ± 2	94 ± 4	88 ± 4
Au[(Gly-Tyr-TrCys)$_2$B]	24 h	98 ± 1	96 ± 1*	93 ± 1**	90 ± 1**
Viability (%)	48 h	95 ± 2	100 ± 2	95 ± 3	87 ± 2*
Measured interference (%)		96 ± 3	90 ± 6	85 ± 7	76 ± 6
Au[(Gly-Tyr-Met)$_2$B]	24 h	96 ± 1	96 ± 1*	96 ± 1*	91 ± 2**[a]
Viability (%)	48 h	94 ± 1	91 ± 6*	81 ± 6**	71 ± 5**[a]
Measured interference (%)		95 ± 2	92 ± 2	90 ± 4	88 ± 4
Au[(Met)$_2$B]	24 h	97 ± 1	96 ± 0.4*	93 ± 0.4**	94 ± 2**[a]
Viability (%)	48 h	97 ± 1	91* ± 3	88 ± 4**	68 ± 4 **[a]
Measured interference (%)		93 ± 1	91±	91 ± 2	89 ± 5
Au[(TrCys)$_2$B]	24 h	98 ± 1	97 ± 1	92 ±2*	88 ± 1**
Viability (%)	48 h	94 ± 4	93 ± 1	88 ± 2 **	77 ± 1**
Measured interference (%)		95 ± 1	93±	91 ± 3	87 ± 4

Also shown are the measured interferences in percent (%) of the control. Average values of three independent measurements are presented (mean ± SEM). Bold emphasis is used to signal the most stable AuNP; *P < 0.05 and **P < 0.01, significant differences from control values. [a]Significant differences between response to 24- and 48-h exposure.

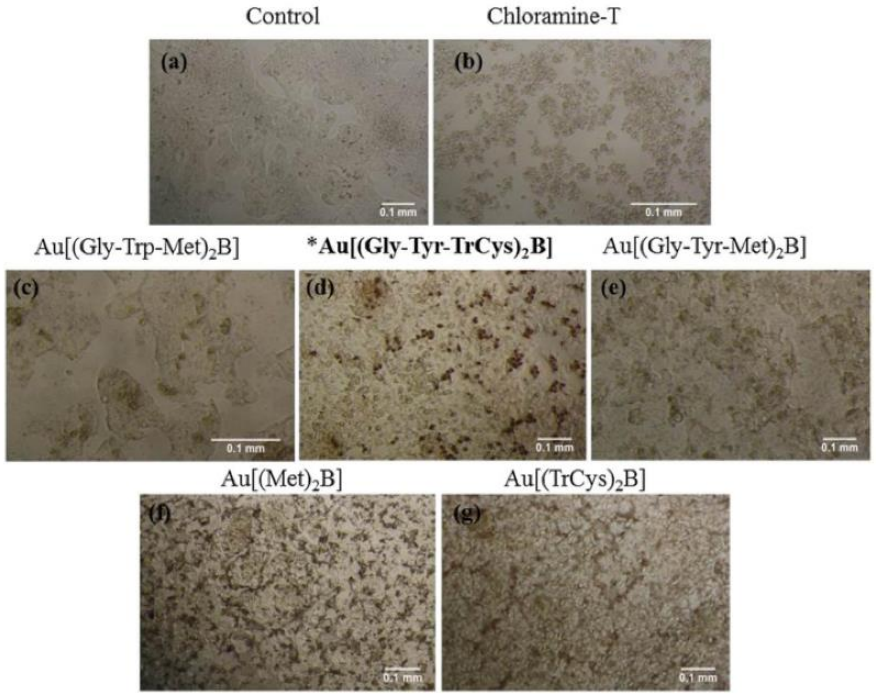

Figure 10 Optical microscope images of the morphology of Hep G2 cells. (a) untreated **(b)** after 24-h incubation with chloramine-T (positive control) and after 24-h exposure to AuNP preparations **(c)** Au[(Gly-Trp-Met)$_2$B], **(d)** Au[(Gly-Tyr-TrCys)$_2$B], **(e)** Au[(Gly-Tyr-Met)$_2$B], **(f)** Au[(Met)$_2$B] and **(g)** Au[(TrCys)$_2$B] in EMEM/S-; asterisk and bold letters are used to signal the most stable AuNP.

the medium culture had less of an effect on the AuNPs Au[(Gly-Tyr-TrCys)$_2$B]. Interestingly, sizes up to micron scale were recorded for Au[(Met)$_2$B] (1,568 nm) almost immediately upon contact with the EMEM/S- medium. UV–vis analysis of this AuNP suspension over time revealed red shifts in the SPR band, with a slight broadening, suggesting agglomeration of NPs in that medium. For Au[(Gly-Trp-Met)$_2$B], Au[(Gly-Tyr-Met)$_2$B] and Au[(Met)$_2$B], which contain methionine, a minimal decrease in the intensity band was observed over time, probably caused by the adsorption of amino acids of the culture medium. In contrast, in the UV–vis spectrum of Au[(Gly-Tyr-TrCys)$_2$B], the decrease in the intensity of SPR band was not observed, suggesting that the steric bulk and the strong interaction of (Gly-Tyr-TrCys)$_2$B with the gold prevents the adsorption of compounds from culture medium. Only after 24-h incubation, the UV–vis spectrum shows a shoulder in the range of 550 to 800 nm. It seems that the aggregation process occurs slower than in other samples. AuNP agglomeration and interaction with medium over time was also confirmed with TEM analysis.

Differences in the structure of the PBH capping agents used in this study led to distinct associations between individual AuNPs and their environment. The stability of Au[(Gly-Tyr-TrCys)$_2$B] and Au[(Gly-Tyr-Met)$_2$B] differed in cell culture conditions. This difference could be attributed to the stabilising effect of the TrCys group in comparison with the Met group. TrCys and Met residues are involved in binding to the gold surface. The higher binding of the PBH (Gly-Tyr-TrCys)$_2$B to the gold in comparison with the PBH (Gly-Tyr-Met)$_2$B is due to the additional aromatic interactions of the TrCys residue. The bulkier group, TrCys, may contribute to protecting individual NPs from assembling into larger agglomerates, thereby leading to the stability of Au[(Gly-Tyr-TrCys)$_2$B] agglomerates. In addition, as revealed by elemental analysis, Au[(Gly-Tyr-TrCys)$_2$B] was stabilised by 40 PBH units in comparison with 7 PBH units for Au[(Gly-Tyr-Met)$_2$B]. Similar considerations can be made for Au[(TrCys)$_2$B] and Au[(Met)$_2$B]. Au[(TrCys)$_2$B] was stable up to 4 h and formed smaller agglomerates over time compared to Au[(Met)$_2$B]. The stabilisation of Au[(TrCys)$_2$B] was achieved with 97 PBH units compared to 57 units for Au[(Met)$_2$B]. It appears that the TrCys group also conferred stability upon Au[(TrCys)$_2$B]. Overall, these findings suggest that the TrCys residue and the steric bulk of PBH (Gly-Tyr-TrCys)$_2$B are responsible for the remarkable stability of Au[(Gly-Tyr-TrCys)$_2$B] agglomerates.

The observations reported here have a major implication for the use of specific PBH capping agents in nanomaterial science. By applying PBH capping agents with different structures, the physico-chemical properties of AuNPs

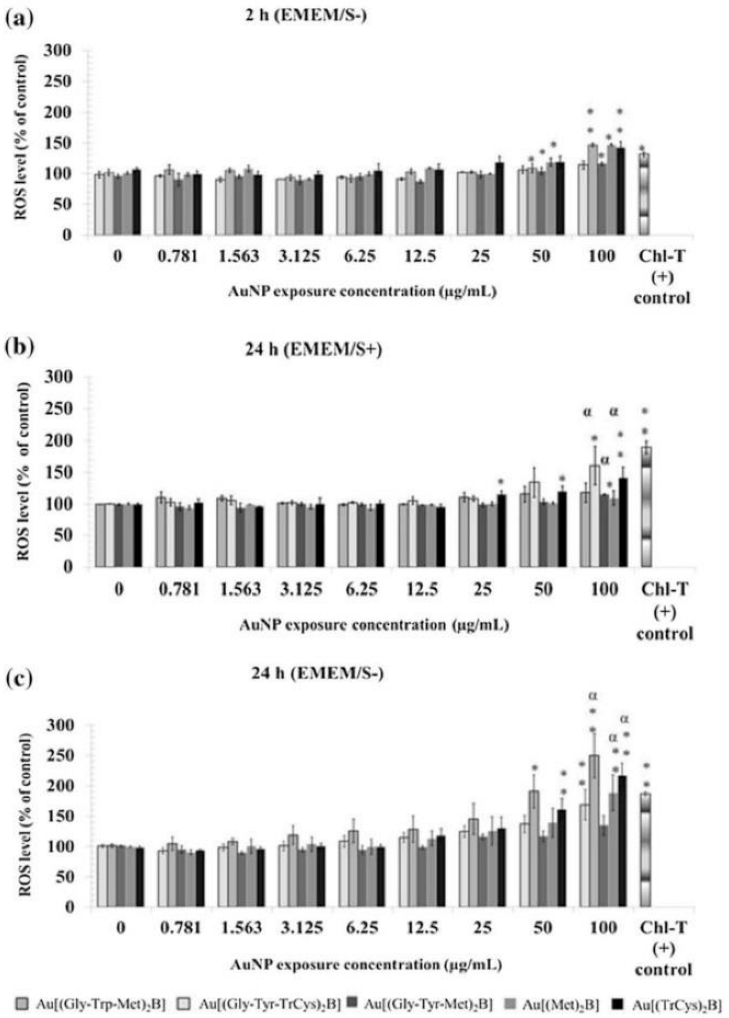

Figure 11 Comparison of oxidative stress response in Hep G2 cell line. (a) Two and **(b)** 24 h of exposure to AuNP under EMEM/S- and **(c)** after 24 h of exposure to EMEM/S+ assay conditions. Average values of three independent measurements are presented (mean ± SEM). Significant differences from control values are shown (*$P < 0.05$, **$P < 0.01$). α indicates significant differences between responses, as shown by pair-wise comparison analysis.

can be manipulated, thus affording tunability in diverse environments.

Interestingly, we observed that the two PBH-capped AuNPs that showed increased stability, namely Au[(Gly-Tyr-TrCys)$_2$B] and Au[(TrCys)$_2$B], also produced the highest increase in ROS levels. However, significant ROS production was detected only at the two highest doses (50 and 100 μg/ml), thus indicating the feasibility of use at lower concentrations. Oxidative stress induction has been proposed as the principal mechanism of toxicity for many forms of NPs [57-59], including AuNPs [60]. Although the exact biological mechanism behind the action of the AuNPs was not determined in this study, we reveal that they all have the capacity to produce increased levels of ROS. However, the extent of this production differed depending on the PBH structures attached to the AuNP and the medium environment. ROS levels twofold higher than control levels were recorded after exposure to 100 μg/ml Au[(Gly-Tyr-TrCys)$_2$B]. In contrast, exposure to the same concentration of Au[(Gly-Tyr-Met)$_2$B] elicited only a slight increase in ROS production, which was 50% higher than control levels. The presence or absence of serum also influenced the oxidative stress response to the PBH-capped AuNPs. Those that caused the highest increase in ROS levels in EMEM/S- had a significantly attenuated capacity to induce ROS in the Hep G2 cells in EMEM/S+ medium. For instance, Au[(Gly-Tyr-TrCys)$_2$B] AuNPs elicited the highest levels of ROS in EMEM/S-, and this effect was weakened in EMEM/S+, despite this NP having the same size distribution in both mediums

(±10 nm). It could therefore be assumed that the attenuated ROS induction observed for all the NPs in EMEM/S+ is not related to size but specifically to serum coating. Merhi et al. [61] showed that endocytosis decreases when NPs are exposed to increasing concentrations of fetal calf serum and bovine serum albumin.

How the AuNPs interact with the cells or whether the different PBH capping agents influence the capacity of the particles to enter cells were not addressed extensively in this study. However, some observations and remarks can be made on the basis of our results. It is known that differently charged functional groups have different associations with cells. In this study, all zeta potentials were negative due to the presence of carboxylate (COO^-) groups on the attached peptide-biphenyl coatings. Using silica NPs modified with amine and carboxyl functional groups and the murine macrophage cell line (RAW264.7), Nabeshi et al. [62] showed that while amine-functionalised silica NPs absorbed to the plasma membrane, carboxyl functionalities penetrated deeper intracellularly. This finding would suggest that these carboxyl groups bury themselves inside the cell membrane. Thus, the increased biological activity of Au[(Gly-Tyr-TrCys)$_2$B] may be explained not only by its stability, remaining in individual AuNP agglomerates of approximately 200 nm in size but also by the presence of free carboxyl groups interacting with cellular components. In addition, studies show that the aromatic structures of tyrosine residues are important regulators of NP cellular uptake (referred to as the aromatic structure hypothesis) [63]. According to these studies, the tyrosine residues in the PBH cap of Au[(Gly-Tyr-TrCys)$_2$B] NPs might enhance the cellular uptake. Using Hep G2 cells, Yuan et al. [64] demonstrated that hydroxyapatite NPs as large as 175 nm are taken up by the cells but do not penetrate the nuclear membrane and are confined to the perinuclear region. However, Johnston et al. [65], who also studied the uptake and intracellular fate of NPs in Hep G2 cells, came to the conclusion that the internalisation of 200 nm negatively charged carboxylated polystyrene NPs was limited because of size.

If the PBH-capped AuNPs are taken up, their strong affinity for GSH, together with the significant increase in ROS production, as illustrated in this study, would suggest that the AuNPs act on the same mechanism of oxidative stress as that proposed by Gao et al. [66]. These authors hypothesised that AuNP-induced oxidative stress in the HL7702 human liver cell line is related to the binding of these NPs to endogenous antioxidants (GSH), leading to complete depletion after 48 h. The increase in surface area associated with the decrease in size allows for more GSH binding and thus depletion. They also reported that the extent of oxidative stress depends on NP access to cytosolic GSH or mitochondrial GSH reserves. Hence, increased oxidative stress may occur with smaller NPs. This notion would explain the different levels of ROS production observed in this study, in particular the higher ROS levels elicited by Au[(Gly-Tyr-TrCys)$_2$B] (the AuNPs present in the smallest hydrodynamic size, as shown by DLS).

Evidence of dark assemblies in Hep G2 cells exposed to AuNP Au[(Gly-Tyr-TrCys)$_2$B] would suggest cellular interaction/internalisation; however, further studies are needed. Cells undergoing autophagy have clearly visible autophagosomes, which form around degraded cellular components. The dark assemblages present in Hep G2 cells after exposure to Au[(Gly-Tyr-TrCys)$_2$B] resemble these autophagosomes. Li et al. [67] proposed a cell survival mechanism of autophagy upon exposure to AuNPs. This mechanism has been studied further by Ma et al. [68], who showed that AuNPs that are taken up and accumulate in lysosomes induce autophagosome accumulation through the blockage of the autophagy flux. This observation supports the findings in this study for Au[(Gly-Tyr-TrCys)$_2$B]. In this case, despite the high levels of ROS produced, the cells did not succumb to the same loss in viability as that registered for the other NPs at 48 h of exposure. This phenomenon was observed only for cells exposed to the AuNP Au[(Gly-Tyr-TrCys)$_2$B], thus suggesting that the unique state of this NP in the culture medium influences the NP-cell interaction.

In fact, AuNPs eliciting the lowest increase in ROS levels after 24 h also showed the greatest loss in viability after 48 h of incubation: exposure to Au[(Gly-Trp-Met)$_2$B], Au[(Gly-Tyr-Met)$_2$B] and Au[(Met)$_2$B] reduced viability to 69%, 71% and 68%, respectively. These AuNPs all formed large agglomerates and had Met groups in their PBH-capping agents.

Several considerations need to be made when studying NP toxicity. One must be aware that NPs may interact unfavourably with assay components. The AuNPs described herein absorb at the same wavelength as those used for the MTT cytotoxicity assay (570 nm) and NRU assay (550 nm). NP interferences with commonly used toxicity assays, such as NRU and MTT, have been reported previously [69,70]. In addition, AuNP interference was also observed when carrying out the GSH/GSSG ratio assay. Care should be taken when interpreting results in order to avoid false positive results. One should also consider that the physico-chemical state of the NP under distinct assay conditions may also lead to differences in levels of interference. All of these factors must not be overlooked.

Conclusions

Here, we prepared AuNPs using several PBHs as capping agents and studied the influence of the structure of these agents on the physico-chemical state and biocompatibility of the resulting NPs. All the AuNPs tested showed excellent

dispersibility in water and form stable agglomerates under culture conditions when serum was present. One PBH-capped AuNP preparation, namely (Au[(Gly-Tyr-TrCys)$_2$B]), showed unique physico-chemical properties presenting agglomerates (approximately 200 nm) that remained in the same size distribution under cell culture conditions as when suspended in water, even in the absence of serum. Interestingly, these AuNPs elicited the highest oxidative stress response, with evidence of a unique biological interaction that did not lead to a reduction in Hep G2 cell viability after 48 h of exposure. Our findings suggest that these particular PBH-capped AuNPs exerts a distinct effect on the Hep G2 cell line that is governed by their particular conformation, which is controlled by the chemical structure of their capping agent (Gly-Tyr-TrCys)$_2$B. Given the distinct cellular morphology after exposure to these AuNPs and previous reports of AuNP mechanisms of interactions with biological systems, we propose that the Hep G2 cells undergo a cell survival mechanism of autophagy upon exposure to these AuNPs, thus supporting the notion of a cellular interaction/internalisation of these AuNPs. Given the relevance of interaction/internalisation, further research efforts should address the applicability of these AuNPs in drug delivery systems.

Additional files

Additional file 1: Synthesis of PBHs.

Additional file 2: Figure S1. 1H NMR spectrum of free PBH (Met)2B (top) in DMSO-d6 and 1H NMR spectrum of AuNP Au[(Met)2B] (bottom) in D2O.

Additional file 3: Figure S2. UV–vis absorption spectra of AuNPs **(a)** Au[(Gly-Tyr-Met)2B], (**b**) Au[(Gly-Tyr-TrCys)2B], **(c)** Au[(Gly-Trp-Met)2B], **(d)** Au[(Met)2B] and **(e)** Au[(TrCys)2B], in water and EMEM/+, each at a concentration of 100 μg/ml and a different time 0, 2, 4 and 24 h after incubation at 37°C.

Competing interests

The authors declare that they have no competing interests.

Authors' contributions

YP, BH and EM were all involved in the chemical synthesis and design of the peptide-biphenyl hybrid-capped AuNPs. YP and MC performed the physico-chemical characterization of the AuNPs. All toxicity studies were validated and performed by MC and supervised and coordinated by MLFC. MLFC and JMN were involved in the conceptual design of toxicity experiments, data analysis and interpretation and assisted in the preparation of the manuscript. MC and YP drafted the manuscript and figures. All authors read and approved the final manuscript.

Acknowledgements

This research was performed under the Environmental ChemOinformatics (ECO) Marie Curie Initial Training Network (ITN) programme, funded by the Seventh Research Framework Programme (FP7) of the European Union (238701). We also thank Mapfre research grants 2010, the Spanish Ministry of Economy and Competitiveness (MINECO project CTQ 2010–19295) and the Instituto Nacional de Investigación y Tecnología Agraria y Alimentaria (Project AT 2011–001) for financial support.

Author details

[1]Departamento de Medio Ambiente, Instituto Nacional de Investigación y Tecnología Agraria y Alimentaria (INIA), Carretera de la Coruña Km 7.5, Madrid 28040, Spain. [2]Universidad Rey Juan Carlos, Tulipán s/n, Móstoles, Madrid 28933, Spain. [3]Consejo Superior de Investigaciones Científicas (CSIC), Instituto de Química Orgánica General, Juan de la Cierva 3, Madrid 28006, Spain.

Received: 9 April 2013 Accepted: 27 June 2013
Published: 6 July 2013

References

1. Ghosh P, Han G, De M, Kim CK, Rotello VM: **Gold nanoparticles in delivery applications.** *Adv Drug Deliv Rev* 2008, **60:**1307–1315.
2. Dreaden EC, Mackey MA, Huang X, Kang B, El-Sayed MA: **Beating cancer in multiple ways using nanogold.** *Chem Soc Rev* 2011, **40:**3391–3404.
3. De Long RK, Reynolds CM, Malcolm Y, Schaeffer A, Severs T, Wanekaya A: **Functionalized gold nanoparticles for the binding, stabilization, and delivery of therapeutic DNA, RNA, and other biological macromolecules.** *Nanotechnol Sci Appl* 2010, **3:**53–63.
4. Parveen S, Misra R, Sahoo SK: **Nanoparticles: a boon to drug delivery, therapeutics, diagnostics and imaging.** *Nanomed Nanotechnol* 2012, **8:**147–166.
5. Lasagna-Reeves C, Gonzalez-Romero D, Barria MA, Olmedo I, Clos A, Sadagopa-Ramanujam VM, Urayama A, Vergara L, Kogan MJ, Soto C: **Bioaccumulation and toxicity of gold nanoparticles after repeated administration in mice.** *Biochem Bioph Res Co* 2010, **393:**649–655.
6. Gu YJ, Cheng J, Lin CC, Lam YW, Cheng SH, Wong WT: **Nuclear penetration of surface functionalized gold nanoparticles.** *Toxicol Appl Pharmacol* 2009, **237:**196–204.
7. Bai X, Ma H, Li X, Dong B, Zheng L: **Patterns of gold nanoparticles formed at the air / water interface: effects of capping agents.** *Langmuir* 2010, **26:**14970–14974.
8. Asharani PV, Lianwu Y, Gong Z, Valiyaveettil S: **Comparison of the toxicity of silver, gold and platinum nanoparticles in developing zebrafish embryos.** *Nanotoxicology* 2011, **5:**43–54.
9. Pérez Y, Mann E, Herradón B: **Preparation and characterization of gold nanoparticles capped by peptide-biphenyl hybrids.** *J Colloid Interf Sci* 2011, **359:**443–453.
10. Herradón B, Montero A, Mann E, Maestro MA: **Crystallization-induced dynamic resolution and analysis of the noncovalent interactions in the crystal packing of peptide–biphenyl hybrids.** *Cryst Eng Commun* 2004, **6:**512–521.
11. Mann E, Montero A, Maestro MA, Herradón B: **Synthesis and crystal structure of peptide-2, 2-biphenyl hybrids.** *Helv Chim Acta* 2002, **85:**3624–3638.
12. Montero A, Alonso M, Benito E, Chana A, Mann E, Navas JM, Herradón B: **Studies on aromatic compounds: inhibition of calpain I by biphenyl derivatives and peptide-biphenyl hybrids.** *Bioorg Med Chem Lett* 2004, **14:**2753–2757.
13. Bendová L, Jureka P, Hobza P, Vondrášek J: **Model of peptide bond-aromatic ring interaction: correlated *ab initio* quantum chemical study.** *J Phys Chem B* 2007, **111:**9975–9979.
14. Nishio M, Umezawa Y, Honda K, Tsuboyama S, Suezawa H: **CH/π hydrogen bonds in organic and organometallic chemistry.** *Cryst Eng Commun* 2009, **11:**1757–1788.
15. Heaton MJ, Bello P, Herradón B, Campo A, Jimenez-Barbero J: **NMR study of intramolecular interactions between aromatic groups: Van der Waals charge-transfer, or quadrupolar interactions?** *J Am Chem Soc* 1998, **120:**12371–12384.
16. Ranganathan D, Haridas V, Gilardi R, Karle IL: **Self-assembling aromatic-bridged serine-based cyclodepsipeptides (serinophanes): a demonstration of tubular structures formed through aromatic π – π interactions.** *J Am Chem Soc* 1998, **120:**10793–10800.
17. Mann E, Rebek JJ: **Deepened chiral cavitands.** *Tetrahedron* 2008, **64:**8484–8487.
18. Lévy R, Thanh NT, Doty RC, Hussain I, Nichols RJ, Schiffrin DJ, Brust M, Fernig DG: **Rational and combinatorial design of peptide capping ligands for gold nanoparticles.** *J Am Chem Soc* 2004, **126:**10076–10084.
19. Jiang J, Oberdörster G, Biswas P: **Characterization of size, surface charge, and agglomeration state of nanoparticle dispersions for toxicological studies.** *J Nanopart Res* 2009, **11:**77–89.
20. Warheit DB: **How meaningful are the results of nanotoxicity studies in the absence of adequate material characterization?** *Toxicol Sci* 2008, **101:**183–185.
21. Nel A, Xia T, Mädler L, Li N: **Toxic potential of materials at the nano level.** *Science* 2006, **311:**622–627.

22. Studer AM, Limbach LK, Duc LV, Krumeich F, Athanassiou EK, Gerber LC, Moch H, Stark WJ: **Nanoparticle cytotoxicity depends on intracellular solubility: comparison of stabilized copper metal and degradable copper oxide nanoparticles.** *Toxicol Lett* 2010, **197**:169–174.
23. Auffan M, Rose J, Wiesner MR, Bottero JY: **Chemical stability of metallic nanoparticles: a parameter controlling their potential cellular toxicity *in vitro*.** *Environ Pollut* 2009, **157**:1127–1133.
24. Pan Y, Neuss S, Leifert A, Fischler M, Wen F, Simon U, Schmid G, Brandau W, Jahnen-Dechent W: **Size-dependent cytotoxicity of gold nanoparticles.** *Small* 2007, **3**:1941–1949.
25. Li Y, Sun L, Jin M, Du Z, Liu X, Guo C, Li Y, Huang P, Sun Z: **Size-dependent cytotoxicity of amorphous silica nanoparticles in human hepatoma HepG2 cells.** *Toxicol In Vitro* 2011, **25**:1343–1352.
26. Liu Y, Meyer-Zaika W, Franzka F, Schmid G, Tsoli M, Kuhn H: **Gold-cluster degradation by the transition of B-DNA into A-DNA and the formation of nanowires.** *Angew Chem Int Ed* 2003, **42**:2853–2857.
27. Tsoli M, Kuhn H, Brandau W, Esche H, Schmid G: **Cellular uptake and toxicity of Au55 clusters.** *Small* 2005, **1**:841–844.
28. Pan Y, Leifert A, Ruau D, Neuss S, Bornemann J, Schmid G, Brandau W, Simon U, Jahnen-Dechent W: **Gold nanoparticles of diameter 1.4 nm trigger necrosis by oxidative stress and mitochondrial damage.** *Small* 2009, **5**:2067–2076.
29. Li T, Albee B, Alemayehu M, Diaz R, Ingham L, Kamal S, Rodriguez M, Bishnoi SW: **Comparative toxicity study of Ag, Au, and Ag–Au bimetallic nanoparticles on *Daphnia magna*.** *Anal Bioanal Chem* 2010, **398**:689–700.
30. Farkas J, Christian P, Urrea JAG, Roos N, Hassellöv M, Tollefsen KE, Thomas KV: **Effects of silver and gold nanoparticles on rainbow trout (*Oncorhynchus mykiss*) hepatocytes.** *Aquat Toxicol* 2010, **96**:44–52.
31. Patra HK, Banerjee S, Chaudhuri U, Lahiri P, Dasgupta AK: **Cell selective response to gold nanoparticles.** *Nanomed Nanotechnol* 2007, **3**:111–119.
32. Ponti J, Colognato R, Franchini F, Gioria S, Simonelli F, Abbas K, Uboldi C, Kirkpatrick CJ, Holzwarth U, Rossi F: **A quantitative *in vitro* approach to study the intracellular fate of gold nanoparticles: from synthesis to cytotoxicity.** *Nanotoxicology* 2009, **3**:296–306.
33. Li JJ, Lo SL, Ng CT, Gurung LR, Hartono D, Hande PM, Ong CN, Bay BH, Yung LLY: **Genomic instability of gold nanoparticle treated human lung fibroblast cells.** *Biomaterials* 2011, **32**:5515–5523.
34. Hirn S, Semmler-Behnke M, Schleh C, Wenk A, Lipka J, Schäffler M, Takenaka S, Möller W, Schmid G, Simon U, Kreyling WG: **Particle size-dependent and surface charge-dependent biodistribution of gold nanoparticles after intravenous administration.** *Eur J Pharm Biopharm* 2011, **77**:407–416.
35. Wang L, Li YF, Zhou L, Liu Y, Meng L, Zhang K, Wu X, Zhang L, Li B, Chen C: **Characterization of gold nanorods *in vivo* by integrated analytical techniques: their uptake, retention, and chemical forms.** *Anal Bioanal Chem* 2010, **396**:1105–1114.
36. Kroll A, Pillukat MH, Hahn D, Schnekenburger J: **Current *in vitro* methods in nanoparticle risk assessment: limitations and challenges.** *Eur J Pharm Biopharm* 2009, **72**:370–377.
37. Kang KA, Wang J, Jasinski JB, Achilefu S: **Fluorescence manipulation by gold nanoparticles: from complete quenching to extensive enhancement.** *J Nanobiotechnology* 2011, **9**:1–13.
38. Stobiecka M, Coopersmith K, Hepel M: **Resonance elastic light scattering (RELS) spectroscopy of fast non-Langmuirian ligand-exchange in glutathione-induced gold nanoparticle assembly.** *J Colloid Interface Sci* 2010, **350**:168–177.
39. Jadzinsky PD, Calero G, Ackerson CJ, Bushnell DA, Kornberg RD: **Structure of a thiol monolayer-protected gold nanoparticle at 1.1 Å resolution.** *Science* 2007, **318**:430–433.
40. Cho CE, Zhang Q, Xia Y: **The effect of sedimentation and diffusion on cellular uptake of gold nanoparticles.** *Nat Nanotechnol* 2011, **6**:385–391.
41. Mosmann T: **Rapid colorimetric assay for cellular growth and survival: application to proliferation and cytotoxicity assays.** *J Immunol Methods* 1983, **65**:55–63.
42. Borenfreund E, Puerner JA: **Toxicity determined *in vitro* by morphological alterations and neutral red absorption.** *Toxicol Lett* 1985, **24**:119–124.
43. O'Brien J, Wilson I, Orton T, Pognan F: **Investigation of the alamar blue (resazurin) fluorescent dye for the assessment of mammalian cell cytotoxicity.** *Eur J Biochem* 2000, **267**:5421–5426.
44. Wang H, Joseph AJ: **Quantifying cellular oxidative stress by dichlorofluorescein assay using microplate reader.** *Free Radical Bio Med* 1999, **27**:612–616.
45. Allen S, Shea JM, Felmet T, Gadra J, Dehn PF: **A kinetic microassay for glutathione in cells plated on 96-well microtiter plates.** *Methods Cell Sci* 2001, **22**:305–312.
46. Krpetic Z, Nativo P, Porta F, Brust M: **A multidentate peptide for stabilization and facile bioconjugation of gold nanoparticles.** *Bioconjug Chem* 2009, **20**:619–624.
47. Liu X, Atwater M, Wang J, Huo Q: **Extinction coefficient of gold nanoparticles with different sizes and different capping ligands.** *Colloids Surf B* 2007, **58**:3–7.
48. Si S, Dinda E, Mandal TK: ***In situ* synthesis of gold and silver nanoparticles by using redox-active amphiphiles and their phase transfer to organic solvents.** *Chem Eur J* 2007, **13**:9850–9861.
49. Lyon JL, Fleming DA, Stone MB, Schiffer P, Williams ME: **Synthesis of Fe oxide core/Au shell nanoparticles by iterative hydroxylamine seeding.** *Nano Lett* 2004, **4**:719–723.
50. Murphy CJ, Gole AM, Hunyadi SE, Stone JW, Sisco PN, Alkilany A, Kinard BE, Hankins P: **Chemical sensing and imaging with metallic nanorods.** *Chem Commun* 2008, **5**:544–557.
51. Zhang XD, Wu D, Shen X, Liu PX, Fan FY, Fan SJ: ***In vivo* renal clearance, biodistribution, toxicity of gold nanoclusters.** *Biomaterials* 2012, **33**:4628–4638.
52. Lynch I, Cedervall T, Lundqvist M, Cabaleiro-Lago C, Linse S, Dawson KA: **The nanoparticle–protein complex as a biological entity; a complex fluids and surface science challenge for the 21st century.** *Adv Colloid Interface Sci* 2007, **134–135**:167–174.
53. Alkilany AM, Murphy C: **Toxicity and cellular uptake of gold nanoparticles: what we have learned so far?** *J Nanopart Res* 2010, **12**:2313–2333.
54. Zhu Y, Li W, Li Q, Li Y, Li Y, Zhang X, Huang Q: **Effects of serum proteins on intracellular uptake and cytotoxicity of carbon nanoparticles.** *Carbon* 2009, **47**:1351–1358.
55. Allouni ZE, Cimpan MR, Høl PJ, Skodvin T, Gjerdet NR: **Agglomeration and sedimentation of TiO_2 nanoparticles in cell culture medium.** *Colloids Surf B Biointerfaces* 2009, **68**:83–87.
56. Ehrenberg MS, Friedman AE, Finkelstein JN, Oberdörster G, McGrath JL: **The influence of protein adsorption on nanoparticle association with cultured endothelial cells.** *Biomaterials* 2009, **30**:603–610.
57. Møller P, Jacobsen NR, Folkmann KJ, Danielsen HP, Mikkelsen L, Hemmingsen GJ, Vesterdal KL, Forchhammer L, Wallin H, Loft S: **Role of oxidative damage in toxicity of particulates.** *Free Radical Res* 2010, **44**:1–46.
58. Choi EJ, Kima S, Ahna HJ, Youna P, Kangb SJ, Park K, Yid J, Ryua DY: **Induction of oxidative stress and apoptosis by silver nanoparticles in the liver of adult zebrafish.** *Aquat Toxicol* 2010, **100**:151–159.
59. Stone V, Shaw J, Brown MD, Macnee W, Faux PS, Donaldson K: **The role of oxidative stress in the prolonged inhibitory effect of ultrafine carbon black on epithelial cell function.** *Toxicol In Vitro* 1998, **12**:649–659.
60. Tedesco S, Doyle H, Blasco J, Redmond G, Sheehan D: **Exposure of the blue mussel, *Mytilus edulis*, to gold nanoparticles and the pro-oxidant menadione.** *Comp Biochem Physiol C* 2010, **151**:167–174.
61. Merhi M, Dombu CY, Brient A, Chang J, Platel A, Le Curieux F, Marzin D, Nesslany F, Betbeder D: **Study of serum interaction with a cationic nanoparticle: implications for *in vitro* endocytosis, cytotoxicity and genotoxicity.** *Int J Pharmaceut* 2012, **423**:37–44.
62. Nabeshi H, Yoshikawa T, Arimori A, Yoshida T, Tochigi S, Hirai T, Akase T, Nagano K, Abe Y, Kamada H, Tsunoda SI, Itoh N, Yoshioka Y, Tsutsumi Y: **Effect of surface properties of silica nanoparticles on their cytotoxicity and cellular distribution in murine macrophages.** *Nanoscale Res Lett* 2011, **6**:1–6.
63. Yang Y, Fung SY, Liu M: **Programming the cellular uptake of physiologically stable peptide-gold nanoparticles hybrids with single amino acids.** *Angew Chem Int Ed* 2011, **50**:9643–9643.
64. Yuan Y, Liu C, Qian J, Wang J, Zhang Y: **Size-mediated cytotoxicity and apoptosis of hydroxyapatite nanoparticles in human hepatoma HepG2 cells.** *Biomaterials* 2010, **31**:730–740.
65. Johnston JH, Semmler-Behnke M, Brown MB, Kreyling W: **Evaluating the uptake and intracellular fate of polystyrene nanoparticles by primary and hepatocyte cell lines *in vitro*.** *Toxicol Appl Pharmacol* 2010, **242**:66–78.
66. Gao W, Xu K, Ji L, Tang B: **Effect of gold nanoparticles on glutathione depletion-induced hydrogen peroxide generation and apoptosis in HL7702 cells.** *Toxicol Lett* 2011, **205**:86–95.
67. Li JJ, Hartono D, Ong CN, Bay BH, Yung LLY: **Autophagy and oxidative stress associated with gold nanoparticles.** *Biomaterials* 2010, **31**:5996–6003.

68. Ma X, Wu Y, Jin S, Tian Y, Zhang X, Zhao Y, Yu L, Liang XJ: **Gold nanoparticles induce autophagosome accumulation through size-dependent nanoparticle uptake and lysosome impairment.** *ACS Nano* 2011, **5**:8629–8639.
69. Belyanskaya L, Manser P, Spohn P, Bruinink A, Wick P: **The reliability and limits of the MTT reduction assay for carbon nanotubes–cell interaction.** *Carbon* 2007, **45**:2643–2648.
70. Ciofani G, Danti S, D'Alessandro D, Moscato S, Menciassi A: **Assessing cytotoxicity of boron nitride nanotubes: interference with the MTT assay.** *Biochem Biophys Res Commun* 2010, **394**:405–411.

doi:10.1186/1556-276X-8-315
Cite this article as: Connolly *et al.*: Peptide-biphenyl hybrid-capped AuNPs: stability and biocompatibility under cell culture conditions. *Nanoscale Research Letters* 2013 **8**:315.

CHAPTER 8

FINDINGS AND GENERAL DISCUSSION

8.1 Toxicity of metal NPs (ZnO, Cu, Ag, and Au) to liver cells

Research presented as part of this thesis sought to assess the hazard associated with metal NP (Ag, Cu, Au, ZnO) exposure to liver cells, using available cell lines. Effects observed in cell lines could be used to infer information on possible effects that could take place in the liver. Taking into account IC_{50} values ZnO ENMs represent an increased hazard (IC_{50} 15.2-26.6 µg/mL) compared to Cu ENMs (IC_{50} 39-55 µg/mL) towards mammalian liver cells (HepG2 cell line) according to a number of assay systems employed and different sized nanoparticle preparations tested. On the other hand, Au ENMs appear rather biocompatible (*research paper 4*).

From an environmental perspective, when using fish liver cells, the group of metal ENMs tested are ranked Ag>ZnO>Cu ENMs in toxicity according to recorded IC_{50} values. The lowest IC_{50} value (10.7 µg/mL) corresponded to the rainbow trout liver cell line, RTL-W1, following 24 h exposure to Ag ENMs. In comparison IC_{50} values of 14.1 and 55 µg/mL were observed following ZnO NP and CuNP exposure, respectively, in the topminnow liver cell line (PLHC-1). All IC_{50} values recorded fall into the toxicity ranking as harmful and moderately toxic (10-100 µg/mL) with Ag ENMs bordering as toxic (1-10 µg/mL) according to classification scheme outlined in the CLP legislation for aquatic species (Regulation (EC) No 1272/2008[29]).

Comparative studies that were performed to investigate any differences in susceptibility to cytotoxic effects of NPs between mammalian and fish liver cells revealed that mammalian liver cells are more sensitive to toxic effects of ENMs (Cu and ZnO ENMs). Mammalian cells are also more sensitive to ionic forms of these metals and thus the role played by differences in tolerances to ions (either released from NPs in the medium environment or intracellularly) may be a key factor in dictating these species specific differences in susceptibility to ENMs and their hazard potential.

In the *introductory paper 3* we have highlighted how the combined effect of such metal ENMs as ZnO and Cu, which have been found simultaneously in the environment, may represent an even greater hazard than each individual ENM alone. A potentiating effect was seen in co-

[29] CLP legislation (REGULATION (EC) No 1272/2008 of the European Parliament and of the council of 16 December 2008 on classification, labelling and packaging of substances and mixtures, amending and repealing Directives 67/548/EEC and 1999/45/EC, and amending Regulation (EC) No 1907/2006).

exposure studies when liver cells were challenged with ZnO ENMs, at non-cytotoxic concentrations, together with Cu ENMs. IC_{50} values decreased from 13 µg/mL, following exposure to Cu ENMs alone, to values as low as 4 µg/mL when cells were co-exposed with ZnO ENMs. Investigating such effects is especially important in the case of ENMs made of metals due to the complex interdependencies of metal regulation in the cell. In this case, heightened toxicity is seen. However other studies comparing the dual cytotoxicity of ZnO and TiO_2 ENMs (commonly found in sunscreens) reveal a protective effect whereby TiO_2 appears to absorb any free Zn^{2+} ions thus reducing their bioavailability (Kathawala et al. 2015). Studies like these highlight the potential hazard associated with exposure to more than one nanoparticle at a time and this is an area which remains largely unexplored.

In vivo exposures (*research paper 3*) incorporated into this research confirmed the relevance of toxicological data obtained from *in vitro* studies to responses *in vivo* and highlighted the liver as a relevant target site for hazards associated with ENM exposure in the environment. Exposures were performed using fish (rainbow trout) and feed spiked with ZnO ENMs. Elevated levels of Zn as well as biochemical disturbances associated with oxidative stress (increased GST activity, decreased ratio of GSH/GSSG) were measured in the livers of fish administered high concentrations of ZnO ENMs. This together with the lack of complete assimilation and elimination from the intestine may point to distinct hazards associated with ZnO ENM exposure *in vivo* in fish (the role of oxidative stress in the mechanism of toxicity of ENMs is discussed in section 8.5.3). Studies have only been performed with ZnO ENMs, with Zn being in general well tolerated by fish. Future studies using different metal ENMs such as AgNPs that have the highest hazard potential according to *in vitro* studies may reveal an increased risk following exposure to this type of ENM.

8.2 Particle properties influencing effects -Is there evidence of a nano-specific effect?

In metal ENM hazard assessment, one of the key questions is do metal-based nanoparticles exert higher toxicity when compared to water-soluble metal compounds or microscale particles of the same metal content? The large surface area to volume ratio that ENMs have facilitates dynamic interactions and often heightened reactivity/activity (quantum confinement). Whether this causes heightened hazard once ENMs are within the cellular environment therefore must be investigated. Also while most metals in their bulk form are poorly soluble, at nanoscale there may be deviations from the classical thermodynamic principles. With decreasing size particles are presumed to exhibit increased dissolution according to the Ostwald-Freundlich equation. This may lead to a significant contribution from dissolved ions to observed effects following ENM exposure.

In the presented studies we have included either a metal salt (soluble ion) or bulk material (all dimensions > 100 nm) preparation in order to compare and contrast toxicological effects. For each of the metal ENMs studied we will discuss findings in relation to nanoparticle-specific effects and the contribution of dissolved ion to any cytotoxicity observed. We have also taken into consideration that it could also be the case that effects are nanoparticle facilitated and ion

mediated, in a sense that the nanoparticles are taken up and subsequently dissolution takes place intracellularly exposing cells to high concentrations of intracellular ions.

8.2.1 CuNPs

Evidence from the here presented studies have shown that Cu exposed to liver cells in nanoparticle suspensions (particles and ions) can exert higher toxicity than equal concentrations of the soluble dissolved copper nitrate salt, $Cu(NO_3)_2$ (*introductory paper 2*). This has also been reported in lung epithelial cells (Karlsson et al. 2008), intestinal cells (Piret et al. 2012) and liver cells by other authors (Cuillel et al. 2014). In fact very similar dose response relationship can be seen in our study and that presented by Karlsson et al. (2008) and Cuillel et al. (2014). IC_{50} values are being approached following exposure to 20 µg Cu/mL in Cu(CuO)NP suspensions while concentrations > 40 µg Cu/mL are needed to reach the same level of loss in viability following exposure to soluble forms of copper salts. The observed cytotoxicity of CuNP suspensions is assumed to be due to the combined effect of the particulate fraction present in the suspensions (NP (particle)) and of the ionic fraction (dissolved Cu^{2+} ions released from the particles) (NP(ion)). Therefore, the solubility of the particles, and their ability to release ions (a process which in turn may lead to modifications in particle physico-chemical properties (e.g. size or stability)) is one essential property that must be taken into account.

In fact we have used a response addition model in introductory paper 2 to estimate the cytotoxic contribution of particle forms and Cu^{2+} in CuNP suspensions. We have found that CuNP forms highly contributed to the toxicity in all cell lines, with much lower IC_{50} values calculated for particle forms than for Cu^{2+} ions. In the *research paper 1* we have investigated further the relative contribution of released Cu^{2+} ions to CuNP toxicity using a CuNP with high dissolution (CuNP 25) and another one with low dissolution (CuNP 78). For the CuNP with high dissolution the concentration of extracellularly dissolved ions was high enough (51.2 µg/ml) to significantly contribute to cytotoxicity. However, in contrast, for the CuNP with low dissolution, copper ion concentrations (6.6 µg/mL) were not high enough to produce cytotoxic effects. Therefore in this case, the nanoparticulate fraction must have an important contribution to the toxicity seen.

To explain such nanoparticle-specific effects one could consider the different cellular uptake and processing mechanisms for ions and particles that may exist. Some studies are emerging looking at subcellular localisations to determine possible differences in processing mechanisms (Fan et al. 2013). In our studies TEM micrographs point to membrane invagination and large aggregates of copper particles in vesicles following exposure to CuNPs which would suggest an endocytotic uptake route and storage of copper in particulate form in intracellular "pools". Thus, copper presented to cells in particulate form may lead to the presence of higher concentrations of copper in the cell than if presented in the form of Cu^{2+}. Uptake, transport, storage and excretion of Cu^{2+} is tightly regulated in cells (Lalioti et al. 2009). Copper (Cu^{2+}) is usually taken up into hepatocytes across the plasma membrane by Ctr protein family members (membrane protein CTR1) (Lee et al. 2002). Once inside the hepatocyte, copper can complex with glutathione (Freedman and Peisach 1989) and copper chaperones such as Atox1 transfer copper to the trans-Golgi network where ATP7B, a Cu-transporting ATPase transports copper for incorporation into ceruloplasmin and absorption into the bloodstream. Excess copper is transported for biliary

excretion into faeces (Bartee and Lutsenko 2007). The cysteine-rich intracellular metallothionein proteins also serve as copper scavengers in hepatocytes and metalochaperones responsible for intracellular copper transfer. The copper ion is almost always associated with biomolecules and proteins and not present free in the cytoplasm. Whether copper nanoparticle uptake and processing (intracellular trafficking) follows the same mechanism as ions and is afforded with such tight regulation is yet to be elucidated. A 75% increase in copper concentration when exposed to cells in nanoparticle form as opposed to in ionic form has been reported (Cuillel et al. 2014). Also toxigenomic analysis points to distinct gene expression profiles following exposure to CuONPs at the molecular level compared to responses from extracellularly released ions in the lung epithelial A549 cell (Hanagata et al. 2011).

Once inside these vesicles CuNPs may remain in particle form or dissolve and thus the cells can be presented with high concentrations of both particulate and ionic copper. The role played by Cu^{2+} ions following CuNP uptake and possible intracellular dissolution has yet to be elucidated. Researchers have used cell permeable Cu chelators (desferoxamine and D–penicillamine) to investigate if intracellular Cu^{2+} was involved in toxic mechanism. Failure of chelation to mitigate cytotoxicity led researchers to conclude that the biological effect of CuO is not mediated by Cu^{2+} release either extracellularily or intracellularily (Fahmy et al. 2009). Minocha and Mumper (2012) evidenced that even CuNPs protected from oxidation by carbon coating caused the same level of toxicity as CuNPs, corroborating the idea of minimal contribution of the ionic fraction to toxicity. All these data corroborate our observations that both ions and particles contribute independently to the toxicity with a major role played by the particle fraction.

We then addressed if specific effects exist for particles in nanometer size when compared to micron-sized particles. Interestingly larger micron-sized Cu particles, caused similar and in some cases heightened toxicity in cell lines compared to CuNP preparations. However physico-chemical characterisation revealed that these particles were present with mean diameter of between 200-600 nm but they transformed under culture conditions leading to cells being exposed to a homogenous distribution of 35 nm nanoparticles of Cu. Therefore it did not represent a true comparison. But it did demonstrate that micron-sized particles can be broken down to smaller particles (be transformed) in different environments and highlights the importance of physico-chemical characterisation under exposure conditions. This is consistent with observations made following exposures of the same preparations to zebrafish embryos (Hua et al. 2014). In both cases transmission electron micrographs reveal large submicron sized particles that appear to be composed of collections of smaller particles according to the propagating edges. Exposure to these micron-sized particle preparations that transformed under culture conditions resulted in the highest cytotoxicity in all cell lines tested showing that even micron sized particles that are susceptible to degradation under specific conditions may act as a source of nanomaterials. It is worth noting that studies performed with stable micron sized preparations have indeed shown that micron-sized Cu based particles are far less toxic to cells compared to nanoforms, supporting size dependent toxicity (Karlsson et al. 2008, Semisch et al. 2014). Also *in vivo* studies have shown that the LD_{50} following exposure in rats was 413 vs > 5000 mg/kg body weight for CuNPs and micron-sized Cu particles respectively (Chen et al. 2006).

Collectively evidence from the research presented supports specific nanoparticulate toxicity associated with CuNP exposure that cannot solely be ascribed to extracellularly released Cu^{2+} ions.

8.2.2 ZnO NPs

In studies assessing the cytotoxicity of ZnO NPs (*introductory paper 1*) we have not included a soluble source of Zn^{2+} (eg. $ZnCl_2$ or $ZnSO_4$) for comparison but instead we have exposed cells to the fractions of dissolved Zn released from ZnO NP preparations during 24 h in cell culture medium. While this was predominantly done to assess the contribution of ions to cytotoxicity (discussed in more detail in section 8.5.1) it allowed us to compare and contrast dose responses to the same mass concentration of Zn in suspension (particle and ion) and the dissolved (ion) form. It is interesting to point out that the fraction of dissolved Zn in cell culture medium ranged from 5.3-30.96% depending on the medium and exposure conditions used (influence of medium composition is discussed further in section 8.3).

According to results, significant reductions in viability were seen at similar mass concentrations of Zn when PLHC-1 cells were exposed to ZnO NP suspensions or dissolved fractions ($\geq$ 9 µg Zn/mL vs $\geq$10 µg Zn/mL respectively). In the case of HepG2 cells the dissolved fraction produced a reduction at lower concentrations (6 µg Zn/mL) with ZnO NP suspensions producing significant reduction in viability between 12-18 µg Zn/mL. However we must point out that this may be related with this mammalian cell lines increased susceptibility to metal ions (discussed in detail in section 8.4). Therefore in general at the same mass Zn concentration both ZnO particle suspensions and dissolved fractions cause similar cytotoxicity.

Similar sensitivity distributions to ZnO nanoparticles and Zn^{2+} have also been reported for a range of aquatic species (Adam et al. 2015). In fact Bondarenko and colleagues have described responses to ZnO NPs and Zn^{2+} ions in different organisms as well as mammalian cells *in vitro* as "stunningly similar" with L(E)C50 of particle exposures correlating well with Zn^{2+} exposures (R^2= 0.85) (Bondarenko et al. 2013). This correlation may lead one to hypothesise that the cytotoxicity of ZnO NP suspensions is related with the dissolved Zn ion. In fact it is the general consensus that toxic effects of ZnO NPs are due to their solubility (Deng et al. 2009). Taking the amount of Zn measured in dissolved fractions obtained from 100 µg/mL ZnO NP suspensions as the solubility of ZnO NPs in the different medium environments, a 9 µg/mL dose of ZnO NPs in EMEM could potentially represent up to 7.7 µg/mL Zn^{2+} and in the case of α-MEM ZnO NPs may be completely dissolved (solubility between 28.3-43.3 µg/mL). As such high concentrations themselves are cytotoxic, the extracellular concentration of dissolved Zn^{2+} may be solely responsible for cytotoxic effects. In fact iron doping has been used to slow the dissolution process and has been shown to reduce the cytotoxicity of ZnO NPs in epithelial and macrophage cell lines (George et al. 2010).

However if the predominant factor driving ZnO NP suspension cytotoxicity in our studies was extracellular dissolution one would expect much higher levels of cytotoxicity to be seen in the PLHC cell line due to the high dissolution levels in α-MEM. Similarly less cytotoxicity should be evidenced in the HepG2 cell line cultured in a medium environment producing lower dissolution rates. The fact that such a distinction was not evidenced, and that both cell lines

showed similar levels of susceptibility to ZnO NP suspensions, may question the role of the extracellular dissolved ion. There is also the possibility of re-precipitation of insoluble ZnO particulates from dissolved Zn^{2+} above a saturation equilibrium in the medium environment. In fact according to DLS analysis of dissolved fractions (assumed to consist of solely Zn^{2+}) there was a particle population present (30-100 nm) most evidently in α-MEM. Therefore the high concentration of Zn present in α-MEM may not have been in free form (Zn^{2+}) but complexed to organic ligands in the media or as precipitates. The formation of insoluble precipitates of either zinc hydrocarbonate (hydrozincite) or zinc phosphate hydrate (hopeite) (30-60 nm in size) when solutions of ZnO NPs or zinc ions are present in culture medium has been witnessed (Reed et al. 2012, Turney et al. 2012).Thus dissolved fractions may also contain insoluble precipitates in the nanometer range that themselves may contribute to cytotoxicity or render Zn^{2+} less bioavailable. This phenomena also makes it difficult to distinguish dissolved ion effects from nanoparticle-specific effects.

There is also evidence to point to nanoparticle-specific effects besides direct comparative studies showing that ZnO NP suspensions have higher cytotoxic effects in a range of mammalian cell types (monocytes, epithelial cells, and lymphoblasts) compared to the same mass concentration of $ZnCl_2$ (Zhang et al. 2014). For example in the *introductory paper 3* we have also evidenced nanoparticle-specific potentiating effects (ZnO NP altering the homeostasis of Cu) in liver cells. Interestingly the same phenomenon was seen in *in vivo* exposures with fish when exposure to $ZnCl_2$ had little effect on Cu liver levels while exposure to ZnO NPs or ZnO NPs and $ZnCl_2$ decreased levels (Amara et al. 2014). To consolidate a nanoparticle-specific effect Moos and colleagues have also demonstrated that direct cell contact with ZnO NPs is required to cause toxicity in RKO colon cancer cells by using a transwell system (Moos et al. 2010). Studies using the water flea *Daphnia magna* incorporating response addition models similar to those we have applied for CuNP exposures (*introductory paper 2*) point to particles dominating effects (Hua et al. 2014).

One must also consider that nanoparticles, if taken up, may be susceptible to intracellular dissolution. How cells deal with ions in their surrounding environment and when internalised will be different. Wang et al. (2014) has proposed that ZnO cytotoxicity is related with the cellular uptake, and subsequent release of large amounts of Zn^{2+} in the cytoplasm and within the low pH environment of lysosomes (for macrophages). We have witnessed large aggregates of ZnO NPs in HepG2 cells exposed to 6.25 μg/mL suspensions of ZnO NPs (19 nm in primary particle size) (*introductory paper 3*) confirming that ZnO NPs are taken up in particulate form and remain present following the 24 h exposure period. The level of ZnO NP intracellular dissolution and the extent to which this may contribute to cytotoxicity was not elucidated. In a similar fashion to copper, zinc bioavailability is thought to be regulated by metalothionein sequestering the metal and preventing absorption, while transport of zinc between the cytosol and vesicles is thought to involve certain zinc transporters. Also vesicular storage sites of zinc in mammalian cells have been identified in cells (zincosomes) that are thought to play a role in zinc redistribution and maintaining zinc homeostasis by accumulating labile zinc (Zalewski et al. 1993, Coyle et al. 1994). If ZnO NPs are conferred with such tight regulation is yet to be confirmed.

As well as the similar levels of cytotoxicity seen for ZnO NP suspensions and dissolved fractions, similar levels of cytotoxicity were also seen for the ZnO NPs and the bulk material (IC50 16.7 vs 16.3 µg/mL). However according to physico-chemical analysis the micron-sized ZnO particles consisted of particles 135 nm in length and therefore they did not act as the most appropriate micron-sized particle for comparative purposes. In spite of this, comparative studies using 70 nm and 420 nm ZnO particles in A549 lung cells showed similar dose response curves (EC50 13.6 vs 14.2 µg/mL) (Lin et al. 2009). Also other authors (Xiong et al. 2011) have reported similar toxicity profiles for ZnO in nano form and bulk corroborating our findings.

The solubility of ZnO NPs and formation of Zn^{2+} appears to play a major role in the cytotoxicity of ZnO NPs. Responses to ZnO NP exposure will be influenced by differences in susceptibility to Zn^{2+}. Also the lack of size dependent influence (difference between nanoparticle and micron-sized particles) supports the predominant role of extracellular dissolution and contribution of Zn^{2+} to cytotoxicity. However we must point out that the presence of particles leads to the potentiation of CuNP cytotoxicity.

8.2.3 AgNPs

Silver in its ionic form is one of the most toxic heavy metals, and whether particle-specific effects exist remains ambiguous (Lubick et al. 2008). *Research paper 2* compares the response of liver cells to the $AgNO_3$ salt, which acted as a source of Ag^+, and AgNPs. In general cytotoxic effects were observed at lower concentrations for the $AgNO_3$ cell exposures than following AgNP cell exposures, which indicated that at respective concentrations of nanoparticle and silver ions, ions are more toxic. IC50 values following exposure to AgNPs were in general higher ranging from 19.8-45 µg/mL according to the specific cell line and toxicity assay endpoint used, compared to 0.4-3.8 µg/mL following exposure to $AgNO_3$. Similar trends have been reported using HepG2 mammalian liver cells with $AgNO_3$ being 100 fold more cytotoxic (IC_{50} 50 µg/mL vs 0.5 µg/mL) (Vrček et al. 2014). In this study AgNP suspensions did not show any dissolution and in fact the intracellular concentration of Ag was the same following exposure to $AgNO_3$ and AgNPs.

Therefore the difference in cytotoxicity may be related to distinct ways in which the cells handle Ag ions and AgNPs. Miyayama and colleagues have shown in bronchial epithelial cells that Ag ions are sequestered by metallothioneins as early as 3 h after treatment and the mechanism of cytotoxicity is associated with Ag ions inhibiting the electron chain transfer of mitochondrial complexes as the concentration of Ag-MT decreases (Miyayama et al. 2014). Similarly Arai and colleagues have shown that the amount of Ag-bound MTs increased in J774.1 macrophage-like cells following exposure to $AgNO_3$ however there was no evidence of Ag bound metallothionein following exposure to AgNPs. Instead large aggregates of AgNPs were found in lysosomes (Arai et al. 2014). AgNPs have been shown to disrupt mitochondrial function by interacting with the cysteine residue of NADH dehydrogenase (Teodoro et al. 2011) (mitochondria as a possible target site is discussed further in section 8.5.2).

In *research paper 2* a physico-chemical characterisation confirmed that the AgNPs tested were present in nanoparticulate form with 95% of particles with an average hydrodynamic diameter of 7 nm and the dispersion was stable over the entire exposure period (24 h). Use of a dispersant assured a stable and homogenous distribution of AgNPs and it was advantageous for comparing

responses across cell types to the same AgNP suspension. However such a dispersion may not reflect what may occur under real exposure situations. In fact we have witnessed an example of how changing the medium environment can lead to destabilisation and complexing of Ag with medium components. It appears that this complexing rendered the AgNPs less bioavailable and thus we see lower cytotoxicity in terms of metabolic activity. Interestingly exposure to complexed AgNP preparations produced distinct and heightened effects on the plasma membrane and lysosomes of cells. Similar IC50 values as $AgNO_3$ exposure were obtained for these preparations when tested using the neutral red assay which monitors lysosomal integrity. Thus the potential dissolution of AgNPs in this compartment may be a possible mechanism of cytotoxicity (discussed in detail in section 8.5.2). Therefore while free Ag^+ represents an increased hazard compared to AgNPs, dissolution of AgNPs either in the environment (extracellularly) or intracellularly can act as a hazardous source of free Ag^+.

Also while a micron-sized particle preparation was not included in this study these complexed Ag preparations formed large particle aggregates (200 nm in size). These preparations did not have the same toxic efficacy in terms of loss in metabolic activity but had equally and even more toxicity using membrane damage and lysosomal dysfunction as an endpoint.

It seems that particle uptake and subsequent dissolution may be acting as an important mechanism of cytotoxicity for AgNPs. This has been proposed first by Park and colleagues in 2010 (Park et al. 2010). In particular the increased sensitivity of the neutral red assay focusing on lysosomes is in line with the proposed "lysosome-enhanced Trojan horse effect" (LETH mechanism) (Sabella et al. 2014) (discussed in more detail in 8.5.2).

8.3 Possible methodological aspects influencing effects-Experimental considerations

Experimental considerations need to be specifically made due to technical issues posed by testing nano-particulate forms using *in vitro* cell culture systems. First, when preparing exposure suspensions it is pertinent to consider the ENMs dispersability[30] in the culture medium environment. Depending on the dispersion state and stability, particles may experience diffusion effects, gravitational settling and agglomeration under culture conditions and such particokinetics[31] can ultimately influence cellular interaction and responses.

The ENMs used in the range of studies presented in this thesis have been either sourced from the manufacturer in powder form (ZnO and CuNPs), supplied already in a colloidal dispersion (AgNP-NM300K) or dispersed in water following synthesis (AuNPs). In all cases, prior to testing, suspensions of ENMs must be prepared in cell culture medium. Besides providing an optimum and nutrient rich environment for cell growth and propagation, the media characteristics can have a direct influence on how ENMs are dispersed in these suspensions. Cell culture medium is a buffered solution that is comprised of a mixture of essential nutrients such as amino acids, carbohydrates, inorganic salts, vitamins, minerals and growth factors. It has a pH of between 7.2-7.4 which is maintained by gaseous CO_2 balances with the $NaHCO_3$ content

[30] degree to which ENM is uniformly distributed in another material (dispersion medium).

[31] First coined by Teeguarden and colleagues in 2007 to describe the solution dynamics of ENMs including diffusion, gravitational settling, and agglomeration (Teeguarden et al. 2007).

of the culture medium. Medium is available with a variety of different formulations depending on the optimum growth conditions for particular cells. Achieving a homogenous and stable dispersion in such an environment is often difficult and technically challenging. Particles in suspension can agglomerate/aggregate, dissolve or sediment depending on their own physico-chemical properties, and that of their dispersion environments. To a certain extent, the laws that govern colloidal chemistry can be applied to ENMs in suspension. Accordingly, the tendency of particles in suspension to aggregate or remain in single particle form in solution is governed by the balance between attractive (van der Waals) and repulsive (electrical double layer) forces. This is the basis of the classical DLVO (Derjaguin, Landau, Verwey, Overweek) theory describing the stability of colloids in suspension based on total/net interaction energy (sum of attractive and repulsive force) (Derjaguin and Landau 1941, Hunter 2001, Verwey and Overbeek 1948). Taking into account the sum of attractive and repulsive forces, an energy barrier is created. The magnitude of this energy barrier depends on the surface potential of the particles and on the ionic strength of the surrounding environment.

The high salt content in culture media used (ranging from 116.359 mM to 136.98 mM) can diminish electrostatic repulsion between individual particles and lead to attractive forces predominating, breakdown of the energy barrier, and particles coming together in agglomerates. This is in fact what we see in the case of most of the ENM suspensions used in our studies upon dispersion in culture medium and their instantaneous agglomeration. Using DLS we have analysed the hydrodynamic size of agglomerates in these suspensions and monitored their stability. Zeta potential can be used as a measure of dispersion stability[32], however blackening of the electrodes and inaccurate measurements will result if the dispersing medium has a high salt concentration (high conductivity). In our studies evidence of large sized agglomerates have been witnessed that continue to increase over time, in some cases reaching hydrodynamic diameters of >3000 nm (ZnO NPs).

In other cases, decreases in agglomerate size associated with the dissolution of metal ions from particles, as well as the transformation (deagglomeration) of particles in the medium environment were evidenced over time (CuNP, *introductory paper 2*). Therefore, particularly in the case of metal ENMs, one must also consider the solubility[33] of such materials in culture medium. The kinetics of dissolution can be influenced by differences in culture medium and the cells culture incubation temperature (Li et al. 2015). Thus, due to culture medias high ionic strength, and metal ENMs susceptibility to dissolution, rapid agglomeration of ENMs and an unstable dispersion was to be expected in most cases, and actually observed in most of the experiments carried out within the studies presented in this thesis.

An important property which will be influenced by such unstable dispersions is dose. The preparation of working suspensions from a heterogeneous unstable stock suspension will lead to the administration of inaccurate doses based on mass concentration. In the *introductory paper 1* losses of, in some cases over 50% of mass concentration dose were seen when preparing working

[32] If the absolute value of the zeta potential is high, there will be high repulsive forces between particles and electrostatic stability, with low agglomeration of particles. However at lower zeta potential values the repulsive forces will be reduced, electrostatic stability will be low and particles will have a tendency to agglomerate.

[33] Maximum mass of a nanomaterial that is soluble in a given volume of a particular solvent under specified conditions) (ISO 7579).

suspensions from stock suspensions, due to the rapid sedimentation of large ZnO particle aggregates. Similar losses (between 23% to 55%) from nominal weighed stock suspensions were also witnessed in the case of the CuNPs test preparations in *introductory paper 2*. In this case the tendency for the particles to adhere to laboratory plastics (microfuge tubes) may have also had an influence. Technical issues such as these involved in dispersion preparation make it very difficult to achieve reproducible concentrations for exposures. Also the use of nominal concentrations in this case would underestimate toxic potencies. To overcome such difficulties we have used ICP-MS to measure "real" administered concentration and used these measured concentrations when calculating dose–response curves and effective concentrations (e.g., IC_{50} values). Thus analytical measurement of exposure concentrations, especially for ENM suspensions that are difficult to disperse, are essential to correctly and accurately determine toxicity.

There is also a need to consider the interaction of NPs with the various components in the culture medium when performing cytotoxicity studies. In *research paper 2*, the cysteine and methionine content of Leibovitz's L-15 medium affected AgNPs dispersion and ultimately the cytotoxic response observed. The presence of large AgNP agglomerates (254 nm in hydrodynamic diameter) together with visible precipitates, and a reduction in cytotoxicity suggest the formation of Ag complexes with Cl^- or bound to cysteine and/or methionine, reducing Ag bioavailability (Behra et al. 2013). Also in the case of ZnO suspensions we have measured particles in supernatants (assumed to only contain dissolved ions) which may suggest reprecipitation of ZnO NPs from Zn^{2+} in the medium environment (*introductory paper 1*). The lack of high levels of cytotoxicity expected if Zn was present in its free ionic form suggests decreased bioavailability in the culture medium and the possible formation of zinc hydrocarbonate (hydrozincite) or zinc phosphate hydrate (hopeite) (Turney et al. 2012). Both these examples highlight how differences in the dispersion state can lead to cells being exposed to different ENM forms, affecting bioavailability, and consequently cytotoxicity.

Different methods can be used to achieve a more homogenous dispersion and avoid the formation of agglomerates of NPs in physiological solutions. Chemical dispersants such as surfactants can be employed to increase the electrostatic repulsive forces. For example in research paper 4, AgNPs were dispersed in 4% polyoxyethylene glycerol trioleate (PGT) and 4% polyoxyethylene sorbitan monolaurate (Tween 20). Both PGT and Tween 20 are non-ionic surfactants that act as emulsifiers. The use of such agents aided suspension stability under certain culture medium conditions (not all).

Biological culture medium is often supplemented with fetal bovine serum (FBS) to enhance cell growth. The presence of FBS also confers increased stability upon the particles due to the abundance of proteins, including albumin, which can absorb to the surface of particles creating a stabilisation effect (Murdock et al. 2008). This stabilisation affect has been witnessed when comparing dispersions of AuNPs in medium with and without FBS (10% FBS) in *research paper 4*. However protein binding has been shown to affect the bioavailability of chemicals and thus may influence the relative potencies of ENMs when incorporated in an *in vitro* system (Seibert et al. 2002). This has divided opinions within the scientific community and whether to incorporate FBS in ENM cytotoxicity test systems or not is under debate.

Using a different mechanism, ENMs can be stabilised through high affinity covalent bonding. In *research paper 4* AuNPs were capped with different peptide biphenyl hybrid (PBH) ligands as stabilizers. These PBHs contain two peptide fragments composed of different combinations of amino acids (glycine (Gly), cysteine (Cys), tyrosine (Tyr), tryptophan (Trp), and methionine (Met)) with a biphenyl scaffold conferring specific conformation. Conjugation of peptides to the gold surface of AuNPs through covalent bonding with either a thiol, amine or carboxylate functional group is easily achieved and thus is routinely used following AuNP synthesis to create stable suspensions. Interestingly, differences in the specific structure of the PBH capping agents used in this study led to distinct associations between individual AuNPs in the culture medium. In particular TrCys (Trityl-Cysteine) residues and the steric bulk of PBH (Gly-Tyr-TrCys)2B were responsible for the remarkable stability of Au[(Gly-Tyr-TrCys)2B] agglomerates in culture medium. As discussed in the corresponding article, the stability of these AuNPs in biological media, together with their ability to enter cells, open up expectations for their potential applicability in drug delivery systems.

Mechanically large agglomerates can be broken up by high shear forces created by ultrasonication (Sato et al. 2008), or simply by mixing or vortexing. In the *introductory papers 2 and 3*, CuNP suspensions were subjected to water bath sonication to improve dispersion. Sonication creates ultrasonic cavitation that is very effective in breaking the van der Waals forces holding agglomerates together. However its efficiency will depend on energy input (which is dependent on time and power/amplitude) (Hielscher 2005) and it may only be a temporary solution, since when the energy input is stopped the smaller particles generated may re-agglomerate into larger ones and precipitate. Publication titles "shaken not stable" have eluded to this limitation (Edri and Regev 2009). There are also other disadvantages associated with the use of such mechanical methods. For example particularly high input energies can lead to re-agglomeration (Kusters et al. 1993) and could theoretically fracture individual particle or change existing surface modifications (OECD 2012a).

Taking all this into account, careful consideration needs to be made regarding the choice of dispersion method. Also the relevance of exposing cells to well-dispersed suspensions that do not occur in "real life scenarios" might also be questioned. In favour of a more representative situation to the environmental one, none of these dispersion techniques were applied to ZnO NP exposure suspensions in the *introductory paper 1*. Instead ZnO NP powders were suspended in serum free-culture medium and simple vortexing was used to disperse the suspensions. Therefore, it is evident from the studies presented that the choice of dispersion technique, whether to use chemical or mechanical means, or to incorporate additional techniques to improve dispersion at all, is at the tester's discretion (currently in absence of established standardised dispersion protocols). This makes it increasingly difficult to make comparisons among studies and to corroborate results that will ultimately aid in validating *in vitro* methods. In a continuous effort to standardize testing, the scientific community has introduced the use of representative ENMs (e.g. NM-300K) and some dispersion protocols (ENPRA 2010, Jensen et al. 2011). For now, when using *in vitro* cell culture systems, techniques such as ICP-MS should be incorporated in order to ensure accurate tested concentrations, and a thorough characterisation of ENM dissolution kinetics and behaviours in different environments made to improve our understanding of particokinetics in *in vitro* cell culture test systems.

8.4 Cell line sensitivity variations: differences between mammalian and fish cell lines

In the *introductory papers 1* and *2* we have performed comparative cytotoxicity studies with a range of different sized ZnO and CuNPs in fish and mammalian liver cell lines. We have included both mammalian (HepG2, H4IIE) and fish liver cell lines (PLHC-1, RTH-149) to assess if they show differences in their sensitivity/susceptibility to toxic effects of such ENMs or if in fact these ENMs exhibit differences in their mechanisms of action at the cellular level across species. Such an approach provides valuable information to assess the hazard posed by nanomaterials across diverse taxa and if the risk of ENMs can be extrapolated across species[34]. While many factors need to be considered for such extrapolations[35], comparing susceptibilities at the cellular level of particular organ systems and identifying particular mechanisms of toxicity will aid in determining levels of uncertainty.

Interestingly, results have revealed that for both ZnO and CuNP exposures mammalian liver cell lines are more sensitive to toxic effects compared to piscine liver cell lines. Higher NOEC values in the fish cell line, PLHC-1 compared to HepG2 following exposure to Zn^{2+} supernatants revealed higher tolerances of this fish cell line to higher concentrations of Zn ions. Similarly, results reveal a clear difference in tolerance to Cu^{2+} between the mammalian and fish cell lines used in this study following exposure to $CuNO_3$ (IC_{50} values ranged between 40- 60 µg/mL for HepG2 and H4IIE vs 100-120 µg/mL for PLHC-1 and RTH-149). This could suggest that differences in tolerances to metal ions (either released from NPs in the medium environment or intracellularly) may be a key factor in determining differences in sensitivity of cell lines towards NPs. Using zebrafish embryos and mammalian cell lines George and colleagues (George et al. 2011) have also shown different sensitivities in the case of AgNPs, pointing to the role of the ions in the case of metal NPs where the ion released from particles as well as the particles themselves can contribute to toxicity.

To understand why these differences in susceptibility exist one needs to consider the environments both taxa inhabit. Fish have evolved to adapt to more variable environments occupying aquatic environment with often diverse salinities, ion compositions and pH values and therefore it is plausible to assume that they may have increased response capacity. The fish cell membrane has a higher phospholipid content compared to mammalian cells with highly polyunsaturated fatty acids giving these cells higher flexibility and lower intrinsic permeability to ions.

Ion regulation itself involves highly evolved uptake, storage, and secretion processes. In all cells ion transport systems are responsible for regulating ionic concentrations across the cell membrane. While ion uptake enzymes are often conserved in amino acid sequence across species their distribution and concentration in cells are often not conserved. Also species may have distinct metal ion storage systems and distribution patterns. For instance, on a cellular level

[34] According to a recent report (Celander et al. 2011) "eventually, predictive models will be developed to extrapolate across species", although they also recognise that "substantial research is still required".

[35] Particularly with regard to ENMs different species may have distinct protein repertoires and longer/shorter circulation times that both will influence the protein coronas formed (Sahneh et al. 2015). Toxicokinetic studies will play a major role in comparing the extent of translocation to different organ systems and tissue burden in different species.

metallothionein (MT)[36] content and functioning has been shown to be different between fish and mammals. Structural differences in the distribution of surface charges and arrangement of amino acids in fish and mammalian MT have been evidenced (Bargelloni et al. 1999, Scudiero et al. 1997, 2005). This can have a direct influence on the kinetics of ion exchange and increase binding flexibility. For example a shift in the C-terminal Cys of MT from the antarctic fish *Notothenia coriiceps* showed better metal exchange capability with respect to mouse MT (D'Auria et al. 2001). Also in the case of fish it appears that MT shows different thermostability, as well as different metal affinity, and different redox properties with respect to mammalian MTs (Isani and Carpenè 2014).

Therefore, and although not studied in this work, difference in metallothionein functioning between mammalian and fish cells may explain differences in ion susceptibility. In fact copper-resistant hepatoma cell lines are characterized by their high levels of MT expression (Capasso et al. 2003).

However results also reveal that despite fish cell lines showing increased resistance to metal ions they were equally as sensitive as mammalian cell lines to NP preparations with low dissolution (CuNP 78) (*research paper 1*). Similar NOEC values, when taking into consideration particle suspension exposures, also prove this is the case for ZnO NPs (*introductory paper 1*). Also if we take into consideration particle forms, trends can even change suggesting that piscine cell lines may be even more vulnerable to particle effects. Therefore while the extent of toxicity and species sensitivity was influenced by the contribution of metal ions, toxicity was also dictated by distinct material effects.

It appears also that there could be differences in the mechanisms of toxic action of NPs depending on the origin of the cell lines. In the case of ZnO NPs, there is a stronger loss in mitochondrial activity in the mammalian HepG2 cell line compared to the PLHC-1 cell lines. This could relate to the contribution of intracellular dissolution in this mammalian cell line (according to the proposed Trojan horse type mechanism of action) which appears to be a more ion sensitive cell line. The extent to which intracellular dissolution contributes to toxicity presently cannot be quantitatively determined due to limitations in analytical techniques although this will be discussed further in section 8.5.1). Similarly, ZnO NPs generate detectable ROS levels only in the PLHC-1 cell line. This could be explained by differences in oxidative coping mechanisms. Differences in natural antioxidant levels of glutathione have been shown to be responsible for differences in sensitivity with cell lines with lower levels having increased sensitivity to metal ENMs, such as for example Ag ENMs (Mukherjee et al. 2012). In accordance with our results, Rau et al. (2004) has also observed that the PLHC-1 cell line was more susceptible to oxidative stress upon exposure to model pro-oxidants compared to the H4IIE rat hepatoma cell line. With regard to CuNPs, the RTH-149 cell line is markedly less susceptible to CuNPs particle fractions than mammalian cell lines, but also than the PLHC-1 fish cell line. This difference is likely not related to specific physico-chemical behaviour in RTH-149 culture medium or culture conditions as no differences in size distribution or dissolution were evidenced. The reduced susceptibility of RTH-149 cells could be related with reduced cellular uptake and the slower metabolism expected for this cell line cultured at lower temperatures. Interestingly in *research paper 2* the

[36] Metallothioneins are low-molecular weight, cysteine-rich proteins provided with high metal binding capacity.

RTH-149 cell line showed comparable sensitivity to AgNP insult compared to other cell lines. Therefore such increased resistance is specific for CuNP exposure and its presentation to the cells. A study has shown minimal metalothionein RNA upregulation by copper compared to those induced by Zn and cadmium in RTH-149 cells (Vergani et al. 2009) what could also contribute to the low sensitivity of these cells towards CuNP toxicity. Therefore it appears that differences in sensitivity is not only influenced by species of origin but the specific cell line used.

To test the sensitivity of liver cell lines in general as test systems in *research paper 2* primary liver cells were included and responses to AgNPs were compared with comparable responses across different fish liver cell lines being evidenced.

8.5 Mechanistic understanding

As well as serving as *in vitro* alternative test systems for ENM hazard assessment, the liver cell lines used in the presented studies provide a valuable platform to investigate the possible mechanisms underlying cytotoxic responses. Cytotoxicity has been assessed using multiple biochemical based assays, each designed to measure perturbation of specific cellular functionality or organelle targeted cytotoxicity. Cells were grown and assays were applied in a high throughput 96-well plate format facilitating a fast and robust cytotoxicity screening. Any differences in the assays sensitivity according to targeted organelle eluded to underlying mechanism of cytotoxicity for the ENMs under investigation.

Understanding the underlying mechanisms of cytotoxicity is becoming increasingly important in an era that is moving away from descriptive approaches, which sought to merely identify adverse effects, towards developing a predictive mechanistic based toxicology framework. Identifying pathways of toxicity at the cellular level is seen as a progressive means to understand and explain observed adverse effects. A pathway of toxicity has been defined as a cellular response pathway that would result in an adverse health effect when sufficiently perturbed (NRC 2007). Such a concept has been developed further to include the point at which a chemical-biological interaction initiates the perturbation of a normal cellular pathway (molecular initiating event, MIE) and the sequence of key cellular and biochemical events (KEs), resulting in adverse health effects. These concepts cumulate into the development of Adverse Outcome Pathways (AOP) for particular effects, that once identified can be tested for using *in vitro* tests systems including those based on cell lines. Once an association between a chemical and a particular AOP is made, identifying the molecular initiating event can serve to develop alerts and create chemical categories that can be used to predict toxicity and thus move toxicology in the direction of a predictive science.

The application of such an AOP framework in testing and hazard assessment is only now being realised (AOP for skin sensitisation, OECD 2012b) and whether such a framework can be applied to ENMs remains to be seen. ENMs are a unique set of materials often each with unique and distinct biological interactions. As well as their chemical composition both intrinsic and extrinsic properties can contribute to specific biological outcomes. On a molecular level ENMs can interact with biological macromolecules which are often in the same size range (e.g. lipids, proteins and nucleic acids) and interfere with their native functioning. This is what makes it

extremely difficult to identify a common mode of action for these class of materials. Some proposed molecular initiating events involve direct or indirect ROS formation, physical disruption of cellular membranes, as well as specific organelle targeted events such as the destabilisation of lysosomes and mitochondrial dysfunction. The assays performed throughout the various studies presented in this thesis were selected in order to investigate each of these sites and try to pinpoint molecular mechanisms underlying the cytotoxicity of the group of metal ENMs under investigation.

We have focused heavily on ROS elicitation, and the extent to which oxidative stress plays a role in these metal ENMs pathways of toxicity. Also due to the uncertainty surrounding the contribution of particle solubility and dissolved ions to ENMs, studies investigating mechanisms of cytotoxicity were performed to provide some insights and will be discussed.

8.5.1 Role of dissolved ion

We have evidenced from comparing responses to exposures with only released ion fractions, that particle forms presented to cells play a key role, independent of extracellularly released ions, in eliciting toxic effects (NP-specific effects have been discussed for each ENM tested in section 8.2). Significantly sharper dose responses following particle suspension exposures suggest that, both in the case of ZnO NPs and CuNPs, particles being present confer a higher toxic potential. NP-specific ROS elicitation from particle suspensions, not seen following exposures to released ions, as well as evidence of uptake of ZnO NPs and CuNPs and their association with intracellular organelles all point to unique biological interactions between cells and these metal ENMs.

However if metal NP cytotoxicity is mechanistically unique compared to metals in ionic form has yet to be clarified. NPs may just be acting as vehicles for large quantities of metal ions in a Trojan-horse type mechanism first proposed by Limbach, which involves NP uptake and subsequent internal ion release (Limbach et al. 2007). Studies since then have extended the concept further with a proposed lysosome-enhanced Trojan-horse type effect (referred to as LETH mechanism) pinpointing the lysosome as a vulnerable site, due to metal NP susceptibility to dissolution in lysosomal acidic environments (pH 4.5) (Sabella et al. 2014). Techniques such as X-ray absorption near edge structure (XANES) analysis has been used by researchers to monitor intracellular ion release from Ag and ZnO NPs in different cell types corroborating such a mechanism of cytotoxicity for NPs. Results revealed that 14.2% of silver taken up into cells was oxidised to Ag after 12h incubation in CHO-K1 hamster ovary cells (Jiang et al. 2015) while there was complete dissolution of ZnO NPs intracellularly after 1 h in BEAS-2B human bronchial epithelium cells (Gilbert et al. 2012).

In the *introductory paper 1* we have employed both the MTT and NRU assays to focus specifically on adverse effects associated with a reduction in metabolic activity or lysosomal damage, respectively. We did not witness any increased sensitivity between the assays following ZnO NP exposure either in the HepG2 or PLHC-1 cell lines. However the increase in response according to the NRU assay when cells were exposed jointly to particle and ion fractions, compared to ion fractions only, may suggest that in the presence of particles the lysosome

susceptibility may play a greater role in cytotoxicity. In contrast, similar levels of reduced viability according to the MTT assay were seen following exposure to joint particle and ion exposure and ions only.

Specifically in the case of AgNPs (NM300K) we have witnessed in general increased cytotoxicity in fish cell lines exposed to $AgNO_3$ (source of Ag^+) compared to AgNP suspensions. However for AgNP suspensions prepared in cysteine-rich and high chloride content L-15 medium (Ag complex formation) specific lysosomal destabilisation effects became apparent with a reduction in IC50 values measured to the same level recorded following Ag^+ exposure. This observation pinpoints the lysosome as an important target and perhaps implies a role for the Ag^+ released intracellularly from AgNPs in the mechanism of cytotoxicity.

Also in *research paper 3* we discuss the possible role of ions released from ZnO NPs in the gastrointestinal tract of the rainbow trout and the form in which Zn accumulates in the liver, intestine and gills. On a cellular level a hypothetical mechanical toxicological pathway has been proposed involving ZnO dissolution to Zn^{2+} in endosomes and subsequent disruption of Zn^{2+} ion homeostasis (Kao et al. 2012).

Overall it is difficult to determine the extent to which intracellular dissolution contributes to toxicity and the involvement of metal ions in ENMs mechanism of cytotoxicity presently is not clear. However there is strong evidence (discussed in section 8.2) to suggest unique and distinct toxic contributions from metal ions and metal ENMs.

8.5.2 Toxicity at the subcellular level

In the studies presented, through the use of an array of classical cytotoxicity assays (test battery) and their combination, we sought to provide important insights into potential subcellular targets and mechanisms of toxicity of the ENMs tested. Assays assessing the cells general overall metabolic status (either based on tetrazolium or resazurin reduction, MTT and AlamarBlue, respectively) were included in all studies as well as, in some cases, assays looking at specific organelle targeted effects (plasma membrane and lysosomal damage). The relative sensitivity of these assays was used as indicative of potential target sites of cytotoxicity of the ENMs tested. This is discussed specifically below.

8.5.2.1 Plasma Membrane

As the first point of contact following exposure to ENM dispersions in an *in vitro* cell culture system, the cells plasma membrane is an important site to focus on and investigate if damage occurs. The plasma membrane acts as a protective barrier to the cell. It is composed of two layers of phospholipids in a lipid bilayer structure (5 nm in thickness) that is impermeable to water-soluble molecules, including ions and most biological molecules, while allowing smaller particles with no charge to pass (carbon dioxide and oxygen). Proteins embedded in the membrane regulate the exchange of substances into and out of the cell through passive (diffusion, carrier mediated) and active transport (endocytosis, exocytosis) (Cooper 2000). ENMs may enter into cells by any of these transport processes. However the properties that control specific uptake

routes have not been fully elucidated. It must also be taken into consideration that NP-membrane interaction may result in physical damage to membranes.

The integrity of the plasma membrane following exposure to the ENMs in the presented studies was either measured according to the cells capability to retain lactate dehydrogenase (LDH assay) (ZnO NPs, *introductory paper 1*) or carboxyfluorescein (CFDA-AM assay) (AgNPs, *research paper 2*). In both cases these assays identify specific cytotoxic effects associated with membrane disruption, however in neither cases do we see increased sensitivity compared to the other cytotoxicity assays employed. This would point to plasma membrane disruption as a downstream consequence of global cytotoxicity and not the specific cause.

TEM analysis of H4IIE liver cells exposed to sublethal concentrations of CuNPs show that aggregates of these CuNPs (with hydrodynamic diameters of ~1000 nm) interact with the membrane and are taken up by cells as a whole (*research paper 1*). The presence of these aggregates and their compartmentalisation in vesicles without any obvious observable membrane damage suggest an endocytotic uptake process. Interestingly, in the *introductory paper 3* there was also evidence of CuNPs present free in the cytoplasm. In this study particle suspensions were prepared in serum-free medium and exposures were performed for 48 h. Again uptake was observed at non-cytotoxic concentrations without any evidence of plasma membrane damage. In the same study ZnO NPs appear to have been taken up by cells by non-endocytotic processes, with again no evidence of cytotoxicity associated with plasma membrane damage. It is only when both CuNPs and ZnO NPs are present intracellularly that we see cytotoxicity, but no indication of specific plasma membrane disruption. In fact the lysosomes are the most affected organelle (lysosome as target will be discussed in detail in the section below).

In contrast to the lack of specific membrane disruption for the ZnO NPs, CuNPs and AgNPs tested, specific plasma membrane damage has been reported and proposed to play a key role in graphene nanoplatelets mechanism of cytotoxicity (Lammel et al. 2013). While specifically cationic polymeric nanomaterials such as organic dendrimers have been reported to create "holes" in the plasma membrane of cells (Hong et al. 2004). Such initiating events targeting membranes can lead to lipid peroxidation, loss in membrane flexibility, a drop in transmembrane potential, permeability to ions, and ultimately cell death.

The transport of ENMs across cell membranes is an area of intensive research in the field of toxicology. Model cell membranes have been used to show that ENMs can permeabilise lipid bilayers (e.g. silica nanospheres (de Planque et al. 2011)) and that positively charged NPs are electrostatically attracted to membranes. However investigations must be performed to see if results will translate to what occurs under real conditions in the case of heterogenous and complex membranes. Particle aggregation and adsorption to proteins (from cell culture medium) under biological conditions can lead to an unknown effective diameter or a specific surface chemistry which will ultimately dictate specific interactions. For example, perhaps the presence or absence of serum is dictating specific CuNP uptake and processing pathways in *introductory paper 3* and *research paper 1*, respectively. Once we begin to fully understand the factors that dictate specific interactions and uptake processes we can seek to design safer ENMs or circumvent effects by modifying surface chemistries.

In fact in the area of nanomedicine, the use of nanomaterials decorated with peptides (cell penetrating peptides) is seen as a promising drug delivery system especially for hydrophilic drugs showing low penetration. For example we have seen in *research paper 4* the influence of a range of different peptides present on the surface of AuNPs on the behaviour of these NPs in the biological environment and cellular interaction. Once fully understood, it can be fully capitalised on.

8.5.2.2 Lysosomes

The presence of ENMs inside cells may lead to direct interaction between NPs and intracellular organelles. The relevance of NP-lysosome interaction lies in lysosomes role in the degradation of macromolecules delivered via the endocytotic and autophagic pathways. Endocytosis has been highlighted as a major cellular uptake pathway for many ENMs. Once taken up into intracellular vesicles, according to the endo/lysosomal pathway of processing (Huotari and Helenius 2011), fusion of vesicles with lysosome will take place and NP-lysosomal interaction is expected.

Lysosomes themselves are described as single membrane-bound organelles present in the cytoplasm. As highlighted above, CuNPs appear to be internalised using endocytotic processes and later may be processed in late endocytotic vesicles interacting with what resembles lysosomes (dense and finely granular under TEM) (*research paper 1*). An assay to specifically assess lysosomal destabilisation based on the ability of lysosomes to retain neutral red dye (NRU assay) following ENM exposure was included in the study. While there was no evidence of lysosomal dysfunction as a specific target following exposure to CuNPs, interestingly in co-incubation studies with sublethal concentrations of CuNPs and ZnO NPs, cells experienced a significant increase in cytotoxicity, most evidently according to the NRU assay. This suggests that lysosomes were targeted. Interestingly this specific targeting was only evidenced in mammalian cells and not seen in co-incubation studies using fish liver cells (Hernández-Moreno et al. 2016) (role of species specific cellular properties discussed in section 8.4). Within the lumen of lysosomes, NPs will be exposed to acidic pH together with a myriad of hydrolases, both of which may lead to dissolution of metal ions or breakdown of any protein coatings. For example lysosomal destabilisation as a result of dissolution of zinc ions from ZnO NPs has been proposed as a mechanism of toxicity for ZnO NPs (Cho et al. 2011), while the degradation of protective protein coating and physical disruption of lysosomes by polystyrene NPs leading to cytosolic release of lysosome content and apoptosis has also been reported (Wang et al. 2013). To pinpoint whether any or either of these processes was occurring in the co-incubation studies would need further investigations. However what is clear is that distinct mechanisms are operating for the particles exposed alone and when in co-incubation.

Findings presented in *research paper 2* may also point to the lysosome as a potential target of toxicity for AgNPs. Specifically in the case of AgNPs (NM300K) and Ag^{+} suspensions prepared in medium with a high cysteine and chloride content (L-15 medium), rainbow trout liver cells were protected somewhat against a loss in metabolic activity and membrane damage (possibly due to a passivation effect) (Loza et al. 2014). However, remarkably lower IC50 values were recorded according to the NRU assay. This may suggest the uptake of Ag chloride nanoparticles

formed from precipitation of silver ions and subsequent liberation of Ag ions under acidic pH of lysosomes. Such targeting was specific only for AgNPs dispersed in L-15 medium. This highlights the important influence of medium composition on effects, which has also been highlighted by Yue and colleagues using cit-AgNP prepared in medium with varying ionic strength and chloride concentration by monitoring effects in rainbow trout gill cells (RTgill-W1 cells line) (Yue et al. 2015).

Together with the presented evidence for lysosomal targeting for CuNPs and ZnO NPs in co-exposures and AgNP suspensions prepared in L-15 medium, lysosomes have recently been highlighted by other authors as critical organelles in ENM mediated cytotoxicity (Fröhlich et al. 2012, Stern et al. 2012). A recent paper has shown the lysosome targeted cytotoxicity of AgNPs in the human alveolar basal epithelial A549 cell line using bafilomycin A1, the lysosomal acidification inhibitor (Miyayama and Matsuoka 2016). Subsequent events following lysosomal membrane destabilisation include an increase in lysosomal pH (acidity), swelling of compartments through accumulation of intracellular phospholipids, release of hydrolases, and ultimately the triggering of apoptotic cell death cascade (Boya et al. 2008).

However to determine fully the lysosomes role and validate lysosomal destabilisation or lysosomal membrane permeabilisation (LMP) as a molecular initiating event more research is needed.

8.5.2.3 Cellular metabolic status

Cellular damage will inevitably result in loss of the ability of the cell to maintain and provide energy for metabolic cell function and growth. However toxicants can also alter cellular metabolism without causing cell death, therefore biomarkers of more general functions such as metabolic activity can be very sensitive systems. In fact in most cases in the studies presented (with the exception of the instances discussed above) the assays assessing metabolic status (MTT and AlamarBlue) proved even more sensitive than specific organelle targeted assays (e.g. NRU, LDH, CFDA-AM).

Metabolic activity was monitored by the cells ability to reduce MTT or resazurin depending on the study presented. In the *introductory paper 1* the MTT assay gave the highest sensitivity in both cell lines following exposure to ZnO NPs. This assay measures the activity of mitochondrial dehydrogenases, which play a fundamental role in the mitochondrial electron transport chain that provides energy for the cell (Berridge and Tan 1993). Mitochondria themselves are scattered throughout the cytoplasm and their number is dictated by specific cell type and energy requirements. Cells in the liver have particularly high energy requirements and therefore possess large numbers of mitochondria (1000–2000 per cell and one-fifth of the cell volume) (Alberts et al. 2002). Therefore, once internalised and present free in the cytoplasm in liver cells, there is a high likelihood of NP-mitochondria interaction. However the mitochondria is protected by a double membrane system; an outer membrane that restricts access to nuclear-encoded proteins through a complex set of import receptors and proteins (mitochondrial protein translocase, MPT family) and an inner membrane impermeable to all molecules except O_2, CO_2, and H_2O (Cooper

2000b). The exact interactions of ENMs with these organelles or how they affect their function has yet to be elucidated.

For ZnO NPs a putative mechanism of cytotoxicity has emerged in which authors have shown that ZnO NPs when in direct contact with mitochondria have the ability to increase the inner membrane permeability and disturb the mitochondrial respiratory chain leading to oxidative stress, release of cytochrome c, induction of caspases and apoptotic cell death (Li et al. 2012). From TEM analysis ZnO NPs are present free in the cytoplasm and thus such a mechanism may be plausible. Such a pathway may also be specific for ZnO NPs since no obvious drop in membrane potential following exposure to TiO_2 NPs was observed in mammalian hepatocytes (Filippi et al. 2015).

Also an alternative toxicity pathway for ZnO NPs has been proposed involving Zn^{2+} release from ZnO NPs in endosomes and an increase in cytosolic Zn^{2+} leading to a collapse in the mitochondrial membrane potential (Kao et al. 2012). Zn^{2+} has also previously been shown to strongly inhibit ATP synthesis by inhibiting both the mitochondrial electron transport chain and the Krebs cycle (for a review of the effects of Zn^{2+} on energy metabolism, see Dineley et al. 2003). In our study, the fact that IC_{50} values following 24 h exposure to all ZnO NP suspensions could only be determined for mammalian cells (cells showing increased susceptibility to ions) also suggest Zn^{2+} mediated mitochondrial dysfunction.

The AlamarBlue assay (employed to screen for loss in general metabolic activity[37]) also proved the most sensitive in detecting a reduction in viability following exposure to the silver ion ($AgNO_3$) in primary liver cells. However there was no indication of increased sensitivity following exposure to AgNPs. Therefore loss in metabolic activity may prove as a sensitive biomarker of effects of Ag^+ however its role in AgNPs mechanism of cytotoxicity is not as clear.

Studies are emerging in which isolated liver mitochondria are being used to study the effects of NP-mitochondria interaction showing ENMs ability to cause mitochondrial inner membrane permeability and impairment of mitochondrial energetics (Teodoro et al. 2011). In future such systems may provide more specific information on how NPs interact with mitochondria and affect their function, while in our studies using liver cells both the MTT and AlamarBlue assays proved their relevance and sensitivity as part of a cytotoxicity screening strategy for ENM hazard assessment.

8.5.3 Role of oxidative stress

Oxidative stress is a cellular state that results from a redox imbalance between the generation of reactive oxygen species (ROS) and the compensatory response from the cells endogenous antioxidant network. For a wide range of ENMs (including the metal and metal oxide group of ENMs under investigation) ROS-associated perturbation and oxidative stress-mediated toxicity has been reported.

[37] AlamarBlue can be reduced by a range of enzymes NADPH, FADH, FMNH, NADH as well as the cytochromes (Ahmed 1994).

In fact there is a proposed oxidative stress pathway of toxicity for ENMs represented in a 3 tier hierarchical model first proposed by Li and colleagues in 2003 as a paradigm to explain the role of oxidative stress in particulate matter-induced adverse health effects (Li et al. 2003). Such tiers are the following: Tier 1, increased ROS leading to activation of anti-oxidant defence; Tier 2, redox imbalance leading to pro-inflammatory effects; Tier 3, anti-oxidant defence systems overwhelmed and high ROS levels lead to mitochondrial dysfunction and cell death by apoptosis cytotoxicity (Xia et al. 2006).

However if oxidative stress is a universal mechanism to explain NP-induced cytotoxicity has been questioned, as examples of non-oxidative stress-mediated cellular damage resulting from direct physical interference of NPs with cellular structures are emerging (Shvedova et al. 2012). A challenging question, but one of paramount importance, is if oxidative stress is merely a secondary effect associated with cell death (consequence) or if ROS increase is a key event (or molecular initiating event) in ENMs mechanism of toxicity leading to redox imbalance and activation of events within the proposed oxidative stress pathway of toxicity that once perturbed leads to an adverse outcome (cytotoxicity (cellular level)/oxidant injury (organismal level)) (as defined by the "pathway of toxicity"). If such an association was established it would provide a valuable mechanistic paradigm that could be used in ENMs hazard assessment and regulatory decision making.

There is already a putative AOP for an ENM-induced adverse liver outcome (Gerloff et al. 2015) and the OECD have recently launched an AOP development programme workplan. The idea is that *in vitro* test systems such as cell lines can be used to investigate the various proposed key events along such an AOP to validate proposed pathways of toxicity. Focusing specifically on the proposed oxidative stress pathway of cytotoxicity for ENMs in liver cells, the DCFH-DA probe was used in the studies presented here to quantify levels of intracellular ROS following ENM exposure. For the array of ZnO NPs and bulk forms, increased intracellular ROS levels were only seen in PLHC-1 cells at the highest concentrations tested ($\geq$40 μg/mL) and did not correlate with cytotoxic effects seen already at much lower concentrations. Levels of ROS were also quantified following exposure to CuNPs, in this case there was an evident dose dependent elevation in levels of ROS, correlating with concentrations at which cytotoxic effects were evidenced using the AlamarBlue assay. Also interesting to point out is that a much higher increase in ROS levels were seen in mammalian cells, correlating to their increased susceptible to the cytotoxic effects of CuNPs. This points to the likelihood that ZnO and CuNPs are acting through different mechanisms of cytotoxicity and in fact there probably exists a high degree of variability in the mechanisms among the wide range of ENMs that exist even within groupings.

The underlying mechanism of ROS generation may involve possible oxidative properties of the ENMs themselves upon photoactivation (e.g. ZnO NPs and TiO_2 NPs) which has been capitalised upon on in their application as antimicrobials. Metal and metal oxide ENM dissolution can lead to the release of transition metals that can produce ROS as a general pathway of toxicity through Fenton or Fenton-like reactions (Stohs and Bagchi 1995). At the same time, high levels of intracellular ROS can be caused by interaction of ENMs with cellular components and disruption of endogenous stores (Sailini et al. 2016). For example the cells mitochondria acts as a major store of ROS. Therefore elevation in ROS could be a downstream consequence of

mitochondrial disruption. However, the elevation of ROS can also be the cause of mitochondrial disruption. Therefore it is interesting to investigate if an increase in intracellular ROS is the cause or consequence of cellular damage that leads to cytotoxicity. Oxidative stress is associated with many types of cell death (apoptosis, necrosis, autophagy) (Ryter et al. 2007) however if ROS increase could be linked to a molecular initiating event following ENM exposure, this would provide a valuable mechanistic paradigm to follow for ENMs toxicity assessment.

In *research paper 1* we have investigated further the role of ROS in CuNPs mechanism of cytotoxicity using only the mammalian H4IIE cell line, which proved the most susceptibility to CuNP toxicity and showed the highest ROS induction. We employed two CuNP preparations, one with a high dissolution and one with a low dissolution, to infer the toxic contribution of ion vs NP both in cytotoxicity and ROS generation. Results revealed that ROS elicitation was NP-specific. However, we also focused on the proposed oxidative stress pathway of toxicity and delved deeper to analyse if in fact the high levels of ROS lead to redox disequilibrium. The ratio of reduced to oxidised glutathione (colorimetric DTNB enzymatic recycling assay) in cells was measured as an important indication of cellular redox status. Results revealed a dose dependent reduction in GSH/GSSG ratios indicating high levels of GSSG (oxidised glutathione), a redox imbalance, and cells under oxidative stress.

To monitor to what extent oxidative stress dictates CuNP toxicity, a co-incubation strategy targeting specific pathways was used. Cells were simultaneously exposed to CuNPs and beta-naphthoflavone (BNF) to activate the aryl hydrocarbon receptor (AhR) signalling pathway and its associated gene battery of antioxidants. We hypothesised that through simultaneous activation of the AhR signalling pathway, and its gene battery, by BNF the anti-oxidative response would be upregulated and may bring the cells redox status back into equilibrium following CuNP insult. Strikingly when the cells redox status was brought into equilibrium there was evidence of a non-oxidative stress-mediated loss in cell viability. Similarly, Fahmy and Cormier (2009) have reported that while resveratrol protected human laryngeal epithelial cells (HEp-2 cell line) against oxidative insult, it afforded only partial protection from the cytotoxicity associated with CuO exposure. Results from the studies presented, as well as those reported in the literature suggest that ROS elicitation and oxidative stress while associated with CuNP exposure does not appear to be an initiating event or key event in CuNPs cytotoxicity in H4IIE liver cells. Instead transmission electron micrographs suggest a major role of organelle disruption (e.g. lysosomes) (discussed in section above). Similarly, and while not directly investigated in these studies Park and colleagues have suggested that the generation of ROS was a secondary effect of AgNP exposure rather that the primary cause of cytotoxicity (Park et al. 2011). Therefore one must be careful in using oxidative stress as a pathway of toxicity and recognise that other possible modes of action may exist.

Other authors have used different approaches to test the oxidative stress pathway of toxicity. For example, authors have used overexpression of microsomal glutathione transferase 1 (MGST1), which contributes to the reduction of oxidative stress, to protect against nanomaterial-induced cytotoxicity. However, while protection was evidenced against SiO_2 NPs, the overexpression did not protect cells against ZnO-induced cytotoxic effects (Shi et al. 2012). This would imply distinct mechanism of cytotoxicity for ENMs and in the case of ZnO NPs suggest perhaps an

oxidative stress independent mechanism of cytotoxicity. The use of N-acetylcysteine, a thiol compound that can act as a cysteine source for the repletion of intracellular GSH and can act as a direct scavenger of ROS, is often used to study the consequences of maintaining redox balance. Sulforaphane, a glucosinolate-derived isothiocyanate (ITCs) from cruciferous vegetables, has also been used as a potent inducers of phase II antioxidant/detoxification enzymes. It has afforded the protection against CdSe QD-induced cytotoxicity in human hepatocytes and the livers of mice with the mechanisms of protection being reported mainly via modulation of cellular GSH levels through activation of Nrf2-ARE pathways (Wang et al. 2015). Protection from such compounds have also been witnessed for CuO NPs in fibroblasts (Aktar et al. 2012).

From the studies presented it is likely that there is a high degree in variability in the mechanisms of cytotoxicity, dictated by distinct properties and cell types. Evidence from studies would suggest that in the case of CuNPs an increase in ROS levels and oxidative stress, while associated with CuNP cytotoxicity, may be more of a consequence than a cause. However more research is needed to determine the exact mechanism of cytotoxicity.

It appears that a link can be made between the ROS elicitation seen specifically in fish cells (*introductory paper 1*) to the biochemical disturbances associated with oxidative stress in ZnO NP *in vivo* exposure studies using rainbow trout (*research paper 3*). However such a link does not translate to a pathological outcome. No overt signs of toxicity were witnessed following a 14 day ZnO NP exposure period in rainbow trout despite a significant decrease in GSH/GSSG ratios pointing to a loss in redox balance in the liver and gills and possible targeting of oxidative stress pathway of toxicity. Instead it appears that the level of biochemical disturbance (decrease in GSH/GSSG ratios) which may have been associated with oxidative stress did not exceed the capability of the fish's endogenous antioxidant/physiological environment to respond. Therefore an organism's adaptive capability must be considered.

In the future, using cell lines together with systems biology approaches (genomics, proteomics and metabolomics) may be very useful in elucidating further the exact cellular and molecular pathways of toxicity for metal and metal oxide ENMs and in validating such pathways of toxicity as oxidative stress as a metric to predict their hazard.

8.6 The value and relevance of liver cell lines as experimental models/test systems for nanomaterial hazard assessment.

The liver as a relevant organ for investigating the hazard associated with metal ENM exposure has been introduced in section 1.4.1. Following entry into the blood/systemic circulation (either through translocation from the lungs, GI tract, skin or direct intravenous administration) ENMs have the potential to be distributed to multiple organs. However, the liver has been identified as one of the main sites of ENMs accumulation. In fact ENMs rapid clearance from circulation by the liver, as well as the spleen (mononuclear phagocyte system), is seen as one of the biggest limitations for the use of ENMs in drug delivery systems seeking to target different organ types (Petros et al. 2010). Also specifically in the case of metal ENMs, different physiological environments can lead to not only the potential translocation of ENMs to the liver but the dissolution of metal ENMs and absorption of metal ions into circulation (in fact most studies do

not distinguish whether the metal is distributed in particulate form or as metal ions). Therefore ENMs can also act as vehicles of high concentrations of metal ions that can subsequently be distributed to the liver. This knowledge, together with pioneering studies reporting adverse effects associated with metal ENM distribution and the lack of elimination (bioaccumulation) in the liver (Chen et al. 2006) as well as damage to liver cells (Hussain et al. 2005), formed the scientific rationale for studies in this thesis investigating the hazards associated with metal ENM exposure to liver cells.

Available liver cell lines were chosen as appropriate *in vitro* test systems to investigate potential hepatotoxicity. *In vitro* test systems such as cell lines may serve as an important component in an integrated testing strategy (ITS) for hazard assessment. An ITS refers to "a tiered approach by which chemicals are tested using the chemical properties, quantitative structure activity relationships (QSARS), *in vitro* tests and other computational models like physiologically based pharmacokinetic (PBPK) and pharmacodynamics modelling". Using such a strategy enables potential hazards to first be identified by alternative approaches, such as *in vitro* test systems, and then together such information can be used to appropriately design *in vivo* studies. This is also the scientific rationale for the use of *in vitro* cell culture in the studies performed in this thesis. Ultimately such an ITS will facilitate a predictive toxicological platform and reduce the amount of animal testing (Hartung et al. 2011, 2013). Recently this vision has been reiterated in the area of nanomaterial science by Nel and colleagues in their publication entitled "Nanomaterial toxicity testing in the 21st century: use of a predictive toxicological approach and high-throughput screening" (Nel et al. 2013). This proposed strategy is also consistent with the 2007 report from the US National Academy of Sciences, "Toxicity Testing in the 21st Century: A Vision and a Strategy", which recommends the use of *in vitro* methods involving human cells and cell lines for mechanistic pathway-based toxicity studies (Gibb 2008).

Research presented in this thesis used in total 6 different liver cell lines from both mammalian, including humans, and piscine species. Using cell lines from different species facilitated cross species comparisons and allowed evidencing important differences in sensitivities to nanomaterials (*introductour papers 1 and 2*). Also the high throughput nature and economic feasibility allowed testing of 4 different types of metal ENMs (ZnO, Cu, Ag, Au) with a range of different sizes (ZnO NPs, Cu NPs) and an array of different capping agents (Au NPs). Such test systems have provided a testing platform to obtain valuable information on the potential hazards of these particular ENMs and to rank the ENMs in hazard potential (section 8.1). They also provided a controlled environment in which to compare responses to NPs vs ions and thus identify if nanoparticle-specific effects exist (discussed in section 8.2). Multiple biochemical based assay systems based on fluorometric readouts were applied to monitor perturbations of specific cellular processes (e.g. oxidative stress) and to try and identify specific organelles that may be involved in the mechanism of cytotoxicity (e.g. lysosome as target site for AgNPs (*research paper 2*)). The robustness of the *in vitro* cell culture test system was also increased by incorporating multiple assay systems to the same set of cells. For example, a 3 in 1 cytotoxicity assay has been incorporated successfully monitoring disturbances in the plasma membrane, on lysosome functioning and on cellular metabolism (*research paper 2*). We have also applied cell lines for co-exposure studies to monitor how cells deal/cope with insults from multiple ENMs (CuNPs and ZnO NPs) and have shown striking synergistic toxicity (*introductory paper 3*).

Presently information gathered from non-validated *in vitro* systems such as the liver cell lines used in this research can be used in a weight of evidence approach of an ITS according to the Commission Regulation (EC) No 134/2009 concerning the Registration, Evaluation, Authorisation and Restriction of Chemicals (REACH). However the use of liver cell lines in an ITS will only gain regulatory approval after they have been scientifically determined to be reliable (reproducible), and relevant for their intended purpose. However, the reliability of *in vitro* systems using cell lines has been questioned for ENM toxicity testing due basically to the technical issues associated with achieving a homogenous and stable dispersion of ENMs (as discussed in section 8.3) and the potential interference with assay readouts. The importance of using analytical tools to determine real exposure concentrations has been highlighted after important losses during ENM dispersion preparation were evidenced in *introductory papers 1* and *2*. Interferences with fluorescence /absorbance measurements and/or interaction with assay components associated with ENMs unique physico-chemical properties is also an important aspect (AuNPs in *research paper 4*) often overlooked when performing NP toxicity studies. Also the interaction of NPs with the various components in the culture medium can influence ENM behaviour, how ENMs are presented to cells and their bioavailability (AgNPs, *research paper 2*). Through increased awareness of such factors and by taking specific experimental considerations, reproducibility when testing ENMs can be improved.

Besides ENM specific considerations immortalised cell lines have lost some functional and metabolic activities and as a result responses may not reflect primary cell behaviour. For example, the expression of cytochrome P450s in HepG2 was found to be extremely low compared with expression in primary human hepatocytes (Wilkening et al. 2003). In *research paper 2* we have compared responses between a range of liver cell lines and liver cells freshly isolated from rainbow trout, to investigate if cell lines are representative models. The cell lines showed comparable responses to primary cells following AgNP and $AgNO_3$ exposure, thus proving such liver cell lines as good representative models. Studies have also been performed comparing responses to ENM exposure in the human hepatoblastoma cell line (C3A), and human primary hepatocytes showing that the overall responses[38] are very similar between both test systems to a panel of ENMs (Kermanizadeh et al. 2012).

By their very nature cell lines can only be used to test for a toxic insult at the cellular level, and thus do not take into consideration adaptive responses at the whole organism's levels or toxico-kinetics. Therefore they cannot be seen as a replacement for the use of animals. However to address their value, in terms of relevance of such systems to biological outcomes *in vivo*, we have performed *in vivo* exposures in fish and compared results to toxicological data generated *in vitro*. Mechanistically, exposure to ZnO NPs in PLHC-1 liver cells produced increased levels of reactive oxygen species as a hallmark of oxidative stress. The relevance of this toxicological data to potential responses *in vivo* was then tested in *research paper 3* by incorporating a ZnO NP dietary exposure in fish and monitoring biochemical disturbances associated with oxidative stress in the liver. Indeed biochemical disturbances in the livers of fish fed diets spiked with high concentrations of ZnO NPs were observed. This is an important example of how *in vitro* studies

[38] with respect to uptake, cytotoxicity, pro-inflammatory cytokine release, and albumin production.

can be used as a screening technique and how *in vitro* data can provide valuable and meaningful results that have proven to be representative of responses *in vivo*.

While all of this evidence supports the value and relevance of liver cell lines as experimental models/test systems for nanomaterial hazard assessment, recent and future technological advancements can improve still the validity. The liver itself has a complex three dimensional structural architecture with hepatic lobules and a range of interacting cell types. Thus in order to increase the physiological relevance of cell lines grown in flat mono-layers on plastic surfaces, 3D spheroid models are being developed using the HepG2 liver cell line cultured on extracellular matrix-rich hydrogels. Engineering the cell culture micro-environment in this way enables increased cell–cell interactions between hepatocytes, the maintenance of a polarized morphology and has been shown to increase metabolic expression (Ramaiahgari et al. 2014). Also direct and indirect interactions between the different cell types of the liver play a major role in the maintenance of normal liver function. Therefore, co-cultures of two or more relevant liver cell types may serve as a more representative model.

Also more sophisticated *in vitro* systems are being constructed using multiple cell types, and even multiple tissues, in micro-fluidic devices to mimic organs of the body in a "body on a chip" format and to simulate the circulation of ENMs (Bhise et al. 2016). For example researchers have used such a system to mimic the interaction between the gastrointestinal tract and liver tissues to show that ingested ENMs have the potential to cause liver injury (Esch et al. 2014). Technological advances such as these are beginning to bridge the gap between conventional 2D cell culture and living tissue environment by more accurately mimicking the *in vivo* behaviour of cells and thus improving the predictive power of such *in vitro* test systems of responses *in vivo*.

With current and future developments in engineering the use of liver cell lines and *in vitro* liver cell culture models in ENM hazard assessment may be more heavily relied upon in the future.

CHAPTER 9

CONCLUSIONS

The main conclusions obtained from this research are summarized below:

1. Liver cell lines are relevant and valuable test systems that can be used to deepen our understanding of the mechanisms underlying the toxicity of metal ENMs both from an environmental and human health perspective.

2. Important experimental adaptations may need to be taken when testing ENMs using *in vitro* cell culture test systems in order to achieve stable dispersions in the culture media.

3. Technical issues related to the preparation of accurate exposure concentrations outline the necessity of measuring real concentrations instead of using nominal concentrations for estimating cytotoxicity.

4. Interference checks should also be incorporated into the experimental design when testing NPs using *in vitro* cell culture systems to ensure no false positive/negative results due to reactivity or binding of NPs with assay components.

5. The metal ENMs tested can be ranked by their decreasing cytotoxicity to liver cell lines, estimated from the IC_{50} values calculated from responses in liver cells, as Ag>ZnO>Cu>Au

6. ENMs can enter the cells and appear within membrane enclosed bodies such as lysosomes. In addition, the increased effects with the neutral red assay, which monitors lysosomal functionality, supports that this mechanism can play a key role in the cytotoxicity of nanoparticles.

7. Nanoparticle-specific effects were evidenced highlighting the increased hazard from exposure of liver cells to metal ENMs compared to solely dissolved metal ions.

8. Primary particle size does not appear to dictate toxicity as there is no evidence of a size-dependent (nano-specific) cytotoxic relationship.

9. Although it has been claimed that oxidative stress is the most important mechanism of toxicity of ENMs, we have demonstrated that in several cases the toxicity of ENMs is not directly dependent on oxidative stress.

10. Species-specific differences in sensitivity to the cytotoxic effects of ENMs exist that could be related to differences in tolerances of mammalian and piscine cells to metal ions which are released from the ENMs.

11. Fish cell lines do not show necessarily a lower sensitivity than fish liver cells maintained in primary culture so that they appear as a valuable tool for the study of the cytotoxicity of ENMs

12. ZnO ENMs administered to fish through the diet resulted in the preferential accumulation of Zn in their gills and intestine. Zn distribution to the liver causes oxidative disturbances that are recovered by the organism adaptive responses during depuration.

13. The toxicity of each ENM can be strongly influenced by variations in capping agents which opens the door to safe by design approaches.

CONCLUSIONES

Se presentan a continuación las conclusiones más importantes generadas a partir de la investigación realizada:

1. Las líneas celulares obtenidas a partir de hígado constituyen unos sistemas de ensayo de enorme relevancia que pueden usarse para profundizar en nuestro conocimiento sobre los mecanismos subyacentes a la toxicidad de NMs manufacturados, tanto desde una perspectiva ambiental como de salud humana.

2. Al ensayar NMs en cultivos celulares *in vitro* es posible que sea necesario realizar importantes adaptaciones experimentales para conseguir dispersiones estables en el medio de cultivo.

3. El uso de dispersiones de NMs en vez de disoluciones da lugar a problemas técnicos para la consecución de las concentraciones deseadas al realizar diluciones, lo que subraya la necesidad de llevar a cabo medidas de concentraciones reales en vez de utilizar concentraciones nominales.

4. Al estudiar la citotoxicidad de NPs en sistemas celulares *in vitro* es necesario chequear las posibles interferencias de esas NPs con las medidas, interferencias debidas a su reacción o unión con los compuestos usados en el ensayo.

5. Los NMs metálicos utilizados en este estudio pueden ser ordenados siguiendo valores decrecientes de citotoxicidad, estimada a partir de los valores de IC_{50} en líneas celulares de hígado, del siguiente modo: Ag>ZnO>Cu>Au.

6. Los NMs son capaces de entrar en las células apareciendo en el interior de los lisosomas. Además, los importantes efectos observados en las medidas del ensayo de rojo neutro, que refleja alteraciones en el funcionamiento de los lisosomas, sugieren que este mecanismo puede jugar un papel fundamental en la citotoxicidad de las NPs.

7. El tamaño de las partículas no parece ser determinante en la toxicidad puesto que no se ha observado una relación directa entre citotoxicidad y tamaño de las NPs.

8. Se han observado efectos específicos de la fracción nanoparticulada lo que evidencia el mayor peligro de los NMs metálicos para las células de hígado con respecto a los iones metálicos liberados.

9. Aunque se ha propuesto que el estrés oxidativo constituye el mecanismo más importante de citotoxicidad de los NMs, hemos demostrado que en varios casos la citotoxicidad de los NMs no es directamente dependiente del estrés oxidativo.

10. Las diferencias interespecíficas en la sensibilidad a los efectos citotóxicos de los NMs podrían relacionarse con diferencias en la tolerancia de las células de mamíferos y peces a los iones metálicos liberados de los NMs.

11. Las líneas celulares de peces no muestran necesariamente una menor sensibilidad que las células mantenidas en cultivo primario frente a la toxicidad de los NMs, lo que hace de ellas unas valiosas herramientas para el estudio de la citotoxicidad de estas sustancias.

12. La administración de un NM de ZnO a peces a través de la dieta resultó en la acumulación preferencial de Zn en branquias e intestino. Además la llegada de Zn al hígado dio lugar a alteraciones en el equilibrio oxidativo que desaparecieron en la fase de depuración por la respuesta adaptativa del organismo.

13. La toxicidad de cada tipo de NM puede verse fuertemente influenciada por el tipo de agentes de superficie con los que se asocie, lo que abre la puerta a avances en la seguridad de los NMs a través del diseño.

References

Ahamed M, Siddiqui MA, O'Brien MJ, Ahmad I, Pant AB, Alhadlaq HA. 2010. Genotoxic potential of copper oxide nanoparticles in human lung epithelial cells. Biochem Biophys Res Commun. 396(2):578-83.

Akhtar MJ, Ahamed M, Fareed M, Alrokayan SA, Kumar S. 2012. Protective effect of sulphoraphane against oxidative stress mediated toxicity induced by CuO nanoparticles in mouse embryonic fibroblasts BALB 3T3. J Toxicol Sci. 7(1):139–48.

Akhtar MJ, Kumar S, Alhadlaq HA, Alrokayan SA, Abu-Salah KM, Ahamed M. 2016. Dose-dependent genotoxicity of copper oxide nanoparticles stimulated by reactive oxygen species in human lung epithelial cells. Toxicol Ind Health. 32(5):809-21.

Alam J, Stewart D, Touchard C, Boinapally S, Choi AM, Cook JL. 1999. Nrf2, a Cap'n'Collar transcription factor, regulates induction of the heme oxygenase-1 gene. J Biol Chem 274:26071–26078.

Al-Bairuty GA, Shaw BJ, Handy RD, Henry TB. 2013. Histopathological effects of waterborne copper nanoparticles and copper sulphate on the organs of rainbow trout (Oncorhynchus mykiss). Aquat Toxicol.126:104-15.

Alberts B, Johnson A, Lewis J, Raff M, Roberts K, Walter P, Eds. 2002. Molecular Biology of the Cell. 4th edition. New York: Garland Science.

Amara S, Slama IB, Mrad I, Rihane N, Khemissi W, El Mir L, Rhouma KB, Abdelmelek H, Sakly M. 2014. Effects of zinc oxide nanoparticles and/or zinc chloride on biochemical parameters and mineral levels in rat liver and kidney. Hum Exp Toxicol. 33(11):1150-7.

Arai Y, Miyayama T, Hirano S. 2014. Difference in the toxicity mechanism between ion and nanoparticle forms of silver in the mouse lung and in macrophages. Toxicology 328:84–92.

Aschberger K, Micheletti C, Sokull-Klüttgen B, Christensen FM. 2011. Analysis of currently available data for characterising the risk of engineered nanomaterials to the environment and human health--lessons learned from four case studies. Environ Int 37(6):1143-56.

Asharani PV, Lianwu Y, Gong Z, Valiyaveettil S. 2011. Comparison of the toxicity of silver, gold and platinum nanoparticles in developing zebrafish embryos. Nanotoxicology 5(1):43-54.

Auffan M, Rose J, Bottero JY, Lowry GV, Jolivet JP, Wiesner MR. 2009. Towards a definition of inorganic nanoparticles from an environmental, health and safety perspective. Nat Nanotechnol. 4(10):634-41.

Bal W, Christodoulou J, Sadler PJ, Tucker A.1998. Multi-metal binding site of serum albumin. J Inorg Biochem. 70(1):33-9.

Balasubramanian SK, Jittiwat J, Manikandan J, Ong CN, Yu LE, Ong WY. 2010. Biodistribution of gold nanoparticles and gene expression changes in the liver and spleen after intravenous administration in rats. Biomaterials. 31(8):2034-42.

Bargelloni, L, Scudiero R, Parisi E, Carginale V, Capasso C, Patarnello T. 1999. Metallothioneins in Antarctic fish: evidence for independent duplication and gene conversion. Mol. Biol. Evol. 16, 885–897.

Bar-Ilan O, Albrecht RM, Fako VE, Furgeson DY. 2009. Toxicity assessments of multisized gold and silver nanoparticles in zebrafish embryos. Small. 5(16):1897-910.

Bartee MY, Lutsenko S. 2007. Hepatic copper-transporting ATPase ATP7B: function and inactivation at the molecular and cellular level. Biometals 20:627–637

Bastús NG, Sánchez-Tilló E, Pujals S, Farrera C, Kogan MJ, Giralt E, Celada A, Lloberas J, Puntes V. 2009. Peptides conjugated to gold nanoparticles induce macrophage activation. Mol Immunol. 46(4):743-8.

Baun A, Hartmann NB, Grieger K, Kusk KO. 2008. Ecotoxicity of engineered nanoparticles to aquatic invertebrates: a brief review and recommendations for future toxicity testing. Ecotoxicology. 17(5):387-95.

Behra R, Sigg L, Clift MJ, Herzog F, Minghetti M, Johnston B, Petri-Fink A, Rothen-Rutishauser B. 2013. Bioavailability of silver nanoparticles and ions: from a chemical and biochemical perspective. J R Soc Interface 10(87):20130396.

Benn TM, Westerhoff P. 2008. Nanoparticle silver released into water from commercially available sock fabrics. Environ Sci Technol. 42(11):4133-9.

Berridge MV, Tan AS. 1993. Characterization of the cellular reduction of 3-(4,5-dimethylthiazol-2-yl)-2,5 diphenyltetrazolium bromide (MTT): subcellular localization, substrate dependence, and involvement of mitochondrial electron transport in MTT reduction. Arch Biochem Biophys. 303(2):474–82.

Bhise NS, Manoharan V, Massa S, Tamayol A, Ghaderi M, Miscuglio M, Lang Q, Shrike Zhang Y, Shin SR, Calzone G, Annabi N, Shupe TD, Bishop CE, Atala A, Dokmeci MR, Khademhosseini A. 2016. A liver-on-a-chip platform with bioprinted hepatic spheroids. Biofabrication 8(1):014101.

Bihari P, Vippola M, Schultes S, Praetner M, Khandoga AG, Reichel CA, Coester C, Tuomi T, Rehberg M, Krombach F. 2008. Optimized dispersion of nanoparticles for biological *in vitro* and *in vivo* studies. Part Fibre Toxicol. 5 (1):14-28.

Bolyard SC, Reinhart DR, Santra S. 2013. Behavior of engineered nanoparticles in landfill leachate. Environ Sci Technol. 47:8114–22

Bondarenko O, Juganson K, Ivask A, Kasemets K, Mortimer M, Kahru A. 2013. Toxicity of Ag, CuO and ZnO nanoparticles to selected environmentally relevant test organisms and mammalian cells *in vitro*: a critical review. Arch Toxicol. 87(7):1181-200.

Borenfreund and Puerner. 1985. A simple quantitative procedure using monolayer cultures for cytotoxicity assays (HTD/NR-90). Journal of tissue culture methods 9 (1):7-9.

Botelho MC, Costa C, Silva S, Costa S, Dhawan A, Oliveira PA, Teixeira JP. 2014. Effects of titanium dioxide nanoparticles in human gastric epithelial cells *in vitro*. Biomed Pharmacother. 68(1):59-64.

Boya P, Kroemer, G. 2008. Lysosomal membrane permeabilization in cell death. Oncogene 27: 6434–6451.

Boyle D, Al-Bairuty GA, Ramsden CS, Sloman KA, Henry TB, Handy RD. 2013. Subtle alterations in swimming speed distributions of rainbow trout exposed to titanium dioxide nanoparticles are associated with gill rather than brain injury. Aquat. Toxicol. 126 (X): 116–127.

Brown DM, Wilson MR, MacNee W, Stone V, Donaldson K. 2001. Size-dependent proinflammatory effects of ultrafine polystyrene particles: a role for surface area and oxidative stress in the enhanced activity of ultrafines. Toxicol Appl Pharmacol.175(3):191-9.

Brown DM, Kinloch AI, Bangert U, Windle HA, Walter MD, Walker SG, Scotchford CA, Donaldson K, Stone V. 2007. An *in vitro* study of the potential of carbon nanotubes and nanofibres to induce inflammatory mediators and frustrated phagocytosis. Carbon 45 (9):1743–1756.

Brown CL, Whitehouse MW, Tiekink ER, Bushell GR. 2008. Colloidal metallic gold is not bio-inert. Inflammopharmacology. 16(3):133-7.

Bystrzejewska-Piotrowska G, Golimowski J, Urban L. 2009. Nanoparticles: their potential toxicity, waste and environmental management. Waste Management. 29(9):2587–2595.

Campbell JK, Mills CF. 1979. The toxicity of zinc to pregnant sheep. Environ Res. 20(1):1-13.

Capasso C, Carginale V, Crescenzi O, Di Maro D, Parisi E, Spadaccini R, Temussi PA. 2003. Solution structure of MT_nc, a novel metallothionein from the Antarctic fish Notothenia coriiceps. Structure 11(4):435-43.

Cedervall T, Lynch I, Foy M, Berggård T, Donnelly SC, Cagney G, Linse S, Dawson KA. 2007. Detailed identification of plasma proteins adsorbed on copolymer nanoparticles. Angew Chem Int Ed Engl. 46(30):5754-6.

Celander MC, Goldstone JV, Denslow ND, Iguchi T, Kille P, Meyerhoff RD, Smith BA, Hutchinson TH, Wheeler JR. Species extrapolation for the 21st century. Environ Toxicol Chem. 30(1):52-63.

Chairuangkitti P, Lawanprasert S, Roytrakul S, Aueviriyavit S, Phummiratch D, Kulthong K, Chanvorachote P, Maniratanachote R. Silver nanoparticles induce toxicity in A549 cells via ROS-dependent and ROS-independent pathways. Toxicol In Vitro. 27(1):330-8.

Chen Z, Meng H, Xing G, Chen C, Zhao Y, Jia G, Wang T, Yuan H, Ye C, Zhao F, Chai Z, Zhu C, Fang X, Ma B, Wan L. 2006. Acute toxicological effects of copper nanoparticles *in vivo*. Toxicol Lett. 163(2):109-20.

Cho WS, Cho MJ, Jeong J, et al. 2009. Acute toxicity and pharmacokinetics of 13 nm-sized PEG-coated gold nanoparticles. Toxicol Appl Pharmacol. 236:16–24.

Cho WS, Duffin R, Poland CA, Howie SE, MacNee W, Bradley M, Megson IL, Donaldson K. 2010. Metal oxide nanoparticles induce unique inflammatory footprints in the lung: important implications for nanoparticle testing. Environ Health Perspect. 118(12):1699-706.

Cho WS, Duffin R, Howie SE, Scotton CJ, Wallace WA, Macnee W, Bradley M, Megson IL, Donaldson K. 2011. Progressive severe lung injury by zinc oxide nanoparticles; the role of Zn2+ dissolution inside lysosomes. Part Fibre Toxicol. 8:27.

Chen Z, Meng H, Xing G, Chen C, Zhao Y, Jia G, Wang T, Yuan H, Ye C, Zhao F, Chai Z, Zhu C, Fang X, Ma B, Wan L. 2006. Acute toxicological effects of copper nanoparticles *in vivo*. Toxicol Lett. 163(2):109-20.

Choi HS, Liu W, Misra P, Tanaka E, Zimmer JP, Itty Ipe B, Bawendi MG, Frangioni JV. 2007. Renal clearance of quantum dots. Nat Biotechnol. 25(10):1165-70.

Choi JE, Kim S, Ahn JH, Youn P, Kang JS, Park K, Yi J, Ryu DY. 2010. Induction of oxidative stress and apoptosis by silver nanoparticles in the liver of adult zebrafish. Aquat Toxicol. 100(2):151-9.

Colman BP, Arnaout CL, Anciaux S, Gunsch CK, Hochella MF Jr, Kim B, Lowry GV, McGill BM, Reinsch BC, Richardson CJ, Unrine JM, Wright JP, Yin L, Bernhardt ES. 2013. Low

Concentrations of Silver Nanoparticles in Biosolids Cause Adverse Ecosystem Responses under Realistic Field Scenario. PLoS One 8(2): e57189.

Connor EE, Mwamuka J, Gole A, Murphy CJ, Wyatt MD. 2005. Gold nanoparticles are taken up by human cells but do not cause acute cytotoxicity. Small 1(3):325-7.

Cooper MG. 2000a. Mitochondria. The Cell, 2nd edition A Molecular Approach Boston University Sunderland (MA): Sinauer Associates.

Cooper MG. 2000b. Structure of the Plasma Membrane. The Cell, 2nd edition A Molecular Approach Boston University Sunderland (MA): Sinauer Associates.

Coyle P, Zalewski PD, Philcox JC, Forbes IJ, Ward AD, Lincoln SF, Mahadevan I, Rofe AM. 1994. Measurement of zinc in hepatocytes by using a fluorescent probe, Zinquin: relationship to metallothionein and intracellular zinc. Biochem. J. 303 Pt 3):781-6.

Cuillel M, Chevallet M, Charbonnier P, Fauquant C, Pignot-Paintrand I, Arnaud J, Cassio D, Michaud-Soret I, Mintz E. 2014. Interference of CuO nanoparticles with metal homeostasis in hepatocytes under sub-toxic conditions. Nanoscale 6(3):1707-15.

D'Auria S, Carginale V, Scudiero R, Crescenzi O, Di Maro D, Temussi PA, Parisi E, Capasso C. 2001. Structural characterization and thermal stability of Notothenia coriiceps metallothionein. Biochem. J. 354:291–299.

Davis JM, Addison J, Bolton RE, Donaldson K, Jones AD, Smith T. 1986. The pathogenicity of long versus short fibre samples of amosite asbestos administered to rats by inhalation and intraperitoneal injection. Br J Exp Pathol. 67(3):415-30.

De Berardis B, Civitelli G, Condello M, Lista P, Pozzi R, Arancia G, Meschini S. 2010. Exposure to ZnO nanoparticles induces oxidative stress and cytotoxicity in human colon carcinoma cells. Toxicol Appl Pharmacol. 246(3):116-27.

De Jong WH, Hagens WI, Krystek P, Burger MC, Sips AJ, Geertsma RE. 2008. Particle size-dependent organ distribution of gold nanoparticles after intravenous administration. Biomaterials. 29:1912–9.

de la Fuente JM, Berry CC. 2005. Tat peptide as an efficient molecule to translocate gold nanoparticles into the cell nucleus. Bioconjug Chem. 16(5):1176-80.

de Planque MR, Aghdaei S, Roose T, Morgan H. 2011. Electrophysiological Characterization of Membrane Disruption by Nanoparticles. ACS Nano 5(5): 3599–3606.

Deng X, Luan Q, Chen W, Wang Y, Wu M, Zhang H, Jiao Z. Nanosized zinc oxide particles induce neural stem cell apoptosis. Nanotechnology 20(11):115101.

Derjaguin BV, Landau L.1941. Theory of the stability of strongly charged lyophobic sols and the adhesion of strongly charged particles in solutions of electrolytes. Acta Physicochim USSR 14:633–662.

Dietrich C. 2016. Antioxidant Functions of the Aryl Hydrocarbon Receptor. Stem Cells International. Volume 2016 Article ID 7943495.

Di Giulio T R, Linton ED. 2008. The toxicology of fishes. Boca Raton, CRC Press

Dineley KE, Votyakova TV, Reynolds IJ. 2003. Zinc inhibition of cellular energy production: implications for mitochondria and neurodegeneration. J Neurochem. 85(3):563-70.

Donaldson K, Stone V, Clouter A, Renwick L, MacNee W. 2001. Ultrafine particles. Occup. Environ. Med. 58:211-216.

Donaldson K, Tran CL. 2002. Inflammation caused by particles and fibers. Inhal Toxicol. 14(1):5-27.

Donaldson K, Stone V, Tran CL, Kreyling W, Borm PJA. 2004. Nanotoxicology. Occup Environ Med 61:727–8.

dos Santos T, Varela J, Lynch I, Salvati A, Dawson KA. 2011. Effects of transport inhibitors on the cellular uptake of carboxylated polystyrene nanoparticles in different cell lines. PLoS One 6(9):e24438.

ECETOC. 2005. The European Centre for Ecotoxicology and Toxicology of Chemicals WORKSHOP REPORT No. 7. Testing Strategies to Establish the Safety of Nanomaterials 7- 8 November 2005, Barcelona.

Edri E, Regev O. 2009. "Shaken, not stable": dispersion mechanism and dynamics of protein-dispersed nanotubes studied via spectroscopy. Langmuir. 25(18):10459-65.

Elechiguerra JL, Burt JL, Morones JR, Camacho-Bragado A, Gao X, Lara HH, Yacaman MJ. 2005. Interaction of silver nanoparticles with HIV-1. J Nanobiotechnology. 29:3:6.

Eom HJ, Choi J. 2009. Oxidative stress of silica nanoparticles in human bronchial epithelial cell, Beas-2B. Toxicol In Vitro. 23(7):1326-32.

Esch MB, Mahler GJ, Stokol T, Shuler ML. 2014. Body-on-a-chip simulation with gastrointestinal tract and liver tissues suggests that ingested nanoparticles have the potential to cause liver injury. Lab Chip. 14(16):3081-92.

European Commission 2009a. Commission Regulation (EC) No 134/2009 amending Regulation (EC) No. 1907/2006 of the European Parliament and of the Council on the Registration, Evaluation, Authorisation and Restriction of Chemicals (REACH) as regards Annex XI. Available online: http://eur-lex. europa.eu/legalcontent/EN/TXT/?qid=1401782624095&uri=CELEX:32009R0134

European Commission 2009b. Commission Regulation (EU) No. 1223/2009 of the European Parliament and the Council of 30 November 2009 on cosmetic products, Article 19(1)(g)), replacing the Cosmetics Directive (76/768/EEC). Available online: http://eur-lex.europa.eu/legal-content/EN/TXT/PDF/?uri=CELEX:32009R1223&from=EN

European Commission 2011. Commission recommendation 2011/696/EU of 18 October 2011 on the definition of nanomaterial. Available online: https://ec.europa.eu/research/industrial_technologies/pdf/policy/commission-recommendation-on-the-definition-of-nanomater-18102011_en.pdf

European Union 2011. Commission Recommendation of 18 October 2011 on the definition of nanomaterial (2011/696/EU).

Fabrega J, Luoma SN, Tyler CR, Galloway TS, Lead JR. 2011. Silver nanoparticles: behaviour and effects in the aquatic environment. Environ Int. 37(2):517–531.

Fahmy B, Cormier SA. 2009. Copper Oxide Nanoparticles Induce Oxidative Stress and Cytotoxicity in Airway Epithelial Cells. Toxicol In Vitro. 23(7): 1365–1371.

Fan W, Li Q, Yang X, Zhang L. 2013. Zn subcellular distribution in liver of goldfish (carassius auratus) with exposure to zinc oxide nanoparticles and mechanism of hepatic detoxification. PLoS One 8(11):e78123.

Federici G, Shaw BJ, Handy RD. 2007. Toxicity of titanium dioxide nanoparticles to rainbow trout (Oncorhynchus mykiss): gill injury, oxidative stress, and other physiological effects. Aquat Toxicol. 84(4):415-30.

Felbeck T, Behnke T, Hoffmann K, Grabolle M, Lezhnina MM, Kynast UH, Resch-Genger U. 2013. Nile-Red–Nanoclay Hybrids: Red Emissive Optical Probes for Use in Aqueous Dispersion. Langmuir 29(36):11489-97.

Ferin, J, Oberdörster G, Penney DP, Soderholm SC, Gelein R and Piper HC. 1990. Increased pulmonary toxicity of ultrafine particles? Journal of Aerosol Science 21 384-387.

Filippi C, Pryde A, Cowan P, Lee T, Hayes P, Donaldson K, Plevris J, Stone V. 2015. Toxicology of ZnO and TiO2 nanoparticles on hepatocytes: impact on metabolism and bioenergetics. Nanotoxicology. 9(1):126-34.

Fischer PW, Giroux A, L'Abbé MR. 1981. The effect of dietary zinc on intestinal copper absorption. Am J Clin Nutr. 34(9):1670-5.

Fischer PWF, Giroux A, L'Abbe MR. 1983. Effects of zinc on mucosal copper binding and on the kinetics of copper absorption. J. Nutr. 113:462–469.

Fosmire GJ.1990. Zinc toxicity. American Journal of Clinical Nutrition 51: 225.

Freedman JH, Peisach J.1989. Resistance of cultured hepatoma cells to copper toxicity. Purification and characterization of the hepatoma metallothionein. Biochim Biophys Acta. 992(2):145-54.

Fröhlich E, Meindl C, Roblegg E, Ebner B, Absenger M, Pieber TR. 2012. Action of polystyrene nanoparticles of different sizes on lysosomal function and integrity. Part Fibre Toxicol. 9:26.

Gao G, Ze Y, Zhao X, Sang X, Zheng L, Ze X, Gui S, Sheng L, Sun Q, Hong J, Yu X, Wang L, Hong F, Zhang X. 2013. Titanium dioxide nanoparticle-induced testicular damage, spermatogenesis suppression, and gene expression alterations in male mice. J Hazard Mater. 15; 258-259:133-43.

Gatoo MA, Naseem S, Arfat MY, Dar AM, Qasim K, Zubair S. 2014. Physicochemical properties of nanomaterials: implication in associated toxic manifestations. Biomed Res Int. 2014:498420.

George S, Pokhrel S, Xia T, Gilbert B, Ji Z, Schowalter M, Rosenauer A, Damoiseaux R, Bradley KA, Mädler L, Nel AE. 2010. Use of a Rapid Cytotoxicity Screening Approach to Engineer a Safer Zinc Oxide Nanoparticle through Iron Doping. ACS Nano 4(1): 15–29.

George S et al. 2011. Use of a high-throughput screening approach coupled with *in vivo* zebrafish embryo screening to develop hazard ranking for engineered nanomaterials ACS Nano 5:1805–17.

Geranio L, Heuberger M, Nowack B. 2009. The behavior of silver nanotextiles during washing. Environmental Science and Technology 43(21): p. 8113-8.

Gerloff K, Landesmann B, Munn S, Palosaari T, Worth A, Whelan M. 2015) Using AOPs to predict nanoparticle-induced liver toxicity. European Commission, Joint Research Centre,

Institute for Health and Consumer Protection, Ispra, Italy. (Poster, Eurotox 2015) https://eurl-ecvam.jrc.ec.europa.eu/posters-1/poster-eurotox-2015-nano-aop

Gibb S. 2010. Toxicity testing in the 21st century: A vision and a strategy. A review of the National Research Council report. Reproductive Toxicology 25 (1):136–138.

Gilbert B, Fakra SC, Xia T, Pokhrel S, Mädler L, Nel AE. 2012. The fate of ZnO nanoparticles administered to human bronchial epithelial cells. ACS Nano. 6(6):4921-30.

Goodman CM, McCusker CD, Yilmaz T, Rotello VM. 2004. Toxicity of gold nanoparticles functionalized with cationic and anionic side chains. Bioconjug Chem. 15(4):897-900.

Gottschalk F, Kost E, Nowack B. 2013. Engineered nanomaterials in water and soils: a risk quantification based on probabilistic exposure and effect modeling. Environ Toxicol Chem. 32(6):1278-87.

Griffitt RJ, Weil R, Hyndman KA, Denslow ND, Powers K, Taylor D, Barber DS. 2007. Exposure to copper nanoparticles causes gill injury and acute lethality in zebrafish (Danio rerio). Environ. Sci. Technol. 41 (23):8178–8186.

Grosell M, Blanchard J, Brix KV, Gerdes R. 2007. Physiology is pivotal for interactions between salinity and acute copper toxicity to fish and invertebrates. Aquat Toxicol. 84(2):162-72.

Guo LL., Liu XH., Qin DX., Gao L, Zhang HM, Liu JY, Cui YG. 2009. Effects of nanosized titanium dioxide on the reproductive system of male mice. National Journal of Andrology. 15(6): 517-522

Hall AC, Young BW, Bremner I. 1979. Intestinal metallothionein and the mutual antagonism between copper and zinc in the rat. J Inorg Biochem 11:57–66.

Han X, Gelein R, Corson N, Wade-Mercer P, Jiang J, Biswas P, Finkelstein JN, Elder A, Oberdörster G. 2011.Validation of an LDH Assay for Assessing Nanoparticle Toxicity. Toxicology. 287: 99–104.

Hanagata N, Zhuang F, Connolly S, Li J, Ogawa N, Xu M. 2011. Molecular responses of human lung epithelial cells to the toxicity of copper oxide nanoparticles inferred from whole genome expression analysis. ACS Nano 5(12):9326-38.

Handy RD, Sims DW, Giles A, Campbell HA, Musonda MM. 1999. Metabolic trade-off between locomotion and detoxification for maintenance of blood chemistry and growth parameters by rainbow trout (*Oncorhynchus mykiss*) during chronic dietary exposure to copper. AquatToxicol 47:23–41.

Handy RD, Owen R, Valsami-Jones E. 2008a. The ecotoxicology of nanoparticles and nanomaterials: current status, knowledge gaps, challenges, and future needs. Ecotoxicology. 17(5):315-25.

Handy R, Henry T, Scown T, Johnston B, Tyler, C. 2008b. Manufactured nanoparticles: their uptake and effects on fish-a mechanistic analysis. Ecotoxicology 17(5):396-409.

Hao L, Chen L, Hao J, Zhong N. 2013. Bioaccumulation and sub-acute toxicity of zinc oxide nanoparticles in juvenile carp (*Cyprinus carpio*): a comparative study with its bulk counterparts. Ecotoxicol Environ Saf. 91:52-60.

Hartung, T. 2011. From alternative methods to a new toxicology. Eur.J. Pharm. Biopharm. 77:338–349.

Hartung T, Luechtefeld T, Maertens A and Kleensang A. 2013. Food for Thought … Integrated Testing Strategies for Safety Assessments. ALTEX 30(1): 3–18.

Hébert CD, Elwell MR, Travlos GS, Fitz CJ, Bucher JR. 1993. Subchronic toxicity of cupric sulfate administered in drinking water and feed to rats and mice. Fundam Appl Toxicol 21: 461–475.

Hennebert P, Avellan A, Yan J, Aguerre-Chariol O. 2013. Experimental evidence of colloids and nanoparticles presence from 25 waste leachates. Waste Manag. 33(9):1870-81.

Hernández-Moreno D, Li L, Connolly M, Conde E, Fernández M, Schuster M, Navas JM, Fernández-Cruz ML. 2016. Mechanisms underlying the enhancement of toxicity caused by the Co-incubation of ZnO and Cu nanoparticles in a fish hepatoma cell line. Environ Toxicol Chem. 35(10):2562-2570.

Hielscher T. 2005. Ultrasonic Production of Nano-Size Dispersions and Emulsions. ENS 2005, Paris, France. TIMA Editions, pp.138-143. https://hal.archives-ouvertes.fr/hal-00166996/document

Hirasawa F, Sato M, Takizawa Y. 1994. Organ distribution of silver and the effect of silver on copper status in rats. Toxicol Lett. 70(2):193-201.

Hogstrand C, Wood CM. 1996. The physiology and toxicology of zinc in fish. In Aquatic Toxicology (ed. E. W. Taylor), pp. 61–84. Cambridge: Cambridge University Press.

Holder AL, Goth-Goldstein R, Lucas D, Koshland CP.Particle-induced artifacts in the MTT and LDH viability assays. Chem Res Toxicol. 2012 Sep 17; 25(9):1885-92.

Hong S, Bielinska AU, Mecke A, Keszler B, Beals JL, Shi X, Balogh L, Orr BG, Baker JR Jr, Banaszak Holl MM. 2004. Interaction of poly(amidoamine) dendrimers with supported lipid bilayers and cells: hole formation and the relation to transport. Bioconjug Chem. 15(4):774-82.

Hsiao IL, Huang YJ. 2011. Effects of various physicochemical characteristics on the toxicities of ZnO and TiO nanoparticles toward human lung epithelial cells. Sci Total Environ. 409(7):1219-28.

Hsin YH, Chen CF, Huang S. et al. 2008. The apoptotic effect of nanosilver is mediated by a ROS- and JNK-dependent mechanism involving the mitochondrial pathway in NIH3T3 cells. Toxicology Letters 179:130– 139.

Hua J, Vijver MG, Ahmad F, Richardson MK, Peijnenburg WJ. 2014. Toxicity of different-sized copper nano- and submicron particles and their shed copper ions to zebrafish embryos. Environ Toxicol Chem. 33(8):1774-82.

Huang CC, Aronstam RS, Chen DR, Huang YW. 2010. Oxidative stress, calcium homeostasis, and altered gene expression in human lung epithelial cells exposed to ZnO nanoparticles. Toxicol In Vitro 24(1):45-55.

Huang X, Teng X, Chen D, Tang F, He J. 2010. The effect of the shape of mesoporous silica nanoparticles on cellular uptake and cell function. Biomaterials. 31(3):438-48.

Hunter RJ. 2001. Foundations of colloid science. Oxford University Press, New York

Huotari J, Helenius A. 2011. Endosome maturation. EMBO J. 30(17):3481-500.

Hussain SM, Hess KL, Gearhart JM, Geiss KT, Schlager JJ. 2005. *In vitro* toxicity of nanoparticles in BRL 3A rat liver cells. Toxicol In Vitro. 19(7):975-83.

Isani, G., Carpenè, E., 2014. Metallothioneins, unconventional proteins from unconventional animals: a long journey from nematodes to mammals. Biomolecules 4(2): 435–457.

ISO 2016. International Standardization Organization. https://www.iso.org/obp/ui/#iso:std:iso:tr:16196:ed-1:v1:en:term:3.4.

Itoh K, Ishii T, Wakabayashi N, Yamamoto M. 1999. Regulatory mechanisms of cellular response to oxidative stress. Free Radic Res 31:319–324.

Jensen KA, Kembouche Y, Christiansen E, Jacobsen NR, Wallin H, Guiot C, Spalla O, Witschger O. 2011. Final Protocol for producing suitable manufactured nanomaterial exposure media. NANOGENOTOX deliverable report n°3: 34.

Jiang X, Miclăuş T, Wang L, Foldbjerg R, Sutherland DS, Autrup H, Chen C, Beer C. 2015. Fast intracellular dissolution and persistent cellular uptake of silver nanoparticles in CHO-K1 cells: implication for cytotoxicity. Nanotoxicology 9(2):181-9.

Johnston HJ, Semmler-Behnke M, Brown DM, Kreyling W, Tran L, Stone V. 2010. Evaluating the uptake and intracellular fate of polystyrene nanoparticles by primary and hepatocyte cell lines *in vitro*. Toxicol Appl Pharmacol. 242(1):66-78.

Jones N, Ray B, Ranjit KT, Manna AC. 2008. Antibacterial activity of ZnO nanoparticle suspensions on a broad spectrum of microorganisms. FEMS Microbiol Lett. 279(1):71-6.

Kao YY, Chen YC, Cheng TJ, Chiung YM, Liu PS. 2012. Zinc Oxide Nanoparticles Interfere With Zinc Ion Homeostasis to Cause Cytotoxicity. Toxicol Sci. 125(2):462-72.

Kang T, Guan R, Chen X, Song Y, Jiang H, Zhao J. *In vitro* toxicity of different-sized ZnO nanoparticles in Caco-2 cells. Nanoscale Res Lett. 2013 Nov 21;8(1):496.

Karlsson HL, Cronholm P, Gustafsson J, Möller L. 2008. Copper oxide nanoparticles are highly toxic: a comparison between metal oxide nanoparticles and carbon nanotubes. Chem Res Toxicol. 21(9):1726-32.

Karlsson HL, Cronholm P, Hedberg Y, Tornberg M, De Battice L, Svedhem S, Wallinder IO. 2013. Cell membrane damage and protein interaction induced by copper containing nanoparticles--importance of the metal release process. Toxicology. 313(1):59-69.

Kashiwada S. 2006. Distribution of nanoparticles in the see-through medaka (Oryzias latipes). Environ Health Perspect. 114(11):1697-702.

Kashiwada S, Ariza ME, Kawaguchi T, Nakagame Y, Jayasinghe BS, Gärtner K, Nakamura H, Kagami Y, Sabo-Attwood T, Ferguson PL, Chandler GT. 2012. Silver nanocolloids disrupt medaka embryogenesis through vital gene expressions. Environ Sci Technol. 46(11):6278-87.

Kathawala MH, Ng KW, Loo SCJ. 2015. TiO2 nanoparticles alleviate toxicity by reducing free Zn2+ ion in Human Primary Epidermal Keratinocytes exposed to ZnO nanoparticles. Journal of Nanoparticle Research 17:263.

Keller AA, McFerran S, Lazareva A, Suh S. 2013. Global life cycle releases of engineered nanomaterials. J Nanopart Res 15(6).

Kermanizadeh A, Gaiser BK, Ward MB, Stone V. 2013. Primary human hepatocytes versus hepatic cell line: assessing their suitability for *in vitro* nanotoxicology. Nanotoxicology 7(7):1255-71.

Kermanizadeh A, Pojana G, Gaiser BK, Birkedal R, Bilanicová D, Wallin H, Jensen KA, Sellergren B, Hutchison GR, Marcomini A, Stone V. 2013. *In vitro* assessment of engineered nanomaterials using a hepatocyte cell line: cytotoxicity, pro-inflammatory cytokines and functional markers. Nanotoxicology. 7(3):301-13.

Kettler K, Veltman K, van de Meent D, van Wezel A, Hendriks AJ. 2014. Cellular uptake of nanoparticles as determined by particle properties, experimental conditions, and cell type. Environ Toxicol Chem. 33(3):481-92.

Kim, YS, Kim JS, Cho HS, Rha DS, Kim JM, Park JD, Choi BS, Lim R, Chang HK, Chung YH, Kwon IH, Jeong J, Han BS, and Yu IJ. 2008. Twenty-eight-day oral toxicity, genotoxicity, and gender-related tissue distribution of silver nanoparticles in Sprague-Dawley rats. Inhalation toxicology 20(6):575-83.

Kim J, Kim S, Lee S. 2011. Differentiation of the toxicities of silver nanoparticles and silver ions to the Japanese medaka (Oryzias latipes) and the cladoceran Daphnia magna. Nanotoxicology. 5(2):208-14.

Kim JA, Åberg C, Salvati A, Dawson KA. 2012. Role of cell cycle on the cellular uptake and dilution of nanoparticles in a cell population. Nat Nanotechnol. 7(1):62–68.

Kipen HM, Laskin DL. 2005. Smaller is not always better: nanotechnology yields nanotoxicology. Am J Physiol Lung Cell Mol Physiol. 289(5):L696-7.

Klaine SJ, Alvarez PJ, Batley GE, Fernandes TF, Handy RD, Lyon DY, Mahendra S, McLaughlin MJ, Lead JR. 2008. Nanomaterials in the environment: behavior, fate, bioavailability, and effects. Environ Toxicol Chem. 27(9):1825-51.

Klotz LO, Sies H. 2009. Cellular generation of oxidants: relation to oxidative stress. In Redox signaling and regulation in biology and medicine. Jacob C, Winyard PG, eds, pp 45–61. Wiley-VCH Verlag, Weinheim, Germany.

Kong B, Seog JH, Graham LM, Lee SB. 2011. Experimental considerations on the cytotoxicity of nanoparticles. Nanomedicine (Lond). 6(5): 929–941.

Kulthong K, Maniratanachote R, Kobayashi Y, Fukami T, Yokoi T. 2012. Effects of silver nanoparticles on rat hepatic cytochrome P450 enzyme activity. Xenobiotica. 42(9):854-62.

Kusters KA, Pratsinis SE, Thoma SG, Smith DM. 1993. Ultrasonic fragmentation of agglomerate powders. Chem Eng Sci. 48(24):4119–4127.

Kwon JT, Hwang SK, Jin H, Kim DS, Minai-Tehrani A, Yoon HJ, Choi M, Yoon TJ, Han DY, Kang YW, Yoon BI, Lee JK, Cho MH. 2008. Body distribution of inhaled fluorescent magnetic nanoparticles in the mice. J Occup Health. 50(1):1-6.

L'Abbé MR, Fischer PW. 1984. The effects of high dietary zinc and copper deficiency on the activity of copper-requiring metalloenzymes in the growing rat. J Nutr.114(5):813-22.

Lam CW, James JT, McCluskey R, Hunter RL. 2004. Pulmonary toxicity of single-wall carbon nanotubes in mice 7 and 90 days after intratracheal instillation. Toxicol Sci. 77(1):126-34.

Lamb JG, Hathaway LB, Munger MA, Raucy JL, Franklin MR. 2010. Nanosilver particle effects on drug metabolism *in vitro*. Drug Metab Dispos 38:2246–2251.

Lammel T, Boisseaux P, Fernández-Cruz ML, Navas JM. 2013. Internalization and cytotoxicity of graphene oxide and carboxyl graphene nanoplatelets in the human hepatocellular carcinoma cell line Hep G2. Part Fibre Toxicol. 10:27.

Lara HH, Ayala-Núñez VN, Turrent IC del L, Padilla RC. 2010. Bactericidal effect of silver nanoparticles against multidrug-resistant bacteria. World Journal of Microbiology and Biotechnology 26 (4):615-621.

Laurén DJ, McDonald DG. 1986. Influence of water hardness, pH and alkalinity on the mechanisms of copper toxicity in juvenile rainbow trout, Salmo gairdneri. Can. J. Fish. aquat. Sci. 43:1488–1496.

Lee J, Pena MM, Nose Y, Thiele DJ. 2002. Biochemical characterization of the human copper transporter Ctr1. J Biol Chem. 277:4380–4387.

Lee WM, Kim SW, Kwak JI, Nam SH, Shin YJ, An YJ. 2010. Research Trends of Ecotoxicity of Nanoparticles in Soil Environment. Toxicol Res. Dec; 26(4): 253–259.

Levard C, Hotze EM, Lowry GV, Brown GE Jr. 2012. Environmental Transformations of Silver Nanoparticles: Impact on Stability and Toxicity. Environ Sci Technol. 46(13):6900-14.

Li N, Hao M, Phalen RF, Hinds WC, Nel AE. 2003. Particulate air pollutants and asthma: a paradigm for the role of oxidative stress in PM-induced adverse health effects. Clin Immunol.109:250–265.

Li N, Sioutas C, Cho A, Schmitz D, Misra C, Sempf J, Wang M, Oberley T, Froines J, Nel A. 2003. Ultrafine particulate pollutants induce oxidative stress and mitochondrial damage. Environ Health Perspect. 111(4):455-60.

Li Z, Hulderman T, Salmen R, Chapman R, Leonard SS, Young SH, Shvedova A, Luster MI, Simeonova PP. 2007. Cardiovascular Effects of Pulmonary Exposure to Single-Wall Carbon Nanotubes. Environ Health Perspect. 115(3): 377–382

Li N, Xia T, Nel EA. 2008. The Role of Oxidative Stress in Ambient Particulate Matter-induced Lung Diseases and Its Implications in the Toxicity of Engineered Nanoparticles. Free Radic Biol Med. 44(9): 1689–1699.

Li Jia-han, Liu Xiao-rong, Zhang Yue, Tian Fang-fang, Zhao Guang-yuan Yu, Qiu-li-yang, Jiang Feng-lei, Liu Yi. 2012. Toxicity of nano zinc oxide to mitochondria. Toxicol. Res. 1:137-144.

Li L, Fernández-Cruz ML, Connolly M, Schuster M, Navas JM. 2015. Dissolution and aggregation of Cu nanoparticles in culture media: Effects of incubation temperature and particles size. J Nano Res 17:1–11.

Lin D, Xing B. 2007. Phytotoxicity of nanoparticles: inhibition of seed germination and root growth. Environ. Pollut. 150:243–250.

Lin W, Xu Y, Huang CC, Ma Y, Shannon BK, Chen DR, Huang YW. 2009. Toxicity of nano- and micro-sized ZnO particles in human lung epithelial cells. Journal of Nanoparticle Research, 11(1):25-39.

Lin W, Xu Y, Huang CC, Ma Y, Shannon BK, Chen DR, Huang YW. 2009. Toxicity of nano- and micro-sized ZnO particles in human lung epithelial cells. Journal of Nanoparticle Research, 11(1):25-39.

Liner MC, Hazeghazam M. 1996. Copper biochemistry and molecular biology. American Journal of Clinical Nutrition 63:797-811.

Limbach LK, Wick P, Manser P, Grass RN, Bruinink A, Stark WJ. 2007. Exposure of engineered nanoparticles to human lung epithelial cells: influence of chemical composition and catalytic activity on oxidative stress. Environ Sci Technol. 41(11):4158-63.

Lomer MC, Hutchinson C, Volkert S, Greenfield SM, Catterall A, Thompson RP, Powell JJ. 2004. Dietary sources of inorganic microparticles and their intake in healthy subjects and patients with Crohn's disease. Br J Nutr. 92(6):947-55.

Loza K, et al. 2014. The dissolution and biological effects of silver nanoparticles in biological media. J Mater Chem B 2:1634–1643.

Lu SC. 2013. Glutathione synthesis. Biochim Biophys. Acta. 1830:3143–3153.

Lubick N. 2008. Nanosilver toxicity: ions, nanoparticles--or both? Environ Sci Technol.42(23):8617.

Ma H, Kabengi NJ, Bertsch PM, Unrine JM, Glenn TC, Williams PL. 2011. Comparative phototoxicity of nanoparticulate and bulk ZnO to a free-living nematode Caenorhabditis elegans: The importance of illumination mode and primary particle size. Environ Pollut. 159(6):1473-80.

Ma Q, Kinneer K, Bi Y, Chan YJ, Kan WY. 2004. Induction of murine NAD(P)H:quinone oxidoreductase by 2,3,7,8- tetrachlorodibenzo-p-dioxin requires the CNC (cap ‘n’ collar) basic leucine zipper transcription factor Nrf2 (nuclear factor erythroid 2-related factor 2): cross-interaction between AhR (aryl hydrocarbon receptor) and Nrf2 signal transduction. Biochemical Journal, 377 (1): 205–213.

Marcone GPS, Oliveira AC, Almeida G, Umbuzeiro GA, Jardim WF. 2012. Ecotoxicity of TiO2 to Daphnia similis under irradiation. Journal of Hazardous Materials 211:436-442.

Massey GA, Thompson RN, Johnson GFB. 1975. The Chemistry of Copper, Silver and Gold: Pergamon International Library of Science, Technology, Engineering and Social Studies. Elsevier, 6 Jun 2016 - Technology & Engineering – Pergamon texts in inorganic chemistry, Volume 17.

Meng H, Chen Z, Xing G, Yuan H, Chen C, Zhao F, Zhang C, Zhao Y. 2007. Ultrahigh reactivity provokes nanotoxicity: explanation of oral toxicity of nano-copper particles. Toxicol Lett. 175(1-3):102-10.

Minocha S, Mumper RJ. 2012. Effect of carbon coating on the physico-chemical properties and toxicity of copper and nickel nanoparticles. Small 8(21):3289-99.

Miyayama T, Arai Y, Suzuki N, Hirano S. 2014. Cellular distribution and behavior of metallothionein in mammalian cells following exposure to silver nanoparticles and silver ions. Yakugaku zasshi journal of the Pharmaceutical Society of Japan 134(6):723-9.

Miyayama T, Matsuoka M. 2016. Involvement of lysosomal dysfunction in silver nanoparticle-induced cellular damage in A549 human lung alveolar epithelial cells. J Occup Med Toxicol. 11:1.

Montes-Burgos I, Walczyk D, Hole P, Smith J, Lynch I, Dawson K. 2010. Characterisation of nanoparticle size and state prior to nanotoxicological studies. J. Nanopart. Res. 12:47–53.

Moore MN. 2006. Do nanoparticles present ecotoxicological risks for the health of the aquatic environment? Environ Int. 32(8):967-76.

Moos PJ, Chung K, Woessner D, Honeggar M, Cutler NS, Veranth JM. 2010. ZnO particulate matter requires cell contact for toxicity in human colon cancer cells. Chem. Res. Toxicol. 23, 733–739.

Mosmann T. 1983. Rapid colorimetric assay for cellular growth and survival: application to proliferation and cytotoxicity assays. J Immunol Methods 65(1-2):55-63.

Mukherjee SG, O'Claonadh N, Casey A, Chambers G. 2012. Comparative *in vitro* cytotoxicity study of silver nanoparticle on two mammalian cell lines. Toxicol In Vitro 26(2):238-51.

Muller J, Huaux F, Moreau N, Misson P, Heilier JF, Delos M, Arras M, Fonseca A, Nagy JB, Lison D. 2005. Respiratory toxicity of multi-wall carbon nanotubes. Toxicol Appl Pharmacol. 207(3):221-31.

Murdock RC, Braydich-Stolle L, Schrand AM, Schlager JJ, Hussain SM, 2008. Characterization of nanomaterial dispersion in solution prior to *in vitro*. Toxicol Sci 101(2):239-53.

Nativo P, Prior IA., Brust M. 2008. Uptake and intracellular fate of surface-modified gold nanoparticles. ACS Nano 2:1639–1644.

Nel A, Xia T, Mädler L, Li N. 2006. Toxic potential of materials at the nanolevel. Science. 311(5761):622-7.

Nel A, Xia T, Meng H, Wang X, Lin S, Ji Z, Zhang H. 2013. Nanomaterial toxicity testing in the 21st century: use of a predictive toxicological approach and high-throughput screening. Acc Chem Res. 46(3):607-21.

Nielson BK, Wing RD. 1984. Preferential Binding of Copper to the /3 Domain of Metallothione. 259 (8):4941-4946.

Nogueira V, Lopes I, Rocha-Santos T, Santos AL, Rasteiro GM, Antunes F, Gonçalves F, Soares AM, Cunha A, Almeida A, Gomes NC, Pereira R. 2012. Impact of organic and inorganic nanomaterials in the soil microbial community structure. Sci Total Environ. 424:344-50.

NRC. 2007. Toxicity Testing in the 21st Century: A Vision and a Strategy. The National Academies Press, Washington, DC

O'Brien J, Wilson I, Orton T, Pognan F. 2000. Investigation of the Alamar Blue (resazurin) fluorescent dye for the assessment of mammalian cell cytotoxicity. Eur J Biochem. 267:5421–6.

Oberdörster G. 2001. Pulmonary effects of inhaled ultrafine particles. Int Arch Occup Environ Health. 74(1):1-8.

Oberdörster G, Sharp Z, Atudorei V, Elder A, Gelein R, Kreyling W, Cox C. 2004. Translocation of inhaled ultrafine particles to the brain. Inhal Toxicol. 16(6-7):437-45.

Oberdörster G, Oberdörster E, Oberdörster J. 2005. Nanotoxicology: an emerging discipline evolving from studies of ultrafine particles. Environ Health Perspect. 113(7):823-39.

OECD 1992. Guidelines for the Testing of Chemicals, Section 2 Effects on Biotic Systems. Test No. 203: Fish, Acute Toxicity Test. Adopted 17th July 1992. Available online:

http://www.oecdilibrary.org/docserver/download/9720301e.pdf?expires=1436362448&id=id&accname=guest&checksum=A8D02C36BBB106A6AA1FA284F655CE33.

OECD 1998. Guidelines for the Testing of Chemicals, Section 2 Effects on Biotic Systems. Test No. 212: Fish, Short-term Toxicity Test on Embryo and Sac-Fry Stages. Adopted 21st September 1998. Available online: http://www.oecdilibrary.org/docserver/download/9721201e.pdf?expires=1436362738&id=id&accname=guest&checksum=F759653EEFDFD5DEDC2105187004CE09.

OECD 2000. Guidelines for the Testing of Chemicals, Section 2 Effects on Biotic Systems. Test No. 215: Fish, Juvenile Growth Test. Adopted 21st Jan 2000. Available online: http://www.oecdilibrary.org/docserver/download/9721501e.pdf?expires=1436363070&id=id&accname=guest&checksum=5BBF1412C8B2D2E39FD8CCEB911DD902.

OECD 2004. ENV/JM/MONO(2003)15 Description of selected key generic terms used in chemical hazard/risk assessment. OECD Environment, Health and Safety Publications, Series on testing and assessment Number 44.

OECD 2010. ENV/JM/MONO(2010)46 Series on the Safety of Manufactured Nanomaterials No. 27 List of manufactured nanomaterials and list of endpoints for phase one of the sponsorship programme for the testing of manufactured nanomaterials: Revison.

OECD 2012a.Guidance on sample preparation and dosimetry for the safety testing of manufactured nanomaterials. Series on the Safety of Manufactured Nanomaterials No. 36. ENV/JM/MONO(2012)40 Available at : http://www.oecd.org/officialdocuments/publicdisplaydocumentpdf/?cote=ENV/JM/MONO(2012)40&docLanguage=En

OECD 2012b. The Adverse Outcome Pathway for Skin Sensitisation Initiated by Covalent Binding to Proteins. Part 1: Scientific Evidence. Series on Testing and Assessment No. 16 (OECD 2012): http://www.oecd.org/officialdocuments/publicdisplaydocumentpdf/?cote=ENV/JM/MONO(2012)10/PART1&docLanguage=En

OECD 2012c. Guidelines for the Testing of Chemicals, Section 2 Effects on Biotic Systems. Test No. 305: Bioaccumulation in Fish: Aqueous and Dietary Exposure. Adopted 2nd Oct 2012. Available online: http://www.oecdilibrary.org/docserver/download/9712191e.pdf?expires=1436363216&id=id&accname=guest&checksum=F04B9E2E4FEE60D3DDE42C037B8BDFD4.

OECD 2014. ENV/JM/MONO(2014)1 Series on the safety of manufactured nanomaterilas No. 40. Ecotoxicity and environmental fate of manufactured nanomaterials: Test guidelines. Expert meeting report. Available online: http://www.oecd.org/officialdocuments/publicdisplaydocumentpdf/?cote=ENV/JM/MONO%282014%291&doclanguage=en

Ong KJ, MacCormack TJ, Clark RJ, Ede JD, Ortega VA, Felix LC, Dang MKM, Ma GB, Fenniri H, Veinot JGC, Goss GG. 2014. Widespread nanoparticle-assay interference: implications for nanotoxicity testing. PLoS One 9(3) e90650.

Osredkar J, Sustar N. 2011. Copper and Zinc, Biological Role and Significance of Copper/Zinc Imbalance. J Clinic Toxicol S3:001.

Pan Y, Neuss S, Leifert A, Fischler M, Wen F, Simon U, Schmid G, Brandau W, Jahnen-Dechent W. 2007. Size-dependent cytotoxicity of gold nanoparticles. Small. 3(11):1941-9.

Park EJ, Yi J, Kim Y, Choi K, Park K. 2010. Silver nanoparticles induce cytotoxicity by a Trojan-horse type mechanism. Toxicol In Vitro 97: 34–41.

Park MVDZ, Neigh AM, Vermeulen JP. et al. 2011. The effect of particle size on the cytotoxicity, inflammation, developmental toxicity and genotoxicity of silver nanoparticles. Biomaterials 32: 9810-9817.

Park K. 2013.Toxicokinetic differences and toxicities of silver nanoparticles and silver ions in rats after single oral administration. J Toxicol Environ Health A. 76(22):1246-60.

Petros R, DeSimone J. 2010. Strategies in the design of nanoparticles for therapeutic applications. Nat. Rev. Drug Discovery 9:615–627.

Piao MJ, Kang KA, Lee IK, Kim HS, Kim S, Choi JY, Choi J, Hyun JW. 2011. Silver nanoparticles induce oxidative cell damage in human liver cells through inhibition of reduced glutathione and induction of mitochondria-involved apoptosis. Toxicol. Lett. 201:92–100.

Pietroiusti A, Massimiani M, Fenoglio I, Colonna M, Valentini F, Palleschi G, Camaioni A, Magrini A, Siracusa G, Bergamaschi A, Sgambato A, Campagnolo L. 2011. Low doses of pristine and oxidized single-wall carbon nanotubes affect mammalian embryonic development. ACS Nano. 5(6):4624-33.

Piret JP, Vankoningsloo S, Mejia J, Noël F, Boilan E, Lambinon F, Zouboulis CC, Masereel B, Lucas S, Saout C, Toussaint O. 2012. Differential toxicity of copper (II) oxide nanoparticles of similar hydrodynamic diameter on human differentiated intestinal Caco-2 cell monolayers is correlated in part to copper release and shape. Nanotoxicology 6(7):789-803.

Poland CA, Duffin R, Kinloch I, Maynard A, Wallace WA, Seaton A, Stone V, Brown S, Macnee W, Donaldson K. 2008. Carbon nanotubes introduced into the abdominal cavity of mice show asbestos-like pathogenicity in a pilot study. Nat Nanotechnol. 3(7):423-8.

Potera C. 2010. Nanomaterials: Transformation of Silver Nanoparticles in Sewage Sludge. Environ Health Perspect. 118(12): A526–A527.

Powell JJ, Faria N, Thomas-McKay E, Pele LC. 2010. Origin and fate of dietary nanoparticles and microparticles in the gastrointestinal tract. J Autoimmun 34: J226–J233

Powers KW, Brown SC, Krishna VB, Wasdo SC, Moudgil BM, Roberts SM. 2006. Research strategies for safety evaluation of nanomaterials. Part VI. Characterization of nanoscale particles for toxicological evaluation. Toxicol Sci. 90(2):296-303.

Pujalté I, Passagne I, Brouillaud B, Tréguer M, Durand E, Ohayon-Courtès C, L'Azou B. 2011. Cytotoxicity and oxidative stress induced by different metallic nanoparticles on human kidney cells. Part Fibre Toxicol. 3:8:10.

Raghupathi KR, Koodali RT, Manna AC. 2011. Size-dependent bacterial growth inhibition and mechanism of antibacterial activity of zinc oxide nanoparticles. Langmuir. 27(7):4020-8.

Rai MK, Deshmukh SD, Ingle AP, Gade AK. 2012. Silver nanoparticles: the powerful nanoweapon against multidrug-resistant bacteria. J Appl Microbiol.112(5):841-52.

Ramaiahgari SC, den Braver MW, Herpers B, Terpstra V, Commandeur JN, van de Water B, Price LS. 2014. A 3D *in vitro* model of differentiated HepG2 cell spheroids with improved liver‐like properties for repeated dose high‐throughput toxicity studies. Arch Toxicol. 88(5):1083-95.

Ramsden CS, Smith TJ, Shaw BJ, Handy RD. 2009. Dietary exposure to tita-nium dioxide nanoparticles in rainbow trout, (*Oncorhynchus mykiss*): no effecton growth, but subtle biochemical disturbances in the brain. Ecotoxicology 18,939–951.

Rauscher H, Roebben G, Amenta V, Sanfeliu AB, Calzolai L, Emons H, Gaillard C, Gibson N, Linsinger T, Mech A, Pesudo QL, Rasmussen K, Sintes RJ, Sokull-Klüttgen B, Stamm H. 2015. Towards a review of the EC Recommendation for a definition of the term "nanomaterial" Part 1: Compilation of information concerning the experience with the definition. Available online: https://ec.europa.eu/jrc/sites/default/files/lbna26567enn.pdf

Rau MA, Whitaker J, Freedman JH, Di Giulio RT. 2004. Differential susceptibility of fish and rat liver cells to oxidative stress and cytotoxicity upon exposure to prooxidants. Comp Biochem Physiol C Toxicol Pharmacol.137(4):335-42.

Reed RB, Ladner DA, Higgins CP, Westerhoff P, Ranville JF. 2012. Solubility of nano-zinc oxide in environmentally and biologically important matrices. Environ Toxicol Chem. 31(1): 93–99.

Reeves JF, Davies SJ, Dodd NJ, Jha AN. 2008. Hydroxyl radicals (*OH) are associated with titanium dioxide (TiO(2)) nanoparticle-induced cytotoxicity and oxidative DNA damage in fish cells. Mutat Res. 640(1-2):113-22.

Royal Society and Royal Academy of Engineering 2004. Nanoscience and nanotechnologies: opportunities and uncertainties. RS Policy document 19/04. Royal Society: London. Available at: www.nanotec.org.uk/

Russell WMS, Burch RL. 1959. (reprinted 1992): The Principles of Humane Experimental Technique. London: Methuen, 69-154 Universities Federation for Animal Welfare: Wheathampstead, UK.

Ryter SW, Kim HP, Hoetzel A, Park JW, Nakahira K, Wang X et al. 2007. Mechanisms of cell death in oxidative stress. Antioxid Redox Signal 9:49–89.

Sabella S, Carney RP, Brunetti V, Malvindi MA, Al-Juffali N, Vecchio G, Janes SM. 2014. A general mechanism for intracellular toxicity of metal-containing nanoparticles. Nanoscale 6 (12):7052-7061.

Sahneh FD, Scoglio CM, Monteiro-Riviere NA, Riviere JE. 2015. Predicting the impact of bio-corona formation kinetics on inter-species extrapolations of nanoparticle biodistribution modeling. Nanomedicine (Lond) 10:25–33.

Salari-Joo H, Kalbassi MR, Yu IJ, Lee JH, Johari SA. 2013. Bioaccumulation of silver nanoparticles in rainbow trout (Oncorhynchus mykiss): Influence of concentration and salinity. Aquat. Toxicol.140–141:398–406.

Saliani M, Jalal R, Goharshadi KE. 2016. Mechanism of oxidative stress involved in the toxicity of ZnO nanoparticles against eukaryotic cells. Nanomedicine Journal 3 (1):1-14.

Sato K, Li J-G, Kamiya H, Ishigaki T. 2008. Ultrasonic Dispersion of TiO2 Nanoparticles in Aqueous Suspension. J. Am. Ceram. Soc. 91 (8):2481–2487.

Schmid G.2008.The relevance of shape and size of Au55 clusters. Chem Soc Rev. 37(9):1909-30.

Schmid G, Decker M, Ernst H, Fuchs H, Grünwald W, Grunwald A, Hofmann H, Mayor M, Rathgeber W, Simon U, Wyrwa D. 2003. Small Dimensions and Material Properties A

Definition of Nanotechnology. Graue Reihe Nr. 35. Final report of the Europäische Akademie's study group "Miniaturization and Material Properties". Europäische Akademie Publishing.

Scown TM, Santos EM, Johnston BD, Gaiser B, Baalousha M, Mitov S, Lead JR, Stone V, Fernandes TF, Jepson M. et al. 2010. Effects of aqueous exposure to silver nanoparticles of different sizes in rainbow trout. Toxicol. Sci. 115:521–534.

Scudiero R, Carginale V, Riggio M, Capasso C, Capasso A, Kille P, di Prisco G, Parisi E. 1997. Difference in hepatic metallothionein content in Antarctic red-blooded and haemoglobinless fish: undetectable metallothionein levels in haemoglobinless fish is accompanied by accumulation of untranslated metallothionein mRNA. Biochem. J. 322:207–211.

Scudiero R, Temussi PA, Parisi E. 2005. Fish and mammalian metallothioneins: a comparative study. Gene 345, 21–26.

Seibert H, Mörchel S, Gülden M. 2002. Factors influencing nominal effective concentrations of chemical compounds *in vitro*: medium protein concentration. Toxicol In Vitro. 16(3):289-97.

Semisch A, Ohle J, Witt B, Hartwig A. 2014. Cytotoxicity and genotoxicity of nano - and microparticulate copper oxide: role of solubility and intracellular bioavailability. Part Fibre Toxicol. 11:10.

Sereemaspun A, Hongpiticharoen P, Rojanathanes R, Maneewattanapinyo P, Ekgasit S, Warisnoicharoen W. 2008. Inhibition of human cytochrome P450 enzymes by metallic nanoparticles: A preliminary to nanogenomics. Int. J. Pharmacol: 4: 492-495.

Sharma V, Shukla RK, Saxena N, Parmar D, Das M, Dhawan A. 2009. DNA damaging potential of zinc oxide nanoparticles in human epidermal cells. Toxicol Lett. 185(3):211-8.

Sharma V, Anderson D, Dhawan A. 2012. Zinc oxide nanoparticles induce oxidative DNA damage and ROS-triggered mitochondria mediated apoptosis in human liver cells (HepG2). Apoptosis. 17(8):852-70.

Shaw BJ, Al-Bairuty G, Handy RD. 2012. Effects of waterborne copper nanoparticles and copper sulphate on rainbow trout, (*Oncorhynchus mykiss*): physiology and accumulation. Aquat Toxicol. 116-117:90-101.

Shavlovski MM, Chebotar NA, Konopistseva LA, Zakharova ET, Kachourin AM, Vassiliev VB, Gaitskhoki VS. 1995. Embryotoxicity of silver ions is diminished by ceruloplasmin--further evidence for its role in the transport of copper. Biometals. 8(2):122-8.

Shi J, Karlsson HL, Johansson K, Gogvadze V, Xiao L, Li J, Burks T, Garcia-Bennett A, Uheida A, Muhammed M, Mathur S, Morgenstern R, Kagan VE, Fadeel B. 2012. Microsomal Glutathione Transferase 1 Protects Against Toxicity Induced by Silica Nanoparticles but Not by Zinc Oxide Nanoparticles. ACS Nano 6(3):1925-38.

Shvedova AA, Kisin ER, Mercer R, Murray AR, Johnson VJ, Potapovich AI, Tyurina YY, Gorelik O, Arepalli S, Schwegler-Berry D, Hubbs AF, Antonini J, Evans DE, Ku BK, Ramsey D, Maynard A, Kagan VE, Castranova V, Baron P. 2005. Unusual inflammatory and fibrogenic pulmonary responses to single-walled carbon nanotubes in mice. Am J Physiol Lung Cell Mol Physiol. 289(5):L698-708.

Shvedova AA, Pietroiusti A, Fadeel B, Kagan VE. 2012. Mechanisms of carbon nanotube-induced toxicity: Focus on oxidative stress. Toxicol Appl Pharmacol. 261(2):121-33.

Shukla R, Bansal V, Chaudhary M, Basu A, Bhonde RR, Sastry M. 2005. Biocompatibility of gold nanoparticles and their endocytotic fate inside the cellular compartment: a microscopic overview. Langmuir. 21(23):10644-5

Siddiqui MA, Alhadlaq HA, Ahmad J, Al-Khedhairy AA, Musarrat J, Ahamed M. 2013. Copper oxide nanoparticles induced mitochondria mediated apoptosis in human hepatocarcinoma cells. PLoS One. 8(8):e69534.

Sies H. 1991. Oxidative stress: from basic research to clinical application. Am J Med. 91(3C):31S-38S.

Simonet BM, Valcarcel M. 2009. Monitoring nanoparticles in the environment. Anal. Bioanal. Chem. 393:17–21.

Smith CJ, Shaw BJ, Handy RD. 2007. Toxicity of single walled carbon nanotubes on rainbow trout, (*Oncorhynchus mykiss*): respiratory toxicity, organ pathologies, and other physiological effects Aquat. Toxicol. 82:94–109.

Sohn EK, Johari SA, Kim TG, Kim JK, Kim E, Lee JH, Chung YS, Yu IJ. 2015. Aquatic Toxicity Comparison of Silver Nanoparticles and Silver Nanowires. Biomed Res Int. 2015: 893049.

Spry DJ, Wood MC. 1989. A kinetic method for the measurement of zinc influx *in vivo* in the rainbow trout, and the effects of waterborne calcium on flux rates. J. Exp. Biol. 142: 425-446.

Stern ST, Adiseshaiah PP, Crist RM. 2012. Autophagy and lysosomal dysfunction as emerging mechanisms of nanomaterial toxicity. Part Fibre Toxicol. 9:20.

Stohs SJ, Bagchi D. Oxidative mechanisms in the toxicity of metal ions. 1995. Free Radic Biol Med. 18(2):321-36.

Stone V, Johnston H, Schins RP. 2009. Development of *in vitro* systems for nanotoxicology: methodological considerations. Crit Rev Toxicol. 39(7):613-26.

Studer AM, Limbach LK, Van Duc L, Krumeich F, Athanassiou EK, Gerber LC, Moch H, Stark WJ. 2010. Nanoparticle cytotoxicity depends on intracellular solubility: comparison of stabilized copper metal and degradable copper oxide nanoparticles. Toxicol Lett. 197(3):169-74.

Sung JH, Ji JH, Park JD, Yoon JU, Kim DS, Jeon KS, Song MY, Jeong J, Han BS, Han JH, Chung YH, Chang HK, Lee JH, Cho MH, Kelman BJ, Yu IJ. 2009. Subchronic inhalation toxicity of silver nanoparticles. Toxicol. Sci. 108:452–461.

Tang J, Xiong L, Wang S, Wang J, Liu L, Li J, Xi T. 2008. Influence of silver nanoparticles on neurons and blood-brain barrier via subcutaneous injection in rats. Applied Surface Science. 255(2):502-504.

Tang J, Xiong L, Wang S, Wang J, Liu L, Li J, Xi T. 2009. Distribution, translocation and accumulation of silver nanoparticles in rats. Journal of Nanoscience and Nanotechnology 9(8): 4924-32.

Tantra R, Tompkins J, Quincey P. 2010. Characterisation of the de-agglomeration effects of bovine serum albumin on nanoparticles in aqueous suspension. Collid. Surf. A 75:275–281.

Teeguarden JG, Hinderliter PM, Orr G, Thrall BD, Pounds JG. 2007. Particokinetics *in vitro*: dosimetry considerations for *in vitro* nanoparticle toxicity assessments. Toxicol Sci. 95(2):300-12.

Teodoro JS, Simões AM, Duarte FV, Rolo AP, Murdoch RC, Hussain SM, Palmeira CM. 2011. Assessment of the toxicity of silver nanoparticles *in vitro*: a mitochondrial perspective. Toxicol In Vitro 25(3):664-70.

Tseng MT, Lu X, Duan X, Hardas SS, Sultana R, Wu P, Unrine JM, Graham U, Butterfield DA, Grulke EA, Yokel RA. 2012. Alteration of hepatic structure and oxidative stress induced by intravenous nanoceria. Toxicol Appl Pharmacol. 260(2):173-82.

Tsoli M, Kuhn H, Brandau W, Esche H, Schmid G. 2005. Cellular Uptake and Toxicity of Au55 Clusters. Small. 1(8-9):841-4.

Turney TW, Duriska MB, Jayaratne V, Elbaz A, O'Keefe SJ, Hastings AS, Piva TJ, Wright PFA, Feltis BN. 2012. Formation of zinc-containing nanoparticles from Zn2+ ions in cell culture media: Implications for the nanotoxicology of ZnO. Chem. Res. Toxicol. 25:2057−2066.

Turrens FJ. 2003. Mitochondrial formation of reactive oxygen species. J Physiol. 552(Pt 2): 335–344.

Valko M, Morris H, Cronin MT. 2005. Metals, toxicity and oxidative stress. Curr Med Chem. 12(10):1161-208.

Vandebriel J R and De Jong H W. 2012. A review of mammalian toxicity of ZnO nanoparticles. Nanotechnol Sci Appl. 5:61–71.

Verbost PM, Rooij J van, Flik G, Lock RAC, Wendelaar Bonga SE. 1989. The movement of cadmium through freshwater trout branchial epithelium and its interference with calcium transport. J. exp. Biol. 145:185–197.

Vergani L, Lanza C, Scarabelli L, Canesi L, Gallo G. 2009. Heavy metal and growth hormone pathways in metallothionein regulation in fish RTH-149 cell line. Comp Biochem Physiol, Part C 149: 572–580.

Verma A, Stellacci F. 2010. Effect of surface properties on nanoparticle-cell interactions. Small. 6(1):12-21.

Verwey EJW, Overbeek JThG. 1948. Theory of stability of lyophobic colloids. Elsevier, Amsterdam.

Vippola M, Falck GC, Lindberg HK, Suhonen S, Vanhala E, Norppa H, Savolainen K, Tossavainen A, Tuomi T. 2009. Preparation of nanoparticle dispersions for in-vitro toxicity testing. Hum Exp Toxicol. 28(6-7):377-85.

Vrček IV, Žuntar I, Petlevski R, Pavičić I, Dutour Sikirić M, Ćurlin M, Goessler W. 2014. Comparison of *in vitro* toxicity of silver ions and silver nanoparticles on human hepatoma cells. Environ Toxicol. 31(6):679-92.

Walczyk D, Bombelli FB, Monopoli MP, Lynch I, Dawson KA. 2010. What the cell "sees" in bionanoscience. J Am Chem Soc. 132(16):5761-8.

Walser T, Limbach LK, Brogioli R, Erismann E, Flamigni L, Hattendorf B, Juchli M, Krumeich F, Ludwig C, Prikopsky K, Rossier M, Saner D, Sigg A, Hellweg S, Günther D, Stark WJ. 2012. Persistence of engineered nanoparticles in a municipal solid-waste incineration plant. Nat Nanotechnol. 7(8):520-4.

Wang H, Joseph JA.1999. Quantifying cellular oxidative stress by dichlorofluorescein assay using microplate reader. Free Radic Biol Med. 27(5-6):612-6.

Wang J, Zhou G, Chen C, Yu H, Wang T, Ma Y, Jia G, Gao Y, Li B, Sun J, Li Y, Jiao F, Zhao Y, Chai Z. 2007. Acute toxicity and biodistribution of different sized titanium dioxide particles in mice after oral administration. Toxicol Lett. 168(2):176-85.

Wang B, Feng W, Wang M, Wang T, Gu Y, Zhu M, Ouyang H, Shi J, Zhang F, Zhao Y, Chai Z, Wang H, Wang J. 2008. Acute toxicological impact of nano- and submicro-scaled zinc oxide powder on healthy adult mice. Journal of Nanoparticle Research 10(2):263-276.

Wang L, Wang L, Ding W, Zhang F. 2010. Acute toxicity of ferric oxide and zinc oxide nanoparticles in rats. J Nanosci Nanotechnol. 10(12):8617-24.

Wang Y, Aker WG, Hwang HM, Yedjou CG, Yu H, Tchounwou PB. 2011. A study of the mechanism of *in vitro* cytotoxicity of metal oxide nanoparticles using catfish primary hepatocytes and human HepG2 cells. Sci Total Environ. 409(22):4753-62.

Wang Z, Li N, Zhao J, White JC, Qu P, Xing B. 2012.CuO nanoparticle interaction with human epithelial cells: cellular uptake, location, export, and genotoxicity. Chem Res Toxicol. 25(7):1512-21.

Wang F, Yu L, Monopoli MP, Sandin P, Mahon E, Salvati A, Dawson KA. 2013. The biomolecular corona is retained during nanoparticle uptake and protects the cells from the damage induced by cationic nanoparticles until degraded in the lysosomes. Nanomedicine 9(8):1159-68.

Wang B, Zhang Y, Mao Z, Yu D, Gao C. 2014.Toxicity of ZnO nanoparticles to macrophages due to cell uptake and intracellular release of zinc ions. J Nanosci Nanotechnol.14(8):5688-96.

Wang W, He Y, Yu G, Li B, Sexton DW, Wileman T, Roberts AA, Hamilton CJ, Liu R, Chao Y, Shan Y, Bao Y. 2015. Sulforaphane Protects the Liver against CdSe Quantum Dot-Induced Cytotoxicity. PLoS One 10(9):e0138771.

Warheit DB. 2008. How meaningful are the results of nanotoxicity studies in the absence of adequate material characterization? Toxicol Sci. 101(2):183-5.

Westerhoff P, Song GX, Hristovski K, Kiser MA. 2011. Occurrence and removal of titanium at full scale wastewater treatment plants: implications for TiO(2) nanomaterials. Journal of Environmental Monitoring; 13:1195-1203.

Wick P, Malek A, Manser P, Meili D, Maeder-Althaus X, Diener L, Diener PA, Zisch A, Krug HF, von Mandach U. 2010. Barrier capacity of human placenta for nanosized materials. Environmental Health Perspectives 118(3):432-436.

Wijmenga C, Klomp LW. 2004. Molecular regulation of copper excretion in the liver. Proc Nutr Soc. 63(1):31-9.

Wilkening S, Stahl F, Bader A. 2003. Comparison of primary human hepatocytes and hepatoma cell line Hepg2 with regard to their biotransformation properties. Drug Metab Dispos 31(8):1035–1042.

Wood CM. 1992. Flux measurements as indices of H+ and metal effects on freshwater fish. Aquat. Toxicol. 22:239–264.

Woodrow Wilson database 2014. Nanotechnology consumer product inventory. Woodrow Wilson International Centre for Scholars. Available online: http://www.nanotechproject.org/cpi/website (accessed on 10 October 2014).

Wolf K, Quimby MC. 1962. Established eurythermic line of fish cells *in vitro*. Science 135: 1065-6.

Wörle-Knirsch JM, K Pulskamp, HF Krug. 2006. Oops they did it again! Carbon nanotubes hoax scientists in viability assays. Nano Lett 6: 1261-1268.

Wu Q, Nouara A, Li Y, Zhang M, Wang W, Tang M, Ye B, Ding J, Wang D. 2013a. Comparison of toxicities from three metal oxide nanoparticles at environmental relevant concentrations in nematode Caenorhabditis elegans. Chemosphere 90(3):1123-31.

Wu Y, Zhou Q. 2013b. Silver nanoparticles cause oxidative damage and histological changes in medaka (*Oryzias latipes*) after 14 days of exposure. Environ. Toxicol. Chem. 32:165–173.

Xia T, Kovochich M, Brant J, Hotze M, Sempf J, Oberley T, Sioutas C, Yeh JI, Wiesner MR, Nel AE. 2006. Comparison of the abilities of ambient and manufactured nanoparticles to induce cellular toxicity according to an oxidative stress paradigm. Nano Lett. 6(8):1794-1807.

Xia T, Kovochich M, Liong M, Mädler L, Gilbert B, Shi H, Yeh JI, Zink JI, Nel AE. 2008a. Comparison of the mechanism of toxicity of zinc oxide and cerium oxide nanoparticles based on dissolution and oxidative stress properties. ACS Nano 2(10):2121-34.

Xia T, Kovochich M, Liong M, Zink JI, Nel AE. 2008b. Cationic polystyrene nanosphere toxicity depends on cell-specific endocytic and mitochondrial injury pathways. ACS Nano 2(1):85-96.

Xie G, Sun J, Zhong G, Shi L, Zhang D. 2010. Biodistribution and toxicity of intravenously administered silica nanoparticles in mice. Arch Toxicol. 84(3):183-90.

Xiong D, Fang T, Yu L, Sima X, Zhu W. 2011. Effects of nano-scale TiO2, ZnO and their bulk counterparts on zebrafish: acute toxicity, oxidative stress and oxidative damage. Sci Total Environ. 409(8):1444-52.

Yamashita K, Yoshioka Y, Higashisaka K, Mimura K, Morishita Y, Nozaki M, Yoshida T, Ogura T, Nabeshi H, Nagano K, Abe Y, Kamada H, Monobe Y, Imazawa T, Aoshima H, Shishido K, Kawai Y, Mayumi T, Tsunoda S, Itoh N, Yoshikawa T, Yanagihara I, Saito S, Tsutsumi Y. 2011. Silica and titanium dioxide nanoparticles cause pregnancy complications in mice. Nat Nanotechnol. 6(5):321-8.

Yue Y, Behra R, Sigg L, Fernández Freire P, Pillai S, Schirmer K. 2015. Toxicity of silver nanoparticles to a fish gill cell line: role of medium composition. Nanotoxicology 9(1):54-63.

Yoon KY, Hoon Byeon J, Park JH, Hwang J. 2007. Susceptibility constants of Escherichia coli and Bacillus subtilis to silver and copper nanoparticles. Sci Total Environ. 373(2-3):572-5.

Zalewski PD, Forbes IJ, Betts WH. 1993. Correlation of apoptosis with change in intracellular labile Zn(II) using zinquin [(2-methyl-8-p-toluenesulphonamido-6-quinolyloxy)acetic acid], a new specific fluorescent probe for Zn(II). Biochem. J. 296(Pt 2):403–408.

Zhang XD, Wu D, Shen X, Liu PX, Fan FY, Fan SJ. 2012. *In vivo* renal clearance, biodistribution, toxicity of gold nanoclusters. Biomaterials 33(18):4628-38.

Zhang Y, Nguyen KC, Lefebvre DE, et al. 2014. Critical experimental parameters related to the cytotoxicity of zinc oxide nanoparticles. J Nanopart Res. 16(6):2440.

Zhu X, Zhu L, Duan Z, Qi R, Li Y, Lang Y. 2008. Comparative toxicity of several metal oxide nanoparticle aqueous suspensions to Zebrafish (Danio rerio) early developmental stage, J Environ Sci Health A Tox Hazard Subst Environ Eng. 43(3):278-84.

Zitka O, Skalickova S, Gumulec J, Masarik M, Adam V, Hubalek J, Trnkova L, Kruseova J, Eckschlager T, Kizek R. 2012. Redox status expressed as GSH:GSSG ratio as a marker for oxidative stress in paediatric tumour patients. Oncol Lett. 4(6):1247-1253.

Zong WX, Thompson CB. 2006. Necrotic death as a cell fate. Genes Dev. 20(1):1-15.

APPENDICES

Appendix A: Supplementary information for chapter 3- Introductoy paper 2: Species-specific toxicity of copper nanoparticles among mammalian and piscine cell line.

Supplementary Material

Supplementary 1. Supplements of cell culture media

H4IIE and HepG2 cells were maintained at 37ºC and 5% CO_2. EMEM culture medium for H4IIE cells was supplemented with 10% FBS, 1% L-glutamine (200 Mm), 1% of penicillin/streptomycin (10 000 u/mL and 10 mg/mL for penicillin and streptomycin respectively and 1% 100XNEAA. For culturing HepG2, the 1% L-glutamine was replaced by 1 % ultraglutamine (200 mM). PLHC-1 cells were cultured at 30 ºC in a 5% CO_2 atmosphere in α-MEM culture medium supplemented with 5 % FBS, 1 % L-glutamine, and 1 % of penicillin/streptomycin, at the same initial concentrations as indicated before. RTH-149 was cultured at 20 ºC under 5% CO_2 atmosphere in EMEM supplemented with 10 % FBS, 1 % L-glutamine, 1 % penicillin/streptomycin, at the same initial concentrations as indicated before, and 1 % sodium pyruvate (100 mM).

Supplementary 2. An example of subtracting particle profiles from media profiles in the DLS graphs. The culture media profile of H4IIE cell lines has been measured first, which was shown in the upper part of this figure. Then the profiles of CuNPs in H4IIE culture media were measured. The peaks with similar sizes and intensity as H4IIE media profiles were neglected. Only the peaks with higher intensity were taken into consideration to determine the size distribution of CuNPs.

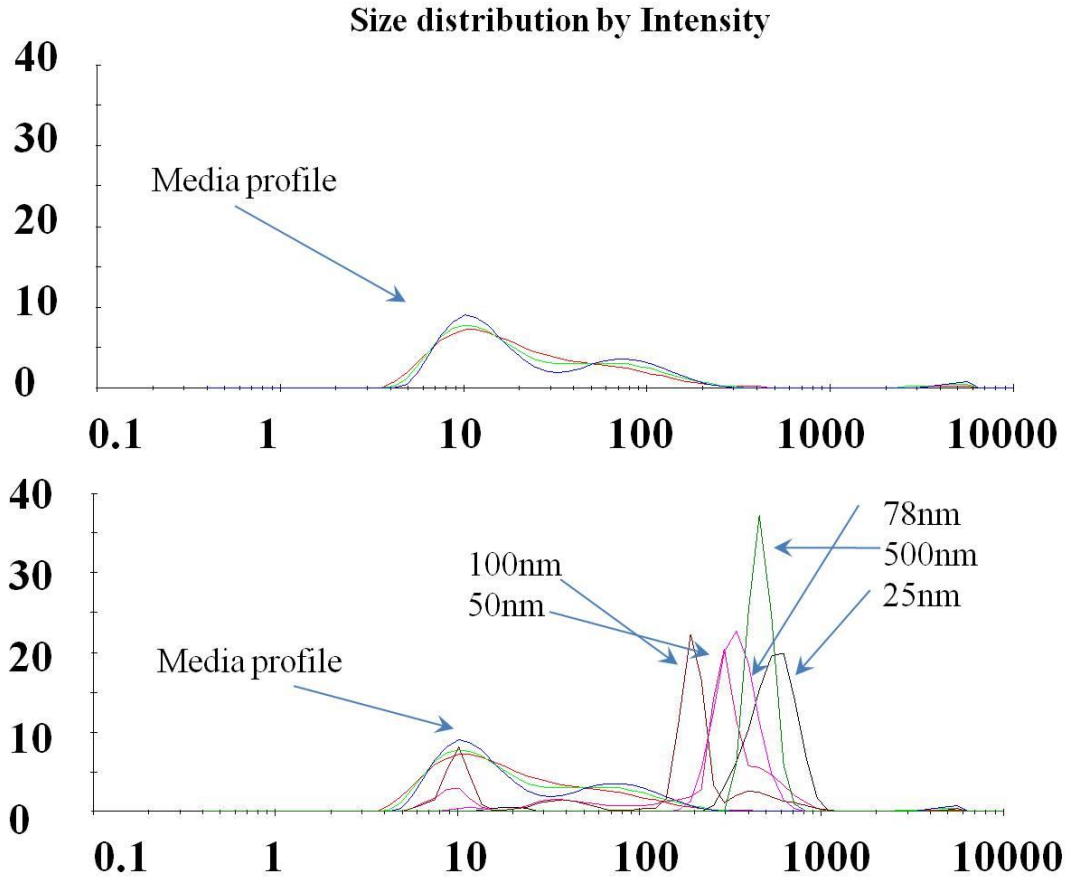

Supplementary 3. ICP-MS measurement

A certified multi-element solution (As, Ba, Be, Bi, Ce, Co, In, Li, Ni, Pb and U - Analytika Ltd, Czech Republic) was used to establish and optimize the operating instrument conditions. Copper quantification was carried out using external calibration and internal standardization (Ga) to minimize the impact of signal instability during the analysis. Calibration standard solutions of copper and internal standard solutions of Ga were prepared daily with subsequent dilutions of the 1000 mg/L Cu in 2 % HNO_3 (v/v) and 1000 mg/L Ga in 2 % HNO_3 (v/v) stock standard solutions (Alfa Aesar, Madrid, Spain), respectively.

Limits of detection (LOD) and limits of quantification (LOQ) were calculated as being respectively three times and ten times the standard deviation of the blank, considering as such each one of the different media studied (H4IIE, HepG2, PLHC-1 and RTH-149) subject to the same treatment as samples. In all cases, the LOD ranged from 0.16 to 0.27 µg/L and the LOQ from 0.53 to 0.90 µg/L. The instrumental response was linear over the calibration range from 0.1 to 100 µg/L, with a relative standard deviation (RSD) < 2 %. For copper concentration measurements, the media from each well was transferred into a polypropylene flask and the well washed twice with nitric acid 2 % (v/v). The rinses were added to the corresponding sample media and made up to a final volume of 10 mL with nitric acid 2% (v/v). Just before ICP-MS analysis, samples were ultrasonicated for five minutes.

Supplementary 4. Size distribution of (a) the pristine micro particles (MPs) prepared in ethanol and (b) 24 h after incubation under culture conditions.

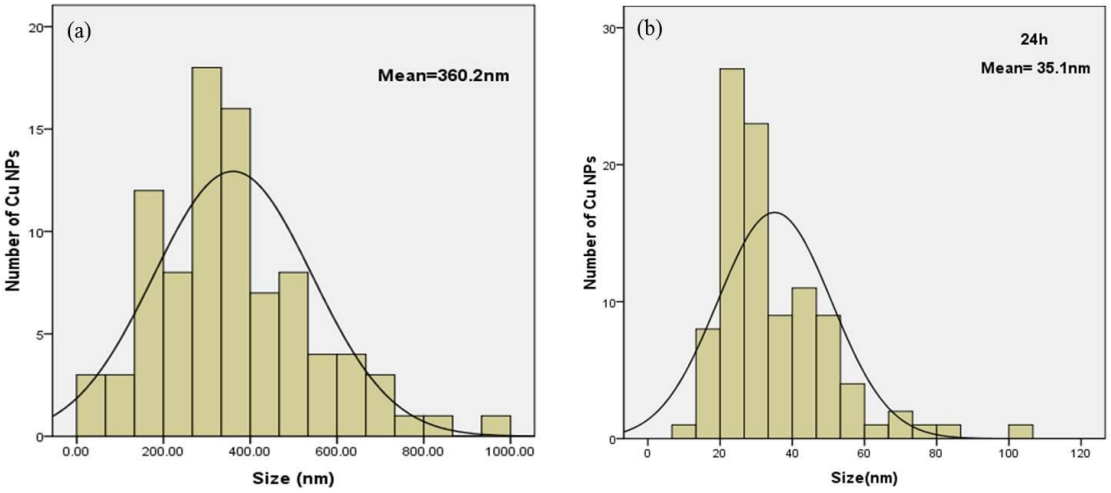

Supplementary 5. IC_{20}, IC_{50} and IC_{80} of each copper suspension after exposure to the four different cell lines after 24 hours and the IC_{20}, IC_{50} and IC_{80} of particle form in each copper suspensions(CuNPs), expressed as mean ± standard deviation (µg Cu /mL of medium suspension).

		H4IIE			HepG2			PLHC-1			RTH-149		
	ICx (µg/ml)	**IC_{20}**	**IC_{50}**	**IC_{80}**	**IC_{20}**	**IC_{50}**	**IC_{80}**	**IC_{20}**	**IC_{50}**	**IC_{80}**	**IC_{20}**	**IC_{50}**	**IC_{80}**
IC_x of copper suspension	**25nm**	10±0*	20±3	70±4	17±4	39±5	68±4	53±13	83±16	124±2	53±18	91±27	144±15
	50nm	20±13	55±15	95±14	22±3	42±2	72±1	45±19	67±20	117±9	63±13	115±12	201±71
	78nm	15±3	56±18	112±55	11±5	48±3	88±5	29±17	58±22	87±28	69±32	182±74	260±13
	100nm	29±0	76±5	136±24	28±2	57±1	81±0	32±5	59±5	88±4	67±30	104±4	166±22
	MPs	6±5	26±12	71±24	15±2	26±12	53±4	38±5	45±18	81±12	35±18	74±14	112±10
	$Cu(NO_3)_2$	18±7	54±9	90±14	18±2	43±4	71±4	79±14	109±10	180±9	68±36	120±15	179±16
ICx of Particle form in copper suspensions	**25nm**	3±0	9±1	15±1	6±2	7±1	17±1	14±3	22±1	29±0	17±7	30±2	43±3
	50nm	16±7	27±10	39±12	19±3	28±2	37±1	23±11	39±7	62±4	49±14	77±10	143±57
	78nm	33±14	77±17	98±43	12±4	44±2	76±5	17±9	35±12	53±14	64±34	139±24	213±15
	100nm	34±6	48±4	62±4	22±2	33±1	44±1	15±2	25±2	36±2	32±2	65±10	98±3
	MPs	1±0	4±3	6±5	4±0	9±1	12±1	6±0	12±7	28±3	6±2	12±2	17±1

*Interpolation from Fig. 6.

Supplementary 6. Significant differences (P<0.05) of $IC_{50\ (total)}$/$IC_{50\ (particle)}$ between different particles (a, b) in the same cell lines and between different cell lines exposed to same particles (c, d), $IC_{50\ (total)}$/$IC_{50\ (particle)}$ were plotted as mean ± standard deviation.

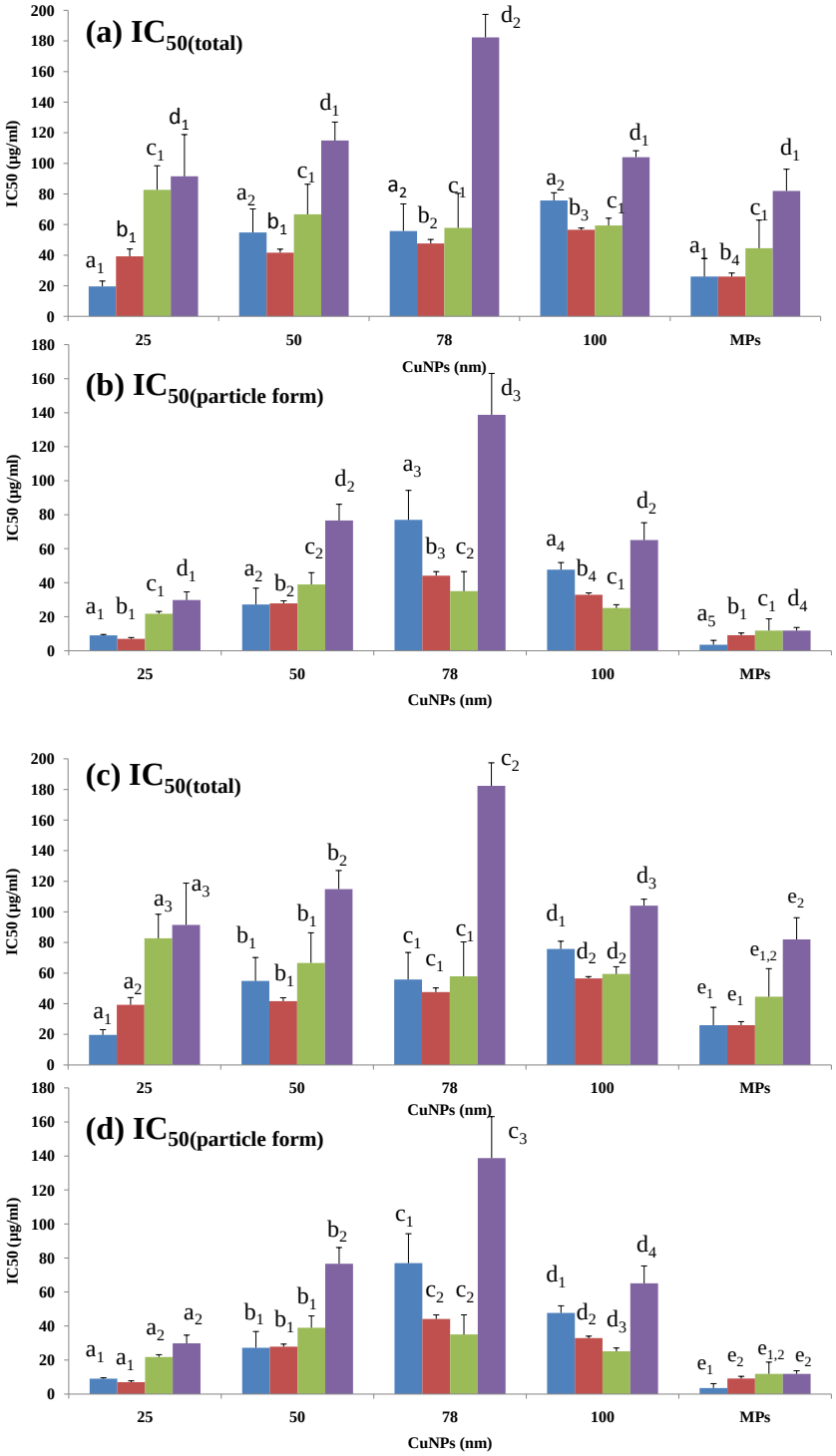

Supplementary 7. Intracellular ROS in hepatocellular cell lines following exposure to a concentration extrapolated from the fitted curves: (a) 50 µg/ml and (b) 80 µg/ml of different types of CuNPs, the MPs and copper nitrate. ROS levels are quantified by measuring the percentage increase in fluorescence with respect to the control (100%). Results are expressed as the mean of three independent assays ± standard error of the mean. Significant differences between CuNPs exposures are represented by (*) (P<0.05) and same numbers designate relationship, while significant differences between cell line responses are represented by (α, β) (P<0.01) and same numbersdesignaterelationship.

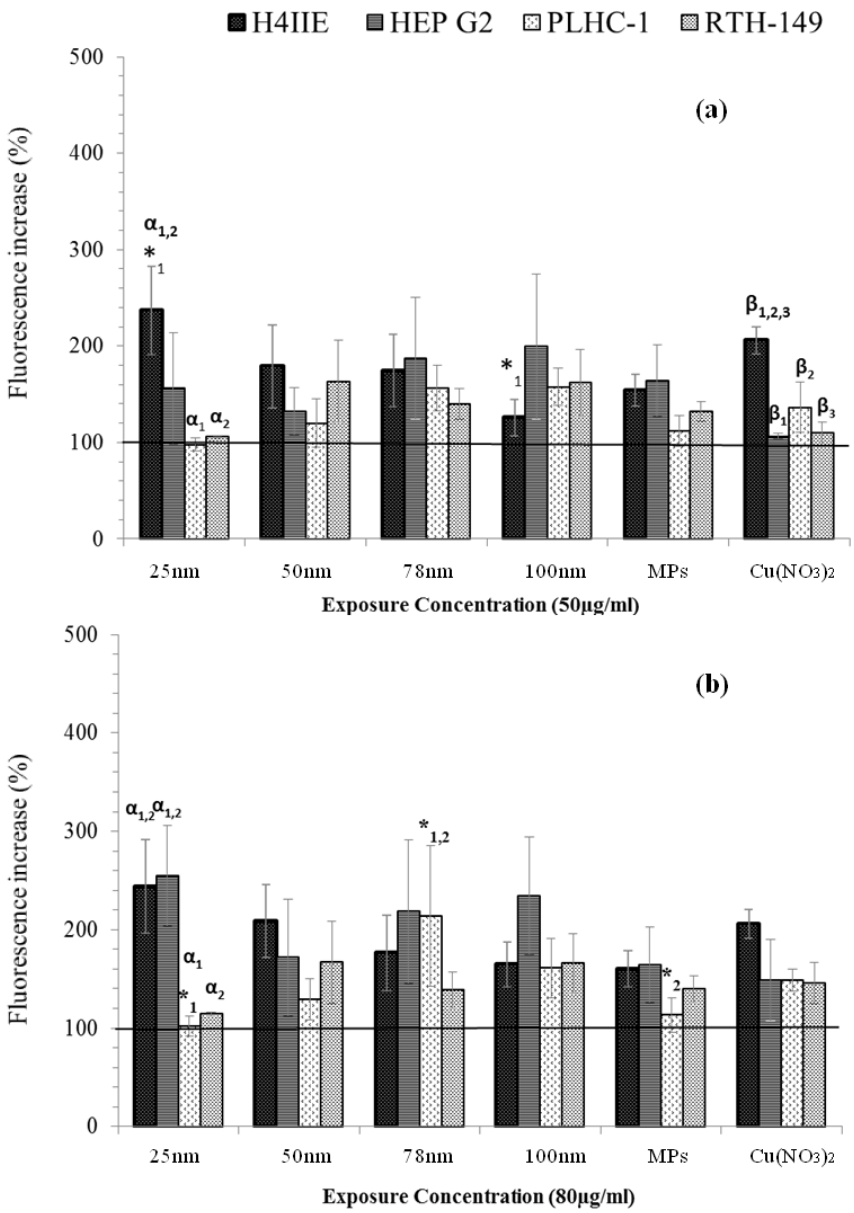

Appendix B: Supplementary information for chapter 4- Research paper 1: Recovery of redox homeostasis altered by CuNPs in H4IIE liver cells does not reduce the cytotoxic effects of these NPs: an investigation using aryl hydrocarbon receptor (AhR) dependent antioxidant activity.

Supplementary Information

Comparative Cytotoxicity Study of Silver Nanoparticles (AgNPs) in a Variety of Rainbow Trout Cell Lines (RTL-W1, RTH-149, RTG-2) and Primary Hepatocytes

Table S1. Composition of L-15, EMEM(pyr), EMEM(NEAA) and M199 complex culture media used to prepare AgNM-300K suspensions and expose the cell lines and primary hepatocytes.

Cell Line	**RTL-W1**	**RTH-149**	**RTG-2**	**Primary Hepatocytes**
Cell culture medium	Leibovitz L-15	EMEM (pyr)	EMEM (NEAA)	M199
Component	Concentration (mg/L)			
Inorganic Salts				
Calcium chloride (CaCl2) (anhyd.)/(dihyd)	140 (anhyd.)	265 (dihyd.)	265 (dihyd.)	200 (anhyd.)
Potassium chloride (KCL)	400	400	400	400
Sodium chloride (NaCL)	8000	6800	6800	6800
Ferric nitrate (monohyd.)	–	–	–	0.720
Magnesium chloride	93.67	–	–	–
Magnesium sulphate (anhyd.)	97.70	200	200	97.67
Sodium acetate (anhydr.)	–	200	200	50
Potassium phosphate (KH_2PO_4)	60			–
Sodium phosphate (NaH_2PO_4) (monohyd.)/(anhyd.) *	190 *	140	140	140
Sodium bicarbonate ($NaHCO_3$)	–	2200	2200	–
Sodium pyruvate	550	110 (Added)	–	–
Amino Acids				
D/L-Alanine	450	–	8.9 (Added)	25
L-Arginine/L-Arginine HCL *	500	126.4 *	126.4 *	70
L-Asparagine	250	–	13.21 (Added)	–
L-Aspartic acid	–		13.30 (Added)	30
L-Cysteine/L-Cysteine HCL (monohyd.) *	120	24	24	26 *
L-Glutamine	292 (Added)	292	292	100
L-Glutamic acid	–	–	14.7 (Added)	67
Glycine	200	–	7.5 (Added)	50
L-Histidine/L-Histidine HCL (monohyd.) *	250	42 *	42 *	21.88 *

Table S1. *Cont.*

Cell Line	RTL-W1	RTH-149	RTG-2	Primary Hepatocytes
D/L-Isoleucine	250	52.4	52.4	20
L-Leucine	125	52.4	52.4	60
L-Lysine/L-Lysine HCL *	75	73 *	73 *	15 *
D/L-Methionine	150	15	15	25
D/L-Phenylalanine	250	33	33	25
L-Serine	200	–	19.5 (Added)	25
L-Proline/Hydroxy L-Proline *	–	–	11.5 (Added)	40/10 *
D/L-Threonine	600	47.6	47.6	30
L-Tyrosine/L-Tyrosine 2Na (dihyd.) *	370 *	36.2	36.2	57.66 *
L-Tryptophan	20	10.2	10.2	10
D/L-Valine	200	46.8	46.8	25
Vitamins				
Ascorbic acid				0.05
Biotin				0.1
Choline chloride	1	1	1	0.5
D/L-Ca Pantothenate	1	1	1	0.01
Ergocalciferol	–			0.1
i-inositol	2	2	2	0.05
Folic acid	1	1	1	0.01
Menadione	–			0.01
Niacin	–			0.025
Nicotinamide	1	1	1	0.025
4-Aminobenzoic acid (PABA)	–			0.05
Pyrridoxal HCL	–			0.025
Pyridoxine HCL	1	1	1	0.025
Riboflavin/Riboflavin -5-PO_4 Na *	0.1 *	0.1	0.1	0.01
Thiamine HCL/Thiamine monophosphate *	1 *	1	1	0.01
DL-α-tocopherol phosphate 2Na	–	–	–	0.01
Vitamin A acetate	–	–	–	0.14
Other components	–	–		
Adenine Sulphate (dihydr.)	–	–	–	10.98
Adenosine 5'-monophosphate (AMP) (monohyd.)	–	–	–	0.2
Adenosine 5'-triphosphate (ATP) 2Na (trihyd.)	–	–	–	1.098
Cholesterol (synthetic)	–	–	–	0.2
2-deoxy-d-ribose	–	–	–	0.5
Dextrose	–	–	–	1000
L-Glutathione (reduced)	–	–	–	0.05

Table S1. *Cont.*

Cell Line	RTL-W1	RTH-149	RTG-2	Primary Hepatocytes
Guanine HCL (monohyd.)	–	–	–	0.3
Hypoxanthine Na	–	–	–	0.345
D-Ribose	–	–	–	0.5
Thymine	–	–	v	0.3
Tween 80	–	–	–	20
Uracil	–	v	–	0.3
D(+)Galactose/Glucose	900	1000	1000	1000
Phenol Red Na	10	10	10	21.24
Penicillin	10000 U/mL	10000 U/mL	10000 U/mL	–
Streptomycin	10	10	10	–
Xanthine Na	–	–	–	0.344
Serum				
Fetal bovine serum (FBS)	10% (Added)	10% (Added)	10% (Added)	10% (Added)

(**a**) (**b**)

Figure 1. Contrasting appearance of NM-300K suspensions (93.45 µg/mL)(right side) prepared in EMEM culture medium (**a**) and L-15 culture medium (**b**) compared to respective medium only (left side).

(a)

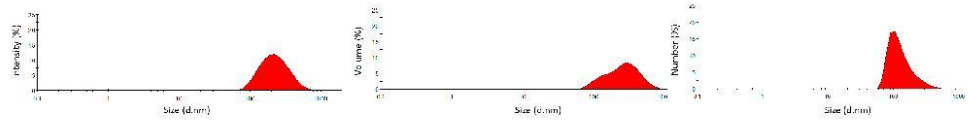

(b)

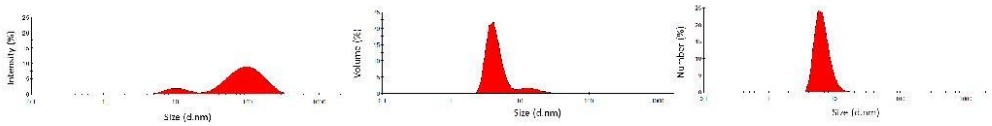

Figure 2. *Cont.*